A FOCUS ON ACTINOBACTERIA: DIVERSITY, DISTRIBUTION, AND SECONDARY METABOLITES

EDITED BY: Yu-Qin Zhang, Louis S. Tisa, Imen Nouioui, Wen-Jun Li and Xin-Peng Tian

PUBLISHED IN: Frontiers in Microbiology

frontiers Research Topics

ISSN 1664-8714
ISBN 978-2-88976-260-6
DOI 10.3389/978-2-88976-260-6

About Frontiers

Frontiers is more than just an open-access publisher of scholarly articles: it is a pioneering approach to the world of academia, radically improving the way scholarly research is managed. The grand vision of Frontiers is a world where all people have an equal opportunity to seek, share and generate knowledge. Frontiers provides immediate and permanent online open access to all its publications, but this alone is not enough to realize our grand goals.

Frontiers Journal Series

The Frontiers Journal Series is a multi-tier and interdisciplinary set of open-access, online journals, promising a paradigm shift from the current review, selection and dissemination processes in academic publishing. All Frontiers journals are driven by researchers for researchers; therefore, they constitute a service to the scholarly community. At the same time, the Frontiers Journal Series operates on a revolutionary invention, the tiered publishing system, initially addressing specific communities of scholars, and gradually climbing up to broader public understanding, thus serving the interests of the lay society, too.

Dedication to Quality

Each Frontiers article is a landmark of the highest quality, thanks to genuinely collaborative interactions between authors and review editors, who include some of the world's best academicians. Research must be certified by peers before entering a stream of knowledge that may eventually reach the public - and shape society; therefore, Frontiers only applies the most rigorous and unbiased reviews.
Frontiers revolutionizes research publishing by freely delivering the most outstanding research, evaluated with no bias from both the academic and social point of view. By applying the most advanced information technologies, Frontiers is catapulting scholarly publishing into a new generation.

What are Frontiers Research Topics?

Frontiers Research Topics are very popular trademarks of the Frontiers Journals Series: they are collections of at least ten articles, all centered on a particular subject. With their unique mix of varied contributions from Original Research to Review Articles, Frontiers Research Topics unify the most influential researchers, the latest key findings and historical advances in a hot research area! Find out more on how to host your own Frontiers Research Topic or contribute to one as an author by contacting the Frontiers Editorial Office: frontiersin.org/about/contact

A FOCUS ON ACTINOBACTERIA: DIVERSITY, DISTRIBUTION, AND SECONDARY METABOLITES

Topic Editors:
Yu-Qin Zhang, Institute of Medicinal Biotechnology, Chinese Academy of Medical Sciences, China
Louis S. Tisa, University of New Hampshire, United States
Imen Nouioui, German Collection of Microorganisms and Cell Cultures GmbH (DSMZ), Germany
Wen-Jun Li, Sun Yat-sen University, China
Xin-Peng Tian, South China Sea Institute of Oceanology, Chinese Academy of Sciences, China

Citation: Zhang, Y.-Q., Tisa, L. S., Nouioui, I., Li, W.-J., Tian, X.-P., eds. (2022). A Focus on Actinobacteria: Diversity, Distribution, and Secondary Metabolites. Lausanne: Frontiers Media SA. doi: 10.3389/978-2-88976-260-6

Table of Contents

frontiers | Frontiers in Microbiology

EDITORIAL
published: 05 May 2022
doi: 10.3389/fmicb.2022.902360

Editorial: A Focus on *Actinobacteria*: Diversity, Distribution, and Secondary Metabolites

Yu-Qin Zhang[1]*, *Xin-Peng Tian*[2], *Louis S. Tisa*[3], *Imen Nouioui*[4] and *Wen-Jun Li*[5]

[1] Institute of Medicinal Biotechnology, Chinese Academy of Medical Sciences and Peking Union Medical College, Beijing, China, [2] Key Laboratory of Marine Bio-resources Sustainable Utilization, Guangdong Key Laboratory of Marine Materia Medica, South China Sea Institute of Oceanology, Chinese Academy of Sciences, Guangzhou, China, [3] Department of Molecular, Cellular, and Biomedical Sciences, University of New Hampshire, Durham, NH, United States, [4] German Collection of Microorganisms and Cell Cultures GmbH (DSMZ), Braunschweig, Germany, [5] State Key Laboratory of Biocontrol, Guangdong Provincial Key Laboratory of Plant Resources and Southern Marine Science and Engineering Guangdong Laboratory (Zhuhai), School of Life Sciences, Sun Yat-sen University, Guangzhou, China

Keywords: ***Actinobacteria*, diversity, biosynthesis gene clusters, secondary metabolites, bioactive compounds**

Editorial on Research Topic

Editorial: A Focus on *Actinobacteria*: Diversity, Distribution, and Secondary Metabolites

Actinobacteria are the most closely related prokaryotic microorganisms of significance to humans. Apart from their significant contribution to soil organic matter turnover (Crowther et al., 2019), they are critical as symbionts in plant-associated microbial communities (Barka et al., 2015), plant-promoting and biocontrol agents (Toumatia et al., 2016; Zahra et al., 2020), and prolific producers of useful natural compounds (Demain and Sanchez, 2009; Idris et al., 2017). As a result, an increasing number of studies have concentrated on the diversity and distribution of actinobacterial resources, as well as the application of novel technologies to explore these microorganisms (Qin et al., 2016). *Actinobacteria* are so intriguing and exciting that has led to considerable novel species, genera, and even higher taxa being proposed and their corresponding novel resources have been collected from diverse ecosystems in recent years (https://lpsn.dsmz.de/phylum/actinobacteria).

After more than a decade of focusing on the diversity of *Actinobacteria* in desert environments, we discovered that members of the family *Geodermatophilaceae* were ubiquitous in various micro-ecosystems in Tengger and Badain Jaran deserts, and that this group of microorganisms played a critical role in determining the bacterial community structure in deserts (Sun et al., 2015, 2018; Jiang et al., 2021). Based on these studies, we hypothesized that *Geodermatophilaceae* represent desert-specific microorganisms and may serve as model organisms for studying the *Actinobacteria*'s resistance to multiple environmental pressures in extreme environments. Thus, we launched the topic "*A Focus on Actinobacteria: Diversity, Distribution, and Secondary Metabolites*" to bring together newly related research findings and ideas to demonstrate the diversity of *Actinobacteria* and their survival mechanisms in various ecosystems, and then to expound on useful *Actinobacteria* in detail.

We are indebted to all the authors for their contributions to this topic, which included one review and eight original research reports. These articles focused on the diversity, function, and biotechnology of *Actinobacteria* from desert, marine, gut, and nodule environments, as well as the application of gene manipulation technologies and metagenome analysis methods to other microorganisms.

Xie and Pathom-aree systematically reviewed recent advances on the technologies to the recovery of novel taxa, ecological functions, and the discovery of previously un-hitherto biotechnological properties of desert *Actinobacteria*.

OPEN ACCESS

Edited by:
George Tsiamis,
University of Patras, Greece

Reviewed by:
Vassiliki Karapapa,
Municipality of Agrinio, Greece

***Correspondence:**
Yu-Qin Zhang
zhyuqin@126.com

Specialty section:
This article was submitted to Systems Microbiology, a section of the journal Frontiers in Microbiology

Received: *23 March 2022*
Accepted: *20 April 2022*
Published: *05 May 2022*

Citation:
Zhang Y-Q, Tian X-P, Tisa LS, Nouioui I and Li W-J (2022) Editorial: A Focus on Actinobacteria: Diversity, Distribution, and Secondary Metabolites. Front. Microbiol. 13:902360. doi: 10.3389/fmicb.2022.902360

(i) After comparing the efficiency of different actinobacterial isolation techniques, this review strongly recommended that *Actinobacteria* can be isolated from desert associated samples using the sprinkling technique. (ii) Whole-genome sequencing was not only effective at resolving taxonomic bottlenecks, but also provided a wealth of information about the ecology and biotechnology potential of desert species. (iii) The PLate Coverage Algorithm (PLCA), a culture-enriched metagenomic approach, may be used to improve the recovery of microbial diversity on any low-abundance microbial communities. This approach was also beneficial in elucidating the mechanisms by which microbial communities interact with their hosts. (iv) Advances in computational techniques and bioinformatics tools have resulted in an enormously richer understanding of *Actinobacteria* biology in desert environments.

Liu et al. further supported the preceding review. They described an investigation into the diversity, novelty, and pharmacological potential of actinobacterial strains isolated from the Taklamakan desert. A batch of newly isolates, representing novel taxa or exhibiting antagonistic activity against "ESKAPE" pathogens, merit further investigation and exploration. Multi-strategies, including high-throughput screening, small-scale fermentation using deep-plates, One Strain Many Compounds (OSMAC), and compound dereplication *via* UPLC-QToF-MS/MS, were proposed to thoroughly investigate the functional *Actinobacteria*.

Distinct from the desert environments, the deep-sea ecological environment has generaly been regarded as another underexplored habitats for undiscovered, potentially pharmaceutical microbial resources. The orders *Gaiellales* and *Rubrobacterales* were discovered to be widespread in marine ecosystems, despite their difficulty in laboratory cultivation (Chen et al.). To obtain their pure cultures, Chen et al. optimized the growth conditions, and found that light, expanding culture time, and low nutrition could promote *Rubrobacterales* survival on media, and some marine factors are indispensable for their growth.

Guerrero-Garzón et al. investigated the antibiotic activity and comparative genomics of *Streptomyces* spp. isolated from marine sponges. The findings indicated that the dominant actinobacterial genus *Streptomyces* is not only a prolific producer of useful natural compounds, but also an ideal model for Synthetic Biology techniques to mine the selected biosynthesis gene clusters (BGCs).

Streptomyces spp. derived compounds have benefited humans for such a long time that it is becoming increasingly difficult to discover new compounds from *Streptomyces* continuously. As a result, it is critical to innovate perspectives, technologies, and strategies for conducting systematic investigations into *Streptomyces*' potential to produce novel compounds. The endophytic *Streptomyces* strain YINM00001, has shown to be strong antimicrobial activity and multiple antibiotic resistances, was predicted as a promising candidate to discover valuable secondary metabolites by genome mining, and proven by using OSMAC approach (Liu et al.).

Besides above approaches, genetic manipulation was another popular strategy for enhancing *Actinobacteria*'s application potential. The genetic manipulation system for genome modification in the rare actinomycete *Pseudonocardia alni* Shahu was carried out, allowing for the delivery of the powerful CRISPR-Cas machinery into this bacterium *via* this approach (Li et al.). This work developed a toolkit to facilitate the development and improvement of strain *P. alni* Shahu, which served as a useful reference for the development of genetic manipulation methods in other rare actinomycetes.

Culture-independent techniques revealed that *Actinobacteria* dominated in nodule environment of Tunisia, with *Frankia* spp. most frequently being detected (Ghodhbane-Gtari et al.). Along a gradient of aridity ranging from humid to arid, *Frankia*'s absolute and relative prevalence decreased at semi-arid and arid sampling locations. Most abundant secondary metabolite biosynthetic gene clusters were predicted in genomes of *Frankia* sp. Therefore, as the niche builder of root nodules, the functional *Frankia* microsymbiont played a keystone role in the nodule environments, especially in shaping and maintaining the diversity and stability of nodule communities.

The core of research on actinobacterial resources is to discover new compounds to combat the growing spread of drug resistance. Mahilkar et al. developed a quantitative model to examine a population's response to two temporal environmental cues and predicted variables that may be relevant for anticipatory regulatory response evolution. After approximately 850 generations of alternating rhamnose and paraquat environments while checking the experimental evolution of *Escherichia coli*, they concluded that pre-exposure to rhamnose resulted in increased fitness in paraquat environment. This anticipatory regulation is encoded by mutations in global regulators, as revealed by genome sequencing. This study advanced our understanding of how the environment shapes the topology of an organism's regulatory networks.

The study by Mao et al. discovered a significantly altered microbial composition in Parkinson's disease (PD) patients by examining the composition of the gut microbiome in PD patients using shotgun metagenomic sequencing. The Cluster of Orthologous Groups protein database, the KEGG Orthology database, and carbohydrate-active enzymes gene category analysis revealed that branched-chain amino acid–related proteins were significantly increased in the PD group, while GH43 was significantly decreased. Functional analysis of the metagenome confirmed differences in microbiome metabolism between the PD and non-PD groups, specifically in the metabolism of short-chain fatty acid precursors.

We are pleased to present this Research Topic in Frontiers in Microbiology. We sincerely hope that readers will find this Research Topic interesting. Surely, we will constantly contribute to the research on *Actinobacteria* and the journal Frontiers in Microbiology.

AUTHOR CONTRIBUTIONS

All authors listed have made a substantial, direct, and intellectual contribution to the work and approved it for publication.

FUNDING

This work has been funded by CAMS Innovation Fund for Medical Sciences (CIFMS, 2021-I2M-1-055), National Natural Science Foundation of China (32170021 and 31670010), and Beijing Natural Science Foundation (5212018).

ACKNOWLEDGMENTS

Great thanks to all the contributing authors and above all to the Frontiers team for their constant support throughout in managing the Research Topic.

REFERENCES

Barka, E. A., Vatsa, P., Sanchez, L., Gaveau-Vaillant, N., Jacquard, C., Meier-Kolthoff, J. P., et al. (2015). Taxonomy, physiology, and natural products of actinobacteria. *Microbiol. Mol. Biol. Rev.* 80, 1–43. doi: 10.1128/MMBR.00019-15

Crowther, T. W., van den Hoogen, J., Wan, J., Mayes, M. A., Keiser, A. D., Mo, L., et al. (2019). The global soil community and its influence on biogeochemistry. *Science.* 365, eaav0550. doi: 10.1126/science.aav0550

Demain, A. L., and Sanchez, S. (2009). Microbial drug discovery: 80 years of progress. *J. Antibiot.* 62, 5–16. doi: 10.1038/ja.2008.16

Idris, H., Goodfellow, M., Sanderson, R., Asenjo, J. A., and Bull, A. T. (2017). Actinobacterial rare biospheres and dark matter revealed in habitats of the chilean atacama desert. *Sci. Rep.* 7, 8373. doi: 10.1038/s41598-017-08937-4

Jiang, Z. M., Zhang, B. H., Sun, H. M., Zhang, T., Yu, L. Y., and Zhang, Y. Q. (2021). Properties of *Modestobacter deserti* sp. nov., a kind of novel phosphate-solubilizing actinobacteria inhabited in the desert biological soil crusts. *Front. Microbiol.* 12, 742798. doi: 10.3389/fmicb.2021.742798

Qin, S., Li, W. J., Dastager, S. G., and Hozzein, W. N. (2016). Editorial: *Actinobacteria* in special and extreme habitats: diversity, function roles, and environmental adaptations. *Front. Microbiol.* 7, 1415. doi: 10.3389/fmicb.2016.01415

Sun, H. M., Zhang, T., Yu, L. Y., Sen, K., and Zhang, Y. Q. (2015). Ubiquity, diversity and physiological characteristics of *Geodermatophilaceae* in shapotou national desert ecological reserve. *Front. Microbiol.* 6, 1059. doi: 10.3389/fmicb.2015.01059

Sun, Y., Shi, Y. L., Wang, H., Zhang, T., Yu, L. Y., Sun, H., et al. (2018). Diversity of bacteria and the characteristics of *Actinobacteria* community structure in Badain Jaran Desert and Tengger Desert of China. *Front. Microbiol.* 9, 1068. doi: 10.3389/fmicb.2018.01068

Toumatia, O., Compant, S., Yekkour, A., Goudjal, Y., Sabaou, N., Mathieu, F., et al. (2016). Biocontrol and plant growth promoting properties of *Streptomyces mutabilis* strain IA1 isolated from a saharan soil on wheat seedlings and visualization of its niches of colonization. *South Afr. J. Bot.* 105, 234–239. doi: 10.1016/j.sajb.2016.03.020

Zahra, T., Hamedi, J., and Mahdigholi, K. (2020). Endophytic *Actinobacteria* of a halophytic desert plant *pteropyrum olivieri*: promising growth enhancers of sunflower. *Biotech.* 3, 10, 514. doi: 10.1007/s13205-020-02507-8

Conflict of Interest: The authors declare that the research was conducted in the absence of any commercial or financial relationships that could be construed as a potential conflict of interest.

Publisher's Note: All claims expressed in this article are solely those of the authors and do not necessarily represent those of their affiliated organizations, or those of the publisher, the editors and the reviewers. Any product that may be evaluated in this article, or claim that may be made by its manufacturer, is not guaranteed or endorsed by the publisher.

frontiers in Microbiology

ORIGINAL RESEARCH
published: 18 March 2020
doi: 10.3389/fmicb.2020.00437

Streptomyces spp. From the Marine Sponge *Antho dichotoma*: Analyses of Secondary Metabolite Biosynthesis Gene Clusters and Some of Their Products

*Jaime Felipe Guerrero-Garzón[1], Martin Zehl[2], Olha Schneider[1], Christian Rückert[3], Tobias Busche[3], Jörn Kalinowski[3], Harald Bredholt[4] and Sergey B. Zotchev[1]**

[1] Department of Pharmacognosy, University of Vienna, Vienna, Austria, [2] Department of Analytical Chemistry, Faculty of Chemistry, University of Vienna, Vienna, Austria, [3] Center for Biotechnology, Bielefeld University, Bielefeld, Germany, [4] Xellia Pharmaceuticals AS, Oslo, Norway

Actinomycete bacteria from marine environments represent a potential source for new antibiotics and anti-tumor drugs. Ten strains belonging to the genus *Streptomyces* isolated from the marine sponge *Antho dichotoma* collected at the bottom of the Trondheim fjord (Norway) were screened for antibiotic activity. Since only few isolates proved to be bioactive in the conditions tested, we decided to gain an insight into their biosynthetic potential using genome sequencing and analysis. Draft genomes were analyzed for the presence of secondary metabolite biosynthesis gene clusters (BGCs) using antiSMASH software. BGCs specifying both known and potentially novel secondary metabolites were identified, suggesting that these isolates might be sources for new bioactive compounds. The results of this analysis also implied horizontal transfer of several gene clusters between the studied isolates, which was especially evident for the lantibiotic- and thiopeptide-encoding BGCs. The latter implies the significance of particular secondary metabolites for the adaptation of *Streptomyces* to the spatially enclosed marine environments such as marine sponges. Two bioactive isolates, one showing activity against both yeast and *Bacillus subtilis*, and one only against yeast were analyzed in details, leading to the identification of cycloheximide, linearmycins, and echinomycins that are presumably responsible for the observed bioactivities.

Keywords: marine sponge, *Streptomyces* spp., genomics, biosynthetic gene clusters, horizontal gene transfer, secondary metabolites

OPEN ACCESS

Edited by:
Imen Nouioui, German Collection of Microorganisms and Cell Cultures GmbH (DSMZ), Germany

Reviewed by:
Johannes F. Imhoff, GEOMAR Helmholtz Centre for Ocean Research Kiel, Germany
Usama Ramadan Abdelmohsen, Minia University, Egypt

****Correspondence:***
Sergey B. Zotchev
sergey.zotchev@univie.ac.at

Specialty section:
This article was submitted to Systems Microbiology, a section of the journal Frontiers in Microbiology

Received: *06 November 2019*
Accepted: *02 March 2020*
Published: *18 March 2020*

Citation:
Guerrero-Garzón JF, Zehl M, Schneider O, Rückert C, Busche T, Kalinowski J, Bredholt H and Zotchev SB (2020) Streptomyces spp. From the Marine Sponge Antho dichotoma: Analyses of Secondary Metabolite Biosynthesis Gene Clusters and Some of Their Products. Front. Microbiol. 11:437. doi: 10.3389/fmicb.2020.00437

INTRODUCTION

Streptomyces are Gram-positive GC rich bacteria of the order Actinomycetales that are ubiquitous in nature and can be isolated from a variety of sources, including terrestrial (soil, insects, animals and plants), as well as marine (sediments, fish, corals and sponges) habitats (Goodfellow et al., 2018; Subramani and Sipkema, 2019). These bacteria remain of significant interest in terms of discovery of biologically active secondary metabolites that can potentially be developed into human medicines such as antimicrobial and anticancer agents, immunosuppressants etc. (Takahashi and Nakashima, 2018). The unprecedented genetic potential of *Streptomyces* to produce diverse secondary metabolites is exemplified by a large number (usually 20–40) of biosynthetic gene

clusters harbored by their genomes (Baltz, 2017). These clusters are usually tightly controlled by sophisticated regulatory networks, and in the laboratory conditions, only a few of them are expressed at the level allowing purification and analyses of the product (Reen et al., 2015). It is tempting to speculate that specific environmental signals are required to induce expression of particular clusters, thus leading to the production of secondary metabolites that would give a certain competitive advantage to the producing organisms. Recent comparative genomics-based studies of *Streptomyces* and other actinomycete bacteria revealed that representatives of the same species isolated from different environments have different sets of secondary metabolite biosynthesis gene clusters (BGCs) (Ian et al., 2014; Ziemert et al., 2014). Consequently, it is plausible that when a particular strain is transferred to a new environment (e.g., by birds, animals, rivers, and ocean currents etc.), some BGCs are lost, while others, specifying production of compounds beneficial for adaptation, are being acquired. Although the exact method of acquisition can vary (e.g., natural transformation, conjugative transfer or transduction), it seems likely that other actinomycete bacteria would be the major source of such BGCs. The latter is probably due to the fact that actinomycetes' genomes have a high GC content (usually around 70%), and a specific codon bias that would increase the probability of gene expression if a BGC is transferred from a related species. It is also worth mentioning that some *Streptomyces* spp. harbor giant linear plasmids (GLPs) that are self-transmissible, frequently carry several BGCs (Kinashi, 2011) and thus can be involved in the transfer of these BGCs to other bacteria, in particular actinomycetes.

Comparative genomics provides excellent opportunities for tracing evolution of the species, and is an invaluable approach to understanding the spread and functional significance of BGCs. It can pinpoint the differences between strains of the same species isolated from different habitats, which are often in the form of so-called "genomic islands" (GIs) (Penn et al., 2009). Apparently, the GIs represent DNA regions acquired from other species in the process of horizontal gene transfer (HGT), and they often contain remains of mobile genetic elements that most likely have been involved in HGT. Such elements may be represented by transposons, often also hosted by GLPs, and many BGCs contain transposon-like elements, or even look like composite transposons themselves, as in the case of the enterocin biosynthetic gene cluster in marine sponge-derived *Streptomyces albus* (Ian et al., 2014). Recently, Jackson et al. reported the analyses of 13 genomes of streptomycetes isolated from various marine sponges (Jackson et al., 2018). Many unique BGCs were identified, suggesting potential of these bacteria in terms of production of novel bioactive secondary metabolites.

Microbial communities associated with marine sponges, which provide relatively enclosed environment, are especially interesting in terms of tracing the HGT events. In the current work, draft genome sequences for 10 phylogenetically diverse *Streptomyces* spp. isolated from the sponge *Antho dichotoma* collected in the Trondheim fjord (Norway) were obtained. Comparative genomics revealed several of them being closely related to terrestrial *Streptomyces*, and BGC analysis allowed identification of the gene clusters that most likely have been subjects to HGT between the isolates. Several of the isolates exhibited antimicrobial activities, and for two of them bioactive compounds, as well as the BGCs specifying their biosynthesis, were identified.

MATERIALS AND METHODS

Sampling and Treatment of Sponge Samples

Sample of marine sponge *A. dichotoma* was collected from Tautra underwater ridge (specific coordinates 63o 36′ 53″ N, 10o 31′ 22″ E) at the depth of 60 m with the aid of a remote operated underwater vehicle equipped with robotic arm. The sample was immediately transferred to a sterile plastic contained filled with sterilized sea water, and transported to the laboratory within 3 h. Sponge piece of ca 2 cm^3 was cut out with a sterile scalpel and transferred to a mortar containing 18 mL of 20% glycerol in sea water. The sample was grinded with a pester for ca 2 min, transferred to a 50 mL plastic tube containing 5 g of 3 mm glass beads, and vortexed for 2 min. 8 mL of the resulting suspension was transferred to a sterile plastic tube, and serial dilutions were plated on various agar media as previously described (Ian et al., 2014). The plates were incubated at 20°C for up to 6 weeks.

Bacterial Strains and Growth Conditions

Streptomyces sp. were maintained on ISP4 agar medium (Difco) and soy flour medium (SFM) (Kieser et al., 2000) with followed preparation of spore suspensions in 20% glycerol. Influence of sea water on the growth of *Streptomyces* isolates was tested using ISP2 agar medium (Difco) prepared with and without artificial sea water. The composition of the artificial sea water was as follows (g/L): NaCl, 26.29; KCl, 0.74; $CaCl_2$, 0.99; $MgCl_2 \cdot 6H_2O$, 6.09; $MgSO_4 \cdot 7H_2O$, 3.94. *Escherichia coli* K12 and *Bacillus subtilis* 168 (received from the Norwegian University of Science and Technology, Norway) were grown in liquid and soil LB-medium, while *Saccharomyces cerevisiae* BY4743 (received from the Joint Bioenergy Institute, United States) was grown on YPD (Sigma) medium. *Streptomyces* strains and *Sa. cerevisiae* were grown at 30°C, *E. coli* and *B. subtilis* at 37°C.

Cultivation, Extracts Preparation, and Bioassays

All ten *Streptomyces* strains were cultivated in PM4-1, 5333 and 5280 media (see below for recipes) and their extracts were tested on antimicrobial activity. For preparation of an overnight culture, 20 ml of TSB medium [Oxoid Tryptone Soya Broth powder (CM129) 30 g/L] was inoculated with 50 µl of *Streptomyces* spore suspension and cultivated for 18–20 h in 250 ml baffled Erlenmeyer flasks by 220 rpm. Next day the main culture was prepared by inoculation of 50 ml of test media with 5% of overnight TSB-culture. Test media were: PM4-1: glucose (15 g/L), soy meal (15 g/L), corn steep solids (Sigma, 5 g/L), $CaCO_3$ (2 g/L), and 6 ml/L Trace Elements Solution (mg/mL): $FeSO_4 \cdot 7H_2O$, 5.0; $CuSO_4 \cdot 5H_2O$, 0.39; $ZnSO_4 \cdot 7H_2O$, 0.44; $MnSO_4 \cdot H_2O$, 0.15; $Na_2MoO_4 \cdot 2H_2O$, 0.01; $CoCl_2 \cdot 6H_2O$, 0.02; HCl, 50;

5333-medium: yeast extract (4 g/L), soluble starch (15 g/L), K_2HPO_4 (1 g/L), $FeSO_4 \cdot 7H_2O$ (0.5 g/L), pH (7.8); 5280-medium: glycerol (30 g/L), NaCl (5 g/L), $CaCO_3$ (1 g/L), pH (7.8).

For the extract preparation 3 mL of culture after 3, 5, and 7 days of cultivation were extracted with 1 ml of butanol and organic phases were tested for the presence of antimicrobial activity against *E. coli* K12, *B. subtilis* 168 and *Sa. cerevisiae* BY4743. The sensitivity of the selected bacteria to extracts was tested by the agar diffusion method by applying 15 µl of extracts on 6 mm filter discs (Whatman) and measuring of growth-inhibition zones.

DNA Isolation, PCR, and Phylogenetic Analysis

Genomic DNAs were extracted from cultures grown in liquid 3% TSB medium (Oxoid, United Kingdom) at 28°C for 24–48 h using the Qiagen DNeasy Blood and Tissue Kit (QIAGEN, Germany). The 16S rRNA gene fragments were amplified by PCR using the universal bacterial 16S rDNA primers F27 and R1492 (Lane, 1991). Obtained PCR products were purified and directly sequenced with the F27 and R1492 primers at EUROFINS (Germany). DNA sequences of almost complete 16S rRNA genes (ca 1400 nucleotides) were compared with those in the GenBank. Phylogenetic tree based on these sequences along with those of the validly named species retrieved using Ez BioCloud[1] as most similar was constructed using the Molecular Evolutionary Genetics Analysis (MEGA) software version 7 (Kumar et al., 2016). The tree was computed using the Neighbor-Joining method, and the resulting tree topology was tested by bootstrap analysis performed with 500 replicates.

Genome Sequencing, Assembly, and Analyses

For genome sequencing of each sample, two WGS sequencing libraries were prepared, using the TruSeq DNA PCR-Free Kit respectively the Nextera Mate Pair Library Preparation Kit (Illumina Inc., San Diego, CA, United States) according to the manufacturer's instructions. The resulting libraries were sequenced on the MiSeq sequencing platform using the MiSeq Reagent Kit v3 in 2 × 300 nt sequencing runs. The sequencing data sets were assembled using the Newbler assembler v2.8 (454 Life Sciences, Branford, CT, United States). In case of ADI95-16, the initial assembly was then manually curated in Consed (Gordon and Green, 2013), resulting in a single contig per replicon for each, the linear chromosome and the four plasmids (three of them linear, one circular). The assembled contigs were annotated using the Prokka pipeline v1.11 (Seemann, 2014), including the annotation of non-coding RNAs. The relevant data for the assembly and genome annotation of the ten strains are listed in **Supplementary Table S1**.

The Whole Genome Shotgun projects have been deposited at DDBJ/ENA/GenBank under the accessions RPGS00000000 (ADI91-18), RPGT00000000 (ADI92-24), RPGU00000000 (ADI93-02), CP033581-CP033585 (ADI95-16), RPGV00000000 (ADI95-17), RPGW00000000 (ADI96-02), RPGX00000000 (ADI96-15), RPGY00000000 (ADI97-07), RPGZ00000000 (ADI98-10), and RPHA00000000 (ADI98-12). The versions described in this paper are version 1 (XXXX01000000).

Analysis of the genomes for secondary metabolite BGCs was done with antiSMASH 5.0 online tool (Blin et al., 2019), and the identified clusters and their genes involved in scaffold assembly were queried against the MiBIG database (Medema et al., 2015).

Construction of the ADI95-16 Knock-Out Mutant

The DNA fragment (0.99 kb), containing the central part of *ftdB* gene identified in the polycyclic tetramate macrolactam (PTM) cluster was amplified by PCR from gDNA of *Streptomyces* spp. ADI95-16; the primers 95-16_C22ko_F and 95-16_C22ko_R were used. These primers included the restriction sites *Eco*RI and *Hin*dIII respectively, to allow proper ligation with the 3.0 kb *Eco*RI-*Hin*dIII fragment from pSOK201 plasmid containing ColE1, *oriT* and Am^R. The resulting construct pPTM95-16KN was introduced in *Streptomyces* sp. ADI95-16 via conjugation from *E. coli* ET12567/pUZ8002. Apramycin (50 µg/mL) was used for selection of recombinant *Streptomyces* strains. Oligonucleotide primers were designed using Clone Manager 9 software (Sci-Ed Software, United States).

Production, Purification, and Identification of Linearmycins and Echinomycins

A 10 mL of TSB medium (Oxoid, United Kingdom) was inoculated with 200 µL of a dense spore suspension of *Streptomyces* spp. ADI95-16 in a 100 mL Erlenmeyer flask and incubated at 28°C with 200 rpm over night to produce seed culture. For the purification of linearmycins, ten 250 mL baffled Erlenmeyer flasks containing each 50 mL of ikarugamycin production medium (starch 2%, cotton seed flour 2%, corn steep liquor 1% and $CaCO_3$ 0.3%, in 1 L of distilled water, pH 6.2) were inoculated with 3 mL of seed culture and fermented at 28°C with 200 rpm for 48 h. The whole culture (0.5 L) was freeze-dried and extracted with 250 mL mixture of chloroform and methanol (1:1) during 2 h. The organic phase was evaporated *in vacuo* to generate a dry layer that was suspended in methanol to generate a concentrated extract. The methanolic crude extract was separated using a Shim-pack GIS C18, 250 mm × 20 mm, 5 µm column (Shimadzu) in a Semi-preparative HPLC Shimadzu LC-20AR equipment. 0.1% aqueous formic acid and acetonitrile were used as mobile phase A and B, respectively. The gradient used was: 5–95% B in 45 min followed by a washing (10 min at 95% B) and re-equilibration step (10 min at 10% B), flow rate was 20 mL/min and 190 nm wave length was used for detection. Linearmycin A eluted with a retention time of 21 min, and linearmycin B with a retention time of 22 min. Approximately 3.0 mg of linearmycin A and 2.5 mg of linearmycin B were obtained.

For the production of echinomycins, 10 mL of TSB medium (Oxoid, United Kingdom) was inoculated with 200 µL of a dense spore suspension of *Streptomyces* spp. ADI96-02 in a 100 mL Erlenmeyer flask and incubated at 28°C with 200 rpm over night

[1] https://www.ezbiocloud.net/

to produce seed culture. Then, a 250 mL baffled flask containing 50 mL of MYM medium (4 g/L maltose, 4 g/L yeast extract, 10 g/L malt extract, 1.9 g/L MOPS) was inoculated with 3 mL of seeding culture. The fermentation was carried out at 200 rpm and 28°C for 7 days. Fermentation culture was harvested and freeze dried. 25 mL of methanol was used to extract the dried material at 200 rpm and room temperature for 1 h. The methanolic extract was concentrated *in vacuo* and analyzed by LC-MS/MS.

LC-MS analyses were performed on two different instruments. All extracts were analyzed on an UltiMate 3000 series system HPLC equipped with a VWD detector (Dionex/Thermo Fisher Scientific, Germering, Germany) that was coupled to a maXis UHR ESI-Qq-TOF mass spectrometer (Bruker Daltonics, Bremen, Germany). Separation was carried out on an Acclaim 120 C18, 2.1 × 150 mm, 3 μm HPLC column (Thermo Fisher Scientific) using water and acetonitrile, both modified with 0.1% formic acid, as mobile phase A and B, respectively. The sample components were separated and eluted with a linear gradient from 5 to 95% B in 45 min followed by an isocratic column cleaning (9.5 min at 95% B) and re-equilibration step (10 min at 5% B). The flow rate was 0.45 mL/min and the column oven temperature was set to 25°C. After passing the UV detector, high-resolution MS and MS/MS spectra were recorded in positive ion mode in the range *m/z* 50–2000. The following ESI ion source settings were applied: capillary voltage: 4.5 kV, nebulizer: 1.2 bar (N_2), dry gas flow: 8.0 L/min (N_2), and dry temperature: 180°C. MS/MS spectra were obtained in automated data-dependent acquisition mode using argon as collision gas, an isolation window of $\Delta m/z$ = 4, and an *m/z*- and charge-dependent fragmentation amplitude. In the case of echinomycin and echinoserine, targeted MS/MS experiments were performed using an isolation window of $\Delta m/z$ = 6 and a fragmentation amplitude of 30 eV to facilitate comparison with literature data (Williamson et al., 1982). The sum formulas of the detected ions were determined using Bruker Compass DataAnalysis 4.0 based on the mass accuracy ($\Delta m/z \leq 5$ ppm) and isotopic pattern matching (SmartFormula algorithm).

Echinomycin (≥98% HPLC) was obtained from Sigma-Aldrich (St. Louis, MO). LC-MS measurements of the ADI96-02 extract, the echinomycin reference standard, and the ADI96-02 extract spiked with the echinomycin reference standard for comparison of the retention time as well as the positive and negative ion mode MS and MS/MS spectra were conducted on a Vanquish Horizon UHPLC system (Thermo Fisher Scientific) coupled to the ESI source of an LTQ Orbitrap Velos mass spectrometer (Thermo Fisher Scientific).

RESULTS

Isolation and Preliminary Characterization of *Streptomyces* spp. From the Marine Sponge *Antho dichotoma*

A sample of the marine sponge collected at the Tautra underwater ridge in the Trondheim fjord (Norway) and classified as *A. dichotoma* was used to isolate actinomycete bacteria (see Materials and Methods). In total, 497 isolates were recovered from different agar media, macromorphology of which suggested them being actinobacteria. One hundred and eight of these isolates were tested for molecular phylogeny using 16S rRNA gene amplicons. Seventy nine of the tested isolates were classified as *Streptomyces*, while the rest was representated by actinobacterial genera *Actinoalloteichus*, *Micromonospora*, *Actinomadura*, *Promicromonospora*, *Isoptericola*, *Rhodococcus*, *Nocardiopsis*, and *Pseudonocardia* (data not shown). Dereplication of the 79 *Streptomyces* isolates based on the 16S rRNA gene fragment sequences (1350–1475 nt) yielded 51 isolates that were considered diverse (**Supplementary Figure S1**). For this study, we selected 10 *Streptomyces* spp. isolates that were both morphologically (visual inspection) and phylogenetically diverse (**Figure 1**). The 16S rRNA gene sequence identities between the selected isolates and their closest validated phylogenetic neighbors were in the range of 98–99%.

These *Streptomyces* isolates were first tested for growth on ISP2 medium with and without sea water. Apparently, the growth and morphological differentiation of nearly all strains was affected by sea water, except for the isolate ADI92-24, which grew equally well on both media (**Table 1**). In order to test whether we can detect the production of antimicrobial compounds in these isolates, all 10 strains were grown in 3 different liquid media (see Materials and Methods) which generally support production of secondary metabolites (unpublished data). The *n*-butanol extracts prepared by liquid-liquid extraction of the cultures sampled after 3, 5, and 7 days of fermentation were used in bioassays against *B. subtilis*, *E. coli*, and *Sa. cerevisiae* (results are shown in **Supplementary Table S1**). Rather surprisingly, and in contrast to what has been observed for *Streptomyces* species isolated from terrestrial sources, very limited bioactivity was revealed in these tests. Only 4 out of 10 isolates showed antibiotic activity in the conditions tested. Considering the fact that *Streptomyces* in general harbor >20 gene clusters for the biosynthesis of secondary metabolites, some of which usually have antibiotic activity, the latter result suggested that media and conditions used were not sufficient to induce biosynthesis of secondary metabolites in most of these isolates.

Comparative Genomics of Sponge-Associated *Streptomyces* Focused on Secondary Metabolite Biosynthesis Gene Clusters

In order to obtain an insight into the secondary metabolite biosynthesis potential of the isolates, and to detect any possible transfer of BGCs between them, draft genome sequences were obtained for all strains. Remarkably, genomes of several sponge isolates showed considerable synteny with the genomes of some terrestrial streptomycetes. In particular, *Streptomyces* sp. ADI98-12 vs. *S. albus* J1074, *Streptomyces* sp. ADI95-16 and ADI91-18 vs. *Streptomyces* sp. Mg1, and *Streptomyces* sp. ADI96-02 vs. *Streptomyces fulvissimus* DSM 40593 (**Supplementary Figures S2–S5**). The draft genomes were then analyzed for the presence of BGCs using antiSMASH 5.0 online software

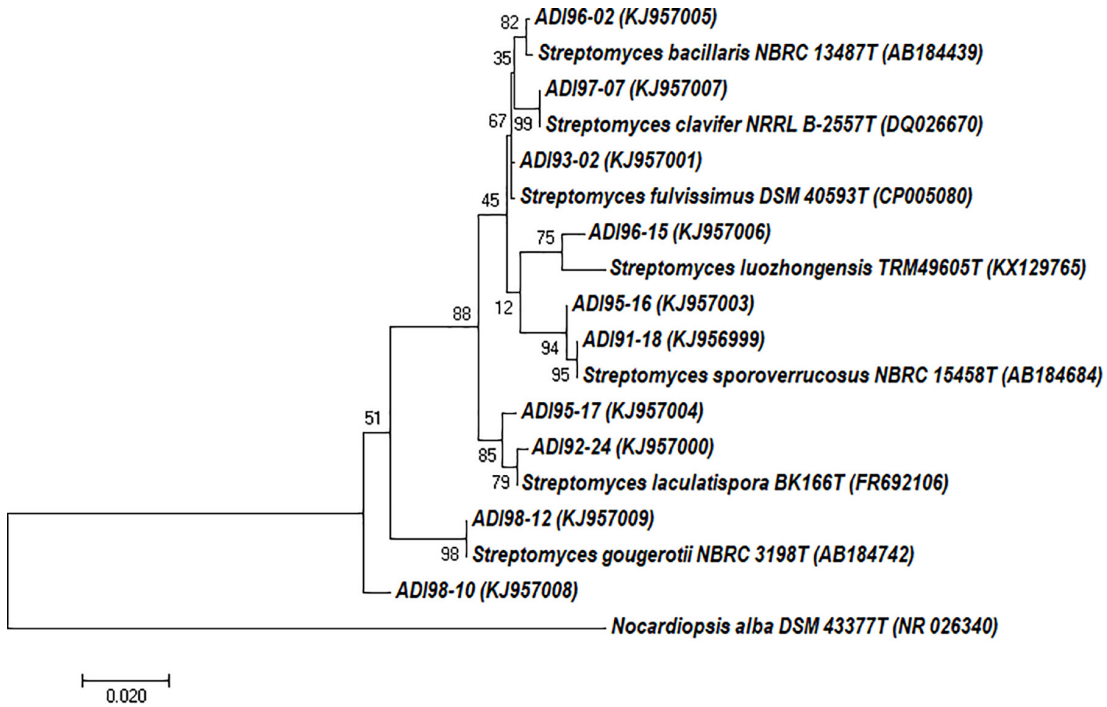

FIGURE 1 | Evolutionary relationships of *Streptomyces* spp. isolated from *Antho dichotoma* based on the 16S rRNA gene sequences. The evolutionary history was inferred by using the Maximum Likelihood method. The tree is drawn to scale, with branch lengths measured in the number of substitutions per site. The analysis involved 18 nucleotide sequences. Evolutionary analyses were conducted in MEGA7 (35).

(Blin et al., 2019). Data obtained with antiSMASH were manually curated to ensure optimized prediction of the gene cluster borders, since the software occasionally considered two adjacent but clearly distinct BGCs as one. In particular, product of each gene was queried against GenBank using BLASTp search engine, and gene encoding proteins without any obvious role in secondary metabolism were considered as flanking the cluster borders. Also, corrections were made when one cluster was split between two or more contigs. A summary of the results of this analysis is presented in **Table 2**, and particular genome features are given in **Supplementary Table S2**. According to this analyses, isolate ADI95-17 has the largest genome of ca 10 Mb which encodes at least 36 BGCs most of which are represented by PKS- and NRPS-type clusters. Isolate ADI96-02 possessed the smallest ca 7 Mb genome among all isolates, which still encoded at least 30 BGCs most of which were represented by RiPPs, terpenoid, and hybrid PKS-NRPS clusters. The largest number of BGSs, was identified in the 9.1 Mb genome of isolate ADI95-16. The majority of these BGCs were represented by PKS, RiPPs and terpenoid clusters. The rest of the isolates had genome sizes that ranged from 7.1 to 9.3 Mb, and harbored between 28 and 34 BGCs per genome.

TABLE 1 | Effect of sea water on the growth of sponge-derived *Streptomyces* spp. on ISP2 medium.

***Streptomyces* isolate**	**ISP2**	**ISP2 + sea water**
ADI91-18	+	−
ADI92-24	−	−
ADI93-02	−	+
ADI95-16	+	−
ADI95-17	−	+
ADI96-02	+	−
ADI96-15	+	−
ADI97-07	−	+
ADI98-10	−	+
ADI98-12	−	+

(+) indicates faster growth and morphological differentiation; (−) no effect (by comparison).

As expected from the high degree of synteny of the draft sequences to genomes of terrestrial *Streptomyces* species, the draft genomes of the sponge-associated streptomycetes were fairly typical, with sequence lengths between 6.99 Mbp and 10.03 Mbp and G + C contents between 70.63 and 73.42%. Likewise, the automated assemblies were also rather typical for MatePair-guided Illumina-only assemblies, with the drafts consisting of 2–18 scaffolds containing 32–377 contigs. Due to the low number of scaffolds and contigs, the genome of ADI95-16 could be finished manually, resulting in just one scaffold/contig for each of the 5 replicons. Finally, the automated annotation revealed some differences concerning the number of ncRNAs detected by INFERNAL (Nawrocki and Eddy, 2013) against the RFAM database (Kalvari et al., 2018), which ranged from 3 up to 33 for the 10 isolates investigated. Closer inspection of the predicted ncRNAs revealed that this large variation is due to the number

TABLE 2 | Secondary metabolite biosynthesis gene clusters in the genomes of sponge-derived *Streptomyces* spp.

Strain	Genome size, Mb	PKS I, II, III	NRPS	PKS/NRPS	RiPP	Terp	Siderophore	Other	Total
ADI91-18	8.64	9	2	3	7	7	3	5	34
ADI92-24	9.31	6	5	3	1	8	1	4	28
ADI93-02	8.41	4	3	2	2	6	2	10	29
ADI95-16	9.11	8	3	3	8	7	3	7	39
ADI95-17	10.03	9	7	3	2	5	1	9	36
ADI96-02	6.99	4	3	5	5	6	2	5	30
ADI96-15	7.08	7	6	4	3	5	2	3	30
ADI97-07	8.35	8	3	5	3	4	3	7	33
ADI98-10	7.72	4	3	2	5	6	2	6	28
ADI98-12	7.24	3	6	6	3	4	2	5	29

The analysis was done using antiSMASH 5.0 online software with subsequent manual curation.

of predicted ASpks and ASdes sRNAs, which range from 1 up to 30. "ASdes TB sRNA" and "ASpks TB sRNA" are two ncRNAs that were initially identified in *Mycobacterium tuberculosis* in the *desA1* and *pks12* genes, respectively. Gene *desA1* encodes an acyl-acyl carrier protein desaturase that catalyzes the introduction of specific double bonds during the biosynthesis of mycolic acids in Mycobacteria, while the *pks12* gene encodes an PKS enzyme responsible for the biosynthesis of lipid moiety of the mycobacterial phospholipid antigen. Similar ncRNAs are found in many *Streptomyces* spp., and are believed to be involved in gene regulation, in particular regulation of BGC expression (Arnvig and Young, 2009).

Some of the BGCs identified in the genomes of the sponge-associated streptomycetes could be linked to already known molecules based on their high similarity to already characterized BGCs (identical gene composition and >75% identity of the gene products) and was annotated in MiBIG database (Medema et al., 2015). Beside BGCs for ectoine, desferrioxamine B, geosmin, 2-methylisoborneol, isorenieratene, melanin, hopanoids, albaflavenone, and spore pigment, commonly present in the streptomycete genomes, the BGCs for less abundant secondary metabolites were also identified (**Table 2**). In addition to the abovementioned BGCs, many of the predicted not-characterized BGCs were unique for each isolate, albeit sometimes being present in the genomes of their terrestrial counterparts or other *Streptomyces* spp. deposited in the public databases. The latter may reflect both different evolutionary origins of the isolates, as well as the timing of their acquisition by the sponge and hence different exposure to the HGT events. However, a number of gene clusters appeared to be either well conserved among certain isolates, suggesting vertical gene transfer (VGT), or might have been recently transmitted via HGT. In particular, the HGT hypothesis concerned gene clusters for lantipeptide and thiopeptide biosynthesis, while VGT could be implied for the gene clusters specifying tetramate macrolactams identified in 8 out of 10 isolates (see below).

Gene Clusters for Lantipeptide and Thiopeptide Biosynthesis

In total, 30 BGCs for lantipeptide biosynthesis were identified in the genomes of 10 sponge-derived *Streptomyces* isolates. Comparison of the amino acid sequences of the lantipeptide precursors revealed striking similarities between some BGCs present in the genomes of different isolates. In particular, similarities between both pre-propeptides and gene organization of a particular cluster were evident in isolates ADI96-02, ADI96-15, and ADI98-10 (**Figure 2A**). Alignment and closer examination of nucleotide sequences of these clusters confirmed their high similarity (70–75% identity), while most differences could be seen in the regulatory regions, especially upstream of the gene encoding the lantipeptide precursor (**Figure 2A**). A similar observation was made for one thiopeptide BGC identified in the isolates ADI96-15, ADI95-16, ADI97-07, and ADI98-12, where the amino acid sequences of pre-propeptides shared even greater homology (**Figure 2B**). Although no apparent direct or inverted repeats could be identified within the DNA regions flanking the abovementioned BGCs, and there were no transposase genes in their vicinity, it seems possible that these clusters have been subjects to a relatively recent HGT. This suggestion is further supported by the phylogenetic diversity of the isolates where highly similar BGCs were found, which makes it less probable that these clusters have been retained due to the VGT. In the process of evolution, their sequences may have changed and diversified as a result of adaptation to the new host's cellular environment and regulatory networks.

Gene Clusters for Polycyclic Tetramate Macrolactam Biosynthesis

Recently, biosynthesis of PTM antibiotics, some of which have antifungal activity, received considerable attention. Biosynthesis of several PTMs was studied in some detail, including heat-stable antifungal factor (HSAF) from *Lysobacter enzymogenes* (Yu et al., 2007), as well as ikarugamycin, frontalamides, and clifednamides from *Streptomyces* spp. (Cao et al., 2010). Chemical structures of these antifungal antibiotics are shown on **Figure 3A**. The BGC for frontalamide (**Figure 3B**) represents a typical PTM biosynthetic gene cluster identified in various *Streptomyces* spp. (Blodgett et al., 2010). The frontalamide BGC encodes a fatty acid hydroxylase FtdA, a hybrid PKS-NRPS FtdB, desaturases FtdC, and FtdD, zinc-dependent dehydrogenase FtdE and P450 monooxygenase FtdF. Precursors for the polycyclic mactrolactam ring, which can vary in size, are synthesized by an iterative

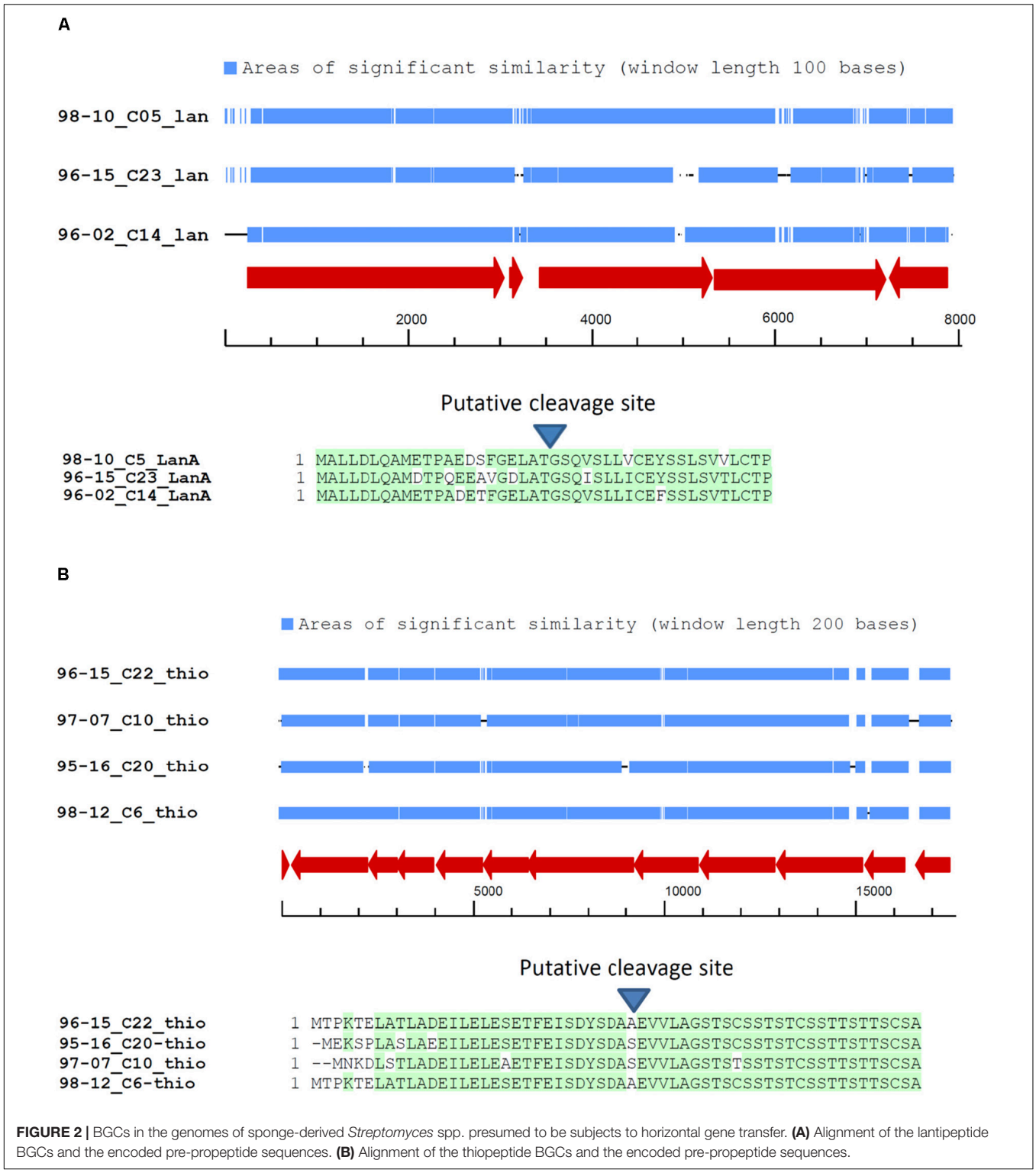

FIGURE 2 | BGCs in the genomes of sponge-derived *Streptomyces* spp. presumed to be subjects to horizontal gene transfer. **(A)** Alignment of the lantipeptide BGCs and the encoded pre-propeptide sequences. **(B)** Alignment of the thiopeptide BGCs and the encoded pre-propeptide sequences.

hybrid PKS-NRPS, such as FtdB, which utilizes malonyl-CoA and ornithine as substrates. The hybrid chain is cyclized via the action of two enzymes belonging the phytoene desaturase family, i.e., Ftd C and FtdD. The fatty acid hydroxylase FtdA installs a hydroxyl group on the macrolactam ring. Some PTM clusters, notably from non-streptomycete bacteria, lack *ftdE* and *ftdF* homologs, which further diversify the PTM structures via changes in the oxidation pattern (Blodgett et al., 2010).

Apparently, BGCs for PTMs are wide-spread in the bacterial kingdom, suggesting that the metabolites they

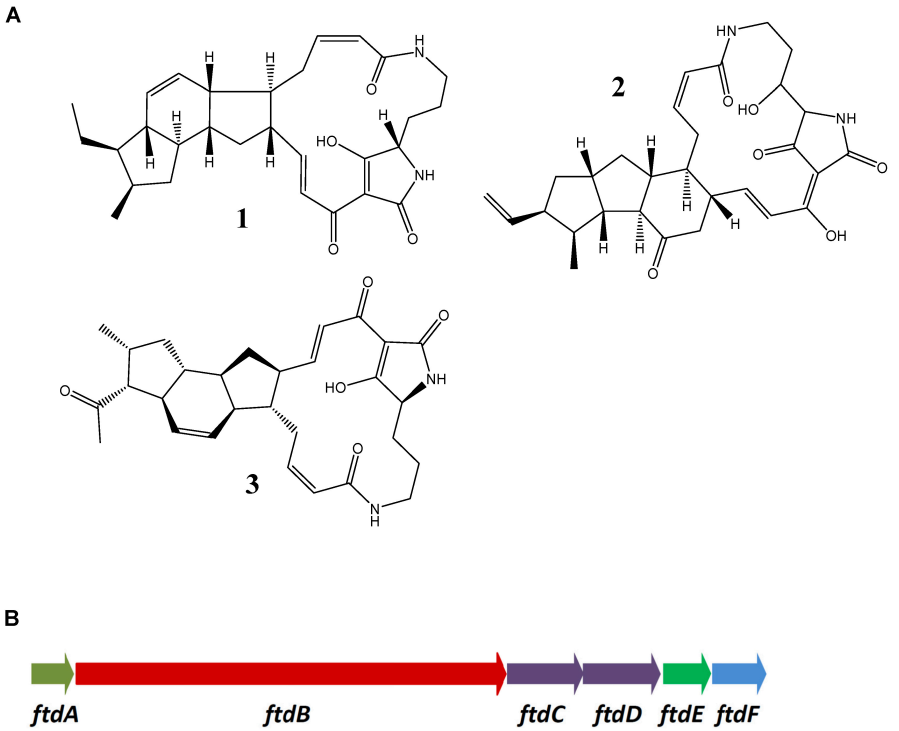

FIGURE 3 | Polycyclic tetramate macrolactams from streptomycetes. **(A)** Ikarugamycin (1), frontalamide B (2), and clifednamide (3). **(B)** BGC for frontalamides from *Streptomyces* sp. SPB78 [17].

specify play an important role in the environmental adaptation (Blodgett et al., 2010). Analysis of the genomes of *Streptomyces* pp. isolated from *A. dichotoma* revealed the presence of PTM BGCs in 8 out of 10 isolates. Six out of eight PTM BGCs identified in the isolates ADI92-24, ADI95-17, ADI96-02, ADI96-15, and ADI98-12 had a gene composition and arrangement identical to that of the frontalamide BGC. The PTM BGCs from ADI91-18 and ADI95-16 (virtually identical on nucleotide level) appeared different in that they lacked the *ftdE* gene homologs. The latter implied that these clusters may encode a novel PTM with unique oxidation pattern. An attempt was made to identify the product of the PTM BGC in isolate ADI95-16, for which a gene transfer system based on intergenic conjugation was established. The strategy for identification was based on construction of a knock-out mutant of the *ftdB* homolog encoding hybrid PKS-NRPS in the PTM cluster, followed by comparison of metabolite profiles of the mutant and the wild type strain. A 0.99 kb DNA fragment representing the central part of this gene was PCR-amplified from the genomic DNA of ADI95-16 and ligated with the part of pSOK201 (Zotchev et al., 2000), generating a suicide knock-out vector pPTM95-16KN. Upon conjugative transfer of this vector to ADI95-16, one knock-out mutant was obtained. Comparative analyses of metabolites produced by the ADI95-16 and its PTM knock-out mutant cultivated in different media using LC-MS/MS did not reveal any relevant differences, suggesting that the cluster is most likely not expressed and the polycyclic macrolactam is not produced under the conditions tested.

Bioactivity of Some Sponge-Derived Streptomycetes Is Due to Production of Linearmycins, Cycloheximide, and Echinomycins

Since isolates ADI95-16 and ADI96-02 displayed good bioactivity against *B. subtilis* and *Sa. cerevisiae*, we decided to identify the compounds responsible for these activities, and to connect the identified molecules with the respective BGCs. Isolate ADI95-16 was cultivated in ikarugamycin production medium (Jomon et al., 1972), and extracts were subjected to bioactivity-guided fractionation that resulted in purification of bioactive compounds. This was followed by the analyses of the bioactive extracts by means of LC-MS/MS. The comparative genome analysis of ADI95-16 resulted in the detection of a BGC for a polyene polyketide by the antiSMASH software, which was at first erroneously annotated as the one for ECO-02301 (McAlpine et al., 2005). Indeed, HPLC and LC-MS analysis of the bioactive $CHCl_3$/MeOH extract showed several main compounds whose UV and mass spectra pointed to this compound class (**Supplementary Figures S6–S10**). A search of the Dictionary of Natural Products and comparison of the obtained MS/MS spectra with literature data identified the two main congeners as linearmycin A and B, antibiotics similar to ECO-02301 that were previously reported from *Streptomyces* sp. Mg1 (Hoefler et al., 2017). The genome of *Streptomyces* sp. Mg1 shares high degree of similarity with that of ADI95-16 and comparison of the complete

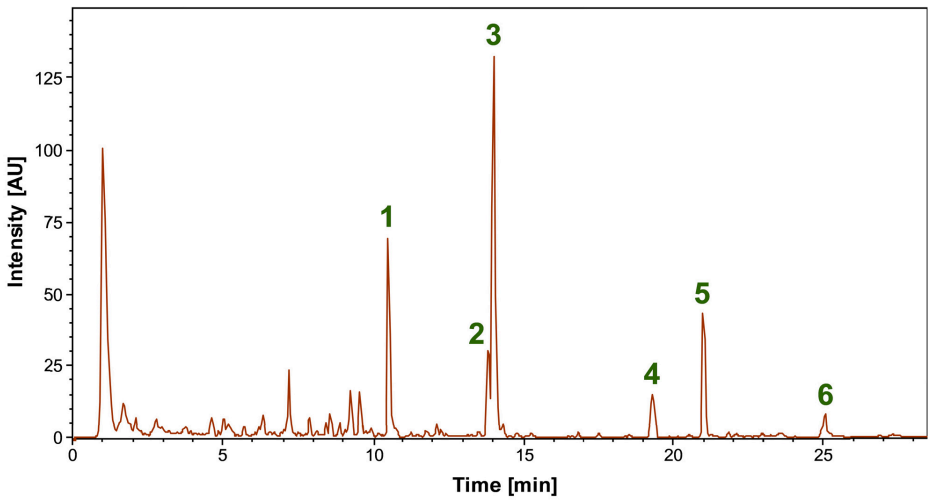

FIGURE 4 | Base peak chromatogram of the bioactive methanolic extract of *Streptomyces* spp. ADI96-02 in the range *m/z* 50-2000. Several main compounds were tentatively identified as nocardamine **(1)**, cycloheximide **(3)**, an isomer of cycloheximide **(2)**, actiphenol **(5)**, echinoserine **(4)**, and echinomycin **(6)**, with the identity of the latter being confirmed by standard addition.

linearmycin gene clusters from ADI95-16 and Mg1 revealed 96% identity on nucleotide level (data not shown). Interestingly, while the two major linearmycin congeners looked identical between the two strains, the profile of the minor congeners was different. In particular, we did not detect the previously reported linearmycin C (Hoefler et al., 2017), but instead found a derivative with the sum formula $C_{71}H_{113}NO_{21}$ (HRESIMS *m/z* 1316.7882 $[M + H]^+$; calculatedd for $C_{71}H_{114}NO_{21}{}^+$, *m/z* 1316.7878, Δ = 0.3 ppm) with similar intensity as linearmycin B (**Supplementary Figures S7, S8**). The fragmentation pattern indicates that a $C_7H_{12}O_5$ group, most likely a methylhexosyl moiety, is attached to the amine group of linearmycin A (**Supplementary Figures S9, S10**). The corresponding derivative of linearmycin B was also detected with lower abundance.

LC-MS analyses of the bioactive methanolic extract of ADI96-02 obtained after strain cultivation in the MYM medium lead to the identification of several main constituents (**Figure 4**), most of them matching the predictions for bioactive compounds by the antiSMASH-based genome analyses (**Table 2**). The highest peak in the base peak chromatogram (**3**) was tentatively assigned to cycloheximide based on the accurate mass (HRESIMS *m/z* 282.1705 $[M + H]^+$; calcd for $C_{15}H_{24}NO_4{}^+$, *m/z* 282.1700, Δ = 1.9 ppm) and a very high similarity of the MS/MS spectrum (**Supplementary Figure S11**) to reference data in the mzCloud database.[2] A less abundant compound with identical mass and fragment ions, most likely an isomer of cycloheximide such as isocycloheximide or naramycin B (**2**), and the related compound actiphenol (**5**) were also detected (**Supplementary Figures S12, S13**) (Yin et al., 2014; Grubbs et al., 2019).

Another main compound (**1**) detected in ADI 96-02 was tentatively identified as the siderophore nocardamine (deferrioxamine E), again by accurate mass (HRESIMS *m/z* 601.3533 $[M + H]^+$; calcd for $C_{27}H_{49}N_6O_9{}^+$, *m/z* 601.3556, Δ = −3.7 ppm) and comparison of the MS/MS spectrum (**Supplementary Figure S14**) to reference data in mzCloud[3] and in literature (Novák et al., 2017). Finally, two peaks could be assigned to the predicted non-ribosomal peptides echinoserine (**4**) and echinomycin (**6**). Echinoserine (HRESIMS *m/z* 1137.4522 $[M + H]^+$; calculated for $C_{51}H_{69}N_{12}O_{14}S_2{}^+$, *m/z* 1137.4492, Δ = 2.6 ppm), which is the non-cyclic form of echinomycin first described in *Streptomyces tendae*, was confirmed with very high certainty by an excellent match of the characteristic MS/MS spectra (**Supplementary Figure S15**) with literature data (Blum et al., 1995; Socha et al., 2009). Despite being the much better investigated congener, no high quality reference MS/MS spectra could be found for echinomycin (HRESIMS *m/z* 1101.4303 $[M + H]^+$; calcd for $C_{51}H_{65}N_{12}O_{12}S_2{}^+$, *m/z* 1101.4281, Δ = 2.2 ppm). Thus, the production of echinomycin in ADI96-02 was unambiguously confirmed by comparison with a commercially available reference standard followed by LC-MS analysis (**Supplementary Figures S16, S17**). Echinomycin is a cytotoxic compound previously reported from *Streptomyces echinatus* (Williamson et al., 1982). Later, the echinomycin BGC from *Streptomyces lasaliensis* was identified and characterized (Watanabe et al., 2006). Interestingly, the echinomycin BGC in ADI96-02 harbored a gene encoding a putative monooxygenase, which was replaced by a transposase in the similar BGC of *S. lasaliensis*. Also, the ADI96-02 cluster contained 2 genes for ABC transporters that were absent on the *S. lasaliensis* counterpart (data not shown).

Additional data on the fragmentation patterns obtained with MS/MS analyses and confirming the identity of linearmycins, echinomycin, echinoserin, cycloheximide, actiphenol, and nocardamine are given in **Supplementary Figures S18–S26**.

[2]https://www.mzcloud.org/DataViewer#Creference2623

[3]https://www.mzcloud.org/DataViewer#Creference7689

Comparative Genomics of Marine *Streptomyces* sp. ADI95-16 and Terrestrial *Streptomyces* sp. Mg1

Due to the high similarity of the genomes of the sponge isolate *Streptomyces* sp. ADI95-16 and the soil-derived *Streptomyces* sp. Mg1 suggested by synteny of draft genomes, it appeared interesting to compare the secondary metabolite biosynthesis potential of these strains. The genomes' similarity was strongly supported by the DDH value calculated using GGDC tool (Meier-Kolthoff et al., 2013), which ranged from 73.2 to 81.0, depending on the calculation formula used. To achieve a full-scale comparison, the genome of ADI95-16 was completely sequenced, revealing a linear chromosome of ca 8.2 Mb, three linear plasmids of 630 kb, 255 kb, 10.7 kb and one circular plasmid of 7 kb. *Streptomyces* sp. Mg1 possessed a linear chromosome of ca 7.9 Mb, two linear plasmids of 530 kb and 184 kb, and one circular plasmid of 135 kb (Hoefler et al., 2013). The latter strain has been reported to produce linearmycins (**Figure 5**), polyketides with antifungal and antibacterial activities (Stubbendieck et al., 2018).

Synteny of the chromosomes and the two largest linear plasmids from the two strains, all of which, according to the antiSMASH analysis, encode secondary metabolite BGCs, are shown in **Figure 6**. Next, we examined the BGCs detected upon antiSMASH analysis followed by manual curation in the

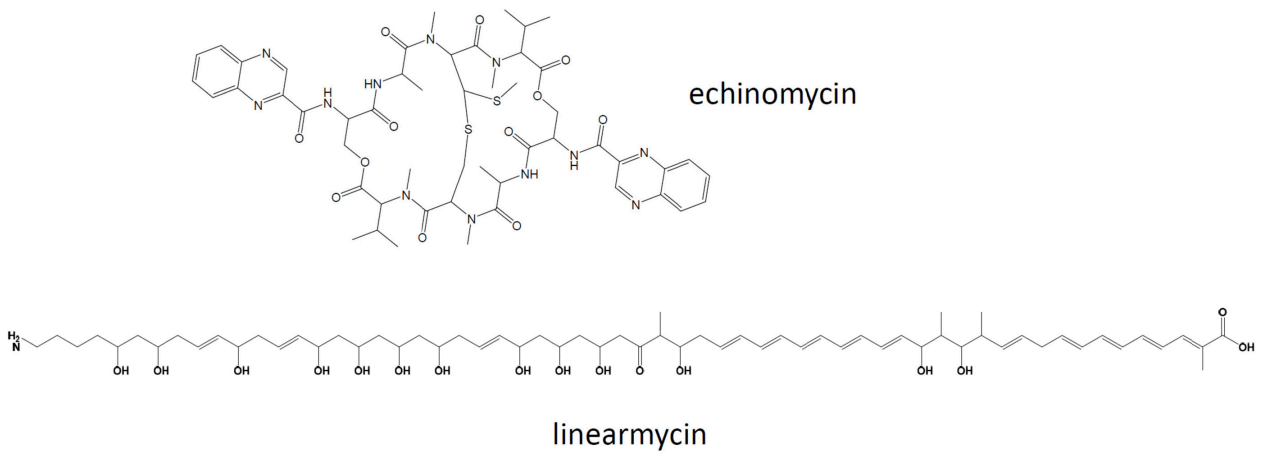

FIGURE 5 | Chemical structures of linearmycin A and echinomycin shown to be produced by *Streptomyces* sp. ADI95-16 and ADI96-02, respectively.

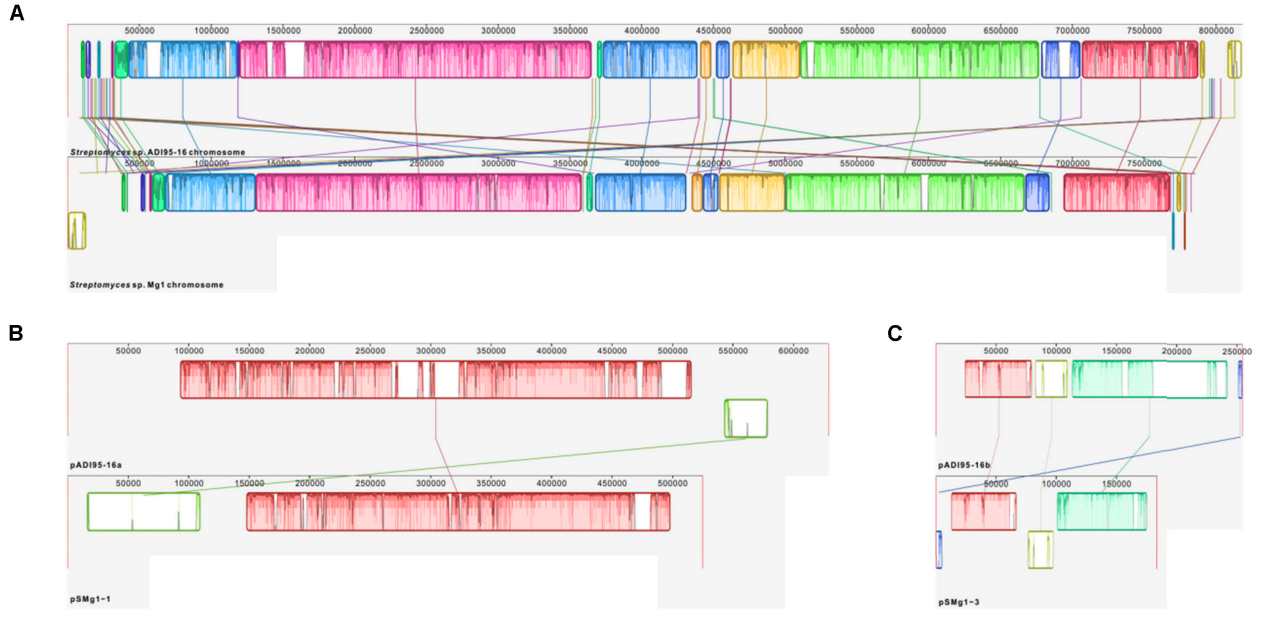

FIGURE 6 | Genomic synteny of *Streptomyces* spp. ADI95-16 and Mg1, based on a progressive alignment with MAUVE (Darling et al., 2010). **(A)** Chromosomes. **(B)** pADI95-16a (reversed) versus pSMg1-1. **(C)** pADI95-16b (reversed) versus pSMg1-3.

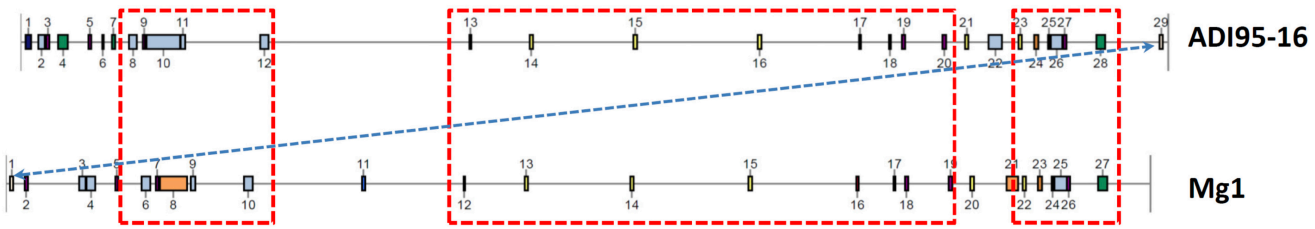

FIGURE 7 | Localization of BGCs on the chromosomes of *Streptomyces* spp. ADI95-16 and Mg1. Largest homologous chromosomal regions harboring identical BGCs are boxed with red dotted lines, and translocation of the nucleoside BGC is indicated by a dotted blue arrow.

genomes of *Streptomyces* spp. ADI95-16 and Mg1. Chromosomes of both strains harbored 23 BGCs that were virtually identical and positioned in the same order on the physical map, with the exception of a putative nucleoside BGC that is located at the opposite chromosomal termini in ADI95-16 and Mg1. In comparison with Mg1, the ADI95-16 chromosome contained unique BGCs for terpene, ectoine, cyclic diketopiperazine, lantipeptide, and NRPS-PKS hybrid-class compounds. Mg1, in comparison to the ADI95-16 counterpart, harbored unique BGCs for a carotenoid, avermitilol, a lasso peptide, a lantipeptide, an unknown terpene, and a chalcomycin-related polyketide. The arrangement of the BGCs in the chromosomes of two strains is shown in **Figure 7**. The largest linear plasmids of both strains, pADI95-16a (630 kb) and pSMg1-1 (530 kb), shared two BGCs for butyrolactones and one for a PKSI-derived polyketide, while pADI95-16a harbored in addition a BGC for a symocyclinone-like compound and a lantipeptide. The smaller linear plasmids of both strains, pADI95-16b (255 kb) and pSMg1-3 (184 kb), contained BGCs for an enedyine, an arylpolyene, and a sporolide-like compound. The latter plasmids differed, however, in that pADI95-16b contained an additional BGC for a butyrolactone, while pSMg1-3 harbored a BGC for a streptonigrin-like compound.

DISCUSSION

Actinomycete bacteria from underexplored habitats may produce novel bioactive secondary metabolites, which can be developed into much needed drugs to fight infections and cancer. Quite often, as it was revealed in recent studies (Ian et al., 2014), such isolates do not produce many bioactive secondary metabolites under standard laboratory conditions. Indeed, only 4 out of 10 *Streptomyces* isolates obtained from a marine sponge and investigated in this work were found to be bioactive in conditions tested. Hence, their genomes were investigated in order to reveal biosynthetic potential of these isolates. Having information on the BGCs, especially those that may potentially specify biosynthesis of novel compounds, opens possibilities for genome mining that can be applied to trigger gene expression of particular BGCs (Sekurova et al., 2019). Also, comparative genomics can be used to trace transfer of BGCs between isolates, which could be expected to happen considering spatial containment within the sponge.

Out of the 10 *Streptomyces* isolates investigated, 9 differed significantly both in terms of taxonomy, genome sizes and BGCs detected. The exception were isolates ADI95-16 and ADI91-18, which were closely related (**Figure 1**), shared most of the BGCs (data not shown), and were apparently also related to the terrestrial isolate *Streptomyces* sp. Mg1. Two other isolates, ADI98-12 and ADI96-02 were also found to have terrestrial counterparts. Thanks to the growing database of characterized BGCs (Medema et al., 2015), we were able to unambiguously assign many BGCs in the sequenced genomes to the known ones (**Table 3**), thus assigning the ability to produce certain secondary metabolites to particular isolates. Together, the 10 *Streptomyces* isolates can potentially produce at least 29 already known secondary metabolites, while judging from their total number of BGCs, this potential exceeds 300 compounds, not counting congeners. This calculation clearly suggests that even this small number of streptomycetes can provide a huge arsenal of bioactive molecules that may benefit their host and protect it from predators and infectious agents.

When looking for potential HGT events, we could rather safely suggest those for BGCs specifying RiPPs, ribosomally synthesized and post-translationally modified peptides that may display a wide range of bioactivities (Arnison et al., 2013). Interestingly, we could detect considerable variation in the amino acid sequences of lantipeptide cores, while the thiopeptide primary amino acid sequences were more conserved (**Figure 2**). This observation may reflect different biological roles that these RiPPs play in their producing hosts, with lantipeptides being more host-specific and thiopeptides more generalistic. Alternatively, thiopeptide BGCs may have been acquired by studied isolates rather recently compared to those for lantipeptides. Notably, the BGCs for PTM were found in 8 out of 10 isolates, and, considering the wide distribution of these clusters in bacteria, their products may play a distinct role in environmental adaptation that is yet to be revealed.

It appeared interesting to compare one of the isolates, ADI95-16, with its terrestrial counterpart *Streptomyces* sp. Mg1, which shared not only homologous chromosomes, but also some linear plasmids. The latter harbor several BGCs, which can be transferred to other species by means of conjugation, thus providing means for distribution of certain BGCs among streptomycetes. Despite the fact that most of the BGCs in the genomes of these strains were identical, several were unique for each strain. It seems likely that the presence of these distinctive

TABLE 3 | Potential of the sponge-derived *Streptomyces* spp. to produce known secondary metabolites deduced from the antiSMASH-based genome analyses followed by manual curation.

Strain	Identified BGC	Compound class	Biological activity	References
ADI91-18	Alkyl-O-dihydrogeranyl-methoxyhydroquinones	Prenylated phenolic lipid	–	Awakawa et al., 2011
	Linearmycins	Polyketide	Antibacterial, antifungal	Stubbendieck et al., 2018
	Avermitilol	Sesquiterpenoid	–	Chou et al., 2010
	SapB peptide	Lantipeptide	Peptidic morphogen	Kodani et al., 2004
ADI92-24	Tomaymycin	Pyrrolobenzodiazepine	Cytotoxic	Li et al., 2009
ADI93-02	Alkyl-O-dihydrogeranyl-methoxyhydroquinones	Prenylated phenolic lipid	–	Awakawa et al., 2011
	Mirubactin	NR peptide	Siderophore	Giessen et al., 2012
	Coelichelin	NR peptide	Siderophore	Challis and Ravel, 2000
	PM100117	Macrolide	Cytotoxic	Salcedo et al., 2016
ADI95-16	Linearmycins	Polyketide	Antibacterial, antifungal	Stubbendieck et al., 2018
	Erythrochelin	Hydroxamate	Siderophore	Robbel et al., 2010
ADI95-17	Mirubactin	NR peptide	Siderophore	Giessen et al., 2012
	Coelichelin	NR peptide	Siderophore	Challis and Ravel, 2000
	Naringenin	Flavonoid	Antioxidant, cytotoxic	Álvarez-Álvarez et al., 2015
ADI96-02	Cycloheximide	Dicarboximide	Antifungal	Yin et al., 2014
	Galbonolides	Macrolide	Antifungal	Kim et al., 2014
	SRO15-3108	Lantipeptide	–	Kersten et al., 2011
	Echinomycin	NR peptide	Cytotoxic	Watanabe et al., 2006
	Alkylresorcinol	Phenolic lipid	–	Funa et al., 2006
	Coelichilin	NR peptide	Siderophore	Challis and Ravel, 2000
ADI96-15	Candicidin	Polyene macrolide	Antifungal	Chen et al., 2003
	Antimycin	NR peptide-polyketide	Cytotoxic	Yan et al., 2012
	Lobophorins	Spirotetronate	Cytotoxic	Yue et al., 2016
	SAL-2242	Lantipeptide	–	Kersten et al., 2011
ADI97-07	Clavams	NR peptide	Antibacterial	Zelyas et al., 2008
	Galbonolides	Macrolide	Antifungal	Kim et al., 2014
	Neocarzilin	Polyketide pyrone	Cytotoxic	Otsuka et al., 2004
	Antimycin	NR peptide-polyketide	Cytotoxic	Yan et al., 2012
	Legonaridin	Linaridin	–	Rateb et al., 2015
	Coelichilin	NR peptide	Siderophore	Challis and Ravel, 2000
ADI98-10	SRO15-2005	Lasso peptide	–	Kersten et al., 2011
	AmfS peptide	Lantipeptide	Peptidic morphogen	Ueda et al., 2002
	Actinomycin	NR peptide	Cytotoxic	Keller et al., 2010
	Alkylresorcinol	Phenolic lipid	–	Funa et al., 2006
	Griseobactin	Catechol-peptide	Siderophore	Patzer and Braun, 2010
ADI98-12	Candicidin	Polyene macrolide	Antifungal	Chen et al., 2003
	Griselimycin	NR peptide	Antibacterial	Kling et al., 2015
	Kirromycin	Polyketide	Antibacterial	Weber et al., 2008

NR – non-ribosomally synthesized.

BGCs reflects different environments where the strains were isolated from, and signifies requirements for adaptation fulfilled by the production of cognate secondary metabolites.

Our investigation of two bioactive isolates, ADI95-16 and ADI96-02, revealed production of compounds already discovered from terrestrial streptomycetes. However, some new derivatives of linearmycin harboring methylhexose attached to the amino group appear to be produced by ADI95-16. Those have never been reported for the related strain *Streptomyces* sp. Mg1. Since no glycosyltransferase gene could be identified in the linearmycin BGC, it is likely that glycosylation is catalyzed by an enzyme encoded someplace else in the ADI95-16 genome, while the same enzyme is absent or not expressed in Mg1. Notably, the BGC for echinomycin and echinoserine, the compounds produced by ADI96-02, was found to be different in at least three genes compared to echinomycin BGC from *S. lasaliensis*. It is possible, that at least the presence of an additional monooxygenase gene in the ADI96-02 echinomycin BGC may provide opportunities for derivatives with altered oxidation pattern.

Taking together, the results of this study further support the significance of *Streptomyces* bacteria for future drug discovery, and open possibilities for targeted genome mining by means of activation or heterologous expression of selected BGCs. Partial marine adaptation of several isolates suggested by the data presented in **Table 1** may also be advantageous in terms of using

these strains for heterologous expression of BGCs originating from marine actinomycetes.

DATA AVAILABILITY STATEMENT

The Whole Genome Shotgun projects have been deposited at DDBJ/ENA/GenBank under the accessions RPGS00000000 (ADI91-18), RPGT00000000 (ADI92-24), RPGU00000000 (ADI93-02), CP033581-CP033585 (ADI95-16), RPGV00000000 (ADI95-17), RPGW00000000 (ADI96-02), RPGX00000000 (ADI96-15), RPGY00000000 (ADI97-07), RPGZ00000000 (ADI98-10), and RPHA00000000 (ADI98-12).

AUTHOR CONTRIBUTIONS

SZ conceptualized the study and supervised the project. SZ, MZ, and HB worked on the methodology. CR, TB, and JK were responsible for the software. JG-G, MZ, OS, CR, and HB carried out the investigation. CR, TB, and JK were responsible for the data curation. JG-G, OS, MZ, CR, and SZ prepared and wrote the original draft.

FUNDING

This research was funded by the University of Vienna, Research Council of Norway and the Norwegian University of Science and Technology.

ACKNOWLEDGMENTS

We are thankful to Geir Johnsen (NTNU, Norway) for help with sponge collection and Hans Tore Rapp (University of Bergen, Norway) for sponge identification. All LC-MS measurements were performed in the Mass Spectrometry Centre of the Faculty of Chemistry, University of Vienna.

SUPPLEMENTARY MATERIAL

The Supplementary Material for this article can be found online at: https://www.frontiersin.org/articles/10.3389/fmicb.2020.00437/full#supplementary-material

REFERENCES

Álvarez-Álvarez, R., Botas, A., Albillos, S. M., Rumbero, A., Martín, J. F., and Liras, P. (2015). Molecular genetics of naringenin biosynthesis, a typical plant secondary metabolite produced by Streptomyces clavuligerus. *Microb. Cell Fact.* 14:178. doi: 10.1186/s12934-015-0373-7

Arnison, P. G., Bibb, M. J., Bierbaum, G., Bowers, A. A., Bugni, T. S., Bulaj, G., et al. (2013). Ribosomally synthesized and post-translationally modified peptide natural products: overview and recommendations for a universal nomenclature. *Nat. Prod. Rep.* 30, 108–160. doi: 10.1039/c2np20085f

Arnvig, K. B., and Young, D. B. (2009). Identification of small RNAs in *Mycobacterium tuberculosis*. *Mol. Microbiol.* 73, 397–408. doi: 10.1111/j.1365-2958.2009.06777.x

Awakawa, T., Fujita, N., Hayakawa, M., Ohnishi, Y., and Horinouchi, S. (2011). Characterization of the biosynthesis gene cluster for alkyl-O-dihydrogeranyl-methoxyhydroquinones in *Actinoplanes missouriensis*. *Chembiochem* 12, 439–448. doi: 10.1002/cbic.201000628

Baltz, R. H. (2017). Gifted microbes for genome mining and natural product discovery. *J. Ind. Microbiol. Biotechnol.* 44, 573–588. doi: 10.1007/s10295-016-1815-x

Blin, K., Shaw, S., Steinke, K., Villebro, R., Ziemert, N., Lee, S. Y., et al. (2019). antiSMASH 5.0: updates to the secondary metabolite genome mining pipeline. *Nucleic Acids Res.* 47, W81–W87. doi: 10.1093/nar/gkz310

Blodgett, J. A., Oh, D. C., Cao, S., Currie, C. R., Kolter, R., and Clardy, J. (2010). Common biosynthetic origins for polycyclic tetramate macrolactams from phylogenetically diverse bacteria. *Proc. Natl. Acad. Sci. U.S.A.* 107, 11692–11697. doi: 10.1073/pnas.1001513107

Blum, S., Fielder, H. P., Groth, I., Kempter, C., Stephan, H., Nicholson, G., et al. (1995). Biosynthetic capacities of actinomycetes. 4. Echinoserine, a new member of the quinoxaline group, produced by Streptomyces tendae. *J. Antibiot.* 48, 619–625. doi: 10.7164/antibiotics.48.619

Cao, S., Blodgett, J. A., and Clardy, J. (2010). Targeted discovery of polycyclic tetramate macrolactams from an environmental *Streptomyces* strain. *Org. Lett.* 12, 4652–4654. doi: 10.1021/ol1020064

Challis, G. L., and Ravel, J. (2000). Coelichelin, a new peptide siderophore encoded by the Streptomyces coelicolor genome: structure prediction from the sequence of its non-ribosomal peptide synthetase. *FEMS Microbiol. Lett.* 187, 111–114. doi: 10.1111/j.1574-6968.2000.tb09145.x

Chen, S., Huang, X., Zhou, X., Bai, L., He, J., Jeong, K. J., et al. (2003). Organizational and mutational analysis of a complete FR-008/candicidin gene cluster encoding a structurally related polyene complex. *Chem. Biol.* 10, 1065–1076. doi: 10.1016/j.chembiol.2003.10.007

Chou, W. K., Fanizza, I., Uchiyama, T., Komatsu, M., Ikeda, H., and Cane, D. E. (2010). Genome mining in *Streptomyces avermitilis*: cloning and characterization of SAV_76, the synthase for a new sesquiterpene, avermitilol. *J. Am. Chem. Soc.* 132, 8850–8851. doi: 10.1021/ja103087w

Darling, A. E., Mau, B., and Perna, N. T. (2010). ProgressiveMauve: multiple genome alignment with gene gain, loss and rearrangement. *PLoS ONE* 5:e11147. doi: 10.1371/journal.pone.0011147

Funa, N., Ozawa, H., Hirata, A., and Horinouchi, S. (2006). Phenolic lipid synthesis by type III polyketide synthases is essential for cyst formation in *Azotobacter vinelandii*. *Proc. Natl. Acad. Sci. U.S.A.* 103, 6356–6361. doi: 10.1073/pnas.0511227103

Giessen, T. W., Franke, K. B., Knappe, T. A., Kraas, F. I., Bosello, M., Xie, X., et al. (2012). Isolation, structure elucidation, and biosynthesis of an unusual hydroxamic acid ester-containing siderophore from *Actinosynnema mirum*. *J. Nat. Prod.* 75, 905–914. doi: 10.1021/np300046k

Goodfellow, M., Nouioui, I., Sanderson, R., Xie, F., and Bull, A. T. (2018). Rare taxa and dark microbial matter: novel bioactive actinobacteria abound in Atacama Desert soils. *Antonie Van Leeuwenhoek* 111, 1315–1332. doi: 10.1007/s10482-018-1088-7

Gordon, D., and Green, P. (2013). Consed: a graphical editor for next-generation sequencing. *Bioinformatics* 29, 2936–2937. doi: 10.1093/bioinformatics/btt515

Grubbs, K. J., Surup, F., Biedermann, P. H., McDonald, B. R., Klassen, J. L., Carlson, C. M., et al. (2019). Cycloheximide-producing *Streptomyces* associated with *Xyleborinus saxesenii* and *Xyleborus affinis* fungus-farming ambrosia beetles. *bioRxiv* [Preprint]

Hoefler, B. C., Konganti, K., and Straight, P. D. (2013). De novo assembly of the *Streptomyces* sp. strain Mg1 genome using PacBio single-molecule sequencing. *Microbiol. Resour. Ann.* 1, e535–e513. doi: 10.1128/genomeA.00535-13

Hoefler, B. C., Stubbendieck, R. M., Josyula, N. K., Moisan, S. M., Schulze, E. M., and Straight, P. D. (2017). A link between linearmycin biosynthesis and extracellular vesicle genesis connects specialized metabolism and bacterial membrane physiology. *Cell Chem. Biol.* 24, 1238–1249. doi: 10.1016/j.chembiol.2017.08.008

Ian, E., Malko, D. B., Sekurova, O. N., Bredholt, H., Ruckert, C., Borisova, M. E., et al. (2014). Genomics of sponge-associated Streptomyces spp. closely related to *Streptomyces albus* J1074: insights into marine adaptation and secondary

metabolite biosynthesis potential. *PLoS ONE* 9:e96719. doi: 10.1371/journal.pone.0096719

Jackson, S. A., Crossman, L., Almeida, E. L., Margassery, L. M., Kennedy, J., and Dobson, A. D. W. (2018). Diverse and abundant secondary metabolism biosynthetic gene clusters in the genomes of marine sponge derived Streptomyces spp. isolates. *Mar. Drugs* 16, E67. doi: 10.3390/md16020067

Jomon, K., Kuroda, Y., Ajisaka, M., and Sakai, H. (1972). A new antibiotic, ikarugamycin. *J. Antibiot.* 25, 271–280. doi: 10.7164/antibiotics.25.271

Kalvari, I., Argasinska, J., Quinones-Olvera, N., Nawrocki, E. P., Rivas, E., Eddy, S. R., et al. (2018). Rfam 13.0: shifting to a genome-centric resource for non-coding RNA families. *Nucleic Acids Res.* 46, D335–D342. doi: 10.1093/nar/gkx1038

Keller, U., Lang, M., Crnovcic, I., Pfennig, F., and Schauwecker, F. (2010). The actinomycin biosynthetic gene cluster of *Streptomyces chrysomallus*: a genetic hall of mirrors for synthesis of a molecule with mirror symmetry. *J. Bacteriol.* 192, 2583–2595. doi: 10.1128/JB.01526-09

Kersten, R. D., Yang, Y. L., Xu, Y., Cimermancic, P., Nam, S. J., Fenical, W., et al. (2011). A mass spectrometry-guided genome mining approach for natural product peptidogenomics. *Nat. Chem. Biol.* 7, 794–802. doi: 10.1038/nchembio.684

Kieser, T., Bibb, M. J., Buttner, M. J., Chater, K. F., and Hopwood, D. A. (2000). *Practical Streptomyces Genetics: A Laboratory Manual*. Norwich: John Innes Centre Foundation.

Kim, H. J., Karki, S., Kwon, S. Y., Park, S. H., Nahm, B. H., Kim, Y. K., et al. (2014). A single module type I polyketide synthase directs de novo macrolactone biogenesis during galbonolide biosynthesis in *Streptomyces galbus*. *J. Biol. Chem.* 289, 34557–34568. doi: 10.1074/jbc.M114.602334

Kinashi, H. (2011). Giant linear plasmids in *Streptomyces*: a treasure trove of antibiotic biosynthetic clusters. *J. Antibiot.* 64, 19–25. doi: 10.1038/ja.2010.146

Kling, A., Lukat, P., Almeida, D. V., Bauer, A., Fontaine, E., and Sordello, S. (2015). Antibiotics. targeting DnaN for tuberculosis therapy using novel griselimycins. *Science* 348, 1106–1112. doi: 10.1126/science.aaa4690

Kodani, S., Hudson, M. E., Durrant, M. C., Buttner, M. J., Nodwell, J. R., and Willey, J. M. (2004). The SapB morphogen is a lantibiotic-like peptide derived from the product of the developmental gene ramS in *Streptomyces coelicolor*. *Proc. Natl. Acad. Sci. U.S.A.* 101, 11448–11453. doi: 10.1073/pnas.0404220101

Kumar, S., Stecher, G., and Tamura, K. (2016). MEGA7: molecular evolutionary genetics analysis version 7.0 for bigger datasets. *Mol. Biol. Evol.* 33, 1870–1874. doi: 10.1093/molbev/msw054

Lane, D. J. (1991). "16S/23S rRNA sequencing," in *Nucleic Acid Techniques in Bacterial Systematic*, eds E. Stackebrandt, and M. Goodfellow (New York, NY: John Wiley and Sons), 115–175.

Li, W., Chou, S., Khullar, A., and Gerratana, B. (2009). Cloning and characterization of the biosynthetic gene cluster for tomaymycin, an SJG-136 monomeric analog. *Appl. Environ. Microbiol.* 75, 2958–2963. doi: 10.1128/AEM.02325-08

McAlpine, J. B., Bachmann, B. O., Piraee, M., Tremblay, S., Alarco, A. M., Zazopoulos, E., et al. (2005). Microbial genomics as a guide to drug discovery and structural elucidation: ECO-02301, a novel antifungal agent, as an example. *J. Nat. Prod.* 68, 493–496. doi: 10.1021/np0401664

Medema, M. H., Kottmann, R., Yilmaz, P., Cummings, M., Biggins, J. B., and Blin, K. (2015). Minimum information about a biosynthetic gene cluster. *Nat. Chem. Biol.* 11, 625–631. doi: 10.1038/nchembio.1890

Meier-Kolthoff, J. P., Auch, A. F., Klenk, H.-P., and Göker, M. (2013). Genome sequence-based species delimitation with confidence intervals and improved distance functions. *BMC Bioinformatics* 14:60. doi: 10.1186/1471-2105-14-60

Nawrocki, E. P., and Eddy, S. R. (2013). Infernal 1.1: 100-fold faster RNA homology searches. *Bioinformatics* 29, 2933–2935. doi: 10.1093/bioinformatics/btt509

Novák, J., Sokolová, L., Lemr, K., Pluháček, T., Palyzová, A., and Havlíček, V. (2017). Batch-processing of imaging or liquid-chromatography mass spectrometry datasets and *de novo* sequencing of polyketide siderophores. *Biochim. Biophys. Acta Proteins Proteom.* 1865, 768–775. doi: 10.1016/j.bbapap.2016.12.003

Otsuka, M., Ichinose, K., Fujii, I., and Ebizuka, Y. (2004). Cloning, sequencing, and functional analysis of an iterative type I polyketide synthase gene cluster for biosynthesis of the antitumor chlorinated polyenone neocarzilin in "*Streptomyces carzinostaticus*". *Antimicrob. Agents Chemother.* 48, 3468–3476. doi: 10.1128/AAC.48.9.3468-3476.2004

Patzer, S. I., and Braun, V. (2010). Gene cluster involved in the biosynthesis of griseobactin, a catechol-peptide siderophore of *Streptomyces* sp. ATCC 700974 *J. Bacteriol.* 192, 426–435. doi: 10.1128/JB.01250-09

Penn, K., Jenkins, C., Nett, M., Udwary, D. W., Gontang, E. A., McGlinchey, R. P., et al. (2009). Genomic islands link secondary metabolism to functional adaptation in marine Actinobacteria. *ISME J.* 3, 1193–1203. doi: 10.1038/ismej.2009.58

Rateb, M. E., Zhai, Y., Ehrner, E., Rath, C. M., Wang, X., Tabudravu, J., et al. (2015). Legonaridin, a new member of linaridin RiPP from a Ghanaian Streptomyces isolate. *Org. Biomol. Chem.* 13, 9585–9592. doi: 10.1039/c5ob01269d

Reen, F. J., Romano, S., Dobson, A. D., and O'Gara, F. (2015). The sound of silence: activating silent biosynthetic gene clusters in marine microorganisms. *Mar. Drugs* 13, 4754–4783. doi: 10.3390/md13084754

Robbel, L., Knappe, T. A., Linne, U., Xie, X., and Marahiel, M. A. (2010). Erythrochelin–a hydroxamate-type siderophore predicted from the genome of Saccharopolyspora erythraea. *FEBS J.* 277, 663–676. doi: 10.1111/j.1742-4658.2009.07512.x

Salcedo, R. G., Olano, C., Gómez, C., Fernández, R., Braña, A. F., Méndez, C., et al. (2016). Characterization and engineering of the biosynthesis gene cluster for antitumor macrolides PM100117 and PM100118 from a marine actinobacteria: generation of a novel improved derivative. *Microb Cell Fact.* 15:44. doi: 10.1186/s12934-016-0443-5

Seemann, T. (2014). Prokka: rapid prokaryotic genome annotation. *Bioinformatics* 30, 2068–2069. doi: 10.1093/bioinformatics/btu153

Sekurova, O. N., Schneider, O., and Zotchev, S. B. (2019). Novel bioactive natural products from bacteria via bioprospecting, genome mining and metabolic engineering. *Microb. Biotechnol.* 12, 828–844. doi: 10.1111/1751-7915.13398

Socha, A. M., Laplante, K. L., Russell, D. J., and Rowley, D. C. (2009). Structure-activity studies of echinomycin antibiotics against drug-resistant and biofilm-forming *Staphylococcus aureus* and *Enterococcus faecalis*. *Bioorg. Med. Chem. Lett.* 19, 1504–1507. doi: 10.1016/j.bmcl.2009.01.010

Stubbendieck, R. M., Brock, D. J., Pellois, J.-P., Gill, J. J., and Straight, P. D. (2018). Linearmycins are lytic membrane-targeting antibiotics. *J. Antibiot.* 71, 372–381. doi: 10.1038/s41429-017-0005-z

Subramani, R., and Sipkema, D. (2019). Marine rare actinomycetes: a promising source of structurally diverse and unique novel natural products. *Mar. Drugs* 17:E249. doi: 10.3390/md17050249

Takahashi, Y., and Nakashima, T. (2018). Actinomycetes, an inexhaustible source of naturally occurring antibiotics. *Antibiotics* 7:E45. doi: 10.3390/antibiotics7020045

Ueda, K., Oinuma, K., Ikeda, G., Hosono, K., Ohnishi, Y., Horinouchi, S., et al. (2002). AmfS, an extracellular peptidic morphogen in *Streptomyces griseus*. *J. Bacteriol.* 184, 1488–1492. doi: 10.1128/jb.184.5.1488-1492.2002

Watanabe, K., Hotta, K., Praseuth, A. P., Koketsu, K., Migita, A., Boddy, C. N., et al. (2006). Total biosynthesis of antitumor nonribosomal peptides in *Escherichia coli*. *Nat. Chem. Biol.* 2, 423–428. doi: 10.1038/nchembio803

Weber, T., Laiple, K. J., Pross, E. K., Textor, A., Grond, S., Welzel, K., et al. (2008). Molecular analysis of the kirromycin biosynthetic gene cluster revealed beta-alanine as precursor of the pyridone moiety. *Chem. Biol.* 15, 175–188. doi: 10.1016/j.chembiol.2007.12.009

Williamson, M. P., Gauvreau, D., Williams, D. H., and Waring, M. J. (1982). Structure and conformation of fourteen antibiotics of the quinoxaline group determined by 1H NMR. *J. Antibiot.* 35, 62–66. doi: 10.7164/antibiotics.35.62

Yan, Y., Zhang, L., Ito, T., Qu, X., Asakawa, Y., Awakawa, T., et al. (2012). Biosynthetic pathway for high structural diversity of a common dilactone core in antimycin production. *Org. Lett.* 14, 4142–5414. doi: 10.1021/ol301785x

Yin, M., Yan, Y. J., Lohman, J. R., Huang, S. X., Ma, M., Zhao, G. R., et al. (2014). Cycloheximide and actiphenol production in *Streptomyces* sp YIM56141 governed by single biosynthetic machinery featuring an acyltransferase-less Type I polyketide synthase. *Org. Lett.* 16, 3072–3075. doi: 10.1021/ol501179w

Yu, F., Zaleta-Rivera, K., Zhu, X., Huffman, J., Millet, J. C., Harris, S. D., et al. (2007). Structure and biosynthesis of heat-stable antifungal factor (HSAF), a broad-spectrum antimycotic with a novel mode of action. *Antimicrob. Agents Chemother.* 51, 64–72. doi: 10.1128/AAC.00931-06

Yue, C., Niu, J., Liu, N., Lü, Y., Liu, M., and Li, Y. (2016). Cloning and identification of the lobophorin biosynthetic gene cluster from marine *Streptomyces olivaceus* strain FXJ7.023. *Pak. J. Pharm. Sci.* 29, 287–293.

Zelyas, N. J., Cai, H., Kwong, T., and Jensen, S. E. (2008). Alanylclavam biosynthetic genes are clustered together with one group of clavulanic acid biosynthetic genes in *Streptomyces clavuligerus*. *J. Bacteriol.* 190, 7957–7965. doi: 10.1128/JB.00698-08

Ziemert, N., Lechner, A., Wietz, M., Millan-Aguinaga, N., Chavarria, K. L., and Jensen, P. R. (2014). Diversity and evolution of secondary metabolism in the marine actinomycete genus Salinispora. *Proc. Natl. Acad. Sci. U.S.A.* 111, E1130–E1139. doi: 10.1073/pnas.1324161111

Zotchev, S., Haugan, K., Sekurova, O., Sletta, H., Ellingsen, T. E., and Valla, S. (2000). Identification of a gene cluster for antibacterial polyketide-derived antibiotic biosynthesis in the nystatin producer *Streptomyces noursei* ATCC 11455. *Microbiology* 146, 611–619. doi: 10.1099/00221287-146-3-611

Conflict of Interest: HB was employed by the company Xellia Pharmaceuticals AS.

The remaining authors declare that the research was conducted in the absence of any commercial or financial relationships that could be construed as a potential conflict of interest.

The handling Editor declared a past co-authorship with one of the authors SZ.

frontiers in Microbiology

ORIGINAL RESEARCH
published: 15 March 2021
doi: 10.3389/fmicb.2021.604999

Bioprospecting of Soil-Derived Actinobacteria Along the Alar-Hotan Desert Highway in the Taklamakan Desert

Shaowei Liu[1,2†], Ting Wang[1†], Qinpei Lu[1], Feina Li[1], Gang Wu[1], Zhongke Jiang[1], Xugela Habden[3], Lin Liu[4], Xiaolin Zhang[5], Dmitry A. Lukianov[6], Ilya A. Osterman[6,7], Petr V. Sergiev[6,7], Olga A. Dontsova[6,7,8] and Chenghang Sun[1,2]*

[1]Department of Microbial Chemistry, Institute of Medicinal Biotechnology, Chinese Academy of Medical Sciences & Peking Union Medical College, Beijing, China, [2]Beijing Key Laboratory of Antimicrobial Agents, Institute of Medicinal Biotechnology, Chinese Academy of Medical Sciences & Peking Union Medical College, Beijing, China, [3]College of Life Science, Xinjiang Normal University, Urumchi, China, [4]School of Traditional Chinese Pharmacy, China Pharmaceutical University, Nanjing, China, [5]School of Life Science and Technology, China Pharmaceutical University, Nanjing, China, [6]Center of Life Sciences, Skolkovo Institute of Science and Technology, Moscow, Russia, [7]Department of Chemistry, A.N. Belozersky Institute of Physico-Chemical Biology, Lomonosov Moscow State University, Moscow, Russia, [8]Shemyakin-Ovchinnikov Institute of Bioorganic Chemistry, Russian Academy of Sciences, Moscow, Russia

OPEN ACCESS

Edited by:
Louis S. Tisa,
University of New Hampshire,
United States

Reviewed by:
Sheng Qin,
Jiangsu Normal University, China
Usman Aftab,
University of Health Sciences,
Pakistan

***Correspondence:**
Chenghang Sun
chenghangsun@hotmail.com

[†]These authors have contributed equally to this work

Specialty section:
This article was submitted to Systems Microbiology, a section of the journal Frontiers in Microbiology

Received: 11 September 2020
Accepted: 22 February 2021
Published: 15 March 2021

Citation:
Liu S, Wang T, Lu Q, Li F, Wu G, Jiang Z, Habden X, Liu L, Zhang X, Lukianov DA, Osterman IA, Sergiev PV, Dontsova OA and Sun C (2021) Bioprospecting of Soil-Derived Actinobacteria Along the Alar-Hotan Desert Highway in the Taklamakan Desert. Front. Microbiol. 12:604999. doi: 10.3389/fmicb.2021.604999

Taklamakan desert is known as the largest dunefield in China and as the second largest shifting sand desert in the world. Although with long history and glorious culture, the Taklamakan desert remains largely unexplored and numerous microorganisms have not been harvested in culture or taxonomically identified yet. The main objective of this study is to explore the diversity, novelty, and pharmacological potential of the cultivable actinomycetes from soil samples at various sites along the Alar-Hotan desert highway in the Taklamakan desert. A total of 590 actinobacterial strains were recovered by the culture-dependent approach. Phylogenetic analysis based on 16S ribosomal RNA (rRNA) gene sequences unveiled a significant level of actinobacterial diversity with 55 genera distributed in 27 families of 12 orders. Thirty-six strains showed relatively low 16S rRNA similarities (<98.65%) with validly described species, among which four strains had already been characterized as novel taxa by our previous research. One hundred and forty-six actinobacterial isolates were selected as representatives to evaluate the antibacterial activities and mechanism of action by the paper-disk diffusion method and a double fluorescent protein reporter "pDualrep2" system, respectively. A total of 61 isolates exhibited antagonistic activity against the tested "ESKAPE" pathogens, among which seven strains could produce bioactive metabolites either to be able to block translation machinery or to induce SOS-response in the pDualrep2 system. Notably, *Saccharothrix* sp. 16Sb2-4, harboring a promising antibacterial potential with the mechanism of interfering with protein translation, was analyzed in detail to gain deeper insights into its bioactive metabolites. Through ultra-performance liquid chromatography (UPLC)-quadrupole time-of-flight (QToF)-MS/MS based molecular networking analysis and databases identification, four families of compounds (**1**–**16**) were putatively identified. Subsequent bioassay-guided

separation resulted in purification of four 16-membered macrolide antibiotics, aldgamycin H (**8**), aldgamycin K (**9**), aldgamycin G (**10**), and swalpamycin B (**11**), and their structures were elucidated by HR-electrospray ionization source (ESI)-MS and NMR spectroscopy. All compounds **8**–**11** displayed antibacterial activities by inhibiting protein synthesis in the pDualrep2 system. In conclusion, this work demonstrates that Taklamakan desert is a potentially unique reservoir of versatile actinobacteria, which can be a promising source for discovery of novel species and diverse bioactive compounds.

Keywords: actinobacteria, diversity, macrolides, Taklamakan desert, novel species, antibacterial metabolites

INTRODUCTION

The finding of novel bioactive compounds is a never-ending process, to meet the everlasting demand for novel drug with antimicrobial properties in order to combat escalating levels of antibiotic resistance in pathogenic microorganisms (Chokshi et al., 2019; Ardal et al., 2020). However, most of the large pharmaceutical and biopharmaceutical companies have terminated their anti-infective research programs due to high risk of failure and relatively low probability to achieve a tangible market success and profit. Until April 2020, there are 41 new antibiotics under global clinical development, but only 13 of them have the potential to treat pathogens on the WHO's critical threat list (Pew Charitable Trusts, 2020). This fact has resulted in today's eminent lack of new antibiotic drug leads, making us face a looming crisis that the emergence of resistance is outpacing the development of new antibiotics (Dickey et al., 2017; Woodworth et al., 2018). The previous admonitory terms of "gloom scenario," "dark horizons," and "back to the pre-antibiotic era" are becoming reality nowadays (Bravo et al., 2018). All these facts impel scientists to rapidly explore new chemical entities for developing novel antibiotics to target the emerging multidrug-resistant microbial pathogens that cause life-threatening infections.

Microorganisms, especially actinobacteria isolated from a diverse range of ecological niches, have been reported as the prolific producers of microbial bioactive secondary metabolites for pharmaceutical and agricultural applications, *etc*. The importance of these organisms is clearly seen from the fact that over 5,000 compounds have been reported from actinobacteria that contributed to the development of 90% of the commercial antibiotics being used for either clinical or research needs (Jose and Jha, 2016), such as Erythromycin, Gentamycin, Neomycin, Streptomycin, Chloramphenicol, Novobiocin, Teicoplanin, Vancomycin, Rifamycin, Chlortetracycline, *etc*. (Shah et al., 2017). However, after decades of exhausted excavation, the discovery of novel compounds from widely explored microbial strains is reaching a stagnation point, since it always yielded disappointing returns due to the frequent rediscovery of already known compounds. Thus, innovative drug discovery approaches are required in order to expedite the antibiotic discovery process.

One promising strategy is to selectively isolate, dereplicate, and screen representatives of novel and rare actinomycetes from neglected and unexplored habitats. The possibility of discovering novel bioactive molecules from extreme biomes could be greatly increased since harsh environmental conditions will give rise to novel actinobacteria with the capacity to synthesize novel metabolites (Goodfellow and Fiedler, 2010; Bull and Asenjo, 2013). As a result, bioprospecting actinobacteria from previously untapped sources, such as hyper-arid deserts, deep-sea sediments, permafrost soils, hydrothermal springs, *etc*. has been proposed as an important strategy to replenish the drug pipeline (Jose and Jha, 2016; Kolter and van Wezel, 2016). Deserts cover approximately 20% of the landmass on the planet (An et al., 2013), and the survival conditions in deserts are a huge challenge for microorganisms, as there is little available water and organic carbon, large temperature fluctuations, high exposure to UV irradiation, intense concentrations of metals and inorganic oxidants, and high salinity, pH in some areas (Koberl et al., 2011; Mohammadipanah and Wink, 2015). However, many surveys in recent years have revealed an extraordinary bacterial diversity across a range of desert environments, such as the Namibian desert (Wink et al., 2003), the Sahara desert (Zitouni et al., 2005; Meklat et al., 2011), the Mongolian desert (Kurapova et al., 2012), the Thar desert (Harwani, 2013; Tiwari et al., 2015), *etc*., and the most extensive studies are focused on the different sites in the Atacama desert in Northern Chile (Bull et al., 2016, 2018; Bull and Goodfellow, 2019). Furthermore, in the last decade, more than 30 novel natural products with diverse chemical structures and various biological activities were discovered from desert-derived actinobacteria, as exemplified by Chaxamycins A–D (Rateb et al., 2011a), Abenquines A–D (Schulz et al., 2011), Atacamycins A–C (Nachtigall et al., 2011), Chaxalactins A–C (Rateb et al., 2011b), Chaxapeptin (Elsayed et al., 2015), Lentzeosides A–F (Wichner et al., 2017), and Asenjonamides A–C (Abdelkader et al., 2018). These findings showed that the desert ecosystem inhabits a promising source of valuable actinobacterial species that can produce novel compounds with interesting chemical and pharmaceutical properties.

Covering as large as 346,905 km^2 in the hinterland of the Tarim Basin in northwest China, the Taklamakan desert is known as the largest dunefield in China and the second largest drift desert in the world (Yang, 2018). It is categorized as harsh, hyper-arid, and continental climate (Yang et al., 2006) characterized by the extremely low water availability [very limited annual rainfall (10–50 mm/year)], strong evaporative potential (2,100–3,400 mm/year), large temperature fluctuations (the highest temperature in summer is 67.2°C and the lowest temperature in winter is −20°C), high ultraviolet radiation (3628.5 MJ/m^2), poor organic carbon, and high osmotic stress

in the soil or on the rock surfaces (Li et al., 2015; Jiang et al., 2019). These harsh living conditions in Taklamakan desert are a challenge for survival of microorganisms. However, a few reports, such as a finding (An et al., 2013) based on a metagenomic analysis of surface sand samples from Taklamakan desert indicated an unexpectedly large bacterial diversity residing in the harsh environment. To the best of our knowledge, up to the end of June 2020, a total of 19 novel species including one novel genus of actinobacteria have been reported from the Taklamakan desert. Our previous efforts to isolate endophytic actinobacteria from psammophytes in Taklamakan desert (Wang et al., 2020a) have successfully described a series of new species from genera, including *Prauserella*, *Nesterenkonia*, *Labedella*, and *Aeromicrobium* (Liu et al., 2015a,b; Li et al., 2019b,c). Although studies on the Chinese deserts are increasing in recent years, the exploration of the diversity of actinobacteria from the Taklamakan desert, to our knowledge, is still very limited. Furthermore, reports on the capability of actinobacteria to produce bioactive substances from Taklamakan desert are even rare. These facts demonstrate that the microbial ecology and their microbiota endowed with the potential to produce novel bioactive metabolites in Taklamakan desert need to be further studied.

In the present study, we continued an investigation on the biodiversity of cultivable actinobacteria sampled from eight arid soil samples along the Alar-Hotan desert highway in the Taklamakan desert and their antibacterial activity and capability to produce bioactive secondary metabolites were deeply explored. Meanwhile, a highlysensitive screening model, defined as double fluorescent protein reporter "pDualrep2" system, was implemented as a high-throughput screening model to distinguish the mechanism of action of bioactive metabolites secreted by actinobacterial strains. Finally, secondary metabolites of the *Saccharothrix* sp. 16Sb2-4 were examined in detail by analysis with comprehensive approaches, including hyphenated technique, MS/MS-based molecular networking analysis, databases identification, bioassay-guided separation, and NMR spectra analysis. Through this study, we wish to expand knowledge on the potential of actinobacteria residing in the Taklamakan desert, and attract more concerted efforts for discovery of new actinobacterial species and prominent antibiotic candidates from the harsh environment.

MATERIALS AND METHODS

Site Description and Sample Collection

A total of eight soil samples, coded as S1, S2, S3, S4, S5, S6, S7, and S8, were collected from various sites along the Alar-Hotan desert highway located in the Taklamakan desert, Xinjiang Uygur Autonomous Region, China in October 2016. The samples were collected at a depth of 10–15 cm from the surface. Sampling sites were at least 8 km away from each other as showed in **Figure 1**, and the sampling information

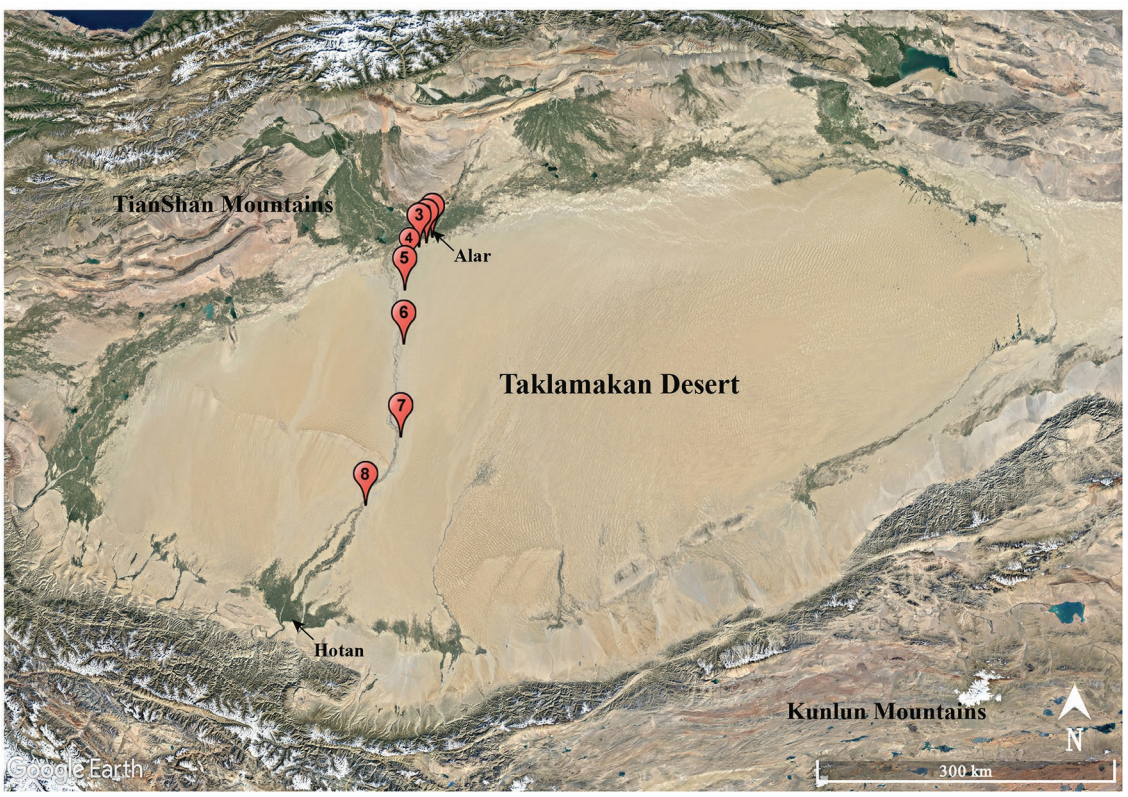

FIGURE 1 | Geographic distribution of the sampling sites (S1–S8) along the Alar-Hotan desert highway in the Taklamakan desert, Xinjiang Uygur Autonomous Region, China.

in detail is listed in **Supplementary Table S1**. All the samples were collected into 50 ml labeled sterile Falcon tubes and stored at 4°C before transporting to our laboratory for further processing.

Samples Processing and Isolation of Actinobacteria

Soil samples were first processed by air-dry at room temperature in the laminar flow hood for 8 h. Actinobacterial strains were isolated according to the standard serial dilution plating technique as described by Li et al. (2019a). Ten different isolation media supplemented with 1% (*v*/*v*) soil leaching liquor were prepared to isolate the actinobacterial strains (**Supplementary Table S2**). To inhibit the growth of Gram-negative bacteria and fungi, all media were supplemented with nalidixic acid, cycloheximide, and potassium dichromate to the final concentration of 20, 50, and 50 mg/l, respectively. The plates were incubated for 2–12 weeks at 30°C, and colonies that displayed differentiable morphologies were picked up from the original isolation plates and then sub-cultured on the Yeast-Malt Extract Agar (International Streptomyces Projects 2, ISP 2; Shirling and Gottlieb, 1966) plates to recover pure cultures with uniform colony morphology. The purified cultures were maintained on ISP 2 medium slants at 4°C and stored in 20% (*v*/*v*) glycerol suspensions at −80°C.

Molecular Identification and Phylogenetic Analysis

Genomic DNAs for the 16S ribosomal RNA (rRNA) gene sequence analysis were extracted as described by Li et al. (2007). The 16S rRNA gene was amplified by PCR with two universal primers 27F (5'-AGAGTTTGATCMTGGCTCAG-3') and 1492R (5'-GGTTACCTTGTTACGACTT-3'), according to the method described by Liu et al. (2014). The PCR products were purified and then sequenced by an ABI PRISMTM 3730XL DNA Analyzer (Thermo Fisher Scientific, United States). The affiliation of the strains at genus-level was validated using the EzBioCloud's Identify service (https://www.ezbiocloud.net/identify; Yoon et al., 2017) and the BLAST tool in GenBank NCBI database.[1] The corresponding sequences of closely related type species were retrieved from the GenBank database. Multiple alignments were made using the Clustal_X tool in MEGA version 7.0 (Kumar et al., 2016). Phylogenetic tree based on the neighbor-joining algorithm (Saitou and Nei, 1987) was constructed under the Kimura's two-parameter model (Kimura, 1980) with 1,000 bootstrap replicates. The 16S rRNA gene sequences obtained in this study were deposited in GenBank under the accession numbers: MT682401-MT682454, MT682461-MT682490, MT705160-MT705204, MH287062, MK787305, MH244160, and MK947033.

Antibacterial Assay

Based on the phenotypic and phylogenetic analyses, 146 strains were selected to examine their antibacterial potentials. Each strain was transferred to three 500 ml Erlenmeyer flasks containing 100 ml of ISP 2 medium and then cultivated for 4–10 days at 30°C with rotated shaking at 180 rpm. The 300 ml fermentation broth for each isolate was centrifuged at 4,500 rpm for 20 min to separate the mycelium portion. The supernatants of fermentation broth were extracted twice with ethyl acetate (1:1, *v*/*v*) to get the organic layer and water layer. The whole organic layer and 50 ml water layer were dried up by rotary evaporation and dissolved in 3 ml methanol, respectively. The mycelium portion was soaked in acetone overnight, and then the leach liquor was concentrated under vacuum, and finally dissolved in 3 ml 50% methanol-water. Consequently, three kinds of samples were obtained from each strain for antibacterial assay by the paper-disk diffusion method. The methanol sample (60 μl) was dripped on a 6 mm paper disk in diameter. Besides, 60 μl methanol was used as the negative control, and levofloxacin solution (10 μl, 0.1 mg/ml) was used as the positive control. After dried up in the biosafety hood, the paper disks were transferred to agar plates with indicator bacteria and were incubated at 37°C for 24 h. Finally, the antibacterial activity was evaluated by measuring the diameters of the inhibition zone with a vernier caliper. The indicator bacteria used in antimicrobial assay were six sets of "ESKAPE" pathogenic bacteria, including *Enterococcus faecalis* (ATCC 33186 and 310682), *Staphylococcus aureus* (ATCC 29213 and ATCC 33591), *Klebsiella pneumonia* (ATCC 10031 and ATCC 700603), *Acinetobacter baumannii* (2799 and ATCC 19606), *Pseudomonas aeruginosa* (ATCC 27853 and 2774), and *Escherichia coli* (ATCC 25922 and ATCC 35218). Each set consisted of two strains, the former was drug-sensitive strain and the latter was drug-resistant strain. Strain 310682 was a clinical isolate resistant to vancomycin; Strain 2774 was a clinical isolate resistant to aminoglycosides and carbapenems. Indicator bacteria were obtained from American Type Culture Collection (ATCC) or the clinic and deposited in the Institute of Medicinal Biotechnology, Chinese Academy of Medical Sciences & Peking Union Medical College.

Assay Based on Antibacterial Mechanism

A specific double fluorescent protein reporter system "pDualrep2" described previously was used to probe the mechanism action of compounds secreted by the antibacterial strains (Osterman et al., 2016). In brief, 100 μl ethyl acetate extract of each strain was dried up and then dissolved in 100 μl DMSO as the testing sample. About 2 μl of each sample solution was spotted on agar plates containing a lawn of the reporter strain *E. coli* JW5503. After overnight incubation at 37°C, the plate was scanned by ChemiDoc Imaging System (Bio-Rad Laboratories, United States) with two channels, "Cy3-blot" (553/574 nm, green pseudocolor) for red fluorescent protein (RFP) fluorescence, and "Cy5-blot" (588/633 nm, red pseudocolor) for Katushka2S fluorescence. Induction of expression of Katushka2S is triggered by translation inhibitors, while RFP is upregulated by DNA damage-induced SOS response. Levofloxacin (Lev, 50 μg/ml, 1 μl) and erythromycin (Ery, 5 mg/ml, 1 μl) were used as

[1]http://www.ncbi.nlm.nih.gov/

positive controls for inhibitors of DNA and protein biosynthesis, respectively.

Large-Scale Fermentation and Extracts Preparation of *Saccharothrix* sp. 16Sb2-4

Based on results from antibacterial activity assay and preliminary mechanism detection, strain *Saccharothrix* sp. 16Sb2-4 with striking antibacterial activity was selected for large-scale fermentation and further chemical analysis. The strain was seeded in a 500 ml Erlenmeyer flask containing 100 ml of ISP 2 broth at 28°C for 2 days on a rotary shaker at 180 rpm. Then, 100 ml of seed culture was transferred into a 5 L Erlenmeyer flask containing 1 L of ISP 2 broth and fermented on a rotary shaker at 180 rpm at 28°C for 6 days. A total of 15 L fermented broth was collected and then centrifuged at 4,000 rpm at 25°C for 20 min. The cell-free supernatant was extracted three times with an equal volume of ethyl acetate. The organic phase was separated by a separatory funnel and then evaporated *in vacuo* to afford semi-solid crude extract (0.9 g). The extracted residue was suspended in methanol for next ultra-performance liquid chromatography (UPLC)-quadrupole time-of-flight (QToF)-MS/MS analysis and further chemical purification. Concomitantly, 1 L sterilized ISP 2 broth without addition of actinobacterial cells was extracted with ethyl acetate and evaporated to dryness parallelly, used as a medium control in metabolomic profiling of strain 16Sb2-4.

UPLC-QToF-MS/MS Analysis

About 1 mg crude extract of strain 16Sb2-4 was dissolved in 1 ml methanol, and then was analyzed by UPLC coupled with QToF tandem mass spectrometry system (ACQUITY UPLC/Xevo G2-XS QTOF, Waters, United States) equipped with an electrospray ionization source (ESI). The sample (2 μl) was separated on the Waters ACQUITY UPLC BEH C18 column (2.1 × 100 mm, 1.7 μm) equipped with a Waters ACQUITY UPLC PDA detector at a flow rate of 0.3 ml/min. The column was eluted with a gradient mobile phase of acetonitrile-water containing 0.1% formic acid solution: 10% acetonitrile for 2 min, 10–90% acetonitrile for following 28 min, and finally, 90% acetonitrile for 3 min. The UV absorbance of the eluate was monitored by PDA detector from 190 to 400 nm. MS spectra were acquired by data-independent acquisition mode (MS^E) for UNIFI analysis (Waters, United States) and data-dependent acquisition (DDA) for Global Natural Products Social Molecular Networking (GNPS) analysis, respectively. MS^E was carried out by operating the instrument at positive ion mode, applying the MS and MS/MS functions with 6 V low energy and 20–45 V high energy collision to collect the mass to charge ratio (*m/z*) from 100 to 2,500 Da. DDA was performed in positive ion mode, and the full MS survey scan was performed for 0.05 s time in the range of 100–2,500 Da, while MS/MS scanned over a mass range of 50–2,500 Da by the same scan time. The five most intense ions were further scanned for MS/MS fragmentation spectra. Data were collected and analyzed using the MassLynx V4.1 software (Waters, United States).

Molecular Networking Analysis and Dereplication

The raw data obtained from DDA acquisition were used to create a molecular network. The DDA data were converted to the 32-bit mzML format using the MSConvert software (Chambers et al., 2012), and then uploaded on the GNPS web-platform (http://gnps.ucsd.edu; Wang et al., 2016a). The MS/MS molecular network was constructed using the "Classic" online workflow (METABOLOMICS-SNETS-V2) at GNPS. The precursor ion mass tolerance and MS/MS fragment ion tolerance were all set to 0.02 Da. A network was then created where edges were filtered to have a cosine score above 0.6 and more than three matched peaks. Further, edges between two nodes were kept in the network if and only if each of the nodes appeared in each other's respective top 10 most similar nodes. The spectra in the network were then searched against GNPS spectral libraries to annotate and identify metabolites through the database search of MS/MS spectra. The library spectra were filtered in the same manner as the input data. The molecular network was visualized using Cytoscape software v3.8.0 (Shannon et al., 2003). To improve the dereplication, a manual annotation was conducted in UNIFI informatics platform (Waters, United States) by searching the microbial natural products database, The Natural Products Atlas (www.npatlas.org; Van Santen et al., 2019) based on the predicted accurate mass value. Sample of the medium control was analyzed in the same procedure as above.

Isolation and Identification of Bioactive Metabolites Produced by *Saccharothrix* sp. 16Sb2-4

To trace the bioactive metabolites produced by *Saccharothrix* sp. 16Sb2-4, bioassay-guided fractionation was performed with the methicillin-resistant *S. aureus* (MRSA) ATCC 33591 as the indicator bacterium. The crude extract dissolved in methanol was subjected to Sephadex LH-20 column chromatography with elution of methanol to obtain different fractions. Each fraction was screening for antibacterial activity against the indicator bacterium. The bioactive fractions were merged and further subjected to flash chromatography (Biotage, United States) using a reversed-phase C18 column with a gradient elution of 20, 40, 60, 70, and 80% (*v/v*) MeOH/H_2O mixtures to yield 10 subfractions (subfrs. 1–10). Each subfraction was assayed by anti-MRSA activity, and the bioactive subfractions (subfrs. 5–8) were analyzed by UPLC-MS/MS to seek compounds of interest. According to the UPLC-MS/MS results, the bioactive subfractions with targeted compounds were combined and further purified by semi-preparative high-performance liquid chromatography (HPLC, Agilent 1200, Agilent Technologies Inc., United States) equipped with an Agilent ZORBAX SB-C18 column (9.4 × 250 mm, 5 μm). Subfrs. 5–6 were combined and purified by HPLC (solvent, 50% MeOH in H_2O; flow rate, 2.0 ml/min; detection, UV 254 nm) to yield compounds **8** (7.8 mg, t_R = 43 min) and **9** (3.1 mg, t_R = 47 min). Subfrs. 7–8 were merged and purified by HPLC (solvent, 58% MeOH in H_2O; flow rate, 2.0 ml/

min; detection, UV 254 nm) to afford compounds **10** (4.6 mg, t_R = 41 min) and **11** (5.3 mg, t_R = 43 min).

The structures of four metabolites were determined by the analysis of HR-ESI-MS, ^{1}H and ^{13}C NMR data. The HR-ESI-MS data were recorded on a Xevo G2-XS QTof mass spectrometer (Waters, United States). The ^{1}H and ^{13}C NMR spectral data were recorded on the Brucker Avance III 600 (600 MHz) spectrometer (Bruker, Germany). The purified compounds were dissolved in chloroform-*d*/methanol-d_4, and the residual solvent signals were used for referencing spectra in ^{1}H and ^{13}C dimensions (Gottlieb et al., 1997).

RESULTS

Biodiversity of Cultivable Actinobacteria Derived From Soil Samples of Taklamakan Desert

A total of 860 strains were isolated from the eight soil samples collected in the Taklamakan desert. The phylogeny of the strains was evaluated based on the comparative analysis of their partial 16S rRNA gene sequences (approximately 800 bp) in EzBioCloud database. The results showed 590 out of 860 isolates were confirmed as actinobacterial strains and assigned to 55 genera in 27 families of 12 orders (**Supplementary Table S3**), which was further supported by analysis of their 16S rRNA gene sequence-based dendrogram (**Figure 2**). Analyzing the relative abundance at the order level, nearly half of the 590 actinobacterial strains were affiliated to *Micrococcales* (49.2%, 290 strains), followed by *Streptomycetales* (26.7%, 157 strains), and *Propionibacteriales* (6.9%, 41 strains). The others belonged to order *Streptosporangiales* (29 strains), *Micromonosporales* (23 strains), *Kineosporiales* (16 strains), *Geodermatophilales* (14 strains), *Pseudonocardiales* (9 strains), *Mycobacteriales* (6 strains), *Jiangellales* (2 strains), *Solirubrobacterales* (2 strains), and *Nakamurellales* (1 strain). At the genus level, the predominant genus was *Streptomyces* (26.7%, 157 strains), and among the rest 433 non-*Streptomyces* strains, the dominant genus was *Microbacterium* (16.1%, 95 strains), followed by *Aeromicrobium* (6.4%, 38 strains), *Kocuria* (4.9%, 29 strains), *Nocardiopsis* (4.4%, 26 strains), and *Brachybacterium* (4.4%, 26 strains).

The genera distribution of 590 actinobacterial strains in eight samples and 10 media are displayed in **Figure 3**. Sample 4 gave the highest diversity (21 genera), followed by sample 5 (19 genera), sample 3 (18 genera), samples 2 and 8 (17 genera), samples 1 and 6 (14 genera), and sample 7 (11 genera). The isolation media played a major influence on the diversity of isolates recovered. The CMKA medium (Lai et al., 2014; M5) was the most effective in terms of the number and diversity of isolates obtained (100 strains distributed in 25 genera); three different isolation media, including modified Gauze's NO. 1 synthetic medium (M1), ISP 2 (M2), and R2A (M3) media also resulted in relatively efficient isolations, and 24 genera were retrieved by each of media above; meanwhile, 18, 15, 15, and 11 genera were obtained from Raffinose-Histidine medium (M6), Proline medium (M8), Casein-Glucose medium (M9), and Modified Cellulose-Casein medium (M4), respectively. Trehalose-Proline medium (M7) yielded the lowest diversity with only eight strains distributed in two genera (*Streptomyces* and *Saccharopolyspora*). The high-salt medium (M10) was used to isolate halophilic or halotolerant strains in desert samples, and 10 strains belonged to five genera (*Brachybacterium*, *Nocardiopsis*, *Streptomyces*, *Microbacterium*, and *Zhihengliuella*) were isolated from this medium. Among the 55 genera of actinobacteria, *Streptomyces* spp. seemed to be the most abundant since they could be recovered in all of the isolated media from all of the samples.

Novelty of Cultivable Actinobacteria

Based on comparative results with EzBiocloud database, 36 strains exhibited less than 98.65% similarities (the threshold for differentiating two species Kim et al., 2014) in 16S rRNA gene sequences with validly described species (**Supplementary Table S4**), indicating that these isolates could be regarded as primary candidates for novel taxon. These 36 putative novel isolates were preliminarily affiliated into 12 families, including *Microbacteriaceae* (10 strains), *Dermabacteraceae* (5 strains), *Promicromonosporaceae* (3 strains), *Cellulomonadaceae* (3 strains), *Nocardioidaceae* (3 strains), *Nocardiopsaceae* (3 strains), *Streptomycetaceae* (3 strains), *Kineosporiaceae* (2 strains), *Bogoriellaceae* (1 strain), *Geodermatophilaceae* (1 strain), *Nakamurellaceae* (1 strain), and *Patulibacteraceae* (1 strain). Notably, 10 putative novel isolates showed close relationships with members of family *Microbacteriaceae*. Pairwise comparison of 16S rRNA gene sequences from the 10 isolates showed they shared the highest sequence identities of 97.29–98.44% to the closest recognized species of family *Microbacteriaceae*. Further phylogenetic analysis of the 10 *Microbacteriaceae*-like isolates based on the neighbor-joining tree is shown in **Supplementary Figure S1**. Phylogenetic analysis indicated that these isolates were diversely distributed within the family *Microbacteriaceae* and formed distinct clusters within the neighbor-joining tree. Isolate 15S1-1, sharing the highest 16S rRNA gene similarity of 97.95% to the type strain of *Agromyces arachidis*, formed a distinct branch within the lineage of the genus *Agromyces*, suggesting that isolate 15S1-1 might represent a novel species of the genus *Agromyces*. Isolates 20Sb5-7 and 16Sc5-2 formed a statistically well supported cluster with one another and fell into a coherent subclade with *Microbacterium wangchenii* dk512^T within the *Microbacterium* group. The 16S rRNA gene sequences of 20Sb5-7 and 16Sc5-2, respectively showed 98.16 and 98.44% identities to the nearest neighbor *M. wangchenii* dk512^T, indicating that the two isolates might be identified as new species of the genus *Microbacterium*. Four isolates, 21Sb5-5, 21Sc5-12, 21Sb2-13, and 15S6-12, showing the highest similarity values of 97.76–98.15% to *Salinibacterium hongtaonis* 194^T, gathered in one monophyletic cluster that was independent from other subclusters corresponding to the established genera of the family *Microbacteriaceae*, indicating that they might represent novel species of a new genus. Similarly, strains 20Sb3-5 and 16Sc1-5 formed a distinct monophyletic clade within the family *Microbacteriaceae* and they showed the highest 16S rRNA gene

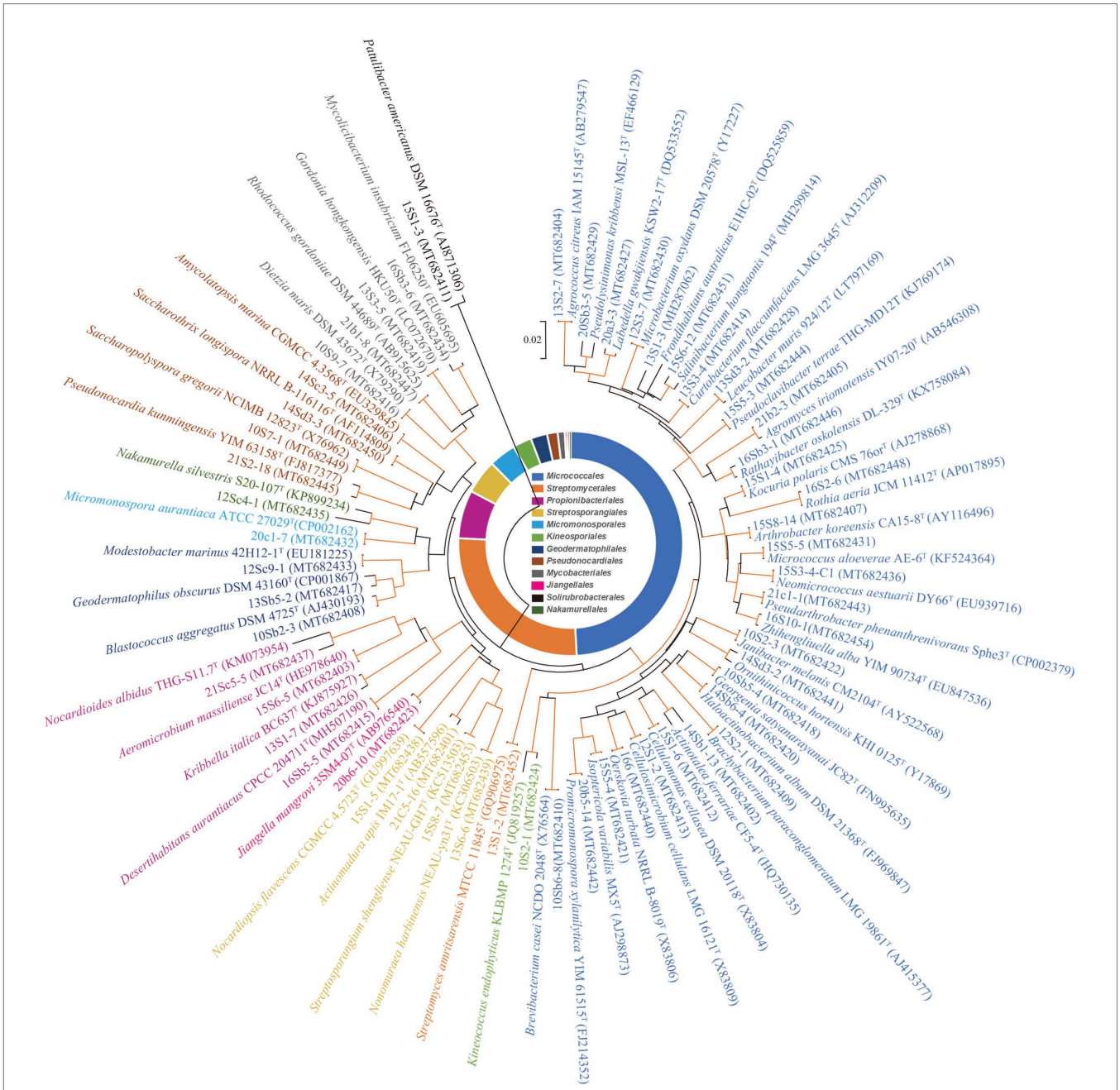

FIGURE 2 | Phylogenetic tree based on 16S ribosomal RNA (rRNA) genes using neighbor-joining method with 1,000 bootstrap replications for 55 representative actinobacterial strains and their closely related type strains. Red lines indicate bootstrap support values >70% for the branch. Strains in the same color belong to the same order. Bar, 2 nt substitutions per 100 nt.

similarities, 98.13 and 98.16%, to the closest type strain of *Pseudolysinimonas kribbensis*, suggesting that isolates 20Sb3-5 and 16Sc1-5 might belong to a new genus. Above nine putative novel species will be further characterized by the polyphasic approach to determine their taxonomic positions. In addition, strain 13S1-3 has been characterized as a novel species of a new genus in the family *Microbacteriacea* by our polyphasic taxonomic analyses with the proposed name "*Planctomonas deserti*" (Liu et al., 2019a). Besides the 10 isolates in family *Microbacteriaceae*, three isolates were characterized as type species of new taxa based on our previous study of polyphasic taxonomy. Strain 12Sc4-1 has been characterized as a new species of the genus *Nakamurella* with the proposed name *Nakamurella deserti* (Liu et al., 2019b); strain 21Sc5-5 has been characterized as a new species of the genus *Nocardioides* with the proposed name *Nocardioides vastitatis* (Liu et al., 2020a);

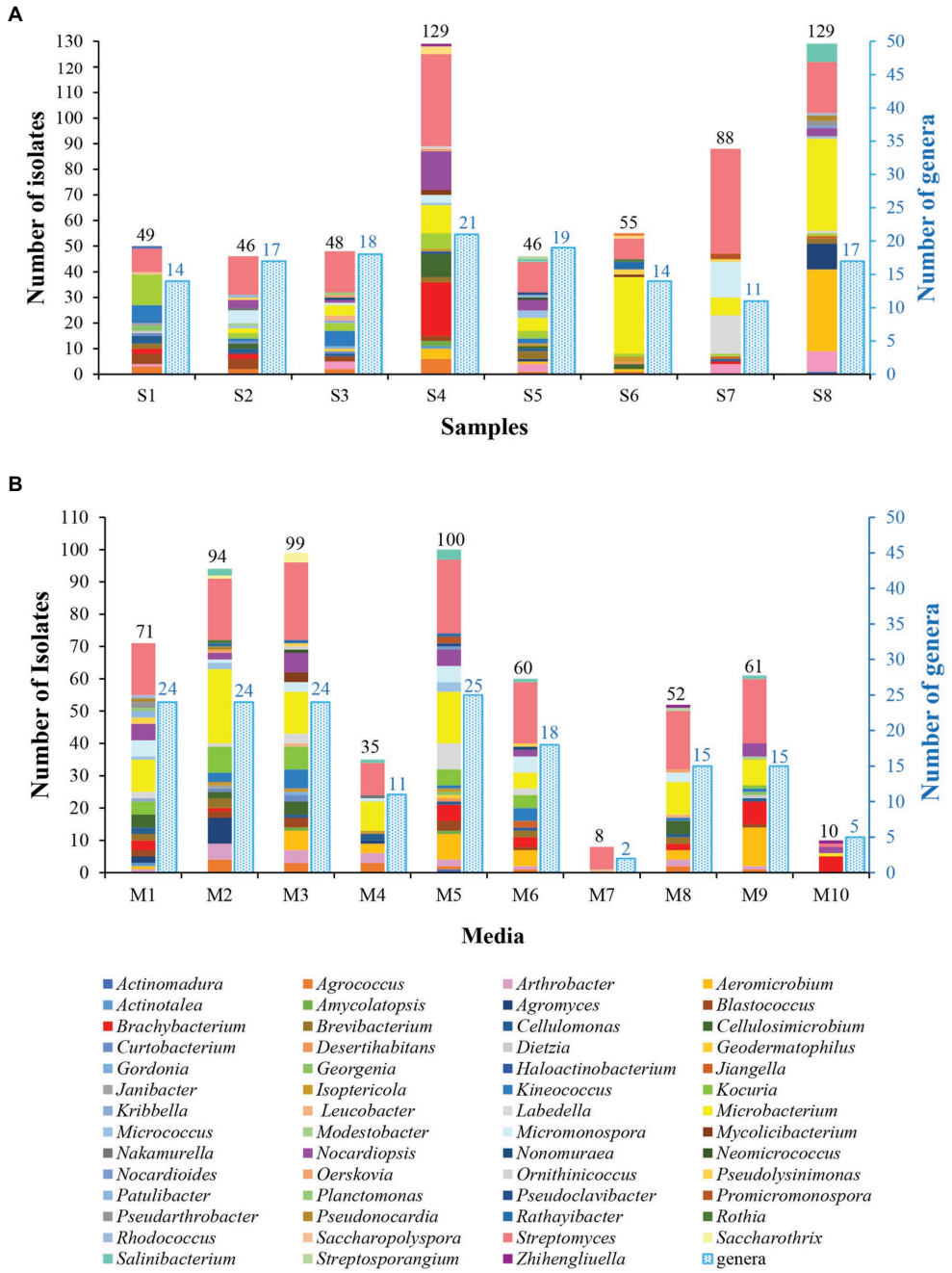

FIGURE 3 | Diversity of cultivable actinobacteria isolated from soil samples collected in Taklamakan desert. **(A)** Actinobacterial isolates recovered from different sampling sites. **(B)** Actinobacterial isolates recovered from the different culture media.

and strain 16Sb5-5 has been characterized as a new species of the genus *Desertihabitans* with the proposed name *Desertihabitans brevis* (Liu et al., 2020b). Notably, although the similarity of 16S rRNA gene sequence between 16Sb5-5 and its closest neighbor *Desertihabitans aurantiacus* CPCC 204711^{T} was as high as 99.6%, the average nucleotide identity (ANI) and *in silico* DNA-DNA hybridization (DDH) values were all less than the widely accepted thresholds to distinguish two species [95% for ANI (Richter and Rossello-Mora, 2009) and 70% for DDH (Chun et al., 2018)]. Therefore, strain 16Sb5-5^{T} has been proved as a novel species of the genus *Desertihabitans* (May and Grabowicz, 2018). Phylogenetic analysis of the other 24 potential novel strains based on the neighbor-joining trees constructed with 16S rRNA gene sequences are shown in **Supplementary Figures S2A–J**. The presence of these rare actinobacteria emphasizes the unique microbial diversity

characteristics of the Taklamakan desert and supports the idea of extreme ecological environments being an important resource for novel species and chemical entities.

Antibacterial Activity

Based on results of phylogenetic and morphological analyses, 146 actinobacterial isolates affiliated to 55 different genera were selected as representatives to evaluate the antimicrobial potential against a panel of "ESKAPE" bacteria. Among the 146 tested isolates, 61 strains (41.8%) exhibited antagonistic activity against at least one of the tested pathogens (**Supplementary Table S5**). The 61 antibacterial strains were affiliated to 19 genera, including *Streptomyces* (37 strains), *Nocardiopsis* (3 strains), *Micromonospora* (3 strains), *Cellulosimicrobium* (2 strains), *Microbacterium* (2 strains), *Saccharothrix* (2 strains), *Actinomadura* (1 strain), *Aeromicrobium* (1 strain), *Blastococcus* (1 strain), *Cellulomonas* (1 strain), *Planctomonas* (1 strain), *Janibacter* (1 strain), *Kineococcus* (1 strain), *Kocuria* (1 strain), *Leucobacter* (1 strain), *Pseudolysinimonas* (1 strain), *Desertihabitans* (1 strain), and *Pseudonocardia* (1 strain). The antimicrobial profile of the actinobacteria against different pathogenic bacteria was shown in **Figure 4**. Out of the 61 antimicrobial isolates, 25 isolates exhibited antagonistic activity against both Gram-negative and Gram-positive bacteria; 29 isolates exhibited antibacterial activity against only Gram-positive bacteria; and seven isolates against only Gram-negative bacteria. Regarding the drug-sensitive pathogens tested, inhibitory zones were observed most frequently against the Gram-positive bacteria such as *S. aureus* (50 isolates) and *E. faecalis* (30 isolates), followed by Gram-negative bacteria, such as *K. pneumonia* (23 isolates), *A. baumannii* (17 isolates), *E. coli* (15 isolates), and *P. aeruginosa* (9 isolates). Concerning the drug-resistant pathogens tested, activity against Gram-positive bacteria remained the most frequent where 44 of the 146 tested strains presented inhibitory zones against MRSA and 30 strains against vancomycin-resistant *E. faecalis* (VRE). The activity against the Gram-negative bacterium *P. aeruginosa* was still the least frequent (five isolates), and 16, 15, and 14 isolates were active against *E. coli*, *A. baumannii*, and *K. pneumonia*, respectively. This phenomenon could be attributed to the sophisticated outer membrane and multiple efflux pumps possessed by Gram-negative bacteria, which served as a robust permeability barrier for preventing many antibiotics from reaching their intracellular targets (Miller, 2016; May and Grabowicz, 2018). Five isolates, including *Nocardiopsis* sp. 14Sc5-11, *Saccharothrix* sp. 16Sb2-4, *Microbacterium* sp. 14Sc5-17, and *Streptomyces* sp. 14Sb4-3 and 13S9-1, appeared to have a broad spectrum of antimicrobial activity against at least 11 test strains. Among them, *Saccharothrix* sp. 16Sb2-4 showed the highest inhibitory activities against VRE and methicillin-sensitive *S. aureus* (MSSA) with inhibition zones 24 and 23 mm in diameter, respectively. Notably, in some cases, only one type of extract demonstrated activity against one or some indicator pathogens, for example, antibacterial activity was observed only from ethyl acetate extracts of cultural broth of *Streptomyces* sp. 15S4-1, 10Sb5-5, and 10S9-4. On the contrary, only mycelia extracts of *Nocardiopsis* sp. 12Sb1-6, *Micromonospora* sp. 12Sd5-1, and *Streptomyces* sp. 12S1-1 showed antibacterial activities against *P. aeruginosa*.

Antibacterial Mechanism Assay

Sixty-one desert-derived actinobacterial strains are potential candidates to produce antibiotics with different mechanisms of action. To distinguish strains with different antibacterial mechanisms, ethyl acetate extracts from culture broth of 61 bioactive strains were screened by the double fluorescent protein reporter "pDualrep2" system, which is a highlysensitive screening model for probe of compounds that inhibit protein translation or DNA biosynthesis (Osterman et al., 2016). The screening

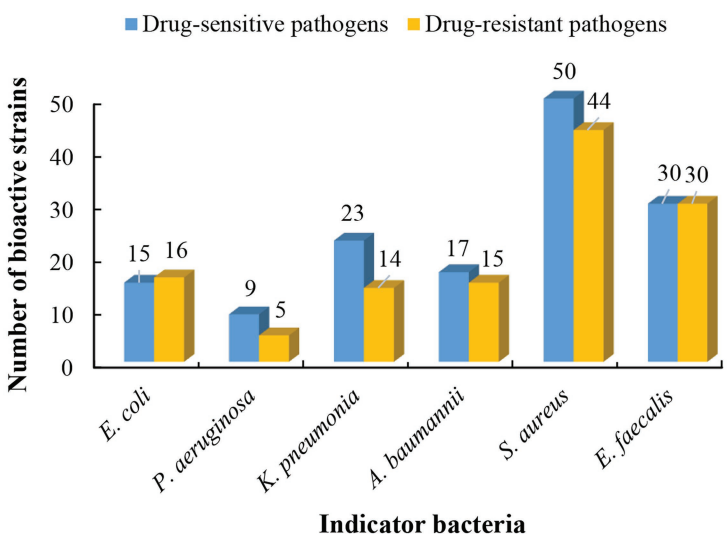

FIGURE 4 | The antibacterial profile of the desert-derived actinobacteria against "ESKAPE" pathogens.

results are shown in **Figure 5A**. Four strains, including two *Streptomyces* sp. (13S2-11 and 21Sa10-2) and two *Saccharothrix* sp. (14Sd3-3 and 16Sb2-4) could induce expression of far-RFP reporter Katushka2S, acting as typical inhibitors of protein translation as the erythromycin did. Meanwhile, three *Streptomyces* strains (14Sb4-3, 10Sb5-5, and 20S9-6) could induce expression of RFP reporter, triggering DNA damage-induced SOS response as the levofloxacin did.

Metabolites Identification of *Saccharothrix* sp. 16Sb2-4 Using MS/MS-Based Molecular Networking

In order to highlight antimicrobial potential of the desert-derived isolates, analysis of the metabolites should perform with a potent antimicrobial metabolite-producing isolate. Strain 16Sb2-4 in genus *Saccharothrix* showed a promising inhibitory activity against both Gram-positive and Gram-negative "ESKAPE" pathogens, especially multi-drug resistant (MDR) bacteria, such as *P. aeruginosa* (16.8 mm), *A. baumannii* (13 mm), and *K. pneumoniae* (10.7 mm), MRSA (22.8 mm), and VRE (24.2 mm). Meanwhile, the strain exhibited activity to block translation machinery in the pDualrep2 system. Blast analysis based on the 16S rRNA gene sequence showed strain 16Sb2-4 shared the highest nucleotide sequence similarity (99.7%) with *Saccharothrix xinjiangensis* NBRC 101911^T, a strain that was previously isolated from Tianchi Lake, Xinjiang Uygur Autonomous Region, China (Hu et al., 2004). Strain of *S. xinjiangensis* has ever been reported to produce a range of bioactive compounds, such as the tianchimycins A and B (Wang et al., 2013), cyanogriside I and J, caerulomycin A and F (Lahoum et al., 2019), and caerulomycin M and saccharopyrone (Babadi et al., 2020). Taking these facts into consideration, strain 16Sb2-4 was prioritized to conduct a chemical analysis to gain deeper insights into its bioactive metabolites.

Ultra-performance liquid chromatography coupled with QToF-HR-MS can offer a high degree of mass resolution, sensitivity, and accuracy for identification of chemical components, especially for trace level ingredients in complex natural product extracts (Kaufmann, 2014; Deng et al., 2016). Therefore, an UPLC-QToF-MS/MS based untargeted metabolite profiling was carried out for a comprehensive understanding of chemical diversity in the cultural broth of strain 16Sb2-4. GNPS platform was employed to detect the MS/MS structural relatedness among molecules in an automated manner; then the software generated a molecular network wherein molecules with related scaffolds clustered together (Wang et al., 2016a). A MN-based network representing the ions detected in the crude extract of *Saccharothrix* sp. 16Sb2–4 was constructed, revealing 981 nodes representing unique spectra in total, of which 600 nodes were clustered in 80 spectral families conformed with at least 2 nodes (**Supplementary Figure S3**). Not all the network nodes correspond to a single molecule since some nodes represent adducts.

Global Natural Products Social Molecular Networking dereplication based on matching with its MS/MS spectral database allowed annotation of two families of potent bioactive compounds (Family A and B, **Figure 6**). Family A was identified as known lipopeptides, including surfactin C (**1**), surfactin C14 (**2**), and [val7]-surfactin C15 (**3**); Family B was annotated as cyclic depsipeptides including xenotetrapeptide (**4**) and YM-47142 (**5**). Detailed information for these annotated peak ions to known metabolites is displayed in **Supplementary Table S6**. The surfactins are cyclic lipopeptides produced by multiple genera of bacteria, such as *Bacillus*,

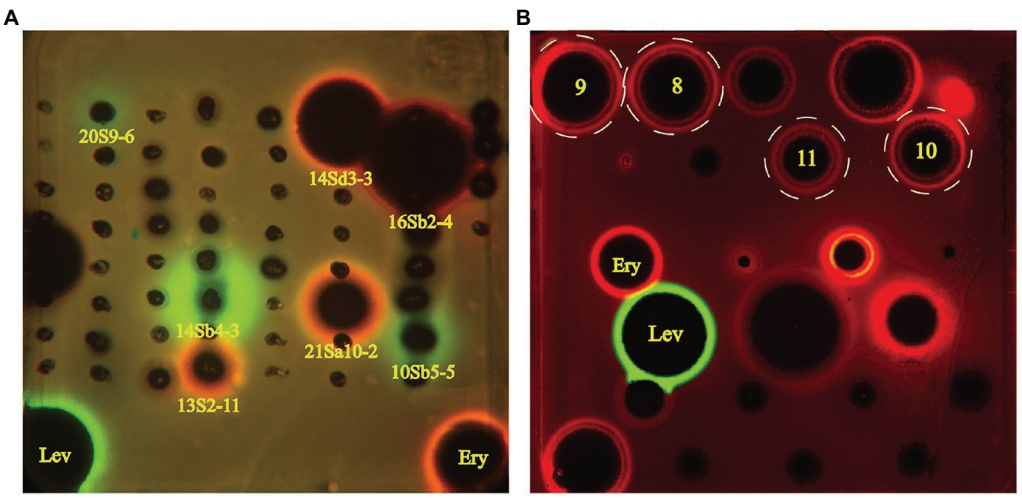

FIGURE 5 | Induction of two-color dual reporters in pDualrep2 system by inhibitors of the ribosome progression or inhibitors of DNA replication, respectively. Spots of erythromycin (Ery), levofloxacin (Lev), and tested samples were placed on the surface of an agar plate containing *Escherichia coli ΔtolC* cells transformed with the pDualrep2 reporter plasmid. Shown is the fluorescence of the lawn of *E. coli* cells scanned at 553/574 nm (green pseudocolor) for red fluorescent protein (RFP) fluorescence and 588/633 nm (red pseudocolor) for Katushka2S fluorescence. Induction of expression of Katushka2S is triggered by translation inhibitors, while RFP is upregulated by induction of DNA damage SOS response. **(A)** Screening results of crude extracts of 61 strains; **(B)** Evaluation of compounds **8–11** (indicated in white dotted circles) isolated from *Saccharothrix* strain 16Sb2-4.

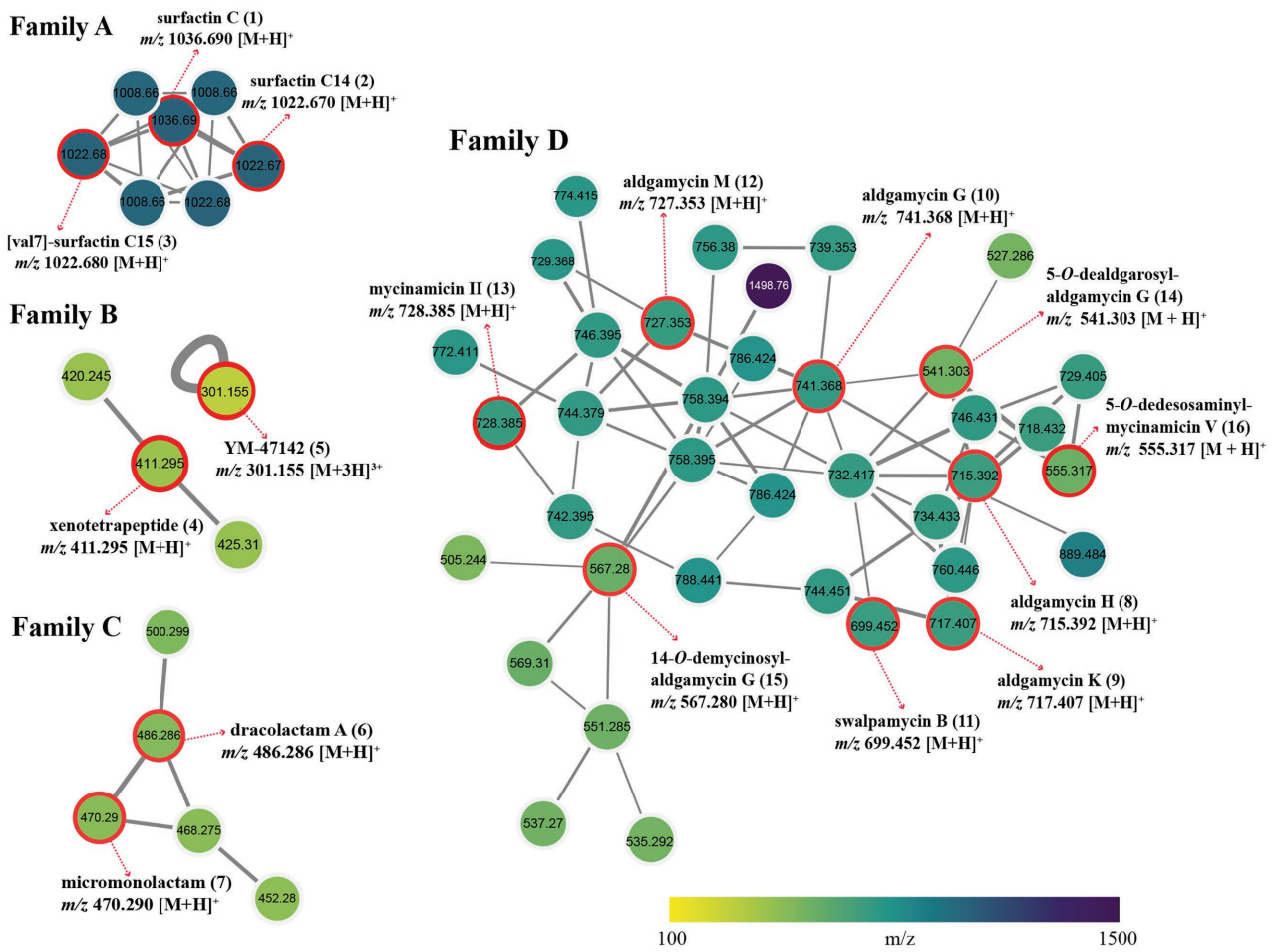

FIGURE 6 | Four identified metabolite families in molecular network of strain *Saccharothrix* sp. 16Sb2-4. Each node represents *m/z* value of the parent ion and the edge thickness signifies cosine score similarity. Family A, surfactin lipopeptides; Family B, cyclic depsipeptides; Family C, polyene macrolactams; and Family D, 16-membered macrolides.

Streptomyces, *Micromonospora*, and *Pseudomonas*. This chemical class is not only regarded as a powerful lipopeptide biosurfactant, but also acts as effective antibiotic agents due to the ability to penetrate cell membranes of Gram-positive and Gram-negative bacteria, as well as fungi (Seydlová and Svobodová, 2008; Meena and Kanwar, 2015). The cyclic depsipeptide YM-47142 was isolated from the fermented broth of a *Flexibacter* bacterium as a potential inhibitor of human leucocyte elastase (HLE) enzyme, which involved in the pathogenesis of a variety of inflammatory diseases, such as emphysema, acute respiratory distress syndrome, and rheumatoid arthritis (Orita et al., 1995). Xenotetrapeptide was a NRPS-derived cyclic tetrapeptide produced by *Xenorhabdus nematophila*, but its activities have not yet to be characterized (Kegler et al., 2014). In addition, some synthetic contaminants such as phthalates (dibutyl phthalate and dioctyl phthalate) commonly occur from plasticware used in experiments were also detected; some dubious compounds readily formed from medium components, such as dipeptides (Ile-Tyr and Tyr-Pro), diketopiperazines [cyclo (Phe-Pro), cyclo (Val-Phe), cyclo (Leu-Phe), and cyclo (Leu-Pro)], and fatty acids (Conjugated linoleic acid and 9-Octadecenamide) were also found in metabolomic profiling of media controls (**Supplementary Figure S3**). These non-metabolites were easy to be precluded through GNPS dereplication.

Many nodes in crude extract of *Saccharothrix* sp. 16Sb2-4 did not match with the large datasets of the GNPS repository, indicating the putative presence of new metabolites or the absence of similar compounds from the GNPS repository. Therefore, an additional manual dereplication was conducted in UNIFI informatics platform by search of the spectral data against the bacterial and fungal natural products database, the Natural Products Atlas (www.npatlas.org; Van Santen et al., 2019). The annotation of these compounds was supported by comparison of the precursor ion *m/z* values, fragmentation pattern, and UV spectra with reference data. The manual dereplication allowed annotation of another two families of compounds presented in the molecular network (Family C and D, **Figure 6**). The Family C subnetwork containing five

spectral nodes was identified as the cluster of macrolactam compounds. Two known 22-membered polyene macrolactams, dracolactam A (**6**) and its biosynthetic precursor micromonolactam (**7**), were annotated in the extract of the strain. Meanwhile, another three structurally related nodes [*m/z* 452.280, 468.275, and 500.299 $(M+H)^+$] identified as derivatives of dracolactam can be found in this molecular cluster. Although no bioactivities were reported for dracolactam (Hoshino et al., 2017) and micromonolactam (Skellam et al., 2013), in the previous studies, it is worthy to concern this class of derivatives due to some polyene macrolactams were reported to display antibacterial, antiprotozoal, or cytotoxic activities (Skellam et al., 2013; Hoshino et al., 2017; Lim et al., 2018). The Family D subnetwork containing 38 spectral nodes with a strong spectral similarity score (cosine score > 0.6) was annotated as the cluster of the 16-membered macrolides. Nine compounds belonging to the 16-membered macrolide family were tentatively identified, *viz*. aldgamycin H (**8**), aldgamycin K (**9**), aldgamycin G (**10**), swalpamycin B (**11**), aldgamycin M (**12**), mycinamicin II (**13**), as well as three deglycosylated derivatives, 5-*O*-dealdgarosyl-aldgamycin G (**14**), 14-*O*-demycinosyl-aldgamycin G (**15**), and 5-*O*-dedesosaminyl-mycinamicin V (**16**). Annotation of these diagnostic 16-membered macrolide antibiotics is of significance, as this class of antibiotics is well-known inhibitor of bacterial protein synthesis, and characterized as among the safest antibacterial reagents in wide clinical use. Many macrolides have successfully been used to treat infections caused by Gram-positive organisms, certain Gram-negative and anaerobic bacteria (Elshahawi et al., 2015; Tang et al., 2016; Arsic et al., 2018; Karpinski, 2019). This finding further emphasized to continue our effort on targeted isolation, identification and activity evaluation of these putative 16-membered macrolides.

Bioactive Macrolides Produced by *Saccharothrix* sp. 16Sb2-4

The crude extract from large-scale fermentation of strain 16Sb2-4 was successively fractionated by Sephadex LH-20 column chromatography, reversed-phase C18 column chromatography, and semi-preparative HPLC. Bioassay against MRSA coupling with UPLC-MS/MS analysis was used to monitor the presences of bioactive 16-membered macrolide antibiotics. Four targeted compounds (**8–11**) were obtained and their structures were determined using HR-ESI-MS, NMR (**Supplementary Figures S4–S11**; **Supplementary Table S7**) as well as comparison with spectral data from the literatures. As suggested by molecular networking analysis, the four compounds were indeed afore-mentioned 16-membered macrolides, *viz*. aldgamycin H (**8**; Zitouni et al., 2007), aldgamycin K (**9**; Wang et al., 2016b), aldgamycin G (**10**; Mizobuchi et al., 1986; Zitouni et al., 2007), and swalpamycin B (**11**; Zitouni et al., 2007; Wang et al., 2013), as shown their structures in **Figure 7**. The antibacterial mechanism of compounds **8–11** was evaluated by the pDualrep2 system. As shown in **Figure 5B**, compounds **8–11** could induce Katushka2S expression, exerting their antibacterial effects by inhibiting protein synthesis. This finding was corresponding to the

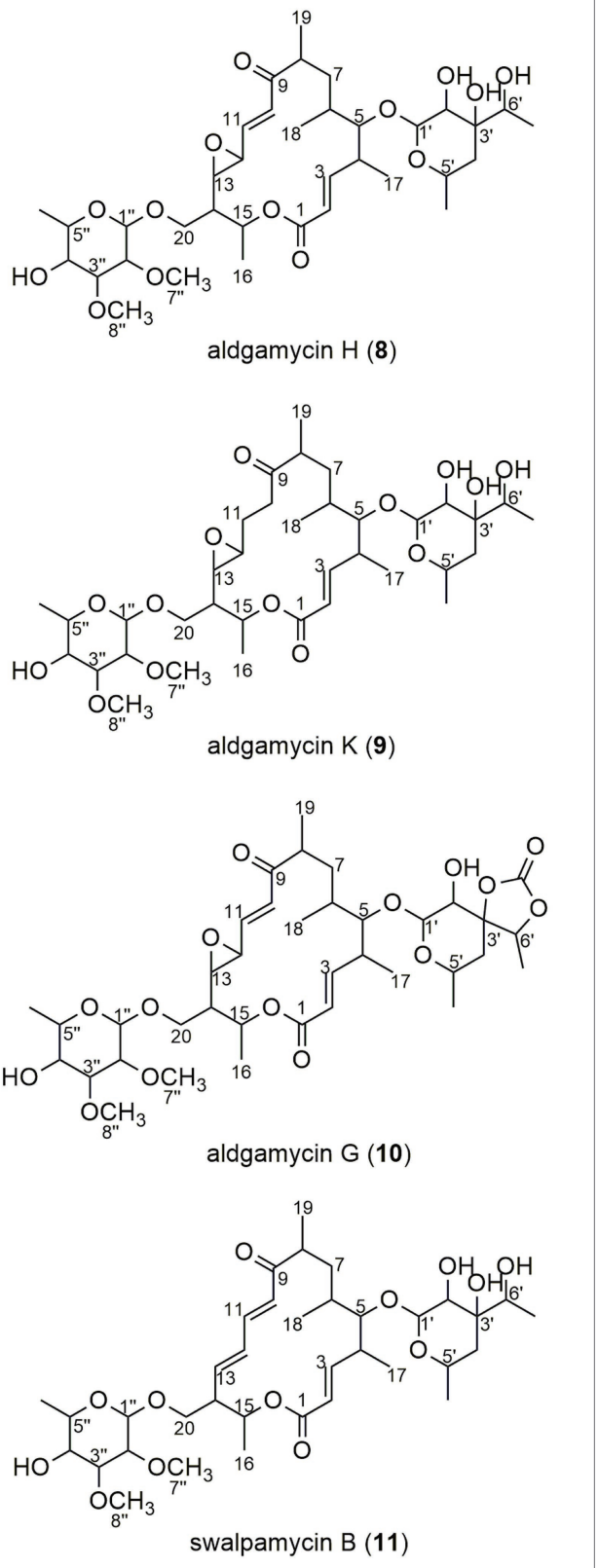

FIGURE 7 | Chemical structures of compounds **8–11** isolated from cultural broth of *Saccharothrix* sp. 16Sb2-4.

preliminary screening result of the crude extract of strain 16Sb2-4 (**Figure 5A**). Given the fact that compounds **8–11** were main bioactive metabolites isolated under guidance of anti-MRSA activities, the activity against Gram-positive bacteria in the cultural broth of strain 16Sb2-4 can be explained mostly by the accumulation of these macrolide antibiotics. In addition, some additional nodes that were structurally related identified aldgamycins in the molecular network but could not be assigned to any of the previously reported compounds, suggesting the potential of strain 16Sb2-4 for producing novel bioactive metabolites. Further purification and structural elucidation of these new putative compounds are still ongoing.

DISCUSSION

Deserts are thought to possess relatively harsh environments that are still poorly explored and waiting for more scientific interventions to search for pharmaceutical microorganisms. Many previous studies have suggested *Actinobacteria* are the major taxa in the phylum-level composition of bacteria in many arid desert soil (Mohammadipanah and Wink, 2015), as exemplified by the Atacama Desert (Crits-Christoph et al., 2013), where *Actinobacteria* were the most dominant phylum (72–88%). Analysis of bacterial diversity of sandy arid soil in southeast Morocco revealed that *Actinobacteria* were the most frequent groups (57%; Gommeaux et al., 2010). The bacterial communities in Namib Desert soils were dominated by the phylum *Actinobacteria* (49%; Makhalanyane et al., 2013). In some arid areas, *Actinobacteria* are among the three most abundant phyla (usually along with the *Firmicutes* and *Proteobacteria*), such as the desert soil of Aridic Calcisols in Kazakhstan (Lynch et al., 2014), a shrub root zone of desert (Steven et al., 2012), and a high elevation desert (Lynch et al., 2014). This is unsurprising, since actinobacteria were proved to possess unique capacity for sporulation, wide metabolic and degradative capacity, competitive advantages *via* secondary metabolite synthesis, and multiple UV repair mechanisms. (McCarthy and Williams, 1992; Chater and Chandra, 2006; Gao and Garcia-Pichel, 2011; Makhalanyane et al., 2015).

Although several pilot studies have been carried out to investigate the bacterial diversity in the Taklamakan desert, the knowledge of its microbial communities and the potential of microbiota to produce bioactive metabolites is still little and patchy. Bao et al. (2011) investigated bacterial diversity of soils collected from *Populus Euphratica* forest in the hinterland of Taklamakan desert. Twenty-seven strains obtained fell into 13 genera in four bacterial phyla, in which 16 strains were actinobacteria with *Streptomyces* and *Kocuria* as the dominant genera. All isolates demonstrated certain enzymatic activity which can be used as inoculants for silage and biofertilizer. Dong et al. (2013) explored the diversity and bioactivity of actinomycetes at the south edge of the Taklamakan desert. One hundred and sixty-five actinobacterial strains were isolated, and they distributed in 24 different genera in 16 families with the dominant genera *Streptomyces* and *Nocardiopsis*. Meanwhile, nearly two thirds strains exhibited antifungal or antibacterial activities. Yu et al. (2015) isolated 52 strains of radiation-resistant bacteria from the soil sample of Taklamakan desert, in which 32 strains were affiliated into phylum *Actinobacteria* including the genera *Agrococcus*, *Arthrobacter*, *Cellulomonas*, *Kocuria*, *Knoella*, and *Nocardioides*. All strains were found to possess reactive oxygen species (ROS)-scavenging enzymes to protect cells against oxidative damage and ionizing radiation. In our recent publication, 320 endophytic actinobacterial strains, assigned to 23 genera in 14 families, were isolated from psammophytes collected in Taklamakan desert with *Streptomyces* as the dominant genus (Wang et al., 2020a). In the present study, a considerable diversity of cultivable actinobacteria was obtained from eight different soil samples along the Alar-Hotan desert highway in the Taklamakan desert. A total of 590 actinobacterial strains were assigned to 55 genera in 27 families of 12 orders, suggesting that enormous actinobacterial strains are widespread throughout this arid region. Comparing with previous studies, this is the first time to recover such magnitude of diversity of cultivable actinobacteria from the Taklamakan desert merely in eight soil samples. Notably, genera *Pseudarthrobacter*, *Oerskovia*, *Patulibacter*, and *Neomicrococcus*, to our knowledge, are the first time to be detected from the desert ecosystem.

Streptomyces species were dominantly isolated from the Taklamakan desert soil, which is congruent with many previous studies in desert ecosystems worldwide (Hozzein et al., 2008; Okoro et al., 2009; Selvameenal et al., 2009; Tiwari et al., 2015). Apart from the ubiquitous genus *Streptomyces*, some rare genera found in this study can be classified as indigenous desert types, as they have been often detected in desert-like environments (arid environments). For example, members of the family *Geodermatophilaceae*, notably the genera *Geodermatophilus*, *Blastococcus*, and *Modestobacter* are known to be resistant to desiccation, low nutrition, strong ionizing radiation, UV-light, and heavy metals (Sghaier et al., 2016). Members of *Actinomadura*, *Micromonospora*, and *Streptosporangium* are thermotolerant species widespread in desert soils (Kurapova et al., 2012). Species of *Gordonia*, *Nocardioides*, and *Amycolatopsis* are reported to be desiccation-resistant (Mohammadipanah and Wink, 2015); *Micrococcus*, *Brachybacterium*, *Nocardia*, *Microbacterium*, *Kocuria*, *Kineococcus*, and *Micrococcus* are reported to be radiation-resistant (Mohammadipanah and Wink, 2015; Yu et al., 2015; Sayed et al., 2020). Genera *Nocardiopsis*, *Haloactinobacterium*, *Kocuria*, *Saccharopolyspora*, and *Nesterenkonia* are mostly halotolerant or halophilic actinomycetes isolated from salty desert environment (Hamedi et al., 2013). Deriving of these unique genera of actinobacteria not only demonstrates the rich actinobacterial diversity in Taklamakan desert but also provides more desert-derived strains for further study on their potential in medicine and biological function in ecology.

In the antibacterial assay, 61 isolates affiliated to 19 genera exhibited antagonistic activity against the tested "ESKAPE" pathogens. Analysis of composition of 61 positive strains in genus level, *Streptomyces* strains accounted for over half (37 strains). It is quite reasonable, since *Streptomyces* are a well-established source of diverse bioactive compounds possessing antimicrobial activity in the microbial world discovered

(Masand et al., 2018; Olanrewaju and Babalola, 2019; Pham et al., 2019). *Nocardiopsis* and *Micromonospora* are the second prevalent genera in the active strains, and each with three strains displayed antibacterial activities. It is noteworthy that two *Nocardiopsis* strains including 14Sc5-11 and 15S9-2, showed less than 98.65% 16S rRNA similarities with the validly reported species in genus *Nocardiopsis*, therefore they might represent two strains in novel species of the genus *Nocardiopsis*. Meanwhile, *Nocardiopsis* species were reported to produce a wide variety of chemical classes of compounds with diverse pharmacological and biological activities (Bennur et al., 2016; Ibrahim et al., 2018). In this context, it would be interesting to explore if novel bioactive metabolites can be identified from the two potential new *Nocardiopsis* strains. Furthermore, five potential new species, including *Cellulosimicrobium* sp. 14Sb3-13 and 14Sb1-5, *Kineococcus* sp. 13S2-4, *Cellulomonas* sp. 10Sc3-5, and *Streptomyces* sp. 20Sb6-6 also showed inhibitory activities against tested pathogens (**Supplementary Table S5**). Thorough investigations will be carried out further to deepen our knowledge on the antibacterial substances of these potential novel strains.

The action of antimicrobial agents can be generally categorized in five mechanisms: inhibition of cell wall synthesis, alteration of cell membranes structure, inhibition of protein synthesis, inhibition of nucleic acid synthesis, and disruption of the metabolic pathways (such as folic acid and mycolic acid; Wilson, 2014; Kapoor et al., 2017; O'Rourke et al., 2020). In this study, a unique high-throughput model based on a double fluorescent protein reporter "pDualrep2" system was implemented to gain preliminary insights into the mechanism of antibacterial action of bioactive strains. This reporter system can early identify the antibacterial inhibitors targeting three mechanisms in "one-pot" format: DNA damage (expression of rfp reporter), inhibition of protein translation (expression of katushka2S reporter), and others (inhibition of bacterial growth targeting on neither DNA replication nor protein synthesis; Osterman et al., 2016; Ivanenkov et al., 2019a). Sensitivity of this system was highly increased by applying an *E. coli* strain with lacking the *tolC* gene that coded for an essential component of several efflux systems in outer membrane (Zgurskaya et al., 2011; Osterman et al., 2016). Both these effects are clearly observed within the sublethal concentration of an antibacterial sample where it does not kill bacteria but substantially attenuates translation or trigger the SOS response. As a biosensor of antimicrobial activity, the described assay was reported to be successfully applied for identification of a series of promising antibiotics whose antibacterial activity had not been reported previously, such as 2-Guanidino-quinazolines (Komarova et al., 2017), N-pyridyl-substituted carboxypiperidine amides (Ivanenkov et al., 2019b), and N-substituted triazolo-azetidines (Ivanenkov et al., 2019c). Furthermore, in our previous study, this platform contributed to effective discovery of some novel antibiotics that act *via* the translation inhibition mechanism, such as Beilunmycin (Jiang et al., 2020), Hetiamacin E and F (Wang et al., 2020b), acetyl-griseoviridin, and desulphurizing griseoviridin (Wang et al., 2020a). In the present research, two *Streptomyces* strains and two *Saccharothrix* strains induced Katushka2S expression, demonstrating the protein inhibitory activities in their ethyl acetate extractions. Three *Streptomyces* strains demonstrated their inhibition activity against DNA biosynthesis by inducing the RFP expression. Investigation of these strains could be prioritized to find potential antibacterial compounds.

It is generally accepted that rare actinobacterial genera possess more potential in terms of secondary metabolites novelty (Schorn et al., 2016; Bundale et al., 2019; Ding et al., 2019). Thus, exploration of bioactive chemicals from rare actinobacterial strains will be more promising and efficient. In the present study, a *Saccharothrix* strain was analyzed firstly to gain deeper insights into its bioactive metabolites. At the time of writing, the genus *Saccharothrix* encompasses 21 species and 2 subspecies with validly published names, in which eight species were isolated from deserts (Liu et al., 2020c). The genus *Saccharothrix* was found to be a potential producer of novel specialized metabolites, and these chemical entities exhibited a broad range of biological functions, such as antibacterial (Takahashi et al., 1986; Isshiki et al., 1989; Takeuchi et al., 1992), antifungal (Igarashi et al., 1997), antitumor (Vértesy et al., 2001), antivirus (Tomita et al., 1991), pro-inflammatory (Gibson et al., 2005), and other activities (Kimura et al., 1995; Yoshimura et al., 1995; Koguchi et al., 2000) of medical and industrial importance. For instance, at least 14 dithiolopyrrolone compounds with strong activities against a panel of bacteria, yeasts, and filamentous fungi were isolated naturally or using biosynthetic method from *Saccharothrix algeriensis* NRRL B-24137 (Lamari et al., 2002; Bouras et al., 2008; Merrouche et al., 2010, 2011). More than 20 macrolides were isolate from different *Saccharothrix* sp., including cytotoxic 10/11-membered macrolides saccharothriolides A–K, X (Lu et al., 2015, 2016) and 20-membered macrolides ammocidins A–D (Murakami et al., 2001, 2009); antibacterial 16-membered macrolides Tianchimycins A and B (Wang et al., 2013), aldgamycins G, H, and swalpamycin B (Mizobuchi et al., 1986; Zitouni et al., 2007; Wang et al., 2013); and antifungal 16-membered macrolides formamicin (Igarashi et al., 1997). Recently, new antibacterial congeners cyanogriside J and M were isolated from strain ABH26, which was closely related to *S. xinjiangensis* NBRC 101911^T (Lahoum et al., 2019); and new cytotoxic compounds, caerulomycin M, saccharopyrone and saccharonoic acid were isolated from *S. xinjiangensis* Act24Zk (Skellam et al., 2013). These promising results emphasize the need to continue the research in the genus *Saccharothrix*. In this research, *Saccharothrix* strain 16Sb2-4 presented a promising antimicrobial potential against all the tested "ESKAPE" pathogens and demonstrated its antibacterial mechanism of interfering with protein translation, thus was given priority for metabolites exploration to discover bioactive compounds from the Taklamakan desert.

To gain a comprehensive understanding of chemical diversity in the cultural broth of strain 16Sb2-4, UPLC-QTof-MS/MS-based dereplication analyses coupled with molecular networking were performed prior to the metabolites isolation. Many researches have reported the successful application of molecular networking for effective chemical dereplication and novel metabolite discovery (Duncan et al., 2015; Kleigrewe et al., 2015; Esposito et al., 2017;

Nothias et al., 2018; Lu et al., 2019), especially in our latest research on endophytic actinobacteria from psammophytes in Taklamakan desert, it has successfully contributed to the discovery of two new griseoviridin-type antibiotics from the fermentation broth of an endophytic *Streptomyces* strain (Wang et al., 2020a). In the present study, four families of bioactive compounds were observed and predicted from the crude extract of strain 16Sb2-4, including lipopeptides, cyclic depsipeptides, 22-membered macrolactams, and 16-membered macrolides. The prediction of 16-membered macrolides was further confirmed by efficient isolation and structure elucidation of compounds **8–11**, which evidenced that molecular networking can accelerate dereplication and compound identification, and moreover, can rationalize isolation procedure for targeted purification of bioactive natural products.

Four known 16-membered macrolides, aldgamycin G, aldgamycin H, aldgamycin K, and swalpamycin B, were isolated and identified from *Saccharothrix* sp. 16Sb2-4 by subsequent targeted separation. Meanwhile, all of them exerted the bacteriostatic effect by interfering with protein translation in the pDualrep2 reporter system. These four compounds are all assigned to be 16-membered macrolides containing a rare branched octose unit at C-5 of the macrolactone ring. Many macrolides were reported to often have a bacteriostatic effect on susceptible organisms, caused by inhibition of RNA-dependent protein synthesis through binding to the 50S subunit of the bacterial ribosome (Bolhuis et al., 2011). The sugar substituent at C-5 plays an essential role in their antibacterial activity by direct interaction with 23S RNA (Bolhuis et al., 2011; Karpinski, 2019). It has been reported that aldgamycin G, H and swalpamycin B showed antibacterial activity against Gram-positive bacteria (Mizobuchi et al., 1986; Zitouni et al., 2007; Wang et al., 2013). Although aldgamycin K did not exhibit antimicrobial activity against tested bacteria and fungi in previous report (Wang et al., 2016b), it revealed its antibacterial potential by inhibiting protein synthesis in the highly-sensitive pDualrep2 system in our study. In terms of the biological source, aldgamycin G, aldgamycin H, and swalpamycin B were ever isolated from *Saccharothrix* species before, meanwhile aldgamycin G and swalpamycin B have also been isolated from *Streptomyces* strains (Mizobuchi et al., 1986; Chatterjee et al., 1987). This is the first report of production of aldgamycin K by the genus *Saccharothrix*, which was reported to be produced only by *Streptomyces* strains in previous study (Wang et al., 2016b).

CONCLUSION

The study reported a relatively integrated investigation on the diversity, novelty, and pharmacological potential of actinobacterial strains isolated from eight soil samples at various sites along the Alar-Hotan desert highway in the Taklamakan desert. These actinobacterial strains were affiliated to 55 genera in 27 families of 12 orders, which implied significant actinobacterial diversity inhabited in the harsh environment. Over 40% of the 146 tested isolates exhibited bioactive potential against at least one of the tested "ESKAPE" pathogens, among which seven strains demonstrated their ability either to block translation machinery or induce SOS-response in the pDualrep2 system. One strain, *Saccharothrix* sp. 16Sb2-4 as an example was studied to prove the capability to produce diverse secondary metabolites based on in-depth chemical profiling, and four bioactive macrolide antibiotics were purified as secondary metabolites from ISP 2 cultural medium. Exploration of the other bioactive isolates by combination of different strategies, including high-throughput screening, small scale fermentation based on deep-plates, One Strain Many Compounds (OSMAC), and compound dereplication by UPLC-QToF-MS/MS, *etc*., is the subject of our further investigation. It is believed that new antibiotics will be discovered from these desert-derived actinobacterial strains, which will support the idea that the Taklamakan desert represents an undeveloped reservoir of pharmaceutical actinobacteria with possessing a significant capacity to produce novel metabolites with unique antibacterial activity.

DATA AVAILABILITY STATEMENT

The datasets presented in this study can be found in online repositories. The names of the repository/repositories and accession number(s) can be found in the article/ **Supplementary Material**.

AUTHOR CONTRIBUTIONS

CS conceived the whole study, supervised the project, and helped in preparing the manuscript. SL and TW carried out the experiments and prepared the manuscript. CS, FL, and XH contributed in sampling from deserts. QL, GW, ZJ, LL, and XZ helped to prepare some experiments. DL, IO, PS, and OD were responsible for screening the mechanisms of action for samples by means of a double fluorescent protein reporter system. All authors contributed to the article and approved the submitted version.

FUNDING

The research work was supported by grant from the National Natural Science Foundation of China (grant numbers 82011530051 and 81373308), CAMS Innovation Fund for Medical Sciences (grant number CAMS 2017-I2M-B&R-08 and 2017-I2M-1-012), Russian Foundation for Basic Research (grant number 18-34-20055), and Russian Science Foundation (grant number 20-74-10031).

SUPPLEMENTARY MATERIAL

The Supplementary Material for this article can be found online at: https://www.frontiersin.org/articles/10.3389/fmicb.2021.604999/full#supplementary-material

REFERENCES

Abdelkader, M., Philippon, T., Asenjo, J. A., Bull, A. T., Goodfellow, M., Ebel, R., et al. (2018). Asenjonamides A-C, antibacterial metabolites isolated from *Streptomyces asenjonii* strain KNN 42.F from an extreme-hyper arid Atacama desert soil. *J. Antibiot.* 71, 425–431. doi: 10.1038/s41429-017-0012-0

An, S., Couteau, C., Luo, F., Neveu, J., and DuBow, M. S. (2013). Bacterial diversity of surface sand samples from the Gobi and Taklamaken deserts. *Microb. Ecol.* 66, 850–860. doi: 10.1007/s00248-013-0276-2

Ardal, C., Balasegaram, M., Laxminarayan, R., McAdams, D., Outterson, K., Rex, J. H., et al. (2020). Antibiotic development—economic, regulatory and societal challenges. *Nat. Rev. Microbiol.* 18, 267–274. doi: 10.1038/s41579-019-0293-3

Arsic, B., Barber, J., Cikos, A., Mladenovic, M., Stankovic, N., and Novak, P. (2018). 16-membered macrolide antibiotics: a review. *Int. J. Antimicrob. Agents* 51, 283–298. doi: 10.1016/j.ijantimicag.2017.05.020

Babadi, Z. K., Sudarman, E., Ebrahimipour, G. H., Primahana, G., Stadler, M., and Wink, J. (2020). Structurally diverse metabolites from the rare actinobacterium *Saccharothrix xinjiangensis*. *J. Antibiot.* 73, 48–55. doi: 10.1038/s41429-019-0223-7

Bao, H., Wang, W., Wang, N., Fang, S., and Zhan, F. (2011). Bacteria diversity of soil of Populus Euphratica forest in the hinterland of Taklimakan desert. *Wei Sheng Wu Xue Bao* 19, 462–467. doi: 10.3724/SP.J.1011.2011.00462

Bennur, T., Ravi, K. A., Zinjarde, S. S., and Javdekar, V. (2016). *Nocardiopsis* species: a potential source of bioactive compounds. *J. Appl. Microbiol.* 120, 1–16. doi: 10.1111/jam.12950

Bolhuis, M. S., Panday, P. N., Pranger, A. D., Kosterink, J. G., and Alffenaar, J. W. (2011). Pharmacokinetic drug interactions of antimicrobial drugs: a systematic review on oxazolidinones, rifamycines, macrolides, fluoroquinolones, and beta-lactams. *Pharmaceutics* 3, 865–913. doi: 10.3390/pharmaceutics3040865

Bouras, N., Merrouche, R., Lamari, L., Mathieu, F., Sabaou, N., and Lebrihi, A. (2008). Precursor-directed biosynthesis of new dithiolopyrrolone analogs by *Saccharothrix algeriensis* NRRL B-24137. *Process Biochem.* 43, 1244–1252. doi: 10.1016/j.procbio.2008.07.008

Bravo, A., Ruiz-Cruz, S., Alkorta, I., and Espinosa, M. (2018). When humans met superbugs: strategies to tackle bacterial resistances to antibiotics. *Biomol. Concepts* 9, 216–226. doi: 10.1515/bmc-2018-0021

Bull, A. T., Andrews, B. A., Dorador, C., and Goodfellow, M. (2018). Introducing the Atacama desert. *Antonie Van Leeuwenhoek* 111, 1269–1272. doi: 10.1007/s10482-018-1100-2

Bull, A. T., and Asenjo, J. A. (2013). Microbiology of hyper-arid environments: recent insights from the Atacama Desert, Chile. *Antonie Van Leeuwenhoek* 103, 1173–1179. doi: 10.1007/s10482-013-9911-7

Bull, A. T., Asenjo, J. A., Goodfellow, M., and Gomez-Silva, B. (2016). The Atacama desert: technical resources and the growing importance of novel microbial diversity. *Annu. Rev. Microbiol.* 70, 215–234. doi: 10.1146/annurev-micro-102215-095236

Bull, A. T., and Goodfellow, M. (2019). Dark, rare and inspirational microbial matter in the extremobiosphere: 16 000 m of bioprospecting campaigns. *Microbiology* 165, 1252–1264. doi: 10.1099/mic.0.000822

Bundale, S., Singh, J., Begde, D., Nashikkar, N., and Upadhyay, A. (2019). Rare actinobacteria: a potential source of bioactive polyketides and peptides. *World J. Microbiol. Biotechnol.* 35:92. doi: 10.1007/s11274-019-2668-z

Chambers, M. C., Maclean, B., Burke, R., Amodei, D., Ruderman, D. L., Neumann, S., et al. (2012). A cross-platform toolkit for mass spectrometry and proteomics. *Nat. Biotechnol.* 30, 918–920. doi: 10.1038/nbt.2377

Chater, K. F., and Chandra, G. (2006). The evolution of development in *Streptomyces* analysed by genome comparisons. *FEMS Microbiol. Rev.* 30, 651–672. doi: 10.1111/j.1574-6976.2006.00033.x

Chatterjee, S., Reddy, G. C. S., Franco, C. M. M., Rupp, R. H., and Ganguli, B. N. (1987). Swalpamycin, a new macrolide antibiotic II. Structure elucidation. *J. Antibiot.* 40, 1368–1374. doi: 10.7164/antibiotics.40.1368

Chokshi, A., Sifri, Z., Cennimo, D., and Horng, H. (2019). Global contributors to antibiotic resistance. *J. Global Infect. Dis.* 11:36. doi: 10.4103/jgid.jgid_110_18

Chun, J., Oren, A., Ventosa, A., Christensen, H., Arahal, D. R., Da, C. M., et al. (2018). Proposed minimal standards for the use of genome data for the taxonomy of prokaryotes. *Int. J. Syst. Evol. Microbiol.* 68, 461–466. doi: 10.1099/ijsem.0.002516

Crits-Christoph, A., Robinson, C. K., Barnum, T., Fricke, W. F., Davila, A. F., Jedynak, B., et al. (2013). Colonization patterns of soil microbial communities in the Atacama Desert. *Microbiome* 1:28. doi: 10.1186/2049-2618-1-28

Deng, L., Shi, A. M., Liu, H. Z., Meruva, N., Liu, L., Hu, H., et al. (2016). Identification of chemical ingredients of peanut stems and leaves extracts using UPLC-QTOF-MS coupled with novel informatics UNIFI platform. *J. Mass Spectrom.* 51, 1157–1167. doi: 10.1002/jms.3887

Dickey, S. W., Cheung, G., and Otto, M. (2017). Different drugs for bad bugs: antivirulence strategies in the age of antibiotic resistance. *Nat. Rev. Drug Discov.* 16, 457–471. doi: 10.1038/nrd.2017.23

Ding, T., Yang, L., Zhang, W., and Shen, Y. (2019). The secondary metabolites of rare actinomycetes: chemistry and bioactivity. *RSC Adv.* 9, 21964–21988. doi: 10.1039/C9RA03579F

Dong, Y., Guo, L., Habden, X., Liu, J., Chen, C., Jiang, Z., et al. (2013). Study on diversity and bioactivity of actinomycetes isolated from the south edge of the Taklamakan Desert. *Chin. J. Antibiot.* 38, 241–247. doi: 10.3969/j.issn.1001-8689.2013.04.001

Duncan, K. R., Crusemann, M., Lechner, A., Sarkar, A., Li, J., Ziemert, N., et al. (2015). Molecular networking and pattern-based genome mining improves discovery of biosynthetic gene clusters and their products from *Salinispora* species. *Chem. Biol.* 22, 460–471. doi: 10.1016/j.chembiol.2015.03.010

Elsayed, S. S., Trusch, F., Deng, H., Raab, A., Prokes, I., Busarakam, K., et al. (2015). Chaxapeptin, a lasso peptide from extremotolerant *Streptomyces leeuwenhoekii* strain C58 from the Hyperarid Atacama Desert. *J. Organomet. Chem.* 80, 10252–10260. doi: 10.1021/acs.joc.5b01878

Elshahawi, S. I., Shaaban, K. A., Kharel, M. K., and Thorson, J. S. (2015). A comprehensive review of glycosylated bacterial natural products. *Chem. Soc. Rev.* 44, 7591–7697. doi: 10.1039/C4CS00426D

Esposito, M., Nothias, L. F., Retailleau, P., Costa, J., Roussi, F., Neyts, J., et al. (2017). Isolation of premyrsinane, myrsinane, and tigliane diterpenoids from *euphorbia pithyusa* using a chikungunya virus cell-based assay and analogue annotation by molecular networking. *J. Nat. Prod.* 80, 2051–2059. doi: 10.1021/acs.jnatprod.7b00233

Gao, Q., and Garcia-Pichel, F. (2011). Microbial ultraviolet sunscreens. *Nat. Rev. Microbiol.* 9, 791–802. doi: 10.1038/nrmicro2649

Gibson, K. J. C., Gilleron, M., Constant, P., Sichi, B., Puzo, G., Besra, G. S., et al. (2005). A lipomannan variant with strong TLR-2-dependent pro-inflammatory activity in *Saccharothrix aerocolonigenes*. *J. Biol. Chem.* 280, 28347–28356. doi: 10.1074/jbc.M505498200

Gommeaux, M., Barakat, M., Montagnac, G., Christen, R., Guyot, F., and Heulin, T. (2010). Mineral and bacterial diversities of desert sand grains from south-East Morocco. *Geomicrobiol J.* 27, 76–92. doi: 10.1080/01490450903393066

Goodfellow, M., and Fiedler, H. P. (2010). A guide to successful bioprospecting: informed by actinobacterial systematics. *Antonie Van Leeuwenhoek* 98, 119–142. doi: 10.1007/s10482-010-9460-2

Gottlieb, H. E., Kotlyar, V., and Nudelman, A. (1997). NMR chemical shifts of common laboratory solvents as trace impurities. *J. Organomet. Chem.* 62, 7512–7515. doi: 10.1021/jo971176v

Hamedi, J., Mohammadipanah, F., and Ventosa, A. (2013). Systematic and biotechnological aspects of halophilic and halotolerant actinomycetes. *Extremophiles* 17, 1–13. doi: 10.1007/s00792-012-0493-5

Harwani, D. (2013). Biodiversity of rare thermophilic actinomycetes in the great Indian Thar desert: an overview. *Indo Am J. Pharm. Res.* 3, 934–939. doi: 10.13140/2.1.5102.4005

Hoshino, S., Okada, M., Awakawa, T., Asamizu, S., Onaka, H., and Abe, I. (2017). Mycolic acid containing bacterium stimulates tandem cyclization of polyene macrolactam in a lake sediment derived rare actinomycete. *Org. Lett.* 19, 4992–4995. doi: 10.1021/acs.orglett.7b02508

Hozzein, W. N., Ali, M. I. A., and Rabie, W. (2008). A new preferential medium for enumeration and isolation of desert actinomycetes. *World J. Microbiol. Biotechnol.* 24, 1547–1552. doi: 10.1007/s11274-007-9641-y

Hu, Y. T., Zhou, P. J., Zhou, Y. G., Liu, Z. H., and Liu, S. J. (2004). *Saccharothrix xinjiangensis* sp. nov., a pyrene-degrading actinomycete isolated from Tianchi Lake, Xinjiang, China. *Int. J. Syst. Evol. Microbiol.* 54, 2091–2094. doi: 10.1099/ijs.0.63143-0

Ibrahim, A. H., Desoukey, S. Y., Fouad, M. A., Kamel, M. S., Gulder, T., and Abdelmohsen, U. R. (2018). Natural product potential of the genus *Nocardiopsis*. *Mar. Drugs* 16:147. doi: 10.3390/md16050147

Igarashi, M., Nakamura, H., Naganawa, H., and Takeuchi, T. (1997). Formamicin, a novel antifungal antibiotic produced by a strain of *Saccharothrix* sp. II. Structure elucidation of formamicin. *J. Antibiot.* 50, 932–936. doi: 10.7164/antibiotics.50.932

Isshiki, K., Sawa, T., Naganawa, H., Matsuda, N., Hattori, S., Hamada, M., et al. (1989). 3-*O*-isobutyrylkinamycin C and 4-deacetyl-4-*O*-isobutyrylkinamycin C, new antibiotics produced by a *Saccharothrix* species. *J. Antibiot.* 42, 467–469. doi: 10.7164/antibiotics.42.467

Ivanenkov, Y. A., Komarova Andreyanova, E. S., Osterman, I. A., Sergiev, P. V., Yamidanov, R. S., Deineka, E. V., et al. (2019b). N-Pyridyl-substituted carboxypiperidine amides: a new class of prokaryote translation inhibitors. *Pharm. Chem. J.* 53, 225–229. doi: 10.1007/s11094-019-01984-3

Ivanenkov, Y. A., Yamidanov, R. S., Osterman, I. A., Sergiev, P. V., Aladinskiy, V. A., Aladinskaya, A. V., et al. (2019c). Identification of N-substituted triazolo-azetidines as novel antibacterials using pDualrep2 HTS platform. *Comb. Chem. High Throughput Screen.* 22, 346–354. doi: 10.2174/1386207322666190412165316

Ivanenkov, Y. A., Zhavoronkov, A., Yamidanov, R. S., Osterman, I. A., Sergiev, P. V., Aladinskiy, V. A., et al. (2019a). Identification of novel antibacterials using machine learning techniques. *Front. Pharmacol.* 10:913. doi: 10.3389/fphar.2019.00913

Jiang, H., Chen, T. J., Chi, Z., Hu, Z., Liu, G. L., Sun, Y., et al. (2019). Macromolecular pullulan produced by *Aureobasidium melanogenum* 13-2 isolated from the Taklimakan desert and its crucial roles in resistance to the stress treatments. *Int. J. Biol. Macromol.* 135, 429–436. doi: 10.1016/j.ijbiomac.2019.05.190

Jiang, Z. K., Hu, X. X., Xiao, L. L., Ren, Y. R., Shakhtina, A. N., Lukianov, D. A., et al. (2020). Beilunmycin, a new virginiamycins antibiotic from mangrove-derived *Streptomyces* sp. 2BBP-J2 and the antibacterial activity by inhibiting protein translation. *J. Asian Nat. Prod. Res.* 1–9. doi: 10.1080/10286020.2020.1830379 [Epub ahead of print]

Jose, P. A., and Jha, B. (2016). New dimensions of research on actinomycetes: quest for next generation antibiotics. *Front. Microbiol.* 7:1295. doi: 10.3389/fmicb.2016.01295

Kapoor, G., Saigal, S., and Elongavan, A. (2017). Action and resistance mechanisms of antibiotics: a guide for clinicians. *J. Anaesthesiol. Clin. Pharmacol.* 33, 300–305. doi: 10.4103/joacp.JOACP_349_15

Karpinski, T. M. (2019). Marine macrolides with antibacterial and/or antifungal activity. *Mar. Drugs* 17:241. doi: 10.3390/md17040241

Kaufmann, A. (2014). Combining UHPLC and high-resolution MS: a viable approach for the analysis of complex samples? *TrAC Trends Anal. Chem.* 63, 113–128. doi: 10.1016/j.trac.2014.06.025

Kegler, C., Nollmann, F. I., Ahrendt, T., Fleischhacker, F., Bode, E., and Bode, H. B. (2014). Rapid determination of the amino acid configuration of xenotetrapeptide. *ChemBioChem* 15, 826–828. doi: 10.1002/cbic.201300602

Kim, M., Oh, H. S., Park, S. C., and Chun, J. (2014). Towards a taxonomic coherence between average nucleotide identity and 16S rRNA gene sequence similarity for species demarcation of prokaryotes. *Int. J. Syst. Evol. Microbiol.* 64, 346–351. doi: 10.1099/ijs.0.059774-0

Kimura, M. (1980). A simple method for estimating evolutionary rates of base substitutions through comparative studies of nucleotide sequences. *J. Mol. Evol.* 16, 111–120. doi: 10.1007/BF01731581

Kimura, T., Nakamura, K., and Takahashi, E. (1995). Phosphonothrixin, a novel herbicidal antibiotic produced by *Saccharothrix* sp. ST-888. II. Structure determination. *J. Antibiot.* 48, 1130–1133. doi: 10.7164/antibiotics.48.1130

Kleigrewe, K., Almaliti, J., Tian, I. Y., Kinnel, R. B., Korobeynikov, A., Monroe, E. A., et al. (2015). Combining mass spectrometric metabolic profiling with genomic analysis: a powerful approach for discovering natural products from cyanobacteria. *J. Nat. Prod.* 78, 1671–1682. doi: 10.1021/acs.jnatprod.5b00301

Koberl, M., Muller, H., Ramadan, E. M., and Berg, G. (2011). Desert farming benefits from microbial potential in arid soils and promotes diversity and plant health. *PLoS One* 6:e24452. doi: 10.1371/journal.pone.0024452

Koguchi, Y., Kohno, J., Suzuki, S., Nishio, M., Takahashi, K., Ohnuki, T., et al. (2000). TMC-86A, B and TMC-96, new proteasome inhibitors from *Streptomyces* sp. TC 1084 and *Saccharothrix* sp. TC 1094. II. Physico-chemical properties and structure determination. *J. Antibiot.* 53, 63–65. doi: 10.7164/antibiotics.53.63

Kolter, R., and van Wezel, G. P. (2016). Goodbye to brute force in antibiotic discovery? *Nat. Microbiol.* 1:15020. doi: 10.1038/nmicrobiol.2015.20

Komarova, A. E., Osterman, I. A., Pletnev, P. I., Ivanenkov, Y. A., Majouga, A. G., Bogdanov, A. A., et al. (2017). 2-Guanidino-quinazolines as a novel class of translation inhibitors. *Biochimie* 133, 45–55. doi: 10.1016/j.biochi.2016.11.008

Kumar, S., Stecher, G., and Tamura, K. (2016). MEGA7: molecular evolutionary genetics analysis version 7.0 for bigger datasets. *Mol. Biol. Evol.* 33, 1870–1874. doi: 10.1093/molbev/msw054

Kurapova, A. I., Zenova, G. M., Sudnitsyn, I. I., Kizilova, A. K., Manucharova, N. A., Norovsuren, Z., et al. (2012). Thermotolerant and thermophilic actinomycetes from soils of Mongolia desert steppe zone. *Microbiology* 81, 98–108. doi: 10.1134/S0026261712010092

Lahoum, A., Sabaou, N., Bijani, C., Bouras, N., Pont, F., Snini, S. P., et al. (2019). Antimicrobial activities of novel bipyridine compounds produced by a new strain of *Saccharothrix* isolated from Saharan soil. Saudi. *Pharm. J.* 27, 56–65. doi: 10.1016/j.jsps.2018.07.019

Lai, H., Wei, X., Jiang, Y., Chen, X., Li, Q., Jiang, Y., et al. (2014). *Halopolyspora alba* gen. Nov., sp. nov., isolated from sediment. *Int. J. Syst. Evol. Microbiol.* 64, 2775–2780. doi: 10.1099/ijs.0.057638-0

Lamari, L., Zitouni, A., Dob, T., Sabaou, N., Lebrihi, A., Germain, P., et al. (2002). New dithiolopyrrolone antibiotics from *Saccharothrix* sp. SA 233. II. Physicochemical properties and structure elucidation. *J. Antibiot.* 55, 702–706. doi: 10.7164/antibiotics.55.702

Li, C., Lei, J., Zhao, Y., Xu, X., and Li, S. (2015). Effect of saline water irrigation on soil development and plant growth in the Taklimakan Desert highway shelterbelt. *Soil Tillage Res.* 146, 99–107. doi: 10.1016/j.still.2014.03.013

Li, F., Liao, S., Liu, S., Jin, T., and Sun, C. (2019b). *Aeromicrobium endophyticum* sp. nov., an endophytic actinobacterium isolated from reed (*Phragmites australis*). *J. Microbiol.* 57, 725–731. doi: 10.1007/s12275-019-8705-7

Li, F., Liu, S., Lu, Q., Zheng, H., Osterman, I. A., Lukyanov, D. A., et al. (2019a). Studies on antibacterial activity and diversity of cultivable actinobacteria isolated from mangrove soil in Futian and Maoweihai of China. *Evid. Based Complement. Alternat. Med.* 2019:3476567. doi: 10.1155/2019/3476567

Li, F., Lu, Q., Liao, S., Jin, T., Li, W., and Sun, C. (2019c). *Labedella phragmitis* sp. nov. and *Labedella populi* sp. nov., two endophytic actinobacteria isolated from plants in the Taklamakan Desert and emended description of the genus *Labedella*. *Syst. Appl. Microbiol.* 42:126004. doi: 10.1016/j.syapm.2019.126004

Li, W. J., Xu, P., Schumann, P., Zhang, Y. Q., Pukall, R., Xu, L. H., et al. (2007). *Georgenia ruanii* sp. nov., a novel actinobacterium isolated from forest soil in Yunnan (China), and emended description of the genus *Georgenia*. *Int. J. Syst. Evol. Microbiol.* 57, 1424–1428. doi: 10.1099/ijs.0.64749-0

Lim, Y. H., Wong, F. T., Yeo, W. L., Ching, K. C., Lim, Y. W., Heng, E., et al. (2018). Auroramycin: a potent antibiotic from *Streptomyces roseosporus* by CRISPR-Cas9 activation. *ChemBioChem*. doi: 10.1002/cbic.201800266 [Epub ahead of print]

Liu, J., Habden, X., Guo, L., Tuo, L., Jiang, Z., Liu, S., et al. (2015a). *Prauserella endophytica* sp. nov., an endophytic actinobacterium isolated from *Tamarix taklamakanensis*. *Antonie Van Leeuwenhoek* 107, 1401–1409. doi: 10.1007/s10482-015-0435-1

Liu, S. W., Li, F. N., Liu, H. Y., Yu, L. Y., and Sun, C. H. (2020b). *Desertihabitans brevis* sp. nov., an actinobacterium isolated from sand of the Taklamakan desert, and emended description of the genus *Desertihabitans*. *Int. J. Syst. Evol. Microbiol.* 70, 1166–1171. doi: 10.1099/ijsem.0.003896

Liu, S. W., Li, F. N., Qi, X., Xie, Y. Y., and Sun, C. H. (2019b). *Nakamurella deserti* sp. nov., isolated from rhizosphere soil of *Reaumuria* in the Taklamakan desert. *Int. J. Syst. Evol. Microbiol.* 69, 214–219. doi: 10.1099/ijsem.0.003132

Liu, S. W., Li, F. N., Zheng, H. Y., Qi, X., Huang, D. L., Xie, Y. Y., et al. (2019a). *Planctomonas deserti* gen. Nov., sp. nov., a new member of the family *Microbacteriaceae* isolated from soil of the Taklamakan desert. *Int. J. Syst. Evol. Microbiol.* 69, 616–624. doi: 10.1099/ijsem.0.003095

Liu, J., Sun, Y., Liu, J., Wu, Y., Cao, C., Li, R., et al. (2020c). *Saccharothrix deserti* sp. nov., an actinomycete isolated from desert soil. *Int. J. Syst. Evol. Microbiol.* 70, 1882–1887. doi: 10.1099/ijsem.0.003989

Liu, J., Tuo, L., Habden, X., Guo, L., Jiang, Z., Liu, X., et al. (2015b). *Nesterenkonia populi* sp. nov., an actinobacterium isolated from *Populus euphratica*. *Int. J. Syst. Evol. Microbiol.* 65, 1474–1479. doi: 10.1099/ijs.0.000123

Liu, Q. Q., Wang, Y., Li, J., Du, Z. J., and Chen, G. J. (2014). *Saccharicrinis carchari* sp. nov., isolated from a shark, and emended descriptions of the genus *Saccharicrinis* and *Saccharicrinis fermentans*. *Int. J. Syst. Evol. Microbiol.* 64, 2204–2209. doi: 10.1099/ijs.0.061986-0

Liu, S. W., Xue, C. M., Li, F. N., and Sun, C. H. (2020a). *Nocardioides vastitatis* sp. nov., isolated from Taklamakan desert soil. *Int. J. Syst. Evol. Microbiol.* 70, 77–82. doi: 10.1099/ijsem.0.003718

Lu, S., Nishimura, S., Hirai, G., Ito, M., Kawahara, T., Izumikawa, M., et al. (2015). Saccharothriolides A-C, novel phenyl-substituted 10-membered macrolides isolated from a rare actinomycete *Saccharothrix* sp. *Chem. Commun.* 51, 8074–8077. doi: 10.1039/C5CC01953B

Lu, S., Nishimura, S., Ito, M., Tsuchida, T., and Kakeya, H. (2016). Isolation and structure elucidation of cytotoxic saccharothriolides D to F from a rare actinomycete *Saccharothrix* sp. and their structure-activity relationship. *J. Nat. Prod.* 79, 1891–1895. doi: 10.1021/acs.jnatprod.6b00372

Lu, Q. P., Ye, J. J., Huang, Y. M., Liu, D., Liu, L. F., Dong, K., et al. (2019). Exploitation of potentially new antibiotics from mangrove actinobacteria in maowei sea by combination of multiple discovery strategies. *Antibiotics* 8:236. doi: 10.3390/antibiotics8040236

Lynch, R. C., Darcy, J. L., Kane, N. C., Nemergut, D. R., and Schmidt, S. K. (2014). Metagenomic evidence for metabolism of trace atmospheric gases by high-elevation desert actinobacteria. *Front. Microbiol.* 5:698. doi: 10.3389/fmicb.2014.00698

Makhalanyane, T. P., Valverde, A., Gunnigle, E., Frossard, A., Ramond, J. B., and Cowan, D. A. (2015). Microbial ecology of hot desert edaphic systems. *FEMS Microbiol. Rev.* 39, 203–221. doi: 10.1093/femsre/fuu011

Makhalanyane, T. P., Valverde, A., Lacap, D. C., Pointing, S. B., Tuffin, M. I., and Cowan, D. A. (2013). Evidence of species recruitment and development of hot desert hypolithic communities. *Environ. Microbiol. Rep.* 5, 219–224. doi: 10.1111/1758-2229.12003

Masand, M., Sivakala, K. K., Menghani, E., Thinesh, T., Anandham, R., Sharma, G., et al. (2018). Biosynthetic potential of bioactive streptomycetes isolated from arid region of the thar desert, Rajasthan (India). *Front. Microbiol.* 9:687. doi: 10.3389/fmicb.2018.00687

May, K. L., and Grabowicz, M. (2018). The bacterial outer membrane is an evolving antibiotic barrier. *Proc. Natl. Acad. Sci. U. S. A.* 115, 8852–8854. doi: 10.1073/pnas.1812779115

McCarthy, A. J., and Williams, S. T. (1992). Actinomycetes as agents of biodegradation in the environment-a review. *Gene* 115, 189–192. doi: 10.1016/0378-1119(92)90558-7

Meena, K. R., and Kanwar, S. S. (2015). Lipopeptides as the antifungal and antibacterial agents: applications in food safety and therapeutics. *Biomed. Res. Int.* 2015:473050. doi: 10.1155/2015/473050

Meklat, A., Sabaou, N., Zitouni, A., Mathieu, F., and Lebrihi, A. (2011). Isolation, taxonomy, and antagonistic properties of halophilic actinomycetes in Saharan soils of Algeria. *Appl. Environ. Microbiol.* 77, 6710–6714. doi: 10.1128/AEM.00326-11

Merrouche, R., Bouras, N., Coppel, Y., Mathieu, F., Monje, M., Sabaou, N., et al. (2010). Dithiolopyrrolone antibiotic formation induced by adding valeric acid to the culture broth of *Saccharothrix algeriensis*. *J. Nat. Prod.* 73, 1164–1166. doi: 10.1021/np900808u

Merrouche, R., Bouras, N., Coppel, Y., Mathieu, F., Sabaou, N., and Lebrihi, A. (2011). New dithiolopyrrolone antibiotics induced by adding sorbic acid to the culture medium of *Saccharothrix algeriensis* NRRL B-24137. *FEMS Microbiol. Lett.* 318, 41–46. doi: 10.1111/j.1574-6968.2011.02246.x

Miller, S. I. (2016). Antibiotic resistance and regulation of the gram-negative bacterial outer membrane barrier by host innate immune molecules. *MBio* 7, e01541–e01616. doi: 10.1128/mBio.01541-16

Mizobuchi, S., Mochizuki, J., Soga, H., Tanba, H., and Inoue, H. (1986). Aldgamycin G, a new macrolide antibiotic. *J. Antibiot.* 39, 1776–1778. doi: 10.7164/antibiotics.39.1776

Mohammadipanah, F., and Wink, J. (2015). Actinobacteria from arid and desert habitats: diversity and biological activity. *Front. Microbiol.* 6:1541. doi: 10.3389/fmicb.2015.01541

Murakami, R., Shinozaki, J., Kajiura, T., Kozone, I., Takagi, M., Shin-Ya, K., et al. (2009). Ammocidins B, C and D, new cytotoxic 20-membered macrolides from *Saccharothrix* sp. AJ9571. *J. Antibiot.* 62, 123–127. doi: 10.1038/ja.2008.23

Murakami, R., Tomikawa, T., Shin-ya, K., Shinozaki, J., Kajiura, T., Seto, H., et al. (2001). Ammocidin, a new apoptosis inducer in ras-dependent cells from *Saccharothrix* sp. II. Physico-chemical properties and structure elucidation. *J. Antibiot.* 54, 714–717. doi: 10.7164/antibiotics.54.714

Nachtigall, J., Kulik, A., Helaly, S., Bull, A. T., Goodfellow, M., Asenjo, J. A., et al. (2011). Atacamycins A-C, 22-membered antitumor macrolactones produced by *Streptomyces* sp. C38. *J. Antibiot.* 64, 775–780. doi: 10.1038/ja.2011.96

Nothias, L. F., Nothias-Esposito, M., Da, S. R., Wang, M., Protsyuk, I., Zhang, Z., et al. (2018). Bioactivity-based molecular networking for the discovery of drug leads in natural product bioassay-guided fractionation. *J. Nat. Prod.* 81, 758–767. doi: 10.1021/acs.jnatprod.7b00737

Okoro, C. K., Brown, R., Jones, A. L., Andrews, B. A., Asenjo, J. A., Goodfellow, M., et al. (2009). Diversity of culturable actinomycetes in hyper-arid soils of the Atacama Desert, Chile. *Antonie Van Leeuwenhoek* 95, 121–133. doi: 10.1007/s10482-008-9295-2

Olanrewaju, O. S., and Babalola, O. O. (2019). *Streptomyces*: implications and interactions in plant growth promotion. *Appl. Microbiol. Biotechnol.* 103, 1179–1188. doi: 10.1007/s00253-018-09577-y

Orita, M., Yasumuro, K., Kokubo, K., Shimizu, M., Abe, K., Tokunaga, T., et al. (1995). YM-47141 and YM-47142, new elastase inhibitors produced by *Flexibacter* sp. Q17897. Part 2. Structure elucidation. *J. Antibiot.* 48, 1425–1429. doi: 10.7164/antibiotics.48.1425

O'Rourke, A., Beyhan, S., Choi, Y., Morales, P., Chan, A. P., Espinoza, J. L., et al. (2020). Mechanism-of-action classification of antibiotics by global transcriptome profiling. *Antimicrob. Agents Chemother.* 64, e01207–e01219. doi: 10.1128/AAC.01207-19

Osterman, I. A., Komarova, E. S., Shiryaev, D. I., Korniltsev, I. A., Khven, I. M., Lukyanov, D. A., et al. (2016). Sorting out antibiotics' mechanisms of action: a double fluorescent protein reporter for high-throughput screening of ribosome and DNA biosynthesis inhibitors. *Antimicrob. Agents Chemother.* 60, 7481–7489. doi: 10.1128/AAC.02117-16

Pew Charitable Trusts (2020). Tracking the global pipeline of antibiotics in development, April 2020. Available at: https://www.pewtrusts.org/en/research-and-analysis/issue-briefs/2020/04/tracking-the-global-pipeline-of-antibiotics-in-development (Accessed September 6, 2020).

Pham, J. V., Yilma, M. A., Feliz, A., Majid, M. T., Maffetone, N., Walker, J. R., et al. (2019). A review of the microbial production of bioactive natural products and biologics. *Front. Microbiol.* 10:1404. doi: 10.3389/fmicb.2019.01404

Rateb, M. E., Houssen, W. E., Arnold, M., Abdelrahman, M. H., Deng, H., Harrison, W. T., et al. (2011a). Chaxamycins A-D, bioactive ansamycins from a hyper-arid desert *Streptomyces* sp. *J. Nat. Prod.* 74, 1491–1499. doi: 10.1021/np200320u

Rateb, M. E., Houssen, W. E., Harrison, W. T., Deng, H., Okoro, C. K., Asenjo, J. A., et al. (2011b). Diverse metabolic profiles of a *Streptomyces* strain isolated from a hyper-arid environment. *J. Nat. Prod.* 74, 1965–1971. doi: 10.1021/np200470u

Richter, M., and Rossello-Mora, R. (2009). Shifting the genomic gold standard for the prokaryotic species definition. *Proc. Natl. Acad. Sci. U. S. A.* 106, 19126–19131. doi: 10.1073/pnas.0906412106

Saitou, N., and Nei, M. (1987). The neighbor-joining method: a new method for reconstructing phylogenetic trees. *Mol. Biol. Evol.* 4, 406–425. doi: 10.1093/oxfordjournals.molbev.a040454

Sayed, A. M., Hassan, M., Alhadrami, H. A., Hassan, H. M., Goodfellow, M., and Rateb, M. E. (2020). Extreme environments: microbiology leading to specialized metabolites. *J. Appl. Microbiol.* 128, 630–657. doi: 10.1111/jam.14386

Schorn, M. A., Alanjary, M. M., Aguinaldo, K., Korobeynikov, A., Podell, S., Patin, N., et al. (2016). Sequencing rare marine actinomycete genomes reveals high density of unique natural product biosynthetic gene clusters. *Microbiology* 162, 2075–2086. doi: 10.1099/mic.0.000386

Schulz, D., Beese, P., Ohlendorf, B., Erhard, A., Zinecker, H., Dorador, C., et al. (2011). Abenquines A-D: aminoquinone derivatives produced by *Streptomyces* sp. strain DB634. *J. Antibiot.* 64, 763–768. doi: 10.1038/ja.2011.87

Selvameenal, L., Radhakrishnan, M., and Balagurunathan, R. (2009). Antibiotic pigment from desert soil actinomycetes; biological activity, purification and chemical screening. *Indian J. Pharm. Sci.* 71, 499–504. doi: 10.4103/0250-474X.58174

Seydlová, G., and Svobodová, J. (2008). Review of surfactin chemical properties and the potential biomedical applications. *Cent. Eur. J. Med.* 3, 123–133. doi: 10.2478/s11536-008-0002-5

Sghaier, H., Hezbri, K., Ghodhbane-Gtari, F., Pujic, P., Sen, A., Daffonchio, D., et al. (2016). Stone-dwelling actinobacteria *Blastococcus saxobsidens*, *Modestobacter marinus* and *Geodermatophilus obscurus* proteogenomes. *ISME J.* 10, 21–29. doi: 10.1038/ismej.2015.108

Shah, A. M., Shakeel-U-Rehman, Hussain, A., Mushtaq, S., Rather, M. A., Shah, A., et al. (2017). Antimicrobial investigation of selected soil actinomycetes

isolated from unexplored regions of Kashmir Himalayas, India. *Microb. Pathog.* 110, 93–99. doi: 10.1016/j.micpath.2017.06.017

Shannon, P., Markiel, A., Ozier, O., Baliga, N. S., Wang, J. T., Ramage, D., et al. (2003). Cytoscape: a software environment for integrated models of biomolecular interaction networks. *Genome Res.* 13, 2498–2504. doi: 10.1101/gr.1239303

Shirling, E. B., and Gottlieb, D. (1966). Methods for characterization of *Streptomyces* species. *Int. J. Syst. Bacteriol.* 16, 313–340. doi: 10.1099/00207713-16-3-313

Skellam, E. J., Stewart, A. K., Strangman, W. K., and Wright, J. L. (2013). Identification of micromonolactam, a new polyene macrocyclic lactam from two marine *Micromonospora* strains using chemical and molecular methods: clarification of the biosynthetic pathway from a glutamate starter unit. *J. Antibiot.* 66, 431–441. doi: 10.1038/ja.2013.34

Steven, B., Gallegos-Graves, L. V., Starkenburg, S. R., Chain, P. S., and Kuske, C. R. (2012). Targeted and shotgun metagenomic approaches provide different descriptions of dryland soil microbial communities in a manipulated field study. *Environ. Microbiol. Rep.* 4, 248–256. doi: 10.1111/j.1758-2229.2012.00328.x

Takahashi, A., Hotta, K., Saito, N., Morioka, M., Okami, Y., and Umezawa, H. (1986). Production of novel antibiotic, dopsisamine, by a new subspecies of *Nocardiopsis mutabilis* with multiple antibiotic resistance. *J. Antibiot.* 39, 175–183. doi: 10.7164/antibiotics.39.175

Takeuchi, M., Takahashi, S., Enokita, R., Sakaida, Y., Haruyama, H., Nakamura, T., et al. (1992). Galacardins a and B, new glycopeptide antibiotics. *J. Antibiot.* 45, 297–305. doi: 10.7164/antibiotics.45.297

Tang, X. L., Dai, P., Gao, H., Wang, C. X., Chen, G. D., Hong, K., et al. (2016). A single gene cluster for chalcomycins and aldgamycins: genetic basis for bifurcation of their biosynthesis. *ChemBioChem* 17, 1241–1249. doi: 10.1002/cbic.201600118

Tiwari, K., Upadhyay, D. J., Mösker, E., Süssmuth, R., and Gupta, R. K. (2015). Culturable bioactive actinomycetes from the great Indian Thar Desert. *Ann. Microbiol.* 65, 1901–1914. doi: 10.1007/s13213-014-1028-3

Tomita, K., Oda, N., Hoshino, Y., Ohkusa, N., and Chikazawa, H. (1991). Fluvirucins A_1, A_2, B_1, B_2, B_3, B_4 and B_5, new antibiotics active against influenza a virus II structure determination. *J. Antibiot.* 44, 940–948. doi: 10.7164/antibiotics.44.940

Van Santen, J. A., Jacob, G., Singh, A. L., Aniebok, V., Balunas, M. J., Bunsko, D., et al. (2019). The natural products atlas: an open access knowledge base for microbial natural products discovery. *ACS Cent. Sci.* 5, 1824–1833. doi: 10.1021/acscentsci.9b00806

Vértesy, L., Barbone, F. P., Cashman, E., Decker, H., Ehrlich, K., Jordan, B., et al. (2001). Pluraflavins, potent antitumor antibiotics from *Saccharothrix* sp. DSM 12931. *J. Antibiot.* 54, 718–729. doi: 10.7164/antibiotics.54.718

Wang, M., Carver, J. J., Phelan, V. V., Sanchez, L. M., Garg, N., Peng, Y., et al. (2016a). Sharing and community curation of mass spectrometry data with global natural products social molecular networking. *Nat. Biotechnol.* 34, 828–837. doi: 10.1038/nbt.3597

Wang, C. X., Ding, R., Jiang, S. T., Tang, J. S., Hu, D., Chen, G. D., et al. (2016b). Aldgamycins J-O, 16-membered macrolides with a branched octose unit from *Streptomycetes* sp. and their antibacterial activities. *J. Nat. Prod.* 79, 2446–2454. doi: 10.1021/acs.jnatprod.6b00200

Wang, T., Li, F., Lu, Q., Wu, G., Jiang, Z., Liu, S., et al. (2020a). Studies on diversity, novelty, antimicrobial activity, and new antibiotics of cultivable endophytic actinobacteria isolated from psammophytes collected in Taklamakan Desert. *J. Pharm. Anal.* doi: 10.1016/j.jpha.2020.06.004 (in press).

Wang, T., Lu, Q., Sun, C., Lukianov, D., Osterman, I. A., Sergiev, P. V., et al. (2020b). Hetiamacin E and F, new amicoumacin antibiotics from *Bacillus subtilis* PJS using MS/MS-based molecular networking. *Molecules* 25:4446. doi: 10.3390/molecules25194446

Wang, X., Tabudravu, J., Jaspars, M., and Deng, H. (2013). Tianchimycins A–B, 16-membered macrolides from the rare actinomycete *Saccharothrix xinjiangensis*. *Tetrahedron* 69, 6060–6064. doi: 10.1016/j.tet.2013.05.094

Wichner, D., Idris, H., Houssen, W. E., McEwan, A. R., Bull, A. T., Asenjo, J. A., et al. (2017). Isolation and anti-HIV-1 integrase activity of lentzeosides A-F from extremotolerant *lentzea* sp. H45, a strain isolated from a high-altitude Atacama Desert soil. *J. Antibiot.* 70, 448–453. doi: 10.1038/ja.2016.78

Wilson, D. N. (2014). Ribosome-targeting antibiotics and mechanisms of bacterial resistance. *Nat. Rev. Microbiol.* 12, 35–48. doi: 10.1038/nrmicro3155

Wink, J., Kroppenstedt, R. M., Seibert, G., and Stackebrandt, E. (2003). *Actinomadura namibiensis* sp. nov. *Int. J. Syst. Evol. Microbiol.* 53, 721–724. doi: 10.1099/ijs.0.02286-0

Woodworth, K. R., Walters, M. S., Weiner, L. M., Edwards, J., Brown, A. C., Huang, J. Y., et al. (2018). Vital signs: containment of novel multidrug-resistant organisms and resistance mechanisms-United States, 2006-2017. *MMWR Morb. Mortal. Wkly Rep.* 67, 396–401. doi: 10.15585/mmwr.mm6713e1

Yang, W. (2018). *Atlas of sandy deserts in China*. China: Science press.

Yang, X., Preusser, F., and Radtke, U. (2006). Late quaternary environmental changes in the Taklamakan Desert, western China, inferred from OSL-dated lacustrine and aeolian deposits. *Quat. Sci. Rev.* 25, 923–932. doi: 10.1016/j.quascirev.2005.06.008

Yoon, S. H., Ha, S. M., Kwon, S., Lim, J., Kim, Y., Seo, H., et al. (2017). Introducing EzBioCloud: a taxonomically united database of 16S rRNA gene sequences and whole-genome assemblies. *Int. J. Syst. Evol. Microbiol.* 67, 1613–1617. doi: 10.1099/ijsem.0.001755

Yoshimura, S., Tsurumi, Y., Takase, S., and Okuhara, M. (1995). WS5624 a and B, new endothelin converting enzyme inhibitors isolated from *Saccharothrix* sp. no. 75624 II. Structure elucidation of WS75624 a and B. *J. Antibiot.* 48, 1073–1075. doi: 10.7164/antibiotics.48.1073

Yu, L. Z., Luo, X. S., Liu, M., and Huang, Q. (2015). Diversity of ionizing radiation-resistant bacteria obtained from the Taklimakan Desert. *J. Basic Microbiol.* 55, 135–140. doi: 10.1002/jobm.201300390

Zgurskaya, H. I., Krishnamoorthy, G., Ntreh, A., and Lu, S. (2011). Mechanism and function of the outer membrane channel TolC in multidrug resistance and physiology of enterobacteria. *Front. Microbiol.* 2:189. doi: 10.3389/fmicb.2011.00189

Zitouni, A., Boudjella, H., Lamari, L., Badji, B., Mathieu, F., Lebrihi, A., et al. (2005). *Nocardiopsis* and *Saccharothrix* genera in Saharan soils in Algeria: isolation, biological activities and partial characterization of antibiotics. *Res. Microbiol.* 156, 984–993. doi: 10.1016/j.resmic.2005.05.006

Zitouni, A., Sabaou, N., Mathieu, F., and Lebrihi, A. (2007). *Novel saccharothrix strain and antibiotics derived therefrom, i.e. Mutactimycins and aldgamycins*. Washington, DC: U.S. Patent and Trademark Office, U.S. Patent No 20070202574A1.

Conflict of Interest: The authors declare that the research was conducted in the absence of any commercial or financial relationships that could be construed as a potential conflict of interest.

frontiers in Microbiology

ORIGINAL RESEARCH
published: 16 June 2021
doi: 10.3389/fmicb.2021.657072

Diversity and Distribution of Uncultured and Cultured Gaiellales and Rubrobacterales in South China Sea Sediments

Rou-Wen Chen[1,2], Yuan-Qiu He[1,2], Lin-Qing Cui[1,2], Cun Li[1,2], Song-Biao Shi[1,2], Li-Juan Long[1,3] and Xin-Peng Tian[1,3]**

[1] CAS Key Laboratory of Tropical Marine Bio-resources and Ecology, Guangdong Key Laboratory of Marine Materia Medica, RNAM Center for Marine Microbiology, South China Sea Institute of Oceanology, Chinese Academy of Sciences, Guangzhou, China, [2] College of Earth and Planetary Sciences, University of Chinese Academy of Sciences, Beijing, China, [3] Southern Marine Science and Engineering Guangdong Laboratory (Guangzhou), Guangzhou, China

OPEN ACCESS

Edited by:
George Tsiamis,
University of Patras, Greece

Reviewed by:
Huiluo Cao,
The University of Hong Kong, Hong Kong, China
Gaosen Zhang,
Cold and Arid Regions Environmental and Engineering Research Institute, Chinese Academy of Sciences, China
Guangxiu Liu,
Northwest Institute of Eco-Environment and Resources, Chinese Academy of Sciences (CAS), China

***Correspondence:**
Li-Juan Long
longlj@scsio.ac.cn
Xin-Peng Tian
xinpengtian@scsio.ac.cn

Specialty section:
This article was submitted to Systems Microbiology, a section of the journal Frontiers in Microbiology

Received: 22 January 2021
Accepted: 23 April 2021
Published: 16 June 2021

Citation:
Chen R-W, He Y-Q, Cui L-Q, Li C, Shi S-B, Long L-J and Tian X-P (2021) Diversity and Distribution of Uncultured and Cultured Gaiellales and Rubrobacterales in South China Sea Sediments. Front. Microbiol. 12:657072. doi: 10.3389/fmicb.2021.657072

Actinobacteria are ubiquitous in marine ecosystems, and they are regarded as an important, underexplored, potential pharmaceutical resource. The orders Gaiellales and Rubrobacterales are deep taxonomic lineages of the phylum Actinobacteria, both are represented by a single genus and contain only a few species. Although they have been detected frequently by high-throughput sequencing, their functions and characteristics in marine habitats remain unknown due to the lack of indigenous phenotypes. Here, we investigated the status of the orders in South China Sea (SCS) sediments using culture-independent and culture-dependent methods. Gaiellales is the second-most abundant order of Actinobacteria and was widely distributed in SCS sediments at water depths of 42–4,280 m, and four novel marine representatives in this group were successfully cultured. Rubrobacterales was present at low abundance in energy-limited marine habitats. An isolation strategy for Rubrobacterales from marine samples was proposed, and a total of 138 mesophilic Rubrobacterales strains were isolated under conditions of light and culture time combined with high-salinity or low-nutrient media. Marine representatives recovered in this study formed branches with a complex evolutionary history in the phylogenetic tree. Overall, the data indicate that both Gaiellales and Rubrobacterales can adapt to and survive in extreme deep-sea environments. This study lays the groundwork for further analysis of the distribution and diversity of the orders Gaiellales and Rubrobacterales in the ocean and provides a specific culture strategy for each group. The results open a window for further research on the ecological roles of the two orders in marine ecosystems.

Keywords: Actinobacteria, Gaiellales, Rubrobacterales, marine sediment, culture

INTRODUCTION

The deep sea is a permanently dark, low-temperature, high hydrostatic pressure, nutrient-limited habitat that possesses great diversity in microbial organisms. The deep sea is considered a resource for mining new and potentially valuable microbial species (Hassan and Shaikh, 2017). Actinobacteria are an important component of the bacterial community and are widely distributed

in marine environments (Lam, 2006; Ward and Bora, 2006). Since the discovery of novel bioactive compounds such as salinosporamides (Marizomib) from marine actinobacteria, searching for new or rare marine actinobacteria has become a focus of marine microbial research (Dhakal et al., 2017).

The orders Gaiellales and Rubrobacterales were established by Albuquerque et al. (2011) and Stackebrandt et al. (1997), respectively. They are two deep monogenetic branches in the phylogenetic tree of the phylum Actinobacteria (Salam et al., 2020), which is of considerable evolutionary importance. Members of the two orders are aerobic and chemoheterotrophic but are difficult to culture, severely restricting the study of their function. The order Gaiellales was proposed as a separate order from Rubrobacterales and contains only one species, *Gaiella occulta* (Albuquerque et al., 2011). The obligate cultivation strategy and insufficient data concerning cultivated species of Gaiellales has hindered its identification in marine ecosystems. Previous research revealed that Gaiellales was predominant in various extreme environments such as weathered serpentine rock (Khilyas et al., 2019), mangrove wetlands (Liu et al., 2019), saline–alkaline soil (Peng et al., 2017), wastewater treatment plants (Shu et al., 2015), and marine ascidians (Steinert et al., 2015). Rubrobacterales is an extremophilic actinobacteria that is abundant in sunlight-exposed biofilms and in the highly irradiated Chernobyl area (Ragon et al., 2011), and dominates in desiccated areas such as speleothems (Vardeh et al., 2018), the Atacama desert (Crits-Christoph et al., 2013), and arid soils (Bachar et al., 2012). The genus *Rubrobacter* is known for the first radiation-resistant species *Rubrobacter radiotolerans*, which was isolated from a radioactive spring (Yoshinaka et al., 1973; Suzuki et al., 1988). *Rubrobacter* species from terrestrial habitats are a potential source of bioactive compounds with ecological applications such as radiation-resistant, desiccant-resistant, and enzymatic radical scavengers (Albuquerque et al., 2014), but they are rarely isolated from marine habitats due to their slow growth and the difficulty of recovery (Kämpfer et al., 2014; Chen et al., 2018).

The limitation of detecting unculturable taxa in marine bacterial communities has been partially conquered via the application of molecular ecological technology (Daae et al., 2013). Most indigenous marine bacteria play key roles in the marine ecosystem but have not been cultured due to insufficient understanding of their physiology and environmental interactions (Vartoukian et al., 2010; Stewart, 2012). Hence, endeavors to devise specific cultivation strategies are important. It is widely accepted that culture-dependent and culture-independent surveys yield different insights into actinobacterial diversity (Vaz-Moreira et al., 2011; Maldonado et al., 2018). Both molecular-based and cultivation-based approaches have been applied in exploring the broad diversity of the obligate marine actinomycete genus *Salinispora* from marine sediments (Mincer et al., 2005). Combining these two approaches to describe actinobacterial diversity is feasible, as they are complementary and partly compensate each other's inherent limitations (Sun et al., 2010).

In this study, we used culture-independent and culture-dependent analyses to examine the distribution, abundance, diversity, and evolutionary status of the two less-studied actinobacterial orders Gaiellales and Rubrobacterales in the South China Sea (SCS). Our study provides a specific culture strategy for each group. Using this method, we obtained hundreds of pure strains within these two groups. We also demonstrate that there are many potentially new taxa in the orders Gaiellales and Rubrobacterales in marine sedimentary environments.

MATERIALS AND METHODS

Sediment Samples

Sampling was conducted during two open cruises in the SCS by R/V Shiyan 1 and R/V Shiyan 3. Twenty-nine sediment samples distributed over the SCS area from depths ranging from 42 to 4,280 m were collected from the sites shown in **Figure 1**. The name and site location information of samples are listed in **Supplementary Table 1**. A surface layer of sandy mud from 0 to 1 cm was obtained as a subsample aseptically after collecting using a grab-bucket collection sampler. The 29 sediment samples of the SCS were prepared for culture-independent experiments and stored at −20°C without pretreatment. All sediment samples were transported to the laboratory for further culture-dependent experiments.

DNA Extraction, PCR Amplification, and Illumina Hiseq Sequencing

Total environmental DNA of the marine sediments was extracted using a DNeasy Power Soil Kit (MoBio, United States) following the manufacturer's instructions. The V4 hypervariable region, about 400 bp of bacterial 16S rDNA, was amplified with prokaryotic universal primers 515F (5′-GTGCCAGCMGCCGCGGTAA-3′) and 806R (5′-GGACTACVSGGGTATCTAAT-3′) (Caporaso et al., 2011). PCR amplification was performed using TaKaRa Premix Taq version 2.0 (TaKaRa Biotechnology Co., Dalian, China) in a mixture with a final volume of 50 μl that contained 60 ng of DNA as a template, 10 μM of each primer, 25 μl of 2×Premix Taq, and nuclease-free water. The amplification was carried out using a BioRad S1000 (Bio-Rad Laboratory, CA, United States) thermocycler using the following procedure: 94°C for 5 min, 30 cycles of denaturation at 94°C for 30 s, primer annealing at 52°C for 30 s, and extension at 72°C for 30 s followed by a final extension at 72°C for 10 min and holding at 4°C. Each genomic DNA sample was amplified in triplicate. The quality of the purified PCR products was detected by 1% agarose gel electrophoresis. The PCR products for each sample were between 290 and 310 bp after concentration using GeneTools analysis software (Version 4.03.05.0, SynGene) (Beisvag et al., 2006). The required volume of PCR product for each replicate was calculated for each sample in accordance with the principle of equal quality. The mixture was recovered by an EZNA Gel Extraction Kit (Omega, United States) for further analysis. The amplicon library of purified PCR products of each sample was prepared using a NEBNext Ultra DNA Library Prep Kit (New England Biolabs, United States) following standard procedures. The construction of an amplification library of paired-end sequences was carried

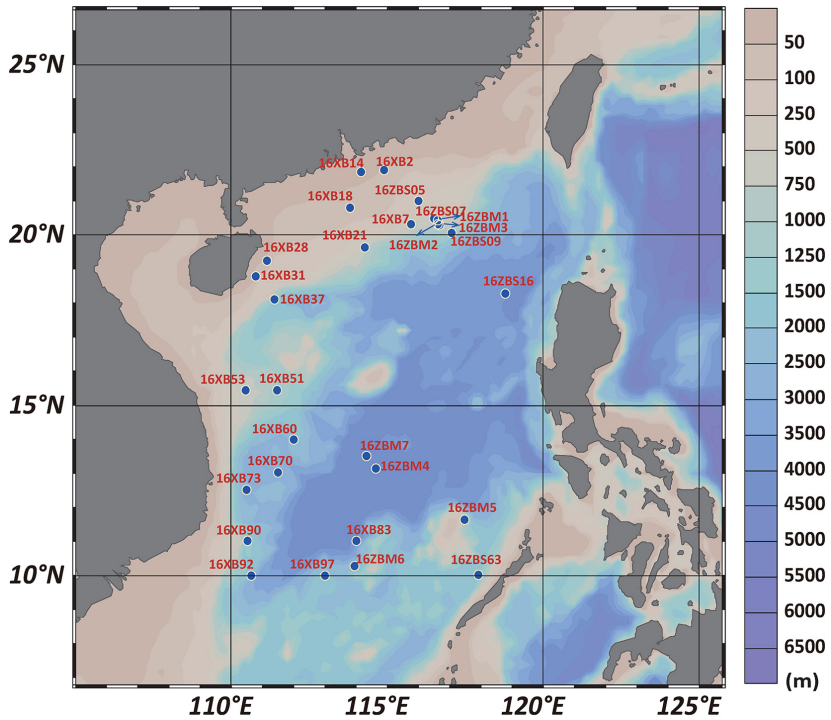

FIGURE 1 | Map of sampling site locations in the SCS area.

out on an Illumina Hiseq 2500 platform for PE250 sequencing according to the standard protocol (Guangdong Magigene Biotechnology Co., Ltd. Guangzhou, China).

Sequence Processing and Analyzing

Raw reads of Illumina data were quality filtered by Trimmomatic (V0.33) (Bolger et al., 2014). Paired-end clean reads were retrieved after barcodes and primers were removed by Mothur software (V1.35.1) (Schloss et al., 2009). Paired-end clean reads were then concatenated by FLASH (V1.2.11) (Magoc and Salzberg, 2011). The sequences assigned to operational taxonomic units (OTUs) were clustered at the level of 97% sequence similarity by USEARCH (V8.0.1517) (Edgar, 2010). OTUs annotation was performed using QIIME against the Greengenes database (V13_5) (DeSantis et al., 2006). The rarefaction curves were calculated using QIIME packages (Caporaso et al., 2010), and the values of Shannon, Simpson, and Margalef indices were calculated by PRIMER 6 (Clarke and Gorley, 2006). Maps of the distribution and abundance of uncultured phenotypes in the SCS were generated by Ocean Data View (Schlitzer, 2002).

Cultivation and Bacterial Taxonomic Classification

Samples were diluted two-fold with sterile seawater and mixed by vortexing before a 200 μl suspension was evenly spread on solid medium. Duplicated plates instead of triplicated plates of each medium were prepared for each sediment sample. Various types of separation media were designed and combined in the cultivation experiment for different nutritional requirements of the bacteria (**Supplementary Table 2**). Actinomycete Isolation Agar (AIA) medium, Marine Agar (MA)/MA-Starch media, and R2A medium were prepared with concentration gradients of various nutrients. The concentration of each medium was diluted to half, one-fifth, and one-tenth with water. Considering that some *Rubrobacter* species were reported to be moderately salt tolerant (Albuquerque et al., 2014), 10% (w/v) NaCl was added in some optimized media. Complex media and synthetic media were chosen and optimized by referring to published media for rare Actinobacteria, e.g., Acidimicrobiia, Thermoleophilia, and Rubrobacteria (Cleaver et al., 2007; Matsumoto et al., 2009; Matsumoto et al., 2013; He et al., 2020). The cultivation strategies were performed at different temperatures of 25–28, 37, and 55°C in petri dishes of two sizes (90 and 150 mm) and in the dark or under incandescent illumination of 8–12 μmol E m^{-2} s^{-1} at different time settings of 2–3 days, 7–14 days, and 1–3 months.

All colonies were selected to subculture on Marine Agar 2216E (MA, BD Difco^{TM}) medium. At least three rounds of subculturing were performed to obtain pure cultures. Purified isolates were maintained in glycerol suspensions (20%, w/v) at −80°C. Genomic DNA of isolates was extracted by 100 μl of a reagent consisting of 5% (w/v) chelax-100 resin dissolved with distilled water as described by Walsh et al. (1991). PCR amplification of the 16S rRNA gene was performed with bacterial general primers 27F (5′-GAGTTTGATCCTGGCTCAG-3′) and 1492R (5′-GGTTACCTTGTTACGACTT-3′) as described by Rainey et al. (1996). The 16S rRNA gene sequence was assembled via the SeqMan program (version 7.1.0), and low-quality

sequences were removed by the BioEdit program (Kimura, 1980). The nearly complete 16S rRNA gene sequence similarity analysis was carried out using EzBioCloud.[1]

Phylogenetic Analysis

The OTU sequences from the 16S rRNA gene amplicon sequencing and the nearly complete 16S rRNA gene sequences from cultured strains were selected for phylogenetic reconstruction. The reference representatives were retrieved from the GenBank database. Phylogenetic analysis was calculated using the Kimura two-parameter model, and the cladogram was constructed by neighbor joining (Saitou and Nei, 1987) in the MEGA X software (Kumar et al., 2018) and visualized by the interactive Tree of Life (iTOL v4) tool (Letunic and Bork, 2019).

PCA Analysis

Principal component analysis (PCA) allowed us to summarize and visualize the information concerning strains cultivated using multiple factors, including light intensity, culture time, salinity, dish size, temperature, and nutrient concentration. The cultured strains were divided into four groups: Gaiellales, Rubrobacterales, Actinomycetales, and non-Actinobacteria. The data were standardized automatically by the function PCA in FactoMineR (Le et al., 2008). The results provided a list of matrices (coordinates, correlations between variables and axes, squared cosine and sine contributions) for the variables that were extracted using the function get_pca_var, and similar results for the cultured strains were extracted using the function get_pca_ind from the PCA output in the factoextra R package (Kassambara and Mundt, 2020). The function fviz_pca_biplot in the factoextra R package was used to construct a biplot of cultured strains and variables (Kassambara and Mundt, 2020).

RESULTS

Illumina Hiseq Sequencing Information

In this study, a total of 785,421 high-quality effective sequences were gained from the sample libraries, and the average length of these overlapping paired-end sequences was about 374 bp. There were from 16,549 to 55,059 sequences of 2,170 to 6,821 OTUs obtained from the samples (**Supplementary Table 3**). The rarefaction curve tended to approach the saturation plateau, indicating that the sampling sizes were sufficient (**Supplementary Figure 1**). A total of 536,417 sequences of bacteria were obtained, with from 11,794 to 37,153 sequences distributed in 29 samples assigned to 16,825 OTUs (**Supplementary Table 3**). The number of OTUs ranged from 1,839 to 6,042, and 93 OTUs were shared among all samples, indicating that the bacteria were well distributed in different samples from various water depths.

Taxa of Uncultured Actinobacteria

A total of 22,074 sequences of 377 OTUs were assigned to the phylum Actinobacteria, and the average relative abundance of Actinobacteria was about 4.05%, ranging from 0.17 to 8.42%. The Shannon indices indicated that the actinobacterial diversity ranged from 2.77 to 6.25, while the Simpson indices ranged from 0.03 to 0.36. The Margalef indices indicated the actinobacterial species richness to be in the range 7.19 to 25.91 (**Supplementary Table 3**). Acidimicrobiales was the most abundant, accounting for 81.21% of Actinobacteria on average (**Figure 2** and **Supplementary Figure 2**). The orders Gaiellales, Actinomycetales, and Solirubrobacterales were the next most dominant groups detected in all sediment samples in the SCS, accounting for 5.8, 3.81, and 3.34% of Actinobacteria on average, respectively. The remaining Actinobacteria were mainly from known or Candidatus orders, including group *OPB41*, group *WCHB1-81,* and Rubrobacterales (**Supplementary Figure 2**). The groups *OPB41* and *WCHB1-81* and the order Rubrobacterales were rare with low relative abundance in partial samples from the SCS (**Figure 2**).

Taxa of Uncultured and Cultured Gaiellales and Rubrobacterales

There were 31 Gaiellales OTUs from 1,216 sequences detected in all sediment sample sites, and the relative abundance of the order was from 2.32 to 11.38% of the Actinobacteria (**Supplementary Table 4**). OTU 218 and OTU 484 were most frequently detected in the SCS, and OTUs 341 and 591 had the highest numbers in the 460 m depth environment sample (16ZBS07) (**Supplementary Table 5**). Thirty-one uncultured Gaiellales OTUs clustered with known Gaiellales representatives and formed multiple independent branches in the phylogenetic tree (**Figure 3**). Based on the culture-dependent method, only four Gaiellales strains were isolated from sediment samples taken at depths of 320–460 m, they were slow-growing on SN-Mn and MA plates and were better maintained in liquid MB media. They represented two potential new species by showing relatively low similarity (<89.0%) to the only known species *Gaiella occulta*. Four cultured strains were clustered with six uncultured OTUs and two unclassified species (*Gaiella* sp. EBR4-RS1 and *Gaiella* sp. EBR4-R2), they formed a separate cluster (named clade Gaiel II) far from the only known species *G. occulta* with a clear divergence and thus represent a new family group.

The order Rubrobacterales comprised a small proportion of Actinobacteria, with extremely low relative abundance (from 0.00 to 4.42% of Actinobacteria). The order was distributed sporadically in the SCS and occurred more in deep sea sediments than in the shallows. Four Rubrobacterales OTUs with 72 sequences were detected in nearly half of all samples, and two ubiquitous representatives, OTU 18976 and OTU 639, showed the highest numbers in the 3,503 m depth environmental sample (16XB83) (**Supplementary Table 5**). Finally, 138 strains assigned to the order Rubrobacterales were isolated from nine samples at depths from 323 to 4,280 m. Samples at water depths of 2,061, 3,448, and 460 m yielded 65, 34, and 21 *Rubrobacter* strains, respectively. The clustering tree of uncultured and cultured organisms revealed that they spanned five divergent phylogenetic lineages of the order Rubrobacterales (**Figure 3**). Hundreds of *Rubrobacter* strains and OTU 10386 were clustered together with two known species, *Rubrobacter aplysinae* and

[1]https://www.ezbiocloud.net/identify

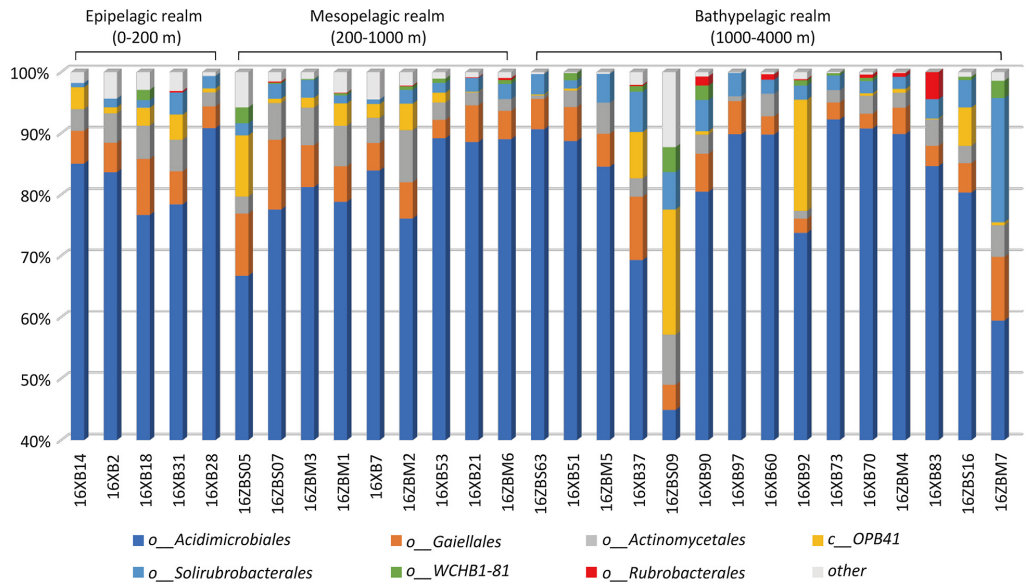

FIGURE 2 | Actinobacterial composition in 29 deep-sea sediments.

Rubrobacter bracarensis, as a part of clade Rubro I. Two sister groups, Rubro II and Rubro III, were ubiquitous in SCS sediments. Species *R. radiotolerans* and *R. indicoceani* were representative of the clades Rubro II and Rubro III, respectively; each had corresponding marine cultured strains and uncultured categories. Nine strains clustering with OTU 7567 formed a distinct phylogenetic cluster named clade Rubro IV and showed a great degree of novelty at the level of species diversity, with the highest similarity to other known species below 95%. Among these strains, we reported two strains as novel *Rubrobacter* species, *R. tropicus* and *R. marinus* (Chen et al., 2020). Moreover, the obtained 16S rRNAs of marine Rubrobacterales were most closely related to four species, *R. aplysinae*, *R. bracarensis*, *R. indicoceani,* and *R. radiotolerans.* However, no marine sequences in this study were related to Rubro V, which is composed of several terrestrial thermophilic species.

The Cultivation of Gaiellales and Rubrobacterales

To explore the relationships between cultured species in the orders Gaiellales and Rubrobacterales and to compare the results with normal bacterial growth, six culture factors (culture time, salinity, dish size, temperature, and nutrient concentration) and 3,504 cultured strains were analyzed using PCA (**Figure 4**). The first two principal components explained 67.2% of the variance. The closer a variable is to the correlation ellipse, the better its representation on the factor map. In the biplot, the variables light, time, and salinity contributed the most to dimensions 1 and 2. Cultured Rubrobacterales strains yielded high values for four factors (light, culture time, salinity, and dish size), but had low values for variables temperature and nutrient concentration. The PCA results were consistent with the culture results. Under optimal light conditions, 109 *Rubrobacter* strains were cultured. The high-salinity (over 10% (w/v) NaCl) media (YJSF, AIAS, and CAAM) yielded the greatest number of halo-tolerant *Rubrobacter* isolates (**Supplementary Figure 3**). Although the oligotrophic media (AIAE, SN, and ZANT) obtained the second largest number of *Rubrobacter* isolates, marine Rubrobacterales isolates required sufficient nutrition for growth; this was shown by the addition of 1% glucose to the medium. In this study, Gaiellales and Rubrobacterales formed visible colonies on isolation media when the cultivation time extended to at least one month at 25–28°C incubation. Only four marine Gaiellales strains were isolated from the inorganic medium with manganese metal ions and MA medium; this result needs further research to find the root causes or bottlenecks for bacterial growth and to design additional cultivation strategies.

DISCUSSION

Actinobacterial Vertical Distribution and Composition in the SCS

Actinobacteria are distributed globally in various marine habitats, including continental shelves, open ocean, and the deep sea (Ward and Bora, 2006; Jensen and Lauro, 2008). Previous studies have revealed the abundance of Actinobacteria in SCS sediment (relative abundance 4–10% of total sequences), which is more common in the deep sea than in the shallows (Zhu et al., 2013). In this study, the normally uneven fluctuation of actinobacterial abundance was generally stable in sediment environments (about 4.05%) (**Supplementary Figure 4**), but the diversity and species richness of Actinobacteria OTUs in shallow samples were higher than in deep samples (**Supplementary Table 3**). The composition of marine Actinobacteria at the level of order was remarkably similar to earlier research results (Durbin and Teske, 2011;

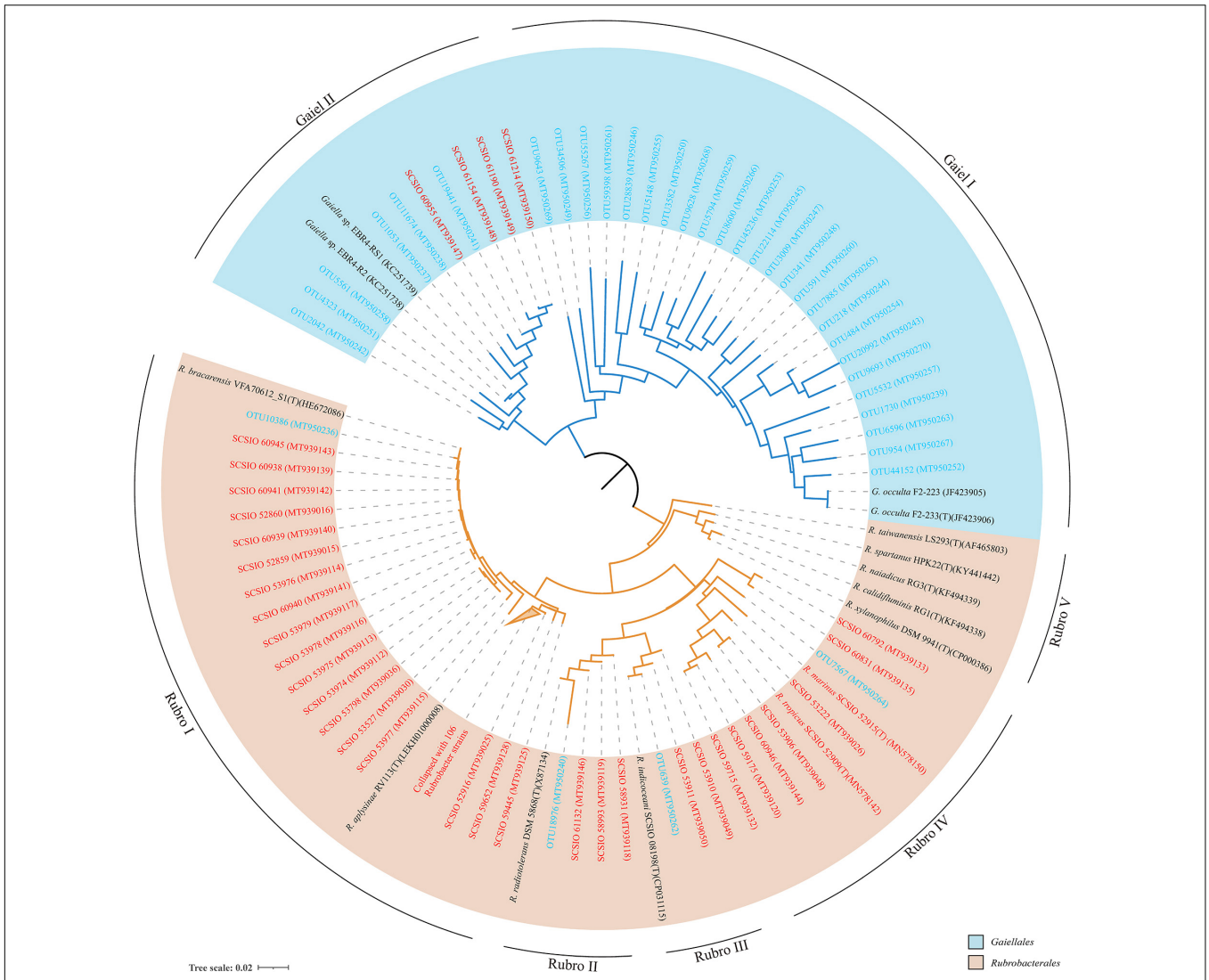

FIGURE 3 | The neighbor-joining tree showing phylogenetic relationships of cultured and uncultured Gaiellales and Rubrobacterales based on nearly full-length 16S rRNA gene sequences (>1,300 bp) and OTUs using 374 unambiguous nucleotides. Tree bar, 0.02 sequence divergence. The similar *Rubrobacter* strains were collapsed with a 2% threshold of dissimilarity. Red font indicates isolated strains; blue font indicates the environmental OTUs. GenBank accession numbers used are given in parentheses.

Chen et al., 2016). The most abundant Actinobacteria group was Acidimicrobiales, and the next most dominant groups were the orders Gaiellales, Actinomycetales, and Solirubrobacterales while Rubrobacterales comprised a minor fraction of the Actinobacteria. The actinobacterial taxa composition difference in the samples may be related to niche adaptation for inhabiting marine environments.

Distribution of Gaiellales and Rubrobacterales in the Deep Sea

Our study revealed that uncultured Gaiellales sequences were widely distributed from 42 to 4,280 m in SCS sediment environments, and Gaiellales was the second dominated uncultured marine Actinobacteria. Previous studies also showed that the order Gaiellales was predominant in a variety of marine habitats, such as submarine permafrost water, permafrost sediments (Mitzscherling et al., 2017), mangrove wetlands (Liu et al., 2019) and deep sea (Chen et al., 2016). The distribution patterns calculated by the diversity indices (Shannon, Simpson, and Margalef) showed that there was no obvious trend in the diversity of the two orders with the depth of sediment environments (**Supplementary Figure 5**). But the OTUs belonging to the clade Gaiel I were particularly abundant in the mesopelagic sediments (**Supplementary Table 5**) where the temperature ranged from about 8 to 2.5°C (Yang et al., 2018). Although it is unclear whether this high abundance is related to the adaptation to the middle and deep sea, this result further illustrated that Gaiellales is ubiquitous and widely distributed in SCS sediments, and also has a stronger ability to adapt to marine environment than the order Rubrobacterales.

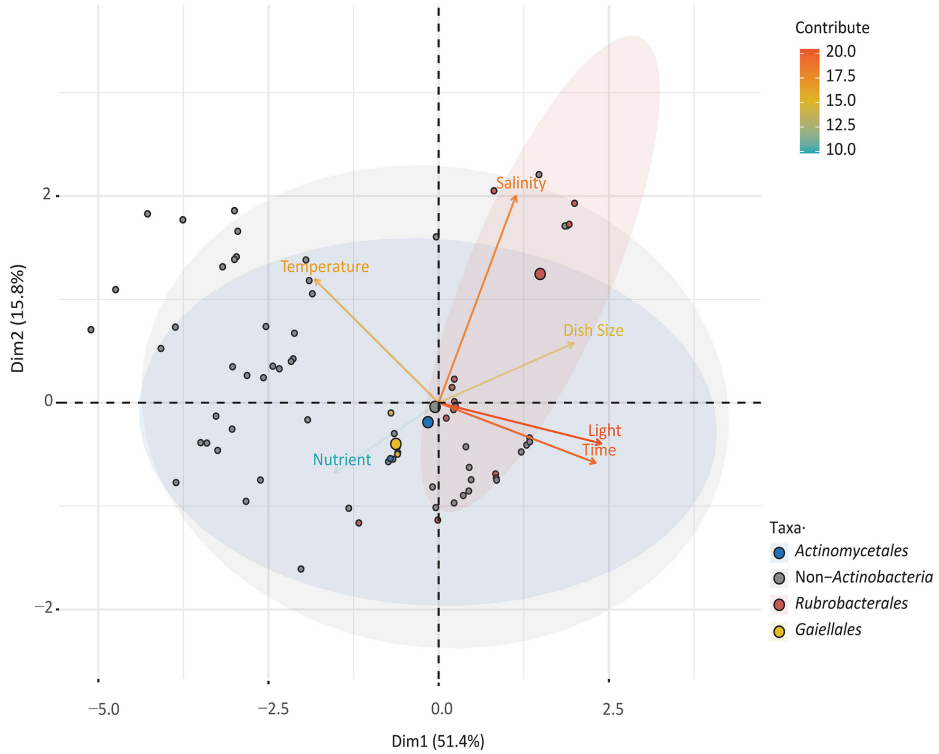

FIGURE 4 | Principal component analysis (PCA) illustrating the relationship between culturable taxa with cultivation variables.

The order Rubrobacterales was a ubiquitous group and had greater natural diversity, such as ancient vestiges (Schabereiter-Gurtner et al., 2001; Mihajlovski et al., 2017), rocky coasts (Molina-Menor et al., 2019), Arctic desert endostromatolites (Pellerin et al., 2009), etc. Rubrobacterales were also detected by high-throughput sequencing although the group comprised only a small proportion of the microorganisms in marine habitats (Brown and Bowman, 2001; Kochling et al., 2011). Similar results were also obtained in this study using the culture-independent method. But for the culture-dependent method, the optimal growth occurred when adding 1% glucose to the media, which implied that the bacteria may be restricted to deep sea sediments where nutrients are limited. They are actually found in deep sea sediments, where they were not detected by the uncultured method. The bacteria mainly exist in the bathypelagic sediments at depths of over 2,000 m, where the temperature is generally below 2.5°C (Yang et al., 2018). Therefore, we postulate that the order Rubrobacterales has cells with a slow growth disadvantage, and they may struggle to survive in nutritionally limited marine habitats.

Diversity of Gaiellales and Rubrobacterales in the Deep Sea

Previous results from interspecies heterogeneity of 16S rRNA genes showed that Gaiellales had a more complex genetic evolutionary history than Rubrobacterales, and this order may have undergone more evolutionary events in the marine environment (Steinert et al., 2015). However, only one valid published species in the order Gaiellales is not enough to supply the representative Candidatus for classifying cultured-independent OTUs, which severely limits the study of the order's diversity and phylogeny. New marine representative species and marine OTUs in this study were clustered into two separated groups named Gaiel I and Gaiel II, that represent potential new marine-derived higher-level taxa. The results support Gaiellales as having a large family tree with complex branches and a high level of evolution in the ocean, a hypothesis that is consistent with their wide distribution and high abundance in marine habitats.

For the order Rubrobacterales, previous study illustrated the limitations of analyzing its diversity and phylogeny by culture-independent surveys, due to the low abundance in marine environments (Rappe et al., 1999; Yooseph et al., 2007; Sunagawa et al., 2015). The deeper recognition of the special niche of rare uncultured Rubrobacterales in marine habitats required more pure cultured strains or genus-specific primers (Castro et al., 2019). In this study, four OTUs and 138 cultured strains clustered in four groups were found to be associated with oceans, expanding the phylogenetic tree of Rubrobacterales. And clade Rubro IV was clearly novel, as shown by the independence and the marine-derived characteristics. The phylogenetic tree of Rubrobacterales also showed that the evolution of these diverse strains is continuous in the marine ecosystem, a conjecture that perhaps they survived in the ancient, stable oceans and developed unique marine properties to adapt to the extreme deep-sea environments.

Isolation Strategies for Rubrobacterales and Gaiellales

It is necessary to successfully cultivate rare living species through a culture strategy, especially for the communities that are common but have low abundance. These rare species may serve as a potentially inexhaustible reservoir of genomic innovation, a factor that could explain how microbial communities episodically reshape planetary processes (Sogin et al., 2006). To obtain the optimal growth conditions for marine Rubrobacterales, an isolating strategy to improve the survival capacity in the laboratory was designed by simulating their natural environment to reverse the situation of nutritional disadvantage.

The *Rubrobacter* species survive well under illuminated conditions, with the ability to respond to reactive oxidative stress (ROS) and to efficiently repair DNA lesions (Egas et al., 2014). It has been reported that the growth of xero-tolerant heterotrophic *Rubrobacter* spp. can be promoted by decreased humidity and increased temperature combined with enhanced daylight irradiation (Imperi et al., 2007). In this study, compared to other light-sensitive bacteria that live in the dark aphotic zone of the deep ocean, the viability and competitive advantage of cultured Rubrobacterales on plates were enhanced by light, and 109 *Rubrobacter* strains were successfully isolated. Although most *Rubrobacter* species derived from terrestrial habitats are thermophilic (Carreto et al., 1996; Chen et al., 2004; Albuquerque et al., 2014; Norman et al., 2017), no isolates of the order Rubrobacterales showed thermotolerant ability in this study. Instead, 44 *Rubrobacter* strains were isolated from Indian Ocean sediments by incubation at 4°C for one year. Since marine sediments are largely present in low-temperature environments, the presence of low temperature-adapted bacteria with low thermostable enzymes (inactivated at temperatures over 40°C) would be expected (Hardeman and Sjoling, 2007). This is consistent with the result that no growth was observed at temperatures over 40°C in marine *Rubrobacter* species (Kämpfer et al., 2014; Chen et al., 2018).

When designing the synthetic media, the salinity and nutrient levels were first considered. In the present study the greatest numbers of halo-tolerant *Rubrobacter* isolates were obtained from high-salinity media, and the second-highest quantity was obtained using oligotrophic media. We speculate that the high-salinity or oligotrophic media restricted the growth of fast-growing bacteria, and the eutrophic bacteria were intolerant to starvation and ultimately died (Gray et al., 2019). Marine *Rubrobacter* species grew slowly and took a long time to form red colonies on plates (Kämpfer et al., 2014; Chen et al., 2018). Similarly, marine Gaiellales and Rubrobacterales were successfully cultured when the cultivation time was extended to at least one month. The subcultures also required at least two weeks to form rich visible colonies on plates. Recent results show that slow-growing colonies are usually discovered at a nutritional disadvantage status when one fast-growing strain is competing for nutrition resources under the same culture conditions (Carini, 2019). Hence, prolonging the incubation time can increase the ratio of viable counts of rare, slow-growing bacteria on media (Stevenson et al., 2004). Moreover, a drastic increase in the quantity of *Rubrobacter* colonies was discovered in this study using large-size petri dishes (150 mm), perhaps due to competition for the living space and the reduced competitive pressure for slowly growing or poorly adaptable bacteria such as Rubrobacterales and Gaiellales.

For the order Gaiellales, the sole known representative was isolated from a mineral water bottling plant, where the borehole water had a temperature of 28°C, a pH of 5.9, and was poor in mineral ions (Albuquerque et al., 2011). However, the lack of phenotypic and genomic annotated information increased the difficulty of the culture (Severino et al., 2019). One interesting result is that Gaiellales are strict chemoorganotrophs, as inferred by genomic data, but they could be cultured from an inorganic medium (SN-Mn) made up of 50% seawater in this study. This suggests that their growth may depend on certain nutrients in seawater that are not present in the laboratory and thereby make them difficult to culture. Further results showed that marine Gaiellales strains were hygrophilous and halophilic, different from the species *G. occulta*. Therefore, simulating the natural environment, especially its potential key factors, is an effective strategy for isolating novel, rare, or uncultured bacteria (Mu et al., 2020).

CONCLUSION

In this study, we analyzed the status of the orders Gaiellales and Rubrobacterales in marine sediments of the SCS using culture-independent and culture-dependent methods. We concluded the following: (1) The order Gaiellales was the second-most dominant order of Actinobacteria, distributed in all detected sediment samples in different water depths of the SCS, but it could hardly be cultured; the order Rubrobacterales was present in low abundance but displayed a steady existence in over more than half of the marine sediments. (2) Marine Gaiellales are highly diverse in the ocean, and they can be separated into two main branches as higher-level new taxa. Each branch was represented by cultured representatives; marine Rubrobacterales clustered in four groups were associated with four known species, *R. aplysinae*, *R. bracarensis*, *R. indicoceani*, and *R. radiotolerans*. Clade Rubro IV is a novel independent branch from the deep sea. (3) Light, high salinity, culture time, or low nutrient levels at optimal growth temperature were the most effective factors for Rubrobacterales survival under laboratory conditions. The order Gaiellales may depend on certain marine factors for growth, and their ability to be cultured needs to be researched further by mimicking the natural habitat.

DATA AVAILABILITY STATEMENT

The datasets presented in this study can be found in the NCBI database with accession numbers SRR12534320–SRR12534348 and MT939011–MT950270.

AUTHOR CONTRIBUTIONS

X-PT and L-JL designed the workflow. R-WC and Y-QH collected the environmental samples and performed the cultivation and also prepared the manuscript. CL and L-QC helped in data collection and making figure and tables. S-BS helped in improving the manuscript. All authors reviewed and corrected the manuscript.

FUNDING

This research was supported by the Guangdong Local Innovation Team Program (2019BT02Y262), the K.C. Wong Education Foundation (GJTD-2020-12), the Talents Team of Southern Marine Science and Engineering Guangdong Laboratory (Guangzhou) (GML2019ZD0402, GML2019ZD0404), the National Natural Science Foundation of China (No. 41576143, 41276004), and the South China Sea Open Cruise by R/V Shiyan 1 and R/V Shiyan 3, South China Sea Institute of Oceanology, CAS.

SUPPLEMENTARY MATERIAL

The Supplementary Material for this article can be found online at: https://www.frontiersin.org/articles/10.3389/fmicb.2021.657072/full#supplementary-material

REFERENCES

Albuquerque, L., Franca, L., Rainey, F. A., Schumann, P., Nobre, M. F., and da Costa, M. S. (2011). *Gaiella occulta* gen. nov., sp. nov., a novel representative of a deep branching phylogenetic lineage within the class actinobacteria and proposal of Gaiellaceae fam. nov. and *Gaiellales* ord. nov. *Syst. Appl. Microbiol.* 34, 595–599. doi: 10.1016/j.syapm.2011.07.001

Albuquerque, L., Johnson, M. M., Schumann, P., Rainey, F. A., and da Costa, M. S. (2014). Description of two new *thermophilic species* of the genus *Rubrobacter*, *Rubrobacter calidifluminis* sp. nov. and *Rubrobacter naiadicus* sp. nov., and emended description of the genus *Rubrobacter* and the species *Rubrobacter bracarensis*. *Syst. Appl. Microbiol.* 37, 235–243. doi: 10.1016/j.syapm.2014.03.001

Bachar, A., Soares, M. I., and Gillor, O. (2012). The effect of resource islands on abundance and diversity of bacteria in arid soils. *Microb. Ecol.* 63, 694–700. doi: 10.1007/s00248-011-9957-x

Beisvag, V., Junge, F. K., Bergum, H., Jolsum, L., Lydersen, S., Gunther, C. C., et al. (2006). GeneTools–application for functional annotation and statistical hypothesis testing. *BMC Bioinform.* 7:470. doi: 10.1186/1471-2105-7-470

Bolger, A. M., Lohse, M., and Usadel, B. (2014). Trimmomatic: a flexible trimmer for Illumina sequence data. *Bioinformatics* 30, 2114–2120. doi: 10.1093/bioinformatics/btu170

Brown, M. V., and Bowman, J. P. (2001). A molecular phylogenetic survey of sea-ice microbial communities (SIMCO). *FEMS Microbiol. Ecol.* 35, 267–275. doi: 10.1111/j.1574-6941.2001.tb00812.x

Caporaso, J. G., Kuczynski, J., Stombaugh, J., Bittinger, K., Bushman, F. D., Costello, E. K., et al. (2010). QIIME allows analysis of high-throughput community sequencing data. *Nat. Methods* 7, 335–336. doi: 10.1038/nmeth.f.303

Caporaso, J. G., Lauber, C. L., Walters, W. A., Berg-Lyons, D., Lozupone, C. A., Turnbaugh, P. J., et al. (2011). Global patterns of 16S rRNA diversity at a depth of millions of sequences per sample. *Proc. Natl. Acad. Sci. U.S.A.* 108(Suppl 1), 4516–4522. doi: 10.1073/pnas.1000080107

Carini, P. (2019). A "Cultural" renaissance: genomics bathes new life into an old craft. *mSystems* 4:e00092-91. doi: 10.1128/mSystems.00092-19

Carreto, L., Moore, E., Nobre, M. F., Wait, R., Riley, P. W., Sharp, R. J., et al. (1996). *Rubrobacter xylanophilus* sp nov: a new *thermophilic* species isolated from a thermally polluted effluent. *Int. J. Syst. Bacteriol.* 46, 460–465. doi: 10.1099/00207713-46-2-460

Castro, J. F., Nouioui, I., Asenjo, J. A., Andrews, B., Bull, A. T., and Goodfellow, M. (2019). New genus-specific primers for PCR identification of *Rubrobacter strains*. *Anton. Van Leeuwenhoek* 112, 1863–1874. doi: 10.1007/s10482-019-01314-3

Chen, M. Y., Wu, S. H., Lin, G. H., Lu, C. P., Lin, Y. T., Chang, W. C., et al. (2004). *Rubrobacter taiwanensis* sp. nov., a novel *thermophilic*, radiation-resistant species isolated from hot springs. *Int. J. Syst. Evol. Microbiol.* 54(Pt 5), 1849–1855. doi: 10.1099/ijs.0.63109-0

Chen, P., Zhang, L., Guo, X., Dai, X., Liu, L., Xi, L., et al. (2016). Diversity, biogeography, and biodegradation potential of Actinobacteria in the deep-sea sediments along the Southwest Indian Ridge. *Front. Microbiol.* 7:1340. doi: 10.3389/fmicb.2016.01340

Chen, R. W., Li, C., He, Y. Q., Cui, L. Q., Long, L. J., and Tian, X. P. (2020). *Rubrobacter tropicus* sp. nov. and *Rubrobacter marinus* sp. nov., isolated from deep-sea sediment of the South China Sea. *Int. J. Syst. Evol. Microbiol.* 70, 5576–5585. doi: 10.1099/ijsem.0.004449

Chen, R. W., Wang, K. X., Wang, F. Z., He, Y. Q., Long, L. J., and Tian, X. P. (2018). *Rubrobacter indicoceani* sp. nov., a new marine actinobacterium isolated from Indian Ocean sediment. *Int. J. Syst. Evol. Microbiol.* 68, 3487–3493. doi: 10.1099/ijsem.0.003018

Clarke, K. R., and Gorley, R. N. (2006). *PRIMER v6: User Manual/Tutorial, Plymouth Routine in Multivariate Ecological Research*. Plymouth, UK: PRIMER-E Ltd.

Cleaver, A. A., Burton, N. P., and Norris, P. R. (2007). A novel acidimicrobium species in continuous cultures of moderately *thermophilic*, mineral-sulfide-oxidizing acidophiles. *Appl. Environ. Microbiol.* 73, 4294–4299. doi: 10.1128/AEM.02658-06

Crits-Christoph, A., Robinson, C. K., Barnum, T., Fricke, W. F., Davila, A. F., Jedynak, B., et al. (2013). Colonization patterns of soil microbial communities in the Atacama Desert. *Microbiome* 1:28. doi: 10.1186/2049-2618-1-28

Daae, F. L., Okland, I., Dahle, H., Jorgensen, S. L., Thorseth, I. H., and Pedersen, R. B. (2013). Microbial life associated with low-temperature alteration of ultramafic rocks in the Leka ophiolite complex. *Geobiol* 11, 318–339. doi: 10.1111/gbi.12035

DeSantis, T. Z., Hugenholtz, P., Larsen, N., Rojas, M., Brodie, E. L., Keller, K., et al. (2006). Greengenes, a chimera-checked 16S rRNA gene database and workbench compatible with ARB. *Appl. Environ. Microbiol.* 72, 5069–5072. doi: 10.1128/AEM.03006-05

Dhakal, D., Pokhrel, A. R., Shrestha, B., and Sohng, J. K. (2017). Marine rare actinobacteria: isolation, characterization, and strategies for harnessing bioactive compounds. *Front. Microbiol.* 8:1106. doi: 10.3389/fmicb.2017.01106

Durbin, A. M., and Teske, A. (2011). Microbial diversity and stratification of South Pacific abyssal marine sediments. *Environ. Microbiol.* 13, 3219–3234. doi: 10.1111/j.1462-2920.2011.02544.x

Edgar, R. C. (2010). Search and clustering orders of magnitude faster than BLAST. *Bioinformatics* 26, 2460–2461. doi: 10.1093/bioinformatics/btq461

Egas, C., Barroso, C., Froufe, H., Pacheco, J., Albuquerque, L., and Costa, M. S. (2014). Complete genome sequence of the Radiation-Resistant bacterium *Rubrobacter radiotolerans* RSPS-4. *Stand Genom. Sci.* 9, 1062–1075. doi: 10.4056/sigs.5661021

Gray, D. A., Dugar, G., Gamba, P., Strahl, H., Jonker, M. J., and Hamoen, L. W. (2019). Extreme slow growth as alternative strategy to survive deep starvation in bacteria. *Nat. Commun.* 10:890. doi: 10.1038/s41467-019-08719-8

Hardeman, F., and Sjoling, S. (2007). Metagenomic approach for the isolation of a novel low-temperature-active lipase from uncultured bacteria of marine sediment. *FEMS Microbiol. Ecol.* 59, 524–534. doi: 10.1111/j.1574-6941.2006.00206.x

Hassan, S. S. U., and Shaikh, A. L. (2017). Marine actinobacteria as a drug treasure house. *Biomed. Pharmacother.* 87, 46–57. doi: 10.1016/j.biopha.2016.12.086

He, Y. Q., Chen, R. W., Li, C., Shi, S. B., Cui, L. Q., Long, L. J., et al. (2020). *Actinomarinicola tropica* gen. nov. sp. nov., a new marine actinobacterium of the family Iamiaceae, isolated from South China Sea sediment environments. *Int. J. Syst. Evol. Microbiol.* 70, 3852–3858. doi: 10.1099/ijsem.0.004251

Imperi, F., Caneva, G., Cancellieri, L., Ricci, M. A., Sodo, A., and Visca, P. (2007). The bacterial aetiology of rosy discoloration of ancient wall paintings. *Environ. Microbiol.* 9, 2894–2902. doi: 10.1111/j.1462-2920.2007.01393.x

Jensen, P. R., and Lauro, F. M. (2008). An assessment of actinobacterial diversity in the marine environment. *Anton. Van Leeuwenhoek* 94, 51–62. doi: 10.1007/s10482-008-9239-x

Kämpfer, P., Glaeser, S. P., Busse, H. J., Abdelmohsen, U. R., and Hentschel, U. (2014). *Rubrobacter* aplysinae sp. nov., isolated from the marine sponge *Aplysina aerophoba*. *Int. J. Syst. Evol. Microbiol.* 64, 705–709. doi: 10.1099/ijs.0.055152-0

Kassambara, A., and Mundt, F. (2020). *Factoextra: Extract and Visualize the Results of Multivariate Data Analyses. R Package Version 1.0.7*. Available online at: https://CRAN.R-project.org/package=factoextra (accessed April 1, 2020).

Khilyas, I. V., Sorokina, A. V., Elistratova, A. A., Markelova, M. I., Siniagina, M. N., Sharipova, M. R., et al. (2019). Microbial diversity and mineral composition of weathered serpentine rock of the *Khalilovsky massif*. *PLoS One* 14:e0225929. doi: 10.1371/journal.pone.0225929

Kimura, M. (1980). A simple method for estimating evolutionary rates of base substitutions through comparative studies of nucleotide-sequences. *J. Mol. Evol.* 16, 111–120. doi: 10.1007/Bf01731581

Kochling, T., Lara-Martin, P., Gonzalez-Mazo, E., Amils, R., and Sanz, J. L. (2011). Microbial community composition of anoxic marine sediments in the Bay of Cadiz (Spain). *Int. Microbiol.* 14, 143–154. doi: 10.2436/20.1501.01.143

Kumar, S., Stecher, G., Li, M., Knyaz, C., and Tamura, K. (2018). MEGA X: Molecular evolutionary genetics analysis across computing platforms. *Mol. Biol. Evol.* 35, 1547–1549. doi: 10.1093/molbev/msy096

Lam, K. S. (2006). Discovery of novel metabolites from marine actinomycetes. *Curr. Opin. Microbiol.* 9, 245–251. doi: 10.1016/j.mib.2006.03.004

Le, S., Josse, J., and Husson, F. (2008). FactoMineR: an R package for multivariate analysis. *J. Stat. Softw.* 25, 1–18. doi: 10.18637/jss.v025.i01

Letunic, I., and Bork, P. (2019). Interactive tree of life (iTOL) v4: recent updates and new developments. *Nucleic Acids Res.* 47, W256–W259. doi: 10.1093/nar/gkz239

Liu, M., Huang, H., Bao, S., and Tong, Y. (2019). Microbial community structure of soils in *Bamenwan mangrove* wetland. *Sci. Rep.* 9:8406. doi: 10.1038/s41598-019-44788-x

Magoc, T., and Salzberg, S. L. (2011). FLASH: fast length adjustment of short reads to improve genome assemblies. *Bioinformatics* 27, 2957–2963. doi: 10.1093/bioinformatics/btr507

Maldonado, M. J., Albarracin, V. H., Lara, J. A., Ferrero, M. A., and Farias, M. E. (2018). Culture-dependent and - independent methods reveal dominance of halophilic Euryarchaeota in high-altitude Andean lakes. *Aquat. Microb. Ecol.* 81, 171–188. doi: 10.3354/ame01863

Matsumoto, A., Kasai, H., Matsuo, Y., Omura, S., Shizuri, Y., and Takahashi, Y. (2009). *Ilumatobacter fluminis* gen. nov., sp. nov., a novel actinobacterium isolated from the sediment of an estuary. *J. Gen. Appl. Microbiol.* 55, 201–205. doi: 10.2323/jgam.55.201

Matsumoto, A., Kasai, H., Matsuo, Y., Shizuri, Y., Ichikawa, N., Fujita, N., et al. (2013). *Ilumatobacter nonamiense* sp. nov. and *Ilumatobacter coccineum* sp. nov., isolated from seashore sand. *Int. J. Syst. Evol. Microbiol.* 63, 3404–3408. doi: 10.1099/ijs.0.047316-0

Mihajlovski, A., Gabarre, A., Seyer, D., Bousta, F., and Di Martino, P. (2017). Bacterial diversity on rock surface of the ruined part of a French historic monument: the *Chaalis abbey*. *Int. Biodeter. Biodegr.* 120, 161–169. doi: 10.1016/j.ibiod.2017.02.019

Mincer, T. J., Fenical, W., and Jensen, P. R. (2005). Culture-dependent and culture-independent diversity within the obligate marine actinomycete genus *Salinispora*. *Appl. Environ. Microbiol.* 71, 7019–7028. doi: 10.1128/Aem.71.11.7019-7028.2005

Mitzscherling, J., Winkel, M., Winterfeld, M., Horn, F., Yang, S. Z., Grigoriev, M. N., et al. (2017). The development of permafrost bacterial communities under submarine conditions. *J. Geophys. Res Biogeo* 122, 1689–1704. doi: 10.1002/2017jg003859

Molina-Menor, E., Tanner, K., Vidal-Verdu, A., Pereto, J., and Porcar, M. (2019). Microbial communities of the Mediterranean rocky shore: ecology and biotechnological potential of the sea-land transition. *Microb. Biotechnol.* 12, 1359–1370. doi: 10.1111/1751-7915.13475

Mu, D. S., Ouyang, Y., Chen, G. J., and Du, Z. J. (2020). Strategies for culturing active/dormant marine microbes. *Mar. Life Sci. Technol.* 3, 121–131. doi: 10.1007/s42995-020-00053-z

Norman, J. S., King, G. M., and Friesen, M. L. (2017). *Rubrobacter spartanus* sp. nov., a moderately thermophilic oligotrophic bacterium isolated from volcanic soil. *Int. J. Syst. Evol. Microbiol.* 67, 3597–3602. doi: 10.1099/ijsem.0.002175

Pellerin, A., Lacelle, D., Fortin, D., Clark, I. D., and Lauriol, B. (2009). Microbial diversity in endostromatolites (cf. Fissure Calcretes) and in the surrounding permafrost landscape, Haughton impact structure region, Devon Island, Canada. *Astrobiol* 9, 807–822. doi: 10.1089/ast.2008.0302

Peng, M., Jia, H., and Wang, Q. (2017). The effect of land use on bacterial communities in saline–alkali soil. *Curr. Microbiol.* 74, 325–333. doi: 10.1007/s00284-017-1195-0

Ragon, M., Restoux, G., Moreira, D., Moller, A. P., and Lopez-Garcia, P. (2011). Sunlight-exposed biofilm microbial communities are naturally resistant to chernobyl ionizing-radiation levels. *PLoS One* 6:e21764. doi: 10.1371/journal.pone.0021764

Rainey, F. A., Ward-Rainey, N., Kroppenstedt, R. M., and Stackebrandt, E. (1996). The genus *Nocardiopsis* represents a phylogenetically coherent taxon and a distinct actinomycete lineage: proposal of Nocardiopsaceae fam. nov. *Int. J. Syst. Bacteriol.* 46, 1088–1092. doi: 10.1099/00207713-46-4-1088

Rappe, M. S., Gordon, D. A., Vergin, K. L., and Giovannoni, S. J. (1999). Phylogeny of actinobacteria small subunit (SSU) rRNA gene clones recovered from marine bacterioplankton. *Syst. Appl. Microbiol.* 22, 106–112. doi: 10.1016/S0723-2020(99)80033-2

Saitou, N., and Nei, M. (1987). The neighbor-joining method: a new method for reconstructing phylogenetic trees. *Mol. Biol. Evol.* 4, 406–425. doi: 10.1093/oxfordjournals.molbev.a040454

Salam, N., Jiao, J. Y., Zhang, X. T., and Li, W. J. (2020). Update on the classification of higher ranks in the phylum Actinobacteria. *Int. J. Syst. Evol. Microbiol.* 70, 1331–1355. doi: 10.1099/ijsem.0.003920

Schabereiter-Gurtner, C., Pinar, G., Vybiral, D., Lubitz, W., and Rolleke, S. (2001). *Rubrobacter*-related bacteria associated with rosy discolouration of masonry and lime wall paintings. *Arch. Microbiol.* 176, 347–354. doi: 10.1007/s002030100333

Schlitzer, R. (2002). Interactive analysis and visualization of geoscience data with Ocean Data View. *Comput. Geosci.* 28, 1211–1218. doi: 10.1016/S0098-3004(02)00040-7

Schloss, P. D., Westcott, S. L., Ryabin, T., Hall, J. R., Hartmann, M., Hollister, E. B., et al. (2009). Introducing mothur: open-source, platform-independent, community-supported software for describing and comparing microbial communities. *Appl. Environ. Microbiol.* 75, 7537–7541. doi: 10.1128/AEM.01541-09

Severino, R., Froufe, H. J. C., Barroso, C., Albuquerque, L., Lobo-da-Cunha, A., da Costa, M. S., et al. (2019). High-quality draft genome sequence of *Gaiella occulta* isolated from a 150 meter deep mineral water borehole and comparison with the genome sequences of other deep-branching lineages of the phylum Actinobacteria. *Microbiologyopen* 8:e00840. doi: 10.1002/mbo3.840

Shu, D., He, Y., Yue, H., and Wang, Q. (2015). Microbial structures and community functions of anaerobic sludge in six full-scale wastewater treatment plants as revealed by 454 high-throughput pyrosequencing. *Bioresour. Technol.* 186, 163–172. doi: 10.1016/j.biortech.2015.03.072

Sogin, M. L., Morrison, H. G., Huber, J. A., Welch, D. M., Huse, S. M., Neal, P. R., et al. (2006). Microbial diversity in the deep sea and the underexplored "rare biosphere.". *Proc. Natl. Acad. Sci. U.S.A.* 103, 12115–12120. doi: 10.1073/pnas.0605127103

Stackebrandt, E., Rainey, F. A., and WardRainey, N. L. (1997). Proposal for a new hierarchic classification system. Actinobacteria classis nov. *Int. J. Syst. Bacteriol.* 47, 479–491. doi: 10.1099/00207713-47-2-479

Steinert, G., Taylor, M. W., and Schupp, P. J. (2015). Diversity of Actinobacteria associated with the marine ascidian *Eudistoma toealensis*. *Mar. Biotechnol. (N.Y.)* 17, 377–385. doi: 10.1007/s10126-015-9622-3

Stevenson, B. S., Eichorst, S. A., Wertz, J. T., Schmidt, T. M., and Breznak, J. A. (2004). New strategies for cultivation and detection of previously uncultured microbes. *Appl. Environ. Microbiol.* 70, 4748–4755. doi: 10.1128/AEM.70.8.4748-4755.2004

Stewart, E. J. (2012). Growing unculturable bacteria. *J. Bacteriol.* 194, 4151–4160. doi: 10.1128/JB.00345-12

Sun, W., Dai, S., Jiang, S., Wang, G., Liu, G., Wu, H., et al. (2010). Culture-dependent and culture-independent diversity of Actinobacteria associated with the marine sponge Hymeniacidon perleve from the South China Sea. *Anton. Van Leeuwenhoek* 98, 65–75. doi: 10.1007/s10482-010-9430-8

Sunagawa, S., Coelho, L. P., Chaffron, S., Kultima, J. R., Labadie, K., Salazar, G., et al. (2015). Ocean plankton. Structure and function of the global ocean microbiome. *Science* 348:1261359. doi: 10.1126/science.1261359

Suzuki, K., Collins, M. D., Iijima, E., and Komagata, K. (1988). Chemotaxonomic characterization of a radiotolerant bacterium, *Arthrobacter radiotolerans*: description of *Rubrobacter radiotolerans* gen. nov., comb. nov. *FEMS Microbiol. Lett.* 52, 33–39. doi: 10.1111/j.1574-6968.1988.tb02568.x

Vardeh, D. P., Woodhouse, J. N., and Neilan, B. A. (2018). Microbial diversity of speleothems in two Southeast Australian limestone cave arches. *J. Cave Karst Stud.* 80, 121–132. doi: 10.4311/2017mb0119

Vartoukian, S. R., Palmer, R. M., and Wade, W. G. (2010). Strategies for culture of 'unculturable' bacteria. *FEMS Microbiol. Lett.* 309, 1–7. doi: 10.1111/j.1574-6968.2010.02000.x

Vaz-Moreira, I., Egas, C., Nunes, O. C., and Manaia, C. M. (2011). Culture-dependent and culture-independent diversity surveys target different bacteria: a case study in a freshwater sample. *Anton. Van Leeuwenhoek* 100, 245–257. doi: 10.1007/s10482-011-9583-0

Walsh, P. S., Metzger, D. A., and Higuchi, R. (1991). Chelex 100 as a medium for simple extraction of DNA for PCR-based typing from forensic material. *Biotechniques* 10, 506–513. doi: 10.2144/000114018

Ward, A. C., and Bora, N. (2006). Diversity and biogeography of marine actinobacteria. *Curr. Opin. Microbiol.* 9, 279–286. doi: 10.1016/j.mib.2006.04.004

Yang, X., Shi, X. Z., Junfeng, Y., Chuanhai, G., Hongfang, C., Aihua, L., et al. (2018). Bottom water temperature measurements in the South China Sea, eastern Indian Ocean and western Pacific Ocean. *J. Tro. Oceanogr.* 37, 86–97. doi: 10.11978/2017113

Yooseph, S., Sutton, G., Rusch, D. B., Halpern, A. L., Williamson, S. J., Remington, K., et al. (2007). The sorcerer II global ocean sampling expedition: expanding the universe of protein families. *PLoS Biol.* 5:e16. doi: 10.1371/journal.pbio.0050016

Yoshinaka, T., Yano, K., and Yamaguchi, H. (1973). Isolation of highly radioresistant bacterium. *Arthrobacter. radiotolerans* nov. sp. *Agric. Biol. Chem.* 37, 2269–2275. doi: 10.1080/00021369.1973.10861003

Zhu, D., Tanabe, S. H., Yang, C., Zhang, W., and Sun, J. (2013). Bacterial community composition of South China Sea sediments through pyrosequencing-based analysis of 16S rRNA genes. *PLoS One* 8:e78501. doi: 10.1371/journal.pone.0078501

Conflict of Interest: The authors declare that the research was conducted in the absence of any commercial or financial relationships that could be construed as a potential conflict of interest.

frontiers in Microbiology

ORIGINAL RESEARCH
published: 28 September 2021
doi: 10.3389/fmicb.2021.728479

Cross-Sectional Study on the Gut Microbiome of Parkinson's Disease Patients in Central China

Liangwei Mao[1†], Yu Zhang[2†], Jing Tian[2], Ming Sang[2], Guimin Zhang[1], Yuling Zhou[1] and Puqing Wang[2*]*

[1] State Key Laboratory of Biocatalysis and Enzyme Engineering, Hubei Collaborative Innovation Center for Green Transformation of Biological Resources, School of Life Sciences, Hubei University, Wuhan, China, [2] Hubei Clinical Research Center of Parkinson's Disease, Xiangyang No. 1 People's Hospital, Hubei University of Medicine, Xiangyang, China

OPEN ACCESS

Edited by:
Yu-Qin Zhang, Institute of Medicinal Biotechnology, Chinese Academy of Medical Sciences, China

Reviewed by:
Maria Jose Gosalbes, Centre for Biomedical Network Research (CIBER), Spain
Ping-Hua Qu, Guangdong Provincial Hospital of Chinese Medicine, China

***Correspondence:**
Yuling Zhou
zyl609@hubu.edu.cn
Puqing Wang
wpq20110328@qq.com

[†] These authors have contributed equally to this work

Specialty section:
This article was submitted to Systems Microbiology, a section of the journal Frontiers in Microbiology

Received: *21 June 2021*
Accepted: *27 August 2021*
Published: *28 September 2021*

Citation:
Mao L, Zhang Y, Tian J, Sang M, Zhang G, Zhou Y and Wang P (2021) Cross-Sectional Study on the Gut Microbiome of Parkinson's Disease Patients in Central China. Front. Microbiol. 12:728479. doi: 10.3389/fmicb.2021.728479

Gastrointestinal dysfunction plays an important role in the occurrence and development of Parkinson's disease (PD). This study investigates the composition of the gut microbiome using shotgun metagenomic sequencing in PD patients in central China. Fecal samples from 39 PD patients (PD group) and the corresponding 39 healthy spouses of the patients (SP) were collected for shotgun metagenomics sequencing. Results showed a significantly altered microbial composition in the PD patients. *Bilophila wadsworthia* enrichment was found in the gut microbiome of PD patients, which has not been reported in previous studies. The random forest (RF) model, which identifies differences in microbiomes, reliably discriminated patients with PD from controls; the area under the receiver operating characteristic curve was 0.803. Further analysis of the microbiome and clinical symptoms showed that *Klebsiella* and *Parasutterella* were positively correlated with the duration and severity of PD, whereas hydrogen-generating *Prevotella* was negatively correlated with disease severity. The Cluster of Orthologous Groups of protein database, the KEGG Orthology database, and the carbohydrate-active enzymes of gene-category analysis showed that branched-chain amino acid–related proteins were significantly increased, and GH43 was significantly reduced in the PD group. Functional analysis of the metagenome confirmed differences in microbiome metabolism in the PD group related to short-chain fatty acid precursor metabolism.

Keywords: Parkinson's disease, gut-brain-axis, shotgun metagenomic sequencing, gastrointestinal dysbiosis, short-chain fatty acids

INTRODUCTION

Parkinson's disease (PD) is a progressive neurodegenerative disease whose prevalence rate among central nervous system (CNS) diseases is only second to that of Alzheimer's disease in the elderly population. The burden of PD will continue to rise with the increase in population size and aging (Castillo et al., 2019). Globally, there were 6.2 million PD patients in 2015; of these, 0.117

million patients died of PD (Mortality, 2016). Most PD cases are sporadic, and the average age at onset is 60 years (Cook Shukla et al., 1993). The pathogenesis of PD is complex, with some of the pathological features being the loss of dopaminergic neurons in the substantia nigra and intracytoplasmic inclusions (Lewy bodies) in the remaining intact nigral neurons (Braak and Braak, 2000).

Dysbiosis of the gut microbiome can affect both the enteric nervous system and the CNS. Previous studies have revealed the existence of the brain–gut–microbiome axis whose bidirectional interaction between the gut microbiome and the human nervous system can cause CNS disease (Cox and Weiner, 2018). In recent years, metagenomics studies have further revealed the correlation between PD and abnormal gut microbiome, which is also an extension of the gastrointestinal hypothesis in PD (Holmqvist et al., 2014). Gastrointestinal dysfunction, as well as changes in microbiome metabolites, can lead to inflammation, impaired epithelial barrier function, and an increase in the translocation of lipopolysaccharides and short-chain fatty acids (SCFAs), thereby causing systemic inflammatory reactions. Inflammatory cytokines pass through the blood–brain barrier to activate the microglia and astrocytes, which leads to neuroinflammation, altered cognition and behaviors, stress, and finally PD (Sampson et al., 2016; Sun and Shen, 2018). Previous studies have noted distinct alterations in the gut microbiome of PD patients, specifically SCFAs and other metabolites (Sampson et al., 2016; Unger et al., 2016; Hill-Burns et al., 2017; Sun et al., 2018).

Currently, the majority of studies use 16S rRNA amplicon sequencing technology to analyze gut microbiome diversity. However, the 16S rRNA primers used for different regions may lead to inconsistent results, because not only does the corresponding flanking conservative region have obvious binding affinity, but also the resolution of each variable region in the taxonomic group is also different (Soergel et al., 2012). Although shotgun metagenomics is expensive, it provides higher resolution and better strain identification potential, which enhances specific classification of the taxon and function (Norman et al., 2015). Only one study, conducted in Germany, has reported the use of this method in PD to date. This study produced results that could not be obtained by the use of 16S rRNA amplicon sequencing technology and revealed the differences in microbiome and microbiome metabolic pathways between L-DOPA–naive PD patients and the control group. Moreover, the study further analyzed the abundances of prophages, plasmids, and total virus (Bedarf et al., 2017). However, shotgun metagenomics has not been applied in studies of PD patients in Central China.

In China, a total of five institutions, in Beijing (Li et al., 2017c), Shanghai (Qian et al., 2018), Guangzhou (Lin et al., 2018), Changchun (Li C. et al., 2019), and Jinzhou (Li F. et al., 2019), have analyzed gut microbiome diversity using 16S rRNA amplicon sequencing technology. However, in consideration of the strong impact that geographic (Rehman et al., 2016; Kushugulova et al., 2018) and population (Deschasaux et al., 2018) factors have on the gut microbiome, shotgun metagenomics was used in this study to analyze the gut microbiome of PD populations in central China. Studies have shown that long-term habitual diets can change the structure of the gut microbiome (David et al., 2014; Krautkramer et al., 2016). Comparison of people from different families has shown that couples share a similar gut microbiome (Song et al., 2013). Therefore, in this study, PD patients' spouses were recruited (the SP group) in order to minimize the impact of diet and living habits. Shotgun metagenomics analysis revealed significant differences in the gut microbiome composition and function between the PD patients and their spouses, further demonstrating the existence of proinflammatory dysbiosis in PD.

MATERIALS AND METHODS

Patient Cohorts

This was a cross-sectional study, and the study subjects were recruited from the Neurology Department of Xiangyang No. 1 People's Hospital. The study was approved by the Ethics Committee of Xiangyang No. 1 People's Hospital. All subjects gave their consent to participate in the study in accordance with the informed consent regulations of the institution where the research was conducted. In order to reduce the potential impact of diet, daily schedule, and other related factors, all the subjects were couples in which one spouse was a PD patient (PD), whereas the other was healthy for comparison purposes (SP). PD patients were diagnosed using the PD diagnostic criteria in the movement disorder society (MDS) 2015 (Li et al., 2017a). The core standard of diagnosis was to identify if the patient had PD symptoms. The patient was considered as having PD syndromes if he/she had bradykinesia in combination with static tremor and/or muscular rigidity. Upon diagnosis with PD syndrome, further diagnosis was made based on the inclusion and exclusion criteria and warning signs to ensure that the patient was a clinical PD patient. The exclusion criteria for the experimental group based on previous literature (Keshavarzian et al., 2015) were as follows: (1) administration or infusion of antibiotics or probiotics in the recent 3 months; (2) serious disease of the gastrointestinal tract; (3) severe mental disorder; (4) too low platelet count (80×10^9/L); (5) prothrombin time > 15 s; (6) History of hemorrhage in any of the visceral organs. There was no detailed dietary plan put in place for all the study subjects, and fecal samples were collected from the first defecation on the day. General demographic parameters and clinical symptoms of the study participants are shown in **Table 1**, while **Supplementary Table 1** shows detailed patient clinical information.

Abbreviations: AUC, area under the curve; BCAA, branched-chain amino acid; BMI, body mass index; CAZymes, carbohydrate-active enzymes; CH, Calinski–Harabasz; CNS, central nervous system; COG, Cluster of Orthologous Groups; FDR, false discovery rate; HUMAnN2, HMP unified metabolic analysis network 2; IBD, inflammatory bowel disease; IBS, irritable bowel syndrome; IBS-C, irritable bowel syndrome with constipation predominance; IBS-D, irritable bowel syndrome with diarrhea predominance; IQR, interquartile range; JSD, Jensen–Shannon divergence; KO, KEGG Orthology; LEfSe, linear discriminant analysis effect size; LOOCV, leave one out cross validation; LPS, lipopolysaccharides; MetaPhlAn2, metagenomic phylogenetic analysis v2.0; MDA, decreases in accuracy; PAM, partitioning around medoids; PCoA, principal coordinate analysis; PD, Parkinson's disease; PERMANOVA, permutational multivariate analysis of variance; RF, random forest; ROC, receiver operating characteristic; SCFAs, short-chain fatty acids; SD, standard deviation; STAMP, statistical analysis of metagenomic profiles.

TABLE 1 | General demographic parameters and clinical manifestations.

	PD group	SP group
Demographics		
No. of participants	39	39
Age (years, mean ± SD)	63.95 ± 6.92	64.82 ± 6.86
Male	21	18
BMI (kg/m^2, IQR)	23.15 (20.67–25.39)	24.2 (20.2–26.02)
Clinical data		
Age at onset (years, mean ± SD)	60.49 ± 6.54	–
Duration (years)		
≥3 years	21	–
>3 ≤ 5 years	11	–
>5 ≤ 10 years	6	–
>10 years	1	–
H&Y stage		
1	12	–
1.5	8	–
2	6	–
2.5	6	–
3	3	–
3.5	1	–
4	3	–
UPDRS-III score (mean ± SD)	34.92 ± 20.25	–

DNA Library Construction and Sequencing Using the BGISEQ-500 Platform

DNA was extracted from the fecal sample as previously described using the MetaHIT protocol (Qin et al., 2012). Qubit (Invitrogen) was used to estimate the DNA concentration. After DNA extraction, genomic libraries were prepared following the manufacturer's standard instructions (MGI, China). To establish a paired-end library with the insertion of 350 bp, 500 ng DNA was used, and sequencing was performed using a BGISEQ-500 sequencer through PE100 mode (Fang et al., 2018). The 1,761.8 GB original sequencing data were deposited in the Sequence Read Archive under the accession number of PRJNA588035.

Taxonomical Analysis

All shotgun metagenomics data were handled according to the Microbiome Helper standard operating procedures (Comeau et al., 2017). FastQC tool[1] was used to check the quality of raw reads of the metagenome. KneadData[2] was used to trim the low-quality sequences (parameter: "SLIDINGWINDOW: 4: 20 MINLEN: 50") and delete any unwanted human genome (HG19) reads (parameter: –very-sensitive –dovetail). The default parameters of MetaPhlAn 2.0 software (Truong et al., 2015) were used for taxonomic profiling and estimation of the reads' abundance after processing. This software utilizes unique clade-specific marker genes to test the taxonomic clade present in the microbiome sample and estimate their relative abundance. Thus, relative abundances were multiplied by the number of sequences and rounded (Segata et al., 2011). Shannon and Chao1 indices were used to estimate α-diversity. β-Diversity was evaluated based on the Bray–Curtis dissimilarity index. The abundance of genera in all the samples was subjected to non-parametric permutational multivariate analysis of variance (PERMANOVA) to evaluate the sample cluster under various predictive factors such as disease status, gender, and age. Principal coordinate analysis (PCoA) was used to visualize the data. For PERMANOVA analysis, we used the "adonis" procedure in the vegan 2.5–4 package. Linear discriminant analysis (LDA) effect size (LEfSe) was used to identify biomarkers in the two groups. Only the taxa with $p < 0.05$ (Kruskal–Wallis test) and LDA score > 2 were considered to show statistically significant enrichment.

SeqKit software was used to convert fastq format to fasta format in order to evaluate the number of phages and plasmids (Bedarf et al., 2017). Further, the sensitive mode of Diamond software was used to map the reads to the ACLAME database (Leplae et al., 2010) after kneadData processing. Among them, the mapping reads with an *e* value < 1e-7 were considered to be valid hits. The reads' quantity of each sample mapped to the plasmid and phage database was divided by clean reads to ensure standardization. The Mann–Whitney *U* test was used to test for the differences between groups in the R environment.

Enterotype Analysis

An enterotype is the objective aggregation effect of gut microbiome, which is presented in the high-dimensional feature space and is another general measure of the gut microbiome (Arumugam et al., 2011; Ding and Schloss, 2014). Jensen–Shannon divergence (JSD) distances and Partitioning Around Medoids (PAM) clustering algorithm were used for cluster analysis of all the samples based on the relative abundance of genera. The Calinski–Harabasz (CH) index was used to evaluate the optimal cluster number. The χ^2 test was used to explore whether the distribution of enterotypes was influenced by disease status.

Gut Microbiome–Clinical Manifestation Correlation Analysis

Spearman correlation between the relative abundance of genera and clinical manifestation with more than 40% distribution among all patients was tested to evaluate the relationship between the gut microbiome and clinical manifestation. Only the genus with a clinical manifestation correlation parameter of $p < 0.1$ and $\rho > 0.25$ was used for visualization. This step was realized in the R environment, and the packages used included ggstatsplot (0.0.10), data.table (1.12.2), dplyr (0.8.0.1), tidyr (0.8.3), and ggplot2 (3.1.1).

Establishment of the Disease Classification Model

The RF model was established based on the relative abundance of genera of the gut microbiome in all subjects in order to confirm the features of fecal bacteria for disease classification of the metagenome samples. Leave-one-out cross-validation was

[1]https://www.bioinformatics.babraham.ac.uk/projects/fastqc/

[2]https://huttenhower.sph.harvard.edu/kneaddata

used to verify the accuracy of the model (Bedarf et al., 2017; Wang et al., 2019). The number of decision trees in the RF was set to be 5,000 (ntree = 5,000), whereas the number of preselected features at each tree node was determined as the square root of the number of features minus one, and the seed was set to be 2,019,613. The variable with the strongest classification capacity was determined based on the mean decrease accuracy (MDA), and the RF model was established. Receiver operating characteristic (ROC) curve was developed, and the areas under the curve (AUCs) of ROC were calculated to evaluate the accuracy of the new criteria for disease prediction. The work was completed in R (4.6-14, RF package).

Gene Catalog Construction and Differential Gene Analysis

The assembly software MEGAHIT (v1.2.9) (Li et al., 2015) based on the principle of De Bruijn graphs was used to assemble the quality-filtered metagenomic sequences of each sample, and the obtained contigs were evaluated by QUAST (v5.0.2) (Gurevich et al., 2013). The prediction of protein-coding genes was performed using Prokka (v1.13) software (Seemann, 2014) with the "—metagenome –kingdom Archaea, Bacteria, Viruses" option. The open reading frame (ORF) of each sample was clustered using CD-HIT tool (v4.8.1) (Li et al., 2001) with parameters "-aS 0.9 -c 0.95 -G 0 -M 0 -T 9 -g 1" in order to obtain an initial non-redundant gene catalog (nrGC) with 95% sequence identity and 90% coverage. Unigene annotation was performed by running Diamond against the eggNOG database (Huerta-Cepas et al., 2019) and dbCAN2 database (Zhang et al., 2018). Salmon (v1.3.0) (Patro et al., 2017) was used to determine the relative abundances of genes in each sample successfully mapped to the initial nrGC. Protein abundances were quantified as counts per million, calculated by the raw valid counts (number of valid alignments) divided by the library sizes and multiplied by one million. Statistical analyses were performed using Statistical Analysis of Metagenomic Profiles (STAMP) (Parks et al., 2014).

Pathway Analysis

Compared with taxology analysis, functional analysis aims to quantify metabolic pathways contributed by known and characterless microbiome members (Franzosa et al., 2015). HMP Unified Metabolic Analysis Network (HUMAnN2) (Franzosa et al., 2018) directly determines the gene family abundance, metabolic pathway abundance, and metabolic pathway coverage of each sample from the read after preliminary treatment. In this study, emphasis was placed on analysis in the output of metabolic pathway abundance. STAMP software was used to identify the pathways for which statistical differences existed between groups (Parks et al., 2014). Welch *t* test was used to compare cases versus controls with a Storey FDR < 0.1 as a cutoff for significance.

RESULTS

Quality Metrics of Metagenomics Data

The gut microbiome of the two groups was analyzed and compared by shotgun metagenomics. After trimming and filtration using kneadData software, more than 4.05×10^9 100-bp high-quality paired-end reads were obtained, among which the total number of human reads was 4.52×10^7, accounting for 1.12%. After elimination of host contamination, the average number of reads per PD patient was $5.31 \times 10^7 \pm 1.58 \times 10^7$, and that for the SP group was $4.95 \times 10^7 \pm 2.26 \times 10^7$ (Mann–Whitney *U* test, $p = 0.24$) (**Supplementary Table 2**). The average number of host reads in the PD patients was $6.07 \times 10^5 \pm 1.01 \times 10^6$, and that of the SP group was $5.53 \times 10^5 \pm 1.71 \times 10^6$ (Mann–Whitney *U* test, $p = 0.03$) (**Supplementary Table 2**). Significant increases in host reads in PD patients may reflect alterations in intestinal permeability and pathological status.

The relative abundances in the gut microbiome were measured for each sample by MetaPhlan2. The complete information for the taxonomic levels is provided in **Supplementary Table 3**. The majority of the reads of the tested sample of the PD group and SP group were 98.61% ± 5.45% and 99.87% ± 0.41% (Mann–Whitney *U* test, $p = 0.67$), respectively, which were all mapped to the kingdom Bacteria. The ratio corresponding to the kingdom Virus was less than that for the kingdom Bacteria: 1.36% ± 5.42% in the PD group and 0.13% ± 0.41% in the SP group (Mann–Whitney *U* test, $p = 0.89$), whereas the kingdoms Archaea and Eukaryota were almost non-existent in the samples (**Supplementary Table 3**).

Differences in the Gut Microbiome

In this study, the microbiome Shannon and Chao1 indices were all analyzed at the genus and species levels, respectively. The genus Shannon (Mann–Whitney *U* test, $p = 0.0002287$) and Chao1 (Mann–Whitney *U* test, $p = 0.007892$) indices of the PD group were significantly higher than those for the SP group (**Figures 1A,B**). At the species level, the Shannon (Mann–Whitney *U* test, $p = 0.02734$) and Chao1 (Mann–Whitney *U* test, $p = 0.0245$) indices also showed similar trends (**Figures 1C,D**). The results revealed that the diversity of the gut microbiome in the PD patients was significantly higher than in the healthy group. Therefore, a higher gut microbiome Shannon and Chao1 indices may not be indicative of a healthy gut microbiome, but rather of an overgrowth of pathogenic bacteria in PD patients.

β-Diversity was analyzed at the genus level based on the disease, age, and gender status in order to estimate community diversity between the samples, using PERMANOVA. Further, the relationship between the factors and gut microbiome composition was analyzed. Between-group differences were visualized in the PCoA using the Bray–Curtis dissimilarity. The results showed that the disease status was related to the change in the between-group gut microbiome. PCoA further revealed the separation between the healthy SP group and PD group. The resolution of the top two principal coordinates was 41.40 and 13.83%, respectively (**Figure 1E**). However, the effects of age and gender were independent (**Supplementary Table 4**). This implied that the gut microbiome dysbiosis in PD patients was mainly caused by the disease itself and was not related to age and gender.

All the clean reads were mapped to the ACLAME database and standardized to estimate the known mobile elements in the

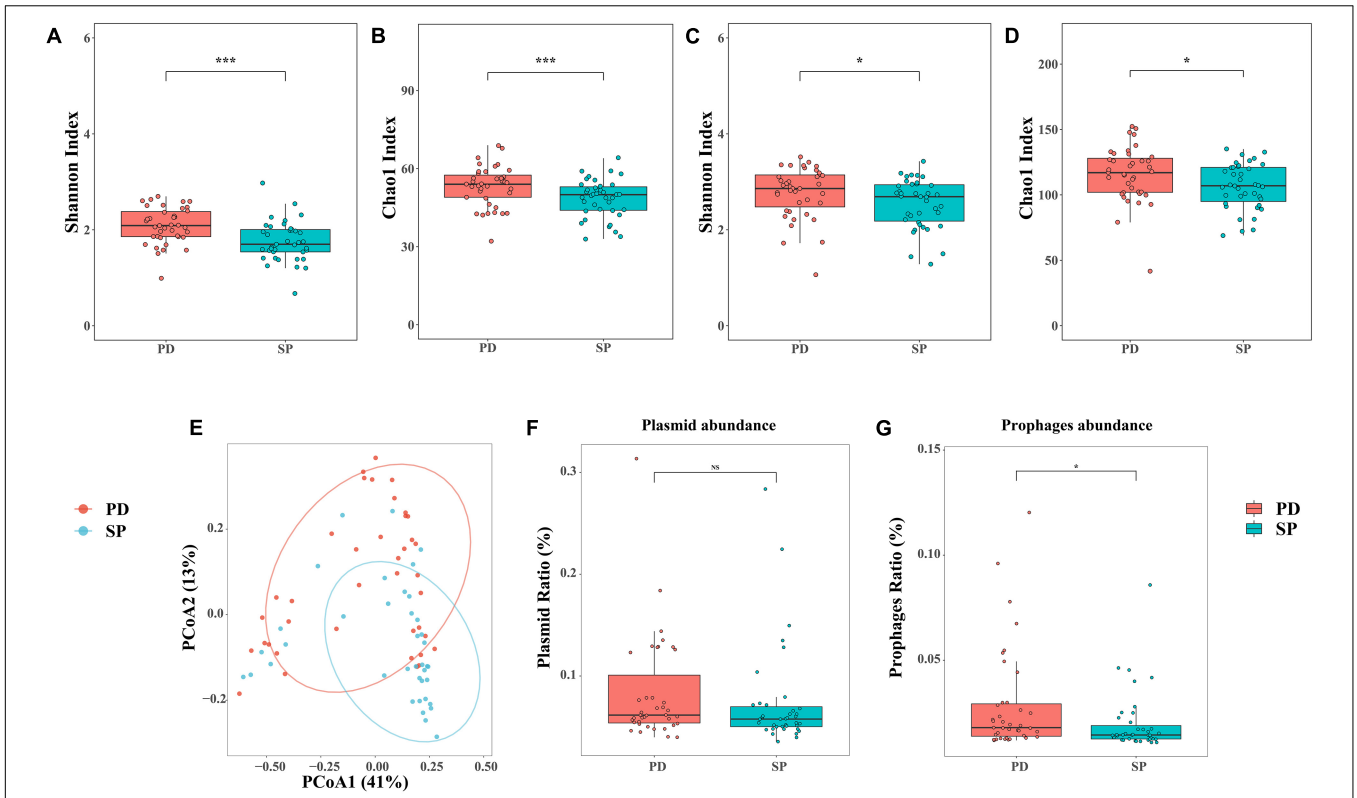

FIGURE 1 | Diversity analysis and quantity of phages and plasmids. **(A,B)** Shannon and Chao1 indices of the two cohorts at the genus level. **(C,D)** Shannon and Chao1 indices of the two cohorts at the species level. **(E)** PCoA analysis of Bray–Curtis dissimilarity index between samples at the genus level. The percentage of diversity explained by each axis is indicated on the figure. **(F,G)** Relative abundance of phages and plasmids between two groups. Asterisk represents statistical significance (*$p < 0.05$, ***$p < 0.01$).

metagenome. There were no significant differences in plasmid abundance between the PD and SP groups (0.083 ± 0.052 vs. 0.073 ± 0.050, Mann–Whitney *U* test, $p = 0.8223$, **Figure 1F**). However, phage abundance in the PD patients was higher (0.029 ± 0.025 vs. 0.020 ± 0.014, Mann–Whitney *U* test, $p = 0.01579$, **Figure 1G**).

Taxonomic Changes in the Gut Microbiome

The gut microbiome was found to be mainly composed of three phyla, namely, *Bacteroidetes* (PD was 54.79% ± 16.42%, SP was 61.49% ± 12.88%, Mann–Whitney *U* test, $p = 0.09$), *Firmicutes* (PD was 28.90% ± 14.76%, SP was 30.34% ± 13.17%, Mann–Whitney *U* test, $p = 0.47$), and *Proteobacteria* (PD was 12.34% ± 17.36%, SP was 7.04% ± 6.82%, Mann–Whitney *U* test, $p = 0.43$) (**Supplementary Figure 1**). Two phyla that were present in small proportions, namely, *Actinobacteria* (PD was 1.54% ± 2.11%, SP was 0.56% ± 0.77%, Mann–Whitney *U* test, $p = 0.01$) and *Synergistetes* (PD was 2.52% ± 7.26%, SP was 0.33% ± 1.12%, Mann–Whitney *U* test, $p = 0.01$), exhibited significant differences, and the abundance in the PD group was significantly increased. These results showed that there were differences in the gut microbiome of the PD and SP groups at a high taxonomic level and that at a lower taxonomic level, corresponding changes could also be observed.

A total of 71 taxa were identified to have notable differences between groups. The LEfSe algorithm revealed differences in 1 phylum, 2 classes, 3 orders, 7 families, 14 genera, and 44 species; details are provided in **Supplementary Table 5**. The enrichment at the genus and species level is shown in **Figures 2A,B**, respectively. In the PD group, phylum *Actinobacteria*, class *Actinobacteria*, order *Bifidobacteriales*, family *Bifidobacteriaceae*, and genus *Scardovia* were enriched at different taxonomic levels in the same clade. In addition, class *Deltaproteobacteria*, order *Desulfovibrionales*, family *Desulfovibrionaceae*, genus *Desulfovibrio*, and genus *Bilophila* also showed consistent enrichment in the PD group (**Figure 2C**). In the SP group, family *Bacteroidaceae* and genus *Bacteroides* shared the same clade and showed a similar trend of enrichment (**Figure 2C**).

Enterotype Analysis

The classification of microbiome structures based on enterotypes has potential clinical significance. The existence of discrete enterotypes widely impacts on the study of microbiome-related human diseases. To date, studies have reported a phenotypic correlation between enterotypes (or major drive species) and human diseases (Qureshi and Mehler, 2013; Li et al., 2017b; Castano-Rodriguez et al., 2018; Cheng and Ning, 2019). Based on the microbiome, individualized diagnosis and treatment can be easily provided if patients are grouped according to enterotypes.

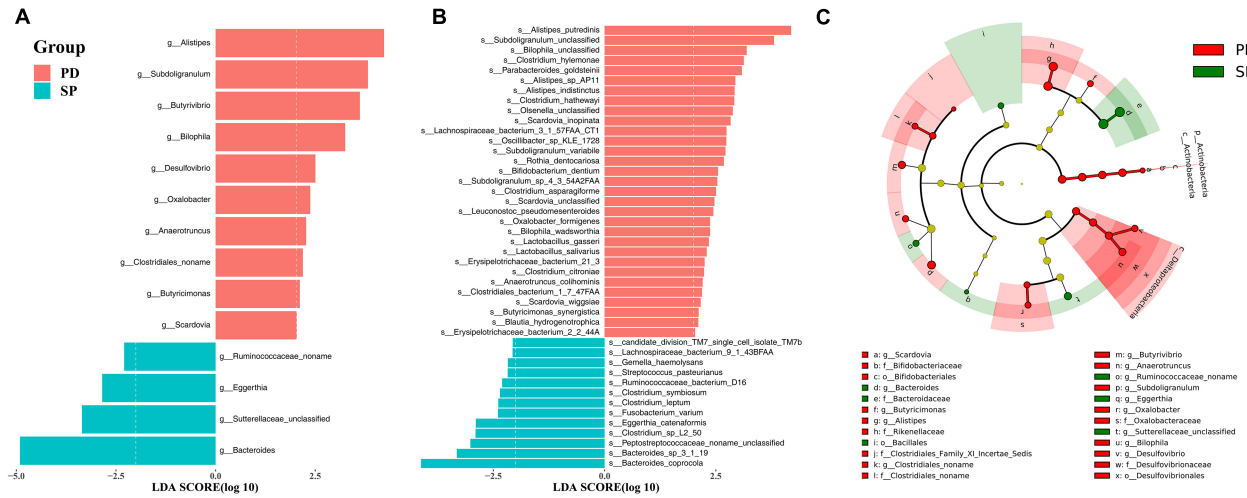

FIGURE 2 | The stool microbiota profile in PD and SP groups. Differential abundance of genera **(A)** and species **(B)** between PD and SP groups identified by LEfSe. **(C)** Cladogram of the gut microbial taxa associated with PD and SP; PD-enriched taxa are in red, and SP-enriched taxa are in green.

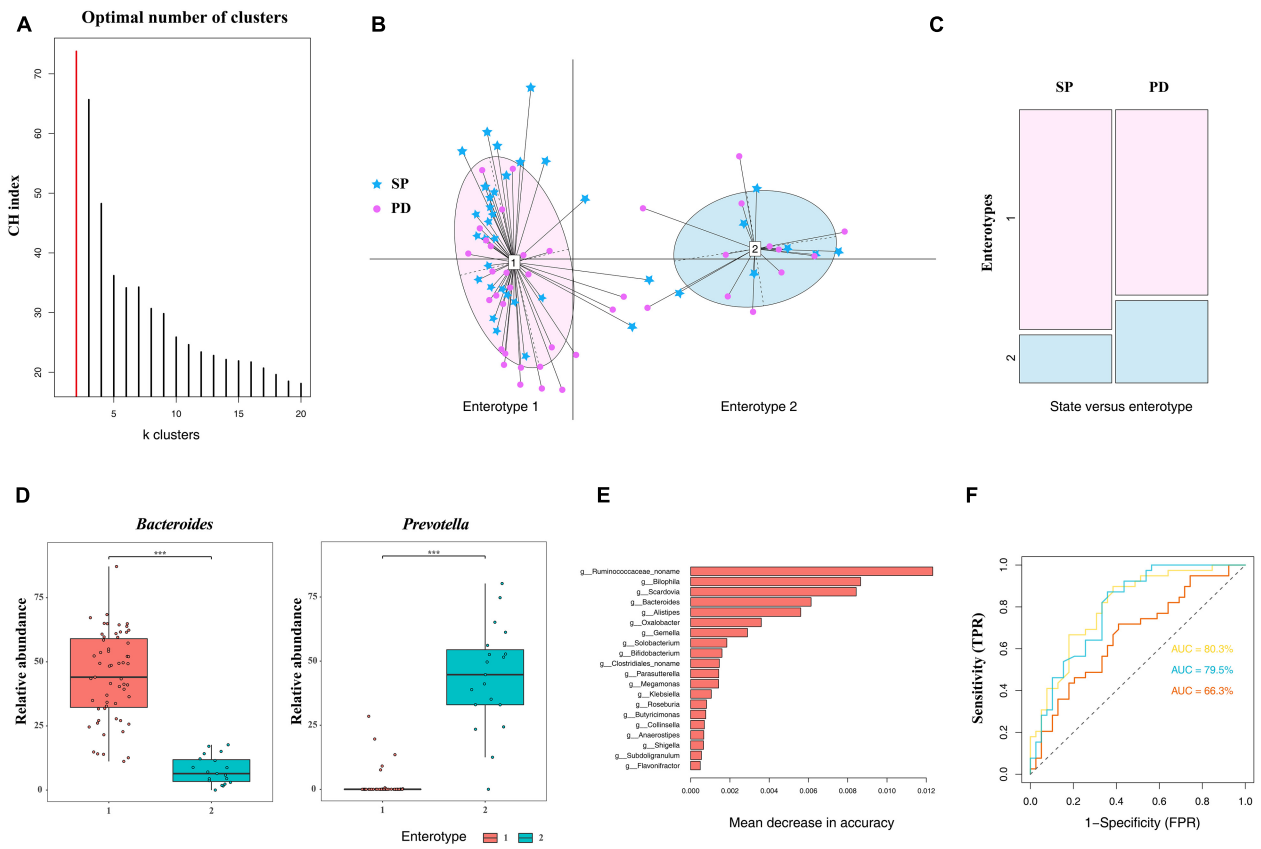

FIGURE 3 | Difference in community types and taxonomic biomarkers for judging health status between PD and SP. **(A)** CH index indicates optimal classification into two community types. **(B)** Plot for PCoA of enterotypes. **(C)** Distribution of the healthy control and PD patient samples in the two enterotypes. **(D)** Relative abundances of *Bacteroides* and *Prevotella* in each enterotype. **(E)** Top 20 MDA genera were identified by applying RF classifier. **(F)** The ROC curve for predicting the occurrence of PD in 78 samples. The genus abundance profile can be used to identify microbiota samples extracted from PD patients. The dotted line represents the performance of the probabilistic model, the yellow line represents the performance of top 20 MDA variables model, the blue line represents the performance of the top 10 MDA variables model, and the orange line represents the performance of all variables. Asterisk represents statistical significance (***$p < 0.01$).

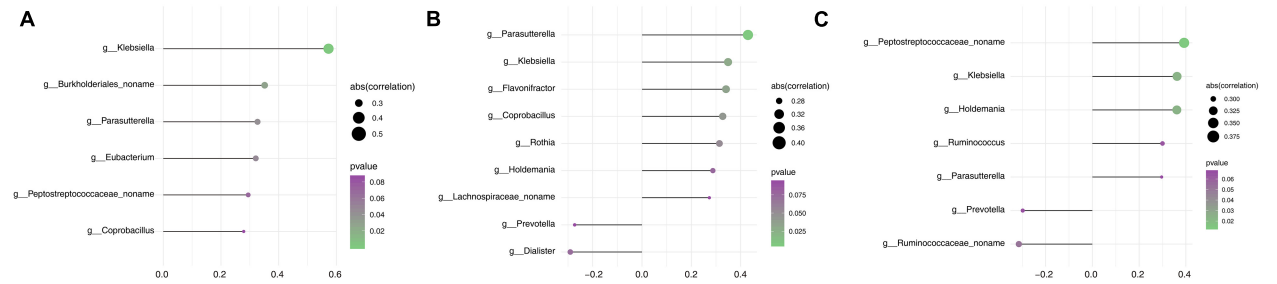

FIGURE 4 | Assessment of the correlation between gut microbiota and clinical phenotype in the PD group. **(A)** Correlation analysis between PD duration and the relative abundance of genera. **(B)** Correlation analysis between H&Y stage and the relative abundance of genera. **(C)** Correlation analysis between the UPDRS III score and the relative abundance of genera. The size of node represents the degree of correlation; the gradient ramp from purple to green represents the *p* value from larger to small values.

In this study, all samples were divided into two clusters using the PAM clustering method (**Figure 3A**), and each cluster comprised PD patients and the control group (**Figure 3B**). The differences in enterotype discreteness between the patient and control were not statistically significant (**Figure 3C**, χ^2 test, $p = 0.1872$). Enterotype 1 was dominated by genus *Bacteroides*, whereas enterotype 2 was dominated by the genus *Prevotella* (**Figure 3D**). Therefore, the enterotypes studied in PD should be further investigated in a larger patient population.

Parkinson's Disease Differentiation Based on the Composition of the Gut Microbiome

The RF algorithm was used to classify samples and establish a diagnostic model. One of the advantages of the RF model is that it can estimate the importance of each feature and the identification of the most important features in the classification process. Based on the measurement of the MDA, the five most important genera in the RF model were *Bilophila*, *Scardovia*, *Bacteroides*, *Alistipes*, and a novel unclassified genus of the family *Ruminococcaceae*. To improve the RF classifier results, the top 10 and 20 MDA variables were used as features to establish the model (**Figure 3E**). ROC curve and AUC were used to evaluate the performance of the binary classifier. We were able to distinguish the PD from the SP with AUC of 0.677 using all genera, whereas the AUC were 0.795 and 0.803 using the top 10 and 20 MDA variables, respectively, which improved diagnostic accuracy (**Figure 3F**). Therefore, based on these findings, differences in microbiome compositions can enable PD classification; furthermore, these can serve as biomarkers in PD diagnosis, prognosis, and therapeutic evaluation in central China.

Correlation Between the Relative Abundance of Genera and Clinical Manifestation

Parkinson's disease clinical manifestations including PD duration and disease severity (UPDRS III and H&Y stage) were quantified in correlation analysis with gut microbiome composition. Based on the Spearman correlation matrix, the correlation between clinical manifestation and relative abundance in 57 genera in which the distribution of the tested samples was greater than 40% was validated. PD duration was positively correlated to *Klebsiella* ($R^2 = 0.573$, $p = 0.0001$); a novel unclassified genus of the family *Burkholderiales* ($R^2 = 0.351$, $p = 0.028$), *Parasutterella* ($R^2 = 0.327$, $p = 0.042$), and *Eubacterium* ($R^2 = 0.321$, $p = 0.047$); and a novel unclassified genus of the family *Peptostreptococcaceae* ($R^2 = 0.294$, $p = 0.069$) and *Coprobacillus* ($R^2 = 0.279$, $p = 0.086$) (**Figure 4A**). Hoehn and Yahr (H&Y) stage showed a positive correlation with *Parasutterella* ($R^2 = 0.430$, $p = 0.006$), *Klebsiella* ($R^2 = 0.349$, $p = 0.030$), *Flavonifractor* ($R^2 = 0.341$, $p = 0.034$), *Coprobacillus* ($R^2 = 0.327$, $p = 0.042$), *Rothia* ($R^2 = 0.314$, $p = 0.052$), and *Holdemania* ($R^2 = 0.287$, $p = 0.076$); a novel unclassified genus of the family *Lachnospiraceae* ($R^2 = 0.273$, $p = 0.093$); and a negative correlation with *Dialister* ($R^2 = -0.291$, $p = 0.073$) and *Prevotella* ($R^2 = -0.273$, $p = 0.093$) (**Figure 4B**). UPDRS III score showed a positive correlation with a novel unclassified genus of the family *Peptostreptococcaceae* ($R^2 = 0.392$, $p = 0.013$), *Klebsiella* ($R^2 = 0.362$, $p = 0.023$), *Holdemania* ($R^2 = 0.361$, $p = 0.024$), *Ruminococcus* ($R^2 = 0.300$, $p = 0.064$), and *Parasutterella* ($R^2 = 0.296$, $p = 0.067$) and a negative correlation with a novel unclassified genus of the family *Ruminococcaceae* ($R^2 = -0.315$, $p = 0.0515$) and *Prevotella* ($R^2 = -0.298$, $p = 0.065$) (**Figure 4C**). Based on these findings, *Klebsiella* and *Parasutterella* showed a positive correlation with PD duration and disease severity, whereas *Prevotella* showed a negative correlation with disease severity.

Significant Difference in Protein Abundance Between the Two Groups

This study aims to bridge the gap between previous 16S rRNA sequencing studies and functional studies by using high-resolution shotgun metagenomic sequencing to identify gut microbiome taxonomic and functional profiles. Given the high diversity between individuals, we performed *de novo* assembly on each sample independently. The data show that the total contig length is 14.24 Gb. The N50 of the PD group was 4,604 ± 1,596 bp, and the N50 of the SP group was 4,723 ± 1,782 bp (**Supplementary Table 6**). There was no statistical difference in the assembly results between the two groups (Mann–Whitney *U* test, $p = 0.9761$). The

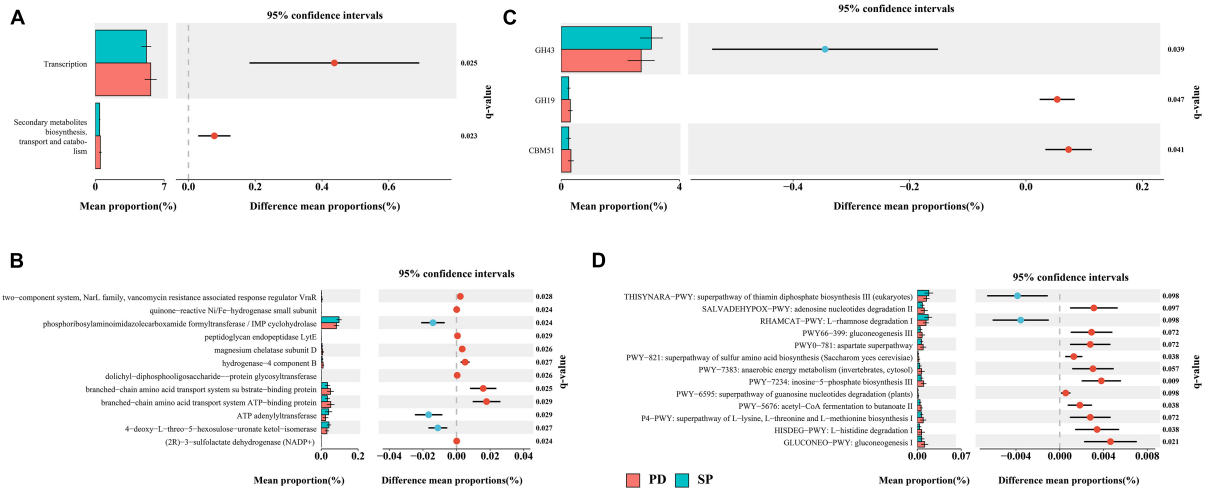

FIGURE 5 | Differentially abundant proteins and functional alterations between PD and SP. **(A)** Differences in relative abundances of COG functional categories. **(B)** Differences in relative abundances of KO functional categories. Only *q* values (false discovery rate–adjusted *p* value) of <0.03 are shown. **(C)** Differences in relative abundances of CAZyme functional categories. **(D)** Metagenomic profile comparisons of differentially abundant pathways between PD and SP group samples; features with $q < 0.1$ were considered significant and were thus retained. A positive difference between proportions denotes higher abundance in PD (red), whereas a negative difference between proportions shows higher abundance in SP (blue).

final non-redundant gut gene set in this study contained 3,365,331 ORFs, among which more than 100 amino acids accounted for 72.79%. All unigenes were aligned to the EggNOG Database and dbCAN2 to classify the functions of the predicted unigenes. Among them, 2,101,873(62.46%), 1,364,199(40.54%), and 301,563(8.96%) unigenes were annotated according to the Cluster of Orthologous Groups (COG) of protein database, KEGG Orthology (KO) database, and dbCAN2 database, respectively. STAMP was used to evaluate the relative enrichment of COG, KO, and carbohydrate-active enzymes (CAZymes) gene categories between the PD and control metagenomes. Enrichment analysis of COG-annotated proteins shows that transcription and secondary metabolite biosynthesis, transport, and catabolism were significantly higher in the PD patient group (**Figure 5A**). Based on the findings for the KO annotated proteins, 86 proteins were found to be significantly different between PD patients and controls (**Figure 5B**). In regard to CAZymes, the study found that GH43 was significantly reduced, whereas GH19 and CBM51 were significantly higher in PD patients (**Figure 5C**). The complete information is provided in **Supplementary Table 7**.

Pathway Analysis

A total of 474 biologically specific pathways (**Supplementary Table 7**) were identified in the two sample sets using the MetaCyc database in order to determine the differences in metabolic potential of the gut microbiome between PD patients and controls. The majority of the pathways were related to bacteria, and this was similar to the taxon results in MetaPhlAn2. PERMANOVA analysis based on the Bray–Curtis dissimilarity index showed that when the health status was used as the grouping variable, the difference in abundance of metabolic pathways distinguished the PD group from the SP group ($P = 0.063$, $R^2 = 0.039$). In STAMP, 13 metabolic pathways were identified to have significant differences between the PD and SP groups (Welch *t* test, storey FDR $q < 0.1$) (**Figure 5D**). The L-rhamnose degradation I (RHAMCAT-PWY) and superpathway of thiamin diphosphate biosynthesis III (THISYNARA-PWY) were found to be enriched in the gut microbiome in the SP group, whereas gluconeogenesis I (GLUCONEO-PWY); L-histidine degradation I (HISDEG-PWY); superpathway of L-lysine, L-threonine, and L-methionine biosynthesis I (P4-PWY); acetyl-CoA fermentation to butanoate II (PWY-5676); superpathway of guanosine nucleotides degradation (PWY-6595); inosine-5′-phosphate biosynthesis III (PWY-7234); anaerobic energy metabolism (PWY-7383); superpathway of sulfur amino acid biosynthesis (PWY-821); aspartate superpathway (PWY0-781); gluconeogenesis III (PWY66-399); and adenosine nucleotides degradation II (SALVADEHYPOX-PWY) were found to be enriched in the PD group. These results show that there were significant differences in the generation of precursor metabolites and energies between the two groups and also in the biological synthesis of amino acids.

DISCUSSION

Main Findings

The gut microbiome is a vast and complex miniecosystem established in the human intestinal tract. It generates various metabolites that significantly affect the physiology, steady state of energy, inflammatory processes, and immunologic functions of the host, playing an important role in maintaining host health (de Clercq et al., 2016; Clavel et al., 2017; Espinoza and Minami, 2018). The advent of high-throughput sequencing technology has completely changed the

understanding of the relationship between the gut microbiome and human health. In this study, the shotgun metagenomic sequencing method is used for the first time to analyze the gut microbiome in PD patients and their healthy spouses in central China. The findings reveal significant differences in the composition and function of the gut microbiome between the PD patients and their spouses. β-Diversity analysis identifies significant differences between the PD and SP groups, revealing that the differences in the gut microbiome are caused by disease status. Moreover, the bacteriophage abundance in the PD group is significantly higher than in the SP group. Therefore, the gut microbiome compositions in the PD and SP groups show significant differences at all taxonomic levels except at the kingdom level. Enterotype analysis, as one of the methods for the classification of microbial community structure, is likely to be used as an index for the evaluation of health status in the future (Hildebrand et al., 2013; Costea et al., 2018). However, no significant dispersion trend was observed between the two groups. At the genus level, the RF model, after selection of features, distinguished between the PD patients and the SP group with very high accuracy (AUC = 0.803). Correlation analysis of clinical manifestation and microbiome composition has significant value in the study of disease progression. In addition, our findings reveal differences in gene categories and microbiome metabolism, for example, branched-chain amino acid (BCAA) transport system–related proteins, GH43, and the acetyl-CoA fermentation to butanoate II pathway, which are related to the generation of precursor metabolites of SCFAs.

Analysis of the Microbiome

Previous studies comparing the gut microbiome between PD patients and the SP group have been mainly carried out at the level of genus and above because of limitations in research methods (Li et al., 2017c; Qian et al., 2018). In this study, significant differences were identified between the composition of the gut microbiome of the PD and the SP groups at all taxonomic levels except the kingdom level. Thus, our results further strengthen the "gastrointestinal hypothesis" of PD. In the following section, we focus on the differences between the two groups at family, genus, and species levels. At the family level, the PD group showed *Bifidobacteriaceae* enrichment. This is consistent with recent studies (Scheperjans et al., 2015; Hill-Burns et al., 2017; Hopfner et al., 2017; Lin et al., 2018). No study has reported a high abundance of *Oxalobacteraceae*, *Desulfovibrionaceae*, *Rikenellaceae*, and *Clostridiales_Family_XI_Incertae_Sedis* and a novel unclassified family of the order *Clostridiales* in PD. The genera enriched in PD showed evolutionary relationships with family levels to some extent; these genera were *Desulfovibrio*, *Alistipes*, *Oxalobacter*, *Bilophila*, and *Scardovia*. In a recent study, fecal analysis of regressive infantile autism patients by pyrosequencing technology showed that *Desulfovibrio* was more common among infantile autism patients relative to the control group (Finegold, 2011). Such bacteria can generate important virulence factors that can account for several pathologic features of infantile autism. Interestingly, PD patients also suffer from depression, cognitive disorders, and other non-motor symptoms (Chen et al., 2013). The genera enriched in PD that showed no evolutionary relationship included *Butyricimonas*, *Butyrivibrio*, *Subdoligranulum*, and *Anaerotruncus*. A previous study has shown that PD patients exhibit *Ruminococcaceae* family enrichment (Li F. et al., 2019); however, this was not the case in this study. Our results show that a novel unclassified genus of the family *Ruminococcaceae* was enriched in the SP group. In addition, we found that *Bacteroides* were enriched in the control group. Study has shown that *Bacteroides* can actively improve the intestinal environment, for example, by reducing intracellular oxygen levels, thereby allowing the growth of strict anaerobes (Wexler and Goodman, 2017). Of interest is that inflammation is a central component of PD pathology. Recently, there has emerged a clear understanding that several species of *Bacteroides* express an integrase that can rapidly recruit white blood cells to kill the immune cells that cause inflammatory bowel disease and prevent the occurrence of IBD (Hebbandi Nanjundappa et al., 2017). This study further identified PD microbial markers and established a diagnostic model from the 20 MDA biomarkers with high diagnostic accuracy. Therefore, gut microbiome analysis represents a tool for the development of targeted non-invasive biomarkers for PD diagnosis.

Key Species

It is still necessary to identify the key species in the gut microbiome that correlate with specific metabolites or disease phenotypes in order to understand the ecological interactions among them and between them and their hosts (Zhang and Zhao, 2016). We further identified enrichment of a species that has never been mentioned previously in the intestinal microbiota of PD patients, that is, *Bilophila wadsworthia*. This bacterium erodes the mucus layer of the colon, allowing bacterial entry into the lining cells (Ribaldone et al., 2018). A previous study has shown that the glycyl radical enzyme enhances the production of H_2S by *B. wadsworthia* (Peck et al., 2019). H_2S is highly toxicogenomic and causes ulcerative colitis and colorectal cancer (Attene-Ramos et al., 2010). This metabolite can also reduce the disulfide bond in the mucous layer of the enteric epithelium, thereby damaging the intestinal barrier (Ijssennagger et al., 2016). During aging, the increase in the permeability of the intestinal epithelium may aggravate damage to the integrity of the intestinal barrier (Camilleri et al., 2012), which could lead to PD under the combined action of several factors. Studies show that hydrogen may provide energy required for the growth of *B. wadsworthia* (da Silva et al., 2008). Thus, overgrowth of such bacteria may accelerate consumption of hydrogen in the intestinal tract. Notably, hydrogen gas selectively neutralizes toxic hydroxyl radicals, downregulates the expression of proinflammatory factors, and maintains cerebrovascular reactivity (Ostojic, 2018). Therefore, the changes in PD microbiome composition impact antioxidant processes in the gut.

Phage Analysis

Our study shows that phages were significantly enriched in the PD group. Currently, it is not known how phages affect the structure and function of the gut microbiome in the healthy human (Manrique et al., 2016). However, some evidence indicates

that phages may reflect the health status of an individual (De Sordi et al., 2019; Hsu et al., 2019). A study found that the number of phages in the intestinal tract was significantly increased in type 2 diabetes patients, and many of these phages were of an unknown type (Ma et al., 2018). Intestinal-tract phages may have various possible roles in the pathogenic mechanism underlying PD, which provides potential novel ways to elucidate the mechanisms of the gut microbiome in PD patients.

Correlation of the Intestinal Microbiota With Clinical Manifestations of Parkinson's Disease

In this study, some genera were related to clinical manifestations of PD, including disease duration and severity. Notably, *Klebsiella* and *Parasutterella* were positively correlated with clinical manifestations in PD, and *Prevotella* was negatively correlated with disease severity. Currently, there is no evidence supporting the relationship between hydrogen produced in the intestinal tract and PD. Some studies indicate that changes in the hydrogen-generating microbiome in PD may cause serious damage, compromising motor functions (Keshavarzian et al., 2015; Scheperjans et al., 2015). Our results also suggest that the abundance of hydrogen-generating *Prevotella* is negatively correlated with two clinical manifestations that reflect disease severity, namely, UPDRS III and H&Y stage. H_2 is produced by intestinal microorganisms that may play a role in the pathogenesis of PD as a mediator of the brain–gut–microbiome axis (Ostojic, 2018). Although the data show that the correlation is not particularly strong, we believe that a trend exists. The above results may be due to the small number of participants, resulting in a certain degree of randomness. Larger population data are therefore needed for further research. In addition, this is a cross-sectional study, and a time-series study is required for further verification of the findings.

Gene Enrichment Analysis

The human body carries more than 10 times the number of microbes than human cells and 100 times more microbial genes than its own (Zhu et al., 2010; Thursby and Juge, 2017). It is the gene products of these microbiota that interact with the intestinal microecosystem, and their potential functions can provide some insights into the occurrence and development of diseases. From the results of the study, it can be observed that the function class "secondary metabolites biosynthesis, transport, and catabolism" was found to be slightly enriched in PD. It is worth noting that in KO-based annotations, BCAA transport system–related proteins increased significantly in the PD group, namely, BCAA transport system ATP-binding protein, BCAA transport system permease protein, and BCAA transport system substrate-binding protein. Valine, leucine, and isoleucine are considered essential amino acids because they cannot be synthesized *de novo* and must be obtained from the diet. They participate indirectly and directly in a variety of biochemical functions in the peripheral nervous system and CNS (Fernstrom, 2005; Brosnan and Brosnan, 2006; Sperringer et al., 2017). In addition, BCAAs are considered key nitrogen donors involved in interorgan and intracellular nitrogen shuttling. Although vital for normal physiological function, excessive amounts of BCAAs are considered toxic and can cause severe tissue damage, especially to the CNS, as evidenced from the neuropathology associated with maple syrup urine disease, an autosomal recessive metabolic disorder that is caused by excessive BCAA levels (Menkes et al., 1954). Studies have shown that amino acids can be used by intestinal bacteria for the production of SCFAs and BCAAs (Elsden and Hilton, 1978). Pathway analysis results showed that the amino acid synthesis pathway was enriched in the PD group. A limitation of our study is that it is observational, limiting our ability to establish a causal relationship between BCAAs and PD. If a causal relationship between BCAAs and PD can be found, PD can be prevented in the future by modulating the dietary intake and metabolism of these amino acids.

In this study, we also found that GH43 was significantly reduced in PD patients. Studies of the human gut microbiome have identified GH43 enzymes to be among the most abundant CAZymes present (El Kaoutari et al., 2013; Wu et al., 2015). It is well known that diet is a key determinant of the structure and function of intestinal communities. Phytochemicals that enter the circulatory system may be beneficial to health through the induction of stress resistance mechanisms (autophagy, DNA repair, mitochondrial biogenesis, and expression of detoxification and antioxidant enzymes) (Martel et al., 2020). The GH43 family has emerged as important in biomass deconstruction efforts, because studies have found this family in a number of plant cell wall–degrading microorganisms (Kohler et al., 2015). Generally, the carbohydrate composition in the intestine has a profound impact on and may be one of the main driving forces shaping the composition of the intestinal microbiota. The CAZyme profile reflects the adaptability of the gut microbial communities. Therefore, we evaluated the differences in the CAZyme profiles between the two groups to further clarify the possible effects of differences in protein function on physiological functions.

Pathways in Parkinson's Disease

To explore dysbiosis of the microbiome according to taxonomic composition, we further analyzed metabolic pathways. Although 13 pathways differed between the two groups, this study focused more on SCFA production–related pathways. SCFAs, such as acetate, propionate, and butyrate, are products of dietary fiber fermentation by the gut microbiome and are thought to mediate microbiota–gut–brain communication (Dalile et al., 2019). They promote health by increasing the integrity of the enteric epithelium, specific antibody reactions, and the number of regulatory T cells in the colon (Arpaia et al., 2013; Smith et al., 2013). Of note is that a previous study found SCFAs to be sufficient for inducing α-syn pathology and microglial activation in α-syn–overexpressing mice (Sampson et al., 2016). Consistent with this, this study shows, for the first time, that the pathway by which acetyl coenzyme A is fermented to butyric acid II was enriched in PD patients. These results imply that at physiological concentrations in the intestinal tract, SCFAs may suppress inflammatory reactions.

Integration of Research in China's Mainland

Integrating research data on PD and the microbiome in five cities of China, namely, Beijing (Li et al., 2017c), Shanghai (Qian et al., 2018), Guangzhou (Lin et al., 2018), Changchun (Li C. et al., 2019), and Jinzhou (Li F. et al., 2019) (**Supplementary Table 8**), revealed low microbiome overlap among regions and even contradictory results. Geographical factors exert a strong effect on the human intestinal microbiota, and this partly explains the inconsistent dysbiosis patterns reported in small-scale studies in some Chinese mainland cities. However, it is important to identify microbiota associated with cross-regional consensus risk, because consistent signals can be valuable for future research in large populations. The results of the study were consistent with those of previous studies to a certain extent. This study and the Guangzhou study (Lin et al., 2018) found that, at the family level, *Desulfovibrionaceae* and *Bifidobacteriaceae* are elevated in PD patients; at the genus level, findings for *Alistipes* in the Changchun study (Li C. et al., 2019) and *Anaerotruncus* in the Shanghai study (Qian et al., 2018) are consistent with this study and have been confirmed to be elevated in PD patients. *Bacteroides* has been shown to be decreased in PD patients in both the Jinzhou study (Li F. et al., 2019) and this study. Except for the impact of geographic location, this result is not surprising, given that the human microbiome is highly heterogeneous at the genomic level and varies among individuals. Several other factors may account for the different conclusions, such as the physiological state of host, selection of study subjects, sample type, experimental method, and bioinformatics analysis. In addition, none of the studies provide information on antibiotic use in early life or previous *Clostridium difficile* infections, which are known to have profound and long-lasting effects on gut microbiota.

CONCLUSION AND FUTURE PERSPECTIVES

In summary, in this study, we performed shotgun metagenomics analysis of the gut microbiome of PD patients in central China. To our knowledge, this is the first analysis of the PD gut microbiome in central China at the level of lower taxa. This study explains the changes in microbial composition, gene categories, and metabolic pathways based on analysis of fecal samples from PD patients. The principal objective of this study was to determine whether there is evidence for proinflammatory dysbiosis in PD. Further research is necessary to develop effective preventive and therapeutic strategies for PD based on microbiome manipulation.

DATA AVAILABILITY STATEMENT

The datasets presented in this study can be found in online repositories. The names of the repository/repositories and accession number(s) can be found below: https://www.ncbi.nlm.nih.gov/, PRJNA588035.

ETHICS STATEMENT

The studies involving human participants were reviewed and approved by Ethics Committee of Xiangyang No. 1 People's Hospital. The patients/participants provided their written informed consent to participate in this study.

AUTHOR CONTRIBUTIONS

LM participated in the study design, designed statistical tests to test hypothesis, interpreted bioinformatics data, and drafted the manuscript. YZ participated in the study design and analyzed and interpreted clinical data. JT and MS participated in patients' recruitment and analyzed and interpreted clinical data. GZ participated in data analysis and drafted the manuscript. YZ participated in the study design, interpreted bioinformatics data, drafted the manuscript, and instructed and supervised this study. PW participated in the study design and patients' recruitment, analyzed and interpreted clinical data, and instructed and supervised this study. All authors critically reviewed the article and approved the final version.

ACKNOWLEDGMENTS

We would like to thank all the participants.

SUPPLEMENTARY MATERIAL

The Supplementary Material for this article can be found online at: https://www.frontiersin.org/articles/10.3389/fmicb.2021.728479/full#supplementary-material

Supplementary Figure 1 | Distribution of phyla in all samples.

Supplementary Table 1 | Clinical information for all PD samples.

Supplementary Table 2 | Sequencing data generated for each sample.

Supplementary Table 3 | Relative abundance of all taxa for each sample.

Supplementary Table 4 | PERMANOVA of the influence of a single factor on the gut microbiome.

Supplementary Table 5 | Details of LEfSe results between the two groups at different taxonomic levels; the LDA scores (log10) > 2 and $p < 0.05$ are listed.

Supplementary Table 6 | The results of *de novo* sequence assembly of each sample.

Supplementary Table 7 | Differentially abundant proteins and functional alterations between groups.

Supplementary Table 8 | Altered gut microbiota composition in patients with PD observed across different studies in Chinese mainland.

REFERENCES

Arpaia, N., Campbell, C., Fan, X., Dikiy, S., van der Veeken, J., deRoos, P., et al. (2013). Metabolites produced by commensal bacteria promote peripheral regulatory T-cell generation. *Nature* 504, 451–455. doi: 10.1038/nature12726

Arumugam, M., Raes, J., Pelletier, E., Le Paslier, D., Yamada, T., Mende, D. R., et al. (2011). Enterotypes of the human gut microbiome. *Nature* 473, 174–180. doi: 10.1038/nature09944

Attene-Ramos, M. S., Nava, G. M., Muellner, M. G., Wagner, E. D., Plewa, M. J., and Gaskins, H. R. (2010). DNA damage and toxicogenomic analyses of hydrogen sulfide in human intestinal epithelial FHs 74 Int cells. *Environ. Mol. Mutagen* 51, 304–314. doi: 10.1002/em.20546

Bedarf, J. R., Hildebrand, F., Coelho, L. P., Sunagawa, S., Bahram, M., Goeser, F., et al. (2017). Functional implications of microbial and viral gut metagenome changes in early stage L-DOPA-naive Parkinson's disease patients. *Genome Med.* 9:39. doi: 10.1186/s13073-017-0451-z

Braak, H., and Braak, E. (2000). Pathoanatomy of Parkinson's disease. *J. Neurol.* 247(Suppl. 2), II3–II10. doi: 10.1007/PL00007758

Brosnan, J. T., and Brosnan, M. E. (2006). Branched-chain amino acids: enzyme and substrate regulation. *J. Nutr.* 136(Suppl. 1), 207S–211S. doi: 10.1093/jn/136.1.207S

Camilleri, M., Madsen, K., Spiller, R., Greenwood-Van Meerveld, B., and Verne, G. N. (2012). Intestinal barrier function in health and gastrointestinal disease. *Neurogastroenterol. Motil.* 24, 503–512. doi: 10.1111/j.1365-2982.2012.01921.x

Castano-Rodriguez, N., Underwood, A. P., Merif, J., Riordan, S. M., Rawlinson, W. D., Mitchell, H. M., et al. (2018). Gut microbiome analysis identifies potential etiological factors in acute gastroenteritis. *Infect. Immun.* 86:e00060-18. doi: 10.1128/IAI.00060-18

Castillo, X., Castro-Obregon, S., Gutierrez-Becker, B., Gutierrez-Ospina, G., Karalis, N., Khalil, A. A., et al. (2019). Re-thinking the etiological framework of neurodegeneration. *Front. Neurosci.* 13:728. doi: 10.3389/fnins.2019.00728

Chen, H., Burton, E. A., Ross, G. W., Huang, X., Savica, R., Abbott, R. D., et al. (2013). Research on the premotor symptoms of Parkinson's disease: clinical and etiological implications. *Environ. Health Perspect.* 121, 1245–1252. doi: 10.1289/ehp.1306967

Cheng, M., and Ning, K. (2019). Stereotypes about enterotype: the old and new ideas. *Genomics Proteomics Bioinformatics* 17, 4–12. doi: 10.1016/j.gpb.2018.02.004

Clavel, T., Gomes-Neto, J. C., Lagkouvardos, I., and Ramer-Tait, A. E. (2017). Deciphering interactions between the gut microbiota and the immune system via microbial cultivation and minimal microbiomes. *Immunol. Rev.* 279, 8–22. doi: 10.1111/imr.12578

Comeau, A. M., Douglas, G. M., and Langille, M. G. (2017). Microbiome helper: a custom and streamlined workflow for microbiome research. *mSystems* 2:e00127-16. doi: 10.1128/mSystems.00127-16

Cook Shukla L, Schulze, J., Farlow, J., Pankratz, N. D., Wojcieszek, J., and Foroud, T. (1993). *Parkinson Disease Overview*, eds M. P. Adam, H. H. Ardinger, R. A. Pagon, S. E. Wallace, L. J. H. Bean, K. Stephens, et al. (Seattle, Was: GeneReviews).

Costea, P. I., Hildebrand, F., Arumugam, M., Backhed, F., Blaser, M. J., Bushman, F. D., et al. (2018). Publisher correction: enterotypes in the landscape of gut microbial community composition. *Nat. Microbiol.* 3:388. doi: 10.1038/s41564-018-0114-x

Cox, L. M., and Weiner, H. L. (2018). Microbiota signaling pathways that influence neurologic disease. *Neurotherapeutics* 15, 135–145. doi: 10.1007/s13311-017-0598-8

da Silva, S. M., Venceslau, S. S., Fernandes, C. L., Valente, F. M., and Pereira, I. A. (2008). Hydrogen as an energy source for the human pathogen Bilophila wadsworthia. *Antonie Van Leeuwenhoek* 93, 381–390. doi: 10.1007/s10482-007-9215-x

Dalile, B., Van Oudenhove, L., Vervliet, B., and Verbeke, K. (2019). The role of short-chain fatty acids in microbiota-gut-brain communication. *Nat. Rev. Gastroenterol. Hepatol.* 16, 461–478. doi: 10.1038/s41575-019-0157-3

David, L. A., Maurice, C. F., Carmody, R. N., Gootenberg, D. B., Button, J. E., Wolfe, B. E., et al. (2014). Diet rapidly and reproducibly alters the human gut microbiome. *Nature* 505, 559–563. doi: 10.1038/nature12820

de Clercq, N. C., Groen, A. K., Romijn, J. A., and Nieuwdorp, M. (2016). Gut microbiota in obesity and undernutrition. *Adv. Nutr.* 7, 1080–1089. doi: 10.3945/an.116.012914

De Sordi, L., Lourenco, M., and Debarbieux, L. (2019). The battle within: interactions of bacteriophages and bacteria in the gastrointestinal tract. *Cell Host Microbe* 25, 210–218. doi: 10.1016/j.chom.2019.01.018

Deschasaux, M., Bouter, K. E., Prodan, A., Levin, E., Groen, A. K., Herrema, H., et al. (2018). Depicting the composition of gut microbiota in a population with varied ethnic origins but shared geography. *Nat. Med.* 24, 1526–1531. doi: 10.1038/s41591-018-0160-1

Ding, T., and Schloss, P. D. (2014). Dynamics and associations of microbial community types across the human body. *Nature* 509, 357–360. doi: 10.1038/nature13178

El Kaoutari, A., Armougom, F., Gordon, J. I., Raoult, D., and Henrissat, B. (2013). The abundance and variety of carbohydrate-active enzymes in the human gut microbiota. *Nat. Rev. Microbiol.* 11, 497–504. doi: 10.1038/nrmicro3050

Elsden, S. R., and Hilton, M. G. (1978). Volatile acid production from threonine, valine, leucine and isoleucine by clostridia. *Arch. Microbiol.* 117, 165–172. doi: 10.1007/BF00402304

Espinoza, J. L., and Minami, M. (2018). Sensing bacterial-induced DNA damaging effects via natural killer group 2 member D immune receptor: from Dysbiosis to autoimmunity and carcinogenesis. *Front. Immunol.* 9:52. doi: 10.3389/fimmu.2018.00052

Fang, C., Zhong, H., Lin, Y., Chen, B., Han, M., Ren, H., et al. (2018). Assessment of the cPAS-based BGISEQ-500 platform for metagenomic sequencing. *Gigascience* 7, 1–8. doi: 10.1093/gigascience/gix133

Fernstrom, J. D. (2005). Branched-chain amino acids and brain function. *J. Nutr.* 135(Suppl. 6), 1539S–1546S. doi: 10.1093/jn/135.6.1539S

Finegold, S. M. (2011). Desulfovibrio species are potentially important in regressive autism. *Med. Hypotheses* 77, 270–274. doi: 10.1016/j.mehy.2011.04.032

Franzosa, E. A., Hsu, T., Sirota-Madi, A., Shafquat, A., Abu-Ali, G., Morgan, X. C., et al. (2015). Sequencing and beyond: integrating molecular 'omics' for microbial community profiling. *Nat. Rev. Microbiol.* 13, 360–372. doi: 10.1038/nrmicro3451

Franzosa, E. A., McIver, L. J., Rahnavard, G., Thompson, L. R., Schirmer, M., Weingart, G., et al. (2018). Species-level functional profiling of metagenomes and metatranscriptomes. *Nat. Methods* 15, 962–968. doi: 10.1038/s41592-018-0176-y

Gurevich, A., Saveliev, V., Vyahhi, N., and Tesler, G. (2013). QUAST: quality assessment tool for genome assemblies. *Bioinformatics* 29, 1072–1075. doi: 10.1093/bioinformatics/btt086

Hebbandi Nanjundappa, R., Ronchi, F., Wang, J., Clemente-Casares, X., Yamanouchi, J., Sokke Umeshappa, C., et al. (2017). A gut microbial mimic that hijacks diabetogenic autoreactivity to suppress colitis. *Cell* 171, 655–667.e17. doi: 10.1016/j.cell.2017.09.022

Hildebrand, F., Nguyen, T. L., Brinkman, B., Yunta, R. G., Cauwe, B., Vandenabeele, P., et al. (2013). Inflammation-associated enterotypes, host genotype, cage and inter-individual effects drive gut microbiota variation in common laboratory mice. *Genome Biol.* 14:R4. doi: 10.1186/gb-2013-14-1-r4

Hill-Burns, E. M., Debelius, J. W., Morton, J. T., Wissemann, W. T., Lewis, M. R., Wallen, Z. D., et al. (2017). Parkinson's disease and Parkinson's disease medications have distinct signatures of the gut microbiome. *Mov. Disord.* 32, 739–749. doi: 10.1002/mds.26942

Holmqvist, S., Chutna, O., Bousset, L., Aldrin-Kirk, P., Li, W., Bjorklund, T., et al. (2014). Direct evidence of Parkinson pathology spread from the gastrointestinal tract to the brain in rats. *Acta Neuropathol.* 128, 805–820. doi: 10.1007/s00401-014-1343-6

Hopfner, F., Kunstner, A., Muller, S. H., Kunzel, S., Zeuner, K. E., Margraf, N. G., et al. (2017). Gut microbiota in Parkinson disease in a northern German cohort. *Brain Res.* 1667, 41–45. doi: 10.1016/j.brainres.2017.04.019

Hsu, B. B., Gibson, T. E., Yeliseyev, V., Liu, Q., Lyon, L., Bry, L., et al. (2019). Dynamic modulation of the gut microbiota and metabolome by bacteriophages in a mouse model. *Cell Host Microbe* 25, 803–814.e5. doi: 10.1016/j.chom.2019.05.001

Huerta-Cepas, J., Szklarczyk, D., Heller, D., Hernandez-Plaza, A., Forslund, S. K., Cook, H., et al. (2019). eggNOG 5.0: a hierarchical, functionally and

phylogenetically annotated orthology resource based on 5090 organisms and 2502 viruses. *Nucleic Acids Res.* 47, D309–D314. doi: 10.1093/nar/gky1085

Ijssennagger, N., van der Meer, R., and van Mil, S. W. C. (2016). Sulfide as a mucus barrier-breaker in inflammatory bowel disease? *Trends Mol. Med.* 22, 190–199. doi: 10.1016/j.molmed.2016.01.002

Keshavarzian, A., Green, S. J., Engen, P. A., Voigt, R. M., Naqib, A., Forsyth, C. B., et al. (2015). Colonic bacterial composition in Parkinson's disease. *Mov. Disord.* 30, 1351–1360. doi: 10.1002/mds.26307

Kohler, A., Kuo, A., Nagy, L. G., Morin, E., Barry, K. W., Buscot, F., et al. (2015). Convergent losses of decay mechanisms and rapid turnover of symbiosis genes in mycorrhizal mutualists. *Nat. Genet.* 47, 410–415. doi: 10.1038/ng.3223

Krautkramer, K. A., Kreznar, J. H., Romano, K. A., Vivas, E. I., Barrett-Wilt, G. A., Rabaglia, M. E., et al. (2016). Diet-microbiota interactions mediate global epigenetic programming in multiple host tissues. *Mol. Cell* 64, 982–992. doi: 10.1016/j.molcel.2016.10.025

Kushugulova, A., Forslund, S. K., Costea, P. I., Kozhakhmetov, S., Khassenbekova, Z., Urazova, M., et al. (2018). Metagenomic analysis of gut microbial communities from a Central Asian population. *BMJ Open* 8:e021682. doi: 10.1136/bmjopen-2018-021682

Leplae, R., Lima-Mendez, G., and Toussaint, A. (2010). ACLAME: a classification of mobile genetic elements, update 2010. *Nucleic Acids Res.* 38, D57–D61. doi: 10.1093/nar/gkp938

Li, C., Cui, L., Yang, Y., Miao, J., Zhao, X., Zhang, J., et al. (2019). Gut microbiota differs between Parkinson's disease patients and healthy controls in Northeast China. *Front. Mol. Neurosci.* 12:171. 10.3389/fnmol.2019.00171 N

Li, D., Liu, C. M., Luo, R., Sadakane, K., and Lam, T. W. (2015). MEGAHIT: an ultra-fast single-node solution for large and complex metagenomics assembly via succinct de Bruijn graph. *Bioinformatics* 31, 1674–1676. doi: 10.1093/bioinformatics/btv033

Li, F., Wang, P., Chen, Z., Sui, X., Xie, X., and Zhang, J. (2019). Alteration of the fecal microbiota in North-Eastern Han Chinese population with sporadic Parkinson's disease. *Neurosci. Lett.* 707:134297. doi: 10.1016/j.neulet.2019.134297

Li, W., Wu, X., Hu, X., Wang, T., Liang, S., Duan, Y., et al. (2017c). Structural changes of gut microbiota in Parkinson's disease and its correlation with clinical features. *Sci. China Life Sci.* 60, 1223–1233. doi: 10.1007/s11427-016-9001-4

Li, J., Jin, M., Wang, L., Qin, B., and Wang, K. (2017a). MDS clinical diagnostic criteria for Parkinson's disease in China. *J. Neurol.* 264, 476–481. doi: 10.1007/s00415-016-8370-2

Li, J., Zhao, F., Wang, Y., Chen, J., Tao, J., Tian, G., et al. (2017b). Gut microbiota dysbiosis contributes to the development of hypertension. *Microbiome* 5:14. doi: 10.1186/s40168-016-0222-x

Li, W., Jaroszewski, L., and Godzik, A. (2001). Clustering of highly homologous sequences to reduce the size of large protein databases. *Bioinformatics* 17, 282–283. doi: 10.1093/bioinformatics/17.3.282

Lin, A., Zheng, W., He, Y., Tang, W., Wei, X., He, R., et al. (2018). Gut microbiota in patients with Parkinson's disease in southern China. *Parkinsonism Relat. Disord.* 53, 82–88. doi: 10.1016/j.parkreldis.2018.05.007

Ma, Y., You, X., Mai, G., Tokuyasu, T., and Liu, C. (2018). A human gut phage catalog correlates the gut phageome with type 2 diabetes. *Microbiome* 6:24. doi: 10.1186/s40168-018-0410-y

Manrique, P., Bolduc, B., Walk, S. T., van der Oost, J., de Vos, W. M., and Young, M. J. (2016). Healthy human gut phageome. *Proc. Natl. Acad. Sci. U.S.A.* 113, 10400–10405. doi: 10.1073/pnas.1601060113

Martel, J., Ojcius, D. M., Ko, Y. F., and Young, J. D. (2020). Phytochemicals as prebiotics and biological stress inducers. *Trends Biochem. Sci.* 45, 462–471. doi: 10.1016/j.tibs.2020.02.008

Menkes, J. H., Hurst, P. L., and Craig, J. M. (1954). A new syndrome: progressive familial infantile cerebral dysfunction associated with an unusual urinary substance. *Pediatrics* 14, 462–467.

Mortality, G. B. D. (2016). Causes of death C. Global, regional, and national life expectancy, all-cause mortality, and cause-specific mortality for 249 causes of death, 1980-2015: a systematic analysis for the Global Burden of Disease Study 2015. *Lancet* 388, 1459–1544. doi: 10.1016/S0140-6736(16)31012-1

Norman, J. M., Handley, S. A., Baldridge, M. T., Droit, L., Liu, C. Y., Keller, B. C., et al. (2015). Disease-specific alterations in the enteric virome in inflammatory bowel disease. *Cell* 160, 447–460. doi: 10.1016/j.cell.2015.01.002

Ostojic, S. M. (2018). Inadequate production of H2 by gut microbiota and Parkinson disease. *Trends Endocrinol. Metab.* 29, 286–288. doi: 10.1016/j.tem.2018.02.006

Parks, D. H., Tyson, G. W., Hugenholtz, P., and Beiko, R. G. (2014). STAMP: statistical analysis of taxonomic and functional profiles. *Bioinformatics* 30, 3123–3124. doi: 10.1093/bioinformatics/btu494

Patro, R., Duggal, G., Love, M. I., Irizarry, R. A., and Kingsford, C. (2017). Salmon provides fast and bias-aware quantification of transcript expression. *Nat. Methods* 14, 417–419. doi: 10.1038/nmeth.4197

Peck, S. C., Denger, K., Burrichter, A., Irwin, S. M., Balskus, E. P., and Schleheck, D. (2019). A glycyl radical enzyme enables hydrogen sulfide production by the human intestinal bacterium Bilophila wadsworthia. *Proc. Natl. Acad. Sci. U.S.A.* 116, 3171–3176. doi: 10.1073/pnas.1815661116

Qian, Y., Yang, X., Xu, S., Wu, C., Song, Y., Qin, N., et al. (2018). Alteration of the fecal microbiota in Chinese patients with Parkinson's disease. *Brain Behav. Immun.* 70, 194–202. doi: 10.1016/j.bbi.2018.02.016

Qin, J., Li, Y., Cai, Z., Li, S., Zhu, J., Zhang, F., et al. (2012). A metagenome-wide association study of gut microbiota in type 2 diabetes. *Nature* 490, 55–60. doi: 10.1038/nature11450

Qureshi, I. A., and Mehler, M. F. (2013). Towards a 'systems'-level understanding of the nervous system and its disorders. *Trends Neurosci.* 36, 674–684. doi: 10.1016/j.tins.2013.07.003

Rehman, A., Rausch, P., Wang, J., Skieceviciene, J., Kiudelis, G., Bhagalia, K., et al. (2016). Geographical patterns of the standing and active human gut microbiome in health and IBD. *Gut* 65, 238–248. doi: 10.1136/gutjnl-2014-308341

Ribaldone, D. G., Pellicano, R., and Actis, G. C. (2018). Inflammation: a highly conserved, Janus-like phenomenon-a gastroenterologist' perspective. *J. Mol. Med.* 96, 861–871. doi: 10.1007/s00109-018-1668-z

Sampson, T. R., Debelius, J. W., Thron, T., Janssen, S., Shastri, G. G., Ilhan, Z. E., et al. (2016). Gut microbiota regulate motor deficits and neuroinflammation in a model of Parkinson's disease. *Cell* 167, 1469–1480.e12. doi: 10.1016/j.cell.2016.11.018

Scheperjans, F., Aho, V., Pereira, P. A., Koskinen, K., Paulin, L., Pekkonen, E., et al. (2015). Gut microbiota are related to Parkinson's disease and clinical phenotype. *Mov. Disord.* 30, 350–358. doi: 10.1002/mds.26069

Seemann, T. (2014). Prokka: rapid prokaryotic genome annotation. *Bioinformatics* 30, 2068–2069. doi: 10.1093/bioinformatics/btu153

Segata, N., Izard, J., Waldron, L., Gevers, D., Miropolsky, L., Garrett, W. S., et al. (2011). Metagenomic biomarker discovery and explanation. *Genome Biol.* 12:R60. doi: 10.1186/gb-2011-12-6-r60

Smith, P. M., Howitt, M. R., Panikov, N., Michaud, M., Gallini, C. A., Bohlooly, Y. M., et al. (2013). The microbial metabolites, short-chain fatty acids, regulate colonic Treg cell homeostasis. *Science* 341, 569–573. doi: 10.1126/science.1241165

Soergel, D. A., Dey, N., Knight, R., and Brenner, S. E. (2012). Selection of primers for optimal taxonomic classification of environmental 16S rRNA gene sequences. *ISME J.* 6, 1440–1444. doi: 10.1038/ismej.2011.208

Song, S. J., Lauber, C., Costello, E. K., Lozupone, C. A., Humphrey, G., Berg-Lyons, D., et al. (2013). Cohabiting family members share microbiota with one another and with their dogs. *Elife* 2:e00458. doi: 10.7554/eLife.00458.018

Sperringer, J. E., Addington, A., and Hutson, S. M. (2017). Branched-chain amino acids and brain metabolism. *Neurochem. Res.* 42, 1697–1709. doi: 10.1007/s11064-017-2261-5

Sun, M. F., and Shen, Y. Q. (2018). Dysbiosis of gut microbiota and microbial metabolites in Parkinson's disease. *Ageing Res. Rev.* 45, 53–61. doi: 10.1016/j.arr.2018.04.004

Sun, M. F., Zhu, Y. L., Zhou, Z. L., Jia, X. B., Xu, Y. D., Yang, Q., et al. (2018). Neuroprotective effects of fecal microbiota transplantation on MPTP-induced Parkinson's disease mice: gut microbiota, glial reaction and TLR4/TNF-alpha signaling pathway. *Brain Behav. Immun.* 70, 48–60. doi: 10.1016/j.bbi.2018.02.005

Thursby, E., and Juge, N. (2017). Introduction to the human gut microbiota. *Biochem. J.* 474, 1823–1836. doi: 10.1042/BCJ20160510

Truong, D. T., Franzosa, E. A., Tickle, T. L., Scholz, M., Weingart, G., Pasolli, E., et al. (2015). MetaPhlAn2 for enhanced metagenomic taxonomic profiling. *Nat. Methods* 12, 902–903. doi: 10.1038/nmeth.3589

Unger, M. M., Spiegel, J., Dillmann, K. U., Grundmann, D., Philippeit, H., Burmann, J., et al. (2016). Short chain fatty acids and gut microbiota differ between patients with Parkinson's disease and age-matched controls. *Parkinsonism Relat. Disord.* 32, 66–72. doi: 10.1016/j.parkreldis.2016.08.019

Wang, S., Li, N., Zou, H., and Wu, M. (2019). Gut microbiome-based secondary metabolite biosynthetic gene clusters detection in Parkinson's disease. *Neurosci. Lett.* 696, 93–98. doi: 10.1016/j.neulet.2018.12.021

Wexler, A. G., and Goodman, A. L. (2017). An insider's perspective: *Bacteroides* as a window into the microbiome. *Nat. Microbiol.* 2:17026. doi: 10.1038/nmicrobiol.2017.26

Wu, M., McNulty, N. P., Rodionov, D. A., Khoroshkin, M. S., Griffin, N. W., Cheng, J., et al. (2015). Genetic determinants of in vivo fitness and diet responsiveness in multiple human gut *Bacteroides*. *Science* 350:aac5992. doi: 10.1126/science.aac5992

Zhang, C., and Zhao, L. (2016). Strain-level dissection of the contribution of the gut microbiome to human metabolic disease. *Genome Med.* 8:41. doi: 10.1186/s13073-016-0304-1

Zhang, H., Yohe, T., Huang, L., Entwistle, S., Wu, P., Yang, Z., et al. (2018). dbCAN2: a meta server for automated carbohydrate-active enzyme annotation. *Nucleic Acids Res.* 46, W95–W101. doi: 10.1093/nar/gky418

Zhu, B., Wang, X., and Li, L. (2010). Human gut microbiome: the second genome of human body. *Protein Cell* 1, 718–725. doi: 10.1007/s13238-010-0093-z

Conflict of Interest: The authors declare that the research was conducted in the absence of any commercial or financial relationships that could be construed as a potential conflict of interest.

Publisher's Note: All claims expressed in this article are solely those of the authors and do not necessarily represent those of their affiliated organizations, or those of the publisher, the editors and the reviewers. Any product that may be evaluated in this article, or claim that may be made by its manufacturer, is not guaranteed or endorsed by the publisher.

frontiers in Microbiology

ORIGINAL RESEARCH
published: 02 December 2021
doi: 10.3389/fmicb.2021.749760

Alone Yet Not Alone: *Frankia* Lives Under the Same Roof With Other Bacteria in Actinorhizal Nodules

Faten Ghodhbane-Gtari[1,2,3], Timothy D'Angelo[4†], Abdellatif Gueddou[3], Sabrine Ghazouani[3], Maher Gtari[1,3] and Louis S. Tisa[4]*

[1] Laboratoire Microorganismes et Biomolécules Actives, Faculté des Sciences de Tunis, Université de Tunis El Manar, Tunis, Tunisia, [2] Institut Supérieur de Biotechnologie de Sidi Thabet, Université de la Manouba, Sidi Thabet, Tunisia, [3] Unité de Bactériologie Moléculaire et Génomique, Centre Urbain Nord, Institut National des Sciences Appliquées et de Technologie, Université de Carthage, Tunis, Tunisia, [4] Department of Molecular, Cellular, and Biomedical Sciences, University of New Hampshire, Durham, NH, United States

OPEN ACCESS

Edited by:
F. L. Consoli, University of São Paulo, Brazil

Reviewed by:
Monali C. Rahalkar, Agharkar Research Institute, India
Luis Wall, National University of Quilmes, Argentina

***Correspondence:**
Louis S. Tisa
louis.tisa@unh.edu

† Present address:
Timothy D'Angelo, Bigelow Laboratory for Ocean Sciences, East Boothbay, ME, United States

Specialty section:
This article was submitted to Systems Microbiology, a section of the journal Frontiers in Microbiology

Received: *29 July 2021*
Accepted: *08 November 2021*
Published: *02 December 2021*

Citation:
Ghodhbane-Gtari F, D'Angelo T, Gueddou A, Ghazouani S, Gtari M and Tisa LS (2021) Alone Yet Not Alone: Frankia Lives Under the Same Roof With Other Bacteria in Actinorhizal Nodules. Front. Microbiol. 12:749760. doi: 10.3389/fmicb.2021.749760

Actinorhizal plants host mutualistic symbionts of the nitrogen-fixing actinobacterial genus *Frankia* within nodule structures formed on their roots. Several plant-growth-promoting bacteria have also been isolated from actinorhizal root nodules, but little is known about them. We were interested investigating the *in planta* microbial community composition of actinorhizal root nodules using culture-independent techniques. To address this knowledge gap, 16S rRNA gene amplicon and shotgun metagenomic sequencing was performed on DNA from the nodules of *Casuarina glauca.* DNA was extracted from *C. glauca* nodules collected in three different sampling sites in Tunisia, along a gradient of aridity ranging from humid to arid. Sequencing libraries were prepared using Illumina NextEra technology and the Illumina HiSeq 2500 platform. Genome bins extracted from the metagenome were taxonomically and functionally profiled. Community structure based off preliminary 16S rRNA gene amplicon data was analyzed *via* the QIIME pipeline. Reconstructed genomes were comprised of members of *Frankia*, *Micromonospora*, *Bacillus*, *Paenibacillus*, *Phyllobacterium,* and *Afipia*. *Frankia* dominated the nodule community at the humid sampling site, while the absolute and relative prevalence of *Frankia* decreased at the semi-arid and arid sampling locations. Actinorhizal plants harbor similar non-*Frankia* plant-growth-promoting-bacteria as legumes and other plants. The data suggests that the prevalence of *Frankia* in the nodule community is influenced by environmental factors, with being less abundant under more arid environments.

Keywords: actinorhizal symbiosis, microbiome, endophyte, symbiont, plant-growth-promoting bacteria

INTRODUCTION

Casuarinaceae family comprises four plant genera (*Allocasuarina*, *Casuarina*, *Ceuthostoma,* and *Gymnostoma*) and approximately 86 species and 13 subspecies indigenous to Australia (Steane et al., 2003; Gtari and Dawson, 2011; Diagne et al., 2013; Normand et al., 2014) that are frequently introduced into approximately 150 tropical and subtropical countries where they play an important role for land reclamation, crop protection and as windbreaks (Diagne et al., 2013;

Potgieter et al., 2014). Large-scale planting of casuarinas has proven to have a strong impact especially in China, Senegal, Egypt, and Tunisia (Gtari and Dawson, 2011). In arid and semi-arid areas, salinization of soils and groundwater is a serious problem causing a drastic reduction in agricultural production (Munns, 2005; Rengasamy, 2006)[1]. Over 800 million hectares of land throughout the world are salt affected. A common method for dealing with salt stress problems is to reclaim saline soils with multipurpose, fast-growing salt-tolerant tree species such as *Casuarina* tree. Casuarina are notable for high salt tolerance (Tani and Sasakawa, 2003) and have been used as a green barrier. Despite the applied interests, substantial global invasion consequences for *Casuarina* has noted in Florida and the Mascarene Islands (Potgieter et al., 2014).

Actinorhizal plants, like *Casuarina,* form a nitrogen-fixing symbiosis with the Actinobacteria *Frankia* that results in the formation of root nodule structures where the bacteria are located (Chaia et al., 2010; Normand et al., 2014). Besides *Frankia*, actinorhizal plants are known to associate with mycorrhizae including both ectomycorrhizal or endomycorrhizal fungi (Zhong et al., 1995; Duponnois et al., 2003; Diagne et al., 2013; Zhou et al., 2017). The symbioses with *Frankia* and mycorrhizae allow actinorhizal host plants to colonize harsh environmental terrains including highly contaminated, dry, poorly drained, nutrient-poor, and salinized soils (Diagne et al., 2013, 2015).

Besides *Frankia*, several other non-*Frankia* bacteria have been isolated as a by-product of *Frankia* isolation attempts (Ghodhbane-Gtari and Tisa, 2014). Large numbers of other bacteria were collected from these actinorhizal nodules, occupying the same microniche as *Frankia*. Most of these isolates were ignored or discarded as being irrelevant to the plants. However, these non-*Frankia* Actinobacteria have consistently been isolated from several actinorhizal plants including *Casuarina* (Guillén et al., 1993; Niner et al., 1996; Valdes et al., 2005; Ghodhbane-Gtari et al., 2010), and consist of Actinobacteria from *Micromonospora* (Valdes et al., 2005; Ghodhbane-Gtari et al., 2010), *Nocardia* (Ghodhbane-Gtari et al., 2010, 2019) and *Streptomyces* genera (Ghodhbane-Gtari et al., 2010). Similarly, non-symbiotic bacteria, such as *Azospirillum*, *Bacillus*, *Pseudomonas,* and *Streptomyces,* are known to be auxiliary bacteria in several *Rhizobium*-legume symbioses (Iruthayathas et al., 1983; Grimes and Mount, 1984; Li and Alexander, 1990). In this case, both wild and cultivated legume nodules are not exclusively inhabited by rhizobia, but contain diverse assemblages of non-rhizobial bacteria (Dudeja et al., 2012; Aserse et al., 2013; Martínez-Hidalgo and Hirsch, 2017). These nodule non-rhizobial communities may be influenced more by soil type rather plant genotype (Leite et al., 2017).

During the last decade, culture-dependent and –independent approaches have been used to intensively investigate these effects. For legume nodules, rhizobial, and non-rhizobial endophytes communities have been initiated (Martínez-Hidalgo and Hirsch, 2017; Zhang et al., 2018; Mayhood and Mirza, 2021), but very little is known about microbial communities and their structure associated with actinorhizal nodules. Endophytic bacteria can be found between cells, while others are associated in an intimate relation with the plant. For that intimate association to occur, complex relationships are required during the colonization of plant tissues. Plant endophytes are described as having the ability to restrain pathogen infection, to accelerate seedling emergence, and to promote plant growth. Thus, they can be considered as biocontrol agents (Ryan et al., 2008; Eljounaidi et al., 2016; Santoyo et al., 2016).

In this study, we investigated the structure and function of bacterial communities found in *Casuarina glauca* nodules and associated rhizosphere soils and bulk soils from three different bioclimates in Tunisia. We used both high-throughput amplicon (targeting of the 16S rRNA gene) and whole metagenome shotgun sequencing of *C. glauca* nodules found from the different bioclimates: humid, semi-arid and arid condition. For comparative purposes, high-throughput amplicon sequencing was performed on rhizosphere soils, and bulk soils for these three sites.

MATERIALS AND METHODS

Sampling

Samples of *Casuarina glauca* root nodules, rhizosphere, and bulk soils. Samples were collected in February 2015 from three sites in Tunisia that represented different bioclimatic regions (**Figure 1**). Sample sites were in Tamra (37°3′26″ N 9°14′17″ E), Sidi Bouzid (35°2′ 7.58″ N 9° 29′2.18″ E), and Medenine (33°21′17″ N 10°30′19″ E), representing Mediterranean-humid, semi-arid and arid bioclimatic regions, respectively. Three to four root nodules were used for each replicate and three replicate samples were taken for each site. For the soil and rhizosphere samples, triplicate samples of 5 g soil were collected from each site. Bulk soil was soil that was not in contact with the root system of any plant. Rhizosphere soil was collected by removing organic litter and 15 cm of the surrounding soil from around the *C. glauca* roots. Soil that was attached to roots after removal of the surrounding soil was collected. The samples were placed in sterile plastic tubes and stored at −20°C until analysis. DNA extractions were performed within 24 h of sampling.

DNA Extractions

For the rhizosphere and bulk soil samples, genomic DNA (gDNA) was extracted from 0.5 g of soil using the Qiagen DNA extraction kit as described previously (Ghodhbane-Gtari et al., 2010, 2014). For the *C. glauca* root nodule samples, three to four nodules were used per gDNA extraction and nodules were surface sterilized as described previously (Ghodhbane-Gtari et al., 2019). Root nodules were thoroughly rinsed with water. Surface sterilization conducted by shaking in 30% (v/v) H_2O_2 for 30 min. Sterilized nodules were rinsed thoroughly several times with sterile water. The final wash liquid was tested for microbial growth and only nodules resulting in a sterile final washing liquid were further considered for DNA extraction. The nodule was then aseptically powdered in liquid nitrogen using a sterile mortar and the resulting powder was used for DNA extraction using Qiagen DNA Plant Mini-kit following the manufacturer's protocol.

[1]http://fao.org

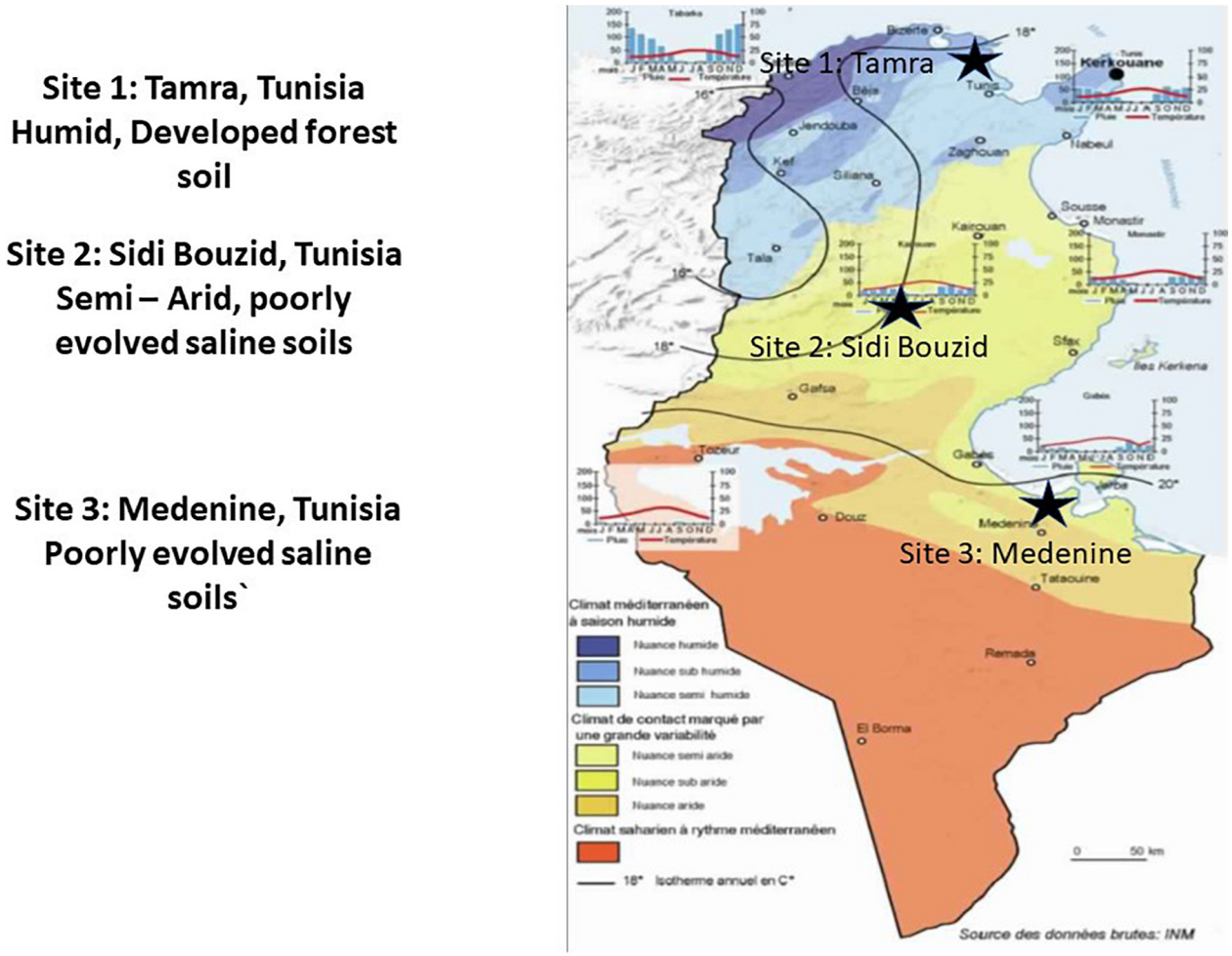

FIGURE 1 | Map and schematic of amplicon survey sampling design: For each sample type from each site, 3 replicates were sampled. Modified from Hénia (2008).

Amplicon and Whole Genome Shotgun Sequencing

To investigate the prokaryotic community profiles of different DNA extracted, sequences corresponding to the V4 hypervariable region the 16S subunit rRNA gene were amplified by PCR using the Earth Microbiome Project 515F/806R universal primers under conditions described previously (Caporaso et al., 2012). For each sample, triplicate amplifications were performed. The triplicates were pooled, and all samples were normalized to equal DNA concentrations. Paired-end sequencing of the amplification product was performed using the Illumina HiSeq 2500 platform at the Hubbard Center for Genome Studies (University of New Hampshire, Durham, NH, United States). Read lengths of 250 bp were obtained and processed as described below.

To generate metagenomes for the *C. glauca* root nodule samples, whole genome shotgun sequencing was performed. Sequencing libraries for the samples were prepared using the Illumina NextEra Library Preparation protocol according to the manufacturer's instructions and were sequenced on an Illumina HiSeq 2500. The same triplicate nodule DNA extractions were used for both the metabarcoding and metagenome shotgun sequencing methods, and metagenome libraries for both methods were sequenced at 150 bp read lengths at the Hubbard Center for Genome Studies (University of New Hampshire, Durham, NH, United States).

Amplicon Sequence Data Processing

The 16S rRNA gene amplicon sequences for each sample were initially processed with Quantitative Insights into Microbial Ecology (QIIME) pipeline (Caporaso et al., 2010b). Paired-end reads were joined using Fastq-join (Aronesty, 2011). Paired-end reads were truncated from positions where nucleotides received a Phred score of 20 or less. Reads with more than three consecutive low-quality nucleotides were discarded. Reads with less than 75% high-quality base-call scores were also discarded. This processing resulted in a total of 176,319 reads with an average length of 253 base pairs.

The reads were clustered as described in the open reference-based protocol provided in QIIME (version 1.9.0-dev) (Rideout et al., 2014). OTUs were clustered by UCLUST, using a 97%

percent identity threshold to define an OTU (Edgar, 2010). Taxonomy was assigned to each OTU cluster using the UCLUST consensus taxonomy assigner by aligning the centroid sequence of each cluster to the Green Genes 13_8 rRNA database with PyNAST (DeSantis et al., 2006; Caporaso et al., 2010a; Edgar, 2010). OTUs that were unable to be aligned to the Green Genes 13_8 database were excluded from downstream analysis. OTUs that only contained one sequence (singletons) were also excluded from downstream analysis. The resulting OTU tables were filtered to exclude all unassigned sequences, and sequences that assigned to mitochondrial or chloroplast taxonomy.

Data Normalization

The OTU table resulting from the process above was rarified to an equal sampling depth based on the smallest library size (1,762 reads) by random sub-sampling of all samples. Alternatively, Cumulative Sum Scaling (CSS), available through the metagenomeSeq R package and facilitated through QIIME, was used to normalize the OTU table (Paulson et al., 2013). Because choice of normalization method has been shown to effect downstream analysis (McMurdie and Holmes, 2014), both methods were used to compare results of normalization techniques. For Alpha diversity analysis, the original OTU table was converted to closed-reference format and corrected for variation in 16S rRNA copy number using the online Galaxy server version of PICRUSt (Langille et al., 2013). This correction was also performed on CSS normalized OTU tables and raw OTU tables in order to assess effects on ordination results.

Amplicon Sequence Data Analysis

Alpha diversity for each sample was calculated based on the Shannon Diversity Index (Shannon, 1948) and significant differences in diversity based on sample type (Nodule, Rhizosphere, or Soil) were determined using ANOVA and the *t*-test in Microsoft Excel. Alpha diversity was also calculated in the similar manner for nodule samples from individual sampling locations. Community beta diversity among samples was measured by the UniFrac distance (Lozupone and Knight, 2005). Both the weighted (quantitative) and unweighted (qualitative) versions of the distance metric were used. Both of these metrics can yield different but complementary results from the same dataset (Lozupone et al., 2007). Distance matrices produced using these metrics were ordinated using Principle Coordinates Analysis (PCoA). Ordinations were created for distance matrices produced by CSS (for both 16S copy number corrected and not corrected), for raw OTU tables with 16S operon copy number correction and for evenly rarefied OTU tables.

Jackknifing, which is the repeated subsampling of a dataset, was used to determine the confidence level in Beta diversity analysis. This technique was performed by randomly subsampling 100 sequences per sample from the rarefied OTU table. For each subsampling, an Unweighted Pair Group Method with Arithmetic Mean (UPGMA) tree was created using the unweighted UniFrac distance matric between samples, based on those 100 randomly subsampled reads. This process was repeated 100 times. A consensus tree was built from the 100 trees with jackknife values for each node representing the number of times, out of the 100 jackknifed trees, that the consensus configuration was observed.

Nodule samples were analyzed by two-way cluster analysis to investigate the difference in nodule community structure across the environmental gradient in the sampling design. An OTU table was constructed that was corrected for 16S operon copy number abundance by PICRUSt and summarized to relative abundance at the genus level. The samples were grouped by hierarchical clustering using the average linkage method. The Bray-Curtis distance between each sample based on taxonomic composition was used for sample clustering. The taxa were clustered by their abundance patterns across samples using the Bray-Curtis distance between metric. Clustering was performed using the data for all genera present. However, for visualization purposes, only taxa that made up greater than 1% of the community were displayed.

Multi-Response Permutation Procedures (MRPP) were performed to determine if there were significant differences in phylogenetic distances based on the sample type (Nodule, Soil, or Rhizosphere). MRPP analysis was performed in R (Version 3.2.1) using the Vegan Library (Oksanen et al., 2016). MRPP To determine if nodules formed a statistically significant group based on the weighted and unweighted UniFrac distance matrices, the samples were partitioned into two categories, nodule ($n = 9$) and non-nodule ($n = 18$). Significance was calculated by permutation of the distance matrices 999 times to determine if the groups had within-group distances that were different to what would be expected by chance. All MRPP analysis was performed on the weighted and unweighted UniFrac distance matrices produced by the different normalization methods described previously (Lozupone et al., 2007; McMurdie and Holmes, 2014).

Soil and Rhizosphere samples were analyzed to test the hypothesis that *C. glauca* maintains a unique microbial community within the rhizosphere at the different sampling locations. Soil ($n = 9$) and Rhizosphere ($n = 9$) samples from all sites were pooled together and analyzed independently of nodule samples in the same fashion as described above. To determine if there were significant groupings between soil and rhizosphere by climate type, the soil and rhizosphere samples were grouped into a humid group ($n = 6$) and non-humid group ($n = 18$). MRPP was performed as above with this grouping using the unweighted UniFrac distance matrix. This metric calculates phylogenetic distance between samples based off of the presence or absence of taxa and is thus useful for identifying differences between samples that come from environments that host distinct communities.

Metagenome Assembly and Analysis

Sequencing Reads Preparation and Assembly

Trimmomatic was used to remove Nextera adapters and filter the raw reads based on quality (Bolger et al., 2014). The following parameters were used. Three base-pairs were trimmed from the tailing and leading ends of each read. The reads were scanned with a sliding window of four base-pairs, and sections of reads were discarded when the average quality score of the base-pairs was below 15. After this process, only reads that retained a minimum length of 36 base pairs were used for downstream

processes. Of these resulting reads, only reads that retained both forward and reverse pairs were used for assembly.

In order to perform differential coverage binning of draft genomes, the read sets from each of the three sampling locations were combined *in silico* and a composite co-assembly was created. SPAdes (version 3.6.0) was used to assemble the combined reads using the metagenomic setting, without error correction (Bankevich et al., 2012). The assembly process used Khmer lengths of 22, 33, and 55 to produce the final assembled contigs.

Binning

Metagenomic Assembled Genomes (MAGs) of individual members of the metagenomic community were binned using the mmgenome package (Albertsen et al., 2013) for R[2] using the Rstudio IDE[3]. This package facilitates distinguishing individual genomes from metagenomes primarily by the unique coverage values of assembled sequences belonging to organisms present in multiple samples, but at different abundances. Coverage values for each contig per-site was performed by individually aligning each read-set to the co-assembled contigs using the Bowtie2 alignment tool (Version 2.2.5) (Langmead and Salzberg, 2012). The resulting Sequence Alignment Map (SAM) files were converted to binary format and sorted to the left-most coordinates on the assembled sequences and depth of coverage per-base was calculated using SAMtools (Version: 0.1.19-96b5f2294a) (Li et al., 2009). The resulting files containing coverage per-base per-contig were converted to average coverage per-contig scripts in the Mmgenome package.

Additional information for assembled contigs was generated following the workflow as described by the mmgenome package developers (Albertsen et al., 2013). Open Reading Frames (ORFs) within the assembled metagenomic contigs were predicted and translated to amino acid sequence using the metagenomic setting of Prodigal (Version 2.6.2) (Hyatt et al., 2010). The translated amino acid fasta file of predicted ORFs was searched against Hidden Markov Models (HMMs) of 111 essential prokaryotic single copy genes provided in the mmgenome package using hmmsearch (Eddy, 1998). ORFs identified as essential genes were extracted from the co-assembly using Perl scripts provided by the mmgenome package.

Taxonomic Classification

Taxonomic information was assigned to each ORF identified as essential gene by searching against the RefSeq protein database using BlastP with an *E* value cutoff of $1e^{-5}$, with five maximum target sequences. The resulting BlastP output in XML format was uploaded into MEGAN (Version 5) (Huson et al., 2007). The Lowest Common Ancestor (LCA) algorithm was used to make a consensus taxonomic assignment for each ORF based off of the top five BlastP hits using the following settings: Top Percent = 5, Minimum Support = 1, Rank = Species. The resulting file was parsed using the hmm.majority.vote.pl script to derive a consensus taxonomic assignment for each assembled contig based off of the taxonomy of the ORFs that it contains.

The coverage and taxonomic information produced above was loaded into the Rstudio environment along with the composite metagenomic co-assembly using BioStrings[4]. The GC content and tetranucleotide frequency distribution of each assembled contig was calculated using the mmgenome R package. A principle component analysis (PCA) of normalized tetranucleotide frequencies of all contigs was performed in R using the mmgenome package. The composite co-assembly was visualized in Rstudio and binning was performed using the tools available in the mmgenome R package. The data that was produced as described above and accompanying rmarkdown files allow the reproduction of the binned draft genomes.

Functional Annotation

Reads from each site were assembled individually using SPAdes-3.6.0 using the metagenomic setting (Bankevich et al., 2012). The resulting assembled contigs were annotated using the Prokka annotation pipeline using the metagenomic settings (Seemann, 2014).

Calculation of Coverage and Relative Abundance

Coverage profiles of individual genomes with PCR duplicates removed were calculated to compare genome coverages at different sites. Reads were aligned to the metagenome assembly using the Bowtie2 alignment tool (Version 2.2.5) (Langmead and Salzberg, 2012). The SAM file resulting from alignment with Bowtie2 was converted to BAM format. The aligned reads were sorted to the left-most coordinate on the indexed metagenome assembly using SAMtools (Version: 0.1.19-96b5f2294a) (Li et al., 2009). Duplicate reads were removed using Picard Tools MarkDuplicates[5]. Coverage for the contigs was calculated from the resulting SAM file using Bedtools (v2.17.0) (Quinlan and Hall, 2010). The coverage calculations per-contig were averaged for all the contigs within a given genome bin. The average coverage for the entire genome was normalized by the amount of reads per data set corresponding to the different sampling sites. The percentage of the given read sets that aligned to plant-derived DNA was used to normalize each genome coverage value based on the differing amounts of plant-derived DNA in the different read sets.

The read sets, with plant-derived reads removed, were aligned to the *Frankia* genome using Bowtie2. The percentage of the reads that aligned to the *Frankia* genome bin were recorded from the standard output statistics in order to compare the relative abundance of *Frankia* in the shotgun data in comparison to the replicated amplicon data.

Mining of Metagenome for Plant-Growth-Promoting Genes and Secondary Metabolites

The Genome Feature File (GFF) produced by Prokka was parsed using a custom python script to evaluate the presence and

[2]http://r-project.org
[3]http://Rstudio.com
[4]https://bioconductor.org/packages/Biostrings
[5]http://broadinstitute.github.io/picard/

taxonomy of plant-growth-promoting genes and genes involved in cellulose, chitin, and pectin degradation within the nodule community. Genes known for plant auxin production (Indole acetic acid and Phenyl acetic acid), phosphate solubilization (alkaline phosphatases and phytases), ACC Deaminase activity and degradation of chitin, cellulose and pectin were identified for each of the three data sets. The presence of these enzymes was identified by parsing the GFF file for the Enzyme Commission (EC) number assigned to a given ORF by the Prokka pipeline. Enzymes that were identified by their EC numbers were annotated by aligning the amino acid sequence of the entry against the RefSeq protein database using BlastP with an *E* value cutoff of $1e^{-5}$ and a maximum output of five entries. Cladograms of the BlastP output were constructed using the Lowest Common Ancestor (LCA) algorithm in MEGAN (Version 5.0) using the following settings: Top Percent = 5, Minimum Support = 1, Rank = Genus. A summary of the EC numbers used in this analysis is in **Supplementary Tables 1–3**. The antiSMASH pipeline (version 3.0) was used to identify secondary metabolites in the binned genomes (Weber et al., 2015). antiSMASH was run using the metagenomic setting to improve gene prediction for highly fragmented metagenomic assemblies.

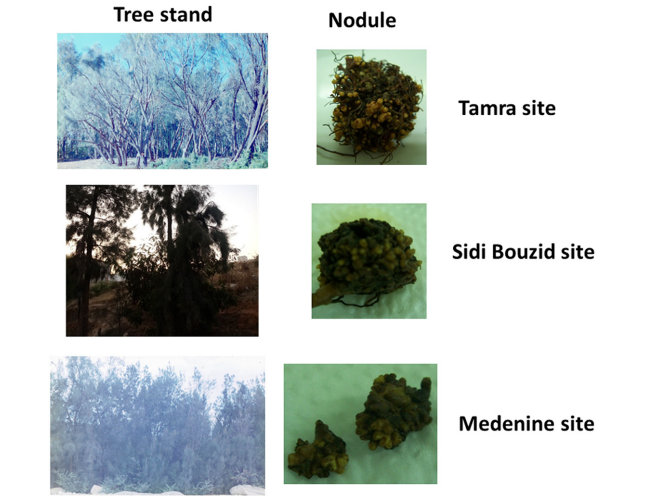

FIGURE 2 | Photograph of *Casuarina* tree stands at the sampling and representative nodules for those trees.

RESULTS

Diversity of the *Casuarina* Nodule Community and Surrounding Soil

Three distinct sites in Tunisia (**Figure 1**) were chosen to assess the effect of environmental conditions on the microbial community structure and diversity for *Casuarina* nodules, rhizosphere and surrounding soil. These sites represented a humid well-developed forest at Tamra, a semi-arid, poorly evolved saline soils of Sidi Bouzid and an arid, poorly evolved saline soils of Medenine. **Figure 2** shows representative *Casuarina* stands from each of these sites and nodules from those stands. There were no obvious differences in nodule shape or size among the three sites and the plants exhibited the same level of general health.

Preprocessing of the 16S rRNA gene amplicon sequences resulted in a total of 7,855 OTUs from the 149,879 paired reads. Individual library sizes ranged from 1,762 to 11,542 reads per sample, with a mean of 5,551 reads per sample. Rarefaction plots were performed in order to estimate the completeness of community sampling at the sequencing depth performed. The rarefaction plots for average observed OTUs per sample type is shown in **Supplementary Figure 1**. These plots show that the nodule samples were sequenced close to saturation, while increased sequencing depth could improve the documentation of rare OTUs for rhizosphere and soil samples.

Alpha Diversity

The Shannon Diversity Index (SDI) was used to measure alpha diversity. This metric was measured on the relative abundance after correction for 16S operon copy number. Diversity measures were grouped by sample type and are as follows; Nodules: 4.47 ± 2.29 (SD), Rhizosphere: 9.33 ± 0.233 (SD) and Soil: 9.52 ± 0.69 (SD), displayed in **Supplementary Figure 2A**. The alpha diversity was significantly less for nodules than for rhizosphere and soil samples (Students *t*-test, $p = 0.00001$). Alpha diversity was calculated for the nodule samples at the three different samples locations. Nodules from Tamra had an average SDI of 2.28 (SD = 0.584), nodules from Sidi Bouzid had an average SDI of 7.32 (SD = 0.389) and nodules from Medenine had an SDI of 3.82 (SD = 0.394) (**Supplementary Figure 2B**).

After correction for 16S operon copy number, the relative abundance of taxa present in the root nodules was analyzed. At the humid sampling site, the relative abundance of *Frankia* was an average of 80% of the nodule community. This prevalence dropped to 1.5% and 0.5% and the semi-arid and arid sampling sites, respectively. These data are like the shotgun sequencing data (**Supplementary Figure 3**), where reads mapping to the binned *Frankia* genome comprised 60% of the humid site read set and that level dropped to 1.71% and 1.63% for the semi-arid and arid sampling sites, respectively. **Supplementary Figure 3** shows the relative abundance of *Frankia* at the three sampling sites using the shotgun and amplicon data. **Figure 3A** gives a taxonomic summary of the nodule samples at the class level. The taxonomic summary of the rhizosphere and bulk soils is shown in **Figure 3B**.

Beta Diversity

Beta diversity was analyzed by measuring the weighted and unweighted UniFrac distances (Lozupone and Knight, 2005). An Unweighted Pair Ground Method with Arithmetic Mean (UPGMA) consensus tree was built from the unweighted UniFrac distance matrix (**Figure 4**). Numbers on the nodes of the tree represent the percentage of trees out of 100 bootstrapped trees that had the configuration of the final consensus tree. The grouping on the tree shows that nodule samples from all sites form one clade when analyzed by the presence or absence of taxa in the samples, after removing one outlier (Sample ID: N3SIDI).

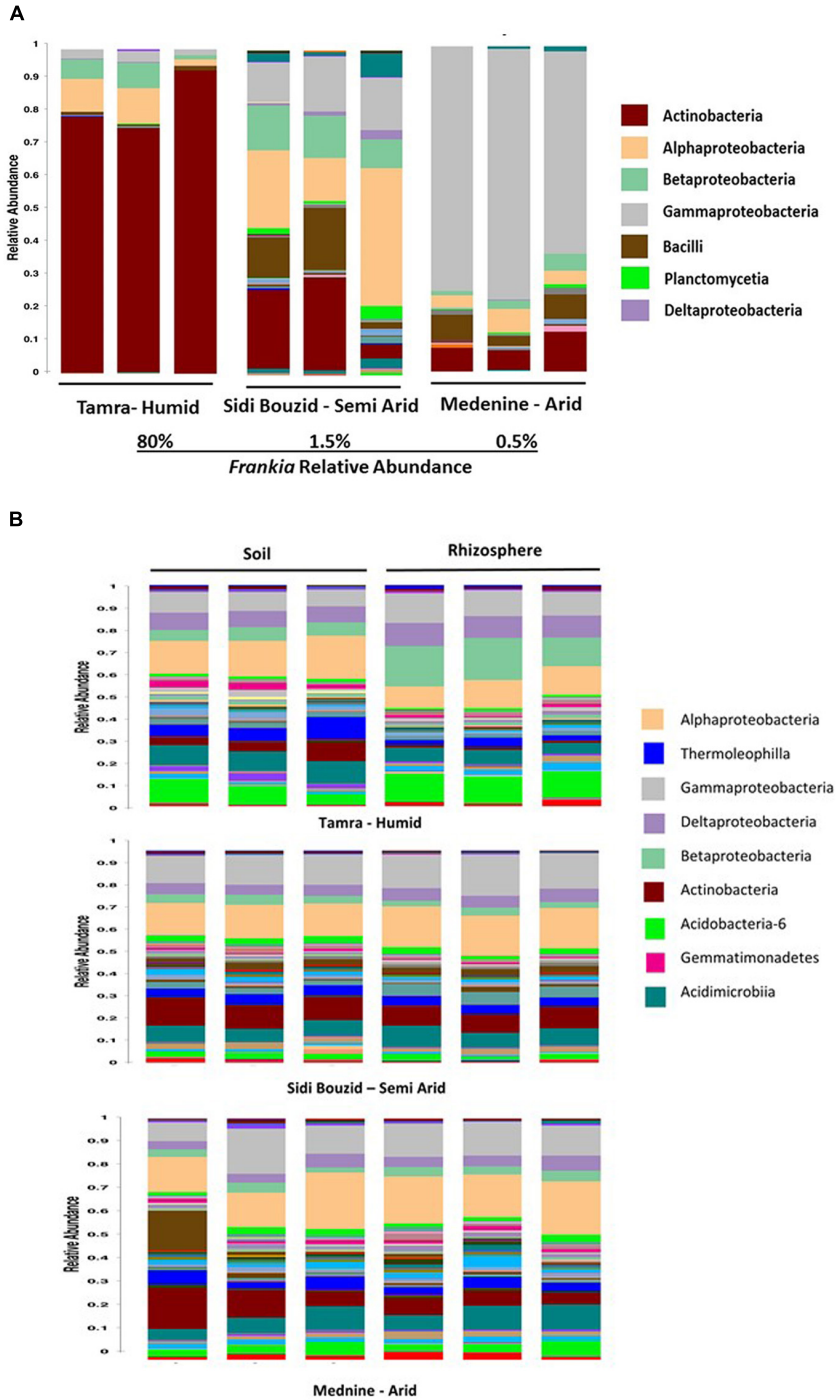

FIGURE 3 | Class level taxonomic summary of nodule, Rhizosphere and soil samples. **(A)** Nodules grouped by site. The relative abundance of the nodule samples was summarized at the class level after corrected for 16S operon copy number variation. The humid and arid samples are significantly less diverse than the semi-arid samples, as can be seen in **(A)**. This can be seen here, as the humid site is dominated by Actinobacteria (the genus *Frankia*), and the arid site is dominated by *Acinetobacter* and *Pseudomonas*. **(B)** Rhizosphere and soil samples grouped by sampling site. These charts show relative abundance of taxa at the class level after correction for 16S operon copy number.

This result shows that although the relative abundance of taxa within the nodule differed from sampling location (**Figure 3** and **Supplementary Figure 3**), the nodules are distinct based on what taxa they host when compared to the soil and rhizosphere samples. The rhizosphere and soil primarily cluster based off the sampling location, this trend is also evident in ordinations

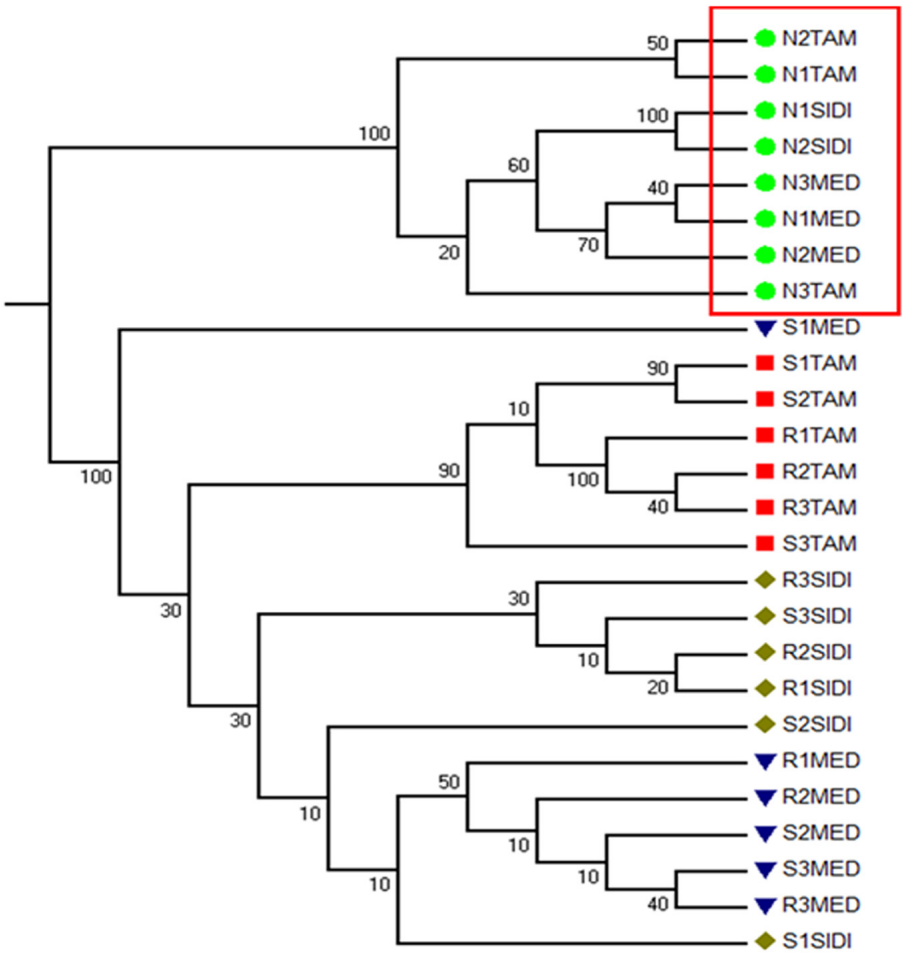

FIGURE 4 | Unweighted pair group method with Arithmetic Mean (UPGMA) Consensus Tree. The tree was constructed from the rarefied unweighted UniFrac distance Matrix. The consensus tree was built by creating 100 trees from 100 randomly subsampled reads from each sample. The numbers on the nodes represent the percentage of the 100 trees that conformed to this configuration. The red box outlines that all nodule samples form one cluster on the tree. The other clades on the tree show that the soil and rhizosphere communities cluster mostly by sampling site.

of the data using the unweighted UniFrac distance metric (**Supplementary Figure 4**).

The beta diversity distance matrices were ordinated using PCoA. Distance matrices were constructed using the weighted and unweighted UniFrac distances on OTU tables that had been normalized by rarefaction, a raw OTU table with ribosomal operon copy number correction and by cumulative sum-scaling (with and without ribosomal operon copy number correction). PCoA ordinations of these distance matrixes can be seen in **Figure 5** and **Supplementary Figures 4**, **5**. For the sake of clarity, **Figure 5** represents weighted UniFrac distances normalized by cumulative sum-scaling without ribosomal operon copy number correction. All of the methods gave similar results (**Supplementary Figure 4**). In all ordinations, nodule samples are separated from the soil and rhizosphere samples along the first Principal Coordinate, which explains the most phylogenetic variation in the data. Multi-response Permutation Procedures (MRPP) agreed with the results seen in the UPGMA tree, with significant grouping of nodules for every normalization type using the both forms of the UniFrac distance metric. **Supplementary Table 4** summarizes the chance-corrected results of the MRPP analysis. The A Statistics, the chance-corrected within-group agreement, is a value between 1 and 0 that describes the within-group heterogeneity of a given group. If all samples in a group are identical A = 1, if the heterogeneity in a group is equal to what would be expected by chance A = 0 (Mielke and Kenneth, 2007).

Nodule Analysis

The results of the UPGMA Tree (**Figure 4**) and the PCoA ordinations (**Figure 5** and **Supplementary Figures 4**, **5**) show that nodules host a distinct prokaryotic community compared to the soil and rhizosphere samples. Ordination and MRPP results show that this grouping is statistically significant whether the unweighted UniFrac or weighted UniFrac is used.

Nodules form a distinct group based on the taxa they host, but the relative composition of this group of taxa changes drastically along the environmental gradient sampled (**Figure 3A**). In

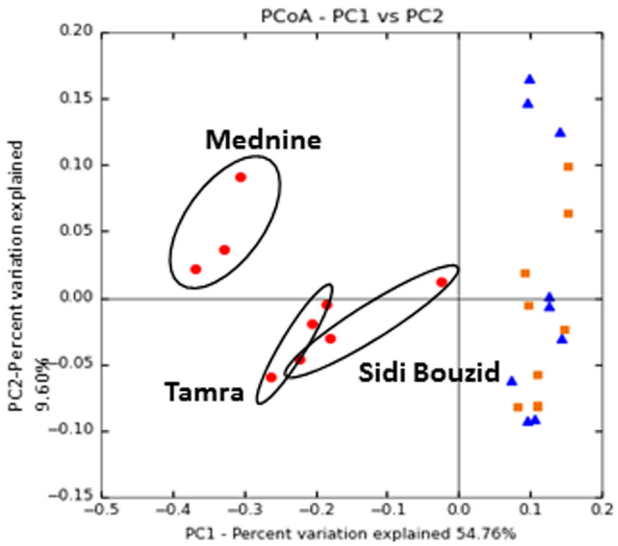

FIGURE 5 | Principal coordinates ordination of CSS normalized UniFrac distance matrices: Ordinations where normalized using Cumulative Sum Scaling. Ordinations was made using the weighted UniFrac distance. Symbols represent: nodules (●), rhizosphere (■), and soil (▲). For all ordinations MRPP showed a statistically significant grouping of the nodule samples, as outlined in **Supplementary Table 4**.

Figure 5, the ordinations show the grouping of nodule samples by location along the second principal coordinate, which explains the second largest amount of taxonomic variation in the dataset.

Rhizosphere and Soil Analysis

To understand differences in the rhizosphere and soil communities across the sampling sites, these samples were analyzed separately from the nodule samples. Rhizosphere soils from all sites were analyzed as one sample category to test the hypothesis that *C. glauca* hosts a distinct microbial community within the rhizosphere across environmental gradients. When soil and rhizosphere samples from all sites were grouped together by type, the MRPP results were inconsistent in their significance, depending on the OTU table normalization strategy. A summary of these results is found in **Supplementary Table 5**. Statistical significance ($P < 0.05$) was only observed with the evenly rarefied OTU table and the raw OUT table that corrected for 16S operon copy number Variation. Ordinations of these data (**Supplementary Figures 4**, **5**) show that the rhizosphere and soil samples formed two clusters only on the raw OTU table and the evenly rarefied OTU table. CSS normalization produces different results with the soil and rhizosphere samples not forming distinct groups.

The ordinations using the unweighted UniFrac distance, which considers the presence and absence of taxa, show that soil and rhizosphere samples clustered based on climate. When the data is ordinated using this metric, two distinct clusters of rhizosphere and soil samples formed **Supplementary Figure 6**. These clusters correspond to the humid sampling site (Tamra) and the two arid sampling sites (Sidi Bouzid and Medenine). For all normalization types, a significant grouping was identified by MRPP (**Supplementary Table 6**), showing that the environmental conditions significantly change the taxa present between the humid and arid soils that were sampled. A taxonomic summary of these samples at the class level are presented in **Figure 3B**.

Shotgun Metagenomic Sequencing

Quality filtering of shotgun metagenomic reads resulted in a total of 83,027,118 paired end reads. The library for Sites 1, 2, and 3 were comprised of 33,051,352, 34,239,886, and 15,735,880 reads, respectively. *In silico* co-assembly of the reads resulted in an assembly contained 3,153,711 contigs totaling 56,964,841 base pairs in length. The statistics for the assembly produced by Quast (Gurevich et al., 2013) are outlined in **Supplementary Table 7**.

Metagenomic Assembled Genomes Reconstructed Using Differential Coverage Binning

Seven predominant genomes were binned using the mmgenome R package. A plot of the metagenomic assembly can be seen in **Figure 6A**. The binned genomes were identified being in the genera *Frankia*, *Micromonospora*, *Bacillus* (two isolates), *Phyllobacterium*, *Paenibacillus,* and *Afipia.*

Two of the binned genomes annotated to the phylum Actinobacteria. The first genome bin contained 4,111 ORFs that annotated to the genus *Frankia*. The annotations for the ORFs in this bin had top hits on many of the *Frankia* clade 1c *Casuarina* infective strains. The most top annotations that hit on a single sequenced strain was 775 of the 4,111 ORFs annotated to *Frankia* sp. BMG5.23, a salt-tolerant Tunisian isolate (Ghodhbane-Gtari et al., 2014). Reads mapping to the binned *Frankia* draft genome comprised 60% of the reads in from the humid sampling site, Tamra. Of the reads from semiarid Sidi Bouzid and arid Gabes, 1.7% and 1.6% of the reads mapped to the *Frankia* genome bin, respectively. Genome bin two resulted in an assembly that contained 6,522 ORFs with 6,053 annotating to the genus *Micromonospora.* The ORFs that annotated to *Micromonospora* were mainly comprised of annotations to *Micromonospora purpureochromogenes,* with 4,565 ORFs. Three genomes that were binned annotated to the phylum Firmicutes. The first contained 6,268 ORFs with 5,866 of them annotating to the genus *Paenibacillus.* The second Firmicutes genome bin contained 4,275 ORFs, 4,060 of which annotated to the genus *Bacillus.* Of those ORFs annotating to the genus *Bacillus*, 3,416 of them annotated to *B. simplex.* The last Firmicutes genome had 4,215 ORFs that also annotated to the genus *Bacillus* with 3,313 of them annotating to *B. aquimaris* and 569 annotating to *B. vietnamensis*. Two of the binned genomes annotated to the phylum proteobacteria. The first binned genome contained 4,370 ORFs that annotated to the genus *Afipia.* The second proteobacteria genome bin contained 3,068 ORFs that annotated to the genus *Phyllobacterium*. General genome characteristics of the binned genomes are summarized in **Table 1**.

Coverage Values for Genome Bins

Genome coverage for binned genomes was calculated in order to compare coverage patterns across sites to the replicated 16S rRNA gene amplicon survey. The only binned genome which followed the same patterns as the replicated analysis was the genome bin that annotated as a member of *Frankia* (**Figure 6A**) compared to the relative abundance of *Frankia* between the two datasets. For those calculations, reads that aligned to plant-derived DNA was first removed. The resulting read sets for each site were aligned to the reassembled *Frankia* genome bin using Bowtie2. The percentage of those reads that aligned to the genome bin was recorded. The *Frankia* genome bin was the dominant member of the humid site, but coverage values were much lower for the semi-arid and arid sampling sites (**Figure 6B**).

Secondary Metabolites Identified in Binned Genomes

The MAGs reconstructed from the metagenomic dataset were analyzed for the presence of secondary metabolite biosynthetic pathways using AnitSMASH (Weber et al., 2015). The secondary metabolite biosynthetic clusters that were identified in the binned genomes are outlined in **Table 2**. Predicted biosynthetic clusters from the binned genomes were predicted to produce siderophores, terpenes, non-ribosomal peptide synthases and other secondary metabolites. The genome *Frankia* and *Micromonospora* genome bins contained the most secondary metabolite biosynthetic clusters about 25 for each bin genome, although only clusters which have a predicted product are listed here.

Functional Mining of Metagenomes

The shotgun metagenomic data was mined for genes of interest with potential functional importance to the actinorhizal symbiosis and *C. glauca* health. Genes potentially responsible for plant–growth-promoting traits were mined from GFF files produced by the Prokka Annotation pipeline (Seemann, 2014). **Figures 7–9** show the results of this analysis as outlined by site. Cladograms for the taxonomy of the genes identified are presented. The number of genes for each function is reported in each figure. The sampling sites 1, 2, and 3 had 159, 183, and 202 genes of interest, respectively. Since shotgun sequencing was not performed with replicates, these results are presented qualitatively as presence or absence data.

DISCUSSION

Prominent Microbial Groups of Nodules, Rhizosphere, and Soil Associated to *Casuarina glauca*

The 16S rRNA gene amplicon analysis of the taxonomic community in nodules showed that they were largely dominated by Actinobacteria, Alphaproteobacteria, and Gammaproteobacteria (**Figure 3**). The remaining sequences matched with Bacilli, Planctomycetia and Deltaproteobacteria. A remarkable change in microbial community dominance was observed across climate stages. In the humid climate zone, represented by Tamra site, Actinobacteria was the most dominant class, while the semiarid (Sidi Bouzid) and arid (Medenine) environments had Alphaproteobacteria and Gammaproteobacteria, respectively, as the most prominent class. This result was surprising because *Frankia* is Actinobacteria and would be expected to dominate the nodule environment.

However, the relative abundance of *Frankia was* drastically affected by the environmental gradient. Nodule occupancy was highest (80%) in plants at the Tamra (humid zone); but was drastically reduced in nodules from the semi-arid Sidi Bouzid (1.5%) and arid Medenine (0.5%). One possible explanation of this phenomenon is that the physical and chemical characteristics of semi-arid and arid environments are not beneficial for the maintenance of the actinorhizal symbiosis or *Frankia* persistence. Soils in the semi-arid and arid regions of Tunisia are poorly evolved calcareous soils (Mtimet, 2001). In these soils, phosphorous is known to be immobilized by formation of complexes with calcium cations (Tunesi et al., 1999). Low phosphorus levels decrease the frequency of *C. cunninghamiana* nodulation by *Frankia* (Yang, 1995) and nodule weight of *Frankia-C. equisetifolia* (Sanginga et al., 1989). Similarly, drying and heat are known to decrease the ability of some *Frankia* strains to infect *C. equisetifolia* (Sayed, 2011). Dryness, high temperature and low levels of available phosphorous are characteristics of soils in arid environments and these factors could be influencing the low abundance and absence of *Frankia* in nodules at these environments. Detecting *Casuarina* infective clades of *Frankia* through plant-trapping assays have proven difficult (Gtari et al., 2002, 2007) and the scarcity of detection of *Casuarinaceae*-infective *Frankia* outside of the plants native range has been demonstrated (Mirza et al., 2007). One possible explanation is that *Casuarina*-infective *Frankia* are more persistent in humid environments that are more similar to the riparian habitat that is preferred by *Casuarina* within their host range. These results are congruent with the need for intentional inoculation with a compatible *Frankia* strain necessary for nodulation in some land reclamation projects in Africa (Gauthier et al., 1985). However, this reasoning does not explain the absence of *Frankia* within mature nodules. The absence of detected *Frankia* in four of the nine nodule samples leads to one hypothesis that another member of the community may be responsible for the formation of nodules on *C. glauca*. *Agrobacterium rhizogenes* will induce pseudonodules on *Elaeagnus angustifolia* that are indistinguishable from *Frankia* – induced nodules (Berg et al., 1992). Our results show an OTU of genus *Agrobacterium* that was as differentially abundant in nodule samples. The genus *Agrobacterium* was present in eight of the nine nodule samples ranging from 0.01% to 2.8% relative abundance. This suggests that a member of this genus could play a role in nodule formation when *Frankia* is in low abundance. Another hypothesis is that this absence is a seasonal variation and part of the life cycle of *Frankia* under semi-arid and arid conditions. As the levels of *Frankia* decreases, other microbes could establish more dominance within the nodule. A seasonal study of the changes in community structure could address this hypothesis.

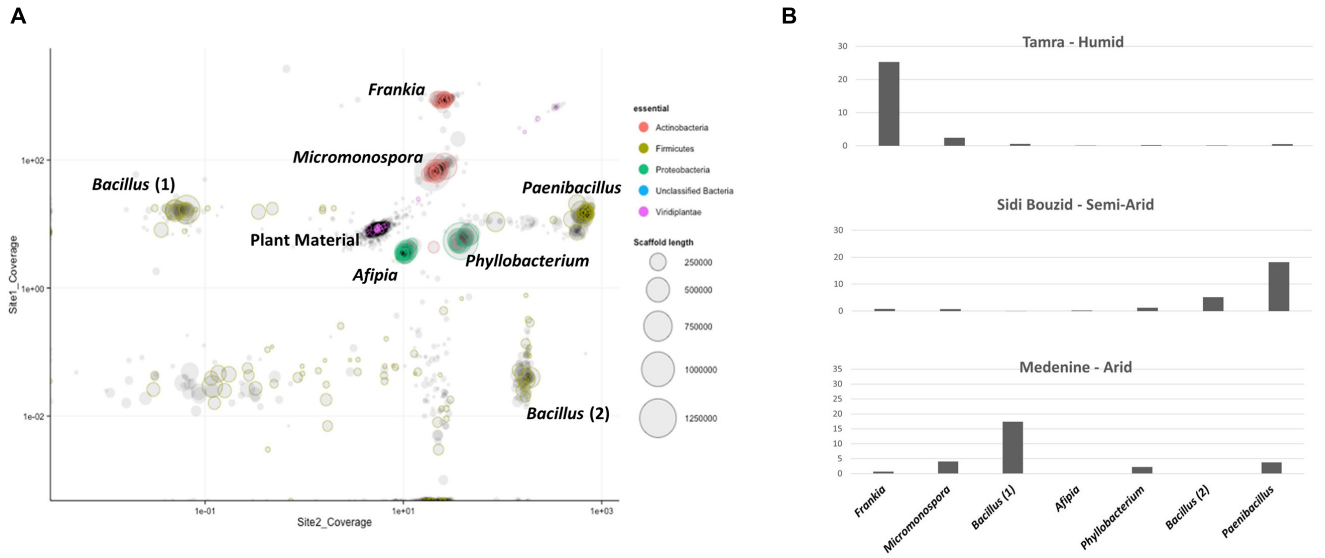

FIGURE 6 | (A) Plot of metagenomic contigs larger than 5 kbp produced by the mmgenome R Package. The seven dominant genomes that were binned using the mmgenome R package are labeled with their annotated genus. The purple and black cluster in the center of the image are contigs derived from *C. glauca* DNA. **(B)** Normalized genome coverage of genome bins. Reads from each of the three sampling sites were aligned to the co-assembled contigs. SAMtools was used to sort and index the coordinates of the aligned reads and Picard MarkDuplicates was used to remove duplicate reads with identical coordinates. Bedtools was then used to calculate coverage per contig per site. Coverage values were normalized by millions of reads per data set and the relative amount of plant DNA that comprised each data set.

TABLE 1 | General assembly characteristics of each binned genome.

Isolate genus	Closest annotation	Assembly length	Open reading frames	GC%
Frankia	*Frankia* sp. BMG5.23	4.92 Mbp	4,111	70.25%
Micromonospora	*M. purpureochromogenes*	7.28 Mbp	6,522	72.26%
Bacillus (1)	*B. simplex*	4.64 Mbp	4,060	40.0%
Bacillus (2)	*B. aquimaris/vietnamensis*	4.7 Mbp	4,215	41.53%
Phyllobacterium	*Phyllobacterium* sp. *UNC302MFCol5.2*	4.8 Mbp	3,068	59.42%
Afipia	*A. broomeae*	5.3 Mbp	4,370	61.64%
Paenibacillus	*Paenibacillus* sp. HGF5	7.0 Mbp	5,866	49.56%

The assembly length and GC content were calculated by Quast. Open reading frames were predicted using Prodigal. Closest annotations were determined after aligning all ORFs to the RefSeq protein database.

Distinct Nodule Community Across Sampling Sites

Multi-response permutation procedures analysis found that nodule samples formed a statistically significant group compared to the rhizosphere and soil samples (**Figure 5** and **Supplementary Figures 4–6**). Nodule samples are separated from the rhizosphere and soil samples by the first principal coordinate axis, which explains the most taxonomic information in the samples. This result is also confirmed with the jackknifed UPGMA tree built from the unweighted UniFrac distance matrix (**Figure 4**), which shows a distinct clade where all nodule samples clustered, despite location. Alpha diversity of the nodule samples was also significantly lower than for the rhizosphere or soil samples (**Supplementary Figure 1**). These observations are similar to comparative analysis of the root microbiome of the model plant *Arabidopsis thaliana,* which has shown that endophytic communities from plants growing in chemically distinct soil types are highly overlapping and less diverse than surrounding soils (Lundberg et al., 2012). The community selected by *C. glauca* was distinct from the soil and rhizosphere communities across a steep environmental gradient and was significantly less diverse, which is like the pattern of the A. *thaliana* microbiome. The similar patterns of microbiome recruitment by *C. glauca* and *A. thaliana* suggests that phylogenetically distant plant groups tend to select for a particular endophytic community across environmental gradients.

Functions of Taxa in Nodules

From metagenome analysis, seven predominant genomes were identified by binning (**Figure 6**) and were assigned to six different genera: *Frankia*, *Micromonospora*, *Bacillus* (two isolates), *Phyllobacterium*, *Paenibacillus,* and *Afipia*. Reads from the humid sampling site Tamra, contains the most reads mapping to the binned *Frankia* draft genome (60%), then

TABLE 2 | Secondary metabolite biosynthetic gene clusters identified each genome bin by antiSMASH.

Bin	Genus	Type	Most similar known cluster	Percent identity
	Frankia	Terpene	Sioxanthin	60%
		Type-Two PKS	Frankiamicin	100%
		Lassopeptide-Type-One PKS	Maklamicin	13%
		Terpene	Hopene	38%
		Other	Streptolydigin	7%
		NRPS	Triostin	16%
		Type-One PKS	Divergolide	13%
		Terpene	Collismycin A	7%
		Type-Two PKS	Medermycin	30%
		Ketide Synthase-Butyrolactone	Abyssomicin	10%
		Other	A47934	10%
		Type-Three Polyketide Synthase	Feglymycin	52%
	Micromonospora			
		T1PKS	Maklamicin	19%
		NRPS-T1PKS	Nostopeptolide	37%
		Other	Diazepinomicin	75%
		Oligosaccharide-PKS-Terpene	Brasilicardin A	54%
		Siderophore	Desferrioxamine B	80%
		T2PKS	Xantholipin	16%
		Terpene	Nocathiacin	4%
		Lantipeptide	Pentalenolactone	15%
		NRPS	Friulimicin	12%
		T3PKS	Alkyl-O-Dihydrogeranyl-Methoxyhydroquinone	71%
		Nrps-T1pks-Lantipeptide	Bleomycin	12%
		Terpene	Sioxanthin	80%
		Nrps-Lantipeptide-T1pks-Others	Naphthyridinomycin	14%
		T1PKS	Calicheamicin	13%
		Terpene-Bacteriocin	Lymphostin	30%
		T1pks-Nrps	Rifamycin	35%
		T1pks	Leucanicidin	100%
	Paenibacillus	Ectoine	Ectoine	75%
		Nrps	Bacillibactin	53%
		Trans-At Pks	Bacillaene	21%
	Bacillus (1)	Siderophore	Desotamide	9%
		Nrps	Koranimine	87%
	Bacillus (2)	Terpene	Carotenoid	33%
		Siderophore		16%
	Afipia	Terpene	Malleobactin	11%
	Phyllobacterium	Nrps	Vicibactin	77%

Sidi Bouzid (1.7%) and Medenine (1.6%). The less abundance of *Frankia* in semi-arid and arid sites can be related to the harsh conditions, dryness and poor composition of soils. Not surprisingly, the *Frankia* MAG closely matched the *Frankia* sp. strain BMG5.23 genome (Ghodhbane-Gtari et al., 2014). This strain was isolated from Tunisian soils and probably represents the local strain in this region.

By the use of the antiSMASH program (Blin et al., 2017), secondary metabolite biosynthetic pathways were predicted from the draft genomes rebuilt from the metagenomic data set (**Table 2**). Not surprisingly, the Actinobacteria, *Frankia* and *Micromonospora,* genomes contained the most secondary metabolite biosynthetic clusters. Actinobacteria are well known for their large assembly of secondary metabolic pathways producing a wide array of natural products.

The presence of non-*Frankia* bacteria within the nodules confirms other observations (Guillén et al., 1993; Niner et al., 1996; Solans and Vobis, 2003; Valdes et al., 2005; Trujillo et al., 2006; Solans, 2007; Ghodhbane-Gtari et al., 2010, 2014, 2019; Solans et al., 2011). In particular, the presence of *Micromonospora* is noteworthy having been identified as an endophyte of actinorhizal and leguminous plants (Trujillo et al., 2006, 2007; Solans et al., 2011) and considered a normal occupant of actinorhizal nodules (Carro et al., 2013). Two different *Bacillus* genomes were identified with one being closely related to *B. simplex* and the other being closely related to *B. aquimaris* and *B. vietnamensis*. *Bacillus simplex* is known for its adaptations to arid environments (Sikorski and Nevo, 2005) and has been shown to acts as a helper-bacteria for the symbiosis between *Pisum sativum* and *Rhizobium leguminosarum* bv. *viciae* (Schwartz et al., 2013). *Bacillus* isolates are helper-bacteria for the *Frankia-Casuarina* symbiosis (Echbab et al., 2004).

Paenibacillus genome revealed secondary metabolic clusters for siderophore production, ectoine, (an osmoprotectant), and bacillaene (an antibiotic). In a nursery trail, co-inoculation of *C. equisetifolia* with *Paenibacillus polymyxa* and *Glomus geosporum* results in the highest seedling quality (Muthukumar and Udaiyan, 2010), showing the potential benefits of this nodule occupant. One hypothesis is that these non-*Frankia* Actinobacteria act as helper-bacteria in the formation of the actinorhizal symbiosis (Ghodhbane-Gtari et al., 2010, 2019; Solans et al., 2011; Ghodhbane-Gtari and Tisa, 2014). The absence of *Nocardia* within these nodule communities was surprising. *Nocardia* strains (BMG51109 and BMG111209) were isolated from *Casuarina glauca* in Tunisia (Ghodhbane-Gtari et al., 2010) and shown to have plant-growth promoting properties (Ghodhbane-Gtari et al., 2019). Co-infection studies showed that *Nocardia casuarinae* strain BMG51109 plays a role as a "helper bacteria" promoting an earlier onset of nodulation (Ghodhbane-Gtari et al., 2019).

Besides generating metagenomes, the shotgun data set was functionally mined to identify potential plant-growth-promoting genes (PGPG) and to phylogenetically analyze these data (**Figures 7–9**) suggesting a wide berth of potential PGPG genetic capability for plant growth promotion. Besides this phylogenetic analysis, these coding regions were predicted to produce enzymes and metabolites of relevance to the benefiting plant health. All three metagenomes contained the 1-aminocyclopropane-1-carboxylate (ACC) deaminase gene. ACC deaminase plays an important role in the nodulation process of leguminous plants

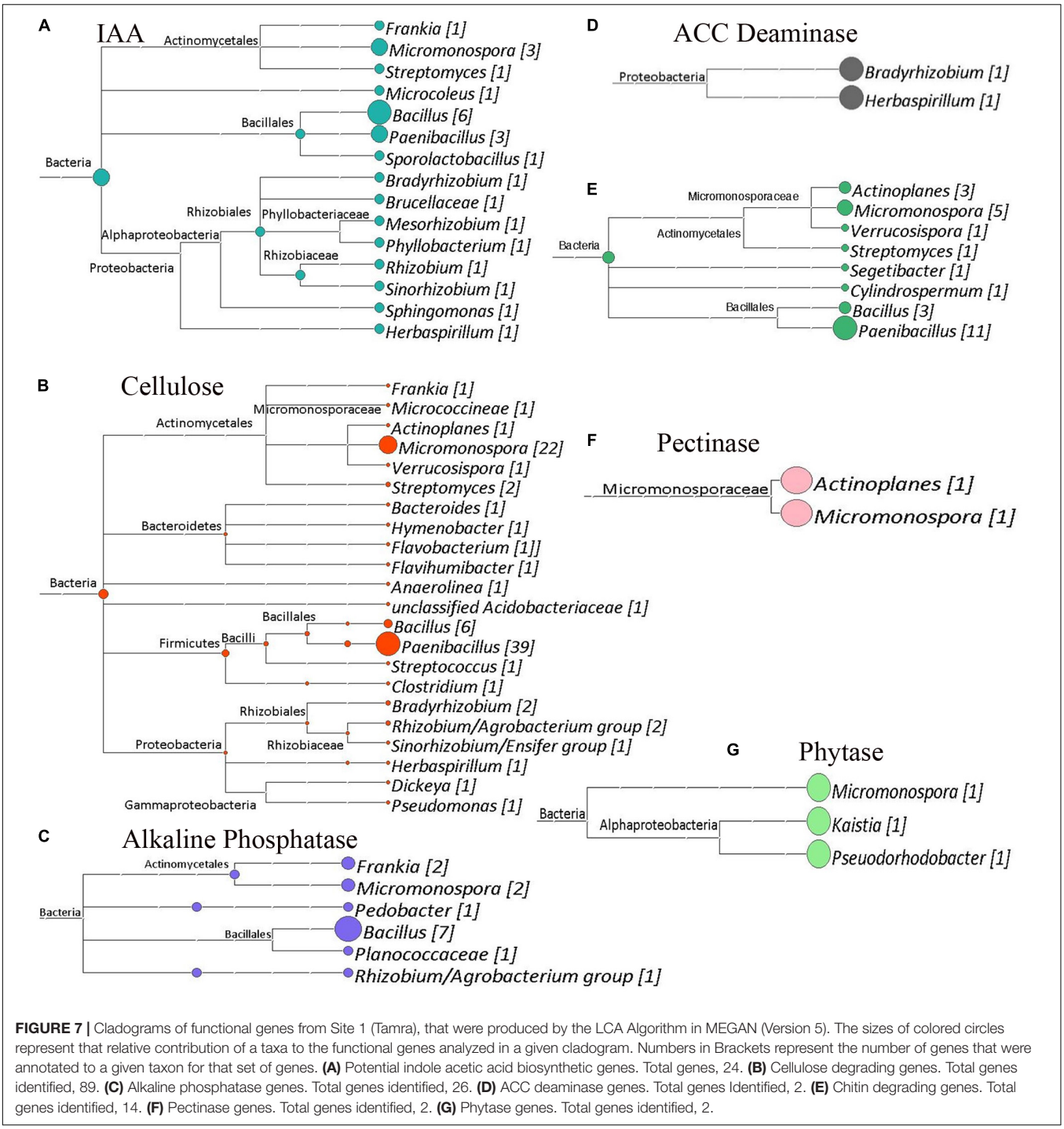

FIGURE 7 | Cladograms of functional genes from Site 1 (Tamra), that were produced by the LCA Algorithm in MEGAN (Version 5). The sizes of colored circles represent that relative contribution of a taxa to the functional genes analyzed in a given cladogram. Numbers in Brackets represent the number of genes that were annotated to a given taxon for that set of genes. **(A)** Potential indole acetic acid biosynthetic genes. Total genes, 24. **(B)** Cellulose degrading genes. Total genes identified, 89. **(C)** Alkaline phosphatase genes. Total genes identified, 26. **(D)** ACC deaminase genes. Total genes Identified, 2. **(E)** Chitin degrading genes. Total genes identified, 14. **(F)** Pectinase genes. Total genes identified, 2. **(G)** Phytase genes. Total genes identified, 2.

(Nascimento et al., 2019) and has been shown to improve plant growth under arid (Bessadok et al., 2020) or saline regions (Orozco-Mosqueda et al., 2020). Other major functions involved in nutrient recycling, suppressing phytopathogens and mineralization of organic matter were also highly abundant within all three metagenomes. The enzymes, chitinase, phytase, cellulase, pectinase and alkaline phosphatase are well known to be involved in the preservation of the plant fertility and maintaining the healthy plant growth (Neeraja et al., 2010; Maksimov et al., 2011; Jain and Singh, 2017). These hydrolytic enzymes serve as an important defense strategy to defend against phytopathogenic fungi (Lynd et al., 2002). These enzymes may serve to help the *Casuarina* to survive from fungal pathogens.

Genes for production of phytohormones were also present at all three sites in variable proportions. Genes for IAA and PAA

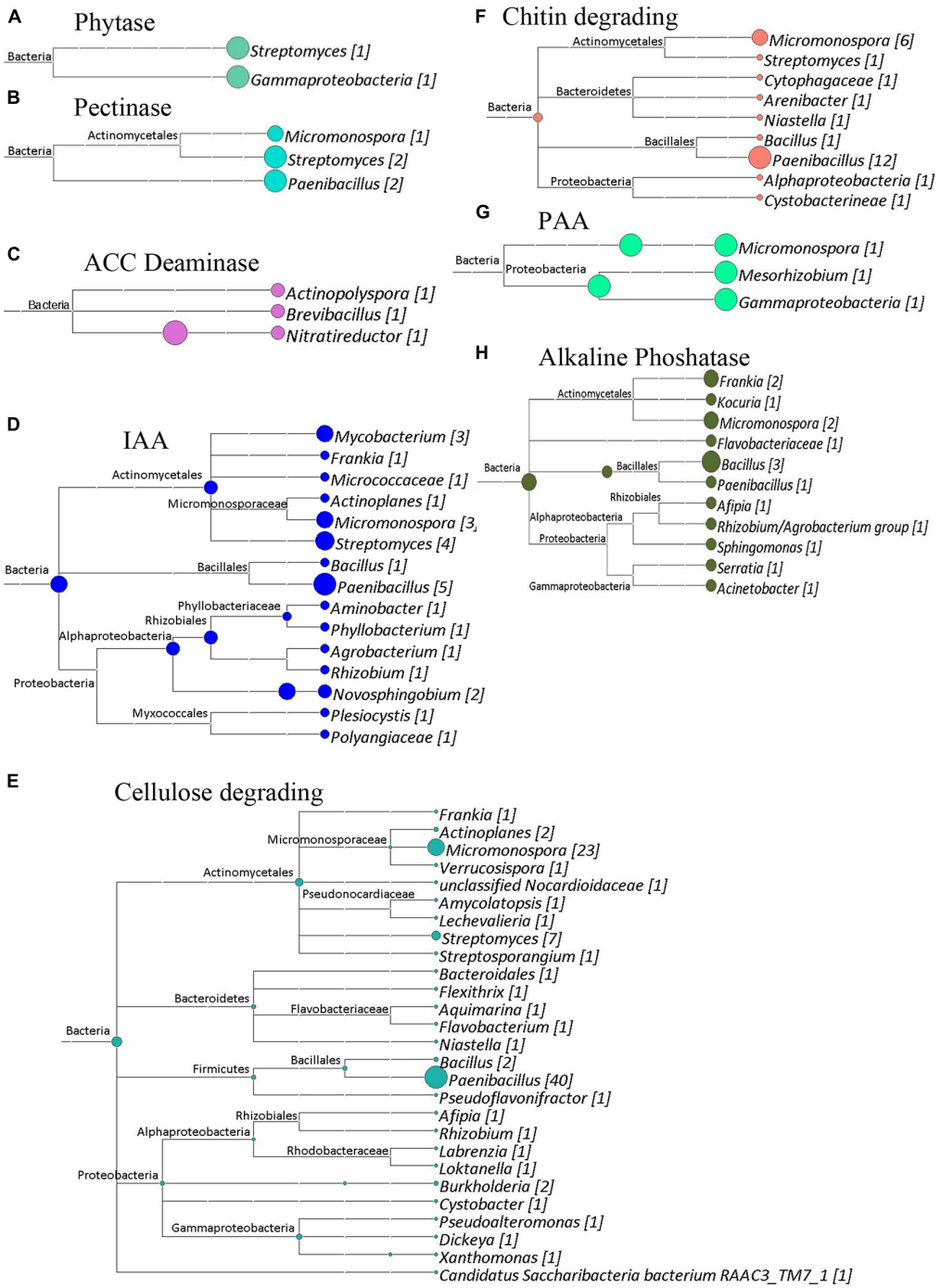

FIGURE 8 | Cladograms of functional genes from Site 2 (Sidi Bouzid), that were produced by the LCA Algorithm in MEGAN (Version 5). The sizes of colored circles represent that relative contribution of a taxa to the functional genes analyzed in a given cladogram. Numbers in Brackets represent that number of genes that annotated to a given taxon for that set of genes. **(A)** Phytase genes. Total genes identified, 8. **(B)** Pectinase enzymes. Total genes identified, 5. **(C)** ACC deaminase genes. Total genes identified, 3. **(D)** Potential indole acetic acid biosynthesis genes. Total genes identified, 27. **(E)** Cellulose degrading enzymes. Total genes identified, 97. **(F)** Chitin degrading enzymes. Total genes identified, 25. **(G)** Potential phenyl acetic acid biosynthesis genes. Total genes identified, 3. **(H)** Alkaline phosphatase genes. Total genes identified, 15.

production were significantly enriched in the semi-arid and arid climates. IAA and PAA play a key role in many aspects of plant growth and cell elongation and division (Champion et al., 2015; Sugawara et al., 2015). The increased number of IAA and PAA genes suggest that these phytohormones may alter the plant physiology to respond to these arid conditions.

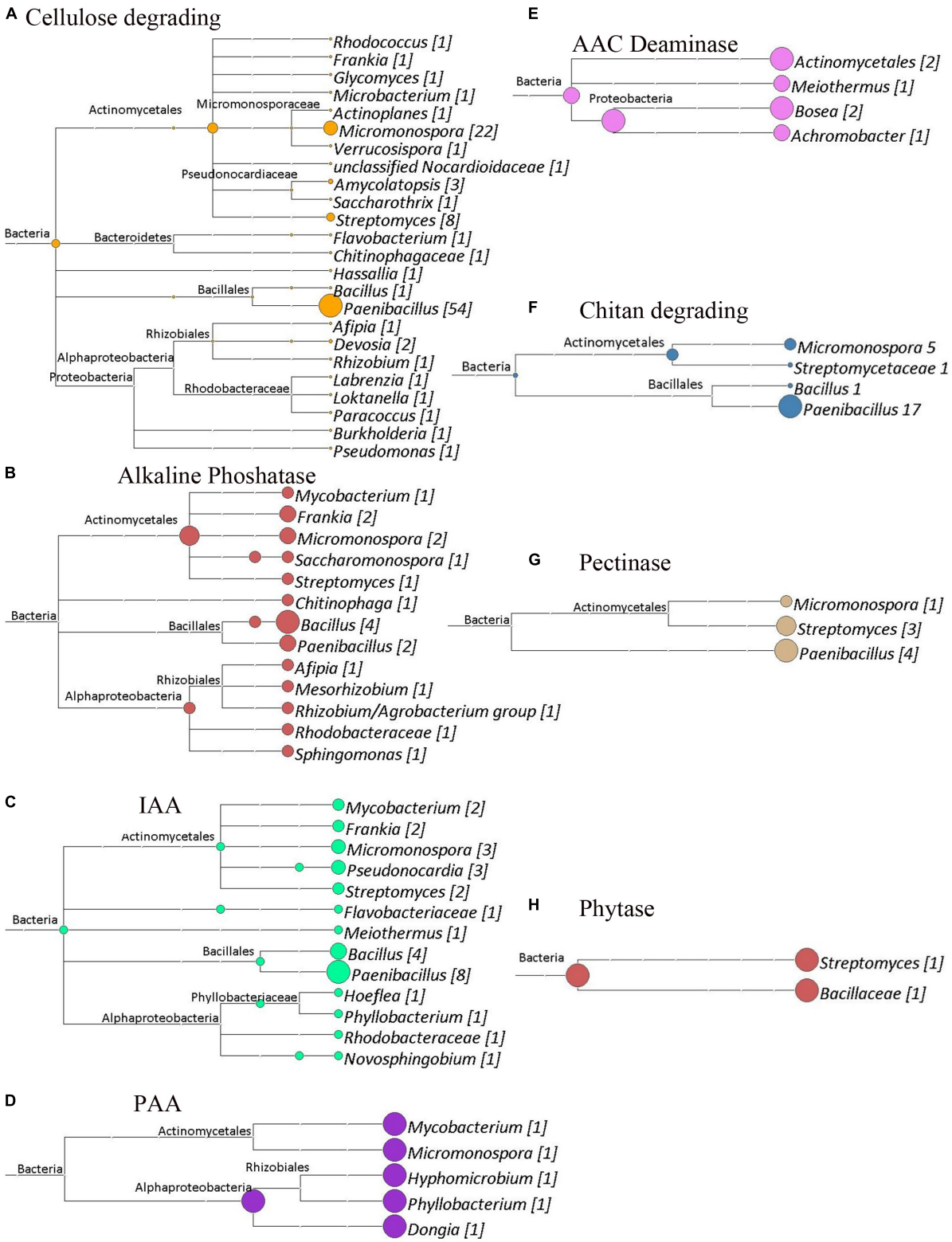

FIGURE 9 | Cladograms of functional genes from Site 3 (Medenine), that were produced by the LCA Algorithm in MEGAN (Version 5). The sizes of colored circles represent that relative contribution of a taxa to the functional genes analyzed in a given cladogram. Numbers in Brackets represent that actual number of genes that annotated to a given taxon for that set of genes. **(A)** Cellulose degrading genes. Total genes identified, 108. **(B)** Alkaline phosphatase genes. Total genes identified, 19. **(C)** Potential indole acetic acid biosynthetic genes. Total genes identified, 30. **(D)** Potential phenyl acetic acid biosynthesis genes. Total genes identified, 5. **(E)** ACC deaminase genes. Total genes identified, 6. **(F)** Chitin degrading genes. Total genes identified, 24. **(G)** Pectinase genes. Total genes identified, 8. **(H)** Phytase genes. Total genes identified, 2.

CONCLUSION

The microbial community of the nodules appears to be shaped by the different bioclimates found in Tunisia. Beside *Frankia* microsymbiont, the niche builder of root nodules, other bacteria may occur within. However, further work is required to understand the PGP mechanisms of the different co-inhabitants of the nodule and more diverse samples from a wide range of actinorhizal plant nodules is needed to deepen this study.

DATA AVAILABILITY STATEMENT

The datasets presented in this study can be found in online repositories. The names of the repository/repositories and accession number(s) can be found below: https://www.ncbi.nlm.nih.gov/bioproject/, PRJNA482626.

AUTHOR CONTRIBUTIONS

FG-G, MG, and LT conceived the study. FG-G and TD'A performed the research. FG-G, TD'A, AG, SG, MG, and LT analyzed the data. FG-G, TD'A, MG, and LT wrote the manuscript. All authors approved the manuscript.

FUNDING

This material is based upon work supported by the New Hampshire Agricultural Experiment Station, through joint funding of the National Institute of Food and Agriculture, United States Department of Agriculture, and State of New Hampshire. This is Scientific Contribution Number 2913. This project (LT) was supported by the USDA National Institute of Food and Agriculture Hatch 1019869 (LT), College of Life Science and Agriculture at the University of New Hampshire, Durham, and Ministère de l'Enseignement Supérieur et de la Recherche Scientifique, Tunisia (LR03ES03) (FG-G).

SUPPLEMENTARY MATERIAL

The Supplementary Material for this article can be found online at: https://www.frontiersin.org/articles/10.3389/fmicb.2021.749760/full#supplementary-material

REFERENCES

Albertsen, M., Hugenholtz, P., Skarshewski, A., Nielsen, K. L., Tyson, G. W., and Nielsen, P. H. (2013). Genome sequences of rare, uncultured bacteria obtained by differential coverage binning of multiple metagenomes. *Nat. Biotechnol.* 31, 533–538. doi: 10.1038/nbt.2579

Aronesty, E. (2011). *ea-utils: "Command-Line Tools for Processing Biological Sequencing Data"*. Available online at: http://code.google.com/p/ea-utils

Aserse, A. A., Rasanen, L. A., Aseffa, F., Hailemariam, A., and Lindstrom, K. (2013). Diversity of sporadic symbionts and nonsymbiotic endophytic bacteria isolated from nodules of woody, shrub, and food legumes in Ethiopia. *Appl. Microbiol. Biotechnol.* 97, 10117–10134. doi: 10.1007/s00253-013-5248-4

Bankevich, A., Nurk, S., Antipov, D., Gurevich, A. A., Dvorkin, M., Kulikov, A. S., et al. (2012). SPAdes: a new genome assembly algorithm and its applications to single-cell sequencing. *J. Comput. Biol.* 19, 455–477. doi: 10.1089/cmb.2012.0021

Berg, R. H., Liu, L. X., Dawson, J. O., Savka, M. A., and Farrand, S. K. (1992). Induction of Pseudoactinorhizae by the plant pathogen agrobacterium-rhizogenes. *Plant Physiol.* 98, 777–779. doi: 10.1104/pp.98.2.777

Bessadok, K., Navarro-Torre, S., Pajuelo, E., Mateos-Naranjo, E., Redondo-Gomez, S., Caviedes, M. A., et al. (2020). The ACC-deaminase producing bacterium Variovorax sp. CT7.15 as a tool for improving *Calicotome villosa* nodulation and growth in Arid regions of Tunisia. *Microorganisms* 8:541. doi: 10.3390/microorganisms8040541

Blin, K., Medema, M. H., Kottmann, R., Lee, S. Y., and Weber, T. (2017). The antiSMASH database, a comprehensive database of microbial secondary metabolite biosynthetic gene clusters. *Nucleic Acids Res.* 45, D555–D559.

Bolger, A. M., Lohse, M., and Usadel, B. (2014). Trimmomatic: a flexible trimmer for illumina sequence data. *Bioinformatics* 30, 2114–2120. doi: 10.1093/bioinformatics/btu170

Caporaso, J. G., Bittinger, K., Bushman, F. D., DeSantis, T. Z., Andersen, G. L., and Knight, R. (2010a). PyNAST: a flexible tool for aligning sequences to a template alignment. *Bioinformatics* 26, 266–267. doi: 10.1093/bioinformatics/btp636

Caporaso, J. G., Kuczynski, J., Stombaugh, J., Bittinger, K., Bushman, F. D., Costello, E. K., et al. (2010b). QIIME allows analysis of high-throughput community sequencing data. *Nat. Methods* 7, 335–336.

Caporaso, J. G., Lauber, C. L., Walters, W. A., Berg-Lyons, D., Huntley, J., Fierer, N., et al. (2012). Ultra-high-throughput microbial community analysis on the illumina HiSeq and MiSeq platforms. *ISME J.* 6, 1621–1624. doi: 10.1038/ismej.2012.8

Carro, L., Pujic, P., Trujillo, M. E., and Normand, P. (2013). *Micromonospora* is a normal occupant of actinorhizal nodules. *J. Biosciences* 38, 685–693. doi: 10.1007/s12038-013-9359-y

Chaia, E. E., Wall, L. G., and Huss-Danell, K. (2010). Life in soil by the actinorhizal root nodule endophyte *Frankia*. A review. *Symbiosis* 51, 201–226. doi: 10.1007/s13199-010-0086-y

Champion, A., Lucas, M., Tromas, A., Vaissayre, V., Crabos, A., Diedhiou, I., et al. (2015). Inhibition of auxin signaling in *Frankia* species-infected cells in *Casuarina glauca* nodules leads to increased nodulation. *Plant Physiol.* 167, 1149–1157. doi: 10.1104/pp.114.255307

DeSantis, T. Z., Hugenholtz, P., Larsen, N., Rojas, M., Brodie, E. L., Keller, K., et al. (2006). Greengenes, a chimera-checked 16S rRNA gene database and workbench compatible with ARB. *Appl. Environ. Microb* 72, 5069–5072. doi: 10.1128/AEM.03006-05

Diagne, N., Diouf, D., Svistoonoff, S., Kane, A., Noba, K., Franche, C., et al. (2013). Casuarina in Africa: distribution, role and importance of arbuscular mycorrhizal, ectomycorrhizal fungi and *Frankia* on plant development. *J. Environ. Manage* 128, 204–209. doi: 10.1016/j.jenvman.2013.05.009

Diagne, N., Ngom, M., Djighaly, P. I., Ngom, D., Ndour, B., Cissokho, M., et al. (2015). "Remediation of heavy-metal-contaminated soils and enhancement of their fertility with actinorhizal plants," in *Heavy Metal Contamination of Soils, Soil Biology*, eds I. Sherameti and A. Varma (Cham: Springer International Publishing), 355–366. doi: 10.1007/978-3-319-14526-6_19

Dudeja, S. S., Giri, R., Saini, R., Suneja-Madan, P., and Kothe, E. (2012). Interaction of endophytic microbes with legumes. *J. Basic Microbiol.* 52, 248–260. doi: 10.1002/jobm.201100063

Duponnois, R., Diédhiou, S., Chotte, J. L., and Sy, M. O. (2003). Relative importance of the endomycorrhizal and (or) ectomycorrhizal associations in *Allocasuarina* and *Casuarina* genera. *Can. J. Microbiol.* 49, 281–287. doi: 10.1139/w03-038

Echbab, H., Prin, Y., Ducousso, M., Nourissier-Mountou, S., Lahlou, H., and Arahou, M. (2004). Helper bacteria associated with *Casuarina cunninghamiana-Frankia* symbiosis: selection of isolates for their effects

on plant growth in axenic conditions. *Acta Bot. Gallica* 151, 429–440. doi: 10.1080/12538078.2004.10515445

Eddy, S. R. (1998). Profile hidden Markov models. *Bioinformatics* 14, 755–763.

Edgar, R. C. (2010). Search and clustering orders of magnitude faster than BLAST. *Bioinformatics* 26, 2460–2461. doi: 10.1093/bioinformatics/btq461

Eljounaidi, K., Lee, S. K., and Bae, H. (2016). Bacterial endophytes as potential biocontrol agents of vascular wilt diseases – Review and future prospects. *Biol. Control* 103, 62–68. doi: 10.1016/j.biocontrol.2016.07.013

Gauthier, D., Diem, H. G., Dommergues, Y. R., and Ganry, F. (1985). Assessment of N-2 fixation by *Casuarina-equisetifolia* inoculated with *Frankia* Ors021001 Using N-15 Methods. *Soil Biol. Biochem.* 17, 375–379. doi: 10.1016/0038-0717(85)90076-8

Ghodhbane-Gtari, F., Essoussi, I., Chattaoui, M., Chouaia, B., Jaouani, A., Daffonchio, D., et al. (2010). Isolation and characterization of non-*Frankia* actinobacteria from root nodules of *Alnus glutinosa*, *Casuarina glauca* and *Elaeagnus angustifolia*. *Symbiosis* 50, 51–57. doi: 10.1007/s13199-009-0029-7

Ghodhbane-Gtari, F., Hurst, S. G. IV, Oshone, R., Morris, K., Abebe-Akele, F., Thomas, W. K., et al. (2014). Draft genome sequence of *Frankia* sp. Strain BMG5.23, a salt-tolerant nitrogen-fixing actinobacterium isolated from the root nodules of *Casuarina glauca* grown in Tunisia. *Genome Announc.* 2:e00520-14. doi: 10.1128/genomeA.00520-14

Ghodhbane-Gtari, F., Nouioui, I., Hezbri, K., Lundstedt, E., D'Angelo, T., McNutt, Z., et al. (2019). The plant-growth-promoting actinobacteria of the genus *Nocardia* induces root nodule formation in *Casuarina glauca*. *Antonie Van Leeuwenhoek* 112, 75–90. doi: 10.1007/s10482-018-1147-0

Ghodhbane-Gtari, F., and Tisa, L. S. (2014). "Ecology and physiology of Non-*Frankia* actinobacteria from actinorhizal plants," in *Plasticity in Plant-Growth-Promoting and Phytopathogenic Bacteria*, ed. E. I. Katsey (New York, NY: Springer), 27–42.

Grimes, H. D., and Mount, M. S. (1984). Influence oF *Pseudomonas* putida on nodulation of *Phaseolus vulgaris*. *Soil Biol. Biochem.* 16, 27–30.

Gtari, M., Brusetti, L., Aouani, M. E., Daffonchio, D., and Boudabous, A. (2002). *Frankia* nodulating *Alnus glutinosa* and *Casuarinaceae* in Tunisia. *Ann. Microbiol.* 52, 145–153.

Gtari, M., Brusetti, L., Hassen, A., Mora, D., Daffonchio, D., and Boudabous, A. (2007). Genetic diversity among *Elaeagnus* compatible *Frankia* strains and sympatric-related nitrogen-fixing actinobacteria revealed by nifH sequence analysis. *Soil Biol. Biochem.* 39, 372–377. doi: 10.1016/j.soilbio.2006.07.005

Gtari, M., and Dawson, J. O. (2011). An overview of actinorhizal plants in Africa. *Funct. Plant Biol.* 38, 653–661. doi: 10.1071/FP11009

Guillén, G. M., Valdès, M., Liao, J., and Hisch, A. M. (1993). Identificacion de actinobacterias aisladas de nodulos de *Casuarina*, por tecnicas tradicionales y moleculares. *Rev. Lat. Amer. Microbiol.* 35, 195–200.

Gurevich, A., Saveliev, V., Vyahhi, N., and Tesler, G. (2013). QUAST: quality assessment tool for genome assemblies. *Bioinformatics* 29, 1072–1075. doi: 10.1093/bioinformatics/btt086

Hénia, L. (2008). *Atlas De L'eau en Tunisie*. Tunis: Université de Tunis, Faculté des Sciences Humaines et Sociales.

Huson, D. H., Auch, A. F., Qi, J., and Schuster, S. C. (2007). MEGAN analysis of metagenomic data. *Genome Res.* 17, 377–386.

Hyatt, D., Chen, G. L., LoCascio, P. F., Land, M. L., Larimer, F. W., and Hauser, L. J. (2010). Prodigal: prokaryotic gene recognition and translation initiation site identification. *BMC Bioinformatics* 11:119. doi: 10.1186/1471-2105-11-119

Iruthayathas, E. E., Gunasekaran, S., and Vlassak, K. (1983). Effect of combined inoculation of *Azospirillum* and *Rhizobium* on nodulation and N2-fixation of winged bean and soybean. *Sci. Hortic.* 20, 231–240.

Jain, J., and Singh, B. (2017). Phytase production and development of an ideal dephytinization process for amelioration of food nutrition using microbial phytases. *Appl. Biochem. Biotech.* 181, 1485–1495. doi: 10.1007/s12010-016-2297-z

Langille, M. G. I., Zaneveld, J., Caporaso, J. G., McDonald, D., Knights, D., Reyes, J. A., et al. (2013). Predictive functional profiling of microbial communities using 16S rRNA marker gene sequences. *Nat. Biotechnol.* 31, 814–821. doi: 10.1038/nbt.2676

Langmead, B., and Salzberg, S. L. (2012). Fast gapped-read alignment with Bowtie 2. *Nat. Methods* 9, 357–359. doi: 10.1038/nmeth.1923

Leite, J., Fischer, D., Rouws, L. F. M., Fernandes, P. I., Hofmann, A., Kublik, S., et al. (2017). Cowpea Nodules Harbor Non-rhizobial bacterial communities that are shaped by soil type rather than plant genotype. *Front. Plant Sci.* 7:2064. doi: 10.3389/fpls.2016.02064

Li, D.-M., and Alexander, M. (1990). Factors affecting co-inoculation with antibiotic-producing bacteria to enhance rhizobial colonization and nodulation. *Plant Soil* 129, 195–201. doi: 10.1007/bf00032413

Li, H., Handsaker, B., Wysoker, A., Fennell, T., Ruan, J., Homer, N., et al. (2009). The sequence alignment/map format and SAMtools. *Bioinformatics* 25, 2078–2079. doi: 10.1093/bioinformatics/btp352

Lozupone, C., and Knight, R. (2005). UniFrac: a new phylogenetic method for comparing microbial communities. *Appl. Environ. Microbiol.* 71, 8228–8235. doi: 10.1128/aem.71.12.8228-8235.2005

Lozupone, C. A., Hamady, M., Kelley, S. T., and Knight, R. (2007). Quantitative and qualitative beta diversity measures lead to different insights into factors that structure microbial communities. *Appl. Environ. Microbiol.* 73, 1576–1585. doi: 10.1128/AEM.01996-06

Lundberg, D. S., Lebeis, S. L., Paredes, S. H., Yourstone, S., Gehring, J., Malfatti, S., et al. (2012). Defining the core *Arabidopsis thaliana* root microbiome. *Nature* 488, 86–90. doi: 10.1038/nature11237

Lynd, L. R., Weimer, P. J., van Zyl, W. H., and Pretorius, I. S. (2002). Microbial cellulose utilization: fundamentals and biotechnology. *Microbiol. Mol. Biol. Rev.* 66, 506–577. doi: 10.1128/mmbr.66.3.506-577.2002

Maksimov, I. V., Abizgil'dina, R. R., and Pusenkova, L. I. (2011). Plant growth promoting rhizobacteria as alternative to chemical crop protectors from pathogens (review). *Appl. Biochem. Microbiol.* 47, 333–345. doi: 10.1134/s0003683811040090

Martínez-Hidalgo, P., and Hirsch, A. M. (2017). The nodule microbiome: N2-fixing rhizobia do not live alone. *Phytobiomes* 1, 70–82. doi: 10.1094/pbiomes-12-16-0019-rvw

Mayhood, P., and Mirza, B. S. (2021). Soybean root nodule and rhizosphere microbiome: distribution of rhizobial and nonrhizobial endophytes. *Appl. Environ. Microbiol.* 87:e02884-20. doi: 10.1128/AEM.02884-20

McMurdie, P. J., and Holmes, S. (2014). Waste not, want not: why rarefying microbiome data is inadmissible. *PLos Comput. Biol.* 10:e1003531. doi: 10.1371/journal.pcbi.1003531

Mielke, P. W. B. Jr., and Kenneth, J. (2007). *Permutation Methods: A Distance Function Approach*. New York, NY: Springer.

Mirza, B. S., Welsh, A., and Hahn, D. (2007). Saprophytic growth of inoculated *Frankia* sp in soil microcosms. *FEMS Microbiol. Ecol.* 62, 280–289. doi: 10.1111/j.1574-6941.2007.00382.x

Mtimet, A. (2001). Soils of Tunisia. *Options Méditer.* 34, 243–268.

Munns, R. (2005). Genes and salt tolerance: bringing them together. *New Phytol.* 167, 645–663. doi: 10.1111/j.1469-8137.2005.01487.x

Muthukumar, T., and Udaiyan, K. (2010). Growth response and nutrient utilization of *Casuarina equisetifolia* seedlings inoculated with bioinoculants under tropical nursery conditions. *New For.* 40, 101–118. doi: 10.1007/s11056-009-9186-z

Nascimento, F. X., Tavares, M. J., Franck, J., Ali, S., Glick, B. R., and Rossi, M. J. (2019). ACC deaminase plays a major role in *Pseudomonas* fluorescens YsS6 ability to promote the nodulation of alpha- and *Betaproteobacteria rhizobial* strains. *Arch. Microbiol.* 201, 817–822. doi: 10.1007/s00203-019-01649-5

Neeraja, C., Anil, K., Purushotham, P., Suma, K., Sarma, P., Moerschbacher, B. M., et al. (2010). Biotechnological approaches to develop bacterial chitinases as a bioshield against fungal diseases of plants. *Crit. Rev. Biotechnol.* 30, 231–241. doi: 10.3109/07388551.2010.487258

Niner, B. M., Brandt, J. P., Villegas, M., Marshall, C. R., Hirsch, A. M., and Valdes, M. (1996). Analysis of partial sequences of genes coding for 16S rRNA of actinomycetes isolated from *Casuarina equisetifolia* nodules in Mexico. *Appl. Environ. Microbiol.* 62, 3034–3036. doi: 10.1128/aem.62.8.3034-3036.1996

Normand, P., Benson, D. R., Berry, A. M., and Tisa, L. S. (2014). "Family Frankiaceae," in *The Prokaryote – Actinobacteria*, eds E. Rosenberg, E. F. DeLong, S. Lory, E. Stackebrandt, and F. Thompson (Berlin: Springer-Verlag), 339–356. doi: 10.1007/978-3-642-30138-4_183

Oksanen, J., Kindt, R., Legendre, P., O'Hara, B., Stevens, M. H. H., and Oksanen, M. J. (2016). The vegan package. *Commun. Ecol. Pack.* 10:719.

Orozco-Mosqueda, M. D., Glick, B. R., and Santoyo, G. (2020). ACC deaminase in plant growth-promoting bacteria (PGPB): an efficient mechanism to counter

salt stress in crops. *Microbiol. Res.* 235:126439. doi: 10.1016/j.micres.2020.126439

Paulson, J. N., Stine, O. C., Bravo, H. C., and Pop, M. (2013). Differential abundance analysis for microbial marker-gene surveys. *Nat. Methods* 10, 1200–1202. doi: 10.1038/nmeth.2658

Potgieter, L. J., Richardson, D. M., and Wilson, J. R. U. (2014). Casuarina: biogeography and ecology of an important tree genus in a changing world. *Biol. Invas.* 16, 609–633. doi: 10.1007/s10530-013-0613-x

Quinlan, A. R., and Hall, I. M. (2010). BEDTools: a flexible suite of utilities for comparing genomic features. *Bioinformatics* 26, 841–842. doi: 10.1093/bioinformatics/btq033

Rengasamy, P. (2006). World salinization with emphasis on Australia. *J. Exp. Bot.* 57, 1017–1023. doi: 10.1093/jxb/erj108

Rideout, J. R., He, Y., Navas-Molina, J. A., Walters, W. A., Ursell, L. K., Gibbons, S. M., et al. (2014). Subsampled open-reference clustering creates consistent, comprehensive OTU definitions and scales to billions of sequences. *PeerJ* 2:e545. doi: 10.7717/peerj.545

Ryan, R. P., Germaine, K., Franks, A., Ryan, D. J., and Dowling, D. N. (2008). Bacterial endophytes: recent developments and applications. *FEMS Microbiol. Lett.* 278, 1–9. doi: 10.1111/j.1574-6968.2007.00918.x

Sanginga, N., Danso, S. K. A., and Bowen, G. D. (1989). Nodulation and growth-response of Allocasuarina and *Casuarina Species* to phosphorus fertilization. *Plant Soil* 118, 125–132. doi: 10.1007/bf02232797

Santoyo, G., Moreno-Hagelsieb, G., Orozco-Mosqueda Mdel, C., and Glick, B. R. (2016). Plant growth-promoting bacterial endophytes. *Microbiol. Res.* 183, 92–99.

Sayed, W. F. (2011). Improving *Casuarina* growth and symbiosis with *Frankia* under different soil and environmental conditions-review. *Folia Microbiol.* 56, 1–9. doi: 10.1007/s12223-011-0002-8

Schwartz, A. R., Ortiz, I., Maymon, M., Herbold, C. W., Fujishige, N. A., Vijanderan, J. A., et al. (2013). *Bacillus* simplex—a little known PGPB with anti-fungal activity—alters pea legume root architecture and nodule morphology when coinoculated with *Rhizobium leguminosarum* bv. viciae. *Agronomy* 3, 595–620. doi: 10.3390/agronomy3040595

Seemann, T. (2014). Prokka: rapid prokaryotic genome annotation. *Bioinformatics* 30, 2068–2069. doi: 10.1093/bioinformatics/btu153

Shannon, C. E. (1948). A mathematical theory of communication. *Bell Syst. Tech. J.* 27, 379–423.

Sikorski, J., and Nevo, E. (2005). Adaptation and incipient sympatric speciation of *Bacillus* simplex under microclimatic contrast at "Evolution Canyons" I and II, Israel. *Proc. Natl. Acad. Sci. U.S.A.* 102, 15924–15929. doi: 10.1073/pnas.0507944102

Solans, M. (2007). *Discaria trinervis – Frankia* symbiosis promotion by saprophytic actinomycetes. *J. Basic Microbiol.* 47, 243–250. doi: 10.1002/jobm.200610244

Solans, M., and Vobis, G. (2003). *Actinomycetes saprophíticos* asociados a la rizósfera de *Discaria trinervis*. *Ecol. Aust.* 13, 97–107.

Solans, M., Vobis, G., Cassan, F., Luna, V., and Wall, L. G. (2011). Production of phytohormones by root-associated saprophytic actinomycetes isolated from the actinorhizal plant *Ochetophila trinervis*. *World J. Microbiol. Biotechnol.* 27, 2195–2202. doi: 10.1007/s11274-011-0685-7

Steane, D. A., Wilson, K. L., and Hill, R. S. (2003). Using matK sequence data to unravel the phylogeny of *Casuarinaceae*. *Mol. Phylogenet. Evol.* 28, 47–59. doi: 10.1016/s1055-7903(03)00028-9

Sugawara, S., Mashiguchi, K., Tanaka, K., Hishiyama, S., Sakai, T., Hanada, K., et al. (2015). Distinct characteristics of indole-3-acetic acid and phenylacetic acid, two common auxins in plants. *Plant Cell Physiol.* 56, 1641–1654. doi: 10.1093/pcp/pcv088

Tani, C., and Sasakawa, H. (2003). Salt tolerance of *Casuarina equisetifolia* and *Frankia* Ceq1 strain isolated from the root nodules of *C-equisetifolia*. *Soil Sci. Plant Nutr.* 49, 215–222.

Trujillo, M. E., Kroppenstedt, R. M., Fernandez-Molinero, C., Schumann, P., and Martinez-Molina, E. (2007). *Micromonospora lupini* sp nov and *Micromonospora saelicesensis* sp nov., isolated from root nodules of *Lupinus angustifolius*. *Int. J. Syst. Evol. Micr.* 57, 2799–2804. doi: 10.1099/ijs.0.65192-0

Trujillo, M. E., Kroppenstedt, R. M., Schumann, P., Carro, L., and Martinez-Molina, E. (2006). *Micromonospora coriariae* sp nov., isolated from root nodules of *Coriaria myrtifolia*. Int. J. Syst. Evol. Micr. 56, 2381–2385. doi: 10.1099/ijs.0.64449-0

Tunesi, S., Poggi, V., and Gessa, C. (1999). Phosphate adsorption and precipitation in calcareous soils: the role of calcium ions in solution and carbonate minerals. *Nutr. Cycling Agroecosyst.* 53, 219–227.

Valdes, M., Perez, N. O., Estrada de los Santos, P., Caballero-Mellado, J., Pena-Cabriales, J. J., Normand, P., et al. (2005). Non-*Frankia* actinomycetes isolated from surface-sterilized roots of *Casuarina equisetifolia* fix nitrogen. *Appl. Environ. Microbiol.* 71, 460–466. doi: 10.1128/AEM.71.1.460-466.2005

Weber, T., Blin, K., Duddela, S., Krug, D., Kim, H. U., Bruccoleri, R., et al. (2015). antiSMASH 3.0-a comprehensive resource for the genome mining of biosynthetic gene clusters. *Nucleic Acids Res.* 43, W237–W243. doi: 10.1093/nar/gkv437

Yang, Y. (1995). The effect of phosphorus on nodule formation and function in the *Casuarina-Frankia* symbiosis. *Plant Soil* 176, 161–169. doi: 10.1007/bf00017686

Zhang, B., Du, N., Li, Y., Shi, P., and Wei, G. (2018). Distinct biogeographic patterns of rhizobia and non-rhizobial endophytes associated with soybean nodules across China. *Sci. Total Environ.* 643, 569–578. doi: 10.1016/j.scitotenv.2018.06.240

Zhong, C. L., Gong, M. Q., Chen, Y., and Wang, F. Z. (1995). Inoculation of *Casuarina* with Ectomycorrhizal fungi, vesicular-arbuscular Mycorrhizal fungi and *Frankia*. *Aciar. Proc.* 62, 122–126.

Zhou, X., Tian, L., Zhang, J. F., Ma, L. N., Li, X. J., and Tian, C. J. (2017). Rhizospheric fungi and their link with the nitrogen-fixing *Frankia* harbored in host plant *Hippophae rhamnoides* L. *J. Basic Microbiol.* 57, 1055–1064. doi: 10.1002/jobm.201700312

Conflict of Interest: The authors declare that the research was conducted in the absence of any commercial or financial relationships that could be construed as a potential conflict of interest.

Publisher's Note: All claims expressed in this article are solely those of the authors and do not necessarily represent those of their affiliated organizations, or those of the publisher, the editors and the reviewers. Any product that may be evaluated in this article, or claim that may be made by its manufacturer, is not guaranteed or endorsed by the publisher.

frontiers in Microbiology

REVIEW
published: 09 December 2021
doi: 10.3389/fmicb.2021.765531

Actinobacteria From Desert: Diversity and Biotechnological Applications

*Feiyang Xie[1] and Wasu Pathom-aree[2]**

[1] Doctor of Philosophy Program in Applied Microbiology (International Program), Faculty of Science, Chiang Mai University, under the CMU Presidential Scholarship, Chiang Mai, Thailand, [2] Research Center of Microbial Diversity and Sustainable Utilization, Department of Biology, Faculty of Science, Chiang Mai University, Chiang Mai, Thailand

Deserts, as an unexplored extreme ecosystem, are known to harbor diverse actinobacteria with biotechnological potential. Both multidrug-resistant (MDR) pathogens and environmental issues have sharply raised the emerging demand for functional actinobacteria. From 2000 to 2021, 129 new species have been continuously reported from 35 deserts worldwide. The two largest numbers are of the members of the genera *Streptomyces* and *Geodermatophilus*, followed by other functional extremophilic strains such as alkaliphiles, halotolerant species, thermophiles, and psychrotolerant species. Improved isolation strategies for the recovery of culturable and unculturable desert actinobacteria are crucial for the exploration of their diversity and offer a better understanding of their survival mechanisms under extreme environmental stresses. The main bioprospecting processes involve isolation of target actinobacteria on selective media and incubation and selection of representatives from isolation plates for further investigations. Bioactive compounds obtained from desert actinobacteria are being continuously explored for their biotechnological potential, especially in medicine. To date, there are more than 50 novel compounds discovered from these gifted actinobacteria with potential antimicrobial activities, including anti-MDR pathogens and anti-inflammatory, antivirus, antifungal, antiallergic, antibacterial, antitumor, and cytotoxic activities. A range of plant growth-promoting abilities of the desert actinobacteria inspired great interest in their agricultural potential. In addition, several degradative, oxidative, and other functional enzymes from desert strains can be applied in the industry and the environment. This review aims to provide a comprehensive overview of desert environments as a remarkable source of diverse actinobacteria while such rich diversity offers an underexplored resource for biotechnological exploitations.

Keywords: actinobacteria, desert, arid environment, diversity, cultivability, bioactive compounds, natural products, plant growth promoting actinomycetes

OPEN ACCESS

Edited by:
Imen Nouioui, German Collection of Microorganisms and Cell Cultures GmbH (DSMZ), Germany

Reviewed by:
Joachim Wink, Helmholtz Centre for Infection Research, Helmholtz Association of German Research Centres (HZ), Germany
Christopher Milton Mathew Franco, Flinders University, Australia

****Correspondence:***
Wasu Pathom-aree
wasu.p@cmu.ac.th

Specialty section:
This article was submitted to Systems Microbiology, a section of the journal Frontiers in Microbiology

Received: *27 August 2021*
Accepted: *08 November 2021*
Published: *09 December 2021*

Citation:
Xie F and Pathom-aree W (2021) Actinobacteria From Desert: Diversity and Biotechnological Applications. Front. Microbiol. 12:765531. doi: 10.3389/fmicb.2021.765531

INTRODUCTION

A serious global health problem caused by pathogenic microorganisms is threatening human lives and welfare at an alarming speed. Due to abusive uses of antibiotics and antimicrobial prescriptions, the effectiveness of drugs and vaccines has been sharply decreased. Worse yet, the reduced interest from large pharmaceutical companies has further compromised the drug development process. To date, growing resistant infections have seriously jeopardized several of the United Nations (UN) Sustainable Development Goals (SDGs) related to the economy, global health, food production, and

environment (Medina et al., 2020). Infectious diseases, such as malaria, HIV/AIDS, tuberculosis, and other communicable diseases, continue to pose risks to global health. In 2018, more than half a million new cases were caused by multidrug-resistant (MDR) pathogenic infections, which remained the top deadly global disease during the past decade (World Health Organization, 2020). The large-scale use of antibiotics as growth promoters in agriculture also contributed to this crisis. As a result, more than 700,000 antimicrobial resistance-related deaths are predicted to happen annually worldwide in 2050, which could further reduce the global economy by $100 trillion as estimated by UN agencies (Medina et al., 2020). In particular, the pharmaceutical industry was unable to deliver effective drugs during the severe acute respiratory syndrome (SARS) epidemic between 2002 and 2003, causing a fatality rate of 11% (Chan-Yeung and Rui-Heng, 2003). Even today, 17 years later, there is still no anti-SARS drug available to cure the disease due to the slow progress in the development of post-epidemic drugs. Therefore, novel bioactive compounds to combat the threat of MDR pathogens and emerging diseases are urgently needed (Choudhary et al., 2016). Microbial natural products are considered as one of the important sources of bioactive compounds. Natural products are secondary metabolites (SMs) synthesized by bacteria and fungi and are not required for the growth, development, and reproduction of the producing organisms. In their native environments, these SMs may function as signaling molecules (Traxler and Kolter, 2015). SMs are attractive for drug discovery programs, in general, owing to their properties such as biochemical specificity, metabolic selectivity, structural diversity, and the potential to pass through eukaryotic outer membranes to block the production of cellular macromolecules and target enzymes (Baltz, 2008). To date, over 23,000 microbial natural products have been identified since the discovery of penicillin (Katz and Baltz, 2016).

Microorganisms isolated from extreme habitats are considered a significant reservoir for the search and discovery of new drugs. The most recent review revealed that 186 novel compounds were produced by 129 microbes (actinobacteria, cyanobacteria, fungi, and other bacteria) isolated from extreme habitats between 2010 and 2018 (Sayed et al., 2020). Cyanobacteria are known to generate antimicrobial (Micallef et al., 2015), antiprotozoal, and anti-inflammatory compounds (Vijayakumar and Menakha, 2015). Other bacteria reported to potentially synthesize bioactive metabolites are *Thermus filiformis*, which produced four antioxidant carotenoids, namely, all-*trans*-zeaxanthin, thermobiszeaxanthins, thermozeaxanthins, and zeaxanthin monoglucoside (Mandelli et al., 2012). Actinobacteria are shown to be the most frequent producer of specialized metabolites as compared to cyanobacteria and other bacteria (Sayed et al., 2020). The exploration of actinobacteria holds great promise in terms of diverse chemical libraries including antimicrobial compounds (erythromycin, gentamicin, vancomycin, daptomycin, and rifamycin), anticancer compounds (bleomycin, actinomycin D, and mitomycin), immunosuppressive compounds (rapamycin and tacrolimus), antiparasitic compounds (avermectins and spinosyns), and herbicidal compounds (bialaphos and glufosinate) and hence continued to drive innovative biotechnology (Krug and Müller, 2014; Katz and Baltz, 2016; Genilloud, 2017; Jose et al., 2021). Thus, actinobacteria are expected to play a significant role in biotechnological applications including in medical and agricultural sectors.

ACTINOBACTERIA: A UNIQUE SOURCE OF BIOACTIVE COMPOUNDS

Actinobacteria is one of the largest Gram-positive bacterial groups with high guanine-plus-cytosine (G + C) content (Barka et al., 2016). Many actinobacteria can produce mycelium, known as aerobic filamentous actinobacteria, and further reproduce by sporulation (Barka et al., 2016). Most actinobacteria are free-living microorganisms that can be found in terrestrial or aquatic habitats, including extreme environments such as caves, deep seas, deserts, and mangroves (Macagnan et al., 2006). These ecosystems are proven to be a prolific source of novel actinobacteria (Hong et al., 2009; Abdel-Mageed et al., 2010; Kamjam et al., 2017; Goodfellow et al., 2018; Bull and Goodfellow, 2019; Rangseekaew and Pathom-aree, 2019). Abundant bioactive metabolites have been produced by actinobacteria, such as antibiotics, anticancer drugs, immunosuppressive drugs, enzymes, enzyme inhibitors, and other therapeutic or biologically active compounds (Adeela et al., 2018; Rateb et al., 2018; Law et al., 2020; Almuhayawi et al., 2021; Jose et al., 2021). There are around 589 novel compounds with various chemical structures reported from actinobacteria between 2015 and 2020, more than half of them (52%) with potential bioactivities, such as antiparasitic, anti-quorum sensing, antiviral, and chelating activities (Jose et al., 2021). Remarkably, members of the actinobacterial taxa, including rare actinobacteria, are responsible for the production of over 10,000 pharmaceutical agents (Jose et al., 2021). With respect to aerobic filamentous actinobacteria, the genus *Streptomyces* is an extremely good source of novel specialized metabolites as it was reported to produce 39% of all known microbial metabolites (Sivalingam et al., 2019). To date, members of the genus *Streptomyces* are responsible for about two-thirds of the frontline antibiotics in clinical use, as well as other anticancer, antifungal, and anthelmintic compounds (Law et al., 2019; Al-Dhabi et al., 2020; Ser et al., 2020; Yi et al., 2020). Rare actinobacteria are generally defined as members of actinobacterial taxa that are difficult to isolate from the environment (Amin D. H. et al., 2020). Members of some rare actinobacteria are comparable to their *Streptomyces* neighbors in term of bioactive compound production. These prolific rare actinobacterial species belong to the families of *Micromonosporaceae* (1,061), *Mycobacteriaceae* (483), *Pseudonocardiaceae* (327), *Streptosporangiaceae* (154), and *Thermomonosporaceae* (633) (Selim et al., 2021). Other unclassified species with reported ability to produce bioactive metabolites belonged to the genera of *Actinosporangium* (30), *Alkalomyces* (1), *Catellatopsora* (1), *Elaktomyces* (3), *Erythrosporangium* (1), *Excelsospora* (3), *Frankia* (7), *Kitasatoa* (5), *Microechinospora* (1), *Microellobosporia* (11), *Salinospora* (1), *Sebekia* (3), *Streptoplanospora* (1), *Synnenomyces* (4), *Waksmania* (3), and *Westerdykella* (6) (Selim et al., 2021). Based

on the metagenomic analyses and rank abundance analyses, diverse rare actinobacterial taxa are detected in the desert with their population significantly higher (over 34%) than that of validly published taxa (Idris et al., 2017a). This diversity has been poorly recovered by current culture-dependent techniques. The improved isolation method could allow researchers to obtain these abundant rare actinobacteria from deserts for bioprospecting programs.

The genome sizes of actinobacteria ranged from 1 to 12 Mb with potent biosynthetic gene clusters (BGCs) encoded by biologically active compounds (Větrovský and Baldrian, 2013). The term "gifted actinobacteria" is first coined by Richard H. Baltz for actinobacteria with a large genome size, coding for more SM production than other taxa (Baltz, 2017). Quantitative analyses of microbial genomes performed by antiSMASH 3.0 revealed that these gifted actinobacteria harbored 20 to 50 SM gene clusters, allocating 0.8–3.0 Mb of the entire genome to SM production (Baltz, 2017, 2018). For example, gifted strains of *Amycolatopsis*, *Micromonospora*, and *Streptomyces* have moderate (about 5.0–7.9 Mb) or large (over 8 Mb) genomes, harboring 19–20 and >30 BGCs, respectively (Baltz, 2017, 2018, 2019; Nouioui et al., 2019). Whole-genome analysis of these gifted genera usually revealed 20–50 BGCs encoding for both known and/or predicted specialized metabolites, which provides strong evidence that actinobacteria are promising producers of diverse novel compounds with various bioactivities (Bentley et al., 2002; Tang et al., 2016). For example, *Streptomyces coelicolor* A3(2) harbors more than 20 BGCs that encode for specialized metabolites such as blue-colored actinorhodin and red-pigment undecylprodigiosin (Bednarz et al., 2021). Similarly, the genome of *Streptomyces* sp. VN1 has shown diverse known and/or novel metabolites encoded by 34 gene clusters, involving a furan-type anticancer agent (Nguyen et al., 2020).

These genome sequence data also allowed the observation of genomic heterogeneity, which provides great insights into the ability of actinobacteria to synthesize diverse specialized metabolites (Jose et al., 2021). Generally, the genome size may correlate with a more complicated environment, implying that the genome encodes significant metabolic and stress-tolerant properties (Baltz, 2018). For example, *Jiangella gansuensis* YIM 002^T isolated from Gansu Desert has a complete genome sequence that identified 45 biosynthetic clusters, suggesting it has high capacity to produce SMs. Compatible solutes, ion transporters, nitrite reductase, and nitrogen fixation proteins were also detected (Jiao et al., 2017). In addition, *J. gansuensis* YIM 002^T has a smaller genome (5.59 Mb) compared to other *Jiangella* species (more than 7 Mb), yet it contains 2,504 functional proteins, implying that it may have discarded many genes for adaptation in the harsh desert environments through its evolution (Jiao et al., 2017). To defend against desert environmental stresses, superfluous and non-essential genes were discarded to improve survival efficiency, resulting in desert strains with higher metabolic capabilities compared with unevolved strains (Burke and Moran, 2011). Genome rearrangements were promoted by mobile DNA, which recombines inactive genes into functional genes, whereas inactivated genes were removed through deletion (Burke and Moran, 2011). This genomic evolution suggested that the reduction in genomic size of desert strains facilitated long-term adaptive evolution.

DESERT: AN UNEXPLORED RESERVOIR FOR NOVEL ACTINOBACTERIA

An increasing number of novel actinobacterial taxa continued to be reported from natural habitats, especially extreme biomes under harsh environmental conditions. These extreme habitats represent a potentially rich resource for novel compounds with biological properties. Particularly, the desert is the largest continental ecosystem on earth with approximately 30% of the total land area while 7% of it is a hyper-arid region with water constraints (Neilson et al., 2012). Desert ecosystems have attracted the increasing interest of microbiologists in the quest for novel bioactive compounds since they are considered an unexplored home of new extremophiles with high tolerance to extreme conditions. Desert environmental conditions are characterized by extremely high or low temperatures, lack of nutrients, very low organic carbon sources, high levels of oxidants and UV radiation or pH or salinity, high concentrations of metals, and other abiotic stresses (Horikoshi et al., 2010; Köberl et al., 2011; Bull et al., 2016; Idris et al., 2017a). The most explored desert soil sample has over 92% new actinobacterial species isolated. However, it is worth to note that the remaining 8% of novel species were found from desert plants, rhizosphere soil, and rock surfaces, respectively. Hence, such extreme conditions in the desert are considered as a selective pressure that shapes diverse actinobacterial communities.

Between 2000 and 2021, numerous diverse newly identified actinobacteria have been recorded from 35 deserts scattered over 11 regions, as summarized in **Figure 1** and **Supplementary Table 1**. These deserts are distributed in the regions of East Asia (31%), Central Asia (3%), Asia (17%), the

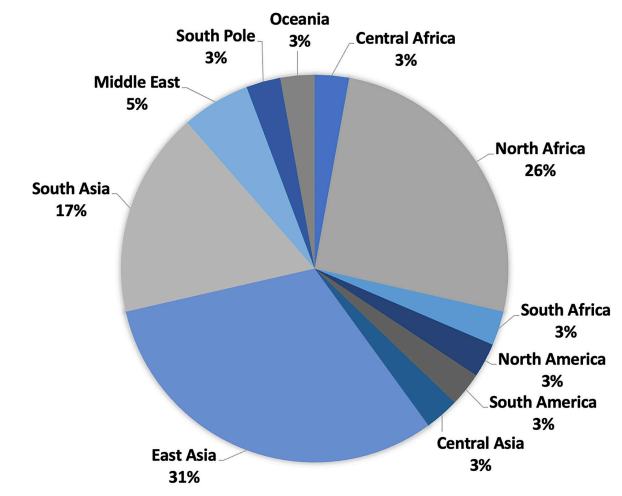

FIGURE 1 | Distribution of desert biomes.

Middle East (4%), North Africa (26%), South America (3%), Central Africa (3%), North America (3%), South Africa (3%), South Pole (3%), and Oceania (3%).

Deserts in East Asia

Most deserts (31%) are distributed in China, East Asia (**Figure 1** and **Supplementary Table 1**), including Badain Jaran Desert, Fukang Desert, Gansu Desert, Gurbantunggut Desert, Hangjin Banner Desert, Isolaginsha Desert, Taklamakan Desert, Tengger Desert, Tibet Autonomous Color Desert, Turpan Desert, and Xinjiang Desert. Taklamakan Desert in southwest Xinjiang is home to the greatest number of new species (14). Despite being the largest desert in China, the Taklamakan Desert is the warmest and driest desert in the country, with an annual temperature of around 39°C (Rittner et al., 2016). Additionally, as the second-largest non-polar and sand-shifting desert in the world, the Taklamakan Desert also experiences an extremely cold temperature (−32°C) in winter and an extremely low average annual rainfall ranging from 10 to 38 mm (Rittner et al., 2016). Such severe environmental circumstances have attracted the attention of researchers for exploration of novel actinobacteria with exceptional tolerance in desert environments.

Deserts in Central and South Asia

Central Asia and South Asia are home to seven deserts, namely, Karakum Desert in Turkmenistan, Central Asia; Cholistan Desert in Pakistan; Kunjam Pass and Lahaul–Spiti Valley, two cold deserts in the Indian Himalayas; the saline desert of Kutch in India; Thal Desert in Pakistan; and Thar Desert in India (**Supplementary Table 1**). The Karakum Desert, in particular, was the isolation source of the most diverse (six genera) and numerous (11 new species) novel actinobacteria in Central and South Asia. It is one of the largest deserts in the world and the hottest desert in Central Asia (Ghassemi and Garzanti, 2019). In comparison to other deserts, the Karakum Desert is inhabited with animals and plants, mainly ephemeral plants, trees, and insects. Ninety-five percent of the area is more or less covered with vegetation, and the remaining 5% is sand dunes (Ghassemi and Garzanti, 2019). The annual average rainfall of Karakum Desert ranges from 70 to 150 mm. Its dry conditions are due to the fact that the coldest temperature of sand reaches −5°C, while the hottest temperature climbs from 55 to 88°C (Ghassemi and Garzanti, 2019). This dry but lively desert led many researchers to devise innovative projects that may benefit agriculture.

Deserts in the Middle East, North Africa, and South America

There are 12 deserts located in the Middle East, North Africa, and South America: Anatolia Desert in Turkey, Saudi Arabia arid area, Beni Suef Governorate Desert, Eastern Desert and saline–alkaline desert in Egypt, Béni Abbès Desert, Béni Isguen Desert and Sahara Desert of Algeria, Sahara Desert in Libya, arid-saline sediment, and Sahara Desert in Tunisia (**Supplementary Table 1**). The Atacama Desert in Chile, being the primary source of new actinobacterial species, accounts for around 20% of all new species (23) and half of all novel compounds (25) in the past two decades. The Atacama Desert is a hyper-arid or an extremely hyper-arid area according to the ratio of mean annual rainfall to mean annual evaporation of less than 0.05 or even below 0.002 (Bull et al., 2016). Being the driest desert in the world, the Atacama Desert has high temperatures during the day that can easily reach over 40–50°C. The soil sample in the desert is very similar to the sample from Mars, with extremely low vegetation and organic carbon (about 2–50 μg of carbon per gram of soil) and high levels of UV radiation (Bull et al., 2016). Microbiologists are interested in the Atacama Desert as despite its harsh conditions, it harbors abundant and diverse actinobacteria with biotechnological potentials.

Deserts in Other Regions

Other new actinobacteria were discovered from the Antarctic Desert (South Pole), arid Australian soils (Oceania), Baja California Desert in Mexico (North America), Namib Desert in Namibia (South Africa), and Sahara Desert in Chad (Central Africa) (**Supplementary Table 1**). The highest number of new species was recorded from the Sahara Desert in Chad (6) and arid Australian soils (5). The Sahara Desert is the world's biggest hot desert, with extremely poor primary productivity, although it does sustain certain organisms that can adapt to arid environments, such as ephemerals (Schuster et al., 2006). The yearly precipitation in the Sahara Desert ranges from 0 to 7.62 cm, with some regions going for years without rain. The daily summer temperature of the Sahara Desert frequently exceeds 38°C during the day but drops to near freezing at night. Arid Australian soils are characterized mainly by mineral or skeletal soils almost without any organic matter (Morton et al., 2011). The hot and dry weather is typical for the Australian arid lands with low annual precipitation (380–635 mm), frequent heatwaves, and high levels of solar radiation.

DIVERSITY OF DESERT ACTINOBACTERIA FROM 2000 TO 2021

Extreme environmental conditions give rise to unique taxa (species and genera), where limited nutrient conditions significantly affect the structure of microbial communities (Hozzein and Goodfellow, 2007). From 2000 to 2021, 129 species in 9 orders, 24 families, and 52 genera were reported from deserts worldwide based on taxonomic studies (**Table 1** and **Figures 2**, **3**). Members of the order *Actinomycetales* (39%) represent the highest number of novel actinobacteria, followed by *Pseudonocardiales* (24%), *Micrococcales* (17%), *Geodermatophilales* (12%), *Micromonosporales* (4%), *Motilibacterales* (1%), *Acidimicrobiales* (1%), *Kineosporiales* (1%), and *Nakamurellales* (1%). Furthermore, members of the *Pseudonocardiaceae* family (23%) are the most abundant, followed by *Streptomycetaceae* (12%), *Geodermatophilaceae* (11%), *Microbacteriaceae* (7%), *Nocardioidaceae* (6%), *Streptosporangiaceae* (6%), *Micrococcaceae* (5%), *Micromonosporaceae* (4%), *Dietziaceae* (3%), *Jiangellaceae* (3%), *Nocardiopsaceae* (2%), *Propionibacteriaceae* (2%), *Bogoriellaceae* (2%), *Intrasporangiaceae* (2%), *Motilibacteraceae*

TABLE 1 | List of new actinobacteria isolated from desert environment from 2000 to 2021.

Order	Family	Genus	Species	References
Acidimicrobiales	*Ilumatobacteraceae*	*Desertimonas*	*Desertimonas flava*	Asem et al., 2018
Actinomycetales	*Actinopolysporaceae*	*Actinopolyspora*	*Actinopolyspora mzabensis*	Meklat et al., 2013
	Cellulomonadaceae	*Cellulomonas*	*Cellulomonas telluris*	Shi et al., 2020
	Dietziaceae	*Dietzia*	*Dietzia kunjamensis*	Mayilraj et al., 2006d
			Dietzia lutea	Li et al., 2009
		Rhodococcus	*Rhodococcus kroppenstedtii*	Mayilraj et al., 2006a
		Williamsia	*Williamsia* sp.	Guerrero et al., 2014
	Jiangellaceae	*Jiangella*	*Jiangella asiatica*	Saygin et al., 2020b
			Jiangella aurantiaca	
			Jiangella ureilytica	
			Jiangella gansuensis	Han et al., 2014
	Nocardioidaceae	*Aeromicrobium*	**Aeromicrobium endophyticum*	Li et al., 2019a
			Aeromicrobium halotolerans	Yan et al., 2016
		Kribbella	*Kribbella deserti*	Sun et al., 2017
			Kribbella turkmenica	Saygin et al., 2019b
		Nocardioides	*Nocardioides deserti*	Tuo et al., 2015
			Nocardioides thalensis	Khan et al., 2017
			Nocardioides vastitatis	Liu et al., 2020b
		Tenggerimyces	*Tenggerimyces mesophilus*	Sun et al., 2015
	Nocardiopsaceae	*Nocardiopsis*	*Nocardiopsis alkaliphila*	Hozzein et al., 2004
			Nocardiopsis benisuefensis	Hozzein et al., 2014
			**Nocardiopsis* sp.	Chen et al., 2015
	Promicromonosporaceae	*Promicromonospora*	*Promicromonospora panici*	Guesmi et al., 2021
	Propionibacteriaceae	*Auraticoccus*	*Auraticoccus cholistanensis*	Cheema et al., 2020
		Desertihabitans	*Desertihabitans aurantiacus*	Sun et al., 2019
			Desertihabitans brevis	Liu et al., 2020a
	Streptomycetaceae	*Streptomyces*	*Streptomyces aburaviensis*	Thumar et al., 2010
			Streptomyces aridus	Idris et al., 2017b
			Streptomyces asenjonii	Goodfellow et al., 2017
			Streptomyces altiplanensis	Cortés-Albayay et al., 2019
			Streptomyces atacamensis	Santhanam et al., 2012b
			Streptomyces cahuitamycinicus	Saygin et al., 2020c
			Streptomyces desertarenae	Li et al., 2019c
			Streptomyces deserti	Santhanam et al., 2012a
			Streptomyces dengpaensis	Li Y. et al., 2018
			Streptomyces bullii	Santhanam et al., 2013
			Streptomyces fukangensis	Zhang et al., 2013
			Streptomyces fragilis	Nithya et al., 2017
			Streptomyces leeuwenhoekii	Rateb et al., 2011a
			**Streptomyces netropsis*	Abdelmoteleb and González-Mendoza, 2020
			Streptomyces sannurensis	Hozzein et al., 2011
			Streptomyces taklimakanensis	Yuan et al., 2020
	Streptosporangiaceae	*Desertiactinospora*	*Desertiactinospora gelatinilytica*	Saygin et al., 2019a
		Nonomuraea	*Nonomuraea deserti*	Saygin et al., 2020d
			Nonomuraea diastatica	
			Nonomuraea longispora	
			Nonomuraea mesophila	
			Nonomuraea terrae	Ay, 2020
		Streptosporangium	*Streptosporangium algeriense*	Boubetra et al., 2016
			Streptosporangium becharense	Chaouch et al., 2016
	Thermomonosporaceae	*Actinomadura*	*Actinomadura deserti*	Cao et al., 2018
			Actinomadura namibiensis	Wink et al., 2003
Geodermatophilales	*Geodermatophilaceae*	*Blastococcus*	*Blastococcus atacamensis*	Castro et al., 2018a
			Blastococcus deserti	Yang et al., 2019

(Continued)

TABLE 1 | Continued

Order	Family	Genus	Species	References
		Geodermatophilus	*Geodermatophilus africanus*	Montero-Calasanz et al., 2013b
			Geodermatophilus arenarius	Montero-Calasanz et al., 2012
			Geodermatophilus chilensis	Castro et al., 2018b
			Geodermatophilus pulveris	Hezbri et al., 2016
			Geodermatophilus sabulis	Hezbri et al., 2015
			Geodermatophilus saharensis	Montero-Calasanz et al., 2013c
			Geodermatophilus siccatus	Montero-Calasanz et al., 2013e
			Geodermatophilus telluris	Montero-Calasanz et al., 2013d
			Geodermatophilus tzadienisis	Montero-Calasanz et al., 2013a
		Modestobacter	*Modestobacter altitudinis*	Goliñska et al., 2020b
			Modestobacter caceresii	Busarakam et al., 2016b
			Modestobacter excelsi	Goliñska et al., 2020a
			Modestobacter multiseptatus	Mevs et al., 2000
Kineosporiales	*Kineosporiaceae*	*Kineococcus*	*Kineococcus xinjiangensis*	Liu et al., 2009
Micrococcales	*Bogoriellaceae*	*Georgenia*	*Georgenia deserti*	Hozzein et al., 2018
			Georgenia alba	Li et al., 2019d
	Intrasporangiaceae	*Janibacter*	*Janibacter* sp.	Khessairi et al., 2014
		Ornithinicoccus	*Ornithinicoccus halotolerans*	Zhang et al., 2016
	Microbacteriaceae	*Agrococcus*	*Agrococcus lahaulensis*	Mayilraj et al., 2006e
		Labedella	**Labedella phragmitis*	Li et al., 2019b
			**Labedella populi*	
		Microbacterium	*Microbacterium album*	Yang et al., 2018b
			Microbacterium deserti	
			**Microbacterium halophytorum*	Li Y. R. et al., 2018
			Microbacterium suaedae	Zhu et al., 2019
			Microbacterium karelineae	Zhu et al., 2021
		Mycetocola	*Mycetocola manganoxydans*	Luo et al., 2012
		Planctomonas	*Planctomonas deserti*	Liu et al., 2019b
	Micrococcaceae	*Arthrobacter*	*Arthrobacter deserti*	Hu et al., 2016
			Arthrobacter mobilis	Ye et al., 2020
		Citricoccus	*Citricoccus alkalitolerans*	Li et al., 2005
		Kocuria	*Kocuria aegyptia*	Li et al., 2006
			Kocuria himachalensis	Mayilraj et al., 2006b
		Nesterenkonia	*Nesterenkonia populi*	Liu et al., 2015b
			Nesterenkonia rhizosphaerae	Wang et al., 2014
	Ornithinimicrobiaceae	*Ornithinimicrobium*	*Ornithinimicrobium kibberense*	Mayilraj et al., 2006c
Micromonosporales	*Micromonosporaceae*	*Actinoplanes*	*Actinoplanes deserti*	Habib et al., 2018
		Micromonospora	*Micromonospora acroterricola*	Carro et al., 2019b
			Micromonospora arida	Carro et al., 2019a
			Micromonospora inaquosa	
			Micromonospora deserti	Saygin et al., 2020a
Motilibacterales	*Motilibacteraceae*	*Motilibacter*	*Motilibacter aurantiacus*	Liu et al., 2020c
			Motilibacter deserti	
Nakamurellales	*Nakamurellaceae*	*Nakamurella*	*Nakamurella deserti*	Liu et al., 2019a
Pseudonocardiales	*Nocardiaceae*	*Nocardia*	*Nocardia sp.*	Zhang et al., 2020
	Pseudonocardiaceae	*Actinoalloteichus*	*Actinoalloteichus spitiensis*	Singla et al., 2005
		Actinophytocola	*Actinophytocola algeriensis*	Bouznada et al., 2016b
			Actinophytocola gilvus	Sun et al., 2014
		Amycolatopsis	*Amycolatopsis australiensis*	Tan et al., 2006
			Amycolatopsis deserti	Busarakam et al., 2016a
			Amycolatopsis granulosa	Zucchi et al., 2012a
			Amycolatopsis ruanii	
			Amycolatopsis thermalba	
			Amycolatopsis thermophila	Zucchi et al., 2012b

(Continued)

TABLE 1 | Continued

Order	Family	Genus	Species	References
			Amycolatopsis viridis	
			Amycolatopsis vastitatis	Idris et al., 2018
		Lechevalieria	*Lechevalieria atacamensis*	Okoro et al., 2010
			Lechevalieria deserti	
			Lechevalieria roselyniae	
		Lentzea	*Lentzea isolaginshaensis*	Wang et al., 2019
			Lentzea chajnantorensis	Idris et al., 2017c
		Prauserella	*Prauserella endophytica*	Liu et al., 2015a
			Prauserella isguenensis	Saker et al., 2015
			Prauserella shujinwangii	Liu et al., 2014
		Pseudonocardia	*Pseudonocardia nigra*	Trujillo et al., 2017
		Saccharopolyspora	*Saccharopolyspora deserti*	Yang et al., 2018a
		Saccharothrix	**Saccharothrix algeriensis*	Zitouni et al., 2004
			Saccharothrix deserti	Liu et al., 2020
			Saccharothrix ghardaiensis	Bouznada et al., 2017
			Saccharothrix hoggarensis	Boubetra et al., 2013b
			Saccharothrix isguenensis	Bouznada et al., 2016a
			Saccharothrix tamanrassetensis	Boubetra et al., 2015
			Saccharothrix tharensis	Ibeyaima et al., 2018
		Yuhushiella	*Yuhushiella deserti*	Mao et al., 2011
			Yuhushiella sp.	Ibeyaima et al., 2016

**Species isolated from plants in desert area.*

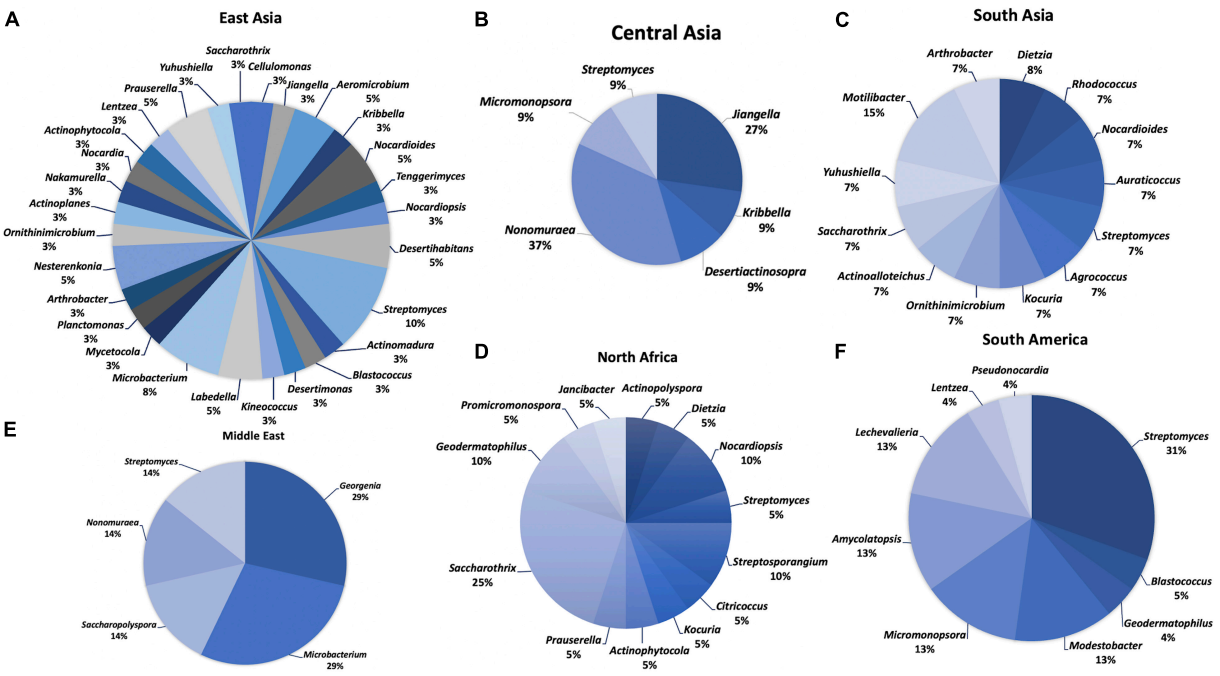

FIGURE 2 | Distribution of desert actinobacteria from different geographical regions: **(A)** East Asia, **(B)** Central Asia, **(C)** South Asia, **(D)** North Africa, **(E)** Middle East, and **(F)** South America.

(2%), *Thermomonosporaceae* (2%), *Actinopolysporaceae* (1%), *Cellulomonadaceae* (1%), *Ilumatobacteraceae* (1%), *Kineosporiaceae* (1%), *Nakamurellaceae* (1%), *Nocardiaceae* (1%), *Ornithinimicrobiaceae* (1%), and *Promicromonosporaceae* (1%).

The two most dominant actinobacteria recovered from deserts are *Streptomyces* and *Geodermatophilus*. *Streptomyces*, the largest genus of actinobacteria, has the greatest number (16) of validly described desert actinobacterial species. To survive in desert

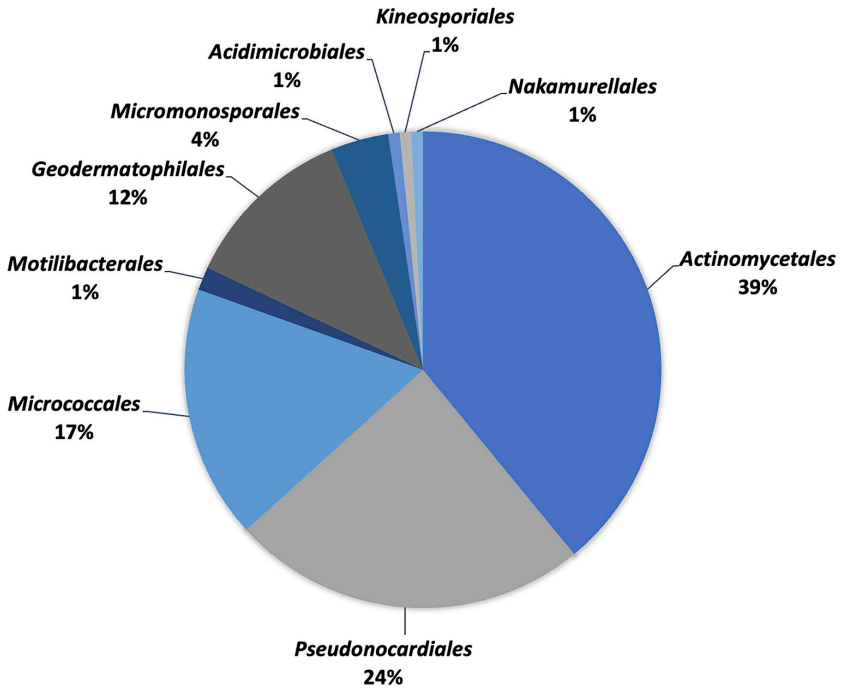

FIGURE 3 | Percentage distribution of different orders of desert actinobacteria.

environments, members of the genus *Streptomyces* have evolved a variety of tolerance mechanisms and bioactive compound potential. Currently, all reported bioactive compounds were derived from desert streptomycetes (Bérdy, 2005). For example, *Streptomyces aburaviensis* (Thumar et al., 2010), *Streptomyces fukangensis* (Zhang et al., 2013), and *Streptomyces sannurensis* (Hozzein et al., 2011) are alkaliphilic actinomycetes, with optimum growth at pH 9 to 11.5. *S. aburaviensis* (Thumar et al., 2010) and *Streptomyces desertarenae* (Li et al., 2019c) are halotolerant species that can adapt to living in high-saline environments (7–15% w/v NaCl), while *Streptomyces asenjonii* (Abdelkader et al., 2018) and *Streptomyces leeuwenhoekii* (Rateb et al., 2011a) were gifted for the synthesis of bioactive compounds with novel chemical structures. It should be noted that the majority of streptomycetes (7) was discovered from the Atacama Desert, including *Streptomyces altiplanensis* (Cortés-Albayay et al., 2019), *Streptomyces atacamensis* (Santhanam et al., 2012b), *Streptomyces deserti* (Santhanam et al., 2012a), and *Streptomyces bullii* (Santhanam et al., 2013), which adapted to the alkaline environments with optimum growth in pH of up to 11; *Streptomyces aridus* (Idris et al., 2017b) is capable of growth in a temperature range between 10 and 40°C, and *S. asenjonii* (Abdelkader et al., 2018) and *S. leeuwenhoekii* (Gran-Scheuch et al., 2018) produced antibacterial metabolites under desert growth conditions. Another dominant group of desert actinobacteria is the genus *Geodermatophilus* with nine new species identified within the same period. Members of this taxon have demonstrated radiation-resistant capabilities, such as *Geodermatophilus pulveris* BMG 825^T and *Geodermatophilus sabuli* BMG 8133^T which are both gamma radiation resistant, whereas *Geodermatophilus tzadiensis* CF5/2^T is a UV-radiation-resistant actinobacterium (Hezbri et al., 2015; Hezbri et al., 2016).

Actinobacterial Diversity in East Asia

Most new actinobacterial species (39) were discovered from East Asia, and they were classified into 28 genera (**Figure 2**). The highest number of novel species was isolated from the Taklamakan Desert (14), belonging to 13 genera: *Aeromicrobium*, *Desertihabitans*, *Labedell*, *Microbacterium*, *Mycetocola*, *Nakamurella*, *Nesterenkonia*, *Nocardioides*, *Nocardioides*, *Nocardiopsis*, *Planctomonas*, *Prauserella*, and *Streptomyces*. Among them, two new species, *Labedella phragmitis* and *Labedella populi*, were obtained from the surface-sterilized flowers of *Phragmites australis* (reed) and branches of *Populus euphratica*, respectively (Li et al., 2019b). Surface-sterilized leaves of *P. australis* (reed) were the isolation source of an endophytic actinobacterium, *Aeromicrobium endophyticum* (Li et al., 2019a). In addition, two actinobacteria, *N. deserti* 12Sc4-1^T and *N. deserti* SC8A-24^T were collected from the rhizosphere of *Reaumuria* and *Alhagi sparsifolia*, respectively. The latter strain showed desiccation tolerance properties (Tuo et al., 2015; Liu et al., 2019a). NaCl tolerance is a common feature among desert actinobacteria; for example, *Desertihabitans brevis* 16Sb5-5^T, isolated from a sand sample in the Taklamakan Desert, tolerates up to 10% NaCl (Liu et al., 2020a). Members of the following genera, *Actinomadura*, *Kineococcus*, *Nocardia*, *Ornithinicoccus*, *Prauserella*, *Saccharothrix*, and *Yuhushiella*, were isolated from Xinjiang Desert. Halotolerant actinobacteria are able to grow under salinity stress, for example, *Ornithinicoccus halotolerans*

EGI 80423^T from Xinjiang Desert which grew in up to 14% NaCl (Zhang et al., 2016). Four genera, *Blastococcus*, *Desertimonas*, *Microbacterium*, and *Streptomyces*, were isolated from the Gurbantunggut Desert. *Actinoplanes*, *Aeromicrobium*, and *Arthrobacter* were recovered from the Turpan Desert. One new species, *Aeromicrobium halotolerans* YIM Y47^T is able to grow in 0%–7% NaCl (Yan et al., 2016). Members of the genera *Cellulomonas* and *Desertihabitans* were isolated from the Badain Jaran Desert, while *Nesterenkonia* and *Streptomyces* strains were reported from the saline–alkaline desert of Fukang. One new species, *Desertihabitans aurantiacus* CPCC 204711^T from the sand of Badain Jaran Desert, could tolerate up to 5% NaCl (Sun et al., 2019). An alkaliphilic actinobacterium, *Nesterenkonia rhizosphaerae* YIM 80379^T, was reported from the rhizosphere soil of *Reaumuria soongorica* grown in the saline–alkaline desert of Fukang (Wang et al., 2014). This strain could grow in up to 15% NaCl and pH 9–10. Another alkaliphile, *S. fukangensis* EGI 80050^T, was also isolated from Fukang Desert with optimal growth observed at pH 9.0–10.0 and 2.5–5.0% NaCl (Zhang et al., 2013). Members of the genera *Jiangella*, *Kribbella*, *Lentzea*, and *Streptomyces* were reported from Gansu Desert, Hangjin Banner Desert, Isolaginsha Desert, and Tibet Autonomous Color Desert, respectively. In Hangjin Banner Desert, a strictly aerobic and non-motile actinobacterium, *Kribbella deserti* SL15-1^T, was isolated from the rhizosphere of *Ammopiptanthus mongolicus* (Sun et al., 2017).

Actinobacterial Diversity in Central and South Asia

Eleven new species of the genera *Jiangella*, *Kribbella*, *Desertiactinospora*, *Nonomuraea*, *Micromonospora*, and *Streptomyces* have been discovered from the Karakum Desert in Central Asia. In South Asia, members of the genera *Actinoalloteichus*, *Agrococcus*, *Kocuria*, *Ornithinimicrobium*, and *Rhodococcus* were found from the Lahaul–Spiti Valley cold desert of the Indian Himalayas. Members of the genera *Auraticoccus*, *Arthrobacter*, and *Motilibacter* were recovered from the Cholistan Desert in Pakistan, while *Saccharothrix* and *Yuhushiella* were discovered from the Indian Thar Desert. Novel species belonging to the genera *Dietzia*, *Nocardioides*, and *Streptomyces* were isolated from the Kunjam Pass cold desert of the Indian Himalayas, the Thal Desert in Pakistan, and the Kutch saline Desert in India, respectively. *S. aburaviensis* strain Kut-8 isolated from the saline desert of Kutch is a halotolerant and alkaliphilic actinobacterium that could grow under saline (15% NaCl) and alkaline (pH 9) conditions (Thumar et al., 2010).

Actinobacterial Diversity in the Middle East, North Africa, and South America

In the Middle East, *Nonomuraea terrae* was isolated from the Anatolia Desert, Turkey, and six new species belong to four genera: *Georgenia*, *Microbacterium*, *Saccharopolyspora*, and *Streptomyces*, which were discovered from the Saudi Arabia arid desert. Three new species, *Georgenia alba* SYSU D8008^T (grew in up to 7% NaCl) (Li et al., 2019d), *Georgenia deserti* SYSU D8004^T (grew in up to 17% NaCl) (Hozzein et al., 2018), and *Saccharopolyspora deserti* SYSU D8010^T (grew in up to 22% NaCl) (Liu et al., 2020), are reported as halotolerant actinobacteria. Representative members of 12 genera were obtained from nine deserts in North Africa. Members of the genera *Actinophytocola*, *Saccharothrix*, and *Streptosporangium* were isolated from the Sahara Desert in Algeria, whereas *Citricoccus*, *Dietzia*, *Nocardiopsis*, and *Streptomyces* were reported from the Eastern Desert of Egypt. A member of the genus *Actinopolyspora, Actinopolyspora mzabensis* H55^T isolated from an Algerian Saharan soil, could tolerate up to 32% NaCl (Saygin et al., 2019a). Alkaliphiles include *Citricoccus alkalitolerans* YIM 70010^T (pH 8–9) (Li et al., 2005), *Nocardiopsis alkaliphila* YIM 80379^T (pH 9.5–10) (Hozzein et al., 2004), and *S. sannurensis* WS 51^T (pH 9.5–10) (Hozzein et al., 2011), which were isolated from the Eastern Desert of Egypt. *Saccharothrix algeriensis* was cultured from a soil sample of palm groves in the Saharan Desert (Zitouni et al., 2004). *Geodermatophilus* and *Promicromonospora* strains were recovered from the Sahara Desert in Tunisia. Other genera, namely, *Nocardiopsis*, *Janibacter*, *Kocuria*, *Prauserella*, and *Streptosporangium*, were described from the Beni Suef Governorate Desert in Egypt, the arid-saline sediment in Tunisia, the saline–alkaline desert in Egypt, the Béni Isguen Desert, and the Béni Abbès Desert in Algeria, respectively. The alkaliphilic strain of *Nocardiopsis benisuefensis* WS65 was isolated from the Beni Suef Governorate Desert in Egypt (Hozzein et al., 2014), while a halotolerant actinobacterium *Prauserella isguenensis* H225^T (grew in up to 25% NaCl) was recovered from the Béni Isguen (Mzab) desert in Algeria (Saker et al., 2015). Twenty-three new species belonging to nine genera (*Amycolatopsis*, *Blastococcus*, *Geodermatophilus*, *Lechevalieria*, *Lentzea*, *Micromonospora*, *Modestobacter*, *Pseudonocardia*, and *Streptomyces*) were reported and described from the Atacama Desert in Chile. One new species, *Pseudonocardia nigra* ATK03^T, was isolated from the rock surface in the Atacama Desert (Trujillo et al., 2017). Two new species recognized as thermophiles, namely, *Amycolatopsis ruanii* NMG112^T and *Amycolatopsis thermalba* SF45^T, could survive under high temperatures (Zucchi et al., 2012a). Another new species, *Modestobacter caceserii* KNN 45-2b^T from the Atacama Desert in Chile, highly adapted to high osmotic stress, cold shock, heat and desiccation, low nutrient, low organic carbon, and high levels of UV radiation (Busarakam et al., 2016b).

Actinobacterial Diversity in Other Regions

Actinomadura namibiensis was isolated from the Namibian Namib Desert in South Africa. *Streptomyces netropsis* was first discovered in North America in the Baja California Desert of Mexico. The Antarctic Desert at the South Pole yielded one new species of *Modestobacter multiseptatus* and *Williamsia* sp., where the former strain was a budding-like psychrophilic actinobacterium isolated from the rock of the Transantarctic Mountains (Mevs et al., 2000). *Williamsia* sp. D3 was considered as a psychrotolerant, able to grow under at a low temperature of 15°C (Guerrero et al., 2014). All new species from the Sahara Desert of Chad in Central Africa and the arid Australian Desert in Oceania were classified in the genera *Geodermatophilus* and *Amycolatopsis*, respectively.

Six new species belonging to the *Geodermatophilus* genus are *Geodermatophilus africanus* (Montero-Calasanz et al., 2013b), *Geodermatophilus arenarius* (Montero-Calasanz et al., 2012), *Geodermatophilus saharensis* (Montero-Calasanz et al., 2013c), *Geodermatophilus siccatus* (Montero-Calasanz et al., 2013e), *Geodermatophilus telluris* (Montero-Calasanz et al., 2013d), and *G. tzadiensis* (Montero-Calasanz et al., 2013a). Two *Geodermatophilus* species, *G. arenarius* CF5/4^T (Montero-Calasanz et al., 2012) and *G. siccatus* CF6/1^T (Montero-Calasanz et al., 2013e) from the Sahara Desert in Chad, have high drought tolerance ability. Members of the genus *Amycolatopsis* were described as *Amycolatopsis australiensis* (Tan et al., 2006), *A. deserti* (Busarakam et al., 2016a), *Amycolatopsis granulosa* (Zucchi et al., 2012a), *Amycolatopsis thermophila*, and *Amycolatopsis viridis* (Zucchi et al., 2012b). Most of them were recognized as thermophiles that could survive under high temperature, including *A. deserti* GY024^T, *A. granulosa* GY307^T, *A. thermophila* GY088^T, and *A. viridis* GY115^T, as well as *A. ruanii* NMG112^T and *A. thermalba* SF45^T from the Atacama Desert in Chile.

ISOLATION AND TAXONOMIC CHARACTERIZATION OF DESERT ACTINOBACTERIA

A bioprospecting strategy to recover actinobacteria from the desert is summarized in **Figure 4**. Most procedures involve the selection of samples from the desert, isolation on selective media, and incubation and selection of representative colonies from the isolation plates for further study (Goodfellow, 2010; Goodfellow and Fiedler, 2010; Tiwari and Gupta, 2013). The low occurrence of rare actinobacteria on the isolation plates clearly reflected the limitations of isolation, cultivation, and maintenance using conventional approaches, which fail to provide optimal growth conditions for desert actinobacteria. Thus, a better or improved isolation method is significant for increasing the number of diverse actinobacterial taxa, which remains an effective strategy for natural product discovery (Jensen, 2010; Jensen et al., 2015).

Selective Isolation of Desert Actinobacteria

Serial Dilution vs. Sprinkling Technique

In general, selective isolation of actinobacteria from desert samples followed the procedure described by Okoro et al. (2009). Serial dilution is commonly used to prepare desert samples for inoculation. Aliquots of soil suspension prepared from serial dilutions were plated onto the selective isolation media, pre-dried in a laminar flow hood for 15 min (Vickers and Williams, 1987). However, there are certain errors associated with sample preparation using a serial dilution method (Ben-David and Davidson, 2014). The first error is related to the initial sample size. If the sample size is larger or smaller than the nominal diluent, under-dilution or over-dilution errors will occur. Similarly, diluent types, mixing method, and mixing time would also cause the same problems. Other errors may occur due to the pipetting technique. It is possible that a non-representative sample will be transferred to the new dilution and finally inoculated on the isolation plates. These errors would lead to a low number of colonies on the isolation plates. Recently, serial dilution, which is part of the conventional culture procedure (CCP), was clearly demonstrated to have limited selectively for even the isolation of members of the genus *Streptomyces*, the most dominant desert actinobacteria (Li et al., 2021).

The sprinkling technique is proposed here as an improved isolation method since few reports have found that it is a simpler and less error-prone way to obtain desert actinobacteria compared to the traditional serial dilution technique, especially for the desert taxa, which may prefer to develop in a reduced-moisture environment, similar to that of the desert, rather than a suspension in a diluent. For example, a greater number of actinobacteria were recorded from selective isolation media using the sprinkling inoculation technique as opposed to the suspensions of the desert sample from Atacama Desert as summarized in **Table 2** (Xie, 2017). This comparative study was carried out using the same selective media supplemented with the same antibiotics under the same incubation conditions. The number of actinobacteria colonies obtained from sprinkling was 10–20 times higher than that acquired via serial dilution. Higher relative abundance was also observed from the sprinkling technique with actinobacterial count representing 85–100% of total bacteria on the isolation plates. The obtained actinobacteria showed antimicrobial activity that is effective against a panel of bacteria, namely, *Bacillus subtilis*, *Escherichia coli*, *Pseudomonas fluorescens*, *Saccharomyces cerevisiae*, and *Staphylococcus aureus*. It is evident that the sprinkling approach clearly provides a higher number of bioactive actinobacteria (141) compared to the serial dilution (97). Again, the number of endophytic actinobacteria acquired from the sprinkling technique is approximately 1.1 times higher than the total population obtained from two improved serial dilution procedures (Qin et al., 2009). Indeed, the isolation medium directly seeded with mineral particles from Atacama Desert soils was found to obtain a higher actinobacterial count than did the serial dilution plates (Idris, 2016). This sprinkling technique allows actinobacterial cells to attach to soil particles in direct contact with the culture media, which increases the isolation efficiency by promoting colony development on the isolation plates (Duddington, 1955; Bailey and Gray, 1989; Qin et al., 2009).

Selective Isolation Media

To maximize the number of actinobacteria, a variety of culture media were employed for the isolation of desert actinobacteria. The effectiveness of the isolation media is closely related to the ecological characteristics of novel actinobacteria from the desert. The media must meet the growth requirements of the target taxa; for example, halophilic strains prefer growth in high-salt-containing media. Selective isolation media resembling the characteristics of the study site increase the success rate of isolation. Carbon and nitrogen sources, growth factors, mineral salts, vitamins, and water are all essential components for the growth of desert actinobacteria on any culture medium (Bonnet et al., 2019). In this aspect, media can be grouped into nutrient-rich media and nutrient-poor media. It is worthy to note that the most effective selective isolation media are specifically

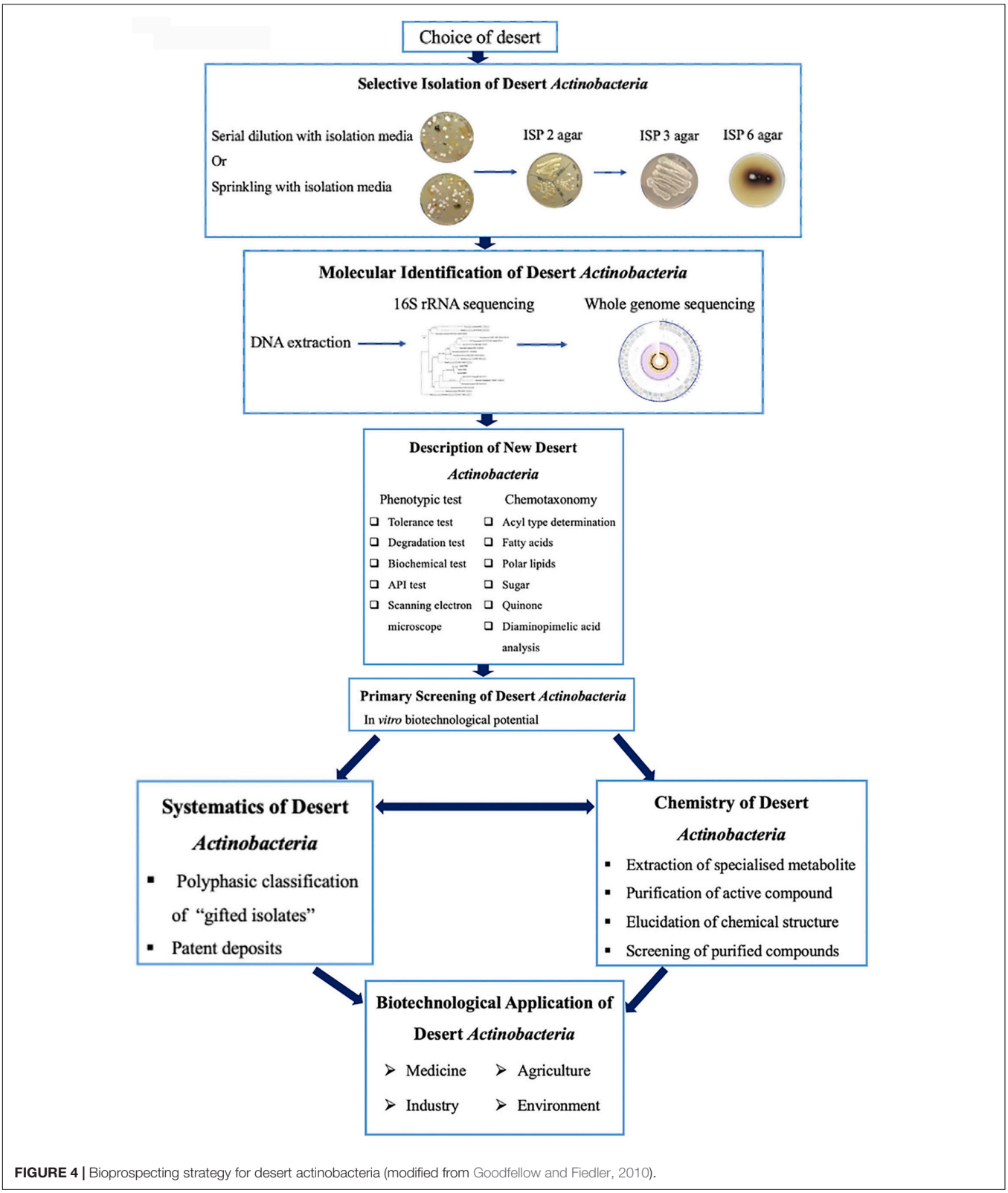

FIGURE 4 | Bioprospecting strategy for desert actinobacteria (modified from Goodfellow and Fiedler, 2010).

designed based on the needs and preferences of actinobacteria, notably nutrient requirements and tolerance preferences of the target taxa. Conventional nutrient-rich media have been widely used to cultivate actinobacteria with limited success. Glucose yeast extract (GYE) agar is recommended as the most suitable medium that can result in a high ratio of actinobacterial count

TABLE 2 | Comparison of serial dilution and sprinkling technique with number and relative abundance of actinobacterial colonies (cfus per gram of dry weight environmental samples) growing on selective media prior to incubation at 28°C for 14 days (modified from Xie, 2017).

Selective medium	Serial dilution			Sprinkling		
	Number of actinobacteria	Relative abundance (%, compared to the total bacteria)	Number of bioactive actinobacteria	Number of actinobacteria	Relative abundance (%, compared to the total bacteria)	Number of bioactive actinobacteria
Valle de la Luna composite sample (VL1 + VL2 + VL3)						
Gauze's no. 1 agar + nalidixic acid (10 μg/ml)	12	65	**5**	**77**	**85**	2
Starch casein agar	31	**72**	3	**87**	62	**6**
HV agar	5	50	0	**80**	**86**	**10**
Valle de la Luna rock scrappings (VLR)						
Gauze's no. 1 agar + nalidixic acid (10 μg/ml)	11	57	3	**177**	**100**	**6**
Starch casein agar	31	45	8	**190**	**76**	**21**
HV agar	1	29	0	**123**	**95**	**14**
Paranal/Paposo composite sample (POP1 + POP2)						
Gauze's no. 1 agar + nalidixic acid (10 μg/ml)	6	75	0	**53**	**76**	**8**
Starch casein agar	39	41	1	**393**	**60**	**9**
HV agar	5	5	0	**107**	**89**	**7**
Yungay composite sample (Y6, 2 and 30 cm)						
Gauze's no. 1 agar + nalidixic acid (10 μg/ml)	196	83	**35**	**513**	**86**	27
Starch casein agar	72	50	18	**453**	**59**	**25**
HV agar	63	43	**24**	**310**	**85**	12

The bolded number indicates the highest value in the comparison of serial dilution and sprinkling technique under the same column items. All media were supplemented with cycloheximide and nystatin (each at 25 μg/ml).

(Agate and Bhat, 1963). Starch casein agar is preferable, especially for saccharolytic organisms, since it contains starch as the sole carbon source as well as sufficient minerals for protein production (Lee et al., 2014). However, recent studies showed that the normally slow-growing rare genera of *Actinobacteria* and *Proteobacteria* failed to grow on commonly used rich media, but growth was observed only from low-nutrient media (Asem et al., 2018; Salam et al., 2021). Approximately 100 novel actinobacteria have been isolated from nutrient-poor media (Salam et al., 2021). This information strongly suggested that nutrient-poor media are more effective for the growth of desert strains as compared to those previously used nutrient-rich media (Bérdy, 2005; Bredholdt et al., 2007; Hozzein et al., 2008). Nutrient-poor media such as soil extract media and a new minimal medium (MM), which reflect the extreme environmental conditions in the desert with low organic matter content, were superior to currently used isolation media for desert actinobacteria (Hozzein et al., 2008). Similarly, humic acid–vitamin (HV) media are also considered as low-nutrient media and are more effective for the isolation of sporulating actinobacteria than are high-nutrient media (Hayakawa, 2008).

Approximately 40 isolation media have been utilized over the last two decades to isolate diverse actinobacterial taxa from the desert (**Supplementary Table 3**). Reasoner's 2A (R2A) agar was the most often used media for desert actinobacterial isolation, representing 25% of reported genera (13): *Blastococcus* (Yang et al., 2019), *Geodermatophilus* (Montero-Calasanz et al., 2013b), *Georgenia* (Li et al., 2019d), *Jiangella* (Saygin et al., 2020b), *Microbacterium* (Yang et al., 2018b), *Micromonospora* (Carro et al., 2019b), *Nocardioides* (Liu et al., 2020), *Nonomuraea* (Saygin et al., 2020c), *Ornithinicoccus* (Zhang et al., 2016), *Saccharopolyspora* (Yang et al., 2018a), *Streptomyces* (Li et al., 2019c), *Tenggerimyces* (Sun et al., 2015), and *Williamsia* (Guerrero et al., 2014). Other media often employed for the isolation of desert taxa include humic acid–vitamin agar and chitin–vitamin agar, which are low-nutrient media comparable to desert environments. Sometimes, media were specially formulated to adjust the nutrient contents to meet the requirements of desert actinobacteria, such as chitin medium, 0.1× tryptic soy agar (TSA) medium, tenfold-diluted trypticase soy broth (TSB) agar, modified 0.3× marine broth agar, and 1/5-strength R2A agar, which were successfully used to recover members of the genera *Labedella* (Li et al., 2019b), *Desertimonas* (Asem et al., 2018), *Kineococcus* (Liu et al., 2009), *Mycetocola* (Luo et al., 2012), and *Tenggerimyces* (Sun et al., 2015). It is worth noting that SM1, SM2, and SM3 agar were specifically designed for the isolation of the *Amycolatopsis* genus (Tan et al., 2006; Zucchi et al., 2012a), whereas medium A was used to recover the alkaliphilic and alkaline-resistant actinobacteria, such as *C. alkalitolerans* (Li et al., 2005), *Nocardiopsis alkaliphile* (Hozzein et al., 2004), and *S. sannurensis* (Hozzein et al., 2011). In addition, media such as starch casein agar and raffinose-histidine agar were used to promote the growth of desert taxa by employing casein and raffinose (selective macromolecules) as nitrogen and carbon sources, respectively. *Saccharothrix tharensis* (Thumar et al., 2010) and *Yuhushiella* sp. (Ibeyaima et al., 2016) were recovered from starch casein agar, while *S. atacamensis* (Santhanam et al., 2012b) and *Streptomyces deserti* (Santhanam et al., 2012a) were isolated from raffinose-histidine agar. Recently, a highly selective culture strategy for the isolation of *Streptomyces* spp. from desert samples was proposed based on the use of minimal medium, actinobacteria isolation agar, and

starch casein agar in combination with a cocktail of selective inhibitors (Li et al., 2021). These authors claimed to increase almost fourfold the number and phylotypes of *Streptomyces* strains isolated from the Gurbantunggut Desert as compared to the conventional approach.

Selective Antibiotics

Another method for increasing the effectiveness of selective isolation of desert actinobacteria is to supplement appropriate antibiotics in the media to enhance the recovery of actinobacteria. Gram-positive (*Bacillus* spp.) and Gram-negative bacteria (*Enterobacteria* and *Escherichia*), as well as fungi (*Alternaria*, *Aspergillus*, *Cladosporium*, *Fusarium*, and *Penicillium*) and yeast, are all frequent contaminants (Bonnet et al., 2019). Thus, selective antibiotics are used to prevent the development of these unwanted fast-growing microorganisms (both bacteria and fungi) that may outcompete actinobacteria on the isolation plates (Entis, 2002; Bonnet et al., 2019). Various antibiotics have been employed to prevent the contaminants from reducing the growth of the desired actinobacteria, summarized in **Supplementary Table 3**. Williams and Davies (1965) initially recommended that a mixture of nystatin (50 μg/ml) and actidione (cycloheximide, 50 μg/ml) was suitable for the enumeration of soil actinobacteria, along with polymyxin B-sulfate (50 μg/ml) and sodium penicillin (10 μg/ml). After that, amphotericin B (20 μg/ml), actidione, calcium propionate (30 mg/ml), cycloheximide (25 μg/ml), nystatin (25 μg/ml), and potassium dichromate (45 mg/L) have been commonly used as antifungal and yeast agents. Penicillin G, bacitracin, and vancomycin were used against Gram-positive bacteria (Bonnet et al., 2019). Polymyxin B (25 mg/L), colistin (2 μg/ml), nalidixic acid (25 mg/l), and ceftazidime (8 μg/ml) were effective for growth inhibition of Gram-negative bacteria. Several antibiotics are active against both Gram-positive and Gram-negative bacteria, including cefalotin, cefamandole, cefixime, ticarcillin, trimethoprim, nitrofurantoin, chloramphenicol, rifampicin (5 μg/ml), oxytetracycline, erythromycin, neomycin (4 μg/ml), gentamicin, fosfomycin, and novobiocin (25 μg/ml) (Bonnet et al., 2019). For the isolation of members of the *Amycolatopsis* genus, SM1 agar was designed to be supplemented with neomycin (1 μg/ml) and cycloheximide and nystatin (each at 25 μg/ml); SM2 agar with neomycin (4 μg/ml), D (+) melezitose (1%, w/v), and nystatin (50 μg/ml); and SM3 agar with cycloheximide (50 μg/ml), nalidixic acid (10 μg/ml), novobiocin (10 μg/ml), and nystatin (50 μg/ml) (Tan et al., 2006). Cycloheximide (50 μg/ml), nalidixic acid (50 μg/ml), and nystatin (100 μg/ml) are often used and responsible for the isolation of 50% of the reported desert actinobacterial genera (27) as shown in **Supplementary Table 3**. Recently, a combination of cycloheximide (25 mg/l), nalidixic acid (25 mg/l), and potassium dichromate (25 mg/L) was used as part of a highly selective culture strategy for the isolation of *Streptomyces* spp. from Gurbantunggut Desert (Li et al., 2021).

Incubation Conditions

Incubation conditions, in particular temperature and incubation duration, are the other important factors in the improvement of isolation (Fang et al., 2017; Ríos-Castillo et al., 2020; **Supplementary Table 3**). It is obvious that the optimal temperature for most actinobacteria is 25–30°C, which could be used as a general incubation temperature for desert actinobacteria. However, extremophilic actinobacteria with specific preference for growth temperature do exist in the desert biomes. For example, one psychrophile, *M. multiseptatus* (Mevs et al., 2000), prefers to grow at a lower temperature (19–21°C), while a thermophile, *Amycolatopsis vastitatis* (Busarakam et al., 2016a), requires an incubation temperature of 45°C. Fourteen new species were recovered from the incubation temperature of 10–50°C. The highest number of new actinobacterial species was obtained at 25–30°C, which is the optimum growth temperature for the majority of desert actinobacteria. Another key factor for selective isolation is the incubation duration. The incubation time which allows actinobacteria to fully grow on the isolation plates ranged from 3 days to 3 months (**Supplementary Table 3**). The fast-growing species are generally allowed abundant growth after 3–14 days, such as *Auraticoccus cholistanensis* (Cheema et al., 2020), *Blastococcus deserti* (Yang et al., 2019), *C. alkalitolerans* (Li et al., 2005), *G. deserti* (Hozzein et al., 2018), *Janibacter* sp. (Khessairi et al., 2014), *Kineococcus xinjiangensis* (Liu et al., 2009), and *K. deserti* (Sun et al., 2017). Slow-growing genera such as *Labedella* (Li et al., 2019b), *Motilibacter* (Liu et al., 2020c), *Modestobacter* (Mevs et al., 2000), *Nonomuraea* (Saygin et al., 2020c), and *Williamsia* (Guerrero et al., 2014) may need more than 4 weeks to fully develop. Nevertheless, the majority of actinobacterial taxa grow well between 2 and 4 weeks. Thus, a specific incubation time allows the recovery of different groups of desert actinobacteria with varied growth rates.

Taxonomic Characterization of Desert Actinobacteria

In general, taxonomic characterization of desert actinobacteria is started with the acquisition of a pure culture of each isolate. Putative actinobacterial colonies from the isolation plates are purified through several rounds of transfer to suitable culture media. Pure isolates of actinobacteria usually develop with different morphological features after being incubated for 2–4 weeks. Morphological characterization of these pure isolated strains was generally observed according to the guidelines proposed by the International *Streptomyces* Project (ISP), including aerial spore mass, substrate mycelial and diffusible pigments, growth, and formation of melanin pigments (Shirling and Gottlieb, 1966). All isolates were further assigned to single- and multi-membered color groups based on the color of the aerial spore mass and substrate mycelial and diffusible pigments. Representative isolates from each morphotype of these assigned color groups are selected for comparative 16S rRNA gene sequence analysis.

The 16S rRNA gene sequencing analysis is routinely the first step for the identification of desert actinobacteria. Genomic DNA of representative isolates can be extracted by various methods such as the phenol-chloroform extraction (Sagova-Mareckova et al., 2008) or solid-phase DNA extraction method such as the bead beating technique (Fujimoto et al., 2004). Several DNA extraction kits are commercially available. The commonly used kits include the MN DNA extraction kit (Macherey-Nagel, Düren,

Germany) (Nithya et al., 2018) and Qiagen Genomic 500 DNA kit (Qiagen, Hilden, Germany) (Jiao et al., 2017). Nucleotide primers for 16S rRNA gene amplification were summarized in **Table 2** including primers 27F and 1492R, which are commonly employed in the study of actinobacteria from deserts.

The information from the 16S rRNA gene sequence is also valuable in delineating actinobacteria from the subspecies to genus levels (Hayashi Sant'Anna et al., 2019). Strains showing less than 98.7% similarity are generally assigned as potential new species (Chun et al., 2018). However, the 16S rRNA genes of members of some closely related species can be too conserved that they cannot be used to differentiate between strains at the species level. Strains of related species with almost identical 16S rRNA gene sequences might belong to different genomic species, as exemplified by members of the genera *Amycolatopsis* (Sangal et al., 2018) and *Streptomyces* (Idris et al., 2017b). It is recommended to obtain a genome sequence for comparison to circumscribe novel species. Nevertheless, 16S rDNA sequence data remain invaluable as they can be used to select appropriate reference strains for whole-genome analysis, thereby reducing the number of marker strains that need to be examined.

The description of new taxa is based on application of the polyphasic taxonomic approach based on a combination of genotypic and phenotypic data. Genotypic data are derived from analyses of nucleic acids and phenotypic data from cultural, chemotaxonomic, morphological, nutritional, and other expressed features. Phenotypic tests involve several biochemical properties and ranges of physiological properties such as pH, temperature, and the concentration of NaCl. Enzymatic activities are currently investigated using the API ZYM (bioMérieux) commercial system (Saygin et al., 2019a). For actinobacterial systematics, it is also critical to investigate the chemotaxonomic properties of new species across closely related taxa (Goodfellow et al., 2012). Developments in molecular systematics have been seen by some to question the continued significance of chemosystematics, but this view is unwarranted as the two approaches are complementary. The most valuable chemical characters are derived from analyses of cellular fatty acids, menaquinones, mycolic acids, muramic acid types, peptidoglycan types, polar lipids, and whole-organism sugars (Goodfellow, 1989). Some of these methods provide quantitative or semiquantitative data, as in the case of cellular fatty acid and menaquinone analyses, but others yield qualitative information, as exemplified by muramic acid, mycolic acid, peptidoglycan, phospholipid, and whole-organism sugar determinations.

Whole-genome sequencing provides the most comprehensive and reliable tool for comparative genome (Ekblom and Wolf, 2014). With the advent of whole-genome sequencing, the weakness of 16S rRNA gene sequencing is being compensated. The genome relatedness thresholds were established to determine whether the compared desert strains can be classified into the same taxon. The overall genome-related index (OGRI) is proposed to replace DNA–DNA hybridization for delineating new species (Chun et al., 2018). OGRI can be used to calculate the relatedness between the genome sequences of isolated strains and closely related strain types of a species. In this aspect, average nucleotide identity (ANI) and digital DDH (dDDH) are the two most widely used OGRI. The proposed and generally accepted species boundary for ANI and dDDH values are 95–96 and 70%, respectively (Goris et al., 2007; Richter and Rosselló-Móra, 2009; Meier-Kolthoff et al., 2013; Chun et al., 2018). These ANI and dDDH values represent a high correlation for the species delineation by a DDH cutoff value of 70% (Kim et al., 2014). Currently, genome sequences provided by Illumina (United States), Ion Torrent (Thermo Fisher Scientific, United States), and Pacific Biosciences (United States) platforms have been shown to generate high-quality DNA sequence data that meet the general standards for taxonomic purposes (Chun et al., 2018). It is evident that polyphasic taxonomy will be a standard approach for the taxonomic characterization of desert actinobacteria as it provides a reliable, reproducible, and stable delineation of taxa.

BIOTECHNOLOGICAL APPLICATIONS OF DESERT ACTINOBACTERIA

Desert actinobacteria generally undergo primary screening to have their interesting bioactivity profiles examined *in vitro* (**Figure 4**). For example, the obtained actinobacteria are subjected to a standard plug assay against a panel of wild-type microorganisms and *B. subtilis* reporter strains (Fiedler, 2004). Those exhibiting an extensive inhibition zone against Gram-positive and Gram-negative bacteria, fungi, and yeasts are assigned as potential antibacterial- or antifungal-producing strains. Similarly, plant beneficial traits, such as phytohormone production, siderophore production, and phosphate solubilization can be screened using qualitative assays to determine their agricultural potential (Allali et al., 2019). Potential actinobacteria are selected for the fermentation study of SMs followed by the purification of the obtained bioactive compounds. The chemical structure of the purified compounds will then be elucidated and tested for their biological properties. Desert actinobacteria with the unique ability to produce novel bioactive compounds could also be deposited as patent strains in public culture collections. In this section, we provide evidences for the potential applications of desert actinobacteria in agriculture, the environment, healthcare, and industry.

Healthcare Applications

Actinobacteria isolated from the desert are potential sources of diverse SMs through their unique metabolic pathways, which adapt for survival under extreme habitats. Recently, the extreme biosphere is the focus of research on the discovery of bioactive compounds to combat MDR pathogens and diseases such as cancer, dementia, and epilepsy (Bull and Goodfellow, 2019). During the past two decades, more than 50 novel natural products have been isolated and identified from desert actinobacteria worldwide (**Table 3**) with potential antiallergic, antibacterial, anticytotoxic, antifungal, anti-inflammatory, antitumor, and antiviral activities. Particularly, members of the genus *Streptomyces* are responsible for more than half of the reported novel compounds.

TABLE 3 | Novel natural products from desert actinobacteria between 2000 and 2021.

Organisms	Location	Structure class	Compound	Bioactivity	References
Jiangella gansuensis YIM 002^T	Desert soil of Gansu, China	Pyrrol-2-aldehyde derivatives	Jiangrines A–E	Anti-inflammatory	Han et al., 2014, Jiao et al., 2017
		Glycolipid	Jiangolide		
		Indolizine derivative	Jiangrine F	Weak cytotoxicity	
Lentzea chajnantorensis H45^T	Atacama Desert, Chile	New diene and monoene glycosides	Lentzeosides A–F	Anti-HIV-1 integrase activity	Wichner et al., 2017
Nocardia sp. XJ31	Xinjiang Desert, China	Ga-siderophores	Nocardimicins J–R	Virus polymerase inhibitory	Zhang et al., 2020
		Benz[α]anthraquinones	Brasiliquinone E	Anti-*Bacillus* Calmette–Guérin (BCG) activity	
Saccharothrix algeriensis SA 233^T	Saharan soil, Algeria	Butanoyl-pyrrothine (BUP)	Dithiolopyrrolone antibiotics	Antibacterial and antifungal activities	Lamari et al., 2002, Zitouni et al., 2004, Strub et al., 2008
		Senecioyl-pyrothine (SEP)			
		Tigloyl-pyrrothine (TIP)			
Saccharothrix algeriensis NRRL B-24137		Crotonyl-pyrrothine	Dithiolopyrrolone PR2	Antibacterial, antifungal, and anti-yeast activities	Merrouche et al., 2011
		Sorbyl-pyrrothine	Dithiolopyrrolone PR8		
		2-Hexonyl-pyrrothine	Dithiolopyrrolone PR9		
		2-Methyl-3-pentenyl-pyrrothine	Dithiolopyrrolone PR10		
		Iso-hexanoyl-pyrrothine	Dithiolopyrrolone PR11		Merrouche et al., 2019
Saccharothrix sp. SA198		$C_{29}H_{30}O_8$	Antibiotic A4	Antifungal and antibacterial activities	Boubetra et al., 2013a
		$C_{30}H_{32}O_8$	Antibiotic A5		
Streptomyces asenjonii KNN 42. f	Atacama Desert, Chile	β-Diketones	Asenjonamides A–C	Antibacterial activity	Abdelkader et al., 2018
Streptomyces leeuwenhoekii C34^T		New 22-membered macrolactone polyketides	Chaxalactins A–C	Antibacterial activity	Rateb et al., 2011b
		New ansamycin-type polyketides	Chaxamycins A–C	Anti-intrinsic ATPase activity of heat shock protein 90 (Hsp), anti-methicillin-resistant *Staphylococcus aureus* (MRSA), and antibacterials	Rateb et al., 2011a
			Chaxamycin D		
		Novel lasso peptide	Leepeptin	ND	Gomez-Escribano et al., 2019
Streptomyces leeuwenhoekii C38		New family of 22-membered antitumor macrolactones	Atacamycins A-C	Antibacterial, antitumor, and cytotoxic activities	Nachtigall et al., 2011
Streptomyces leeuwenhoekii C58		New lasso peptide	Chaxapeptin	Anti-human lung cancer cell line A549	Elsayed et al., 2015
Streptomyces sp. 8P21H-1	Taklamakan Desert, China	New streptogramin-type antibiotics	Acetyl-griseoviridin	No antibacterial activity	Wang et al., 2021
			Desulfurizing griseoviridin	Antibacterial activity	
Streptomyces sp. DA3-7	Saudi Arabian desert	New pyridine alkaloid	Pyridine alkaloid: pyridine-2,5-diacetamide	Antimicrobial activity	Nithya et al., 2018
Streptomyces sp. DB634	Atacama Desert, Chile	Aminoquinone derivatives	Abenquines A–D	Antibacterial, anti-dermatophytic fungal, and anti-phosphodiesterase type 4b activities	Schulz et al., 2011
Streptomyces sp. SAS02	Thar Desert, Rajasthan (India)	New anthracyclines	Non-named	Anticancer activity	Masand et al., 2018
Streptomyces sp. SAS09		New anthracycline glycoside		Antibacterial activity	
		New macrolide			
Streptomyces sp. SAS13		New anthracycline glycoside			
		New macrolide			
Streptomyces sp. SAS15		New macrolide			

Antibacterial and Antifungal Compounds

Diverse novel bioactive compounds produced from several desert actinobacteria have potential antibacterial and antifungal activities. A halotolerant actinobacterium, *J. gansuensis* YIM 002^T, was isolated from a desert soil sample of Gansu. Its whole-genome analysis identified 60 functional gene clusters with the potential to produce pristinamycin, a known antibiotic effective for staphylococcal infections, and other antibiotics (Jiao et al., 2017). One new anthraquinone, brasiliquinone E produced by *Nocardia* sp. XJ31 from the Xinjiang Desert, demonstrated modest anti-*Bacillus* Calmette-Guérin (BCG) activity in an antituberculosis (anti-TB) assay (Zhang et al., 2020). The anti-TB activity indicated that brasiliquinone E can be used as a potential treatment for MDR TB. Three novel dithiolopyrrolone antibiotics, butanoyl-pyrrothine (BUP), senecioyl-pyrrothine (SEP), and tigloyl-pyrrothine (TIP), along with the known benzoyl-pyrrothine, iso-butyropyrrothine (ISP), and thiolutine, were produced from *S. algeriensis* SA 233^T (Lamari et al., 2002; Zitouni et al., 2004; Strub et al., 2008). Dithiolopyrrolones produced by this Saharan Desert (Algeria) strain were highly inhibitory against Gram-positive bacteria such as *Bacillus coagulans*, *B. subtilis*, and *Micrococcus luteus*. Three dithiolopyrrolones, ISP, and thiolutine are also effective against Gram-negative bacteria including *Klebsiella pneumoniae*. In addition, SEP and TIP showed greater activity against *S. cerevisiae*, *Mucor ramannianus*, and other phytopathogenic fungi (*Fusarium culmorum*, *Fusarium oxysporum* f.sp. *albedinis*, and *F. oxysporum* f.sp. *lini*), compared to thiolutine and ISP (Lamari et al., 2002). Two more Saharan Desert strains from Algeria are also capable of producing novel compounds. *Saccharothrix* strain SA198 generated two new antibiotics designated as A4 and A5, which inhibited both Gram-positive bacteria (*B. subtilis*, *Enterococcus faecalis*, and *Listeria monocytogenes*) and Gram-negative bacteria (*E. coli*, *K. pneumoniae*, and *Pseudomonas aeruginosa*) (Boubetra et al., 2013a). A4 and A5 also exhibited modest antifungal ability against filamentous fungi such as *Ascochyta fabae*, *Aspergillus carbonarius*, *F. culmorum*, *Fusarium equiseti*, *M. ramannianus*, and *Penicillium expansum*. By incorporating sorbic acid into its culture medium, *S. algeriensis* NRRL B-24137 produced five novel dithiolopyrrolone antibiotics: PR2, PR8, PR9, PR10, and PR11 (Merrouche et al., 2011, 2019). These five antibiotics showed antimicrobial activity against Gram-positive bacteria, filamentous fungi, and yeasts, including *B. subtilis*, *B. coagulans*, *L. monocytogenes*, *M. luteus*, *S. aureus*, *A. carbonarius*, *F. oxysporum* f.sp. *lini*, *Fusarium moniliforme*, *F. equiseti*, *F. culmorum*, *Fusarium graminearum*, *M. ramannianus*, *P. expansum*, *Candida albicans*, and *S. cerevisiae*.

Four strains obtained from the Atacama Desert were discovered to produce antibiotics with effective antibacterial and antifungal activities. *S. asenjonii* KNN 42.f generated asenjonamides A–C, three new bioactive β-diketones (Abdelkader et al., 2018). All compounds showed inhibitory activity against a panel of Gram-positive and Gram-negative bacteria, such as *S. aureus*, *B. subtilis*, *E. coli*, *E. faecalis*, and *Mycobacterium smegmatis*. Three new compounds named chaxalactins A–C (22-membered macrolactone polyketides), identified from *S. leeuwenhoekii* C34^T, displayed strong inhibitory activity against Gram-positive bacteria (*S. aureus*, *L. monocytogenes*, and *B. subtilis*) and weak activity against Gram-negative bacteria (*E. coli* and *Vibrio parahaemolyticus*) (Rateb et al., 2011b). Another four new ansamycin-type polyketides, chaxamycins A–D, were shown to be active against *S. aureus*, *E. coli*, and a panel of methicillin-resistant *S. aureus* (MRSA) clinical isolates (epidemic MRSA and Scottish MRSA) (Rateb et al., 2011a). *S. leeuwenhoekii* C38 synthesized atacamycins A–C, three new 22-membered macrolactone antibiotics (Nachtigall et al., 2011). The antibacterial assay revealed that atacamycins were effective against Gram-positive and Gram-negative bacteria, including *B. subtilis*, *Brevibacterium epidermidis*, *Dermabacter hominis*, *K. pneumoniae*, *Propionibacterium acnes*, *P. aeruginosa*, *S. aureus*, *Staphylococcus epidermidis*, *Staphylococcus lentus*, and *Xanthomonas campestris*. Atacamycins A–C also slightly inhibited the growth of the phytopathogenic bacterium *Ralstonia solanacearum* DSM 9544 (Nachtigall et al., 2011). Four aminoquinone derivatives, abenquines A–D, isolated from *Streptomyces* sp. DB634, showed antibacterial and antifungal activities, in particular anti-dermatophytic fungi, against *Trichophyton rubrum*, *Trichophyton mentagrophytes*, and *Microsporum canis*, as well as slightly inhibiting *B. subtilis* and mouse fibroblasts (NIH-3T3 cell line) (Schulz et al., 2011).

Other desert actinobacterial strains also produced bioactive compounds, although their structures are unknown. *Streptomyces* sp. BS30 generated two undetermined compounds that are anti-*Aspergillus niger* 2CA936 and anti-yeast (Souagui et al., 2017). *Streptomyces* sp. Wb2n-11 has moderate antifungal, antibacterial, and antinematicidal activities against *F. culmorum*, *Rhizoctonia solani*, *Verticillium dahliae*, *R. solanacearum*, and root-knot nematode (*Meloidogyne incognita*) (Köberl et al., 2015). Several Thar Desert *Streptomyces* strains show bioactivity against MDR pathogens such as *C. albicans*, *E. coli* ATCC 3739, MRSA, *P. aeruginosa* ATCC 10145, and vancomycin-resistant *Enterococcus* (Masand et al., 2018). Three actinobacteria, *S. aburaviensis* Kut-8 (Thumar et al., 2010; Ramirez-Rodriguez et al., 2018), *S. asenjonii* KNN35.1b^T (Goodfellow et al., 2017), and *Yuhushiella* sp. TD-032 (Ibeyaima et al., 2016), were reported to inhibit Gram-positive bacteria including *S. aureus*, *Bacillus cereus*, *Bacillus megaterium*, and *B. subtilis*. *Micromonospora arida* LB32^T and *Micromonospora inaquosa* LB39^T were found to have antibacterial and antifungal abilities, especially against MDR *K. pneumoniae* ATCC 700603 (Carro et al., 2019a). *Nocardiopsis* sp. 38-7L-1 was able to treat the pathogen *P. aeruginosa* (Chen et al., 2015).

Anticancer and Antitumor Compounds

Chaxamycins A–D derived from *S. leeuwenhoekii* C34^T can be used as anticancer drugs based on their ability to inhibit the intrinsic ATPase activity of heat shock protein 90 (Hsp90) (Rateb et al., 2011a). Another strain, *S. leeuwenhoekii* C38, produced chaxapeptin, a new lasso peptide with a substantial inhibitory effect in the human lung cancer cell line A549 according to the cell invasion assay (Elsayed et al., 2015). Three

antitumor compounds were also derived from *S. leeuwenhoekii* C38, atacamycins A–C, which moderately inhibited the enzyme phosphodiesterase (PDE-4B2) (Nachtigall et al., 2011). Furthermore, atacamycins A and B showed clear cytotoxic activities against a panel of 42 different human tumor cell lines. Atacamycin A was the most active in cell lines of colon cancer (CXF DiFi), breast cancer (MAXF 401NL), and uterus cancer (UXF 1138L), whereas atacamycin B showed significant antiproliferative activity against colon RKO cells (Nachtigall et al., 2011). *Micromonospora chalcea* LB4 and LB41 showed antitumor activity against human hepatocellular carcinoma (HepG2) cells (Carro et al., 2019a).

Anti-inflammatory Compounds

Jiangella gansuensis YIM 002^T was collected from Gansu Desert in China and produced seven new compounds, jiangrines A–F and jiangolide, as well as pyrrolezanthine, a known compound (Han et al., 2014). Jiangrines A–E and jiangrine F are pyrrol-2-aldehyde derivatives and an indolizine derivative, respectively. All of them, including pyrrolezanthine, demonstrated significant anti-inflammatory activity by inhibiting NO production in LPS-treated RAW 264.7 macrophage cells. Jiangolide is a glycolipid with weak cytotoxicity based on a low inhibitory ratio (<20%) of the cell viability assay (Han et al., 2014). Abenquines A–D isolated from *Streptomyces* sp. DB634 showed moderate anti-inflammatory activity against phosphodiesterase type 4 (PDE4b), which can be used to treat inflammatory diseases, such as chronic obstructive pulmonary disease (Schulz et al., 2011).

Antiviral Compounds

Lentzeosides A–F are six new diene and monoene glycosides derived from *Lentzea chajnantorensis* H45^T isolated from the Atacama Desert (Wichner et al., 2017). These novel compounds clearly inhibited HIV-1 integrase, one of the key enzymes in the HIV replication cycle. Thus, lentzeosides might be used as HIV integrase inhibitors for the treatment of HIV-1 infections, HIV-1 replication, and other virus strains resistant to multi-antiretroviral drugs (Wichner et al., 2017). *Nocardia* sp. XJ31, isolated from the Xinjiang Desert, generated nine new siderophores (nocardimicins J–R), which were found to inhibit viral infection by binding affinities with the four 3′′-RNA pockets of viral polymerases (>90%) (Zhang et al., 2020).

Antioxidant Compounds

Streptomyces sp. D25, isolated from Thar Desert, Rajasthan, showed antioxidant potential based on free radical scavenging activity using DPPH and nitric oxide assays (Radhakrishnan et al., 2016). It is also moderately effective against biofilm-forming bacteria, including *Alcaligenes* sp. M28, *Alcaligenes* sp. P8, *Bacillus* sp. M38, *Bacillus* sp. P13, *Kurthia* sp. P3, *Lactobacillus* sp. M6, *Lactobacillus* sp. M51, *Lactobacillus* sp. P4, *Micrococcus* sp. M50, *Pseudomonas* sp. P1, and *Staphylococcus* sp. M1.

Agricultural Applications

Actinobacteria from the desert showed a broad range of plant growth-promoting and biocontrol properties. Their ability to survive under extreme environments allows them to enhance the growth of plants under severe abiotic stresses, especially drought and salinity. Since 2013, 37 actinobacteria from the desert have been reported to have agricultural potential, mostly from members of the genus *Streptomyces* as summarized in **Table 4**. All these studies highlight the potential application of desert actinobacteria in agriculture under stress environments.

Plant Growth Promotion

Plant growth-promoting properties displayed by desert actinobacteria include 1-aminocyclopropane-1-carboxylic acid (ACC) deaminase production, auxin production, gibberellic acid (GA) production, indole-3-acetic acid (IAA) production, siderophore production, nitrogen fixation, and P and K solubilization. For example, a high-IAA-producing strain of *Kocuria turfanensis* 2M4 recovered from a saline desert in India significantly increased the total length and fresh biomass of groundnut after 15 days of germination by pot study (*Arachis hypogaea* L.) (Goswami et al., 2014). *Streptomyces mutabilis* IA1 from Saharan soil produced IAA and GA, which are responsible for the promotion of wheat growth after incubation in a phytotronic growth chamber for 10 days (Toumatia et al., 2016). *Nocardiopsis dassonvillei* MB22 was isolated from the Algerian Sahara soil and can stimulate the growth of durum wheat seedlings (shoot and root lengths and dry weight) by a variety of properties (chitinolytic activity, hydrogen cyanide production, IAA production, siderophore production, and inorganic phosphate solubilization) (Allali et al., 2019). Three plant growth-promoting *Streptomyces* isolated from the desert plant *Pteropyrum olivieri* could enhance the yield and biochemical contents of sunflower in greenhouse and field experiments under normal conditions (Zahra et al., 2020). These streptomycetes could also improve salt and drought tolerance in inoculated sunflower seedlings. In addition, they can act as plant probiotics by supplying the host plant with three major traits: acquisition of nutrients, growth hormone, and stress tolerance. *Microbacterium* sp. WLJ053 and *Streptomyces* sp. WLJ079 from the rhizosphere of *A. sparsifolia* harbored a nitrogen-fixation gene *nif*H, which improved maize growth by increasing stem and root lengths, fresh and dry weights after 1 month planting, and cultivation in the greenhouse (Wang et al., 2017). In addition, *S. netropsis* A-ICA from *Larrea tridentata* in the Baja California Desert of Mexico enhanced root elongation and development of wheat by the production of IAA, siderophores, and GA and phosphate solubilization after 4 days of germination in semisolid plates (Abdelmoteleb and González-Mendoza, 2020).

Mitigation Potential for Abiotic Stress in Plants

Streptomyces sp. AC5 from the semi-arid environment of Saudi Arabia could mitigate the negative effects of drought on the growth and physiology of maize, discovered from 6 weeks of cultivation in a controlled greenhouse (Selim et al., 2019). This IAA- and siderophore-producing *Streptomyces* sp. AC5 positively enhanced the growth and drought tolerance ability of maize by reducing H_2O_2 accumulation and lipid peroxidation through the production of antioxidants (total ascorbate, glutathione, tocopherols, phenolic acids, and flavonoids) and compatible solutes (sucrose, total soluble sugar, proline, arginine, and

TABLE 4 | Agricultural applications from desert actinobacteria between 2000 and 2021.

Organism	Location	PGP traits	Target	References
Arthrobacter sp. AF3	Atacama Desert, Chile	Siderophore production, auxin (AIA) production, nitrogen fixation, ACC deaminase activity and phosphate solubilization	ND	Gaete et al., 2020
Cryobacterium sp. S5				
Frondihabitans sp. R8				
Microbacterium spp. M1-B and M2-A				
Paeniglutamicibacter spp. L1D and L2D				
Pseudarthrobacter spp. M1, M3, M2, and L2				
Rhodococcus sp. D4				
Streptomyces sp. M1-A				
Cellulosimicrobium sp. JZ28	Saudi Arabia, Jizan and Al Wahbah	Chitinase activity	Pathogens	Eida et al., 2020
		β-Glucosidases	Degradation of cellulose biopolymers	
		Osmoprotectants	Oxidative, osmotic, and salinity stresses	
		Volatiles: hydrogen sulfide	Biotic and abiotic stress	
Kocuria turfanensis 2M4	Saline desert of Little Rann of Kutch, Gujarat, India	IAA	Groundnut (*Arachis hypogaea* L.)	Goswami et al., 2014
Microbacterium sp. WLJ053	The rhizosphere of desert plant *Alhagi sparsifolia*	Plant growth-promoting activity	Maize	Wang et al., 2017
Streptomyces sp. WLJ079				
Nocardiopsis dassonvillei MB22	Sahara, Algeria	Biocontrol activity	Common root rot pathogen caused by *Bipolaris sorokiniana* LB12	Allali et al., 2019
		IAA, siderophore, hydrogen cyanide, chitinolytic activity, and solubilized inorganic phosphates	Durum wheat (cv. Vitron)	
Streptomyces mutabilis IA1	Saharan, Algeria	Biocontrol activity	Temperate crop	Toumatia et al., 2016
		IAA and GA3	Soft wheat (*Triticum aestivum* L.)	
Streptomyces netropsis A-ICA	Baja California, Mexico	Antifungal activity	*Macrophomina phaseolina*, *Fusarium oxysporum*, *Fusarium solani*, *Fusarium equiseti*, *Botrytis cinerea*, *Alternaria alternata*, and *Colletotrichum gloeosporioides*	Abdelmoteleb and González-Mendoza, 2020
		Inorganic phosphate solubilization	ND	
		IAA, GA	Tomato (*Solanum lycopersicum*)	
Streptomyces sp. AC5	Saudi Arabia, Jouf	Flavonoid, phytohormone, and siderophore production	Maize (*Zea mays* L.) under drought condition	Selim et al., 2019
Streptomyces sp. MM40	Monte Desert, NW of Patagonia, Neuquén	Auxin, cytokines, zeatins, and siderophores	ND	Solans et al., 2021
		Exoenzymes: proteases, phospholipase, and lipases		
Streptomyces sp. RD1 and RD5		Phosphorous solubilization	Native vegetation	
Streptomyces sp. MNB-1, MNB-2, MNB-3, MNC-1, MNC-2, MNC-3, MNC-4, MNT-1	Merzouga, Morocco	IAA, siderophore production, N_2 fixation, P and K solubilization	ND	Nafis et al., 2019
Streptomyces sp. PT2	The Algerian Sahara	Crude IAA	Tomato	Goudjal et al., 2013
Streptomyces sp. UTMC 2482, UTMC 2483, and UTMC 3136	Salt Lake Qom, Iran	IAA, ethylene via ACC deaminase, and siderophores	Sunflower	Zahra et al., 2020
Streptomyces sp. Wb2n-11	Sinai Desert, Egypt	Antifungal	*Fusarium culmorum*; *Rhizoctonia solani*; *Verticillium dahliae*	Köberl et al., 2015
		Antibacterial	*Ralstonia solanacearum*	
		Antinematicidal	*Meloidogyne incognita* (soilborne phytopathogens)	

ND, not determined.

glycine betaine). The IAA and siderophores were suggested to promote root architecture and water and nutrient uptake from drought-affected soil (Selim et al., 2019). Similarly, *Cellulosimicrobium* sp. JZ28 was isolated from *Panicum turgidum* in the Saudi Arabia Desert, and its whole-genome sequence indicated that several genes were responsible for protecting the plant from environmental stresses, such as the ability to synthesize osmoprotectants and volatile compounds in order to withstand abiotic and biotic stresses (Eida et al., 2020).

Biocontrol Potential

Streptomyces mutabilis IA1 from Saharan soil exhibited biocontrol property to decrease severity (79.6%) and reduce occurrence (64.7%) of fungal infection caused by *F. culmorum* evaluated from 10 days young wheat (*Triticum aestivum* L.) seedlings in a phytotronic growth chamber (Toumatia et al., 2016). *N. dassonvillei* MB22, a powerful antifungal producing strain isolated from Algerian Sahara soil, could be used as a biocontrol agent to ensure crop health (Allali et al., 2019). This strain has the potential for controlling several soil-borne phytopathogens (*Bipolaris sorokiniana* LB12, *R. solani* LRS1, *F. culmorum* LF18, *F. graminearum* LF21 and *F. oxysporum* f.sp. *radices lycopersici* LF30). *Streptomyces* sp. UTMC 2482, UTMC 2483, and UTMC 3136 isolated from desert plant *P. olivieri* produced several lytic enzymes namely amylase, cellulase, chitinase, lipase and protease, which can inhibit growth of plant pathogens such as *A. niger*, *F. oxysporum* and *Mucor hiemalis* (Zahra et al., 2020). A rhizobacterium *S. netropsis* A-ICA from *Larrea tridentata* in the Baja California Desert of Mexico demonstrated high inhibitory activity on fungal growth (*Alternaria alternata*, *Botrytis cinerea*, *Colletotrichum gloeosporioides*, *F. equiseti*, *F. oxysporum*, *Fusarium solani,* and *Macrophomina phaseolina*) due to the production of hydrolytic enzymes (cellulases, chitinase, and glucanase) and antifungal compounds (Abdelmoteleb and González-Mendoza, 2020). The culture filtrate of *S. netropsis* A-ICA strongly suppressed the mycelial development of two fungal pathogens, *Botrytis cinerea* and *Macrophomina phaseolina*. The presence of chitinase genes suggested that *Cellulosimicrobium* sp. JZ28 isolated from *P. turgidum* in the Saudi Arabia Desert has a biocontrol potential against fungal pathogens, such as *B. cinerea*, *F. oxysporum* and *V. dahliae* (Eida et al., 2020).

Industrial and Environmental Application

To adapt for living in the extreme arid ecosystems, various functional enzymes were synthesized by actinobacteria, and these enzymes can be applied for industrial and environmental uses. Those studies shown below provide supporting evidence for potential applications of desert actinobacteria in the environment and industry.

Pentachlorophenol Remediation

Pentachlorophenol (PCP) is a commonly utilized technique in some industries, such as the preservation of wood and leather (Kao et al., 2004). However, PCP is also toxic, and its exposure can induce acute pancreatitis, cancer, immunodeficiency, and neurological problems, as well as inhibiting oxidative phosphorylation (Sai et al., 2001; Shen et al., 2005). A halotolerant *Janibacter* sp. FAS23 strain obtained from arid and saline Tunisia terrain can degrade PCP (Khessairi et al., 2014). Strain FAS23 was able to degrade PCP up to 300 mg/L and could be used for PCP bioremediation in PCP-contaminated environments.

Industrial Potential

Two new oxidative enzymes, type I Baeyer-Villiger monooxygenases (BVMOs), industrial potential biocatalysts were discovered from *S. leeuwenhoekii* C34, isolated from Atacama Desert. These new BVMOs enzymes with high melting temperature (45°C) and water-miscible cosolvents tolerance were capable of NADPH-dependent BV oxidation activity on ketones, sulfoxidation activity on sulfides (Gran-Scheuch et al., 2018). In Saudi Arabia, *Streptomyces fragilis* DA7-7 synthesized a thermostable α-amylase, an important enzyme with commercial potential in industries, including brewery, detergent, paper, food, starch saccharification and pharmaceuticals. (Nithya et al., 2017). *Am*-fluorinase, another thermostable enzyme, was found in *A. mzabensis* from Saharan soil in Algeria (Sooklal et al., 2020). This enzyme is responsible for incorporating fluorine into organic molecules to improve the bioactive and biophysical characteristics of compounds and has been widely used in the agrochemical, material and pharmaceutical industries. The *Am*-fluorinase from *A. mzabensis* catalyzed a C-F bond and displayed great thermostability with the optimum temperature at 65°C. *Cellulosimicrobium* sp. JZ28, isolated from *P. turgidum* also contains genes encoding for β-glucosidases enzymes (Eida et al., 2020). This enzyme could be applied to extract the juice and liberate aroma from wine grapes by hydrolyzing bitter compounds, for example, it can enhance the flavor of fruit juice, tea, and wine in food processing industries (Singh et al., 2016).

CONCLUSION AND FUTURE PERSPECTIVES

Diverse actinobacteria from the desert are undoubtedly potential resources for biotechnology. These actinobacteria which thrive under such extreme environmental conditions, exhibit the diversity and their exceptional adaptability from specialized metabolisms. This review explored 129 new species including alkaliphiles, halotolerant, thermophile and psychrotolerant from 35 deserts in the past two decades. Several species showed potential applications in biotechnology in particular bioactive compounds production, biocontrol properties, functional enzymes and plant growth promotion. The survival mechanisms of actinobacteria under extensive environmental stress in the desert offer tremendous possibilities to explore novel bioactive compounds with unique biosynthesis pathways. It is strongly supporting the view that gifted desert actinobacteria with their bioactive potential provide beneficial appropriate solutions to triumph over the increasingly serious threats from MDR pathogens, agricultural stress and environmental problems.

To recover untapped diversity of culturable actinobacteria from desert, it is extremely important and urgently need for develop improved techniques for selective isolation of target

taxa. The progress of actinobacterial diversity depends on the development of such isolation methods which can reflect physicochemical characteristics of the desert environments. Growth of desert actinobacteria is mainly influenced by several physicochemical factors, such as the cation exchange capacity (CEC), the carbon and nitrogen sources, water retention capacity, hydrogen-ion concentration (pH) and temperature (Amin A. et al., 2020). To date, studies have revealed that the efficiency of actinobacterial isolation methods was positively related to the choices of selective media, supplemented inhibitors, inoculation techniques and incubation conditions, which mimics desert environments (Goodfellow, 2010; Goodfellow and Fiedler, 2010; Tiwari and Gupta, 2013). Selective media provide nutrient sources require for the growth and proliferation of target actinobacteria with the help of inhibitors to suppress the growth of unwanted bacteria. Most desert actinobacteria are slow-growing actinobacteria, with a preference for poor nutrient media over nutrient rich media (Li et al., 2021). The supplement of selective antibiotics was significantly promoted the isolation of desert taxa by sharply reduced the number of unwanted bacteria represented by the genus *Bacillus*. Media supplemented with these antibiotics far exceeded in obtaining the target actinobacteria than media without supplementation (Li et al., 2021). In addition, a higher number of isolates were recorded from the isolation media using the sprinkling technique for inoculation as compared with those corresponding plates prepared from the traditional serial dilution method (Idris, 2016; Xie, 2017). As opposed to the isolation plates seeded with soil suspensions, sprinkling technique allowed the mineral particles to be in direct contact with the nutrients in the media, which may stimulate spore germination and improve the growth of actinobacteria. More diversity was recovered from mineral particles inoculated onto selective media supplemented with inhibitor using sprinkling technique as exemplified by Idris (2016) and Xie (2017). Therefore, it is strongly recommended to use the sprinkling technique for the isolation of actinobacteria from desert associated samples.

In addition to culture-dependent studies, next-generation sequencing techniques and metagenomics are widely used in the identification and characterization of actinobacteria to gain an understanding of their diversity and functions in the desert. However, most desert microorganisms cannot be cultured as exemplified by only 1% of them are culturable (Martiny, 2019). Whole-genome sequences seem to be an effective way to resolve these taxonomic bottlenecks with increasing utilization in systematic studies. It provides a deep insight into the ecology and biotechnological potential of desert species. Currently, 16,763 reference genomes are available in the database (Shi et al., 2021). With the increasing availability of genome sequences, the information regarding genes and their functions provides insights into the metabolic potential of desert actinobacteria, which will greatly promote their biotechnology applications. A culture-enriched metagenomic approach named PLate Coverage Algorithm (PLCA) is developed based on the use of 16S rRNA gene sequencing of culture-enriched plates and shotgun metagenomics to identify the microbial community and their functions, which has been succeeded to recover bacteria including actinobacteria from the cystic fibrosis (Whelan et al., 2020). The PLCA improves the recovery of microbial diversity in the sample and provides a better understanding of the mechanisms between microbial communities and the host environment. This method can be used on any low-abundance microbial community in particular low-abundance actinobacterial taxa from desert, such as *Desertiactinospora*, *Tenggerimyces*. Another method for recovering unculturable actinobacteria is the cooperation of 16S rRNA gene metagenomics and commercially available media (Ito et al., 2019). These authors suggested that selective features of media are significantly influenced the recovery of slow-growing taxa on the isolation plates. Successful isolation of novel actinobacteria from commercially available media suggested that uncultured actinobacteria are potentially culturable. This method highlights the high possibility of the recovery of low-abundance taxa in laboratory culture. Besides, computational techniques are continuedly developed since several new algorithms, tools and databases are becoming available, aiming to explore both actinobacterial diversity, their functions and biotechnological potential (Medema, 2021). Several bioinformatics tools are designed specifically for the prediction of bioactive compounds with novel chemical structures from the whole genome sequences (Mikulak-Klucznik et al., 2020; Stokes et al., 2020). An effective biosynthetic pathway for such new compounds can be selected and mined through these genomic data for further engineering purposes. These exciting improvements will undoubtedly provide a tool for the recovery of novel taxa, their ecological functions and the discovery of un-hitherto biotechnological values of these desert actinobacteria. The more comprehensive knowledge should be built upon the principle of "embrace the genome" (Whitman, 2014), which would provide an immensely richer understanding of the biology of actinobacteria in desert environments.

AUTHOR CONTRIBUTIONS

FX wrote the first draft. WP conceived the idea and supervised FX. FX and WP revised the manuscript. Both authors contributed to the article and approved the submitted version.

FUNDING

This research was supported by the Graduate Ph.D's Degree Program in Applied Microbiology, Department of Biology, Faculty of Science, Chiang Mai University, under the CMU Presidential Scholarship. WP is also grateful for partially supported by Chiang Mai University.

SUPPLEMENTARY MATERIAL

The Supplementary Material for this article can be found online at: https://www.frontiersin.org/articles/10.3389/fmicb.2021.765531/full#supplementary-material

REFERENCES

Abdelkader, M., Philippon, T., Asenjo, J. A., Bull, A. T., Goodfellow, M., Ebel, R., et al. (2018). Asenjonamides A-C, antibacterial metabolites isolated from *Streptomyces asenjonii* strain KNN 42.f from an extreme-hyper arid Atacama Desert soil. *J. Antibiot.* 71, 425–431. doi: 10.1038/s41429-017-0012-0

Abdel-Mageed, W. M., Milne, B. F., Wagner, M., Schumacher, M., Sandor, P., Pathom-aree, W., et al. (2010). Dermacozines, a new phenazine family from deep-sea dermacocci isolated from a Mariana Trench sediment. *Org. Biomol. Chem.* 8, 2352–2362. doi: 10.1039/c001445a

Abdelmoteleb, A., and González-Mendoza, D. (2020). A novel Streptomyces rhizobacteria from desert soil with diverse anti-fungal properties. *Rhizosphere* 16:100243. doi: 10.1016/j.rhisph.2020.100243

Adeela, F., Riaz, S., and Sajid, I. (2018). Anti-MRSA potential and metabolic fingerprinting of actinobacteria from Cholistan desert, Pakistan. *Trop. J. Pharm. Res.* 17, 2037–2046. doi: 10.4314/tjpr.v17i10.21

Agate, A. D., and Bhat, J. V. (1963). A method for the preferential isolation of actinomycetes from soils. *Antonie van Leeuwenhoek* 29, 297–304. doi: 10.1007/BF02046072

Al-Dhabi, N. A., Esmail, G. A., Ghilan, A. M., Arasu, M. V., Duraipandiyan, V., and Ponmurugan, K. (2020). Chemical constituents of *Streptomyces* sp. strain Al-Dhabi-97 isolated from the marine region of Saudi Arabia with antibacterial and anticancer properties. *J. Infect. Public. Health.* 13, 235–243. doi: 10.1016/j.jiph.2019.09.004

Allali, K., Goudjal, Y., Zamoum, M., Bouznada, K., Sabaou, N., and Zitouni, A. (2019). *Nocardiopsis dassonvillei* strain MB22 from the Algerian Sahara promotes wheat seedlings growth and potentially controls the common root rot pathogen *Bipolaris sorokiniana*. J. Plant Pathol. 101, 1115–1125. doi: 10.1007/s42161-019-00347-x

Almuhayawi, M. S., Mohamed, M., Abdel-Mawgoud, M., Selim, S., Al Jaouni, S. K., and AbdElgawad, H. (2021). Bioactive potential of several actinobacteria isolated from microbiologically barely explored desert habitat. *Saudi Arabia. Biology.* 10, 235–257. doi: 10.3390/biology10030235

Amin, A., Ahmed, I., Khalid, N., Khan, I. U., Ali, A., Dahlawi, S. M., et al. (2020). Insights on comparative bacterial diversity between different arid zones of Cholistan Desert, Pakistan. *3 Biotech* 10, 224–237. doi: 10.1007/s13205-020-02204-6

Amin, D. H., Abdallah, N. A., Abolmaaty, A., Tolba, S., and Wellington, E. M. (2020). Microbiological and molecular insights on rare Actinobacteria harboring bioactive prospective. *Bull. Natl. Res. Cen.* 44, 1–12. doi: 10.1186/s42269-019-0266-8

Asem, M. D., Shi, L., Jiao, J. Y., Wang, D., Han, M. X., Dong, L., et al. (2018). *Desertimonas flava* gen. nov., sp. nov. isolated from a desert soil, and proposal of Ilumatobacteraceae fam. nov. *Int. J. Syst. Evol. Microbiol.* 68, 3593–3599. doi: 10.1099/ijsem.0.003038

Ay, H. (2020). *Nonomuraea terrae* sp. nov., isolated from arid soil. *Arch. Microbiol.* 202, 2197–2205. doi: 10.1007/s00203-020-01941-9

Bailey, F., and Gray, N. F. (1989). The comparison of isolation techniques for nematophagous fungi from soil. *Ann. Appl. Biol.* 114, 125–132. doi: 10.111/j.1744-7348.1989.tb06792.x

Baltz, R. H. (2008). Renaissance in antibacterial discovery from actinomycetes. *Curr. Opin. Pharmacol.* 8, 557–563. doi: 10.1016/j.coph.2008.04.008

Baltz, R. H. (2017). Gifted microbes for genome mining and natural product discovery. *J. Ind. Microbiol. Biotechnol.* 44, 573–588. doi: 10.1007/s10295-016-1815-x

Baltz, R. H. (2018). Synthetic biology, genome mining, and combinatorial biosynthesis of NRPS-derived antibiotics: a perspective. *J. Ind. Microbiol. Biotechnol.* 45, 635–649. doi: 10.1007/s10295-017-1999-8

Baltz, R. H. (2019). Natural product drug discovery in the genomic era: realities, conjectures, misconceptions, and opportunities. *J. Ind. Microbiol. Biotechnol.* 46, 281–299. doi: 10.1007/s10295-018-2115-4

Barka, E. A., Vatsa, P., Sanchez, L., Gaveau-Vaillant, N., Jacquard, C., Meier-Kolthoff, J. P., et al. (2016). Taxonomy, physiology, and natural products of actinobacteria. *Microbiol. Mol. Biol. Rev.* 80, 1–43. doi: 10.1128/MMBR.00019-15

Bednarz, B., Millan-Oropeza, A., Kotowska, M., Świat, M., Quispe Haro, J. J., Henry, C., et al. (2021). Coelimycin synthesis activatory proteins are key regulators of specialized metabolism and precursor flux in Streptomyces coelicolor A3(2). *Front. Microbiol.* 12:616050. doi: 10.3389/fmicb.2021.616050

Ben-David, A., and Davidson, C. E. (2014). Estimation method for serial dilution experiments. *J. Microbiol. Methods.* 107, 214–221. doi: 10.1016/j.mimet.2014.08.023

Bentley, S. D., Chater, K. F., Cerdeño-Tárraga, A.-M., Challis, G. L., Thomson, N. R., James, K. D., et al. (2002). Complete genome sequence of the model actinomycete *Streptomyces coelicolor* A3(2). *Nature* 417, 141–147. doi: 10.1038/417141a

Bérdy, J. (2005). Bioactive microbial metabolites. *J. Antibiot.* 58, 1–26. doi: 10.1038/ja.2005.1

Bonnet, M., Lagier, J. C., Raoult, D., and Khelaifia, S. (2019). Bacterial culture through selective and non-selective conditions: the evolution of culture media in clinical microbiology. *New Microbes. New Infect.* 34:100622. doi: 10.1016/j.nmni.2019.100622

Boubetra, D., Bouras, N., Zitouni, A., Schumann, P., Spröer, C., Sabaou, N., et al. (2016). *Streptosporangium algeriense* sp. nov., an actinobacterium isolated from desert soil. *Int. J. Syst. Evol. Microbiol.* 66, 1034–1038. doi: 10.1099/ijsem.0.000829

Boubetra, D., Sabaou, N., Zitouni, A., Bijani, C., Lebrihi, A., and Mathieu, F. (2013a). Taxonomy and chemical characterization of new antibiotics produced by *Saccharothrix* SA198 isolated from a Saharan soil. *Microbiol. Res.* 168, 223–230. doi: 10.1016/j.micres.2012.11.005

Boubetra, D., Zitouni, A., Bouras, N., Mathieu, F., Lebrihi, A., Schumann, P., et al. (2013b). *Saccharothrix hoggarensis* sp. nov., an actinomycete isolated from Saharan soil. *Int. J. Syst. Evol. Microbiol.* 63, 549–553. doi: 10.1099/ijs.0.039099-0

Boubetra, D., Zitouni, A., Bouras, N., Schumann, P., Spröer, C., Klenk, H. P., et al. (2015). *Saccharothrix tamanrassetensis* sp. nov., an actinomycete isolated from Saharan soil. *Int. J. Syst. Evol. Microbiol.* 65, 1316–1320. doi: 10.1099/ijs.0.000104

Bouznada, K., Bouras, N., Mokrane, S., Chaabane Chaouch, F., Zitouni, A., Pötter, G., et al. (2016a). *Saccharothrix isguenensis* sp. nov., an actinobacterium isolated from desert soil. *Int. J. Syst. Evol. Microbiol.* 66, 4785–4790. doi: 10.1099/ijsem.0.001430

Bouznada, K., Bouras, N., Mokrane, S., Chaabane Chaouch, F., Zitouni, A., Pötter, G., et al. (2017). *Saccharothrix ghardaiensis* sp. nov., an actinobacterium isolated from Saharan soil. *Antonie van Leeuwenhoek.* 110, 399–405. doi: 10.1007/s10482-016-0812-4

Bouznada, K., Bouras, N., Schumann, P., Spröer, C., Sabaou, N., and Klenk, H. P. (2016b). *Actinophytocola algeriensis* sp. nov., an actinobacterium isolated from Saharan soil. *Int. J. Syst. Evol. Microbiol.* 66, 2760–2765. doi: 10.1099/ijsem.0.001136

Bredholdt, H., Galatenko, O. A., Engelhardt, K., Fjaervik, E., Terekhova, L. P., and Zotchev, S. B. (2007). Rare actinomycete bacteria from the shallow water sediments of the Trondheim fjord, Norway: isolation, diversity and biological activity. *Environ. Microbiol.* 9, 2756–2764. doi: 10.1111/j.1462-2920.2007.01387.x

Bull, A. T., Asenjo, J. A., Goodfellow, M., and Gómez-Silva, B. (2016). The Atacama Desert: technical resources and the growing importance of novel microbial diversity. *Annu. Rev. Microbiol.* 70, 215–234. doi: 10.1146/annurev-micro-102215-095236

Bull, A. T., and Goodfellow, M. (2019). Dark, rare and inspirational microbial matter in the extremobiosphere: 16 000 m of bioprospecting campaigns. *Microbiology.* 165, 1252–1264. doi: 10.1099/mic.0.000822

Burke, G. R., and Moran, N. A. (2011). Massive genomic decay in *Serratia symbiotica*, a recently evolved symbiont of aphids. *Genome Biol. Evol.* 3, 195–208. doi: 10.1093/gbe/evr002

Busarakam, K., Bull, A. T., Trujillo, M. E., Riesco, R., Sangal, V., van Wezel, G. P., et al. (2016b). *Modestobacter caceresii* sp. nov., novel actinobacteria with an insight into their adaptive mechanisms for survival in extreme hyper-arid Atacama Desert soils. *Syst. Appl. Microbiol.* 39, 243–251. doi: 10.1016/j.syapm.2016.03.007

Busarakam, K., Brown, R., Bull, A. T., Tan, G. Y., Zucchi, T. D., da Silva, L. J., et al. (2016a). Classification of thermophilic actinobacteria isolated from arid desert soils, including the description of *Amycolatopsis deserti* sp. nov. *Antonie van Leeuwenhoek.* 109, 319–334. doi: 10.1007/s10482-015-0635-8

Cao, C., Xu, T., Liu, J., Cai, X., Sun, Y., Qin, S., et al. (2018). *Actinomadura deserti* sp. nov., isolated from desert soil. *Int. J. Syst. Evol. Microbiol.* 68, 2930–2935. doi: 10.1099/ijsem.0.002922

Carro, L., Golinska, P., Nouioui, I., Bull, A. T., Igual, J. M., Andrews, B. A., et al. (2019b). *Micromonospora acroterricola* sp. nov., a novel actinobacterium isolated from a high altitude Atacama Desert soil. *Int. J. Syst. Evol. Microbiol.* 69, 3426–3436. doi: 10.1099/ijsem.0.003634

Carro, L., Castro, J. F., Razmilic, V., Nouioui, I., Pan, C., Igual, J. M., et al. (2019a). Uncovering the potential of novel micromonosporae isolated from an extreme hyper-arid Atacama Desert soil. *Sci. Rep.* 9:4678. doi: 10.1038/s41598-019-38789-z

Castro, J. F., Nouioui, I., Sangal, V., Choi, S., Yang, S. J., Kim, B. Y., et al. (2018a). *Blastococcus atacamensis* sp. nov., a novel strain adapted to life in the Yungay core region of the Atacama Desert. *Int. J. Syst. Evol. Microbiol.* 68, 2712–2721. doi: 10.1099/ijsem.0.002828

Castro, J. F., Nouioui, I., Sangal, V., Trujillo, M. E., Montero-Calasanz, M., Rahmani, T., et al. (2018b). *Geodermatophilus chilensis* sp. nov., from soil of the Yungay core-region of the Atacama Desert. *Chile. Syst. Appl. Microbiol.* 41, 427–436. doi: 10.1016/j.syapm.2018.03.005

Chan-Yeung, M., and Rui-Heng, X. (2003). SARS: epidemiology. *Respirology* 8, S9–S14. doi: 10.1046/j.1440-1843.2003.00518.x

Chaouch, C. F., Bouras, N., Mokrane, S., Zitouni, A., Schumann, P., Spröer, C., et al. (2016). *Streptosporangium becharense* sp. nov., an actinobacterium isolated from desert soil. *Int. J. Syst. Evol. Microbiol.* 66, 2484–2490. doi: 10.1099/ijsem.0.001077

Cheema, M. T., Ye, J. J., Li, F. N., Lu, Q. P., Abbas, M., Sajid, I., et al. (2020). *Auraticoccus cholistanensis* sp. nov., an actinomycete isolated from soil of the Cholistan Desert, and emended description of the genus Auraticoccus. *Int. J. Syst. Evol. Microbiol.* 70, 3179–3185. doi: 10.1099/ijsem.0.004152

Chen, C., Liu, J.-M., Jiang, Z.-K., Li, X.-J., Liu, S.-W., Tuo, L., et al. (2015). Endophytic actinomycetes from psammophytes of taklamakan desert against *Pseudomonas aeruginosa* and study on bioactive product of strain 38-7L-1. Chin. *J. Antibiot.* 40, 81–87 and115.

Choudhary, D. K., Kasotia, A., Jain, S., Vaishnav, A., Kumari, S., Sharma, K. P., et al. (2016). Bacterial-mediated tolerance and resistance to plants under abiotic and biotic stresses. *J. Plant. Growth. Regul.* 35, 276–300. doi: 10.1007/s00344-015-9521-x

Chun, J., Oren, A., Ventosa, A., Christensen, H., Arahal, D. R., da Costa, M. S., et al. (2018). Proposed minimal standards for the use of genome data for the taxonomy of prokaryotes. *Int. J. Syst. Evol. Microbiol.* 68, 461–466.

Cortés-Albayay, C., Dorador, C., Schumann, P., Schniete, J. K., Herron, P., Andrews, B., et al. (2019). *Streptomyces altiplanensis* sp. nov., an alkalitolerant species isolated from Chilean Altiplano soil, and emended description of *Streptomyces chryseus* (Krasil'nikov et al. 1965) Pridham 1970. *Int. J Syst. Evol. Microbiol.* 69, 2498–2505. doi: 10.1099/ijsem.0.003525

Duddington, C. L. (1955). Notes on the technique of handling predacious fungi. *Trans. Brit. Mycol. Soc.* 38, 97–103. doi: 10.1016/S0007-1536(55)80021-6

Eida, A. A., Bougouffa, S., Alam, I., Saad, M. M., and Hirt, H. (2020). Complete genome sequence of the endophytic bacterium *Cellulosimicrobium* sp. JZ28 isolated from the root endosphere of the perennial desert tussock grass *Panicum turgidum*. *Arch. Microbiol.* 202, 1563–1569. doi: 10.1007/s00203-020-01859-2

Ekblom, R., and Wolf, J. B. (2014). A field guide to whole-genome sequencing, assembly and annotation. *Evol. Appl.* 7, 1026–1042. doi: 10.1111/eva.12178

Elsayed, S. S., Trusch, F., Deng, H., Raab, A., Prokes, I., Busarakam, K., et al. (2015). Chaxapeptin, a lasso peptide from extremotolerant *Streptomyces leeuwenhoekii* strain C58 from the Hyperarid Atacama Desert. *J. Org. Chem.* 80, 10252–10260. doi: 10.1021/acs.joc.5b01878

Entis, P. (2002). *Food Microbiology: The Laboratory*. Washington DC: The Food Processor Institute.

Fang, B. Z., Salam, N., Han, M. X., Jiao, J. Y., Cheng, J., Wei, D. Q., et al. (2017). Insights on the effects of heat pretreatment, pH, and calcium salts on isolation of rare Actinobacteria from Karstic Caves. *Front. Microbiol.* 8:1535. doi: 10.3389/fmicb.2017.01535

Fiedler, H. P. (2004). "Screening for bioactivity," in *Microbial Diversity and Bioprospecting*, ed. A. T. Bull (Washington, DC: ASM), 324–335.

Fujimoto, S., Nakagami, Y., and Kojima, F. (2004). Optimal bacterial DNA isolation method using bead-beating technique. *Memoirs. Kyushu. Univ. Dep. Health Scis. Med. Sch.* 3, 33–38.

Gaete, A., Mandakovic, D., and González, M. (2020). Isolation and identification of soil bacteria from extreme environments of Chile and their plant beneficial characteristics. *Microorganisms* 8:8. doi: 10.3390/microorganisms8081213

Genilloud, O. (2017). Actinomycetes: still a source of novel antibiotics. *Nat. Prod. Rep.* 34, 1203–1232. doi: 10.1039/c7np00026j

Ghassemi, M. R., and Garzanti, E. (2019). Geology and geomorphology of Turkmenistan: a review. *Geopersia* 9, 125–140. doi: 10.22059/geope.2018.265613.648416

Golińska, P., Montero-Calasanz, M., Świecimska, M., Yaramis, A., Igual, J. M., Bull, A. T., et al. (2020a). *Modestobacter excelsi* sp. nov., a novel actinobacterium isolated from a high altitude Atacama Desert soil. *Syst. Appl. Microbiol.* 43, 126051. doi: 10.1016/j.syapm.2019.126051

Golińska, P., Świecimska, M., Montero-Calasanz, M., Yaramis, A., Igual, J. M., Bull, A. T., et al. (2020b). *Modestobacter altitudinis* sp. nov., a novel actinobacterium isolated from Atacama Desert soil. *Int. J. Syst. Evol. Microbiol.* 70, 3513–3527. doi: 10.1099/ijsem.0.004212

Gomez-Escribano, J. P., Castro, J. F., Razmilic, V., Jarmusch, S. A., Saalbach, G., Ebel, R., et al. (2019). Heterologous expression of a cryptic gene cluster from *Streptomyces leeuwenhoekii* C34T yields a novel lasso peptide, leepeptin. *Appl. Environ. Microbiol.* 85:23. doi: 10.1128/AEM.01752-19

Goodfellow, M. (1989). "Supregeneric classification of actinomycets," in *Bergey's Manual of Systematic Bacteriology*, ed. S. T. Williams (Baltimore, MD: Springer), 2333–2339.

Goodfellow, M. (2010). "Selective isolation of actinobacteria," in *Manual of Industrial Microbiology and Biotechnology*, eds R. H. Baltz, J. E. Davies, A. L. Demain, A. T. Bull, B. Junker, L. Katz, et al. (Washington, DC: ASM Press), 13–27.

Goodfellow, M., Busarakam, K., Idris, H., Labeda, D. P., Nouioui, I., Brown, R., et al. (2017). *Streptomyces asenjonii* sp. nov., isolated from hyper-arid Atacama Desert soils and emended description of Streptomyces viridosporus Pridham et al. 1958. *Antonie van Leeuwenhoek.* 110, 1133–1148. doi: 10.1007/s10482-017-0886-7

Goodfellow, M., and Fiedler, H. P. (2010). A guide to successful bioprospecting: informed by actinobacterial systematics. *Antonie van Leeuwenhoek* 98, 119–142. doi: 10.1007/s10482-010-9460-2

Goodfellow, M., Nouioui, I., Sanderson, R., Xie, F., and Bull, A. T. (2018). Rare taxa and dark microbial matter: novel bioactive actinobacteria abound in Atacama Desert soils. *Antonie van Leeuwenhoek* 111, 1315–1332. doi: 10.1007/s10482-018-1088-7

Goodfellow, M., Whitman, W., and Parte, A. (2012). "The Actinobacteria," in *Bergey's Manual of Systematic Bacteriology Part A and B*, 2nd Edn, eds M. Goodfellow, P. Kämpfer, H. J. Busse, M. E. Trujillo, K. Suzuki, W. Ludwig, et al. (New York, N: Springer).

Goris, J., Konstantinidis, K. T., Klappenbach, J. A., Coenye, T., Vandamme, P., and Tiedje, J. M. (2007). DNA-DNA hybridization values and their relationship to whole-genome sequence similarities. *Int. J. Syst. Evol. Microbiol.* 57, 81–91. doi: 10.1099/ijs.0.64483-0

Goswami, D., Pithwa, S., Dhandhukia, P., and Thakker, J. N. (2014). Delineating Kocuria turfanensis 2M4 as a credible PGPR: a novel IAA-producing bacteria isolated from saline desert. *J. Plant Interact.* 9, 566–576. doi: 10.1080/17429145.2013.871650

Goudjal, Y., Toumatia, O., Sabaou, N., Barakate, M., Mathieu, F., and Zitouni, A. (2013). Endophytic actinomycetes from spontaneous plants of Algerian Sahara: indole-3-acetic acid production and tomato plants growth promoting activity. *World J. Microbiol. Biotechnol.* 29, 1821–1829. doi: 10.1007/s11274-013-1344-y

Gran-Scheuch, A., Trajkovic, M., Parra, L., and Fraaije, M. W. (2018). Mining the Genome of *Streptomyces leeuwenhoekii*: two new type I baeyer-villiger Monooxygenases from Atacama Desert. *Front. Microbiol.* 9:1609. doi: 10.3389/fmicb.2018.01609

Guerrero, L. D., Makhalanyane, T. P., Aislabie, J. M., and Cowan, D. A. (2014). Draft genome sequence of Williamsia sp. strain D3, isolated from the Darwin Mountains. *Antarctica. Genome Announc.* 2, 1. doi: 10.1128/genomeA.01230-13

Guesmi, S., Nouioui, I., Pujic, P., Dubost, A., Najjari, A., Ghedira, K., et al. (2021). Draft genome sequence of *Promicromonospora panici* sp. nov., a novel ionizing-radiation-resistant actinobacterium isolated from roots of the desert plant *Panicum turgidum*. *Extremophiles* 25, 25–38. doi: 10.1007/s00792-020-01207-8

Habib, N., Khan, I. U., Chu, X., Xiao, M., Li, S., Fang, B. Z., et al. (2018). *Actinoplanes deserti* sp. nov., isolated from a desert soil sample. *Antonie van Leeuwenhoek* 111, 2303–2310. doi: 10.1007/s10482-018-1121-x

Han, L., Gao, C., Jiang, Y., Guan, P., Liu, J., Li, L., et al. (2014). Jiangrines A-F and jiangolide from an actinobacterium *Jiangella gansuensis*. *J. Nat. Prod.* 77, 2605–2610. doi: 10.1021/np500402a

Hayakawa, M. (2008). Studies on the isolation and distribution of rare actinomycetes in soil. *Actinomycetologica* 22, 12–19. doi: 10.3209/saj.SAJ220103

Hayashi Sant'Anna, F., Bach, E., Porto, R. Z., Guella, F., Hayashi Sant'Anna, E., and Passaglia, L. (2019). Genomic metrics made easy: what to do and where to go in the new era of bacterial taxonomy. *Crit. Rev. Microbiol.* 45, 182–200. doi: 10.1080/1040841X.2019.1569587

Hezbri, K., Ghodhbane-Gtari, F., Montero-Calasanz, M., Nouioui, I., Rohde, M., Spröer, C., et al. (2016). *Geodermatophilus pulveris* sp. nov., a gamma-radiation-resistant actinobacterium isolated from the Sahara desert. *Int. J. Syst. Evol Microbiol.* 66, 3828–3834. doi: 10.1099/ijsem.0.001272

Hezbri, K., Ghodhbane-Gtari, F., Montero-Calasanz, M., Sghaier, H., Rohde, M., Schumann, P., et al. (2015). *Geodermatophilus sabuli* sp. nov., a γ-radiation-resistant actinobacterium isolated from desert limestone. *Int. J. Syst. Evol Microbiol.* 65, 3365–3372. doi: 10.1099/ijsem.0.000422

Hong, K., Gao, A. H., Xie, Q. Y., Gao, H., Zhuang, L., Lin, H.-P., et al. (2009). Actinomycetes for marine drug discovery isolated from mangrove soils and plants in China. *Mar. Drugs.* 7, 24–44. doi: 10.3390/md7010024

Horikoshi, K., Antranikian, G., Bull, A. T., Robb, F. T., and Stetter, K. O. (2010). *Extremophiles Handbook*. Berlin: Springer Science & Business Media.

Hozzein, W. N., Ali, M. I., Hammouda, O., Mousa, A. S., and Goodfellow, M. (2011). *Streptomyces sannurensis* sp. nov., a new alkaliphilic member of the genus *Streptomyces* isolated from Wadi Sannur in Egypt. *Afri. J. Microbiol. Res.* 5, 1329–1334. doi: 10.5897/AJMR11.200

Hozzein, W. N., Ali, M. I. A., Hammouda, O., and Mousa, A. S. (2014). Characterization of a new alkaliphilic nocardiopsis strain from the desert of Egypt. *J. Pure Appl. Microbiol.* 8, 3285–3290.

Hozzein, W. N., Ali, M. I. A., and Rabie, W. (2008). A new preferential medium for enumeration and isolation of desert actinomycetes. *World. J. Microbiol. Biotechnol.* 24, 1547–1552. doi: 10.1007/s11274-007-9641-y

Hozzein, W. N., and Goodfellow, M. (2007). *Streptomyces synnematoformans* sp. nov., a novel actinomycete isolated from a sand dune soil in Egypt. *Int. J. Syst. Evol. Microbiol.* 57, 2009–2013. doi: 10.1099/ijs.0.65037-0

Hozzein, W. N., Li, W. J., Ali, M., Hammouda, O., Mousa, A. S., Xu, L. H., et al. (2004). *Nocardiopsis alkaliphila* sp. nov., a novel alkaliphilic actinomycete isolated from desert soil in Egypt. *Int. J. Syst. Evol. Microbiol.* 54, 247–252. doi: 10.1099/ijs.0.02832-0

Hozzein, W. N., Yang, Z. W., Alharbi, S. A., Alsakkaf, W., Asem, M. D., Xiao, M., et al. (2018). *Georgenia deserti* sp. nov., a halotolerant actinobacterium isolated from a desert sample. *Int. J. Syst. Evol. Microbiol.* 68, 1135–1139. doi: 10.1099/ijsem.0.002640

Hu, Q. W., Chu, X., Xiao, M., Li, C. T., Yan, Z. F., Hozzein, W. N., et al. (2016). *Arthrobacter deserti* sp. nov., isolated from a desert soil sample. *Int. J. Syst. Evol. Microbiol.* 66, 2035–2040. doi: 10.1099/ijsem.0.000986

Ibeyaima, A., Rana, J., Dwivedi, A., Gupta, S., Sharma, S. K., Saini, N., et al. (2016). Characterization of *Yuhushiella* sp TD-032 from the Thar Desert and its antimicrobial activity. *J. Adv. Pharm. Technol. Res.* 7, 32–36. doi: 10.4103/2231-4040.177201

Ibeyaima, A., Singh, A. K., Lal, R., Gupta, S., Goodfellow, M., and Sarethy, I. P. (2018). *Saccharothrix tharensis* sp. nov., an actinobacterium isolated from the Thar Desert. *India. Antonie van Leeuwenhoek.* 111, 2141–2147. doi: 10.1007/s10482-018-1106-9

Idris, H. (2016). *Actinobacterial Diversity in Atacama Desert Habitats as a road Map to Biodiscovery. dissertation*. Newcastle: Newcastle University.

Idris, H., Goodfellow, M., Sanderson, R., Asenjo, J. A., and Bull, A. T. (2017a). Actinobacterial rare biospheres and dark matter revealed in habitats of the Chilean Atacama Desert. *Sci. Rep.* 7, 1. doi: 10.1038/s41598-017-08937-4

Idris, H., Labeda, D. P., Nouioui, I., Castro, J. F., Del Carmen.Montero-Calasanz, M., Bull, A. T., et al. (2017b). *Streptomyces aridus* sp. nov., isolated from a high altitude Atacama Desert soil and emended description of Streptomyces noboritoensis Isono et al. 1957. *Antonie van Leeuwenhoek* 110, 705–717. doi: 10.1007/s10482-017-0838-2

Idris, H., Nouioui, I., Asenjo, J. A., Bull, A. T., and Goodfellow, M. (2017c). *Lentzea chajnantorensis* sp. nov., an actinobacterium from a very high altitude Cerro Chajnantor gravel soil in northern Chile. *Antonie van Leeuwenhoek* 110, 795–802. doi: 10.1007/s10482-017-0851-5

Idris, H., Nouioui, I., Pathom-Aree, W., Castro, J. F., Bull, A. T., Andrews, B. A., et al. (2018). *Amycolatopsis vastitatis* sp. nov., an isolate from a high altitude subsurface soil on Cerro Chajnantor, northern Chile. *Antonie van Leeuwenhoek* 111, 1523–1533. doi: 10.1007/s10482-018-1039-3

Ito, T., Sekizuka, T., Kishi, N., Yamashita, A., and Kuroda, M. (2019). Conventional culture methods with commercially available media unveil the presence of novel culturable bacteria. *Gut Microbes* 10, 77–91. doi: 10.1080/19490976.2018.1491265

Jensen, P. R. (2010). Linking species concepts to natural product discovery in the post-genomic era. *J. Ind. Microbiol. Biotechnol.* 37, 219–224. doi: 10.1007/s10295-009-0683-z

Jensen, P. R., Moore, B. S., and Fenical, W. (2015). The marine actinomycete genus *Salinispora*: a model organism for secondary metabolite discovery. *Nat. Prod. Rep.* 32, 738–751. doi: 10.1039/c4np00167b

Jiao, J. Y., Carro, L., Liu, L., Gao, X. Y., Zhang, X. T., Hozzein, W. N., et al. (2017). Complete genome sequence of Jiangella gansuensis strain YIM 002T (DSM 44835T), the type species of the genus Jiangella and source of new antibiotic compounds. *Stand. Genomic. Sci.* 12:21. doi: 10.1186/s40793-017-0226-6

Jose, P. A., Maharshi, A., and Jha, B. (2021). Actinobacteria in natural products research: progress and prospects. *Microbiol. Res.* 246:126708. doi: 10.1016/j.micres.2021.126708

Kamjam, M., Sivalingam, P., Deng, Z., and Hong, K. (2017). Deep sea actinomycetes and their secondary metabolites. *Front. Microbiol.* 8:760. doi: 10.3389/fmicb.2017.00760

Kao, C. M., Chai, C. T., Liu, J. K., Yeh, T. Y., Chen, K. F., and Chen, S. C. (2004). Evaluation of natural and enhanced PCP biodegradation at a former pesticide manufacturing plant. *Water Res.* 38, 663–672. doi: 10.1016/j.watres.2003.10.030

Katz, L., and Baltz, R. H. (2016). Natural product discovery: past, present, and future. *J. Ind. Microbiol. Biotechnol.* 43, 155–176. doi: 10.1007/s10295-015-1723-5

Khan, I. U., Hussain, F., Habib, N., Xiao, M., Ahmed, I., Amin, A., et al. (2017). *Nocardioides thalensis* sp. nov., isolated from a desert. *Int. J. Syst. Evol. Microbiol.* 67, 2848–2852. doi: 10.1099/ijsem.0.002032

Khessairi, A., Fhoula, I., Jaouani, A., Turki, Y., Cherif, A., Boudabous, A., et al. (2014). Pentachlorophenol degradation by Janibacter sp., a new actinobacterium isolated from saline sediment of arid land. *Biomed. Res. Int.* 2014, 296472. doi: 10.1155/2014/296472

Kim, M., Oh, H. S., Park, S. C., and Chun, J. (2014). Towards a taxonomic coherence between average nucleotide identity and 16S rRNA gene sequence similarity for species demarcation of prokaryotes. *Int. J. Syst. Evol. Microbiol.* 64, 346–351. doi: 10.1099/ijs.0.059774-0

Köberl, M., Müller, H., Ramadan, E. M., and Berg, G. (2011). Desert farming benefits from microbial potential in arid soils and promotes diversity and plant health. *PLoS One* 6:9. doi: 10.1371/journal.pone.0024452

Köberl, M., White, R. A. III, Erschen, S., El-Arabi, T. F., Jansson, J. K., and Berg, G. (2015). Draft genome sequence of *Streptomyces* sp. strain Wb2n-11, a desert isolate with broad-spectrum antagonism against soilborne phytopathogens. *Genome Announc.* 3:4. doi: 10.1128/genomeA.00860-15

Krug, D., and Müller, R. (2014). Secondary metabolomics: the impact of mass spectrometry-based approaches on the discovery and characterization of microbial natural products. *Nat. Prod. Rep.* 31, 768–783. doi: 10.1039/c3np70127a

Lamari, L., Zitouni, A., Boudjella, H., Badji, B., Sabaou, N., Lebrihi, A., et al. (2002). New dithiolopyrrolone antibiotics from *Saccharothrix* sp. SA 233. I. taxonomy, fermentation, isolation and biological activities. *J. Antibiot.* 55, 696–701. doi: 10.7164/antibiotics.55.696

Law, J. W., Pusparajah, P., Mutalib, N. A., Wong, S., Goh, B., and Lee, L. (2019). A review on mangrove actinobacterial diversity: the roles of Streptomyces and novel species discovery. *Prog. Microbes Mol. Biol.* 2:1. doi: 10.36877/pmmb.a0000024

Law, J. W. F., Letchumanan, V., Tan, L. T. H., Ser, H. L., Goh, B. H., and Lee, L. H. (2020). The rising of "modern actinobacteria" era. *Prog. Microbes Mol. Biol.* 3, 1. doi: 10.36877/pmmb.a0000064

Lee, L. H., Zainal, N., Azman, A. S., Eng, S. K., Goh, B. H., Yin, W. F., et al. (2014). Diversity and antimicrobial activities of actinobacteria isolated from tropical mangrove sediments in Malaysia. *Sci. World J.* 2014:698178. doi: 10.1155/2014/698178

Li, F. N., Liao, S. L., Liu, S. W., Jin, T., and Sun, C. H. (2019a). *Aeromicrobium endophyticum* sp. nov., an endophytic actinobacterium isolated from reed (*Phragmites australis*). *J. Microbiol.* 57, 725–731. doi: 10.1007/s12275-019-8705-7

Li, L. Y., Yang, Z. W., Asem, M. D., Fang, B. Z., Salam, N., Alkhalifah, D., et al. (2019c). *Streptomyces desertarenae* sp. nov., a novel actinobacterium isolated from a desert sample. *Antonie van Leeuwenhoek.* 112, 367–374. doi: 10.1007/s10482-018-1163-0

Li, L. Y., Yang, Z. W., Asem, M. D., Salam, N., Xiao, M., Alkhalifah, D., et al. (2019d). *Georgenia alba* sp. nov., a novel halotolerant actinobacterium isolated from a desert sand sample. *Antonie van Leeuwenhoek* 112, 203–209. doi: 10.1007/s10482-018-1145-2

Li, F. N., Lu, Q., Liao, S. L., Jin, T., Li, W., and Sun, C. H. (2019b). *Labedella phragmitis* sp. nov. and *Labedella populi* sp. nov., two endophytic actinobacteria isolated from plants in the Taklamakan Desert and emended description of the genus *Labedella*. *Syst. Appl. Microbiol.* 42:126004. doi: 10.1016/j.syapm.2019.126004

Li, J., Chen, C., Zhao, G. Z., Klenk, H. P., Pukall, R., Zhang, Y. Q., et al. (2009). Description of *Dietzia lutea* sp. nov., isolated from a desert soil in Egypt. *Syst. Appl. Microbiol.* 32, 118–123. doi: 10.1016/j.syapm.2008.11.007

Li, S., Dong, L., Lian, W. H., Lin, Z. L., Lu, C. Y., Xu, L., et al. (2021). Exploring untapped potential of *Streptomyces* spp. in Gurbantunggut Desert by use of highly selective culture strategy. *Sci. Total Environ.* 790:148235.

Li, W. J., Chen, H. H., Zhang, Y. Q., Kim, C. J., Park, D. J., Lee, J. C., et al. (2005). *Citricoccus alkalitolerans* sp. nov., a novel actinobacterium isolated from a desert soil in Egypt. *Int. J. Syst. Evol. Microbiol.* 55, 87–90. doi: 10.1099/ijs.0.63237-0

Li, W. J., Zhang, Y. Q., Schumann, P., Chen, H. H., Hozzein, W. N., Tian, X. P., et al. (2006). *Kocuria aegyptia* sp. nov., a novel actinobacterium isolated from a saline, alkaline desert soil in Egypt. *Int. J. Syst. Evol. Microbiol.* 56, 733–737. doi: 10.1099/ijs.0.63876-0

Li, Y., Li, Y., Wang, L. W., and Bao, J. (2018). *Streptomyces dengpaensis* sp. nov., an actinomycete isolated from desert soil. *Int. J. Syst. Evol. Microbiol.* 68, 3322–3326. doi: 10.1099/ijsem.0.002994

Li, Y. R., Zhu, Z. N., Li, Y. Q., Xiao, M., Han, M. X., Wadaan, M., et al. (2018). *Microbacterium halophytorum* sp. nov., a novel endophytic actinobacterium isolated from halophytes. *Int. J. Syst. Evol. Microbiol.* 68, 3928–3934. doi: 10.1099/ijsem.0.003092

Liu, J., Sun, Y., Liu, J., Wu, Y., Cao, C., Li, R., et al. (2020). *Saccharothrix deserti* sp. nov., an actinomycete isolated from desert soil. *Int. J. Syst. Evol. Microbiol.* 70, 1882–1887. doi: 10.1099/ijsem.0.003989

Liu, J. M., Habden, X., Guo, L., Tuo, L., Jiang, Z. K., Liu, S. W., et al. (2015a). *Prauserella endophytica* sp. nov., an endophytic actinobacterium isolated from *Tamarix taklamakanensis*. *Antonie van Leeuwenhoek* 107, 1401–1409. doi: 10.1007/s10482-015-0435-1

Liu, J. M., Tuo, L., Habden, X., Guo, L., Jiang, Z. K., Liu, X. F., et al. (2015b). *Nesterenkonia populi* sp. nov., an actinobacterium isolated from *Populus euphratica*. *Int. J. Syst. Evol. Microbiol.* 65, 1474–1479. doi: 10.1099/ijs.0.000123

Liu, M., Peng, F., Wang, Y., Zhang, K., Chen, G., and Fang, C. (2009). *Kineococcus xinjiangensis* sp. nov., isolated from desert sand. *Int. J. Syst. Evol. Microbiol.* 59, 1090–1093. doi: 10.1099/ijs.0.004168-0

Liu, M., Zhang, L., Ren, B., Yang, N., Yu, X., Wang, J., et al. (2014). *Prauserella shujinwangii* sp. nov., from a desert environment. *Int. J. Syst. Evol. Microbiol.* 64, 3833–3837. doi: 10.1099/ijs.0.065425-0

Liu, S. W., Ye, J. J., Lu, Q. P., Cheema, M. T., Abbas, M., Huang, D. L., et al. (2020c). *Motilibacter deserti* sp. nov. and *Motilibacter aurantiacus* sp. nov., two novel actinobacteria isolated from soil of Cholistan Desert and emended description of the genus *Motilibacter*. *Syst. Appl. Microbiol.* 43, 126150. doi: 10.1016/j.syapm.2020.126150

Liu, S. W., Li, F. N., Liu, H. Y., Yu, L. Y., and Sun, C. H. (2020a). *Desertihabitans brevis* sp. nov., an actinobacterium isolated from sand of the Taklamakan desert, and emended description of the genus *Desertihabitans*. *Int. J. Syst. Evol. Microbiol.* 70, 1166–1171. doi: 10.1099/ijsem.0.003896

Liu, S. W., Li, F. N., Zheng, H. Y., Qi, X., Huang, D. L., Xie, Y. Y., et al. (2019b). *Planctomonas deserti* gen. nov., sp. nov., a new member of the family Microbacteriaceae isolated from soil of the Taklamakan desert. *Int. J. Syst. Evol. Microbiol.* 69, 616–624. doi: 10.1099/ijsem.0.003095

Liu, S. W., Li, F. N., Qi, X., Xie, Y. Y., and Sun, C. H. (2019a). *Nakamurella deserti* sp. nov., isolated from rhizosphere soil of Reaumuria in the Taklamakan desert. *Int. J. Syst. Evol. Microbiol.* 69, 214–219. doi: 10.1099/ijsem.0.003132

Liu, S. W., Xue, C. M., Li, F. N., and Sun, C. H. (2020b). *Nocardioides vastitatis* sp. nov., isolated from Taklamakan desert soil. *Int. J. Syst. Evol. Microbiol.* 70, 77–82. doi: 10.1099/ijsem.0.003718

Luo, X., Wang, J., Zeng, X. C., Wang, Y., Zhou, L., Nie, Y., et al. (2012). *Mycetocola manganoxydans* sp. nov., an actinobacterium isolated from the Taklamakan desert. *Int. J. Syst. Evol. Microbiol.* 62, 2967–2970. doi: 10.1099/ijs.0.038877-0

Macagnan, D., Romeiro, R. D. S., de Souza, J. T., and Pomella, A. W. V. (2006). Isolation of actinomycetes and endospore-forming bacteria from the cacao pod surface and their antagonistic activity against the witches' broom and black pod pathogens. *Phytoparasitica* 34, 122–132. doi: 10.1007/BF02981312

Mandelli, F., Miranda, V. S., Rodrigues, E., and Mercadante, A. Z. (2012). Identification of carotenoids with high antioxidant capacity produced by extremophile microorganisms. *World J. Microbiol. Biotechnol.* 28, 1781–1790. doi: 10.1007/s11274-011-0993-y

Mao, J., Wang, J., Dai, H. Q., Zhang, Z. D., Tang, Q. Y., Ren, B., et al. (2011). *Yuhushiella deserti* gen. nov., sp. nov., a new member of the suborder *Pseudonocardineae*. *Int. J. Syst. Evol. Microbiol.* 61, 621–630. doi: 10.1099/ijs.0.019588-0

Martiny, A. C. (2019). High proportions of bacteria are culturable across major biomes. *ISME. J.* 13, 2125–2128. doi: 10.1038/s41396-019-0410-3

Masand, M., Sivakala, K. K., Menghani, E., Thinesh, T., Anandham, R., Sharma, G., et al. (2018). Biosynthetic potential of bioactive *Streptomycetes* isolated from arid region of the Thar Desert, Rajasthan (India). *Front. Microbiol.* 9, 687–698. doi: 10.3389/fmicb.2018.00687

Mayilraj, S., Suresh, K., Kroppenstedt, R. M., and Saini, H. S. (2006d). *Dietzia kunjamensis* sp. nov., isolated from the Indian Himalayas. *Int. J. Syst. Evol. Microbiol.* 56, 1667–1671. doi: 10.1099/ijs.0.64212-0

Mayilraj, S., Krishnamurthi, S., Saha, P., and Saini, H. S. (2006a). *Rhodococcus kroppenstedtii* sp. nov., a novel actinobacterium isolated from a cold desert of the Himalayas, India. *Int. J. Syst. Evol. Microbiol.* 56, 979–982. doi: 10.1099/ijs.0.63831-0

Mayilraj, S., Suresh, K., Schumann, P., Kroppenstedt, R. M., and Saini, H. S. (2006e). *Agrococcus lahaulensis* sp. nov., isolated from a cold desert of the Indian Himalayas. *Int. J. Syst. Evol. Microbiol.* 56, 1807–1810. doi: 10.1099/ijs.0.64247-0

Mayilraj, S., Kroppenstedt, R. M., Suresh, K., and Saini, H. S. (2006b). *Kocuria himachalensis* sp. nov., an actinobacterium isolated from the Indian Himalayas. *Int. J. Syst. Evol. Microbiol.* 56, 1971–1975. doi: 10.1099/ijs.0.63915-0

Mayilraj, S., Saha, P., Suresh, K., and Saini, H. S. (2006c). *Ornithinimicrobium kibberense* sp. nov., isolated from the Indian Himalayas. *Int. J. Syst. Evol. Microbiol.* 56, 1657–1661. doi: 10.1099/ijs.0.64138-0

Medema, M. H. (2021). The year 2020 in natural product bioinformatics: an overview of the latest tools and databases. *Nat. Prod. Rep.* 38, 301–306. doi: 10.1039/d0np00090f

Medina, M. J., Legido-Quigley, H., and Hsu, L. Y. (2020). "Antimicrobial resistance in one health," in *Global Health Security. Advanced Sciences and Technologies for Security Applications*, eds A. Masys, R. Izurieta, and M. Reina Ortiz (Cham: Springer), 209–229.

Meier-Kolthoff, J. P., Auch, A. F., Klenk, H. P., and Göker, M. (2013). Genome sequence-based species delimitation with confidence intervals and improved distance functions. *BMC Bioinform.* 14:60. doi: 10.1186/1471-2105-14-60

Meklat, A., Bouras, N., Zitouni, A., Mathieu, F., Lebrihi, A., Schumann, P., et al. (2013). *Actinopolyspora mzabensis* sp. nov., a halophilic actinomycete isolated from an Algerian Saharan soil. *Int. J. Syst. Evol. Microbiol.* 63, 3787–3792. doi: 10.1099/ijs.0.046649-0

Merrouche, R., Bouras, N., Coppel, Y., Mathieu, F., Sabaou, N., and Lebrihi, A. (2011). A New dithiolopyrrolone antibiotics induced by adding sorbic acid to the culture medium of *Saccharothrix algeriensis* NRRL B-24137. *FEMS Microbiol. Lett.* 318, 41–46. doi: 10.1111/j.15746968.2011.02246.x

Merrouche, R., Yekkour, A., Coppel, Y., Bouras, N., Zitouni, A., Lebrihi, A., et al. (2019). A new dithiolopyrrolone antibiotic triggered by a long fermentation of

Saccharothrix algeriensis NRRL B-24137 in sorbic acid-amended medium. *Lett. Appl. Microbiol.* 69, 294–301. doi: 10.1111/lam.13207

Mevs, U., Stackebrandt, E., Schumann, P., Gallikowski, C. A., and Hirsch, P. (2000). *Modestobacter multiseptatus* gen. nov., sp. nov., a budding actinomycete from soils of the Asgard Range (Transantarctic Mountains). *Int. J. Syst. Evol. Microbiol.* 50, 337–346. doi: 10.1099/00207713-50-1-337

Micallef, M. L., D'Agostino, P. M., Sharma, D., Viswanathan, R., and Moffitt, M. C. (2015). Genome mining for natural product biosynthetic gene clusters in the Subsection V cyanobacteria. *BMC Genom.* 16:1. doi: 10.1186/s12864-015-1855-z

Mikulak-Klucznik, B., Gołębiowska, P., Bayly, A. A., Popik, O., Klucznik, T., Szymkuæ, S., et al. (2020). Computational planning of the synthesis of complex natural products. *Nature* 588, 83–88. doi: 10.1038/s41586-020-2855-y

Montero-Calasanz, M. C., Göker, M., Pötter, G., Rohde, M., Spröer, C., Schumann, P., et al. (2012). *Geodermatophilus arenarius* sp. nov., a xerophilic actinomycete isolated from Saharan desert sand in Chad. *Extremophiles* 16, 903–909. doi: 10.1007/s00792-012-0486-4

Montero-Calasanz, M. C., Göker, M., Pötter, G., Rohde, M., Spröer, C., Schumann, P., et al. (2013b). *Geodermatophilus africanus* sp. nov., a halotolerant actinomycete isolated from Saharan desert sand. *Antonie van Leeuwenhoek* 104, 207–216. doi: 10.1007/s10482-013-9939-8

Montero-Calasanz, M. C., Göker, M., Pötter, G., Rohde, M., Spröer, C., Schumann, P., et al. (2013c). *Geodermatophilus saharensis* sp. nov., isolated from sand of the Saharan desert in Chad. *Arch. Microbiol.* 195, 153–159. doi: 10.1007/s00203-012-0860-8

Montero-Calasanz, M. C., Göker, M., Rohde, M., Schumann, P., Pötter, G., Spröer, C., et al. (2013e). *Geodermatophilus siccatus* sp. nov., isolated from arid sand of the Saharan desert in Chad. *Antonie van Leeuwenhoek.* 103, 449–456. doi: 10.1007/s10482-012-9824-x

Montero-Calasanz, M. C., Göker, M., Pötter, G., Rohde, M., Spröer, C., Schumann, P., et al. (2013d). *Geodermatophilus telluris* sp. nov., an actinomycete isolated from Saharan desert sand. *Int. J. Syst. Evol. Microbiol.* 63, 2254–2259. doi: 10.1099/ijs.0.046888-0

Montero-Calasanz, M. C., Göker, M., Broughton, W. J., Cattaneo, A., Favet, J., Pötter, G., et al. (2013a). *Geodermatophilus tzadiensis* sp. nov., a UV radiation-resistant bacterium isolated from sand of the Saharan desert. *Syst. Appl. Microbiol.* 36, 177–182. doi: 10.1016/j.syapm.2012.12.005

Morton, S. R., Smith, D. S., Dickman, C. R., Dunkerley, D. L., Friedel, M. H., McAllister, R. R. J., et al. (2011). A fresh framework for the ecology of arid Australia. *J. Arid Environ.* 75, 313–329. doi: 10.1016/j.jaridenv.2010.11.001

Nachtigall, J., Kulik, A., Helaly, S., Bull, A. T., Goodfellow, M., Asenjo, J. A., et al. (2011). Atacamycins A-C, 22-membered antitumor macrolactones produced by *Streptomyces* sp. *C38. J. Antibiot.* 64, 775–780. doi: 10.1038/ja.2011.96

Nafis, A., Raklami, A., Bechtaoui, N., El Khalloufi, F., El Alaoui, A., Glick, B. R., et al. (2019). Actinobacteria from extreme niches in morocco and their plant growth-promoting potentials. *Diversity* 11, 139–154. doi: 10.3390/d11080139

Neilson, J. W., Quade, J., Ortiz, M., Nelson, W. M., Legatzki, A., Tian, F., et al. (2012). Life at the hyperarid margin: novel bacterial diversity in arid soils of the Atacama Desert. *Chile. Extremophiles.* 16, 553–566. doi: 10.1007/s00792-012-0454-z

Nguyen, H. T., Pokhrel, A. R., Nguyen, C. T., Pham, V., Dhakal, D., Lim, H. N., et al. (2020). *Streptomyces* sp. VN1, a producer of diverse metabolites including non-natural furan-type anticancer compound. *Sci. Rep.* 10:1756. doi: 10.1038/s41598-020-58623-1

Nithya, K., Muthukumar, C., Biswas, B., Alharbi, N. S., Kadaikunnan, S., Khaled, J. M., et al. (2018). Desert actinobacteria as a source of bioactive compounds production with a special emphases on Pyridine-2,5-diacetamide a new pyridine alkaloid produced by Streptomyces sp. *DA3-7. Microbiol. Res.* 207, 116–133. doi: 10.1016/j.micres.2017.11.012

Nithya, K., Muthukumar, C., Kadaikunnan, S., Alharbi, N. S., Khaled, J. M., and Dhanasekaran, D. (2017). Purification, characterization, and statistical optimization of a thermostable α-amylase from desert actinobacterium *Streptomyces fragilis* DA7-7. *3 Biotech* 7, 350. doi: 10.1007/s13205-017-0981-5

Nouioui, I., Cortés-Albayay, C., Carro, L., Castro, J. F., Gtari, M., Ghodhbane-Gtari, F., et al. (2019). Genomic insights into plant-growth-promoting potentialities of the genus Frankia. *Front. Microbiol.* 10:1457. doi: 10.3389/fmicb.2019.01457

Okoro, C. K., Brown, R., Jones, A. L., Andrews, B. A., Asenjo, J. A., Goodfellow, M., et al. (2009). Diversity of culturable actinomycetes in hyper-arid soils of the Atacama Desert, Chile. *Antonie van Leeuwenhoek* 95, 121–133. doi: 10.1007/s10482-008-9295-2

Okoro, C. K., Bull, A. T., Mutreja, A., Rong, X., Huang, Y., and Goodfellow, M. (2010). *Lechevalieria atacamensis* sp. nov., *Lechevalieria deserti* sp. nov. and *Lechevalieria roselyniae* sp. nov., isolated from hyperarid soils. *Int. J. Syst. Evol. Microbiol.* 60, 296–300. doi: 10.1099/ijs.0.009985-0

Qin, S., Li, J., Chen, H. H., Zhao, G. Z., Zhu, W. Y., Jiang, C. L., et al. (2009). Isolation, diversity, and antimicrobial activity of rare actinobacteria from medicinal plants of tropical rain forests in *Xishuangbanna*, China. *Appl. Environ. Microbiol.* 75, 6176–6186. doi: 10.1128/AEM.01034-09

Radhakrishnan, M., Gopikrishnan, V., Vijayalakshmi, G., and Kumar, V. (2016). *In vitro* antioxidant activity and antimicrobial activity against biofilm forming bacteria by the pigment from Desert soil *Streptomyces* sp D25.J. *Appl. Pharm. Sci.* 6, 148–150. doi: 10.7324/JAPS.2016.60626

Ramirez-Rodriguez, L., Stepanian-Martinez, B., Morales-Gonzalez, M., and Diaz, L. (2018). Optimization of the cytotoxic activity of three *Streptomyces* strains isolated from guaviare river sediments (Colombia, South America). *Biomed. Res. Int.* 2018:2839356. doi: 10.1155/2018/2839356

Rangseekaew, P., and Pathom-aree, W. (2019). Cave actinobacteria as producers of bioactive metabolites. *Front. Microbiol.* 10:387. doi: 10.3389/fmicb.2019.00387

Rateb, M. E., Ebel, R., and Jaspars, M. (2018). Natural product diversity of actinobacteria in the Atacama Desert. *Antonie van Leeuwenhoek* 111, 1467–1477. doi: 10.1007/s10482-018-1030-z

Rateb, M. E., Houssen, W. E., Arnold, M., Abdelrahman, M. H., Deng, H., Harrison, W. T., et al. (2011a). Chaxamycins A-D, bioactive ansamycins from a hyper-arid desert Streptomyces sp. *J. Nat. Prod.* 74, 1491–1499. doi: 10.1021/np200320u

Rateb, M. E., Houssen, W. E., Harrison, W. T., Deng, H., Okoro, C. K., Asenjo, J. A., et al. (2011b). Diverse metabolic profiles of a Streptomyces strain isolated from a hyper-arid environment. *J. Nat. Prod.* 74, 1965–1971. doi: 10.1021/np200470u

Richter, M., and Rosselló-Móra, R. (2009). Shifting the genomic gold standard for the prokaryotic species definition. *Proc. Natl. Acad. Sci. U.S.A.* 106, 19126–19131. doi: 10.1073/pnas.0906412106

Ríos-Castillo, A. G., Ripolles-Avila, C., and Rodríguez-Jerez, J. J. (2020). Detection of *Salmonella* Typhimurium and *Listeria monocytogenes* biofilm cells exposed to different drying and pre-enrichment times using conventional and rapid methods. *Int. J. Food. Microbiol.* 324:108611. doi: 10.1016/j.ijfoodmicro.2020.108611

Rittner, M., Vermeesch, P., Carter, A., Bird, A., Stevens, T., Garzanti, E., et al. (2016). The provenance of Taklamakan desert sand. *Earth Planet. Sci. Lett.* 437, 127–137. doi: 10.1016/j.epsl.2015.12.036

Sagova-Mareckova, M., Cermak, L., Novotna, J., Plhackova, K., Forstova, J., and Kopecky, J. (2008). Innovative methods for soil DNA purification tested in soils with widely differing characteristics. *Appl. Environ. Microbiol.* 74, 2902–2907. doi: 10.1128/AEM.02161-07

Sai, K., Kang, K. S., Hirose, A., Hasegawa, R., Trosko, J. E., and Inoue, T. (2001). Inhibition of apoptosis by pentachlorophenol in v-myc-transfected rat liver epithelial cells: relation to down-regulation of gap junctional intercellular communication. *Cancer Lett.* 173, 163–174. doi: 10.1016/s0304-3835(01)00616-4

Saker, R., Bouras, N., Meklat, A., Zitouni, A., Schumann, P., Spröer, C., et al. (2015). Prauserella isguenensis sp. nov., a halophilic actinomycete isolated from desert soil. *Int. J. Syst. Evol. Microbiol.* 65, 1598–1603. doi: 10.1099/ijs.0.000145

Salam, N., Xian, W. D., Asem, M. D., Xiao, M., and Li, W. J. (2021). From ecophysiology to cultivation methodology: filling the knowledge gap between uncultured and cultured microbes. *Mar. Life Sci. Technol.* 3, 132–147. doi: 10.1007/s42995-020-00064-w

Sangal, V., Goodfellow, M., Blom, J., Tan, G., Klenk, H. P., and Sutcliffe, I. C. (2018). Revisiting the taxonomic status of the biomedically and industrially important genus *Amycolatopsis*, using a phylogenomic approach. *Front. Microbiol.* 9:2281. doi: 10.3389/fmicb.2018.02281

Santhanam, R., Okoro, C. K., Rong, X., Huang, Y., Bull, A. T., Weon, H. Y., et al. (2012b). *Streptomyces atacamensis* sp. nov., isolated from an extreme hyper-arid soil of the Atacama Desert. *Chile. Int. J Syst. Evol. Microbiol.* 62, 2680–2684. doi: 10.1099/ijs.0.038463-0

Santhanam, R., Okoro, C. K., Rong, X., Huang, Y., Bull, A. T., Andrews, B. A., et al. (2012a). *Streptomyces deserti* sp. nov., isolated from hyper-arid Atacama Desert soil. *Antonie van Leeuwenhoek.* 101, 575–581. doi: 10.1007/s10482-011-9672-0

Santhanam, R., Rong, X., Huang, Y., Andrews, B. A., Asenjo, J. A., and Goodfellow, M. (2013). *Streptomyces bullii* sp. nov., isolated from a hyper-arid Atacama

Desert soil. *Antonie van Leeuwenhoek.* 103, 367–373. doi: 10.1007/s10482-012-9816-x

Sayed, A., Hassan, M., Alhadrami, H., Hassan, H., Goodfellow, M., and Rateb, M. (2020). Extreme environments: microbiology leading to specialized metabolites. *J. Appl. Microbiol.* 128, 630–657. doi: 10.1111/jam.14386

Saygin, H., Ay, H., Guven, K., and Sahin, N. (2019b). *Kribbella turkmenica* sp. nov., isolated from the Karakum Desert. *Int. J. Syst. Evol. Microbiol.* 69, 2533–2540. doi: 10.1099/ijsem.0.003538

Saygin, H., Ay, H., Guven, K., Cetin, D., and Sahin, N. (2019a). *Desertiactinospora gelatinilytica* gen. nov., sp. nov., a new member of the family *Streptosporangiaceae* isolated from the Karakum Desert. *Antonie van Leeuwenhoek* 112, 409–423. doi: 10.1007/s10482-018-1169-7

Saygin, H., Ay, H., Guven, K., Cetin, D., and Sahin, N. (2020a). *Micromonospora deserti* sp. nov., isolated from the Karakum Desert. *Int. J. Syst. Evol. Microbiol.* 70, 282–291. doi: 10.1099/ijsem.0.003752

Saygin, H., Ay, H., Guven, K., Cetin, D., and Sahin, N. (2020c). *Streptomyces cahuitamycinicus* sp. nov., isolated from desert soil and reclassification of *Streptomyces galilaeus* as a later heterotypic synonym of Streptomyces bobili. *Int. J. Syst. Evol. Microbiol.* 70, 2750–2759. doi: 10.1099/ijsem.0.004103

Saygin, H., Ay, H., Guven, K., and Sahin, N. (2020b). Genome-based classification of three novel actinobacteria from the Karakum Desert: *Jiangella asiatica* sp. nov., *Jiangella aurantiaca* sp. nov. and *Jiangella ureilytica* sp. nov. *Int. J. Syst. Evol. Microbiol.* 70, 1993–2002. doi: 10.1099/ijsem.0.004011

Saygin, H., Nouioui, I., Ay, H., Guven, K., Cetin, D., Klenk, H. P., et al. (2020d). Polyphasic classification of Nonomuraea strains isolated from the Karakum Desert and description of *Nonomuraea deserti* sp. nov., *Nonomuraea diastatica* sp. nov., *Nonomuraea longispora* sp. nov. and *Nonomuraea mesophila* sp. nov. *Int. J. Syst. Evol. Microbiol.* 70, 636–647. doi: 10.1099/ijsem.0.003808

Schulz, D., Beese, P., Ohlendorf, B., Erhard, A., Zinecker, H., Dorador, C., et al. (2011). Abenquines A-D: aminoquinone derivatives produced by *Streptomyces* sp. strain DB634. *J. Antibiot.* 64, 763–768. doi: 10.1038/ja.2011.87

Schuster, M., Duringer, P., Ghienne, J. F., Vignaud, P., Mackaye, H. T., Likius, A., et al. (2006). The age of the Sahara desert. *Science* 311, 821–821. doi: 10.1126/science.1120161

Selim, M., Abdelhamid, S. A., and Mohamed, S. S. (2021). Secondary metabolites and biodiversity of actinomycetes. *J. Genet. Eng. Biotechnol.* 19:1. doi: 10.1186/s43141-021-00156-9

Selim, S., Hassan, Y. M., Saleh, A. M., Habeeb, T. H., and AbdElgawad, H. (2019). Actinobacterium isolated from a semi-arid environment improves the drought tolerance in maize (*Zea mays* L.). *Plant Physiol. Biochem.* 142, 15–21. doi: 10.1016/j.plaphy.2019.06.029

Ser, H.-L., Law, J. W.-F., Tan, W.-S., Yin, W.-F., and Chan, K.-G. (2020). Whole genome sequence of *Streptomyces colonosanans* strain MUSC 93JT isolated from mangrove forest in Malaysia. *Prog. Microbes Mol. Biol.* 3:1. doi: 10.36877/pmmb.a0000061

Shen, D. S., Liu, X. W., and Feng, H. J. (2005). Effect of easily degradable substrate on anaerobic degradation of pentachlorophenol in an upflow anaerobic sludge blanket (UASB) reactor. *J. Hazard Mater.* 119, 239–243. doi: 10.1016/j.jhazmat.2004.12.024

Shi, W., Sun, Q., Fan, G., Hideaki, S., Moriya, O., Itoh, T., et al. (2021). gcType: a high-quality type strain genome database for microbial phylogenetic and functional research. *Nucleic Acids Res.* 49, D694–D705. doi: 10.1093/nar/gkaa957

Shi, Y. L., Sun, Y., Ruan, Z. Y., Su, J., Yu, L. Y., and Zhang, Y. Q. (2020). *Cellulomonas telluris* sp. nov., an endoglucanase-producing actinobacterium isolated from Badain Jaran desert sand. *Int. J. Syst. Evol. Microbiol.* 70, 631–635. doi: 10.1099/ijsem.0.003806

Shirling, E. T., and Gottlieb, D. (1966). Methods for characterization of Streptomyces species1. *Int. J. Syst. Evol. Microbiol.* 16, 313–340. doi: 10.1099/00207713-16-3-313

Singh, G., Verma, A. K., and Kumar, V. (2016). Catalytic properties, functional attributes and industrial applications of β-glucosidases. *3 Biotech* 6:3. doi: 10.1007/s13205-015-0328-z

Singla, A. K., Mayilraj, S., Kudo, T., Krishnamurthi, S., Prasad, G. S., and Vohra, R. M. (2005). *Actinoalloteichus spitiensis* sp. nov., a novel actinobacterium isolated from a cold desert of the Indian Himalayas. *Int. J. Syst. Evol. Microbiol.* 55, 2561–2564. doi: 10.1099/ijs.0.63720-0

Sivalingam, P., Hong, K., Pote, J., and Prabakar, K. (2019). Extreme environment Streptomyces: potential sources for new antibacterial and anticancer drug leads? *Int. J. Microbiol.* 2019:5283948. doi: 10.1155/2019/5283948

Solans, M., Pelliza, Y. I., and Tadey, M. (2021). Inoculation with native actinobacteria may improve desert plant growth and survival with potential use for restoration practices. *Microb. Ecol.* 10, 1–13. doi: 10.1007/s00248-021-01753-4

Sooklal, S. A., De Koning, C., Brady, D., and Rumbold, K. (2020). Identification and characterisation of a fluorinase from Actinopolyspora mzabensis. *Protein Expr. Purif.* 166, 105508. doi: 10.1016/j.pep.2019.105508

Souagui, Y., Grosdemange-Billiard, C., Tritsch, D., and Kecha, M. (2017). Antifungal molecules produced by a new salt-tolerant and alkaliphilic *Streptomyces* sp. BS30 isolated from an arid soil. *Proc. Natl. Acad. Sci. India Sect. B. Biol. Sci.* 87, 527–535. doi: 10.1007/s40011-015-0632-8

Stokes, J. M., Yang, K., Swanson, K., Jin, W., Cubillos-Ruiz, A., Donghia, N. M., et al. (2020). A deep learning approach to antibiotic discovery. *Cell* 180, 688–702. doi: 10.1016/j.cell.2020.04.001

Strub, C., Brandam, C., Meyer, X., and Lebrihi, A. (2008). Investigations of Saccharothrix algeriensis growth on synthetic media. *J. Biosci. Bioeng.* 106, 148–153. doi: 10.1263/jbb.106.148

Sun, H. M., Zhang, T., Wei, Y. Z., Liu, H. Y., Yu, L. Y., and Zhang, Y. Q. (2015). *Tenggerimyces mesophilus* gen. nov., sp. nov., a member of the family Nocardioidaceae. *Int. J. Syst. Evol. Microbiol.* 65, 3359–3364. doi: 10.1099/ijsem.0.000421

Sun, H. M., Zhang, T., Yu, L. Y., Lu, X. X., Mou, X. Z., and Zhang, Y. Q. (2014). *Actinophytocola gilvus* sp. nov., isolated from desert soil crusts, and emended description of the genus Actinophytocola Indananda et al. 2010. *Int. J. Syst. Evol. Microbiol.* 64, 3120–3125. doi: 10.1099/ijs.0.061051-0

Sun, J. Q., Xu, L., Guo, Y., Li, W. L., Shao, Z. Q., Yang, Y. L., et al. (2017). *Kribbella deserti* sp. nov., isolated from rhizosphere soil of *Ammopiptanthus mongolicus*. Int. J. Syst. Evol. Microbiol. 67, 692–696. doi: 10.1099/ijsem.0.001697

Sun, Y., Wang, H., Zhang, T., Liu, W. H., Liu, H. Y., Yu, L. Y., et al. (2019). *Desertihabitans aurantiacus* gen. nov., sp. nov., a novel member of the family Propionibacteriaceae. *Int. J. Syst. Evol. Microbiol.* 69, 2486–2491. doi: 10.1099/ijsem.0.003519

Tan, G., Robinson, S., Lacey, E., and Goodfellow, M. (2006). *Amycolatopsis australiensis* sp. nov., an actinomycete isolated from arid soils. *Int. J. Syst. Evol. Microbiol.* 56, 2297–2301. doi: 10.1099/ijs.0.64260-0

Tang, B., Xie, F., Zhao, W., Wang, J., Dai, S., Zheng, H., et al. (2016). A systematic study of the whole genome sequence of *Amycolatopsis methanolica* strain 239T provides an insight into its physiological and taxonomic properties which correlate with its position in the genus. *Synth. Syst. Biotechnol.* 1, 169–186. doi: 10.1016/j.synbio.2016.05.001

Thumar, J. T., Dhulia, K., and Singh, S. P. (2010). Isolation and partial purification of an antimicrobial agent from halotolerant alkaliphilic *Streptomyces aburaviensis* strain Kut-8. *World. J. Microbiol. Biotechnol.* 26, 2081–2087. doi: 10.1007/s11274-010-0394-7

Tiwari, K., and Gupta, R. K. (2013). Diversity and isolation of rare actinomycetes: an overview. *Crit. Rev. Microbiol.* 39, 256–294. doi: 10.3109/1040841X.2012.709819

Toumatia, O., Compant, S., Yekkour, A., Goudjal, Y., Sabaou, N., Mathieu, F., et al. (2016). Biocontrol and plant growth promoting properties of *Streptomyces mutabilis* strain IA1 isolated from a Saharan soil on wheat seedlings and visualization of its niches of colonization. *South Afr. J. Bot.* 105, 234–239. doi: 10.1016/j.sajb.2016.03.020

Traxler, M. F., and Kolter, R. (2015). Natural products in soil microbe interactions and evolution. *Nat. Prod. Rep.* 32, 956–970. doi: 10.1039/C5NP00013K

Trujillo, M. E., Idris, H., Riesco, R., Nouioui, I., Igual, J. M., Bull, A. T., et al. (2017). *Pseudonocardia nigra* sp. nov., isolated from Atacama Desert rock. *Int. J. Syst. Evol. Microbiol.* 67, 2980–2985. doi: 10.1099/ijsem.0.002063

Tuo, L., Dong, Y. P., Habden, X., Liu, J. M., Guo, L., Liu, X. F., et al. (2015). *Nocardioides deserti* sp. nov., an actinobacterium isolated from desert soil. *Int. J. Syst. Evol. Microbiol.* 65, 1604–1610. doi: 10.1099/ijs.0.000147

Větrovský, T., and Baldrian, P. (2013). The variability of the 16S rRNA gene in bacterial genomes and its consequences for bacterial community analyses. *PLoS One* 8:2. doi: 10.1371/journal.pone.0057923

Vickers, J. C., and Williams, S. T. (1987). An assessment of plate inoculation procedures for the enumeration and isolation of soil streptomycetes. *Microbios. Lett.* 35, 113–117.

Vijayakumar, S., and Menakha, M. (2015). Pharmaceutical applications of cyanobacteria—A review. *J. Acute Med.* 5, 15–23. doi: 10.1016/j.jacme.2015.02.004

Wang, H. F., Zhang, Y. G., Chen, J. Y., Hozzein, W. N., Li, L., Wadaan, M., et al. (2014). *Nesterenkonia rhizosphaerae* sp. nov., an alkaliphilic actinobacterium isolated from rhizosphere soil in a saline-alkaline desert. *Int. J. Syst. Evol. Microbiol.* 64, 4021–4026. doi: 10.1099/ijs.0.066894-0

Wang, L., Li, Y., and Li, Y. (2019). *Lentzea isolaginshaensis* sp. nov., an actinomycete isolated from desert soil. *Antonie van Leeuwenhoek* 112, 633–639. doi: 10.1007/s10482-018-1193-7

Wang, L., Xu, L., Sun, J., and Wu, X. (2017). Plant growth-promoting ability of culturable bacteria in the rhizosphere of *Alhagi sparsifolia*. *Chin. J. Appl. Environ. Biol.* 23, 628–634. doi: 10.3724/SP.J.1145.2016.08040

Wang, T., Li, F., Lu, Q., Wu, G., Jiang, Z., Liu, S., et al. (2021). Diversity, novelty, antimicrobial activity, and new antibiotics of cultivable endophytic actinobacteria isolated from psammophytes collected from Taklamakan Desert. *J. Pharm. Anal.* 11, 241–250. doi: 10.1016/j.jpha.2020.06.004

Whelan, F. J., Waddell, B., Syed, S. A., Shekarriz, S., Rabin, H. R., Parkins, M. D., et al. (2020). Culture-enriched metagenomic sequencing enables in-depth profiling of the cystic fibrosis lung microbiota. *Nat. Microbiol.* 5, 379–390. doi: 10.1038/s41564-019-0643-y

Whitman, W. B. (2014). The need for change: embracing the genome. *Methods Microbiol.* 41, 1–12. doi: 10.1016/bs.mim.2014.08.002

Wichner, D., Idris, H., Houssen, W. E., McEwan, A. R., Bull, A. T., Asenjo, J. A., et al. (2017). Isolation and anti-HIV-1 integrase activity of lentzeosides A-F from extremotolerant *Lentzea* sp, H45, a strain isolated from a high-altitude Atacama Desert soil. *J. Antibiot.* 70, 448–453. doi: 10.1038/ja.2016.78

Williams, S. T., and Davies, F. L. (1965). Use of antibiotics for selective isolation and enumeration of actinomycetes in soil. *J. Gen. Microbiol.* 38, 251–261. doi: 10.1099/00221287-38-2-251

Wink, J., Kroppenstedt, R. M., Seibert, G., and Stackebrandt, E. (2003). Actinomadura namibiensis sp. nov. *Int. J. Syst. Evol. Microbiol.* 53, 721–724. doi: 10.1099/ijs.0.02286-0

World Health Organization (2020). *Antimicrobial Resistance*. Available online at: https://www.who.int/news-room/fact-sheets/detail/antimicrobial-resistance (accessed October 13, 2020).

Xie, F. (2017). *New Drug Leads From Filamentous Actinobacteria Isolated From High Altitude Atacama Desert Soils.* master's thesis. Newcastle: Newcastle University.

Yan, Z. F., Lin, P., Chu, X., Kook, M., Li, C. T., and Yi, T. H. (2016). *Aeromicrobium halotolerans* sp. nov., isolated from desert soil sample. *Arch. Microbiol.* 198, 423–427. doi: 10.1007/s00203-016-1196-6

Yang, Z. W., Asem, M. D., Li, X., Li, L. Y., Salam, N., Alkhalifah, D., et al. (2019). *Blastococcus deserti* sp. nov., isolated from a desert sample. *Arch. Microbiol.* 201, 193–198. doi: 10.1007/s00203-018-1604-1

Yang, Z. W., Salam, N., Mohany, M., Chinnathambi, A., Alharbi, S. A., Xiao, M., et al. (2018b). *Microbacterium album* sp. nov. and *Microbacterium deserti* sp. nov., two halotolerant actinobacteria isolated from desert soil. *Int. J. Syst. Evol. Microbiol.* 68, 217–222. doi: 10.1099/ijsem.0.002485

Yang, Z. W., Salam, N., Asem, M. D., Fang, B. Z., Lan, L., Xiao, M., et al. (2018a). *Saccharopolyspora deserti* sp. nov., a novel halotolerant actinobacterium isolated from a desert. *Int. J. Syst. Evol. Microbiol.* 68, 860–864. doi: 10.1099/ijsem.0.002598

Ye, J. J., Liu, S. W., Lu, Q. P., Cheema, M. T., Abbas, M., Sajid, I., et al. (2020). Arthrobacter mobilis sp. nov., a novel actinobacterium isolated from Cholistan desert soil. *Int. J. Syst. Evol. Microbiol.* 70, 5445–5452. doi: 10.1099/ijsem.0.004431

Yi, W., Qin, L., Lian, X. Y., and Zhang, Z. (2020). New antifungal metabolites from the Mariana Trench sediment-associated actinomycete *Streptomyces* sp. *SY1965*. *Mar. Drugs* 18, 385–396. doi: 10.3390/md18080385

Yuan, L. L., Zhang, L. L., Luo, X. X., Xia, Z. F., Sun, B. B., and Zeng, H. (2020). *Streptomyces taklimakanensis* sp. nov., an actinomycete isolated from the Taklimakan desert. *Antonie van Leeuwenhoek* 113, 1023–1031. doi: 10.1007/s10482-020-01416-3

Zahra, T., Hamedi, J., and Mahdigholi, K. (2020). Endophytic actinobacteria of a halophytic desert plant *Pteropyrum olivieri*: promising growth enhancers of sunflower. *3 Biotech* 10, 1–13. doi: 10.1007/s13205-020-02507-8

Zhang, L., Zhang, J., Ren, B., Lu, W., Hou, C., Wang, J., et al. (2020). Characterization of anti-BCG benz[α]anthraquinones and new siderophores from a Xinjiang desert-isolated rare actinomycete *Nocardia* sp. *XJ31*. *Appl. Microbiol. Biotechnol.* 104, 8267–8278. doi: 10.1007/s00253-020-10842-2

Zhang, Y. G., Wang, H. F., Liu, Q., Hozzein, W. N., Wadaan, M. A., Cheng, J., et al. (2013). *Streptomyces fukangensis* sp. nov., a novel alkaliphilic actinomycete isolated from a saline-alkaline soil. *Antonie van Leeuwenhoek* 104, 1227–1233. doi: 10.1007/s10482-013-0045-8

Zhang, Y. G., Wang, H. F., Yang, L. L., Guo, J. W., Xiao, M., Huang, M. J., et al. (2016). *Ornithinicoccus halotolerans* sp. nov., and emended description of the genus Ornithinicoccus. *Int. J. Syst. Evol. Microbiol.* 66, 1894–1899. doi: 10.1099/ijsem.0.000964

Zhu, Q. H., Yang, C. L., Luo, X. X., Zhang, L. L., and Xia, Z. F. (2021). *Microbacterium karelineae* sp. nov. isolated from a halophyte plant in the Taklamakan desert. *Int. J. Syst. Evol. Microbiol.* 71, 2. doi: 10.1099/ijsem.0.004629

Zhu, Z. N., Li, Y. R., Li, Y. Q., Xiao, M., Han, M. X., Wadaan, M., et al. (2019). *Microbacterium suaedae* sp. nov., isolated from Suaeda aralocaspica. *Int. J. Syst. Evol. Microbiol.* 69, 411–416. doi: 10.1099/ijsem.0.003162

Zitouni, A., Lamari, L., Boudjella, H., Badji, B., Sabaou, N., Gaouar, A., et al. (2004). *Saccharothrix algeriensis* sp. nov., isolated from Saharan soil. *Int. J. Syst. Evol. Microbiol.* 54, 1377–1381. doi: 10.1099/ijs.0.02679-0

Zucchi, T. D., Tan, G. Y. A., Bonda, A. N. V., Frank, S., Kshetrimayum, J. D., and Goodfellow, M. (2012a). *Amycolatopsis granulosa* sp. nov., *Amycolatopsis ruanii* sp. nov. and *Amycolatopsis thermalba* sp. nov., thermophilic actinomycetes isolated from arid soils. *Int. J. Syst. Evol. Microbiol.* 62, 1245–1251. doi: 10.1099/ijs.0.031039-0

Zucchi, T. D., Tan, G. Y. A., and Goodfellow, M. (2012b). *Amycolatopsis thermophila* sp. nov. and *Amycolatopsis viridis* sp. nov., thermophilic actinomycetes isolated from arid soil. *Int. J. Syst. Evol. Microbiol.* 62, 168–172. doi: 10.1099/ijs.0.029256-0

Conflict of Interest: The authors declare that the research was conducted in the absence of any commercial or financial relationships that could be construed as a potential conflict of interest.

frontiers in Microbiology

ORIGINAL RESEARCH
published: 11 January 2022
doi: 10.3389/fmicb.2021.796228

Experimental Evolution of Anticipatory Regulation in *Escherichia coli*

*Anjali Mahilkar, Pavithra Venkataraman, Akshat Mall and Supreet Saini**

Department of Chemical Engineering, Indian Institute of Technology Bombay, Mumbai, India

Environmental cues in an ecological niche are often temporal in nature. For instance, in temperate climates, temperature is higher in daytime compared to during night. In response to these temporal cues, bacteria have been known to exhibit anticipatory regulation, whereby triggering response to a yet to appear cue. Such an anticipatory response in known to enhance Darwinian fitness, and hence, is likely an important feature of regulatory networks in microorganisms. However, the conditions under which an anticipatory response evolves as an adaptive response are not known. In this work, we develop a quantitative model to study response of a population to two temporal environmental cues, and predict variables which are likely important for evolution of anticipatory regulatory response. We follow this with experimental evolution of *Escherichia coli* in alternating environments of rhamnose and paraquat for ∼850 generations. We demonstrate that growth in this cyclical environment leads to evolution of anticipatory regulation. As a result, pre-exposure to rhamnose leads to a greater fitness in paraquat environment. Genome sequencing reveals that this anticipatory regulation is encoded *via* mutations in global regulators. Overall, our study contributes to understanding of how environment shapes the topology of regulatory networks in an organism.

Keywords: evolution of anticipatory regulation adaptation, anticipatory regulation, *Escherichia coli*, laboratory evolution, rhamnose, paraquat

OPEN ACCESS

Edited by:
Louis S. Tisa,
University of New Hampshire,
United States

Reviewed by:
Jose Utrilla,
National Autonomous University of Mexico, Mexico
Marie Filteau,
Laval University, Canada

***Correspondence:**
Supreet Saini
saini@che.iitb.ac.in

Specialty section:
This article was submitted to Systems Microbiology, a section of the journal Frontiers in Microbiology

Received: *16 October 2021*
Accepted: *20 December 2021*
Published: *11 January 2022*

Citation:
Mahilkar A, Venkataraman P, Mall A and Saini S (2022) Experimental Evolution of Anticipatory Regulation in Escherichia coli. Front. Microbiol. 12:796228. doi: 10.3389/fmicb.2021.796228

INTRODUCTION

Environmental cues are often cyclical in nature, for instance, temperature in day is higher and night is cooler. Thus, microorganisms have to continuously adapt to this changing environment. Moreover, the changing cues have a strong temporal element associated with them. That is, high temperature precedes the lower temperature of the night. Can the gene expression pattern of a microbial population be tuned to pre-empt the arriving cue? While examples of such anticipatory gene regulation are known from ecological contexts (Tagkopoulos et al., 2008; Mitchell et al., 2009), the dynamics of evolution of anticipatory regulation are not known.

The cellular response to a biological cue is based on specificity of recognition of the cue. Biological systems expend considerable effort toward reducing non-specific substrate binding and reducing crosstalk (Swain and Siggia, 2002; Siryaporn and Goulian, 2008; Skerker et al., 2008; Johnson and Hummer, 2011). However, anticipatory regulation requires that the gene expression

is tuned in response to a yet-to-appear environmental cue. Moreover, regulatory crosstalk between cellular modules is ubiquitous in biology (Ravasz et al., 2002; Shen-Orr et al., 2002). One of the forms of specificity and crosstalk in regulation is between transcription factors and their recognition site on the DNA. Although each transcription factor binds its cognate regulatory site on the DNA, significant non-specific binding, and hence regulatory crosstalk, exists (Wunderlich and Mirny, 2009; Burger et al., 2010).

A particular form of crosstalk between two functional modules is when gene expression changes upon anticipation of an upcoming environmental shift. For example, in *Escherichia coli*, an increase in temperature elicits response to low oxygen conditions, mimicking how these two environments are sequentially encountered by the bacterium in the mammalian gastrointestinal tract (Tagkopoulos et al., 2008). Such anticipatory regulation was also demonstrated to occur between sugars lactose and maltose (Mitchell et al., 2009). Anticipatory regulation is seen in yeast too. Recent studies have demonstrated that yeast anticipates exhaustion of a primary carbon source, and thus, switches to the secondary source in the environment, even before the primary source is exhausted (New et al., 2014; Wang et al., 2015; Venturelli et al., 2015). Thus, fine-tuning of regulatory crosstalk between modules, leading to exhibition of anticipatory regulation, is done in accordance with the precise ecological niche of an organism.

Anticipatory gene regulation, as a strategy, is widespread in pathogens (Brunke and Hube, 2014). In *Mycobacterium*, the different two-component systems (TCSs) in the bacterium are wired so that activation of one leads to partial activation of the downstream TCSs (Agrawal et al., 2015). In *Salmonella*, flagella is assembled prior to assembly of a Type 3 Secretion System (T3SS) (Saini et al., 2010), and regulatory elements in the flagellar cascade are known to activate the SPI1-encoded T3SS genes (Chubiz et al., 2010). *Burkholderia*, in response to high cell density, anticipates stationary phase stress and triggers anticipatory response (Goo et al., 2012). Fungal pathogens have been shown to elicit anticipatory response for protection against attack from the immune system of the host (Pradhan et al., 2020).

Thus, repeated, temporal exposure of environmental cues may have led to evolution of regulatory crosstalk between cellular modules. Despite significant evidence that anticipatory gene expression provides an adaptive advantage to an organism, little is known about how anticipatory regulation can evolve in a population.

In this work, we ask the following question: if a population is exposed to two environmental signals, S1 and S2, sequentially and repeatedly, under what conditions can anticipatory regulation evolve as an adaptive strategy? To answer this question, we use a simple mathematical model to represent exposure of a population to two temporal stimuli [signal1 (S1) and signal2 (S2)] and identify the network and physiological parameters, which maximize fitness in the given conditions. Based on the inputs from our modeling results, we evolve *E. coli* under alternating exposure to a pentose sugar rhamnose (S1) and an oxidative stress molecule, paraquat (PQ) (S2) (see **Supplementary Material 1** for more details).

Repeated, alternating exposure to S1 and S2 for ∼850 generations, leads to evolution of anticipatory regulation, where prior exposure to rhamnose provides an adaptive benefit when the population is shifted to paraquat. This benefit is observed only in lines, which were exposed to alternating S1 and S2; and is only seen when these cells are pre-exposed to rhamnose. Gene expression experiments demonstrate that one of the possible mechanisms of this adaptive benefit is partial activation of *soxS*, upon exposure to rhamnose. Our study thus demonstrates that, in controlled laboratory environment, anticipatory gene regulation can evolve in a short timeframe of a few hundred generations. Genome sequencing of the evolved lines reveals that anticipatory regulation can evolve *via* distinct molecular pathways, often involving mutations in global regulators.

MATERIALS AND METHODS

Model System Description

Two regulatory modules and their possible interaction was studied as follows. A microorganism experiences an environmental signal S1. Upon sensing this signal, it modulates gene expression. As part of this response, a transcription factor R1 gets activated and triggers expression of a target protein T1. After time *t1*, S1 is replaced by another signal S2. In response to S2, the cell activates a transcription factor R2. The activated R2 then positively controls expression of the target protein T2, which confers an adaptive benefit in S2. The signal S2 persists for time *t2* (**Figure 1**).

In the first regulatory design, activated R1 is responsible for response to S1 (controlling expression of T1 only), and activated R2 controls expression of T2. We call this design a no-anticipatory regulation design (**Figure 1A**). In such a setting, when allowed to propagate in alternating S1 and S2 for a long time, the population will evolve and enhance fitness. In our mathematical framework, we solve for parameter values, which maximize fitness for the regulatory topology in **Figure 1A**.

On the other hand, in the design with anticipatory regulation, expression of T2 is controlled by active R1 as well as active R2 (**Figure 1B**). We solve for the values of these biochemical interaction that maximize fitness in this regulatory design. In particular, we are interested in identification of parameter values such that the fitness conferred by design in **Figure 1B** exceeds that by design in **Figure 1A**.

The equations dictating the synthesis and degradation rate of proteins in the cell, upon sensing signal S1 or S2 can be written as below.

$$R1 + [s1] \leftrightarrow R1^{*} \tag{1}$$

and,

$$R2 + [s2] \leftrightarrow R2^{*} \tag{2}$$

is represented as:

$$k_{f1}\,[R1]\,[s1] \leftrightarrow k_{r1}[R1^{*}] \tag{3}$$

and

$$k_{f2}\,[R2]\,[s2] \leftrightarrow k_{r2}[R2^{*}] \tag{4}$$

The dynamics of target protein T2 is represented as described in Equation 5. $R2^*$ is the transcription factor responsible for expression of T2, *Km2* is the Michaelis–Menten kinetic constant for T2 production, b_2 is the maximum production rate of T2, and k_{d2} is the combined degradation and dilution rate of T2 in the cell (Alon, 2006). The parameters k_{f1} (k_{f2}) and k_{r1} (k_{r2}) represent the rate constant of association and disassociation between the regulator R1 (R2) and the signal s1 (s2), respectively. We assume that expression of R1 and R2 is not contingent on the presence or absence of signals (but their activation is).

$$\frac{dT2}{dt} = b_2 \frac{R2^*}{R2^* + K_{m2}} - k_{d2}\, T2 \quad (5)$$

However, in the case when anticipatory regulation controls gene expression (**Figure 1B**), the dynamics of T2 in the cell can be quantified as:

$$\frac{dT2}{dt} = b_1 \frac{R1^*}{R1^* + K_{m12}} + b_2 \frac{R2^*}{R2^* + K_{m2}} - k_{d2}\, T2 \quad (6)$$

Where,

$$K_m = \frac{k\_off}{k\_on}$$

for each transcription factor-DNA interaction, and b_1 (b_2) is the maximal strength of the *T2* promoter when driven by the activated transcription factor R1 (R2). In this manner, given the biochemical parameters of a network, we can quantify the dynamics of protein expression in a cell.

Cost-Benefit Framework

From the time-course data of protein expression, we use a cost-benefit model to understand the cellular fitness, as a result of the gene expression dynamics (Dekel and Alon, 2005; Zaslaver et al., 2006b; Roselius et al., 2014; Fritz et al., 2019). In this formulation, the benefit conferred to the cell by the target protein T2 is given by the following expression:

$$Benefit,\ E = E_{max} \frac{[T2]}{[T2] + K_{mT2}} \quad (7)$$

In addition, protein production is known to have a cost associated with it (Kafri et al., 2016). This cost is a linear function of the amount of protein being synthesized.

$$Cost,\ c = c_o\,[T2] \quad (8)$$

The overall fitness of a cell is given by,

$$Fitness,\ f = E - c \quad (9)$$

Given a set of network topology and the biochemical parameters associated with it, this framework allows us to compute the benefit of production of T2 and track this quantity with time. In the context of this work, we compute the fitness conferred by T2 in the time window [*t1, t2*] and the total cost associated with synthesis of protein T2 in the window [*t0*, *t2*].

Solving for Optimal Fitness

We assume that the parameters associated with changing the regulatory patterns of gene expression (like, *Km* and *b*) are evolvable on a time scale faster than the time needed to change parameters associated with protein property (like, enzyme activity, degradation rate) (Babu et al., 2004; Wray, 2007; Wittkopp and Kalay, 2011; Rubinstein and de Souza, 2013). As a result, we let the parameters, which control regulation evolve, while keeping the others constant. Moreover, in our simulations, the value of each parameters is constrained by the thermodynamics associated with biological processes (**Supplementary Material 2**). The range chosen for each parameter represents the biologically permissible window in which they can take a value (Ozbudak et al., 2002; Rosenfeld et al., 2005, 2007; Mitrophanov and Groisman, 2008; Sneppen et al., 2010).

Given the above, we introduce "mutations" (change parameters) in the network and for each of the two regulatory designs (with and without anticipatory regulation, as defined above), find the parameter set which optimizes fitness. We are particularly interested in finding whether fitness is optimized *via* topology in **Figures 1A** or **B**.

All simulations were performed in Matlab 7.0.

Strain Used

Escherichia coli K12 MG1655 (ATCC 47076) (F^- lambda$^-$) was used in this study. The *soxS* mutant was generated using the primers 5′-CCCCAACAGATGAA TTAACGAACTGAACACTGAAA AGAGG GTGTAGGCTGG AGCTGCTTC-3′ and 5′-GAGCAATTACCCGCGCGGGAGT TAA CGCGCGGGCAATAAACATATGAATATCCTCCTTA-3′ from the parent strain, as per the method described by Datsenko and Wanner (2000).

Media and Reagents

M9 glycerol medium contained 0.2% glycerol unless otherwise stated. M9 salts, trace elements and casamino acids were prepared in concentrated stocks. Stock of a 5× M9 salts solution consisted of 64 g/L $Na_2HPO_4.7H_2O$, 15 g/L KH_2PO_4, 2.5 g/L NaCl, and 5 g/L NH_4Cl dissolved in Milli-Q filtered water. Casamino acids were prepared as 10× solution and were used at a final concentration of 0.05% (w/v) in the growth media. $MgSO_4$ and $CaCl_2$ were prepared at 1M stock solutions each. Stocks of rhamnose and paraquat was prepared at 20% and 5 mM, respectively, and sterilized by filtration through 0.22 μm filters.

Laboratory Evolution Experiment

Rhamnose (S1) and paraquat (S2) at a concentration of 0.2% and 40 μM, respectively, were used as the two stimuli. The evolution experiment was carried out in three replicate lines serially diluted 1:100 in alternating conditions of rhamnose and paraquat every 12 h, as described above. Control lines (in triplicate) were evolved in either 0.2% rhamnose only or 40 μM paraquat only. The control experiment were both the stimuli were added together did not grow beyond four dilutions, hence was dropped out of the experiment.

All cultures were grown at 37°C and 250 rpm. Sub-cultures in fresh media were done every 12 h (1:100) to ensure that cells did not enter stationary phase (Navarro Llorens et al., 2010). The evolution experiment was carried out for a total of 850 generations. Freezer stocks of intermediate time points were made in the experiment. Analysis of the stocks at 300 and 600 generations are presented in this work. Starting from the ancestor, three independent lines were evolved for each environmental condition.

Analysis of Evolved Lines for Anticipatory Regulation

All evolved lines and the ancestor were revived from freezer stocks into 2 ml LB and incubated for 12 h with shaking at 250 rpm at 37°C. The cultures were then sub-cultured 1:100 in 2 ml M9 medium, containing 0.2% glycerol as the carbon source, for 12 h. From each tube, cells were then sub-cultured 1:100 in 2 ml M9 glycerol media (a) with and (b) without 0.2% rhamnose, and allowed to grow for 12 h at 250 rpm at 37°C. After growth for 12 h, all lines were sub-cultured to the same initial OD (0.1) into 2 ml M9 glycerol with PQ (40 μM). A volume of 150 μL of these cultures were transferred to a 96-well clear flat-bottom microplate (Costar) in triplicates. The cultures were grown at 37°C in a microplate reader (Tecan Infinite M200 Pro), until they reached stationary phase. OD600 readings were taken every 30 min with 10 min of orbital shaking at 5 mm amplitude before the readings. A gas permeable *Breathe-Easy* (Sigma-Aldrich) sealing membrane was used to seal the 96-well plates. Growth rate (Malthusian parameter, *r*) was calculated from the time to reach an OD 1.0, assuming exponential growth in this duration. This growth rate is presented in the growth rates in **Figures 4D**, **5**.

Gene Expression Measurements

The evolved lines and wild-type were transformed with *soxS*-GFP, a plasmid-based promoter fusion from Thermo Scientific *E. coli* promoter collection (PEC3877) (Zaslaver et al., 2006a). For estimating the promoter activity, cells were revived from freezer stocks from the −80°C deep freezer into 2 ml LB containing 40 μg/ml Kanamycin and incubated for 12 h at 37°C. The saturated cultures were then sub-cultured 1:100 in 2 ml M9 glycerol medium for 12 h. All lines were then sub-cultured 1:100 into fresh M9 glycerol medium without/with 0.2% rhamnose and allowed to grow for 12 h at 37°C. After this period of growth, 150 μL of these cultures was transferred to a 96-well Black clear flat-bottom microplate (Costar) and Fluorescence (488/525 nm) and OD600 readings taken using a microplate reader.

For *soxS*-GFP expression in presence of paraquat, cells were transferred at a 1:100 dilution from M9 glycerol to M9 glycerol with /without 0.2% rhamnose. The culture were then allowed to grow for 12 h at 37°C. The resulting cultures were diluted to an initial OD600 of 0.1 in 2 ml M9 glycerol media with 40 μM PQ. A volume of 150 μL of these cultures were transferred to a 96-well Black clear flat-bottom microplate in triplicates. The cultures were grown at 37°C in a microplate reader, until they reached stationary phase. Fluorescence (488/525 nm) and OD600 readings were taken every 30 min with 10 min of orbital shaking at 5 mm amplitude before the readings. A gas permeable *Breathe-Easy* (Sigma-Aldrich) sealing membrane was used to seal the 96-well plates. In this assay, the cumulative promoter strength over a period of time is measured.

A two-tailed *t*-test was performed to compare two sets of data. The *p*-value corresponding to four degrees of freedom was obtained using the calculated *t*-statistic for each set.

Whole Genome Sequencing and Variant Calling

Sample Preparation and Sequencing

Genomic DNA of ancestral and evolved lines were isolated following standard zymolyase-based protocol using the kit from FAVORGEN Biotech Corporation. DNA concentrations and quality were measured using a Nano-spectrophotometer from Eppendorf and by gel electrophoresis. Samples were paired-end sequenced on an Illumina HiSeq, with an average read length of 150 bp. Each sample had a minimum coverage of 100×.

Mapping and Variant Calling

A cloud-based web interface system Galaxy[1] was used to perform all sequence data analysis. Illumina paired-end reads were uploaded into the server. The quality of the reads was assessed using FastQC (Version 0.72) (Andrews, n. d.). The reads were mapped to *E. coli* str. K-12 substr. MG1655 genome (GCA_000005845.2) and variant calling was performed using the automated tool Snippy (Version 3.2) (Seemann, 2015), according to the recommendations for evaluating single nucleotide variant calling (Olson et al., 2015). Variants present in the ancestral strain were filtered out manually. Finally, all remaining indels and SNPs were verified using intensive manual curation.

RESULTS

Anticipatory Regulation Is an Adaptive Response for Intermediate Values of Degradation Rates of the Protein T2

We simulate the networks in **Figures 1A,B** for a set of parameter values, chosen from a window typically representing each biochemical interaction in a cell (Ozbudak et al., 2002; Rosenfeld et al., 2005, 2007; Suel et al., 2006; Mitrophanov and Groisman, 2008; Sneppen et al., 2010; Prajapat et al., 2016). For a given value of *kd* (degradation + dilution rate constant for protein T2), we find the regulatory design in **Figure 1**, which leads to a maximal fitness.

Maximal fitness is obtained *via* three distinct regulatory logics, depending on the degradation rate of the protein T2 (**Figure 2A**). These region corresponding to the three designs is as shown in the bands in **Figures 2A,B** (yellow, green, and blue). For small values of the *kd* of T2, the maximal fitness is achieved when control of T2 is entirely under the regulator R1. That is, R2 does not play any role in controlling expression of T2. This can be understood as follows. Expression of T2 by R1 leads to T2

[1] https://usegalaxy.eu/

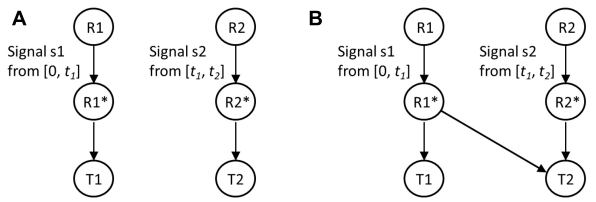

FIGURE 1 | Regulatory designs without **(A)** and with **(B)** anticipatory regulation. In the prevailing environment, signal s1 is present from [0, *t1*] and signal s2 is present from [*t1*, *t2*]. In the first design, activated regulator R1* controls expression of target protein T1, and R2* controls expression of T2. In the second regulatory design, R1*, in addition to controlling expression of T1, also partially/fully controls expression of target protein T2.

production even before signal S2 is present in the environment. As a result, the T2 so produced does not confer any advantage to the cell. Thus, this preemptive production of T2 does not give any benefit to the cell, but does come at an additional cost associated with protein production in the cell. This cost, however, is offset by the enhanced T2 levels inside the cell (and consequently the benefit conferred to the cell), from the time when signal S2 is introduced to the system. When T2 is stable, the steady state T2 in the cell is high, and as a result, the fitness of the cell at the moment S2 is introduced to the system is also high.

At the other extreme, when the *kd* of T2 is high, the regulatory design that optimizes cellular fitness is one where control of expression of T2 is not by R1, but is instead entirely by R2. In such a context, the energetic cost of T2 production in the "futile" time-period [0, *t1*] prior to introduction of signal B, because of the high protein turnover, is high. In such a scenario, the cellular adaptive strategy is control of each target protein by its cognate regulatory partner.

However, at intermediate values of the protein T2 degradation rate constant, for maximal cellular fitness, both b_1 and b_2 are non-zero. This window of the values of the degradation rate constant of T2 represents the scenario where conditioning is the adaptive response in cellular functioning. Such a set up identifies conditions for a distributed regulatory design for control of gene expression (Saini et al., 2010). However, anticipatory regulation may or may not be accessible from a given starting point on the landscape (Blount et al., 2018; Brajesh et al., 2019; Fragata et al., 2019).

Changes in regulatory design can also be incorporated by changing the binding affinity of the transcription factor with the promoter region of the DNA. In the context of the model, we change the parameter k_on, which represents the affinity of the DNA for the transcription factor. Similar to the results obtained above, anticipatory regulation outperforms the regulatory design in **Figure 1A** for intermediate values of the degradation rate of protein T2, when we permit k_on to vary for protein T2 (**Figure 2B**).

Can Anticipatory Regulation Be Evolved in a Laboratory Set-up?

We use the model to text the conditions in which conditioning would be the optimum response (compared to non-conditioning response). When we scan the two parameter region defined by E_{max} (maximum benefit conferred by T2) and *kd* of protein T2, we note that as E_{max} increases, conditioning emerges as the optimal solution for an increasing window of the parameter range *kd* for protein T2 (**Figure 3**).

From these results, we predict that anticipatory regulation is most likely to evolve if the target protein confers a large fitness advantage to the cell. This is perhaps the single most important criteria for anticipatory regulation to emerge as an outcome of an evolutionary experiment. In other words, anticipatory regulation is more likely to be the optimal regulatory design when absence of T2 causes a significant fitness cost to the cell. Therefore, for experimental evolution of anticipatory regulation, we choose a cellular stress as S2.

Evolution of Anticipatory Regulation in *Escherichia coli*

From our modeling exercise, we note that the key parameter for evolution of anticipatory regulation is cost associated with not initiating a rapid response to signal S2. In view of these inputs, we chose a pair of environmental signals, which meet this criteria. We chose the pentose sugar rhamnose as signal S1 and an oxidative stress molecule, paraquat (PQ) as signal

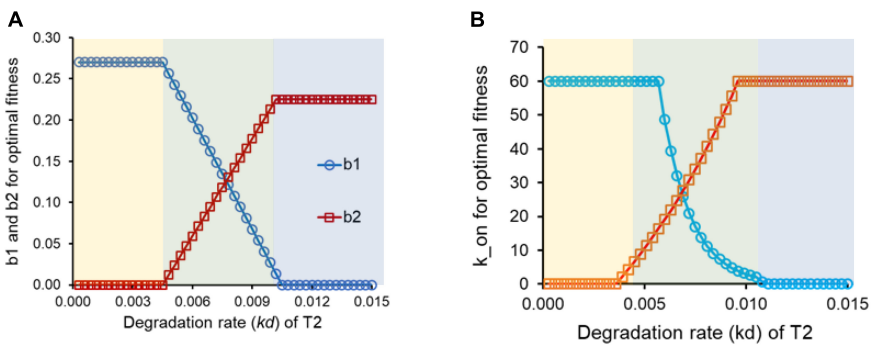

FIGURE 2 | (A) For intermediate values of the degradation rate *kd* for target protein, T2, conditioning is the optimal response. **(B)** For intermediate values of the degradation rate *kd* for target protein, T2, conditioning is the optimal response.

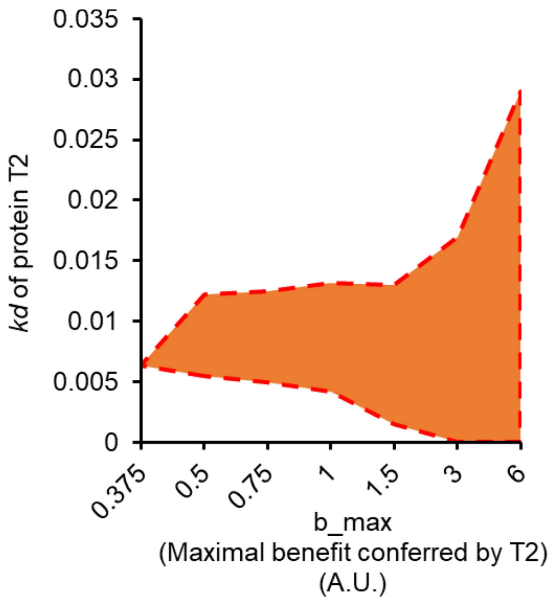

FIGURE 3 | Anticipatory regulation emerges as optimal solution as maximum benefit conferred by T2 increases. The shaded region in orange represents the range of the values of *kd* for protein T2, for which anticipatory regulation is the optimal regulatory design, at a given value of b_{max}.

S2 (see **Supplementary Material 1** for more details of the two systems). To the best of our knowledge, the two systems are not linked by any direct transcriptional regulation. A stress of 40 μM PQ induces a growth defect in *E. coli* (**Figure 4A**). Thus, any anticipated expression of the SoxRS regulon is likely to provide a large adaptive benefit to the individual. With this premise, we performed an evolutionary experiment where the cells were exposed to S1 and S2 alternatively for a total of about 850 generations (**Figure 4B**; see section "Materials and Methods").

In such a context, anticipatory regulation can be said to have evolved when the following two conditions are met. First, after alternating exposure to rhamnose and PQ, pre-exposure to rhamnose confers a growth advantage when the cells are exposed to PQ. Second, that this advantage should only be present in the lines evolved in an environment of alternating rhamnose and PQ.

In **Figure 4C**, growth kinetics of one of the lines from the three experimental conditions are shown. Cells evolved in alternating rhamnose-PQ were pre-grown in (a) glycerol and (b) glycerol and rhamnose. The two cultures were transferred to a M9 glycerol media containing PQ, and the growth kinetics compared. As shown in **Figure 4C**, the cells pre-exposed to rhamnose exhibit a growth advantage in PQ environment. This advantage is absent in the lines evolved in rhamnose-only, or PQ-only. In **Figure 4D**, the growth rate for all three lines in each of the three environments is shown. Among all the lines, only rhamnose-PQ alternating evolved lines show a growth advantage, when pre-exposed to rhamnose. The relative amounts of the advantage vary between the three lines. As expected, the rhamnose-evolved lines show a considerably lower growth rate as compared to the PQ-evolved and the rhamnose-PQ alternating evolved lines.

To test the kinetics of the growth advantage during the course of our evolution experiment, two intermediate time-points (generation 300 and 600) in the evolutionary experiment were also checked for their growth rate. As shown in **Figure 5**, no growth advantage due to anticipatory regulation was observed at 300 generations. By 600 generations, anticipatory regulation was observed in two of the three rhamnose-PQ alternating lines. This trend was exaggerated by generations 850. The growth advantage, associated with a prior exposure to rhamnose, is not observed in rhamnose-only and PQ-only evolved lines. Interestingly, in two of the three rhamnose-evolved lines, fitness decreases in the PQ environment, indicating trade-off (Cooper and Lenski, 2000; Litchman et al., 2015; Ferenci, 2016).

Evolved Lines Lead to Faster Induction of SoxS

SoxS is one of the key proteins responsible for cellular oxidative stress response (Seo et al., 2015). To test if induction of SoxS differs in the evolved and ancestral lines, when the cells are exposed to rhamnose, we grew *E. coli* in M9 glycerol media in the absence and presence of 0.2% rhamnose. As shown in **Figure 6**, in all three lines evolved with alternating exposure to rhamnose and paraquat, *soxS* promoter is activated in presence of 0.2% rhamnose. This rhamnose-dependent activation of the *soxS* promoter is absent in the lines evolved in rhamnose only, or the lines evolved in paraquat only. In addition, rhamnose-dependent activation of the *soxS* promoter is absent in the ancestor strain.

When lines Alt1, Alt2, and Alt3 were transferred from M9 glycerol media with and without rhamnose to M9 glycerol media containing paraquat, cells transferred from environments with rhamnose exhibited a faster induction of the *soxS* promoter (**Supplementary Material 3**).

This data demonstrates that in the lines evolved in alternating rhamnose and paraquat, anticipatory regulation evolves. This anticipatory regulation leads to a growth phenotype. Our results here demonstrate that one of the manifestations of evolution of anticipatory regulation is partial induction of the *soxS* promoter, when cells are grown in rhamnose. This partial induction leads to a faster transition to the ON state, when cells transition to an environment containing paraquat.

Molecular Basis of Anticipatory Regulation

Mutations in the evolved lines were identified from the genome sequencing results. A complete list of the mutations in the evolved lines is in **Supplementary Material 4**. All three lines had SNPs in *glpK*. Glycerol kinase (GlpK) is involved in the utilization of the glycerol moiety of phospholipids and triglycerides after their breakdown into usable forms (Lin et al., 1962; Zwaig and Lin, 1966; Zwaig et al., 1970; Thorner and Paulus, 1973; Herring et al., 2006; Joyce et al., 2006). In several adaptive evolution experiments, growth on glycerol has led to mutations in *glpK* coding region (Honisch et al., 2004; Herring et al., 2006; Applebee et al., 2008, 2011; Cheng et al., 2014). Our studies report three novel *glpK* alleles, which improve growth rate in minimal media containing glycerol.

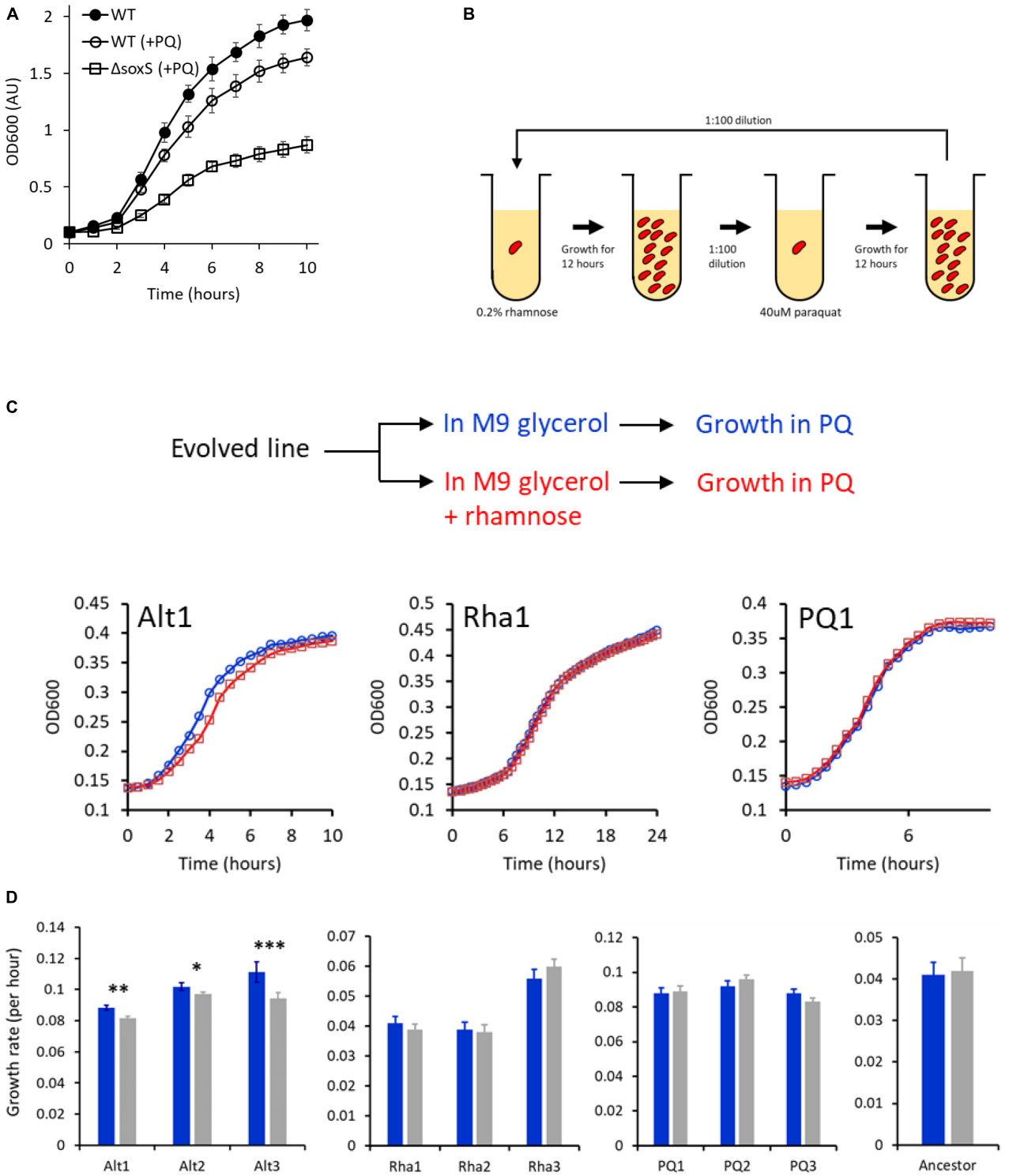

FIGURE 4 | (A) *Escherichia coli* exhibits a growth defect in M9 glycerol media, when grown in the presence of 40 μM PQ. **(B)** Experimental plan for the rhamnose-PQ alternating evolution. Cells were exposed to rhamnose and then PQ for 6–7 generations for a total of 850 generations. **(C)** Anticipatory regulation evolves in rhamnose-PQ alternating lines. Cells from rhamnose-PQ evolved line (line Alt1) (left), rhamnose-only evolved line (line Rha1) (middle), and PQ-only evolved line (PQ1) (right) were grown in M9 minimal glycerol media with (blue) or without (red) rhamnose. The cells were transferred 1:100 to M9 glycerol media with 40 μM PQ, and their growth kinetics observed. (lines 1 from alternating rhamnose-PQ; only rhamnose; and only PQ.) **(D)** Anticipatory regulation provides a growth advantage in all rhamnose-PQ alternating evolved lines. Growth rates of the evolved lines in M9 glycerol media containing 40 μM PQ, when transferred from M9 glycerol media with (blue) or without (gray) 0.2% rhamnose. (***p-value < 0.01; **p-value < 0.02; *p-value < 0.15; two-tailed, paired t-test).

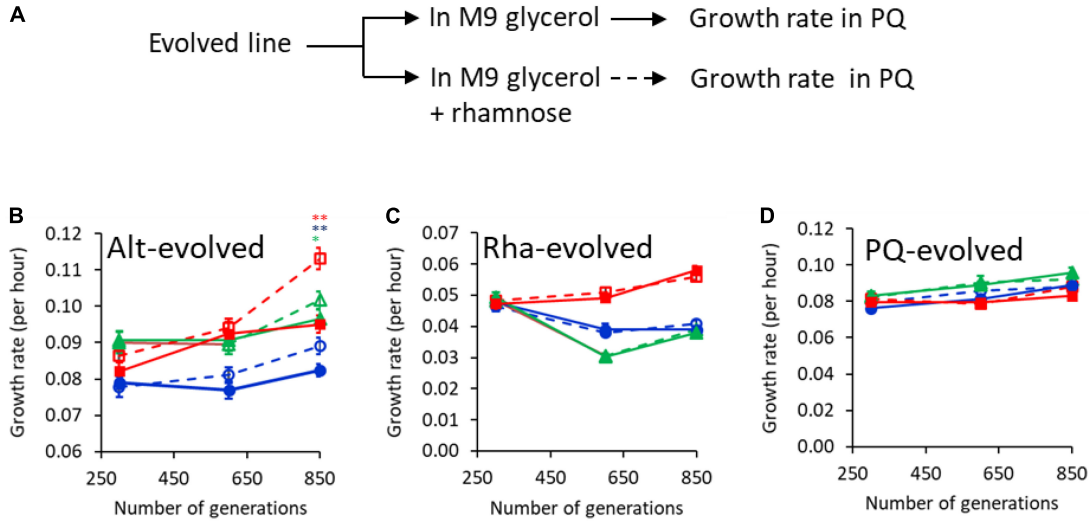

FIGURE 5 | Growth advantage because of evolution of anticipatory regulation takes place around and after 600 generations into the experiment. **(A)** Experimental design. Evolved lines were grown in M9 glycerol and M9 glycerol containing rhamnose separately. The two cultures were transferred to M9 media containing PQ, and growth kinetics monitored. Growth rate of lines 1 (blue), 2 (green), and 3 (red) in rhamnose-PQ alternating conditions **(B)**, rhamnose-only **(C)**, and PQ only **(D)**. Solid and dashed lines represent growth rates of the lines, when transferred from M9 glycerol medium without or with rhamnose, respectively. (* represents p-value < 0.1; ** represents p-value $< 0.0.1$ in two-tailed, paired t-test).

Additionally, each of the three lines acquired other mutations. Adenylate cyclase (encoded by *cyaA*) catalyzes synthesis of cyclic AMP (cAMP). Mutations in cyaA has also been reported to confer high hydrostatic pressure resistance and increased antibiotic resistance in *E. coli* (Nishino et al., 2008; Gayan et al., 2017). Moreover, because of cyclic AMP receptor protein (CRP)-cAMP complex has a global affect on gene regulation, the gene expression patterns in the cell in a *cya* mutant are qualitatively different, compared to the wild-type (Delaney, 1990). A mutation identified in one of the lines (Alt3) is a SNP in the RNA component of the small subunit (30S subunit) of the *E. coli* ribosome. The 16S rRNA is targeted by a number of antibiotic agents (Thompson and Hearst, 1983; Stern et al., 1989; Brimacombe, 1992; Schneider et al., 2003). As a result of this mutation, the proteome profile in the cell is known to be changed, affecting expression levels of more than a hundred proteins. Line Alt2 acquired a mutation in *rpoS*, which regulates transcription of a large number of genes related to sugar metabolism and polyamine metabolism in response to cellular stresses. It also has important roles in nucleic acid synthesis, modification, and turnover (Maciag et al., 2011); and response to oxidative stress (Soo and Wood, 2013). Polymorphisms in *rpoS* that affect fitness across different environments are commonly found in *E. coli* (Notley-McRobb et al., 2002; Zinser and Kolter, 2004; King et al., 2006).

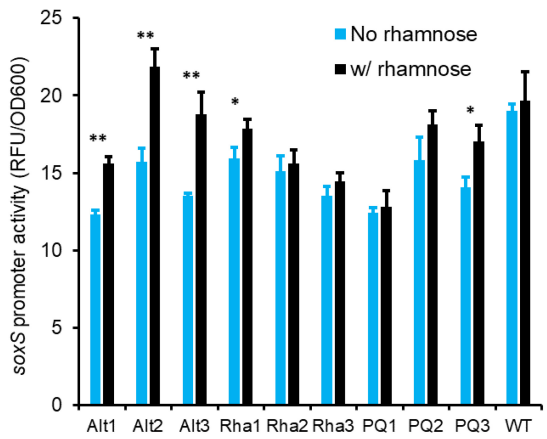

FIGURE 6 | Lines evolved with alternating exposure to rhamnose and paraquat (Alt1, Alt2, and Alt3) exhibit a higher expression from the *soxS* promoter after growth for 8 h in the presence of rhamnose. This rhamnose-dependent activation of the *soxS* promoter is absent in the ancestor (WT), in rhamnose-evolved lines (Rha1, Rha2, and Rha3), and in paraquat-evolved lines (PQ1, PQ2, and PQ3) (** indicates p-value < 0.002, * indicates p-value < 0.02, two-tailed, paired t-test).

Another class of mutations was identified in line Alt1. These include a mutation in *potA*, which impacts susceptibility to oxidative stresses (Tabor and Tabor, 1964; Abraham, 1968; Mitsui et al., 1984; Schuber, 1989; Chattopadhyay et al., 2003). Line Alt1 also acquired a mutation in TrkH, a potassium ion transporter (Dosch et al., 1991; Schlosser et al., 1995). A mutation in *trkH* is often associated with aminoglycoside resistance in bacteria (Lazar et al., 2013; Apjok et al., 2019). It also plays important roles in osmotic response, modulation of membrane potential, pH maintenance, and overall fitness in a variety of bacterial species (Castaneda-Garcia et al., 2011; Ochrombel et al., 2011; Quintero-Yanes et al., 2019).

Overall, while the mechanistic explanation for the observed anticipatory regulation, and the corresponding increase in fitness is difficult to understand fully from the sequencing results, our

results demonstrate how small mutations in global regulators of a cell can bring about fine-tuning of gene expression which leads to changes in timing and strength of gene expression, contributing to cellular fitness.

DISCUSSION AND CONCLUSION

Ecological niches often have cyclical cues – e.g., temperature increase followed by decrease in oxygen availability upon ingestion; nutritional cues are spatial in nature in the small intestine. Presumably, repeated exposure to these cues leads to evolution of anticipatory regulation. However, the timeline, mechanisms *via* which anticipatory regulation evolves is not known. This work is a first attempt toward this question.

Repeated exposure to two cues (rhamnose and PQ) lead to evolution of anticipatory regulation. While the phenomenology is reported in our study, the mechanistic details of this phenomenon is not identified. Our future work is directed toward answering this question. Our results suggest the possibility that *via* mutations in global regulators, the gene expression pattern of the cell is changed so that prior exposure to rhamnose leads to a fitness advantage when cells are exposed to oxidative stress. Interestingly, this phenomenon is observed without mutations in the *rhaSR* region or the *soxSR* region of the *E. coli* genome. The precise mechanistic details of the rhamnose-dependent upregulation of *soxS* remains unknown. Several possibilities exist in this regard. Expression of rhamnose utilization genes could lead to a pleiotropic effect on gene expression, leading to partial expression of genes involved in tackling oxidative stress. Alternatively, change in global regulators (as indicated in the mutations in **Supplementary Table 1**), and an altered metabolic state (due to presence of rhamnose) leads to upregulation of *soxS* and presumably, its regulon. Gene regulation can also be incorporated *via* post-transcription, translation, and/or post-translation mechanisms, while our model only considers transcriptional rewiring. Post-transcriptional modes of regulation can, structurally, be added to the modeling details. However, since most biochemical parameters are unknown, the utility of inputs from these models will likely be limited. On the other hand, our model, albeit simple, predicts the effect that use of a stress as a signal leads to a greater chance of anticipatory regulation to evolve.

In this work, we present experimental evidence of evolution of anticipatory regulation in bacteria. We demonstrate that by evolving *E. coli* in alternating environments of rhamnose and PQ, anticipatory regulation evolves, where prior exposure to rhamnose enhances fitness of the population in PQ. In our experimental set-up this adaptation evolves in the time scale of a few hundred generations. Anticipatory regulation involves mutations in global regulators (like *cya*, *rpoS*, ribosomal subunit), which likely lead to large-scale changes in transcriptional and translational profile of the cell. Mutations which confer a direct fitness advantage in the evolved environment are also reported (e.g., all three lines have a SNP is *glpK*). A previous attempt to evolve anticipatory regulation in yeast was made by choice of two stresses as environmental cues. However, disentangling the effect of the two stresses made the analysis of such a system challenging (Dhar et al., 2013). Overall, our study demonstrates clearly, that anticipatory regulation of gene regulation can evolve in a few hundred generations. Understanding this largely unexplored mode of regulation can help us understand the arrangement of global regulatory patterns in bacteria.

DATA AVAILABILITY STATEMENT

The datasets presented in this study can be found in online repositories. The names of the repository/repositories and accession number(s) can be found in the article/ **Supplementary Material**.

AUTHOR CONTRIBUTIONS

AnM carried out the evolution experiment, performed gene expression measurements, sequence analysis, and wrote the manuscript. PV and AkM performed the simulations and analyzed the data. SS and AnM conceived the study and wrote the manuscript. All authors gave final approval for publication and agreed to be held accountable for the work performed therein.

FUNDING

AnM is supported by the Council of Scientific and Industrial Research (CSIR), Government of India, as a Senior Research Fellow [09/087(0873)/2017-EMR-I].

SUPPLEMENTARY MATERIAL

The Supplementary Material for this article can be found online at: https://www.frontiersin.org/articles/10.3389/fmicb.2021.796228/full#supplementary-material

REFERENCES

Abraham, K. A. (1968). Studies on DNA-dependent RNA polymerase from *Escherichia coli*. 1. The mechanism of polyamine induced stimulation of enzyme activity. *Eur. J. Biochem.* 5, 143–146. doi: 10.1111/j.1432-1033.1968.tb00348.x

Agrawal, R., Pandey, A., Rajankar, M. P., Dixit, N. M., and Saini, D. K. (2015). The two-component signalling networks of Mycobacterium tuberculosis display extensive cross-talk *in vitro*. *Biochem. J.* 469, 121–134. doi: 10.1042/BJ20150268

Alon, U. (2006). *An Introduction to Systems Biology: Design Principles of Biological Circuits*. Boca Raton: Chapman and Hall/CRC.

Andrews, S. (n. d.). *FastQC A Quality Control tool for High Throughput Sequence Data*. Available Online at: http://www.bioinformatics.babraham.ac.uk/projects/fastqc/ (accessed August 15, 2021).

Apjok, G., Boross, G., Nyerges, A., Fekete, G., Lazar, V., Papp, B., et al. (2019). Limited evolutionary conservation of the phenotypic effects of antibiotic resistance mutations. *Mol. Biol. Evol.* 36, 1601–1611. doi: 10.1093/molbev/msz109

Applebee, M. K., Herrgard, M. J., and Palsson, B. O. (2008). Impact of individual mutations on increased fitness in adaptively evolved strains of *Escherichia coli*. *J. Bacteriol.* 190, 5087–5094. doi: 10.1128/JB.01976-07

Applebee, M. K., Joyce, A. R., Conrad, T. M., Pettigrew, D. W., and Palsson, B. O. (2011). Functional and metabolic effects of adaptive glycerol kinase (GLPK) mutants in *Escherichia coli*. *J. Biol. Chem.* 286, 23150–23159. doi: 10.1074/jbc.M110.195305

Babu, M. M., Luscombe, N. M., Aravind, L., Gerstein, M., and Teichmann, S. A. (2004). Structure and evolution of transcriptional regulatory networks. *Curr. Opin. Struct. Biol.* 14, 283–291.

Blount, Z. D., Lenski, R. E., and Losos, J. B. (2018). Contingency and determinism in evolution: replaying life's tape. *Science* 362:eaam5979. doi: 10.1126/science.aam5979

Brajesh, R. G., Dutta, D., and Saini, S. (2019). Distribution of fitness effects of mutations obtained from a simple genetic regulatory network model. *Sci. Rep.* 9:9842. doi: 10.1038/s41598-019-46401-7

Brimacombe, R. (1992). Structure-function correlations (and discrepancies) in the 16S ribosomal RNA from *Escherichia coli*. *Biochimie* 74, 319–326. doi: 10.1016/0300-9084(92)90109-r

Brunke, S., and Hube, B. (2014). Adaptive prediction as a strategy in microbial infections. *PLoS Pathog.* 10:e1004356. doi: 10.1371/journal.ppat.1004356

Burger, A., Walczak, A. M., and Wolynes, P. G. (2010). Abduction and asylum in the lives of transcription factors. *Proc. Natl. Acad. Sci. U. S. A.* 107, 4016–4021. doi: 10.1073/pnas.0915138107

Castaneda-Garcia, A., Do, T. T., and Blazquez, J. (2011). The K+ uptake regulator TrkA controls membrane potential, pH homeostasis and multidrug susceptibility in *Mycobacterium smegmatis*. *J. Antimicrob. Chemother.* 66, 1489–1498. doi: 10.1093/jac/dkr165

Chattopadhyay, M. K., Tabor, C. W., and Tabor, H. (2003). Polyamines protect *Escherichia coli* cells from the toxic effect of oxygen. *Proc. Natl. Acad. Sci. U. S. A.* 100, 2261–2265. doi: 10.1073/pnas.2627990100

Cheng, K. K., Lee, B. S., Masuda, T., Ito, T., Ikeda, K., Hirayama, A., et al. (2014). Global metabolic network reorganization by adaptive mutations allows fast growth of *Escherichia coli* on glycerol. *Nat. Commun.* 5:3233. doi: 10.1038/ncomms4233

Chubiz, J. E. C., Golubeva, Y. A., Lin, D. X., Miller, L. D., and Slauch, J. M. (2010). FliZ Regulates Expression of the *Salmonella* Pathogenicity Island 1 Invasion Locus by Controlling HilD Protein Activity in *Salmonella enterica* Serovar Typhimurium. *J. Bacteriol.* 192, 6261–6270. doi: 10.1128/JB.00635-10

Cooper, V. S., and Lenski, R. E. (2000). The population genetics of ecological specialization in evolving *Escherichia coli* populations. *Nature* 407, 736–739. doi: 10.1038/35037572

Datsenko, K. A., and Wanner, B. L. (2000). One-step inactivation of chromosomal genes in *Escherichia coli* K-12 using PCR products. *Proc. Natl. Acad. Sci. U. S. A.* 97, 6640–6645. doi: 10.1073/pnas.120163297

Dekel, E., and Alon, U. (2005). Optimality and evolutionary tuning of the expression level of a protein. *Nature* 436, 588–592. doi: 10.1038/nature03842

Delaney, J. M. (1990). A cya deletion mutant of *Escherichia coli* develops thermotolerance but does not exhibit a heat-shock response. *Genet. Res.* 55, 1–6. doi: 10.1017/s001667230002512x

Dhar, R., Sagesser, R., Weikert, C., and Wagner, A. (2013). Yeast adapts to a changing stressful environment by evolving cross-protection and anticipatory gene regulation. *Mol. Biol. Evol.* 30, 573–588. doi: 10.1093/molbev/mss253

Dosch, D. C., Helmer, G. L., Sutton, S. H., Salvacion, F. F., and Epstein, W. (1991). Genetic analysis of potassium transport loci in *Escherichia coli*: evidence for three constitutive systems mediating uptake potassium. *J. Bacteriol.* 173, 687–696. doi: 10.1128/jb.173.2.687-696.1991

Ferenci, T. (2016). Trade-off mechanisms shaping the diversity of bacteria. *Trends Microbiol.* 24, 209–223. doi: 10.1016/j.tim.2015.11.009

Fragata, I., Blanckaert, A., Dias Louro, M. A., Liberles, D. A., and Bank, C. (2019). Evolution in the light of fitness landscape theory. *Trends Ecol. Evol.* 34, 69–82. doi: 10.1016/j.tree.2018.10.009

Fritz, G., Walker, N., and Gerland, U. (2019). Heterogeneous timing of gene induction as a regulation strategy. *J. Mol. Biol.* 431, 4760–4774. doi: 10.1016/j.jmb.2019.05.020

Gayan, E., Cambre, A., Michiels, C. W., and Aertsen, A. (2017). RpoS-independent evolution reveals the importance of attenuated cAMP/CRP regulation in high hydrostatic pressure resistance acquisition in E. coli. *Sci. Rep.* 7:8600. doi: 10.1038/s41598-017-08958-z

Goo, E., Majerczyk, C. D., An, J. H., Chandler, J. R., Seo, Y. S., Ham, H., et al. (2012). Bacterial quorum sensing, cooperativity, and anticipation of stationary-phase stress. *Proc. Natl. Acad. Sci. U. S. A.* 109, 19775–19780. doi: 10.1073/pnas.1218092109

Herring, C. D., Raghunathan, A., Honisch, C., Patel, T., Applebee, M. K., Joyce, A. R., et al. (2006). Comparative genome sequencing of *Escherichia coli* allows observation of bacterial evolution on a laboratory timescale. *Nat. Genet.* 38, 1406–1412. doi: 10.1038/ng1906

Honisch, C., Raghunathan, A., Cantor, C. R., Palsson, B. O., and Van Den Boom, D. (2004). High-throughput mutation detection underlying adaptive evolution of *Escherichia coli*-K12. *Genome Res.* 14, 2495–2502. doi: 10.1101/gr.2977704

Johnson, M. E., and Hummer, G. (2011). Nonspecific binding limits the number of proteins in a cell and shapes their interaction networks. *Proc. Natl. Acad. Sci. U. S. A.* 108, 603–608. doi: 10.1073/pnas.1010954108

Joyce, A. R., Reed, J. L., White, A., Edwards, R., Osterman, A., Baba, T., et al. (2006). Experimental and computational assessment of conditionally essential genes in *Escherichia coli*. *J. Bacteriol.* 188, 8259–8271. doi: 10.1128/JB.00740-06

Kafri, M., Metzl-Raz, E., Jona, G., and Barkai, N. (2016). The cost of protein production. *Cell Rep.* 14, 22–31. doi: 10.1016/j.celrep.2015.12.015

King, T., Seeto, S., and Ferenci, T. (2006). Genotype-by-environment interactions influencing the emergence of rpoS mutations in *Escherichia coli* populations. *Genetics* 172, 2071–2079. doi: 10.1534/genetics.105.053892

Lazar, V., Pal Singh, G., Spohn, R., Nagy, I., Horvath, B., Hrtyan, M., et al. (2013). Bacterial evolution of antibiotic hypersensitivity. *Mol. Syst. Biol.* 9:700.

Lin, E. C., Koch, J. P., Chused, T. M., and Jorgensen, S. E. (1962). Utilization of L-alpha-glycerophosphate by *Escherichia coli* without hydrolysis. *Proc. Natl. Acad. Sci. U. S. A.* 48, 2145–2150. doi: 10.1073/pnas.48.12.2145

Litchman, E., Edwards, K. F., and Klausmeier, C. A. (2015). Microbial resource utilization traits and trade-offs: implications for community structure, functioning, and biogeochemical impacts at present and in the future. *Front. Microbiol.* 6:254. doi: 10.3389/fmicb.2015.00254

Maciag, A., Peano, C., Pietrelli, A., Egli, T., De Bellis, G., and Landini, P. (2011). *In vitro* transcription profiling of the sigmaS subunit of bacterial RNA polymerase: re-definition of the sigmaS regulon and identification of sigmaS-specific promoter sequence elements. *Nucleic Acids Res.* 39, 5338–5355. doi: 10.1093/nar/gkr129

Mitchell, A., Romano, G. H., Groisman, B., Yona, A., Dekel, E., Kupiec, M., et al. (2009). Adaptive prediction of environmental changes by microorganisms. *Nature* 460, 220–224.

Mitrophanov, A. Y., and Groisman, E. A. (2008). Positive feedback in cellular control systems. *Bioessays* 30, 542–555.

Mitsui, K., Ohnishi, R., Hirose, S., and Igarashi, K. (1984). Necessity of polyamines for maximum *in vivo* synthesis of beta beta' subunits of RNA polymerase. *Biochem. Biophys. Res. Commun.* 123, 528–534. doi: 10.1016/0006-291x(84)90261-4

Navarro Llorens, J. M., Tormo, A., and Martinez-Garcia, E. (2010). Stationary phase in gram-negative bacteria. *FEMS Microbiol. Rev.* 34, 476–495. doi: 10.1111/j.1574-6976.2010.00213.x

New, A. M., Cerulus, B., Govers, S. K., Perez-Samper, G., Zhu, B., Boogmans, S., et al. (2014). Different levels of catabolite repression optimize growth in stable and variable environments. *PLoS Biol.* 12:e1001764. doi: 10.1371/journal.pbio.1001764

Nishino, K., Senda, Y., and Yamaguchi, A. (2008). CRP regulator modulates multidrug resistance of *Escherichia coli* by repressing the mdtEF multidrug efflux genes. *J. Antibiot. (Tokyo)* 61, 120–127. doi: 10.1038/ja.2008.120

Notley-McRobb, L., King, T., and Ferenci, T. (2002). rpoS mutations and loss of general stress resistance in *Escherichia coli* populations as a consequence of conflict between competing stress responses. *J. Bacteriol.* 184, 806–811. doi: 10.1128/JB.184.3.806-811.2002

Ochrombel, I., Ott, L., Kramer, R., Burkovski, A., and Marin, K. (2011). Impact of improved potassium accumulation on pH homeostasis, membrane potential adjustment and survival of *Corynebacterium glutamicum*. *Biochim. Biophys. Acta* 1807, 444–450. doi: 10.1016/j.bbabio.2011.01.008

Olson, N. D., Lund, S. P., Colman, R. E., Foster, J. T., Sahl, J. W., Schupp, J. M., et al. (2015). Best practices for evaluating single nucleotide variant calling methods for microbial genomics. *Front. Genet.* 6:235. doi: 10.3389/fgene.2015.00235

Ozbudak, E. M., Thattai, M., Kurtser, I., Grossman, A. D., and Van Oudenaarden, A. (2002). Regulation of noise in the expression of a single gene. *Nat. Genet.* 31, 69–73.

Pradhan, A., Ma, Q., De Assis, L. J., Leaves, I., Larcombe, D. E., Rodriguez Rondon, A. V., et al. (2020). Anticipatory stress responses and immune evasion in fungal pathogens. *Trends Microbiol.* 29, 416–427. doi: 10.1016/j.tim.2020.09.010

Prajapat, M. K., Jain, K., Choudhury, D., Raj, N., and Saini, S. (2016). Revisiting demand rules for gene regulation. *Mol. Biosyst.* 12, 421–430. doi: 10.1039/c5mb00693g

Quintero-Yanes, A., Monson, R. E., and Salmond, G. P. C. (2019). Environmental potassium regulates bacterial flotation, antibiotic production and turgor pressure in Serratia through the TrkH transporter. *Environ. Microbiol.* 21, 2499–2510. doi: 10.1111/1462-2920.14637

Ravasz, E., Somera, A. L., Mongru, D. A., Oltvai, Z. N., and Barabasi, A. L. (2002). Hierarchical organization of modularity in metabolic networks. *Science* 297, 1551–1555. doi: 10.1126/science.1073374

Roselius, L., Langemann, D., Muller, J., Hense, B. A., Filges, S., Jahn, D., et al. (2014). Modelling and analysis of a gene-regulatory feed-forward loop with basal expression of the second regulator. *J. Theor. Biol.* 363, 290–299. doi: 10.1016/j.jtbi.2014.08.043

Rosenfeld, N., Young, J. W., Alon, U., Swain, P. S., and Elowitz, M. B. (2005). Gene regulation at the single-cell level. *Science* 307, 1962–1965. doi: 10.1126/science.1106914

Rosenfeld, N., Young, J. W., Alon, U., Swain, P. S., and Elowitz, M. B. (2007). Accurate prediction of gene feedback circuit behavior from component properties. *Mol. Syst. Biol.* 3:143. doi: 10.1038/msb4100185

Rubinstein, M., and de Souza, F. S. (2013). Evolution of transcriptional enhancers and animal diversity. *Philos. Trans. R. Soc. Lond. B Biol. Sci.* 368:20130017. doi: 10.1098/rstb.2013.0017

Saini, S., Slauch, J. M., Aldridge, P. D., and Rao, C. V. (2010). Role of cross talk in regulating the dynamic expression of the flagellar *Salmonella* pathogenicity island 1 and type 1 fimbrial genes. *J. Bacteriol.* 192, 5767–5777. doi: 10.1128/JB.00624-10

Schlosser, A., Meldorf, M., Stumpe, S., Bakker, E. P., and Epstein, W. (1995). TrkH and its homolog, TrkG, determine the specificity and kinetics of cation transport by the Trk system of *Escherichia coli*. *J. Bacteriol.* 177, 1908–1910.

Schneider, D. A., Ross, W., and Gourse, R. L. (2003). Control of rRNA expression in *Escherichia coli*. *Curr. Opin. Microbiol.* 6, 151–156. doi: 10.1016/s1369-5274(03)00038-9

Schuber, F. (1989). Influence of polyamines on membrane functions. *Biochem. J.* 260, 1–10. doi: 10.1042/bj2600001

Seemann, T. (2015). *Snippy: Fast Bacterial Variant Calling From NGS Reads*. Available Online at: https://github.com/tseemann/snippy (accessed August 15, 2021).

Seo, S. W., Kim, D., Szubin, R., and Palsson, B. O. (2015). Genome-wide reconstruction of OxyR and SoxRS transcriptional regulatory networks under oxidative stress in *Escherichia coli* K-12 MG1655. *Cell Rep.* 12, 1289–1299. doi: 10.1016/j.celrep.2015.07.043

Shen-Orr, S. S., Milo, R., Mangan, S., and Alon, U. (2002). Network motifs in the transcriptional regulation network of *Escherichia coli*. *Nat. Genet.* 31, 64–68. doi: 10.1038/ng881

Siryaporn, A., and Goulian, M. (2008). Cross-talk suppression between the CpxA-CpxR and EnvZ-OmpR two-component systems in E-coli. *Mol. Microbiol.* 70, 494–506. doi: 10.1111/j.1365-2958.2008.06426.x

Skerker, J. M., Perchuk, B. S., Siryaporn, A., Lubin, E. A., Ashenberg, O., Goulian, M., et al. (2008). Rewiring the specificity of two-component signal transduction systems. *Cell* 133, 1043–1054. doi: 10.1016/j.cell.2008.04.040

Sneppen, K., Krishna, S., and Semsey, S. (2010). Simplified models of biological networks. *Annu. Rev. Biophys.* 39, 43–59. doi: 10.1146/annurev.biophys.093008.131241

Soo, V. W., and Wood, T. K. (2013). Antitoxin MqsA represses curli formation through the master biofilm regulator CsgD. *Sci. Rep.* 3:3186. doi: 10.1038/srep03186

Stern, S., Powers, T., Changchien, L. M., and Noller, H. F. (1989). RNA-protein interactions in 30S ribosomal subunits: folding and function of 16S rRNA. *Science* 244, 783–790. doi: 10.1126/science.2658053

Suel, G. M., Garcia-Ojalvo, J., Liberman, L. M., and Elowitz, M. B. (2006). An excitable gene regulatory circuit induces transient cellular differentiation. *Nature* 440, 545–550. doi: 10.1038/nature04588

Swain, P. S., and Siggia, E. D. (2002). The role of proofreading in signal transduction specificity. *Biophys. J.* 82, 2928–2933. doi: 10.1016/S0006-3495(02)75633-6

Tabor, H., and Tabor, C. W. (1964). Spermidine, spermine, and related amines. *Pharmacol. Rev.* 16, 245–300.

Tagkopoulos, I., Liu, Y. C., and Tavazoie, S. (2008). Predictive behavior within microbial genetic networks. *Science* 320, 1313–1317. doi: 10.1126/science.1154456

Thompson, J. F., and Hearst, J. E. (1983). Structure-function relations in E. coli 16S RNA. *Cell* 33, 19–24.

Thorner, J. W., and Paulus, H. (1973). Catalytic and allosteric properties of glycerol kinase from *Escherichia coli*. *J. Biol. Chem.* 248, 3922–3932. doi: 10.1016/s0021-9258(19)43821-0

Venturelli, O. S., Zuleta, I., Murray, R. M., and El-Samad, H. (2015). Population diversification in a yeast metabolic program promotes anticipation of environmental shifts. *PLoS Biol.* 13:e1002042. doi: 10.1371/journal.pbio.1002042

Wang, J., Atolia, E., Hua, B., Savir, Y., Escalante-Chong, R., and Springer, M. (2015). Natural variation in preparation for nutrient depletion reveals a cost-benefit tradeoff. *PLoS Biol.* 13:e1002041. doi: 10.1371/journal.pbio.1002041

Wittkopp, P. J., and Kalay, G. (2011). Cis-regulatory elements: molecular mechanisms and evolutionary processes underlying divergence. *Nat. Rev. Genet.* 13, 59–69. doi: 10.1038/nrg3095

Wray, G. A. (2007). The evolutionary significance of cis-regulatory mutations. *Nat. Rev. Genet.* 8, 206–216. doi: 10.1038/nrg2063

Wunderlich, Z., and Mirny, L. A. (2009). Different gene regulation strategies revealed by analysis of binding motifs. *Trends Genet.* 25, 434–440. doi: 10.1016/j.tig.2009.08.003

Zaslaver, A., Mayo, A., Ronen, M., and Alon, U. (2006b). Optimal gene partition into operons correlates with gene functional order. *Phys. Biol.* 3, 183–189. doi: 10.1088/1478-3975/3/3/003

Zaslaver, A., Bren, A., Ronen, M., Itzkovitz, S., Kikoin, I., Shavit, S., et al. (2006a). A comprehensive library of fluorescent transcriptional reporters for *Escherichia coli*. *Nat. Methods* 3, 623–628. doi: 10.1038/nmeth895

Zinser, E. R., and Kolter, R. (2004). *Escherichia coli* evolution during stationary phase. *Res. Microbiol.* 155, 328–336. doi: 10.1016/j.resmic.2004.01.014

Zwaig, N., Kistler, W. S., and Lin, E. C. (1970). Glycerol kinase, the pacemaker for the dissimilation of glycerol in *Escherichia coli*. *J. Bacteriol.* 102, 753–759. doi: 10.1128/jb.102.3.753-759.1970

Zwaig, N., and Lin, E. C. (1966). Feedback inhibition of glycerol kinase, a catabolic enzyme in *Escherichia coli*. *Science* 153, 755–757. doi: 10.1126/science.153.3737.755

Conflict of Interest: The authors declare that the research was conducted in the absence of any commercial or financial relationships that could be construed as a potential conflict of interest.

Publisher's Note: All claims expressed in this article are solely those of the authors and do not necessarily represent those of their affiliated organizations, or those of the publisher, the editors and the reviewers. Any product that may be evaluated in this article, or claim that may be made by its manufacturer, is not guaranteed or endorsed by the publisher.

frontiers in Microbiology

ORIGINAL RESEARCH
published: 10 February 2022
doi: 10.3389/fmicb.2022.831174

Exploration of Diverse Secondary Metabolites From *Streptomyces* sp. YINM00001, Using Genome Mining and One Strain Many Compounds Approach

Tao Liu[1†], Zhen Ren[2†], Wei-Xun Chunyu[3†], Gui-Ding Li[1], Xiu Chen[2], Zhou-Tian-Le Zhang[1], Hui-Bing Sun[1], Mei Wang[1], Tian-Peng Xie[1], Meng Wang[1], Jing-Yuan Chen[1], Hao Zhou[1], Zhong-Tao Ding[1,4]* and Min Yin[1]**

[1] School of Medicine, School of Chemical Science and Technology, Yunnan University, Kunming, China, [2] School of Agriculture and Life Sciences, Kunming University, Kunming, China, [3] Department of Pathogen Biology and Immunology, Kunming Medical University, Kunming, China, [4] College of Pharmacy, Dali University, Dali, China

A talented endophytic bacteria strain YINM00001, which showed strong antimicrobial activity and multiple antibiotic resistances, was isolated from a Chinese medicinal herb *Peperomia dindygulensis* Miq. Phylogenetic analysis based on 16S rRNA gene sequences demonstrated that strain was closely related to *Streptomyces anulatus* NRRL B-2000T (99.93%). The complete genome of strain YINM00001 was sequenced. The RAxML phylogenomic tree also revealed that strain YINM00001 was steadily clustered on a branch with strain *Streptomyces anulatus* NRRL B-2000T under the 100 bootstrap values. The complete genome of strain YINM00001 consists of an 8,372,992 bp linear chromosome (71.72 mol% GC content) and a 317,781 bp circular plasmid (69.14 mol% GC content). Genome mining and OSMAC approach were carried out to investigate the biosynthetic potential of producing secondary metabolites. Fifty-two putative biosynthetic gene clusters of secondary metabolites were found, including the putative cycloheximide, dinactin, warkmycin, and anthracimycin biosynthetic gene clusters which consist with the strong antifungal and antibacterial activities exhibited by strain YINM00001. Two new compounds, peperodione (**1**) and peperophthalene (**2**), and 17 known compounds were isolated from different fermentation broth. Large amounts and high diversity of antimicrobial and/or anticancer compounds cycloheximide, dinactin, anthracimycin, and their analogs had been found as predicted before, which highlights strain YINM00001 as an ideal candidate for further biosynthetic studies and production improvement of these valuable compounds. Meanwhile, several gene clusters that were highly conserved in several sequenced actinomycetes but significantly different from known gene clusters might be silent under proceeding fermentation conditions. Further studies, such as heterologous expression and genetic modification, are needed to explore more novel compounds from this talented endophytic *Streptomyces* strain.

Keywords: *Peperomia dindygulensis*, endophytic actinomycetes, genome mining, OSMAC approach, secondary metabolites

OPEN ACCESS

Edited by:
Yu-Qin Zhang,
Institute of Medicinal Biotechnology, Chinese Academy of Medical Sciences, China

Reviewed by:
Dewu Zhang,
Institute of Medicinal Biotechnology, Chinese Academy of Medical Sciences, China
Geoff Horsman,
Wilfrid Laurier University, Canada
Fuhang Song,
Beijing Technology and Business University, China

***Correspondence:**
Hao Zhou
haozhou@ynu.edu.cn
Zhong-Tao Ding
ztding@ynu.edu.cn
Min Yin
yinmin@ynu.edu.cn;
ym3612003@163.com

† These authors have contributed equally to this work

Specialty section:
This article was submitted to Systems Microbiology, a section of the journal Frontiers in Microbiology

Received: *08 December 2021*
Accepted: *07 January 2022*
Published: *10 February 2022*

Citation:
Liu T, Ren Z, Chunyu W-X, Li G-D, Chen X, Zhang Z-T-L, Sun H-B, Wang M, Xie T-P, Wang M, Chen J-Y, Zhou H, Ding Z-T and Yin M (2022) Exploration of Diverse Secondary Metabolites From Streptomyces sp. YINM00001, Using Genome Mining and One Strain Many Compounds Approach. Front. Microbiol. 13:831174. doi: 10.3389/fmicb.2022.831174

INTRODUCTION

The development of new drugs lags far behind the outbreak of infectious diseases and cancers. It is urgent to find novel natural products. Plenty of bioactive natural products were found from actinomycetes, including clinical and agricultural antibiotics, antitumor drugs, immunosuppressants, and other active drugs. Actinomycetes are responsible for about 10,100 of the 22,500 bioactive microbial metabolites that have been discovered so far; about 150 compounds were directly applied to humans, animals, and agriculture (Berdy, 2005; Newman and Cragg, 2020). However, with the accumulation of strains and compounds year by year, the probability of rediscovery of studied strains and known compounds is greatly increased. In addition, time-consuming and guideless traditional fermentation makes it difficult to find novel natural products. Using new research methods to explore new actinomycetes trains isolated from new habitats might be a new way to discover novel natural products (Shen, 2015; Newman and Cragg, 2020).

Endophytic bacteria, which live in almost all studied plants, are important components of the host ecosystem. Many endophytes could give beneficial feedback to their host in different ways, including growth promotion, pathogen suppression, contaminants remove, phosphate solubilization, nitrogen fixation, etc. (Assmus et al., 1995; Sessitsch et al., 2002; Hardoim et al., 2008). During the long time interaction with their host, Chinese medicinal herb derived endophytic bacteria, especially actinomycetes strains, could produce various bioactive natural products that make them valuable resources for drug leads discovery.

Chinese medicinal herbs have been used as anti-infection and anti-cancer drugs for thousands of years. Many natural products isolated from Chinese medicinal herbs showed considerable antibacterial, antifungal, antiviral, and antitumor activities (Lee, 2000). *Peperomia dindygulensis* Miq. is a fleshy herb mainly found in southern China. Compounds with antitumor, anti-inflammatory, and antiviral activities had been isolated from *Peperomia dindygulensis*, including Secolignans, tetrahydrofuran lignans, chromones, and acylcyclohexane-1,3-diones. It is commonly used for treatment of cough, asthma, measles, burns, and cancers in southwest China (Wang et al., 2012). However, the endophytic bacteria of *Peperomia dindygulensis* are still poorly characterized.

On the basis of the deepening understanding of the biosynthesis mechanism of some secondary metabolites, genome mining has become a new way to explore new natural products. By applying the knowledge of biosynthetic pathways, potential gene clusters can be mined from the genome, skeletal structure of the relative products can be predicted, and some gene clusters can be activated in a variety of ways, so as to discover new natural products. Meanwhile, because some bacteria can potentially produce many more metabolites than they do under determined conditions, the "one strain many compounds" (OSMAC) approach had been widely used in recent years (Bode et al., 2002; Romano et al., 2018). Therefore, using genomic mining and OSMAC approach together to investigate new actinomycetes strains from new habitats may get better results.

In this study, endophytic bacteria, including *Streptomyces* strains, were isolated from *Peperomia dindygulensis* Miq. One of the *Streptomyces* strains, designed YINM00001, showed strong antimicrobial activity and multi-antibiotics resistance and was chosen for secondary metabolites discovery by using genome mining and OSMAC approach. Totally, 19 natural products including two new compounds were found from different fermentation broths of strain YINM00001. Some compounds had been predicted by genome mining before isolation, and several active compounds were consistent with the activities exhibited by strain YINM00001. Our study showed the great potential of genome mining and OSMAC in natural products exploration from novel strains.

MATERIALS AND METHODS

Bacterial Isolation

Fresh *Peperomia dindygulensis* were collected from the Chinese medicinal herb garden in Kunming University, Yunnan Province, China. Ten healthy plants, including leaves, stems, and roots, were randomly chosen from the garden. All the samples were stored at 4°C and processed within 12 h. The whole plants were washed with tap water and distilled water several times, and then immersed in 70% ethanol (v/v) and sodium hypochlorite solution (0.5% available chlorine) for 1 min, respectively. After being washed with distilled water thoroughly three times, the whole plants were smashed into small pieces with a sterilized grinder (Ren et al., 2018). The juice and residues were plated onto ISP2 agar (soytone 4 g, malt extract 10 g, glucose 4 g, agar 20 g, H_2O 1000 ml, pH = 7.2) and Gause's synthetic agar (soluble starch 20 g, sodium chloride 0.5 g, ferrous sulfate 0.01 g, potassium nitrate 1 g, sipotassium hydrogen phosphate 0.5 g, magnesium sulfate 0.5 g, agar 15 g, pH = 7.2) supplemented with nystatin and nalidixic acid (50 μg/ml each) to isolate actinomycetes strains. Then, the plates were incubated at 28°C for up to a month. The actinomycete strains were picked out and purified on ISP2 plates with nystatin and nalidixic acid. The purified cultures were preserved in ISP2 slants and 20% (v/v) glycerol tubes and stored at 4 and −80°C, respectively, for further using. Genomic DNA isolation, 16S rRNA gene amplification, and sequencing were done as described before (Li et al., 2021).

Antimicrobial Activity and Antibiotic Resistance Assay

Fresh cultures of isolated strains were inoculated on ISP2 agar disks and incubated at 28°C for a week. The liquid cultures of activated pathogens, including *Escherichia coli* (CGMCC 1.2385), *Pseudomonas aeruginosa* (CGMCC 1.2387), *Bacillus subtilis* (CGMCC 1.1849), *Staphylococcus aureus* (CGMCC 1.2386), *Mycobacterium tuberculosis* (ATCC 25177), *Fusarium oxysporum* (MW149127.1), *Candida albicans* (CGMCC 2.2086), and *Fusarium fulcrum* (MW149128.1), were mixed well with Mueller-Hinton Agar (beef extract powder 2 g, casein hydrolyzate 17.5 g, starch 1.5 g, agar 12 g, pH = 7.3) 1:1 v/v and then spread on the top of ISP2 agar. Once the top agar had solidified, about 5 mm

diameter ISP2 agar with a single colony of each isolated strains was placed on the top agar and incubated at 28°C for a week.

Fresh cultures of isolated strains were inoculated on ISP2 agar supplemented with chloramphenicol (50 μg/ml), kanamycin (200 μg/ml), levofloxacin (50 μg/ml), vancomycin (50 μg/ml), rifampicin (50 μg/ml), oxytetracycline (50 μg/ml), apramycin (50 μg/ml), and bacitracin (50 μg/ml) and incubated at 28°C for 5 days.

Genome Sequencing and Mining

A single colony of strain YINM00001 was inoculated into 50 ml Tryptic Soy Broth (TSB) medium (casein tryptone 17 g, soy peptone 5 g, sodium chloride 5 g, D-glucose 2.5 g, dipotassium phosphate 2.5 g, H_2O up to 1,000 ml, pH = 7.3) for 36 h at 28°C with 200 rpm vigorous shaking. DNA isolation and purification in strain YINM00001 were carried out according to standard procedures (Pospiech and Neumann, 1995). The quality and quantity of purified genomic DNA were analyzed by using NanoDrop 2000 spectrophotometer (Thermo Scientific, Wilmington, DE, United States) and 0.8% agarose gel electrophoresis.

For Pacbio sequencing, genomic DNA was sheared to 8–10 kb length fragments randomly and a genomic DNA library was constructed. Pacbio clean data were generated by sequencing platform; all the reads were assembled and checked using HGAP software (Rhoads and Au, 2015). For Illumina Hiseq sequencing, genomic DNA was sheared to about 400 bp length fragments randomly and a genomic DNA library was constructed. PE150 pair-end sequencing was carried out, and clean data were obtained. SOAPdenovo V2.04 (Luo et al., 2012) was used to check and assemble all the reads.

The DNA G+C mol% value was obtained from the genomic sequence. The protein coding sequences of the chromosome and plasmid were predicted by Glimmer (v3.02) (Delcher et al., 2007) and GeneMarkS, respectively (Besemer et al., 2001). tRNA and rRNA were predicted with tRNAscan-SE v2.0 (Chan et al., 2021) and Barrnap,[1] respectively. EzTaxon-e database (Yoon et al., 2017) was used to identify phylogenetic neighbors of isolated strains. Phylogenetic tree of 16S rRNA gene was reconstructed based on neighbor-joining (NJ) (Saitou and Nei, 1987) in mega software (version 7.0.14) (Kumar et al., 2016). Evolutionary distances for the analyses were calculated using the Kimura two-parameter model (Kimura, 1980). The genome tree based on the concatenated sequences of 557 protein marker genes was reconstructed using RAxML (Stamatakis, 2014), and fast bootstrapping (Stamatakis et al., 2008) was used to generate the support values in the tree.

Clusters of Orthologous Groups of proteins (COG) and Gene Ontology (GO) programs (Tatusov et al., 2003; Gene Ontology Consortium, 2021) were used to analyze the function of annotated genes. Kyoto Encyclopedia of Genes and Genomes (KEGG) PATHWAY analysis (Kanehisa and Goto, 2000) was carried out to determine the key potential pathways in strain YINM00001. CRISPR finder platform (Grissa et al., 2007) was used to identify CRISPR-Cas sequences on chromosome. PHAST (Zhou et al., 2011) was used to identify putative prophages on the chromosome. Tandem repeats finder (Benson, 1999) and Repeatmasker[2] were used to identify simple tandem repeats and interspersed repeats, respectively. Genomic islands were predicted with IslandViewer 4 (Bertelli et al., 2017). Transposable elements were identified with ISEScan (Xie and Tang, 2017). ResFinder (Zankari et al., 2012) and the Comprehensive Antibiotic Resistance Database (CARD) (Jia et al., 2017) were used to predict resistance genes. The VFDB database (Chen et al., 2016) was used to predict bacterial virulence factors.

The biosynthetic gene clusters for putative secondary metabolites were identified using the antiSMASH 5.0 (Blin et al., 2019) and PRISM 4 programs (Skinnider et al., 2020) and then verified by manual inspection.

One Strain Many Compounds Strategy Fermentation

For small scale fermentation, the strain YINM00001 was activated in MS medium (soya flour 20 g, mannitol 20 g, agar 20 g, H_2O up to 1,000 ml, pH = 7.0) at 28°C for 4 days. The activated strain was inoculated into 500 ml Erlenmeyer flasks containing 100 ml of TSB medium and cultured for 4 days at 28°C and 200 rpm. Then, 5.0 ml of the seed culture was transferred into 500 ml Erlenmeyer flasks containing 100 ml of 10 different types of fermentation media (1#–10#, data not show), respectively.

For large scale fermentation, seed cultures of strain YINM00001 were prepared as described above. Then, 5.0 ml of the seed cultures were transferred into 500 ml Erlenmeyer flasks containing 100 ml of 4# and 9# fermentation media (4# medium, soluble starch 40 g, corn extract 10 g, monopotassium phosphate 0.5 g, magnesium sulfate 0.25 g, zinc sulfate heptahydrate 40 mg, methionine 0.1 g, vitamin B12 0.1 g, calcium carbonate 5 g, H_2O up to 1000 ml, pH = 7.2; 9# medium, glucose 10 g, glycerol 10 ml, corn extract 2.5 g, peptone 5 g, soluble starch 10 g, yeast extract 2 g, calcium carbonate 3 g, sodium chloride 1 g, H_2O up to 1,000 ml, pH = 7.3), respectively, and cultured for 10 days at 28°C and 200 rpm (15 L each).

Isolation and Identification of Compounds

The broth was extracted with equal volume ethyl acetate (EtOAc) three times, and the solvent was removed under vacuum to obtain the EtOAc extract. The crude extract of 4# medium fermentation broth (10.2 g) was separated into four fractions (Fr.1–Fr.4) by LiChroprep RP-18 column, eluting stepwise with a MeOH-H_2O gradient (30% MeOH, 50% MeOH, 70% MeOH, and 100% MeOH). Fr.1 was fractionated by a Sephadex LH-20 column with MeOH to afford Fr.1-1 to Fr.1-4. Then, Fr.1-1 was separated by a Sephadex LH-20 column with MeOH to obtain **10** (34.2 mg). Fr.1-3 was chromatographed using a silica gel column (petroleum ether-acetone, 150:1 to 20:1) to obtain **17** (20.5 mg) and **18** (26.3 mg). Fr.2 was separated by a Sephadex LH-20 column with MeOH to give **3** (36.8 mg) and **4** (15.9 mg). Fr.3 was divided into three parts (Fr.3-1 to Fr.3-3) by a Sephadex LH-20 column with

[1]https://github.com/tseemann/barrnap

[2]http://www.repeatmasker.org

MeOH. Fr.3-1 was purified by a silica gel column with CH_2Cl_2-EtOAc (80:1-9:1) to afford **15** (13.5 mg) and **16** (15.8 mg). Fr.3-2 was separated by a silica gel column (petroleum ether-acetone, 50:1 to 1:1) to obtain **1** (8.9 mg). Fr.3-3 was chromatographed using a silica gel column (CH_2Cl_2-MeOH, 100:1-10:1) to give **5** (8.5 mg) and **6** (8.5 mg). Fr.4 was divided into three parts (Fr.4-1 to Fr.4-3) by a Sephadex LH-20 column with MeOH. Fr.4-1 was fractionated by a silica gel column with CH_2Cl_2-MeOH (100:1-10:1) to afford **19** (16.5 mg). Fr.4-2 was separated by a Sephadex LH-20 column with MeOH to give **11/12** (20.6 mg) and **13/14** (17.9 mg). Fr.4-3 was chromatographed using a silica gel column (CH_2Cl_2-MeOH, 130:1-10:1) to yield **7** (9.5 mg), **8** (14.3 mg), and **9** (11.9 mg). The crude extract of 9# medium fermentation broth (9.1 g) was also separated into four fractions (Fr.1–Fr.4) by LiChroprep RP-18 column, eluting stepwise with a MeOH-H_2O gradient (30% MeOH, 50% MeOH, 70% MeOH, and 100% MeOH). Fr.3 was divided into two parts (Fr.3-1 to Fr.3-2) by a Sephadex LH-20 column with MeOH. Fr.3-2 was chromatographed using a silica gel column (CH_2Cl_2-MeOH, 100:1-20:1) to give **2** (4.2 mg).

The 1D and 2D NMR spectra were measured on a Bruker Avance-400 MHz instrument (Bruker, Karlsruhe, Germany) with tetramethylsilane as the internal standard. HRESIMS data were obtained by an Agilent 1200 Q-TOF mass instrument (Agilent, Santa Clara, CA, United States). Silica gel (200-300 mesh, Qingdao Marine Chemical Group Co., Qingdao, China), Lichroprep RP-18 gel (40-63 mm, Merck, Darmstadt, Germany), and Sephadex LH-20 (GE Healthcare Bio-Science AB, Uppsala, Sweden) were used for column chromatography (CC). Thin-layer chromatography (TLC) was performed on silica gel GF254 plates (Qingdao Haiyang Chemical Co., Ltd., Qingdao, China) and visualized by spraying with anisaldehyde-H_2SO_4 reagent. All solvents used for CC were of analytical grade from Chengdu Titan Chron Chemical Co., Ltd. (Chengdu, China).

RESULTS AND DISCUSSION

Strain Isolation and 16S rRNA Gene Sequence

A total of 39 endophytic bacteria, including 12 actinomycetes, were isolated from *Peperomia dindygulensis*. Phylogenetic analyses of the 16S rRNA gene sequences showed that strains *Streptomyces* sp. YM9, *Streptomyces* sp. YM74, *Streptomyces* sp. YM75, *Streptomyces* sp. YM77, *Streptomyces* sp. YM79, *Streptomyces* sp. YM80, *Streptomyces* sp. YM81, *Streptomyces* sp. YM83, *Streptomyces* sp. YM84, *Streptomyces* sp. YM85, *Streptomyces* sp. YM86, and *Streptomyces* sp. YINM00001 were closely related to *Streptomyces setonii*, *Streptomyces hydrogenans*, *Streptomyces coelescens*, *Streptomyces aurantiacus*, *Streptomyces bottropensis*, *Streptomyces cellulosae*, *Streptomyces lusitanus*, *Streptomyces albogriseolus*, *Streptomyces hydrogenans*, *Streptomyces speibonae*, *Streptomyces aureus*, and *Streptomyces fulvissimus*, respectively. Probably due to the thin stems, roots, and leaves of *Peperomia dindygulensis*, a large number of vulnerable bacteria were killed by surface sterilization with ethanol and sodium hypochlorite solution. Only a few dozen bacteria were isolated. *Streptomyces* spores are highly resistant to sterilization, and isolation media ISP2 and Gause's synthetic agar are suitable for the growth of actinomycetes, which might lead to separation of a variety of *Streptomyces* strains.

Antimicrobial Activity and Antibiotic Resistance of *Streptomyces* YINM00001

Strains of *Streptomyces* genius could produce various types of antibiotics. In this study, eight pathogens, including *Escherichia coli* (CGMCC 1.2385), *Pseudomonas aeruginosa* (CGMCC 1.2387), *Bacillus subtilis* (CGMCC 1.1849), *Staphylococcus aureus* (CGMCC 1.2386), *Mycobacterium tuberculosis* (ATCC 25177), *Fusarium oxysporum* (MW149127.1), *Candida albicans* (CGMCC 2.2086), and *Fusarium fulcrum* (MW149128.1), were chosen for antimicrobial activity screening. Among them, *Streptomyces* sp. YINM00001 showed strong inhibition activities against several gram positive bacterial and fungal pathogens, including *S. aureus*, *M. tuberculosis*, *F. oxysporum*, and *C. albicans*. Other strains showed certain antimicrobial activity against a few pathogens (**Table 1**). Antimicrobial activity test results indicated that *Streptomyces* sp. YINM00001 might have the capacity to produce different types of active antibiotics.

To avoid being killed by the antibiotics produced by the strains themselves, antibiotics resistant genes are often found within or beside the biosynthetic gene clusters. Testing the antibiotic resistance of the strains could unveil their possibility to produce antibiotics. Strain YINM00001 could grow well on ISP2 media with chloramphenicol, vancomycin, oxytetracycline, and bacitracin. Some of the remaining strains could grow on ISP2 media with different antibiotics (**Table 2**). Antibiotic resistance tests indicated that strain YINM00001 might produce chloramphenicol, glycopeptide, tetracycline, and polypeptide antibiotics. Based on the results of antimicrobial activity and antibiotic resistance screening, *Streptomyces* sp. YINM00001 was chosen for genome sequencing.

Genome Sequencing and Analysis of *Streptomyces* sp. YINM00001

The complete genome of strain YINM00001 was obtained by using Pacbio RSII and Illumina Hiseq platform. Approximately 1.62 Gb Pacbio and 1.08 Gb Illumina Hiseq clean data were generated. The average depth of genome coverage was 187-fold. The complete genome of strain YINM00001 was composed of a linear chromosome of 8,372,992 bp with a GC content of 71.72 mol% (accession no. CP086102) and a circular plasmid of 317,781 bp with a GC content of 69.14 mol% (accession no. CP086103).

The chromosome contained 7,506 predicted genes, including 18 rRNA genes, 67 tRNA genes, and 52 sRNA genes (**Figure 1** and **Table 3**). Six 16S rRNA genes were identified in the chromosome of strain YINM00001. The sequence of the 16S rRNA gene was used for phylogenetic analysis. Phylogenetic analyses of the 16S rRNA gene sequences showed that strain YINM00001 was a member of the genus *Streptomyces*. It was evident from the NJ phylogenetic tree that strain YINM00001 formed a cluster with *Streptomyces fulvorobeus* NBRC 15897T and *Streptomyces*

TABLE 1 | Antimicrobial activity assay of Streptomyces strains.

	Pathogens							
	***Escherichia coli* (CGMCC 1.2385)**	***Pseudomonas aeruginosa* (CGMCC 1.2387)**	***Bacillus subtilis* (CGMCC 1.1849)**	***Staphylococcus aureus* (CGMCC 1.2386)**	***Mycobacterium tuberculosis* (ATCC 25177)**	***Fusarium oxysporum* (MW149127.1)**	***Candida albicans* (CGMCC 2.2086)**	***Fusarium fulcrum* (MW149128.1)**
Isolates								
Streptomyces sp. YM83	−	−	++	−	−	−	−	−
Streptomyces sp. YM77	+	−	−	−	−	−	−	−
Streptomyces sp. YM86	+	−	−	+	−	−	−	−
Streptomyces sp. YM79	−	−	−	++	−	−	−	−
Streptomyces sp. YM75	−	+−	−	+	−	−	−	−
Streptomyces sp. YINM00001	−	−	−	+++	++	+++	+++	−
Streptomyces sp. YM74	+	−	−	−	−	−	−	−
Streptomyces sp. YM84	−	−	++	−	−	−	−	−
Streptomyces sp. YM81	+	−	−	+	−	−	−	−
Streptomyces sp. YM9	−	−	−	−	−	−	−	−
Streptomyces sp. YM85	+	+	−	−	−	−	−	−
Streptomyces sp. YM80	+	−	−	−	−	−	−	−

Diameter of inhibitory zone: +, <5 mm; ++, 5–10 mm; +++, >10 mm; -, no inhibitory zone.

TABLE 2 | Antibiotic resistance assay of Streptomyces strains.

	Antibiotics							
	Chloramphenicol (50 μg/ml)	**Kanamycin (200 μg/ml)**	**Levofloxacin (50 μg/ml)**	**Vancomycin (50 μg/ml)**	**Rifampicin (50 μg/ml)**	**Oxytetracycline (50 μg/ml)**	**Apramycin (50 μg/ml)**	**Bacitracin (50 μg/ml)**
Isolates								
Streptomyces sp. YM83	−	−	−	−	−	−	+	++
Streptomyces sp. YM77	−	−	−	−	+	−	+	+
Streptomyces sp. YM86	−	−	−	−	+	+	−	−
Streptomyces sp. YM79	−	−	−	+	−	+	−	+
Streptomyces sp. YM75	−	−	−	−	−	−	−	−
Streptomyces sp. YINM00001	++	−	−	++	−	++	−	++
Streptomyces sp. YM74	−	−	−	+	−	−	−	++
Streptomyces sp. YM84	−	−	−	−	−	−	−	+
Streptomyces sp. YM81	−	−	−	−	−	−	−	−
Streptomyces sp. YM9	+	−	−	+	−	−	−	+
Streptomyces sp. YM85	−	−	−	+	+	−	−	−
Streptomyces sp. YM80	−	−	−	−	−	−	−	−

Growth state: +, grow poorly; ++, grow well; -, did not grow.

microflavus NBRC 13062T. It showed the highest 16S rRNA gene sequence similarity (99.93%) with *Streptomyces anulatus* NRRL B-2000T (**Figure 2**). The RAxML phylogenomic tree demonstrated that strain YINM00001 formed a cluster with strain *S. anulatus* NRRL B-2000T under the 100 bootstrap values (**Figure 3**).

Among the identified genes, 5,628 and 5,165 genes were classified into functional categories based on clusters of orthologous genes of proteins (COG) and GO designation, respectively (**Supplementary Figures 1**, **2**). A total of 2,714 genes of KEGG pathways were assigned (**Supplementary Figure 3**). Fifty putative CRISPR repeat regions were identified on the chromosome of strain YINM00001 (**Table 3**). Two incomplete prophase remnants containing 70 and 25 coding sequences, respectively, were detected on the chromosome; the length of prophages ranges from 8,264 bp to 28,169 bp (**Table 3**). In total, 1,031 simple tandem repeats and 31 interspersed repeats were assigned (**Table 3**). Twenty genomic islands containing 459 genes which may contribute to the diversification and adaptation of microorganisms were found (**Table 3**). A total of 242 genes were assigned to be carbohydrate-active enzymes, including 27 auxiliary activities, 5 carbohydrate-binding modules, 58 carbohydrate esterases, 91 glycoside hydrolases, 55 glycosyl transferases, and six polysaccharide lyases (**Table 3**). One transposable element was found, which contains a 1,568 bp transposase (**Table 3**). In total, 446 genes were identified as

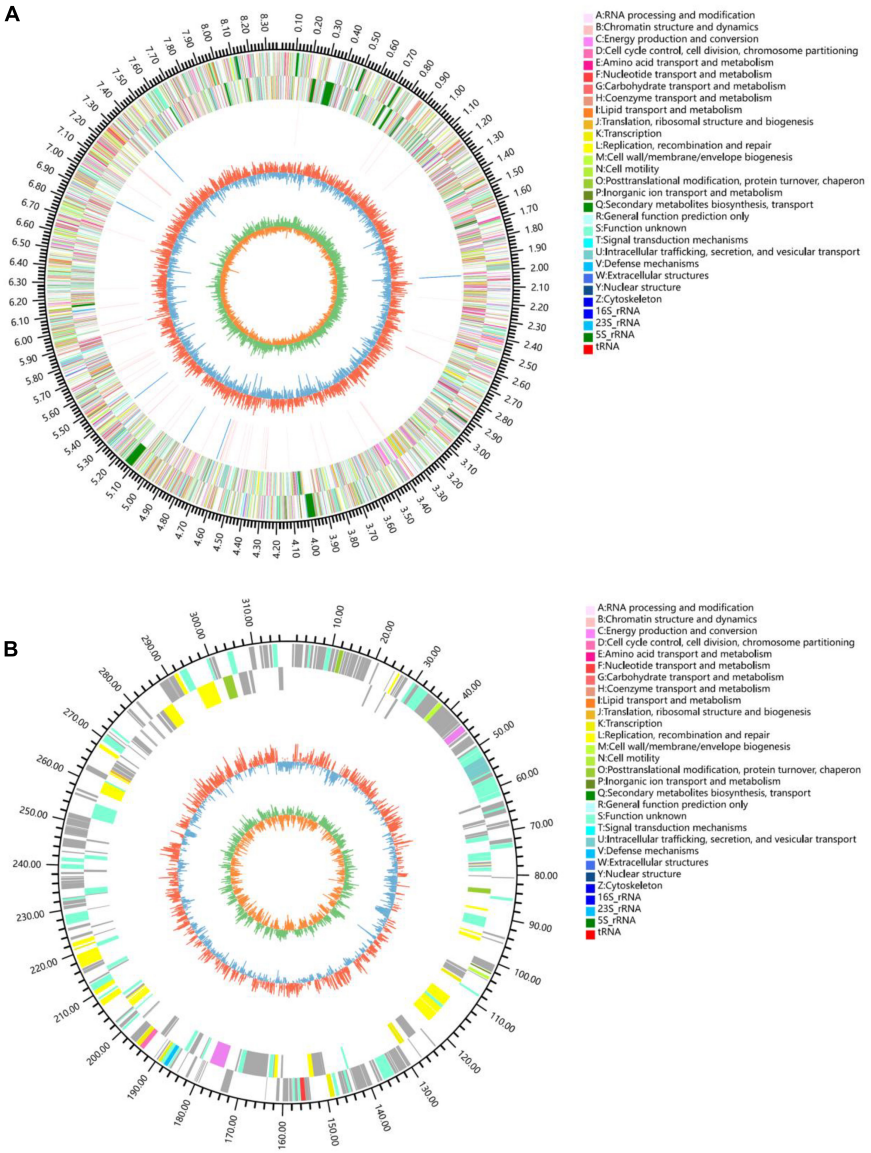

FIGURE 1 | Genome map of strain YINM00001. **(A)** Chromosome. **(B)** Plasmid. Tracks (from outer to inner): (1) genome size, (2) forward strand gene, colored according to COG classification, (3) reverse strand gene, colored according to COG classification, (4) rRNA and tRNA, (5) GC content, (6) GC skew.

antibiotic resistance genes, including one chloramphenicol resistance gene, 21 glycopeptide resistance genes, 31 tetracycline resistance genes, and 15 bacitracin resistance genes, which was consistent with the antibiotics resistance test results (**Table 3**). A total of 606 putative virulence factors were found (**Table 3**).

The circular plasmid contained 309 predicted genes, including 83 function assigned genes and 226 hypothetical proteins (**Figure 1**).

Genome Mining of Secondary Metabolites

Based on genome mining results, 52 putative biosynthetic gene clusters were found (**Table 4**), including 14 saccharides, 6 polyketides, 5 polyketide-non-ribosomal peptides, 5 terpenes, 4 non-ribosomal peptides, 4 fatty acids, 3 lantipeptides, 3 halogenated, 2 siderophores, 2 ectoines, 1 Ripps, 1 melanin, 1 butyrolactone, and 1 thiopeptide. Among them, 14 putative gene clusters showed high similarity (>70% of genes show similarity) to ectoine, dinactin, AmfS, melanin, cycloheximide, alkylresorcinol, SGR PTMs, geosmin, warkmycin, RP-1776, streptobactin, desferrioxamin B, and anthracimycin gene clusters. The presence of the putative cycloheximide (Yin et al., 2014), dinactin (Zhang et al., 2020), warkmycin (Helaly et al., 2013), and anthracimycin (Hensler et al., 2014) biosynthetic gene clusters was consistent with the strong antifungal and antibacterial activities of strain YINM00001. Three putative gene clusters showed moderate similarity (30–70% of genes

TABLE 3 | Genome features of strain YINM00001.

Feature	Chromosome characteristics
Chromosome size (bp)	8,372,992
GC content (%)	71.72%
Predicted genes	7,506
rRNA operons	18
tRNA genes	67
sRNA genes	52
Genes assigned to COG	5,628
Genes assigned to GO	5,165
Genes assigned to KEGG	2,714
CRISPR repeat regions	50
Prophages	2
Simple tandem repeats	1,031
Interspersed repeats	31
Genomic islands	20
Carbohydrate-active enzymes	242
Transposable element	1
Antibiotic resistance genes	446
Virulence factors	606
Secondary metabolite gene clusters	53
Plasmid size (bp)	317,781
Plasmid GC content (%)	69.14
Plasmid predicted genes	309

show similarity) to hopene, nucleocidin, and acarviostatin gene clusters. The existence of these putative gene clusters indicated that strain YINM00001 offers the opportunity to produce these important antibiotics or their analogs. Twenty-three putative gene clusters showed low similarity (<30% of genes show similarity) to reported frigocyclinone, steffimycin D, formicamycins, C-1027, dechlorocuracomycin, stambomycin, collismycin A, enduracidin, phosphonoglycans, retimycin A, CDA, asukamycin, cyclothiazomycin, herboxidiene, coelimycin P1, kanamycin, herboxidiene, SF2575, caniferolide, ficellomycin, kanamycin, and calicheamicin gene clusters. The other 13 putative gene clusters were not conserved relative to any known cluster. Some putative gene clusters were highly conserved in several sequenced actinomycetes but were significantly different from known gene clusters. The existence of these cryptic secondary metabolite biosynthetic gene clusters implied that novel antibiotics might be found from strain YINM00001.

Compounds Isolated Using Genome Mining and One Strain Many Compounds Approach

With the guidance of the genome mining results, strain YINM00001 was fermented using OSMAC approach. Two new compounds, peperodione (**1**) and peperophthalene (**2**), together with 17 known ones, were obtained (**Figure 4**). Their structures were established by extensive spectroscopic analyses.

The chemical investigations of the EtOAc extract of 4# medium fermentation of strain YINM00001 were performed. This led to the discovery of a new nonane-dione, peperodione (**1**), as well as 17 known compounds, actiphenol (**3**), 3-hydroxy-3-[2-(2-hydroxy-3,5-dimethylphenyl)-2-oxoethyl] glutarimide (**4**) (Sun et al., 2014), cycloheximide (**5**) (Schaeffer and Jain, 1963),

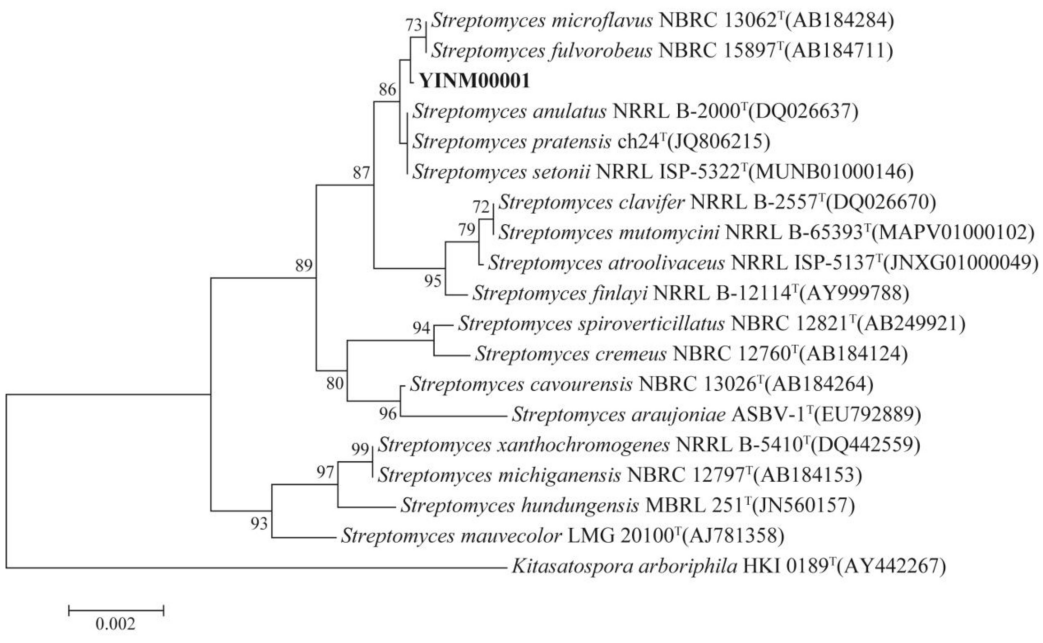

FIGURE 2 | The neighbor-joining phylogenetic tree of strain YINM00001 and its closest relatives from the genus *Streptomyces* based on 16S rRNA genes. Bootstrap values (>70%) based on 1,000 resamplings are given at the nodes. *Kitasatospora arboriphila* NRRL HKI 0189T (accession no. AY442267) was used as outgroup. Bar, 0.002 substitutions per nucleotide position.

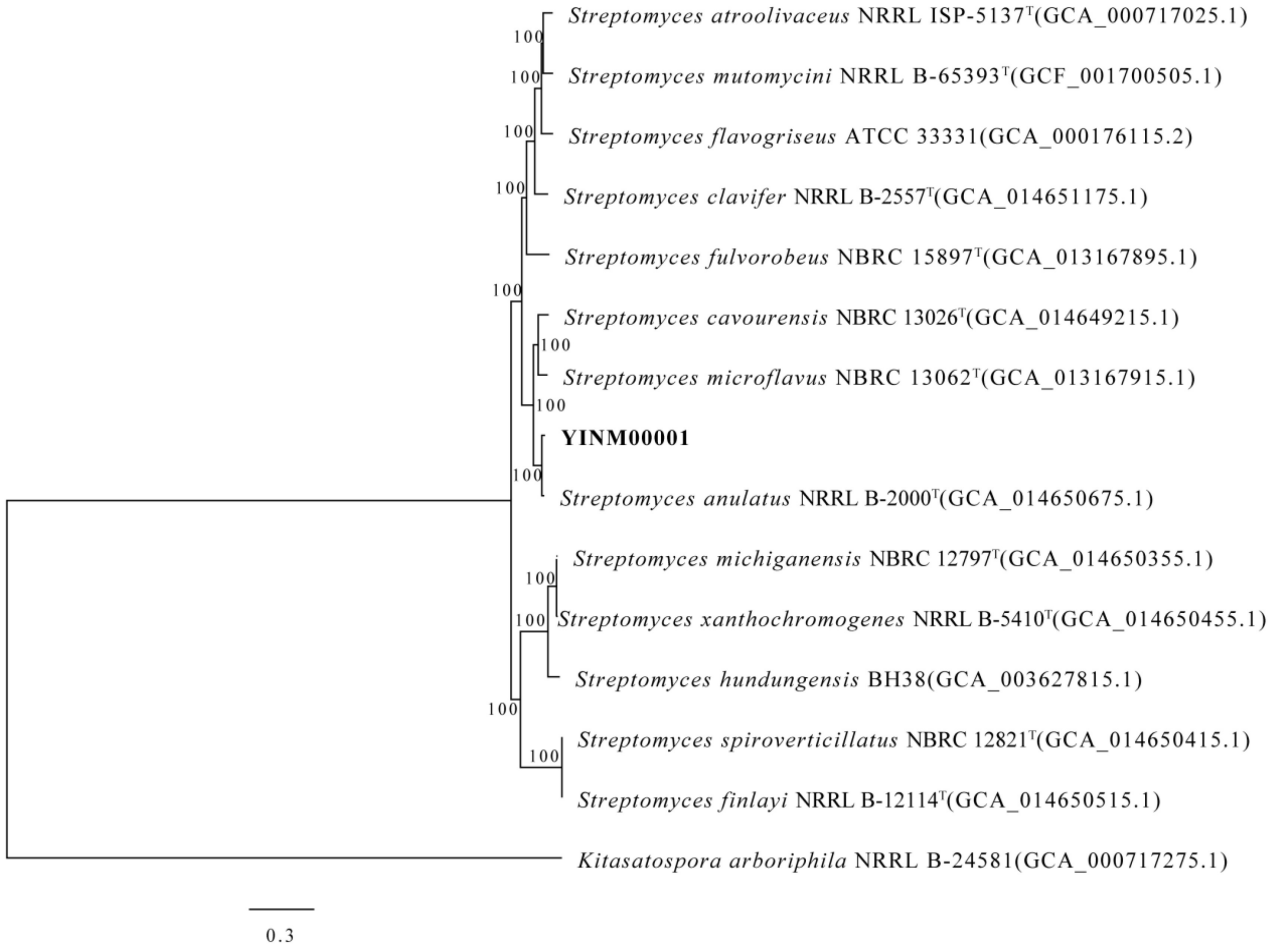

FIGURE 3 | The RAxML phylogenomic tree of strain YINM00001 and its closest relatives from the genus *Streptomyces* based on marker genes. Bootstrap values (>70%) based on 1,000 resamplings are given at the nodes. *Kitasatospora arboriphila* NRRL B-24581 (accession no. GCA_000717275) was used as outgroup. Bar, 0.3 substitutions per nucleotide position.

isocycloheximide (**6**) (Casey et al., 1976), naramycin B (**7**) (Johnson et al., 1965), 4-[2′-(3′′(*R*),5′′(*S*)-3′′,5′′-dimethyl-2′′-oxocyclohexylidene)ethyl]piperidine-2,6-dione (**8**), 4-[2′-(3′′(*S*),5′′(*S*)-3′′,5′′-dimethyl-2′′-oxocyclohexylidene)ethyl] piperidine-2,6-dione (**9**) (Guo et al., 2009), anthracimycin (**10**) (Jang et al., 2013), (±)-nonactic acid (**11/12**), (±)-homononactic acid (**13/14**) (Huang et al., 2015), feigrisolide C (**15**), methoxy-feigrisolide C (**16**) (Kim et al., 2005), bis-nonactic-homononactic trilactone (**17**) (Rezanka et al., 2004), dinactin (**18**) (Xie et al., 2014), and (*E*)-3-(methylthio)propenoic acid (**19**) (Detterbeck and Hesse, 2002). In an attempt to expand the metabolic profile, the strain was cultivated on 9# medium. Then, the research of the extract yielded a new methylnaphthalene, peperophthalene (**2**).

Peperodione (**1**) was isolated as a colorless solid, and its molecular formula was determined to be $C_9H_{14}O_2$ based on the HR-ESIMS data (*m/z* 177.0887 $[M + Na]^+$, calcd for 177.0886), implying the presence of three degrees of unsaturation. The ^{1}H NMR data of **1** revealed the presence of two olefin protons at δ_H 6.79 (1H, dt, J = 16.0, 6.4 Hz) and 6.06 (1H, d, J = 16.0 Hz). The ^{13}C NMR data of **1** (**Table 5**), with the aid of DEPT and HSQC spectral analyses (**Supplementary Figures 5**, **7**), revealed the presence of two carbonyls (at δ_C 209.8 and 198.7), two methyls (at δ_C 27.2 and 8.0), three sp^3 methylenes (at δ_C 40.4, 36.2, and 26.4), and two sp^2 methines (at δ_C 146.7 and 131.9). This analysis brought the total number of unsaturations to three, indicating the nature of being a chain molecule. The ^{1}H-^{1}H COSY spectrum (**Figure 5**) showed the presence of two independent spin systems, H-3/H-4/H-5/H-6 and H-8/H-9. The plane structure of **1** was confirmed by the HMBC correlations (**Figure 5**) from H-1 to C-2 and C-3, from H-3 and H-4 to C-2, from H-8 to C-6, as well as from H-5, H-6, H-8, and H-9 to C-7. Then, the $J_{3,4}$ = 16.0 Hz for H-3, 4 suggested a *trans* double bond in compound **1** as depicted in **Figure 4**.

Peperophthalene (**2**) was isolated as a white solid. A molecular formula of $C_{13}H_{14}O_3$ was assigned by interpretation of positive HRESIMS (*m/z* 219.1018 $[M + H]^+$, calcd for 219.1016), indicating 7 degrees of unsaturation. The ^{1}H NMR data (**Table 5**) displayed characteristic signals for four aromatic singlets at δ_H 7.49, 7.14, 7.05, and 6.55. The ^{13}C NMR and DEPT spectral data (**Table 5** and **Supplementary Figure 11**) allowed 13 carbon

TABLE 4 | Secondary metabolite clusters in strain YINM00001.

Cluster	Type	From	To	Most similar known biosynthetic gene cluster	Similarity
1	PKS-NRPS	84,576	136,796	Kanamycin	2%
2	PKS	193,333	260,857	Cycloheximide	100%
3	PKS	287,907	392,629	Alkylresorcinol	100%
4	Saccharide	396,814	437,537	Herboxidiene	9%
5	PKS-NRPS	479,532	531,991	Dutomycin	4%
6	PKS	550,475	596,892	C-1027	17%
7	PKS-NRPS	685,700	790,947	SGR PTMs	100%
8	NRPS	830,795	881,560	Nucleocidin	47%
9	Terpene	921,379	954,079	Hopene	69%
10	Fatty_acid	1,123,671	1,142,079	NA	
11	Fatty_acid	1,226,558	1,254,030	Dinactins	100%
12	Terpene	1,299,563	1,337,571	Formicamycins	18%
13	Fatty_acid	1,391,530	1,411,546	Asukamycin	9%
14	Saccharide	1,482,920	1,514,707	Dechlorocuracomycin	16%
15	RiPP	1,550,247	1,561,632	NA	
16	Saccharide	1,566,484	1,589,151	Enduracidin	14%
17	PKS	1,624,227	1,732,875	Warkmycin	97%
18	Halogenated	1,778,277	1,797,054	NA	
19	Siderophore	1,907,090	1,920,104	Ficellomycin	3%
20	Terpene	2,372,509	2,430,987	Stambomycin	16%
21	Saccharide	2,483,973	2,504,826	NA	
22	Saccharide	2,638,010	2,665,831	NA	
23	Saccharide	2,716,974	2,740,644	NA	
24	Lanthipeptide	2,771,646	2,804,777	AmfS	100%
25	Melanin	2,832,234	2,842,656	Melanin	100%
26	PKS-NRPS	2,863,825	2,952,386	Frigocyclinone	24%
27	Saccharide	3,015,862	3,043,856	Calicheamicin	2%
28	Saccharide	3,117,380	3,148,637	NA	
29	Halogenated	3,444,989	3,464,863	Caniferolide	4%
30	PKS-NRPS	3,934,309	4,114,251	RP-1776	95%
31	Ectoine	4,831,371	4,840,375	Ectoine	75%
32	PKS	5,085,935	5,173,228	Anthracimycin	73%
33	Saccharide	5,226,715	5,245,804	NA	
34	Saccharide	5,428,844	5,465,067	NA	
35	Siderophore	5,673,906	5,685,684	Desferrioxamin B	80%
36	Lanthipeptide	5,766,480	5,788,895	NA	
37	Saccharide	5,939,603	5,983,999	Phosphonoglycans	14%
38	Lanthipeptide	6,107,105	6,175,310	CDA	10%
39	Fatty_acid	6,201,945	6,221,750	NA	
40	Saccharide	6,415,616	6,444,572	Acarviostatin	33%
41	Saccharide	6,577,910	6,601,547	NA	
42	Saccharide	6,789,625	6,827,138	SF2575	6%
43	Ectoine	6,829,116	6,839,514	Ectoine	100%
44	Terpene	7,276,290	7,295,361	Steffimycin D	19%
45	NRPS	7,614,167	7,659,334	Collismycin A	14%
46	Thiopeptide	7,687,241	7,717,428	Kanamycin	8%
47	Halogenated	7,789,710	7,811,065	NA	
48	PKS	7,944,108	7,997,088	Herboxidiene	6%
49	NRPS	7,997,553	8,047,034	Retimycin A	13%
50	NRPS	8,099,304	8,191,692	Streptobactin	94%
51	Terpene	8,254,330	8,276,543	Geosmin	100%
52	Butyrolactone	8,308,010	8,318,954	Coelimycin P1	8%

resonances to be classified into six non-protonated carbons [at δ_C 154.6 (oxygenated), 146.44 (oxygenated), 146.35 (oxygenated), 134.3, 131.1, and 118.1], four methines (at δ_C 118.3, 109.0, 104.8, and 100.7), along with three methyls [at δ_C 56.1 (oxygenated), 55.6 (oxygenated), and 22.3]. On the basis of the multiple HMBC correlations (**Figure 5** and **Supplementary Figure 13**) from H-1 to C-2, C-4a, C-8, and C-8a, from H-3 to C-2, C-4, and C-4a, from H-5 to C-4a, C-7, and C-8a, from H-7 to C-5 and C-8, combined with from H-10 to C-5, C-6, and C-7, established the methyl naphthalene skeleton in compound **2**. Sequentially, the two methoxy groups attached at C-4 and C-9 were uncovered by the HMBC correlations from H-9 to C-4, and from H-11 to C-8, respectively (**Supplementary Figure 13**). The structure of **2** was therefore assigned as shown in **Figure 4**.

Compounds Consisted With Gene Clusters

Several isolated compounds are consistent with highly conserved gene clusters that are identified by genome mining in the chromosome of strain YINM00001.

Cluster 2 showed 100% similarities with cycloheximide gene cluster, which was consistent with the result that strain YINM00001 could produce cycloheximide and analogs (Yin et al., 2014). These compounds belong to the glutarimide-containing polyketide family, which have been pursued to be promising anti-metastatic drug due to their potent cell migration inhibition activity and cytotoxicity. Cycloheximide could inhibit protein synthesis in eukaryote cells by efficiently inhibiting translation elongation through binding to the 60S ribosomal subunits. It was widely used as fungicide, plant growth regulator, and protein synthesis inhibitor (Schneider-Poetsch et al., 2010). The high yield of cycloheximide and analogs probably accounted for the strong inhibition of strain YINM00001 against fungal pathogens.

Cluster 11 showed 100% similarities with dinactin gene cluster, which was consistent with the result that strain YINM00001 could produce dinactin and analogs (Kwon et al., 2001). These compounds belong to type II polyketide metabolites, which had been isolated from fermentation broth of several *Streptomyces* strains. These compounds use nonactic acid and homononactic acid as building units of ionophoretic character. Dinactin and analogs exhibited a very wide range of effects, including antibacterial, antifungal, antitumor, acaricidal, insecticidal, antiprotozoan, and antiparasitic activities (Zhang et al., 2020). The presence of these dinactins coincided with the antimicrobial activity of strain YINM00001.

Cluster 32 showed 100% similarities with anthracimycin gene cluster, which was consistent with the result that strain YINM00001 could produce anthracimycin (Alt and Wilkinson, 2015). Anthracimycin and analogs, belonging to decalin-containing tricyclic macrolides, were isolated from several marine-derived actinomycete strains. Anthracimycin showed strong antibiotic activities against *Bacillus anthracis* and methicillin resistant *Staphylococcus aureus* (MRSA). Spores of *B. anthracis* have been used as bioterrorism weapons, and MRSA has become a global health challenge. Meanwhile,

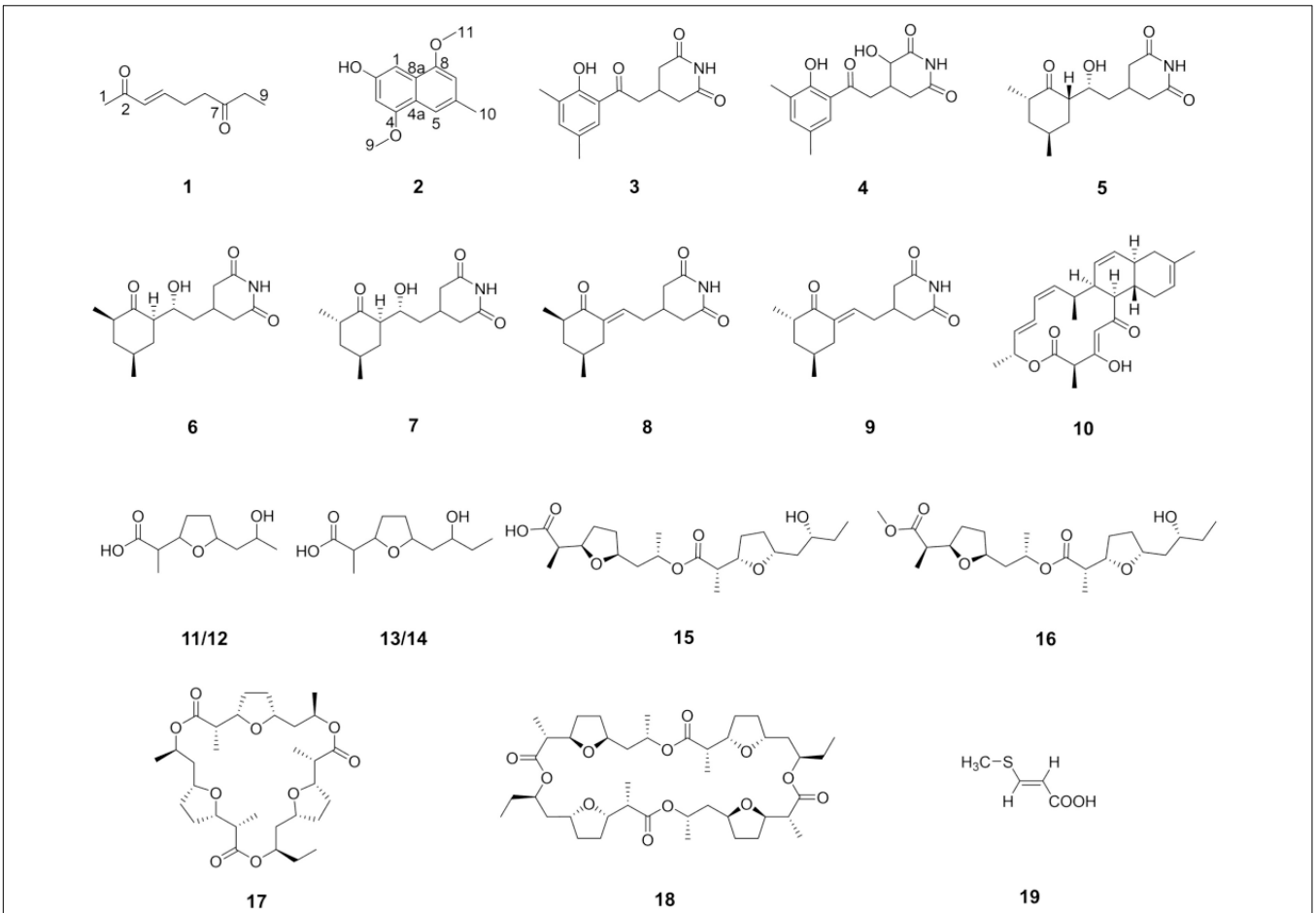

FIGURE 4 | Structures of the compounds isolated from strain YINM00001.

TABLE 5 | ^{1}H (400 MHz) and ^{13}C (100 MHz) NMR data for peperodione (1) and peperophthalene (2) in $CDCl_3$.

Position	1		2	
	δ_C, type	δ_H, (*J* in Hz)	δ_C, type	δ_H, (*J* in Hz)
1	27.2, CH_3	2.23 (s)	100.7, CH	7.49 (s)
2	198.7, C		146.4 (146.44), C	
3	131.9, CH	6.06 (d, 16.0)	109.0, CH	7.14 (s)
4	146.7, CH	6.79 (dt, 16.0, 6.6)	146.4 (146.35), C	
4a			118.8, C	
5	26.4, CH_2	2.50 (overlap)	118.3, CH	7.05 (s)
6	40.4, CH_2	2.60 (t, 7.2)	134.3, C	
7	209.8, C		104.8, CH	6.55 (s)
8	36.2, CH_2	2.44 (q, 7.3)	154.6, C	
8a			131.1, C	
9	8.0, CH_3	1.07 (t, 7.3)	56.1, CH_3	4.03 (s)
10			22.3, CH_3	2.46 (s)
11			55.6, CH_3	3.99 (s)

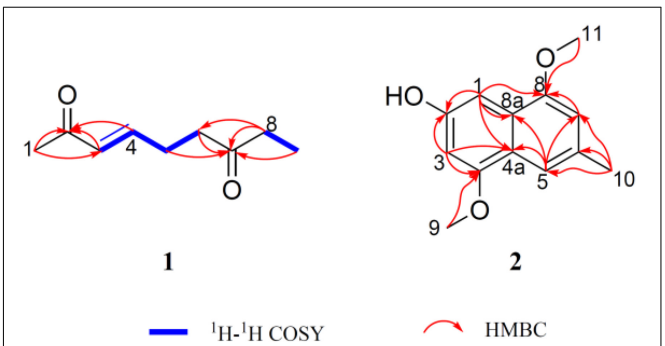

FIGURE 5 | Key ^{1}H-^{1}H COSY and HMBC correlations of peperodione **(1)** and peperophthalene **(2)**.

anthracimycin exhibits anticancer activity (Davison et al., 2020). This is the first time that it has been found from endophytic *Streptomyces* of inland plants. The gene cluster of this compound may have been passed down from ancestors to different offspring long ago, and these strains evolved independently in different environments.

Although biosynthesis of cycloheximide, dinactin, anthracimycin, and their analogs has been studied before, some important biosynthetic mechanisms remain mysterious

(Kwon et al., 2001, 2002; Heine et al., 2014; Yin et al., 2014; Alt and Wilkinson, 2015). Further studies on this talented strain would help us to uncover these secrets.

CONCLUSION

Endophytic bacteria were isolated from a Chinese medicinal herb *Peperomia dindygulensis* Miq. A *Streptomyces* sp. YINM00001 showed strong antimicrobial activity, and multiple antibiotic resistance was chosen for natural products exploration. After using genome mining and OSMAC approach to investigate this *Streptomyces* strain, two new compounds, peperodione (**1**) and peperophthalene (**2**), and 17 known compounds were isolated from different fermentation broth. Among them, cycloheximide, dinactin, anthracimycin, and analogs possess outstanding antimicrobial and/or anticancer activities, which had been pursued to be drug leads for a long time. The appearance of these compounds is not surprising due to the identification of their biosynthetic gene clusters through genome mining before fermentation. The large amount and high diversity of cycloheximide, dinactin, anthracimycin, and analogs produced by strain YINM00001 highlight this talented strain as an ideal candidate for further biosynthetic studies and production improvement of these valuable compounds. Other gene clusters might be silent under proceeding fermentation conditions. Further studies, such as heterologous expression and genetic modification, are needed to explore more novel compounds. Natural products from *Peperomia dindygulensis* endophytic bacteria, especially strain YINM00001, might provide a partial function of this medicinal herb to cure diseases, including cough, asthma, measles, burns, and cancers.

In conclusion, new drug leads research needs to be accelerated to counter the threat of dangerous infectious diseases and cancer. Endophytic *Streptomyces* sp. YINM00001 is a promising candidate to discover valuable secondary metabolites. Using genome mining and OSMAC approach together to investigate new strains from new habitats is a promising way to explore novel natural products.

DATA AVAILABILITY STATEMENT

The complete chromosome and plasmid sequences of strain YINM00001 were deposited in GenBank under accession number CP086102.1 and CP086103.1. This strain had been deposited at the Yunnan University and Guangdong Microbial Culture Collection Center under accession number YINM00001 and GDMCC No. 61693, respectively. The datasets presented in this study can be found in online repositories. The names of the repository/repositories and accession number(s) can be found in the article/**Supplementary Material**.

AUTHOR CONTRIBUTIONS

MY, HZ, and Z-TD designed the study, carried out the data analysis, and wrote the manuscript. TL, ZR, W-XC, G-DL, Z-T-LZ, H-BS, MeiW, T-PX, MengW, and J-YC carried out the experiments and participated in data analysis. All authors have read and approved the manuscript.

FUNDING

This work was supported by the National Natural Science Foundation of China (Grants 31860017 and 82160674 to MY and 31800002 to W-XC) and Yunnan Natural Science Foundation (202101AS070035, 202001BB050069, and YNWR-QNBJ-2019-031 to MY, 202101BA070001-035 and YNWR-QNBJ-2020-096 to ZR, and 2019FE001-131 to W-XC).

SUPPLEMENTARY MATERIAL

The Supplementary Material for this article can be found online at: https://www.frontiersin.org/articles/10.3389/fmicb.2022.831174/full#supplementary-material

REFERENCES

Alt, S., and Wilkinson, B. (2015). Biosynthesis of the novel macrolide antibiotic anthracimycin. *Acs Chem. Biol.* 10, 2468–2479. doi: 10.1021/acschembio.5b00525

Assmus, B., Hutzler, P., Kirchhof, G., Amann, R., Lawrence, J. R., and Hartmann, A. (1995). In situ localization of azospirillum brasilense in the rhizosphere of wheat with fluorescently labeled, rRNA-targeted oligonucleotide probes and scanning confocal laser microscopy. *Appl. Environ. Microbiol.* 61, 1013–1019. doi: 10.1128/aem.61.3.1013-1019.1995

Benson, G. (1999). Tandem repeats finder: a program to analyze DNA sequences. *Nucleic Acids Res.* 27, 573–580. doi: 10.1093/nar/27.2.573

Berdy, J. (2005). Bioactive microbial metabolites. *J. Antibiot.* 58, 1–26. doi: 10.1007/978-1-4757-9522-6_1

Bertelli, C., Laird, M. R., Williams, K. P., Simon Fraser University Research Computing Group, Lau, B. Y., Hoad, G., et al. (2017). IslandViewer 4: expanded prediction of genomic islands for larger-scale datasets. *Nucleic Acids Res.* 45, W30–W35. doi: 10.1093/nar/gkx343

Besemer, J., Lomsadze, A., and Borodovsky, M. (2001). GeneMarkS: a self-training method for prediction of gene starts in microbial genomes. Implications for finding sequence motifs in regulatory regions. *Nucleic Acids Res.* 29, 2607–2618. doi: 10.1093/nar/29.12.2607

Blin, K., Shaw, S., Steinke, K., Villebro, R., Ziemert, N., Lee, S., et al. (2019). antiSMASH 5.0: updates to the secondary metabolite genome mining pipeline. *Nucleic Acids Res.* 47, W81–W87. doi: 10.1093/nar/gkz310

Bode, H. B., Bethe, B., Hofs, R., and Zeeck, A. (2002). Big effects from small changes: possible ways to explore nature's chemical diversity. *Chembiochem* 3, 619–627. doi: 10.1002/1439-7633(20020703)3:7<619::AID-CBIC619>3.0.CO;2-9

Casey, M. L., Paulick, R. C., and Whitlock, H. W. Jr. (1976). A carbon-13 nuclear magnetic resonance study of mollisin and its biosynthesis. *J. Am. Chem. Soc.* 98, 2636–2640. doi: 10.1021/ja00425a037

Chan, P. P., Lin, B. Y., Mak, A. J., and Lowe, T. M. (2021). tRNAscan-SE 2.0: improved detection and functional classification of transfer RNA genes. *Nucleic Acids Res.* 49, 9077–9096. doi: 10.1093/nar/gkab688

Chen, L., Zheng, D., Liu, B., Yang, J., and Jin, Q. (2016). VFDB 2016: hierarchical and refined dataset for big data analysis–10 years on. *Nucleic Acids Res.* 44, D694–D697. doi: 10.1093/nar/gkv1239

Davison, E. K., Freeman, J. L., Zhang, W. L., Wuest, W. M., Furkert, D. P., and Brimble, M. A. (2020). asymmetric total synthesis of the naturally occurring antibiotic anthracimycin. *Org. Lett.* 22, 5550–5554. doi: 10.1021/acs.orglett.0c01913

Delcher, A. L., Bratke, K. A., Powers, E. C., and Salzberg, S. L. (2007). Identifying bacterial genes and endosymbiont DNA with Glimmer. *Bioinformatics* 23, 673–679. doi: 10.1093/bioinformatics/btm009

Detterbeck, R., and Hesse, M. (2002). Synthesis and structure elucidation of open-chained putrescine-bisamides from Aglaia species. *Tetrahedron* 58, 6887–6893. doi: 10.1016/s0040-4020(02)00751-2

Gene Ontology Consortium (2021). The gene ontology resource: enriching a GOld mine. *Nucleic Acids Res.* 49, D325–D334. doi: 10.1093/nar/gkaa1113

Grissa, I., Vergnaud, G., and Pourcel, C. (2007). CRISPRFinder: a web tool to identify clustered regularly interspaced short palindromic repeats. *Nucleic Acids Res.* 35, W52–W57. doi: 10.1093/nar/gkm360

Guo, H. F., Li, Y. H., Yi, H., Zhang, T., Wang, S. Q., Tao, P. Z., et al. (2009). Synthesis, structures and anti-HBV activities of derivatives of the glutarimide antibiotic cycloheximide. *J. Antibiot.* 62, 639–642. doi: 10.1038/ja.2009.87

Hardoim, P. R., Van Overbeek, L. S., and Elsas, J. D. (2008). Properties of bacterial endophytes and their proposed role in plant growth. *Trends Microbiol.* 16, 463–471. doi: 10.1016/j.tim.2008.07.008

Heine, D., Bretschneider, T., Sundaram, S., and Hertweck, C. (2014). Enzymatic polyketide chain branching to give substituted lactone, lactam, and glutarimide heterocycles. *Angew. Chem. Int. Ed. Engl.* 53, 11645–11649. doi: 10.1002/anie.201407282

Helaly, S. E., Goodfellow, M., Zinecker, H., Imhoff, J. F., Sussmuth, R. D., and Fiedler, H. P. (2013). Warkmycin, a novel angucycline antibiotic produced by Streptomyces sp. Acta 2930*. *J. Antibiot.* 66, 669–674. doi: 10.1038/ja.2013.74

Hensler, M. E., Jang, K. H., Thienphrapa, W., Vuong, L., Tran, D. N., Soubih, E., et al. (2014). Anthracimycin activity against contemporary methicillin-resistant *Staphylococcus aureus*. *J. Antibiot.* 67, 549–553. doi: 10.1038/ja.2014.36

Huang, H. R., Lan, X., Wang, Y. L., Tian, L., Fang, Y. X., Zhang, L., et al. (2015). New bioactive derivatives of nonactic acid from the marine *Streptomyces griseus* derived from the plant Salicornia sp. *Phytochem. Lett.* 12, 190–195. doi: 10.1016/j.phytol.2015.04.001

Jang, K. H., Nam, S. J., Locke, J. B., Kauffman, C. A., Beatty, D. S., Paul, L. A., et al. (2013). Anthracimycin, a potent anthrax antibiotic from a marine-derived actinomycete. *Angew. Chem. Int. Ed. Engl.* 52, 7822–7824. doi: 10.1002/anie.201302749

Jia, B., Raphenya, A. R., Alcock, B., Waglechner, N., Guo, P., Tsang, K. K., et al. (2017). CARD 2017: expansion and model-centric curation of the comprehensive antibiotic resistance database. *Nucleic Acids Res.* 45, D566–D573. doi: 10.1093/nar/gkw1004

Johnson, F., Starkovsky, N. A., and Gurowitz, W. D. (1965). Glutarimide antibiotics. Vii. The synthesis of Dl-neocycloheximide and the determination of the cyclohexanone ring stereochemistry of cycloheximide, its isomers, and inactone. *J. Am. Chem. Soc.* 87, 3492–3500. doi: 10.1021/ja01093a038

Kanehisa, M., and Goto, S. (2000). KEGG: kyoto encyclopedia of genes and genomes. *Nucleic Acids Res* 28, 27–30.

Kim, W. H., Jung, J. H., and Lee, E. (2005). Feigrisolide C: structural revision and synthesis. *J. Org. Chem.* 70, 8190–8192. doi: 10.1021/jo051107d

Kimura, M. (1980). A simple method for estimating evolutionary rates of base substitutions through comparative studies of nucleotide sequences. *J. Mol. Evol.* 16, 111–120. doi: 10.1007/BF01731581

Kumar, S., Stecher, G., and Tamura, K. (2016). MEGA7: molecular evolutionary genetics analysis version 7.0 for Bigger datasets. *Mol. Biol. Evol.* 33, 1870–1874. doi: 10.1093/molbev/msw054

Kwon, H. J., Smith, W. C., Scharon, A. J., Hwang, S. H., Kurth, M. J., and Shen, B. (2002). C-O bond formation by polyketide synthases. *Science* 297, 1327–1330. doi: 10.1126/science.1073175

Kwon, H. J., Smith, W. C., Xiang, L. K., and Shen, B. (2001). Cloning and heterologous expression of the macrotetrolide biosynthetic gene cluster revealed a novel polyketide synthase that lacks an acyl carrier protein. *J. Am. Chem. Soc.* 123, 3385–3386. doi: 10.1021/ja0100827

Lee, K. H. (2000). Research and future trends in the pharmaceutical development of medicinal herbs from Chinese medicine. *Public Health Nutr.* 3, 515–522. doi: 10.1017/s1368980000000604

Li, R., Wang, M., Ren, Z., Ji, Y., Yin, M., Zhou, H., et al. (2021). Amycolatopsis aidingensis sp. nov., a halotolerant actinobacterium, produces new secondary metabolites. *Front. Microbiol.* 12:743116. doi: 10.3389/fmicb.2021.743116

Luo, R., Liu, B., Xie, Y., Li, Z., Huang, W., Yuan, J., et al. (2012). SOAPdenovo2: an empirically improved memory-efficient short-read de novo assembler. *Gigascience* 1:18.

Newman, D. J., and Cragg, G. M. (2020). Natural products as sources of new drugs over the nearly four decades from 01/1981 to 09/2019. *J. Nat. Prod.* 83, 770–803. doi: 10.1021/acs.jnatprod.9b01285

Pospiech, A., and Neumann, B. (1995). A versatile quick-prep of genomic DNA from gram-positive bacteria. *Trends Genet.* 11, 217–218. doi: 10.1016/s0168-9525(00)89052-6

Ren, Z., Tang, S., Jiang, Y., Jiang, M., Zheng, S., Liu, W., et al. (2018). High-throughput sequencing analysis of endophytic bacteria diversity in fruits of white and red pitayas from three different origins. *Pol. J. Microbiol.* 67, 27–35. doi: 10.5604/01.3001.0011.6139

Rezanka, T., Spizek, J., Prikrylova, V., Prell, A., and Dembitsky, V. A. (2004). Five new derivatives of nonactic and homo-nonactic acids from Streptomyces globisporus. *Tetrahedron* 60, 4781–4787. doi: 10.1016/j.tet.2004.04.006

Rhoads, A., and Au, K. F. (2015). PacBio Sequencing and Its Applications. *Genomics Proteomics Bioinformatics* 13, 278–289. doi: 10.1016/j.gpb.2015.08.002

Romano, S., Jackson, S. A., Patry, S., and Dobson, A. D. W. (2018). Extending the "One Strain Many Compounds" (OSMAC) principle to marine microorganisms. *Mar. Drugs* 16:244. doi: 10.3390/md16070244

Saitou, N., and Nei, M. (1987). The neighbor-joining method: a new method for reconstructing phylogenetic trees. *Mol. Biol. Evol.* 4, 406–425.

Schaeffer, H. J., and Jain, V. K. (1963). Investigation of the stereochemistry of cycloheximide and its degradation products. *J. Pharm. Sci.* 52, 639–642. doi: 10.1002/jps.2600520707

Schneider-Poetsch, T., Ju, J. H., Eyler, D. E., Dang, Y. J., Bhat, S., Merrick, W. C., et al. (2010). Inhibition of eukaryotic translation elongation by cycloheximide and lactimidomycin. *Nat. Chem. Biol.* 6, 209–217. doi: 10.1038/nchembio.304

Sessitsch, A., Reiter, B., Pfeifer, U., and Wilhelm, E. (2002). Cultivation-independent population analysis of bacterial endophytes in three potato varieties based on eubacterial and Actinomycetes-specific PCR of 16S rRNA genes. *FEMS Microbiol. Ecol.* 39, 23–32. doi: 10.1111/j.1574-6941.2002.tb00903.x

Shen, B. (2015). A new golden age of natural products drug discovery. *Cell* 163, 1297–1300. doi: 10.1016/j.cell.2015.11.031

Skinnider, M. A., Johnston, C. W., Gunabalasingam, M., Merwin, N. J., Kieliszek, A. M., Maclellan, R. J., et al. (2020). Comprehensive prediction of secondary metabolite structure and biological activity from microbial genome sequences. *Nat. Commun.* 11:6058. doi: 10.1038/s41467-020-19986-1

Stamatakis, A. (2014). RAxML version 8: a tool for phylogenetic analysis and post-analysis of large phylogenies. *Bioinformatics* 30, 1312–1313. doi: 10.1093/bioinformatics/btu033

Stamatakis, A., Hoover, P., and Rougemont, J. (2008). A rapid bootstrap algorithm for the RAxML Web servers. *Syst. Biol.* 57, 758–771. doi: 10.1080/10635150802429642

Sun, D., Sun, W., Yu, Y., Li, Z., Deng, Z., and Lin, S. (2014). A new glutarimide derivative from marine sponge-derived Streptomyces anulatus S71. *Nat. Prod. Res.* 28, 1602–1606. doi: 10.1080/14786419.2014.928877

Tatusov, R. L., Fedorova, N. D., Jackson, J. D., Jacobs, A. R., Kiryutin, B., Koonin, E. V., et al. (2003). The COG database: an updated version includes eukaryotes. *BMC Bioinformatics* 4:41. doi: 10.1186/1471-2105-4-41

Wang, Q. W., Yu, D. H., Lin, M. G., Zhao, M., Zhu, W. J., Lu, Q., et al. (2012). Antiangiogenic polyketides from Peperomia dindygulensis Miq. *Molecules* 17, 4474–4483. doi: 10.3390/molecules17044474

Xie, P. F., Ma, M., Rateb, M. E., Shaaban, K. A., Yu, Z. G., Huang, S. X., et al. (2014). Biosynthetic potential-based strain prioritization for natural product discovery: a showcase for diterpenoid-producing actinomycetes. *J. Nat. Prod.* 77, 377–387. doi: 10.1021/np401063s

Xie, Z., and Tang, H. (2017). ISEScan: automated identification of insertion sequence elements in prokaryotic genomes. *Bioinformatics* 33, 3340–3347. doi: 10.1093/bioinformatics/btx433

Yin, M., Yan, Y., Lohman, J. R., Huang, S. X., Ma, M., Zhao, G. R., et al. (2014). Cycloheximide and actiphenol production in Streptomyces sp. YIM56141 governed by single biosynthetic machinery featuring an acyltransferase-less type I polyketide synthase. *Org. Lett.* 16, 3072–3075. doi: 10.1021/ol501179w

Yoon, S. H., Ha, S. M., Kwon, S., Lim, J., Kim, Y., Seo, H., et al. (2017). Introducing EzBioCloud: a taxonomically united database of 16S rRNA gene sequences and whole-genome assemblies. *Int. J. Syst. Evol. Microbiol.* 67, 1613–1617. doi: 10.1099/ijsem.0.001755

Zankari, E., Hasman, H., Cosentino, S., Vestergaard, M., Rasmussen, S., Lund, O., et al. (2012). Identification of acquired antimicrobial resistance genes. *J. Antimicrob. Chemother.* 67, 2640–2644. doi: 10.1093/jac/dks261

Zhang, K., Gu, L., Zhang, Y., Liu, Z., and Li, X. (2020). Dinactin from a new producer, *Streptomyces badius* gz-8, and its antifungal activity against the rubber anthracnose fungus colletotrichum gloeosporioides. *Microbiol. Res.* 240:126548. doi: 10.1016/j.micres.2020.126548

Zhou, Y., Liang, Y., Lynch, K. H., Dennis, J. J., and Wishart, D. S. (2011). PHAST: a fast phage search tool. *Nucleic Acids Res.* 39, W347–W352. doi: 10.1093/nar/gkr485

Conflict of Interest: The authors declare that the research was conducted in the absence of any commercial or financial relationships that could be construed as a potential conflict of interest.

Publisher's Note: All claims expressed in this article are solely those of the authors and do not necessarily represent those of their affiliated organizations, or those of the publisher, the editors and the reviewers. Any product that may be evaluated in this article, or claim that may be made by its manufacturer, is not guaranteed or endorsed by the publisher.

frontiers in Microbiology

ORIGINAL RESEARCH
published: 03 March 2022
doi: 10.3389/fmicb.2022.848964

Enabling Efficient Genetic Manipulations in a Rare Actinomycete *Pseudonocardia alni* Shahu

Jie Li[1,2†], Baiyang Wang[1,3†], Qing Yang[1], Han Si[1], Yuting Zhao[1], Yanli Zheng[1,2] and Wenfang Peng[1*]*

[1]State Key Laboratory of Biocatalysis and Enzyme Engineering, Hubei Engineering Research Center for Bio-enzyme Catalysis, Environmental Microbial Technology Center of Hubei Province, School of Life Sciences, Hubei University, Wuhan, China, [2]College of Life Science and Technology, Wuhan Polytechnic University, Wuhan, China, [3]Department of Microbiology, College of Life Sciences, Wuhan University, Wuhan, China

OPEN ACCESS

Edited by:
Yu-Qin Zhang,
Institute of Medicinal Biotechnology (CAS), China

Reviewed by:
Nan Peng,
Huazhong Agricultural University, China
Haiyan He,
Institute of Medicinal Biotechnology (CAS), China

***Correspondence:**
Yanli Zheng
Yanli.Zheng@whpu.edu.cn
Wenfang Peng
wenfang@hubu.edu.cn

[†]These authors have contributed equally to this work

Specialty section:
This article was submitted to Systems Microbiology, a section of the journal Frontiers in Microbiology

Received: 05 January 2022
Accepted: 01 February 2022
Published: 03 March 2022

Citation:
Li J, Wang B, Yang Q, Si H, Zhao Y, Zheng Y and Peng W (2022) Enabling Efficient Genetic Manipulations in a Rare Actinomycete Pseudonocardia alni Shahu. Front. Microbiol. 13:848964. doi: 10.3389/fmicb.2022.848964

Pseudonocardia species are emerging as important microorganisms of global concern with unique and increasingly significant ecological roles and represent a prominent source of bioactive natural products, but genetic engineering of these organisms for biotechnological applications is greatly hindered due to the limitation of efficient genetic manipulation tools. In this regard, we report here the establishment of an efficient genetic manipulation system for a newly isolated strain, *Pseudonocardia alni* Shahu, based on plasmid conjugal transfer from *Escherichia coli* to *Pseudonocardia*. Conjugants were yielded upon determining the optimal ratio between the donor and recipient cells, and designed genome modifications were efficiently accomplished, including exogenous gene integration based on an integrative plasmid and chromosomal stretch removal by homologous recombination using a suicidal non-replicating vector. Collectively, this work has made the *P. alni* Shahu accessible for genetic engineering, and provided an important reference for developing genetic manipulation methods in other rare actinomycetes.

Keywords: ***Pseudonocardia*, genetic manipulation, conjugal transfer, gene integration, gene deletion**

INTRODUCTION

Bacteria in the rare genus of *Pseudonocardia* belong to *Actinomycetes* that are represented by Gram-positive bacteria with high G + C DNA content (Tiwari and Gupta, 2012). With recent rapid developments in genome sequencing, more and more *Pseudonocardia* genomic data have been accumulated in the database. Many *Pseudonocardia*-specific gene clusters are now available, and their functions, concerning, for example, synthesis of many natural bioactive products (Miyamoto et al., 2014; Caffrey et al., 2016; Won et al., 2017; Geddis et al., 2018; Fang et al., 2019; Strecker et al., 2019; Subramani and Sipkema, 2019), biodegradation of large amounts of industrially discharged environmental pollutants (Grostern et al., 2012; Sales et al., 2013; Inoue et al., 2016; Yamamoto et al., 2018; Qi et al., 2019), defense against invading genetic elements (Doron et al., 2018), have been and will continue

to be deduced or demonstrated, showing great application potentials in human medicine, animal health, and crop protection, etc. Indeed, current applications of *Pseudonocardia* have been summarized very recently (Riahi et al., 2021). These beneficial potentials have attracted a great deal of interest in the *Pseudonocardia* genus. However, the generally poor efficiency or perhaps lack of genetic manipulation tools for *Pseudonocardia* has largely impeded deeper research and further application of this genus.

Introduction of DNAs into actinomycetes is generally difficult, possibly owing to the strong cell wall of such bacteria. Although strategies including protoplast transformation and electroporation of plasmids have been successfully used to introduce DNAs into some *Streptomyces* species, they are either of low efficiency or not adaptable for many of the less easy-to-handle non-model actinomycetes. Fortunately, easy and efficient DNA introduction from *Echerichia coli* to actinomycetes can be achieved *via* conjugal transfer. This method represents probably the most straightforward strategy for genetic manipulation in actinomycetes.

Conjugal transfer of different types of vectors, including replicative plasmids, integrative plasmids, and suicidal non-replicating vectors, has been applied in various actinomycetes. The replicative plasmids are useful for overproduction of heterologous proteins, but their host range is usually restricted to native strains and permanent selective pressure is required for their stable maintenance in the hosts. Advantageously, the other two types of vectors, integrative plasmids and suicidal non-replicating vectors, can introduce stable genomic alterations in many actinomycetes. Integrative plasmids contain genes encoding attachment/integration (*att*/*int*) functions, therein being capable of incorporating DNAs into chromosomes of a range of actinomycete species. Mechanistically, integrases derived from bacteriophages catalyze site-specific recombination between attachment sites, respectively, located on the genomes of phage (*attP*) and bacteria (*attB*), forming *attL* and *attR* hybrid sites (Combes et al., 2002). Currently, the suicidal non-replicating vectors have been extensively used to generate stable DNA inserts into any neutral genomic region, or deletion of genes of interest, *via* homologous recombination.

Here we report a rare actinomycete strain, *Pseudonocardia alni* Shahu, recently isolated from the sediment of a lake in the Shahu Park, Wuhan, China. In order to manipulate *P. alni* Shahu, we established an efficient conjugal transfer system, and *via* which, conjugal transfer of the pSET152 plasmid (Flett et al., 1997) and its derivatives from *E. coli* cells to *P. alni* spores were successfully achieved. Moreover, upon conjugation, the pSET152 derivatives have mediated the accomplishment of stable genomic alterations, including integration of an exogenous *gfp* gene into the chromosome and deletion of the *pgl* genes encoding key elements of a phage growth limitation antiviral defense system (Goldfarb et al., 2015). Collectively, these findings have allowed us to conduct genetic analyses of gene or system functions in *P. alni* Shahu, which, potentially, may serve as an important resource for both theoretical research and practical application in the future.

MATERIALS AND METHODS

Bacterial Strains and Culture Conditions

Pseudonocardia alni Shahu and derivatives constructed in this work, and *E. coli* strains, were listed in **Supplementary Table S1**. *Pseudonocardia alni* Shahu cells were grown at 30°C in an ISP4 medium (10 g/L soluble starch, 1 g/L K_2HPO_4, 1 g/L $MgSO_4$·7H2O, 1 g/L NaCl, 2 g/L $(NH_4)_2SO_4$, 2 g/L $CaCO_3$, 0.001 g/L $FeSO_4·7H_2O$, 0.001 g/L $MnCl_2·4H_2O$, and 0.001 g/L $ZnSO_4·7H_2O$, and pH 7.0–7.4) or on ISP4 agar plates (15 g/L agar in ISP4), while *E. coli* strains at 37°C in Luria broth or on Luria agar plates. When required, the following antibiotics were used: 50 mg/L of apramycin, 25 mg/L of chloramphenicol, and 50 mg/L of kanamycin.

Construction of Plasmids

All the conjugation plasmids were constructed based on the pSET152 vector and listed in **Supplementary Table S1**. The site-specific integration plasmid pInt-green fluorescent protein (GFP) was generated by inserting a GFP-expression cassette into pSET152 at BamH I and Not I sites (**Supplementary Figure S1**). The GFP-expression DNA fragment was synthesized from GenScript (Nanjing, China). To construct the non-replicating suicidal plasmid, we first amplified three DNA fragments by PCR with each containing either the *E. coli ori* (primer set P1 + P2), or the *aac(3)IV* gene encoding the apramycin-resistance marker (P3 + P4), or the elements mediating plasmid transfer, i.e., *traJ* and *oriT* of RK2 (P5 + P6), using pSET152 as a template. These fragments were then ligated together using T4 ligase to generate a base vector, pTSF, for plasmid transfer. Subsequently, the upstream (Up, P7 + P8) and downstream (Down, P9 + P10) sequences of the target *pgl* genes were amplified from the genomic DNA of *P. alni* Shahu by PCR and inserted into pTSF as homologous recombination arms using EcoR I and Sal I, Hind III, and Pvu II sites, respectively, giving pKO-pgl (**Supplementary Figure S1**). All oligonucleotides were synthesized from GenScript (Nanjing, China) and listed in **Supplementary Table S2**. Restriction enzymes and T4 ligase were purchased from New England Biolabs (Beijing) Led (Beijing, China).

Intergeneric Conjugation With *E. coli* and Screening of Recombinants

Pseudonocardia alni Shahu spores and the methylation-deficient *E. coli* strain ET12567 containing pUZ8002 were used as the recipient and the donor, respectively, throughout this study. A culture of the donor cells containing a transfer plasmid was grown to an OD_{600} of 0.4 in the presence of 50 mg/L apramycin, 50 mg/L kanamycin, and 25 mg/L chloramphenicol. The cells were then washed twice with an equal volume of LB to remove the antibiotics and finally resuspended in 0.1 volume of LB. The *P. alni* Shahu spores were resuspended with 0.5 ml of 2 × YT broth (10 g/L yeast extract, 16 g/L trptone, and 5 g/L NaCl). Recipient spores and donor cells were mixed and spread on ISP4 agar plates. After incubation at 30°C for 12–13 h, the plates were overlaid with 1 ml of distilled water containing 0.75 mg

nalidixic acid and 1.25 mg apramycin, and put at 30°C until colonies were observed. Recombinant candidates were screen by colony PCR using primers listed in **Supplementary Table S2**. The PCR products were analyzed by agarose gel electrophoresis and confirmed by Sanger sequencing (GneScript, Nanjing, China).

FACS Analysis

The protocol used for FACS analysis was as previously described with slight modifications (Zheng et al., 2019). The *P. alni* Shahu cells were washed with phosphate buffered saline (PBS) twice and then resuspended into PBS to a concentration of 10^7 cells/ml. Afterwards, the cells were analyzed *via* flow cytometry using Beckman CytoFLEX FCM (Beckman Coulter, Inc., United States) with PBS as the sheath fluid. A 488 nm laser was used as an FITC channel to detect the cell fluorescence of GFP.

RESULTS

Identification and Characterization of *P. alni* Shahu

In order to identify the isolate, based on the complete genome sequence that has been deposited into NCBI with the BioProject accession number PRJNA563468, the 1,540-bp 16S rDNA gene sequence (GenBank accession number MW405797, **Supplementary Table S3**) was phylogenetically characterized *via* BLAST (NCBI) search. In the constructed phylogenetic tree, the isolate falls into the cluster including members of *P. alni*, *Pseudonocardia antarctica*, and *Pseudonocardia carboxydivorans* with a reliability of 86% (**Figure 1A**), suggesting that it belongs to the genus *Pseudonocardia*. To further detail the species of this isolate, its genome sequence was then subjected to a taxonomic analysis with genomes of *Pseudonocardia* available in the NCBI Genome database to estimate pairwise Average Nucleotide Identity (ANI) score using the FastANI method (https://github.com/ParBLiSS/FastANI; Jain et al., 2018). The result showed that the genome of the isolate pairing with that of *P. alni* DSM44104^T or that of *Pseudonocardia* sp. AL041005-10 had ANI values ≥95% (**Figure 1B**), a criterion determining the same species in an existing genus (Jain et al., 2018). Taken together, the isolate was identified to be *P. alni* and assigned the strain name Shahu.

In order to determine a proper antibiotic resistance marker for *P. alni* Shahu, we investigated the resistance profile of this bacterium to common selective antibiotics, including apramycin (50 mg/L), kanamycin (50 mg/L), chloramphenicol (25 mg/L), tetracycline (50 mg/L), streptomycin (50 mg/L), and ampicillin (100 mg/L). About 10^6 pores were plated onto ISP4 agar containing one of the above antibiotics. At the tested concentrations, *P. alni* Shahu was sensitive to apramycin, chloramphenicol, and tetracycline, while fully resistant to kanamycin, streptomycin, and ampicillin.

Accomplishment of Conjugal Transfer Upon Determining the Optimal Donor-to-Recipient Ratio

Conjugal transfer represents one of the most straightforward and efficient methods for introducing foreign DNAs into rare *Antinomycetes*. We initially attempted conjugation between *E. coli* ET12567 (pUZ8002, pSET152) and *P. alni* Shahu following a standard conjugation protocol (Rebets et al., 2017), but failed in obtaining any exconjugant on the plate containing apramycin. This suggested that a modified protocol that specifically works for this strain is required to be established.

Previous studies have reported that an appropriate concentration of Mg^{2+} in the medium, or a suitable heat-shock treatment of the cells, or an optimal ratio of donor-to-recipient could give improved frequency of conjugation (Song et al., 2019; Zhang et al., 2019). We thus individually assessed each of such factors to attain successful conjugation. While, still, no exconjugant could be yielded, neither in the assay examining the various Mg^{2+} concentrations (0, 5, 10, 15, 30, and 50 mM), nor in that testing the heat-shocks with a temperature range from 37 to 65°C (data not shown). Fortunately, when we attempted changing the ratios of donor cells to recipient spores, we saw that different numbers of exconjugants appeared on the selective plates. The number of recipient cells played a more decisive role than that of the donor cells in the efficiency of conjugal transfer between *E. coli* and *P. alni*. When donor and recipient cells were 1×10^8 and 4×10^7, respectively, the highest conjugation efficiency reached 5.53×10^{-6} (**Table 1**). We therefore took this parameter in our following conjugation experiments.

Chromosomal Integration of an Exogenous Gene Using the *Φ*C31 *att*/*int* System

The apramycin-resistance ability of the obtained exconjugants is suggestive of the chromosomal integration of the pSET152 plasmid harboring the *aac(3)IV* apramycin resistance marker gene driven by the *Φ*C31 integrase (**Figure 2A**). Therein, integration of exogeneous genes into the *P. alni* Shahu chromosome could be achievable *via* the *Φ*C31 *att*/*int* system. To test such capability of the system, an integrative plasmid, pInt-GFP, was constructed by inserting a GFP-expressing cassette to pSET152 (**Supplementary Figure S1**). Then, conjugal transfer of pInt-GFP from *E. coli* to *P. alni* was conducted and its subsequent integration into the *P. alni* chromosome was examined.

According to the determined optimal ratio, *E. coli* ET12567 (pUZ8002, pInt-GFP) cells were mixed with *P. alni* Shahu spores for conjugation. Of the conjugants appeared on the plate with apramycin, eight were randomly picked up and grown up in a liquid ISP4 medium containing 50 mg/L of apramycin. To illustrate the chromosomal integration of pInt-GFP in detail, total DNAs were individually extracted from the selected exconjugants and used as templates for PCR analyses with a primer set of either P11 + P12 or P13 + P14 amplifying DNA fragments encompassing the *attL* or *attR* site, respectively (**Figure 2A**). Since P11 and P14 target the genomic sequences while P12 and P13 are located on the plasmid, PCR products can be amplified only when chromosomal integration of plasmid occurs. Agarose gel electrophoresis of the PCR products suggested successful integration of pInt-GFP into the Shahu genome, as PCR products with the expected sizes were amplified from the chromosomal DNAs of the conjugants but not from that

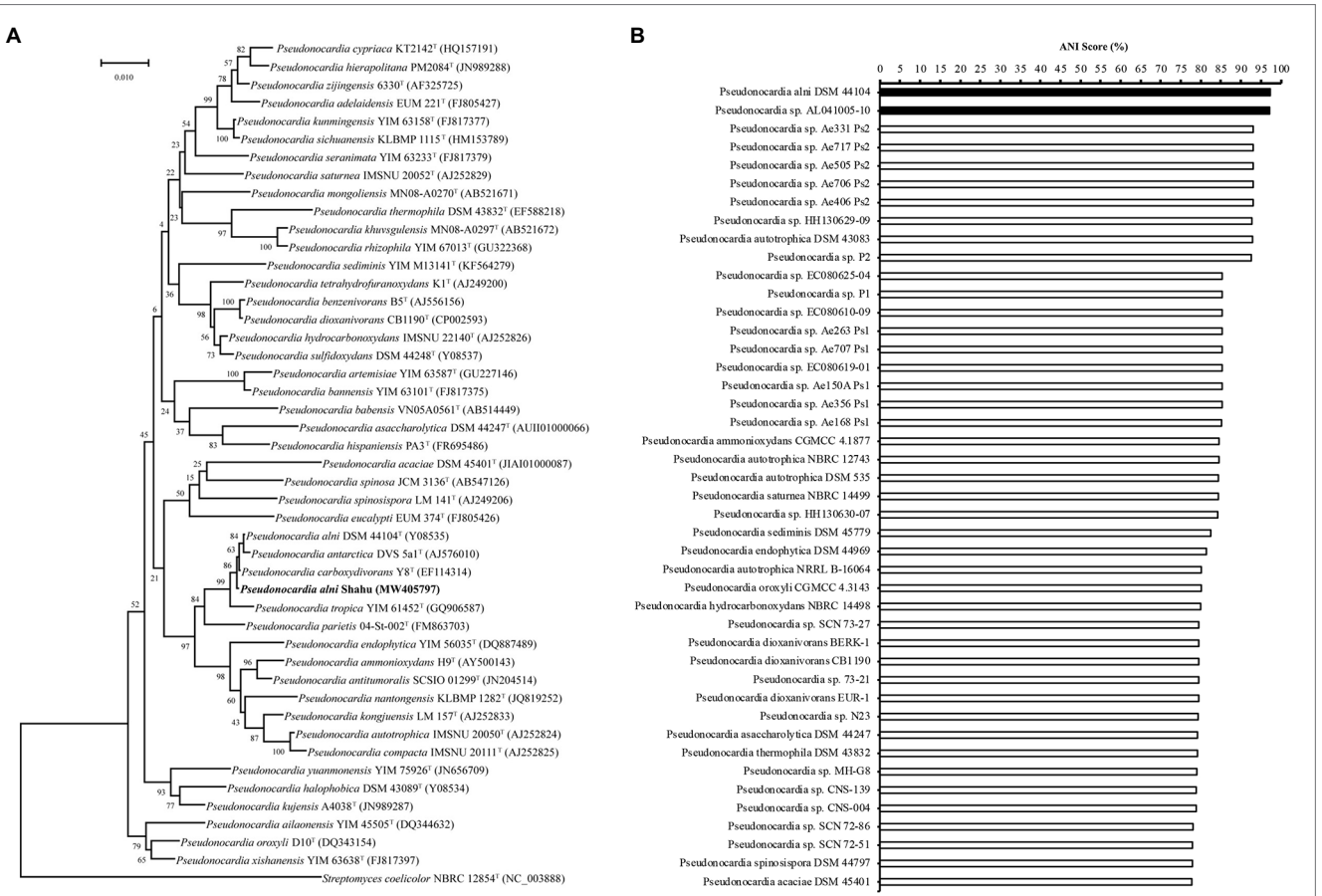

FIGURE 1 | Identification of *Pseudonocardia alni* Shahu. **(A)** Neighbor-joining phylogenetic tree based on 16S rDNA sequences showing the phylogenetic relationships of *P. anli* Shahu and the selected *Pseudonocardia* species. *Streptomyces coelicolor* NBRC 12854^T represents an outgroup reference. **(B)** Taxonomic analysis of *P. anli* Shahu with genomes of *Pseudonocardia* available in the NCBI Genome database. Pairwise Average Nucleotide Identity (ANI) score was estimated, and ANI score over 95% indicated with filled bars.

TABLE 1 | Effects of the donor (*E. coli* cells)-to-recipient (*P. alni* Shahu spores) ratio on transconjugation efficiency. At ratio, three independent conjugations were analyzed.

Number of donor cells	Number of recipient spores	Number of exconjugants
1.0×10^9	1.0×10^9	$(2.51\pm0.17)\times10^{-9}$
	1.0×10^8	$(4.70\pm0.33)\times10^{-7}$
	1.0×10^7	$(7.33\pm0.87)\times10^{-6}$
	1.0×10^6	$(4.12\pm0.54)\times10^{-6}$
1.0×10^8	1.0×10^9	$(3.76\pm0.35)\times10^{-9}$
	1.0×10^8	$(1.22\pm0.22)\times10^{-6}$
	1.0×10^7	$(5.53\pm0.27)\times10^{-6}$
	1.0×10^6	$(3.92\pm0.66)\times10^{-6}$
1.0×10^7	1.0×10^9	$(8.81\pm0.98)\times10^{-9}$
	1.0×10^8	$(7.75\pm0.32)\times10^{-7}$
	1.0×10^7	$(8.63\pm0.23)\times10^{-7}$
	1.0×10^6	$(2.57\pm0.56)\times10^{-6}$

of the wild-type strain (wt; **Figure 2B**). Subsequent Sanger sequencing of the PCR products confirmed the generation of the hybrid sequences of *attL* and *attR* from *attB* and *attP* (**Figure 2C**). In addition, our results detected the fluorescence signal of GFP from all the pInt-GFP exconjugants by flow cytometry, suggesting that the heterologously integrated GFP protein was stably expressed. In contrast, the signal was not detectable in the reference pSET152 exconjugant (**Figure 2D**). All these combined results suggested that the *Φ*C31 *att*/*int* system could be used for efficient chromosomal incorporation of foreign DNAs in *P. alni* Shahu.

Generation of Gene Deletion Mutants of *P. alni* Shahu *via* Homologous Recombination

We next demonstrated removal of exogeneous genes from the *P. alni* Shahu chromosome by using a non-replicating vector to facilitate homologous recombination. A DNA stretch containing the *pgl* genes was chosen as an editing target, since it was reported to be non-essential for cell viability (Goldfarb et al., 2015). The entire sequence of the *Φ*C31 *int* gene, together with that of the *attP* site, was removed from pSET152; while homologous arms of 633 and 733 bp were inserted upstream and downstream, respectively, of the *acc(3)IV* gene, giving the suicidal plasmid, pKO-pgl, for knockout of the *pgl* genes (**Figure 3A**).

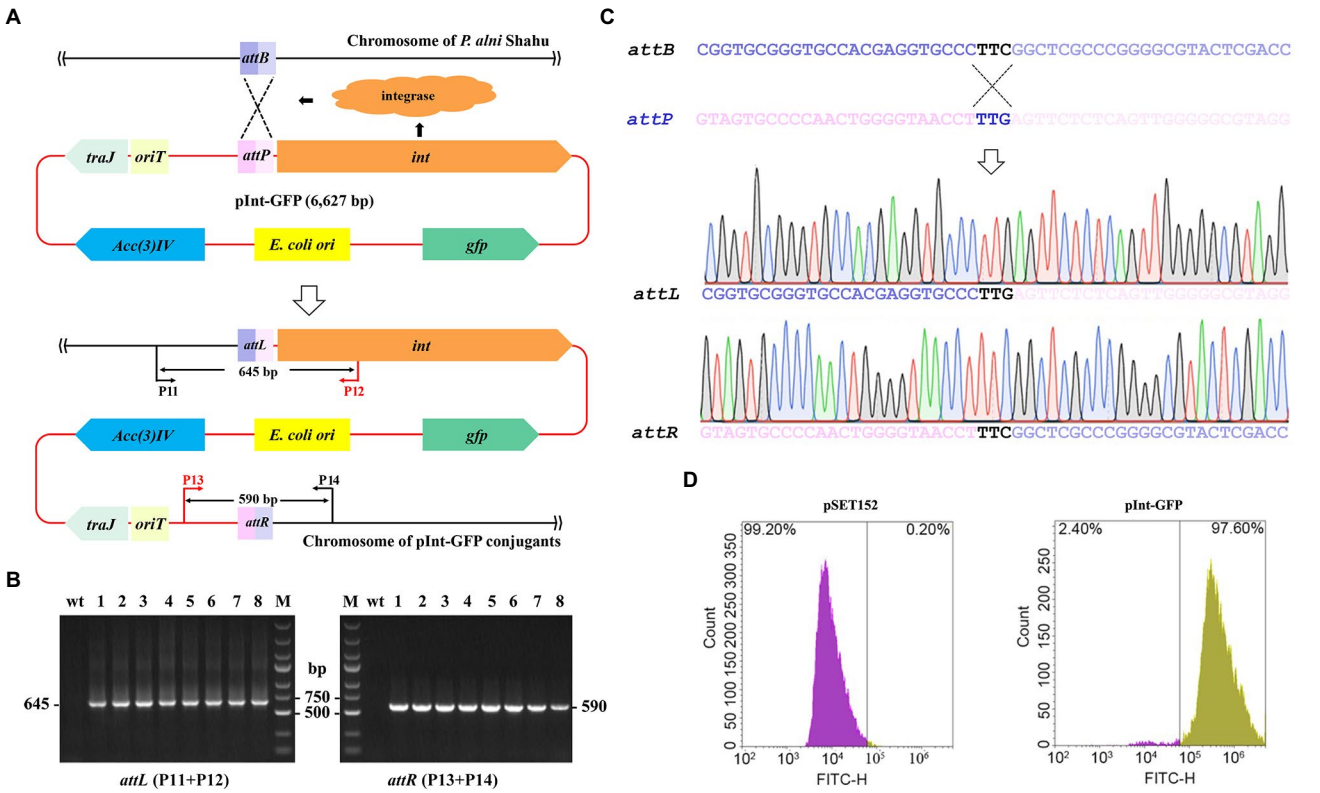

FIGURE 2 | Chromosomal integration of the exogenous *gfp* gene using the ΦC31 *att/int* system. **(A)** Schematic showing integration of the entire pInt-green fluorescent protein (GFP) plasmid into *P. anli* Shahu chromosome. **(B)** Colony PCR analyses of eight randomly taken exconjugants, and the wild-type strain (wt) as a reference, using primer sets of P11 + P12 and P13 + P14 as shown in **(A)**. Predicted sizes of PCR products encompassing the created hybrid *attL* and *attR* sites after integration are indicated. M, DNA size marker. **(C)** Representative chromatographs of Sanger sequencing results of the *attL* and *attR* sites. Original sequences of *attB* in *P. anli* Shahu chromosome and *attP* in pInt-GFP plasmid, respectively, are shown. **(D)** Signal of GFP was detected in the pInt-GFP exconjugant whereas not in the pSET152 exconjugant by flow cytometry.

After conjugal transfer of pKO-PGL into *P. alni* Shahu, colonies were observed on the selective plate containing apramycin, indicative of integration of the *acc(3)IV* gene into the host chromosome. We picked up 16 of the appeared colonies and analyzed their genotypes by PCR and Sanger sequencing. Using the primer set of P15 + P16, DNA products were amplified from total DNAs extracted from the strains that were expected to contain mutant alleles with a predicted size of 2,994 bp. However, the 2,994-bp band was amplified in only 11 of the tested colonies, while, interestingly, a predicted 8,228 bp band was amplified in the remainder (**Figure 3B**). Reasonably, double crossover has resulted in the replacement of the target region (2,260 bp) with the expression cassette of the *acc(3)IV* gene (1,010 bp), allowing for amplification of the 2,994-bp fragments (vs. the wild-type 4,244 bp); whereas a single crossover through either of the homologous arms would occur, leading to chromosomal integration of the entire plasmid and hence explaining the detected 8,228-bp DNA products.

To further corroborate the above observations, we designed an additional primer set, P17 + P18 with each, respectively, targeting a sequence located within the homologous arms, for PCR analyses of the same samples. As expected, PCR products of 3,002 and 1,752-bp were yielded in the wild-type cells and the double crossover recombinants, respectively; while both fragments were amplified in the colonies where single crossovers occurred (**Figure 3C**). These results thus confirmed the homologous recombination events deduced and showcased in **Figure 3A**.

DISCUSSION

Although successful examples of genetic engineering of some model actinobacteria have been accumulated in the literature (Deng et al., 2017; Kormanec et al., 2019), it is, in general, still more difficult to generically manipulate many rare actinomycetes. Methods to genetically manipulate the genome of rare actinomycetes, for example *Pseudonocardia*, might open new avenues toward the demonstration, development, and application of the valuable bacteria. Despite of the importance, until this work, there had been no detailed description of establishing a genetic manipulation system for genome modifications in any *Pseudonocardia* species.

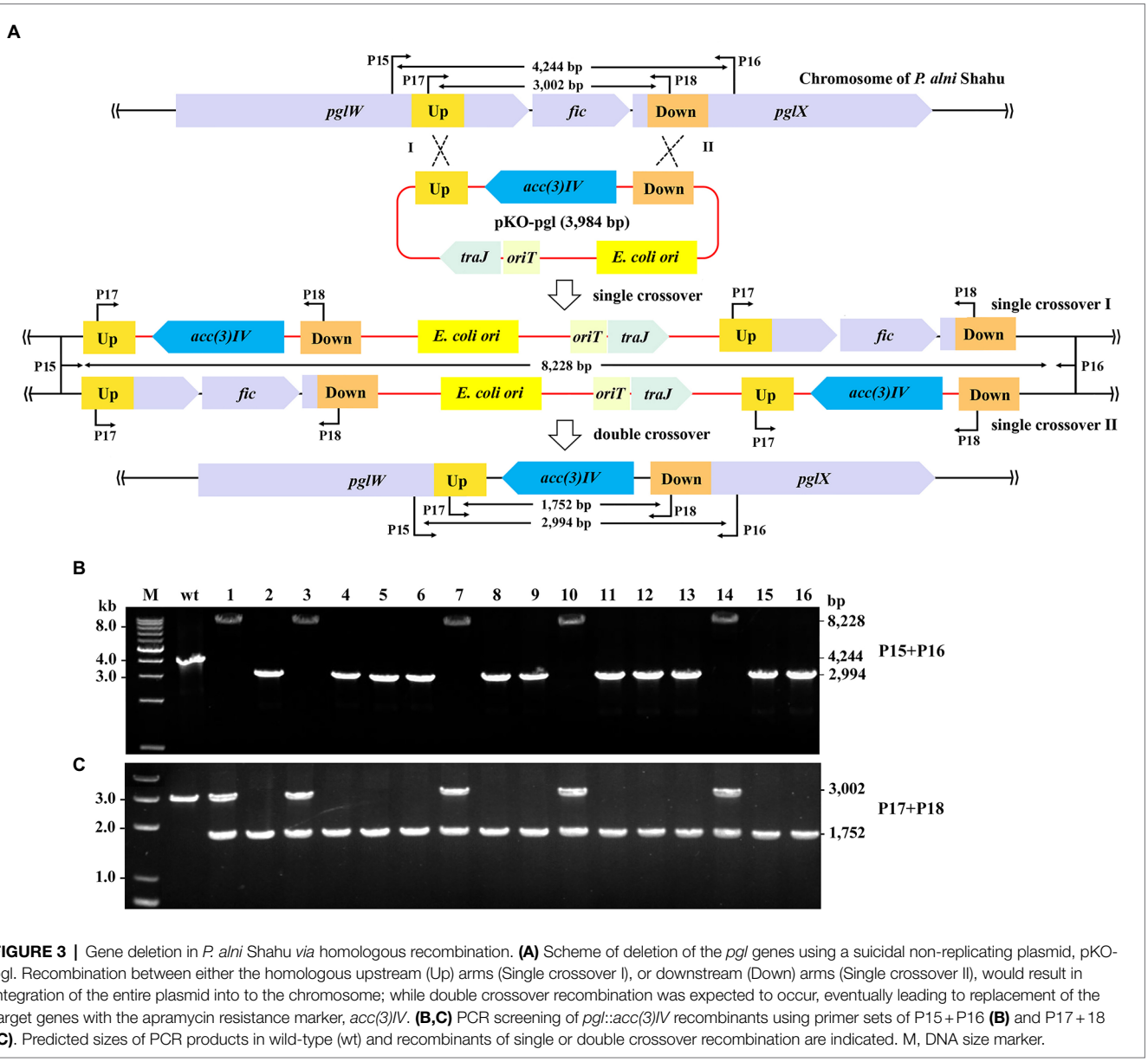

FIGURE 3 | Gene deletion in *P. alni* Shahu *via* homologous recombination. **(A)** Scheme of deletion of the *pgl* genes using a suicidal non-replicating plasmid, pKO-pgl. Recombination between either the homologous upstream (Up) arms (Single crossover I), or downstream (Down) arms (Single crossover II), would result in integration of the entire plasmid into to the chromosome; while double crossover recombination was expected to occur, eventually leading to replacement of the target genes with the apramycin resistance marker, *acc(3)IV*. **(B,C)** PCR screening of *pgl*::*acc(3)IV* recombinants using primer sets of P15 + P16 **(B)** and P17 + 18 **(C)**. Predicted sizes of PCR products in wild-type (wt) and recombinants of single or double crossover recombination are indicated. M, DNA size marker.

The major challenges could include the transfer of the vector harboring the foreign DNAs into the host and the incorporation of DNA into the host chromosome. Intergeneric conjugation has been proven to be one of the most efficient approaches for gene transfer into actinomycetes, and has been already successfully applied to *Streptomyces* species as an example (Netzker et al., 2016; Kormanec et al., 2019). However, it was suggested that conjugation protocols have to be customized for individual species before accomplishing successful conjugation (Marcone et al., 2010), and indeed, our work has confirmed that the standard conjugation protocol (Rebets et al., 2017) is not suitable for *P. alni* Shahu. We figured out the optimal parameters for conjugation and successfully achieved transfer of the pSET152 plasmid and its derivatives from *E. coli* into *P. alni*, therein, making it possible to deliver the powerful CRISPR-Cas machinery and others of interest, into this bacterium by this very approach for high-throughput genome engineering in the future.

We did observe the integration of the transferred pInt-GFP, a pSET152 derivative, into the genome at an *attB* site. Based on the confirmed *attL* and *attR* sequences, we deduced the 51-nt sequence of the *attB* site (**Figure 2C**) and traced it back to the genome of *P. alni* Shahu, seeing that it laid within an OFR coding for a pirin-homolog. This was very similarly to the case of *Streptomyces* species where *attB* sites were exclusively located within pirin-encoding ORFs. We found that this *attB* sequence showed an 89% nt identity to the canonical *attB* sequence possessed by *Streptomyces coelicolor* A3(2) from which the antinophage ΦC31 was originated (Lomovskaya et al., 1972). The sequence identity between the *attB* site of *S. coelicolor*

A3(2) and that of other actinomycetes seemed to play an important role in determining conjugation efficacy (**Supplementary Figure S2**). For example, plasmid transconjugation into *S. ambofaciens* harboring an *attB* sequence identical to that of *S. coelicolor* A3(2) (100% identity) yielded an efficiency of 1.4×10^{-2}, while into *S. clavligerus* yielded an efficiency of 3×10^{-5} as the *attB* identity was 96% (Kim et al., 2008). Furthermore, when the plasmid was transconjugated into a non-*Streptomyces* species *Kitasatospora setae* with a 78% *attB* identity, the efficiency was dropped to 2×10^{-7} (Choi et al., 2004). This thus explained the observed efficiency of foreign DNA integration into *P. alni* Shahu genome (5.5×10^{-6}, **Table 1**) *via* the *Φ*C31 *int/att* system in our work, and might provide a possibility to enhance the conjugation efficiency *via* engineering the *attB* sequence of *P. alni* Shahu to make it as identical as that of *S. coelicolor* A3(2).

An obvious shortcoming of this genetic manipulation system could be the lack of a counterselection marker. Currently, several suicide genes, e.g., *sacB*, *glkA*, *pyrF*, and *rpsL*, have been available as counterselection markers in different bacteria. The *sacB* gene, conferring sucrose sensitivity, was ever used for unmarked gene deletion in actinobacteria species (van der Geize et al., 2001, 2007). However, it was reported that this method was not applicable for *S. lividans* due to lack of sucrose sensitivity of this actinobacterium (Jager et al., 1992). The *glkA*, *pyrF*, and *rpsL*, and others, did play their roles in counterselection but only in the corresponding null mutants (van Wezel and Bibb, 1996; Hosted and Baltz, 1997; Knipfer et al., 1997). Additionally, some toxic genes, such as *mazF* (Zhang et al., 2006), can also be used as suicidal markers, which, however, rely on tightly controlled inducible promoters, thus limiting their applicability in strains with poorly developed molecular toolkits. Other methods may also include the application of temperature-sensitive replicons. For instance, the replicon of pIJ101 has been widely applied in some *Streptomyces* species (Mo et al., 2019). These methods might be also possibly applicable in *P. alni* Shahu, albeit, of course, necessitating the examination and determination of optimal parameters.

It would be also interesting to introduce the advanced CRISPR-Cas-based technologies into this actinobacterium. One of advantages of the technologies is that no selection marker is required due to the potent killing effect of the CRISPR-Cas systems on the bacterial cells. However, we could not get any transconjugant in the conjugation using a plasmid carrying a Cas9-expression cassette, even without a targeting guide RNA (data not shown). Possibly, the Cas9 nuclease *per se* is toxic to the host cells. Similar observations have been reported for other bacteria (Zheng et al., 2020; Hao et al., 2022). Interesting, we found that the chromosome of *P. alni* Shahu encodes a native CRISPR-Cas system. We believe that in the near future this system would be harnessed as a powerful genetic manipulation tool, although thorough demonstration of this system would be essentially needed.

Nevertheless, this work has enabled the generation of stable genome modifications in a rare actinomycetes *P. alni* Shahu with a considerably high efficiency, and thus making this strain amenable to the discovery and design of novel bioactive natural products by genetic engineering.

DATA AVAILABILITY STATEMENT

The datasets presented in this study can be found in online repositories. The names of the repository/repositories and accession number(s) can be found at: https://www.ncbi.nlm.nih.gov/, PRJNA563468; https://www.ncbi.nlm.nih.gov/genbank/, MW405797.

AUTHOR CONTRIBUTIONS

WP and YZe designed the research. JL, BW, QY, HS, and YZa performed the experiments. WP, JL, BW, and YZe wrote the manuscript. All authors contributed to data analyses, read, revised, and approved the final manuscript.

FUNDING

This work was supported by the Open Funding Project of the State Key Laboratory of Biocatalysis and Enzyme Engineering (SKLBEE2021019), and the Innovation Base for Introducing Talents of Discipline of Hubei Province (2019BJH021). YZe and WP acknowledge the support from the State Key Laboratory of Biocatalysis and Enzyme Engineering.

SUPPLEMENTARY MATERIAL

The Supplementary Material for this article can be found online at: https://www.frontiersin.org/articles/10.3389/fmicb.2022.848964/full#supplementary-material

REFERENCES

Caffrey, P., De Poire, E., Sheehan, J., and Sweeney, P. (2016). Polyene macrolide biosynthesis in streptomycetes and related bacteria: recent advances from genome sequencing and experimental studies. *Appl. Microbiol. Biotechnol.* 100, 3893–3908. doi: 10.1007/s00253-016-7474-z

Choi, S. U., Lee, C. K., Hwang, Y. I., Kinoshita, H., and Nihira, T. (2004). Intergeneric conjugal transfer of plasmid DNA from Escherichia coli to *Kitasatospora setae*, a bafilomycin B1 producer. *Arch. Microbiol.* 181, 294–298. doi: 10.1007/s00203-004-0654-8

Combes, P., Till, R., Bee, S., and Smith, M. C. (2002). The streptomyces genome contains multiple pseudo-attB sites for the (phi)C31-encoded site-specific recombination system. *J. Bacteriol.* 184, 5746–5752. doi: 10.1128/JB.184.20.5746-5752.2002

Deng, Y., Zhang, X., and Zhang, X. (2017). Recent advances in genetic modification systems for Actinobacteria. *Appl. Microbiol. Biotechnol.* 101, 2217–2226. doi: 10.1007/s00253-017-8156-1

Doron, S., Melamed, S., Ofir, G., Leavitt, A., Lopatina, A., Keren, M., et al. (2018). Systematic discovery of antiphage defense systems in the microbial pangenome. *Science* 359:eaar4120. doi: 10.1126/science.aar4120

Fang, Z., Chen, S., Zhu, Y., Li, J., Khan, I., Zhang, Q., et al. (2019). A new uridine derivative and a new indole derivative from the coral-associated actinomycete Pseudonocardia sp. SCSIO 11457. *Nat. Prod. Res.* 35, 188–194. doi: 10.1080/14786419.2019.1616729

Flett, F., Mersinias, V., and Smith, C. P. (1997). High efficiency intergeneric conjugal transfer of plasmid DNA from *Escherichia coli* to methyl DNA-restricting streptomycetes. *FEMS Microbiol. Lett.* 155, 223–229. doi: 10.1111/j.1574-6968.1997.tb13882.x

Geddis, S. M., Coroama, T., Forrest, S., Hodgkinson, J. T., Welch, M., and Spring, D. R. (2018). Synthesis and biological evaluation of 1,2-disubsubstituted 4-quinolone analogues of Pseudonocardia sp. natural products. *Beilstein J. Org. Chem.* 14, 2680–2688. doi: 10.3762/bjoc.14.245

Goldfarb, T., Sberro, H., Weinstock, E., Cohen, O., Doron, S., Charpak-Amikam, Y., et al. (2015). BREX is a novel phage resistance system widespread in microbial genomes. *EMBO J.* 34, 169–183. doi: 10.15252/embj.201489455

Grostern, A., Sales, C. M., Zhuang, W. Q., Erbilgin, O., and Alvarez-Cohen, L. (2012). Glyoxylate metabolism is a key feature of the metabolic degradation of 1,4-dioxane by Pseudonocardia dioxanivorans strain CB1190. *Appl. Environ. Microbiol.* 78, 3298–3308. doi: 10.1128/AEM.00067-12

Hao, Y., Wang, Q., Li, J., Yang, S., Zheng, Y., and Peng, W. (2022). Double nicking by RNA-directed Cascade-nCas3 for high-efficiency large-scale genome engineering. *Open Biol.* 12:210241. doi: 10.1098/rsob.210241

Hosted, T. J., and Baltz, R. H. (1997). Use of rpsL for dominance selection and gene replacement in Streptomyces roseosporus. *J. Bacteriol.* 179, 180–186. doi: 10.1128/jb.179.1.180-186.1997

Inoue, D., Tsunoda, T., Sawada, K., Yamamoto, N., Saito, Y., Sei, K., et al. (2016). 1,4-Dioxane degradation potential of members of the genera Pseudonocardia and Rhodococcus. *Biodegradation* 27, 277–286. doi: 10.1007/s10532-016-9772-7

Jager, W., Schafer, A., Puhler, A., Labes, G., and Wohlleben, W. (1992). Expression of the Bacillus subtilis sacB gene leads to sucrose sensitivity in the gram-positive bacterium Corynebacterium glutamicum but not in Streptomyces lividans. *J. Bacteriol.* 174, 5462–5465. doi: 10.1128/jb.174.16.5462-5465.1992

Jain, C., Rodriguez, R. L., Phillippy, A. M., Konstantinidis, K. T., and Aluru, S. (2018). High throughput ANI analysis of 90K prokaryotic genomes reveals clear species boundaries. *Nat. Commun.* 9:5114. doi: 10.1038/s41467-018-07641-9

Kim, M. K., Ha, H. S., and Choi, S. U. (2008). Conjugal transfer using the bacteriophage phiC31 att/int system and properties of the attB site in Streptomyces ambofaciens. *Biotechnol. Lett.* 30, 695–699. doi: 10.1007/s10529-007-9586-0

Knipfer, N., Seth, A., and Shrader, T. E. (1997). Unmarked gene integration into the chromosome of mycobacterium smegmatis via precise replacement of the pyrF gene. *Plasmid* 37, 129–140. doi: 10.1006/plas.1997.1286

Kormanec, J., Rezuchova, B., Homerova, D., Csolleiova, D., Sevcikova, B., Novakova, R., et al. (2019). Recent achievements in the generation of stable genome alterations/mutations in species of the genus Streptomyces. *Appl. Microbiol. Biotechnol.* 103, 5463–5482. doi: 10.1007/s00253-019-09901-0

Lomovskaya, N. D., Mkrtumian, N. M., Gostimskaya, N. L., and Danilenko, V. N. (1972). Characterization of temperate actinophage phi C31 isolated from *Streptomyces coelicolor* A3(2). *J. Virol.* 9, 258–262. doi: 10.1128/jvi.9.2.258-262.1972

Marcone, G. L., Foulston, L., Binda, E., Marinelli, F., Bibb, M., and Beltrametti, F. (2010). Methods for the genetic manipulation of Nonomuraea sp. ATCC 39727. *J. Ind. Microbiol. Biotechnol.* 37, 1097–1103. doi: 10.1007/s10295-010-0807-5

Miyamoto, K. T., Komatsu, M., and Ikeda, H. (2014). Discovery of gene cluster for mycosporine-like amino acid biosynthesis from Actinomycetales microorganisms and production of a novel mycosporine-like amino acid by heterologous expression. *Appl. Environ. Microbiol.* 80, 5028–5036. doi: 10.1128/AEM.00727-14

Mo, J., Wang, S., Zhang, W., Li, C., Deng, Z., Zhang, L., et al. (2019). Efficient editing DNA regions with high sequence identity in actinomycetal genomes by a CRISPR-Cas9 system. *Synth. Syst. Biotechnol.* 4, 86–91. doi: 10.1016/j.synbio.2019.02.004

Netzker, T., Schroeckh, V., Gregory, M. A., Flak, M., Krespach, M. K. C., Leadlay, P. F., et al. (2016). An efficient method to generate gene deletion mutants of the rapamycin-producing bacterium Streptomyces iranensis HM 35. *Appl. Environ. Microbiol.* 82, 3481–3492. doi: 10.1128/AEM.00371-16

Qi, M., Huang, H., Zhang, Y., Wang, H., Li, H., and Lu, Z. (2019). Novel tetrahydrofuran (THF) degradation-associated genes and cooperation patterns of a THF-degrading microbial community as revealed by metagenomic. *Chemosphere* 231, 173–183. doi: 10.1016/j.chemosphere.2019.05.137

Rebets, Y., Kormanec, J., Luzhetskyy, A., Bernaerts, K., and Anne, J. (2017). Cloning and expression of metagenomic DNA in Streptomyces lividans and subsequent fermentation for optimized production. *Methods Mol. Biol.* 1539, 99–144. doi: 10.1007/978-1-4939-6691-2_8

Riahi, H. S., Heidarieh, P., and Fatahi-Bafghi, M. (2021). Genus Pseudonocardia: what we know about its biological properties, abilities and current application in biotechnology. *J. Appl. Microbiol.* 132, 890–906. doi: 10.1111/jam.15271

Sales, C. M., Grostern, A., Parales, J. V., Parales, R. E., and Alvarez-Cohen, L. (2013). Oxidation of the cyclic ethers 1,4-dioxane and tetrahydrofuran by a monooxygenase in two Pseudonocardia species. *Appl. Environ. Microbiol.* 79, 7702–7708. doi: 10.1128/AEM.02418-13

Song, Z. Q., Liao, Z. J., Hu, Y. F., Ma, Z., Bechthold, A., and Yu, X. P. (2019). Development and optimization of an intergeneric conjugation system and analysis of promoter activity in Streptomyces rimosus M527. *J Zhejiang Univ Sci B* 20, 891–900. doi: 10.1631/jzus.B1900270

Strecker, J., Jones, S., Koopal, B., Schmid-Burgk, J., Zetsche, B., Gao, L., et al. (2019). Engineering of CRISPR-Cas12b for human genome editing. *Nat. Commun.* 10:212. doi: 10.1038/s41467-018-08224-4

Subramani, R., and Sipkema, D. (2019). Marine rare actinomycetes: a promising source of structurally diverse and unique novel natural products. *Mar. Drugs* 17:249. doi: 10.3390/md17050249

Tiwari, K., and Gupta, R. K. (2012). Rare actinomycetes: a potential storehouse for novel antibiotics. *Crit. Rev. Biotechnol.* 32, 108–132. doi: 10.3109/07388551.2011.562482

van der Geize, R., Hessels, G. I., van Gerwen, R., van der Meijden, P., and Dijkhuizen, L. (2001). Unmarked gene deletion mutagenesis of kstD, encoding 3-ketosteroid Delta1-dehydrogenase, in Rhodococcus erythropolis SQ1 using sacB as counter-selectable marker. *FEMS Microbiol. Lett.* 205, 197–202. doi: 10.1111/j.1574-6968.2001.tb10947.x

Van der Geize, R., Yam, K., Heuser, T., Wilbrink, M. H., Hara, H., Anderton, M. C., et al. (2007). A gene cluster encoding cholesterol catabolism in a soil actinomycete provides insight into mycobacterium tuberculosis survival in macrophages. *Proc. Natl. Acad. Sci. U. S. A.* 104, 1947–1952. doi: 10.1073/pnas.0605728104

van Wezel, G. P., and Bibb, M. J. (1996). A novel plasmid vector that uses the glucose kinase gene (glkA) for the positive selection of stable gene disruptants in Streptomyces. *Gene* 182, 229–230. doi: 10.1016/S0378-1119(96)00563-X

Won, H. J., Kim, H. J., Jang, J. Y., Kang, S. H., Choi, S. S., and Kim, E. S. (2017). Improved recovery and biological activities of an engineered polyene NPP analogue in Pseudonocardia autotrophica. *J. Ind. Microbiol. Biotechnol.* 44, 1293–1299. doi: 10.1007/s10295-017-1954-8

Yamamoto, N., Saito, Y., Inoue, D., Sei, K., and Ike, M. (2018). Characterization of newly isolated Pseudonocardia sp. N23 with high 1,4-dioxane-degrading ability. *J. Biosci. Bioeng.* 125, 552–558. doi: 10.1016/j.jbiosc.2017.12.005

Zhang, S., Chen, T., Jia, J., Guo, L., Zhang, H., Li, C., et al. (2019). Establishment of a highly efficient conjugation protocol for Streptomyces kanamyceticus ATCC12853. *Microbiology* 8:e00747. doi: 10.1002/mbo3.747

Zhang, X. Z., Yan, X., Cui, Z. L., Hong, Q., and Li, S. P. (2006). mazF, a novel counter-selectable marker for unmarked chromosomal manipulation in Bacillus subtilis. *Nucleic Acids Res.* 34:e71. doi: 10.1093/nar/gkl358

Zheng, Y., Han, J., Wang, B., Hu, X., Li, R., Shen, W., et al. (2019). Characterization and repurposing of the endogenous type I-F CRISPR-Cas system of Zymomonas mobilis for genome engineering. *Nucleic Acids Res.* 47, 11461–11475. doi: 10.1093/nar/gkz940

Zheng, Y., Li, J., Wang, B., Han, J., Hao, Y., Wang, S., et al. (2020). Endogenous type I CRISPR-Cas: from foreign DNA defense to prokaryotic engineering. *Front. Bioeng. Biotechnol.* 8:62. doi: 10.3389/fbioe.2020.00062

Conflict of Interest: The authors declare that the research was conducted in the absence of any commercial or financial relationships that could be construed as a potential conflict of interest.

Publisher's Note: All claims expressed in this article are solely those of the authors and do not necessarily represent those of their affiliated organizations, or those of the publisher, the editors and the reviewers. Any product that may be evaluated in this article, or claim that may be made by its manufacturer, is not guaranteed or endorsed by the publisher.

Advantages of publishing in Frontiers

OPEN ACCESS
Articles are free to read for greatest visibility and readership

FAST PUBLICATION
Around 90 days from submission to decision

HIGH QUALITY PEER-REVIEW
Rigorous, collaborative, and constructive peer-review

TRANSPARENT PEER-REVIEW
Editors and reviewers acknowledged by name on published articles

Frontiers
Avenue du Tribunal-Fédéral 34
1005 Lausanne | Switzerland

Visit us: www.frontiersin.org
Contact us: frontiersin.org/about/contact

REPRODUCIBILITY OF RESEARCH
Support open data and methods to enhance research reproducibility

DIGITAL PUBLISHING
Articles designed for optimal readership across devices

FOLLOW US
@frontiersin

IMPACT METRICS
Advanced article metrics track visibility across digital media

EXTENSIVE PROMOTION
Marketing and promotion of impactful research

LOOP RESEARCH NETWORK
Our network increases your article's readership